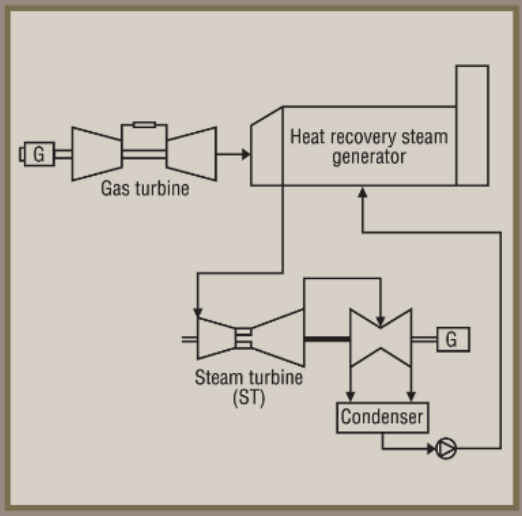
WOODHEAD PUBLISHING SERIES IN ENERGY



Advanced power plant materials, design and technology

Edited by Dermot Roddy

CRC
WP

Advanced power plant materials, design and technology

© Woodhead Publishing Limited, 2010

https://boilersinfo.com/

Related titles:

Developments and innovation in carbon dioxide (CO_2) capture and storage technology:
Volume 1 Carbon dioxide (CO_2) capture, transport and industrial applications
(ISBN 978-1-84569-533-0)
Volume 2 Carbon dioxide (CO_2) storage and utilisation
(ISBN 978-1-84569-797-6)
Carbon dioxide (CO_2) capture and storage (CCS) is the one advanced technology that conventional power generation cannot do without. CCS technology reduces the carbon footprint of power plants by capturing and storing the CO_2 emissions from burning fossil fuels and biomass. Capture technology ranges from post- and pre-combustion capture to combustion-based capture. Storage options range from geological sequestration in deep saline aquifers and utilisation of CO_2 for enhanced oil and gas recovery, to mineral carbonation and biofixation of CO_2. Volume 1 critically reviews carbon capture processes and technology applicable to the conventional power generation sector as well as other high-carbon-footprint industries. Volume 2 reviews carbon storage and utilisation, covering all the main geological, terrestrial and ocean sequestration options and their environmental impacts, as well as other advanced concepts such as utilisation and photocatalytic reduction.

Generating power at high efficiency: Combined cycle technology for sustainable energy production
(ISBN 978-1-84569-433-3)
Combined cycle technology is used to generate power at one of the highest levels of efficiency of conventional power plants. It does this through primary generation from a gas turbine coupled with secondary generation from a steam turbine powered by primary exhaust heat. *Generating power at high efficiency* thoroughly charts the development and implementation of this technology in power plants and looks to the future of the technology, noting the advantages of the most important technical features – including gas turbine, steam generator, combined heat and power and integrated gasification combined cycle (IGCC) – with their latest applications.

Details of these and other Woodhead Publishing materials books can be obtained by:

- visiting our web site at www.woodheadpublishing.com
- contacting Customer Services (e-mail: sales@woodheadpublishing.com; fax: +44 (0) 1223 893694; tel.: +44 (0) 1223 891358 ext. 130; address: Woodhead Publishing Limited, Abington Hall, Granta Park, Great Abington, Cambridge CB21 6AH, UK)

If you would like to receive information on forthcoming titles, please send your address details to: Francis Dodds (address, tel. and fax as above; e-mail: francis.dodds@woodheadpublishing.com). Please confirm which subject areas you are interested in.

© Woodhead Publishing Limited, 2010

https://boilersinfo.com/

Woodhead Publishing Series in Energy: Number 5

Advanced power plant materials, design and technology

Edited by
Dermot Roddy



CRC Press
Boca Raton Boston New York Washington, DC

WOODHEAD PUBLISHING LIMITED
Oxford Cambridge New Delhi

© Woodhead Publishing Limited, 2010

https://boilersinfo.com/

Published by Woodhead Publishing Limited, Abington Hall, Granta Park,
Great Abington, Cambridge CB21 6AH, UK
www.woodheadpublishing.com

Woodhead Publishing India Private Limited, G-2, Vardaan House, 7/28 Ansari Road,
Daryaganj, New Delhi – 110002, India
www.woodheadpublishingindia.com

Published in North America by CRC Press LLC, 6000 Broken Sound Parkway, NW,
Suite 300, Boca Raton, FL 33487, USA

First published 2010, Woodhead Publishing Limited and CRC Press LLC
© Woodhead Publishing Limited, 2010
The authors have asserted their moral rights.

This book contains information obtained from authentic and highly regarded sources. Reprinted material is quoted with permission, and sources are indicated. Reasonable efforts have been made to publish reliable data and information, but the authors and the publishers cannot assume responsibility for the validity of all materials. Neither the authors nor the publishers, nor anyone else associated with this publication, shall be liable for any loss, damage or liability directly or indirectly caused or alleged to be caused by this book.

Neither this book nor any part may be reproduced or transmitted in any form or by any means, electronic or mechanical, including photocopying, microfilming and recording, or by any information storage or retrieval system, without permission in writing from Woodhead Publishing Limited.

The consent of Woodhead Publishing Limited does not extend to copying for general distribution, for promotion, for creating new works, or for resale. Specific permission must be obtained in writing from Woodhead Publishing Limited for such copying.

Trademark notice: Product or corporate names may be trademarks or registered trademarks, and are used only for identification and explanation, without intent to infringe.

British Library Cataloguing in Publication Data
A catalogue record for this book is available from the British Library.

Library of Congress Cataloging in Publication Data
A catalog record for this book is available from the Library of Congress.

Woodhead Publishing ISBN 978-1-84569-515-6 (book)
Woodhead Publishing ISBN 978-1-84569-946-8 (e-book)
CRC Press ISBN 978-1-4398-2727-7
CRC Press order number: N10145

The publishers' policy is to use permanent paper from mills that operate a sustainable forestry policy, and which has been manufactured from pulp which is processed using acid-free and elemental chlorine-free practices. Furthermore, the publishers ensure that the text paper and cover board used have met acceptable environmental accreditation standards.

Typeset by Data Standards Ltd, Frome, Somerset, UK
Printed by TJ International Limited, Padstow, Cornwall, UK

© Woodhead Publishing Limited, 2010

https://boilersinfo.com/

Contents

Contributor contact details *xi*

Woodhead Publishing Series in Energy *xv*

Preface *xvii*

Part I Advanced power plant materials and designs

1 Advanced gas turbine materials, design and technology 3
J. FADOK, Siemens Energy Inc., USA

1.1 Introduction 3
1.2 Development of materials and coatings for gas turbines and turbine components 8
1.3 Higher temperature efficiency operation 15
1.4 Design for hydrogen-rich gases 21
1.5 Design to run at variable generation rates 26
1.6 Future trends 29
1.7 Sources of further information 30
1.8 References 31

2 Gas-fired combined-cycle power plant design and technology 32
A. D. RAO, University of California, USA

2.1 Introduction 32
2.2 Plant design and technology 36
2.3 Applicable criteria pollutants control technologies 41
2.4 CO_2 emissions control technologies 42
2.5 Advantages and limitations of gas-fired combined-cycle plants 46
2.6 Future trends 48
2.7 Sources of further information 52
2.8 References 52

© Woodhead Publishing Limited, 2010

https://boilersinfo.com/

3 Integrated gasification combined cycle (IGCC) power plant design and technology 54
Y. ZHU, Pacific Northwest National Laboratory, USA; and H. C. FREY, North Carolina State University, USA

3.1 Introduction: types of integrated gasification combined cycle (IGCC) plants 54
3.2 IGCC plant design and main processes technologies 60
3.3 Applicable CO_2 capture technologies 67
3.4 Applicable emissions control technologies 69
3.5 Advantages and limitations of coal IGCC plants 75
3.6 Future trends 79
3.7 Sources of further information 83
3.8 References 83

4 Improving thermal cycle efficiency in advanced power plants: water and steam chemistry and materials performance 89
B. DOOLEY, Structural Integrity Associates, Inc., USA; and R. SVOBODA, Svoboda Consulting, Switzerland

4.1 Introduction 89
4.2 Key characteristics of advanced thermal power cycles 91
4.3 Volatility, partitioning and solubility 93
4.4 Deposits and corrosion in the thermal cycle of a power plant 94
4.5 Water and steam chemistry in the thermal cycle with particular emphasis on supercritical and ultra-supercritical plant 100
4.6 Challenges for future ultra-supercritical power cycles 105
4.7 Acknowledgement 107
4.8 References 107

Part II Gas separation membranes, emissions handling, and instrumentation and control technology for advanced power plants

5 Advanced hydrogen (H_2) gas separation membrane development for power plants 111
S. J. DOONG, UOP, a Honeywell Company, USA

5.1 Introduction 111
5.2 Hydrogen membrane materials 113
5.3 Membrane system design and performance 121
5.4 Hydrogen membrane integration with power plant 125
5.5 Hydrogen storage and transportation 132
5.6 Future trends 133

© Woodhead Publishing Limited, 2010

https://boilersinfo.com/

5.7	Sources of further information and advice	135
5.8	References	135
6	Advanced carbon dioxide (CO_2) gas separation membrane development for power plants A. BASILE, Italian National Research Council, Italy; F. GALLUCCI, University of Twente, The Netherlands; and P. MORRONE, University of Calabria, Italy	143
6.1	Introduction	143
6.2	Performance of membrane system	148
6.3	CO_2 membrane materials and design	156
6.4	Membrane modules	161
6.5	Design for power plant integration	169
6.6	Cost considerations	175
6.7	Sources of further information	178
6.8	References	181
7	Advanced flue gas cleaning systems for sulfur oxides (SO_x), nitrogen oxides (NO_x) and mercury emissions control in power plants S. FALCONE MILLER and B. G. MILLER, The Pennsylvania State University, USA	187
7.1	Introduction	187
7.2	Flue gas desulfurization (FGD)	189
7.3	Selective catalytic reduction (SCR)	203
7.4	Selective non-catalytic reduction (SNCR)	207
7.5	Hybrid SNCR/SCR	208
7.6	Activated carbon injection systems	209
7.7	Future trends	212
7.8	Sources of further information	215
7.9	References	215
8	Advanced flue gas dedusting systems and filters for ash and particulate emissions control in power plants B. G. MILLER, The Pennsylvania State University, USA	217
8.1	Introduction	217
8.2	Materials, design, and development for particulate control	219
8.3	Electrostatic precipitators (ESPs)	219
8.4	Fabric filters	229
8.5	Future trends	236
8.6	Sources of further information	241
8.7	References	242

© Woodhead Publishing Limited, 2010

https://boilersinfo.com/

9 Advanced sensors for combustion monitoring in power plants: towards smart high-density sensor networks 244
M. YU and A. K. GUPTA, University of Maryland, USA; and M. BRYDEN, Iowa State University, USA

9.1 Introduction 244
9.2 Combustion behavior 246
9.3 Sensor considerations 248
9.4 Sensor response 251
9.5 Vision of smart sensor networks 255
9.6 Sensor information processing 260
9.7 Conclusions 261
9.8 Acknowledgements 262
9.9 References 262

10 Advanced monitoring and process control technology for coal-fired power plants 264
Y. YAN, University of Kent, UK

10.1 Introduction 264
10.2 Advanced sensors for on-line monitoring and measurement 266
10.3 Advanced control 279
10.4 Future trends 282
10.5 Sources of further information 284
10.6 References 285

Part III Improving the fuel flexibility, environmental impact and generation performance of advanced power plants

11 Low-rank coal properties, upgrading and utilization for improving the fuel flexibility of advanced power plants 291
T. DLOUHÝ, Czech Technical University in Prague, Czech Republic

11.1 Introduction 291
11.2 Properties of low-rank coal 292
11.3 Influence on design and efficiency of boilers 294
11.4 Low-rank coal preparation 294
11.5 Technologies of low-rank coal upgrading 296
11.6 Utilization of low-rank coal in advanced power plants 305
11.7 Future trends in coal upgrading 307
11.8 Sources of further information 309
11.9 Acknowledgement 310
11.10 References 310

© Woodhead Publishing Limited, 2010

https://boilersinfo.com/

12 Biomass resources, fuel preparation and utilization for improving the fuel flexibility of advanced power plants 312
L. ROSENDAHL, Aalborg University, Denmark

12.1 Introduction 312
12.2 Biomass types and conversion technologies 316
12.3 Chemical constituents in biomass fuels 320
12.4 Physical preparation of biomass fuels 324
12.5 Functional biomass mixes 329
12.6 Summary 330
12.7 References 330

13 Development and integration of underground coal gasification (UCG) for improving the environmental impact of advanced power plants 332
M. GREEN, UCG Engineering Ltd, UK

13.1 Introduction 332
13.2 Brief history of UCG 334
13.3 The UCG process 335
13.4 Criteria for siting and geology 341
13.5 Drilling technologies and well construction for UCG 344
13.6 Integration with power plant 346
13.7 Environmental issues and benefits 350
13.8 Future trends 354
13.9 Conclusion and future trends 358
13.10 Sources of further information 359
13.11 Glossary 360
13.12 References 361

14 Development and application of carbon dioxide (CO_2) storage for improving the environmental impact of advanced power plants 364
B. MCPHERSON, The University of Utah, USA

14.1 Introduction 364
14.2 Premise: capture and sequestration of CO_2 from power plants 365
14.3 Fundamentals of subsurface CO_2 flow and transport 366
14.4 Fundamentals of subsurface CO_2 storage 368
14.5 Enhanced oil/gas and coalbed methane recovery 371
14.6 CO_2 storage in deep saline formations 372
14.7 Comparison of storage options: oil/gas versus coal versus deep saline 372
14.8 General site selection criteria 373
14.9 Emissions versus potential subsurface storage capacity 375

© Woodhead Publishing Limited, 2010

https://boilersinfo.com/

14.10 Sealing and monitoring to ensure CO_2 containment 376
14.11 Alternatives to geologic storage 376
14.12 Future trends 377
14.13 Sources of further information and advice 379
14.14 References 379

15 Advanced technologies for syngas and hydrogen (H_2) production from fossil-fuel feedstocks in power plants 383
P. CHIESA, Politecnico di Milano, Italy

15.1 Introduction 383
15.2 Syngas production from gas and light liquids 383
15.3 Syngas conversion and purification 393
15.4 Syngas and hydrogen from heavy feedstocks 399
15.5 Thermal balance of hydrogen production processes 403
15.6 Future trends 408
15.7 Sources of further information 409
15.8 References 410

Index *412*

© Woodhead Publishing Limited, 2010

https://boilersinfo.com/

Contributor contact details

(* = main contact)

Editor

D. Roddy
Science City Professor of Energy
Director, Sir Joseph Swan Institute
Floor 3, Devonshire Building
Newcastle University
Newcastle upon Tyne
NE1 7RU
Email: dermot.roddy@ncl.ac.uk

Chapter 1

J. Fadok
Project Director, Gas Turbine Engineering
Siemens Energy, Inc.
4400 Alafaya Trail
MS Q3-039
Orlando, Florida 32826
Email: joseph.fadok@siemens.com

Chapter 2

A. D. Rao
Advanced Power and Energy Program
University of California
Irvine, California 92697
USA
Email: adr@nfcrc.uci.edu

Chapter 3

Y. Zhu
Energy and Environmental Directorate
Pacific Northwest National Laboratory
902 Battelle Boulevard
Richland
Washington 99354
USA
Email: yunhua.zhu@pnl.gov

H. C. Frey*
Department of Civil, Construction, and Environmental Engineering
North Carolina State University
Raleigh
North Carolina 27695-7908
USA
Email: frey@ncsu.edu

Chapter 4

B. Dooley*
Structural Integrity Associates, Inc.
2616 Chelsea Drive
Charlotte, NC 28209
USA
Email: bdooley@structint.com

R. Svoboda
Svoboda Consulting

© Woodhead Publishing Limited, 2010

https://boilersinfo.com/

Rosenauweg 9A
CH-5430 Wettingen,
Switzerland
Email: r.svoboda@swissonline.ch

Chapter 5

S. J. Doong
UOP, a Honeywell Company
25 East Algonquin Road
Des Plaines, 60017
USA
Email: shain.doong@UOP.com

Chapter 6

A. Basile*
Institute of Membrane Technology
Italian National Research Council
Italy
Email: a.basile@itm.cnr.it

F. Gallucci
Fundamentals of Chemical
Reaction Engineering
Department
IMPACT
University of Twente
Enschede
The Netherlands

P. Morrone
Department of Mechanical
Engineering
University of Calabria
Rende (CS)
Italy

Chapter 7

S. Falcone Miller*
EMS Energy Institute
The Pennsylvania State University
407 Academic Activities Building
University Park, PA 16802
Email: sfm1@psu.edu

B. G. Miller
EMS Energy Institute
The Pennsylvania State University
C214 Coal Utilization Laboratory
University Park, PA 16802
Email: bgm3@psu.edu

Chapter 8

B. G. Miller
EMS Energy Institute
The Pennsylvania State University
C214 Coal Utilization Laboratory
University Park, PA 16802
Email: bgm3@psu.edu

Chapter 9

M. Yu and A. K. Gupta*
University of Maryland
College Park
MD 20742
USA
Email: akgupta@umd.edu

M. Bryden
Iowa State University
Ames
Iowa
IA 50011
USA

Chapter 10

Y. Yan
Instrumentation, Control and
Embedded Systems Group
School of Engineering and Digital
Arts
University of Kent
Canterbury

© Woodhead Publishing Limited, 2010

https://boilersinfo.com/

Kent CT2 7NT
UK
Email: y.yan@kent.ac.uk

Chapter 11

T. Dlouhý
Czech Technical University in Prague
Faculty of Mechanical Engineering
Technická 4
Prague 6
166 07
Czech Republic
Email: tomas.dlouhy@fs.cvut.cz

Chapter 12

L. Rosendahl
Department of Energy Technology
Aalborg University
Pontoppidanstræde 101
DK-9220 Aalborg
Denmark
Email: lar@iet.aau.dk

Chapter 13

M. Green
Founding Director
UCG Engineering Ltd
29/30 Fitzroy Square
London
W1T 6LQ
UK
Email: michael.green@ucgengineering.com

Chapter 14

B. McPherson
Department of Civil and Environmental Engineering
The University of Utah
Salt Lake City
Utah 84112
USA
Email: b.j.mcpherson@utah.edu

Chapter 15

P. Chiesa
Department of Energy
Politecnico di Milano
Via Lambruschini, 4
20156 Milan
Italy
Email: paolo.chiesa@polimi.it

© Woodhead Publishing Limited, 2010

https://boilersinfo.com/

https://boilersinfo.com/

Woodhead Publishing Series in Energy

1 **Generating power at high efficiency: Combined cycle technology for sustainable energy production**
Eric Jeffs

2 **Advanced separation techniques for nuclear fuel reprocessing and radioactive waste treatment**
Edited by Kenneth L. Nash and Gregg J. Lumetta

3 **Bioalcohol production: Biochemical conversion of lignocellulosic biomass**
Edited by Keith Waldron

4 **Understanding and mitigating ageing in nuclear power plants: Materials and operational aspects of plant life management (PLiM)**
Edited by Philip G. Tipping

5 **Advanced power plant materials, design and technology**
Edited by Dermot Roddy

6 **Stand-alone and hybrid wind energy systems: Technology, energy storage and applications**
Edited by J. K. Kaldellis

7 **Biodiesel science and technology: From soil to oil**
Jan C. J. Bart, Natale Palmeri and Stefano Cavallaro

8 **Developments and innovation in carbon dioxide (CO_2) capture and storage technology Volume 1: Carbon dioxide (CO_2) capture, transport and industrial applications**
Edited by M. Mercedes Maroto-Valer

9 **Geological repository systems for safe disposal of spent nuclear fuels and radioactive waste**
Edited by Joonhong Ahn and Mick Apted

© Woodhead Publishing Limited, 2010

https://boilersinfo.com/

10 **Wind energy systems: Optimising design and construction for safe and reliable operation**
Edited by John Dalsgaard Sørensen and Jens Nørkær Sørensen

11 **Solid oxide fuel cell technology: Principles, performance and operations**
Kevin Huang and John Bannister Goodenough

12 **Handbook of advanced radioactive waste conditioning technologies**
Edited by Michael I. Ojovan

13 **Nuclear reactor safety systems**
Edited by Dan Gabriel Cacuci

14 **Materials for energy efficiency and thermal comfort in buildings**
Edited by Matthew R. Hall

15 **Handbook of biofuels production: Processes and technology**
Edited by Rafael Luque, Juan Campelo and James Clark

16 **Developments and innovation in carbon dioxide (CO_2) capture and storage technology Volume 2: Carbon dioxide (CO_2) storage and utilisation**
Edited by M. Mercedes Maroto-Valer

17 **Oxy-fuel combustion for fossil-fuel power plants: Developments and applications for advanced CO_2 capture**
Edited by Ligang Zheng

© Woodhead Publishing Limited, 2010

https://boilersinfo.com/

Preface

These are exciting times for the power supply industry! The world of power plant design is faced with a wide range of challenges and opportunities in response to serious concerns about climate change and energy security as we begin to exhaust the world's cheapest sources of fossil fuels. Developed countries are replacing ageing fleets of power stations with new plants designed to meet present-day expectations. Those expectations include huge reductions in carbon dioxide (CO_2) emissions, continuous improvement in performance with respect to other emissions, and ever-increasing demands for higher energy efficiency. Developing countries are experiencing rapid population growth and ever-increasing expectations of affordable electricity in support of higher standards of living.

There is a growing acceptance that global CO_2 emissions need to be reduced by 60% by 2050, with developed countries aiming for a higher reduction figure of 80% by that date. Uncertainty about the approach to incentivising investment in relevant technologies combined with a recent international financial crisis have led to projected energy gaps that are starting to cause serious concern. Interruptions to cross-border gas supplies have heightened that concern and caused people to consider afresh their views on national energy security.

Much attention has been paid to the development programme for renewable energy, with various roadmaps being developed to chart expected progress of different technologies in different countries over time. As these plans develop and parallel plans for nuclear power are deployed around the world, countries look at their forecast energy gaps and try to figure out what role can be played by fossil fuel plants as part of the energy mix in balancing conflicting demands for low-cost, low-carbon electricity that is secure and flexible. This requires a good understanding of the current state of the art in power plants and their major components. This book sets out to provide that overview.

The book is divided into three parts for ease of reference. Part I looks at complete power plants and explores developments in gas-fired and coal-fired

© Woodhead Publishing Limited, 2010

https://boilersinfo.com/

designs in pursuit of high-efficiency, flexible operation, including various combined-cycle configurations. Part II looks at major equipment developments that are relevant to a range of power plant configurations in pursuit of tighter control, general reductions in emissions and affordable capture of CO_2. Part III looks at improving the envelope within which fossil fuel power plants operate by introducing increased levels of fuel flexibility and more cost-effective ways of reducing CO_2 emissions and storage costs.

The book opens with Fadok's chapter on gas turbine plants, addressing developments aimed at enabling high-temperature operation for higher energy efficiency, enabling plants to run at variable generation rates (which becomes increasingly important as more renewable electricity comes into the mix), and coping with synthetic gaseous fuels (often derived from coal and rich in hydrogen).

The concept of a combined-cycle plant for improved energy efficiency is introduced by Rao, including a useful exposition of the advantages and limitations of gas-fired combined-cycle plants. Zhu and Frey introduce coal through the integrated gasification combined-cycle (IGCC) plant, looking at configurations with and without CO_2 capture. Technologies introduced in this chapter for CO_2 capture and for control of various other emissions are addressed more fully later in the book in dedicated chapters.

This leads into a chapter by Dooley and Svoboda on improving the steam/water cycle in power plants to guard against corrosion and other damage, and the challenge of applying current chemistries to the high-temperature, high-pressure plants that are now being considered.

Part II opens with two chapters on gas separation membranes: one by Doong where the emphasis is on separating out the hydrogen and the other by Basile where the emphasis is on separating out the CO_2. These chapters distinguish between technologies that are ready for commercial deployment on power plants and technologies that are still under development. Chapters by Miller and Miller then examine technologies for controlling emissions of SO_x, NO_x, mercury, dust and particulates, providing a combination of practical design guidelines for well-developed technologies alongside some insights into expected future developments.

The direction of travel for power plant design in a world of tight emissions control, flexible operation and high reliability includes tight control – and therefore reliable measurement – at every point in the process. Yu *et al.* provide forward-looking insights into the intelligent use of multiple sensors in achieving tight control in advanced combustors, while Yan also includes some developments for the difficult solids-handling sections of a coal-fired power plant.

Part III starts by exploring ways of broadening the feedstock supply base. Dlouhý provides a general overview of techniques for low-rank coal upgrading that are not commonly used. Rosendahl takes a different

© Woodhead Publishing Limited, 2010

https://boilersinfo.com/

approach by exploring a range of biomass materials (both specially grown and waste) and ways in which they can be pre-processed to enable their use in displacing all or part of the feedstock for a thermal power plant, reducing the carbon footprint. Green introduces the concept of underground gasification of coal as a means of harnessing the unmineable coal resources that significantly exceed the figures usually quoted for bankable coal reserves, along with the option of linking it to CO_2 capture and storage. This leads into McPherson's chapter on geological storage of CO_2, which explains the often-misunderstood science behind the subject and explores the issues that need to be addressed.

The book concludes with Chiesa's chapter on production of a highly flexible fuel – synthesis gas or syngas – by reforming or gasifying fossil fuels. Here the emphasis is on using the syngas (or hydrogen derived from it) for decentralised power generation, which opens up an opportunity for using rejected heat in a combined heat and power configuration.

A common theme across the book is technology development to improve energy efficiency, increase reliability, reduce generation cost and enhance ability to operate flexibly within grids that are absorbing increasing levels of renewable electricity. Another common theme is the range of approaches being pursued to reduce the carbon footprint associated with power generation from fossil fuels while taking account of other regulatory pressures. There are, of course, tensions between these various requirements, leading to new thinking in the realms of materials, mechanical, electrical and instrument engineering.

This book is aimed at industry practitioners and academic researchers, and contains material from a blend of the two. The aim throughout is to provide a well-referenced appraisal of the state of the art with guidance on where to find further detail and some pointers to likely areas of future development. I hope you find it both informative and inspiring.

Professor Dermot J Roddy
Newcastle University
UK

© Woodhead Publishing Limited, 2010

https://boilersinfo.com/

Part I

Advanced power plant materials and design

© Woodhead Publishing Limited, 2010

https://boilersinfo.com/

https://boilersinfo.com/

1

Advanced gas turbine materials, design and technology

J. FADOK, Siemens Energy Inc., USA

Abstract: This chapter will discuss the technologies and material used in modern industrial gas turbines. Rapid evolution of the gas turbine since its first application to wartime aircraft engines has been made possible through the deployment of advanced materials and technologies. The background of these advancements, their use in the gas turbine, and the drivers for new technologies to achieve higher temperatures and efficiencies will be the main focus. Furthermore, the technologies needed for advanced hydrogen-fuelled gas turbines will be considered.

Key words: gas turbine, advanced materials, turbine, combustion, compressor, IGCC, NGCC, thermal barrier coating, single crystal, hydrogen, Brayton cycle, CO_2 capture, gamma prime phase.

1.1 Introduction

The industrial gas turbine is a key element to meeting the world energy demands today and in the future. The flexibility of this technology facilitates deployment in simple cycle peaking applications as well as combined cycle applications. Evolution from the first industrial gas turbines in the 1940s of about 19% thermal efficiency to today's combined cycle plants at 60% efficiency has been enabled by advancements in materials, design and technology. This chapter will discuss the background of these advancements, their use in the gas turbine, the drivers for new technologies to achieve higher temperatures and efficiencies, and technologies needed for advanced hydrogen-fuelled gas turbines.

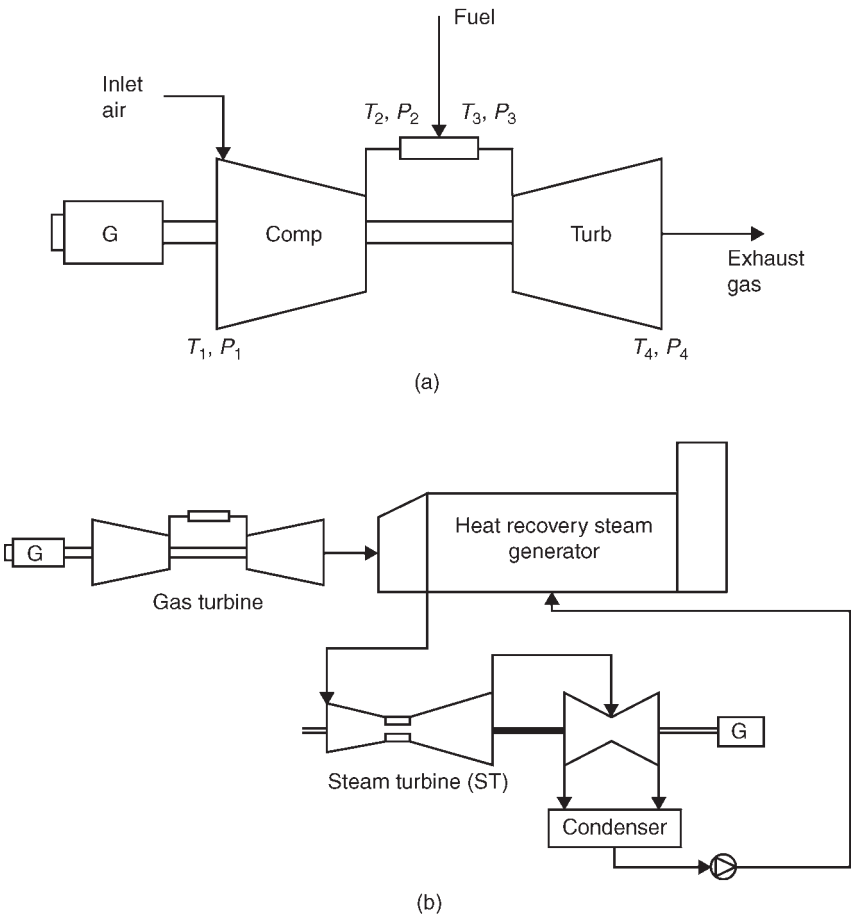
In only 50 years, industrial gas turbines have evolved from the early jet engines for airplanes used in the Second World War to one of the most widely deployed power generation technologies in the world today. Early

© Woodhead Publishing Limited, 2010

https://boilersinfo.com/

applications to power generation were direct adaptations of the jet engine, but, as industrial use increased, especially in combined cycle systems, technologies necessary to advance land-based gas turbines were developed. The first industrial gas turbines went into service in the early 1950s for application in power generation, transportation and mechanical drives. The 1960s saw the development of the combined cycle power plants. By thermodynamically coupling the gas turbine Brayton cycle to the Rankine cycle, an efficiency of 39% was already possible compared to about 30% simple cycle efficiency available at that time (Scalzo and Bannister, 1994). Figure 1.1 shows schematic representations of a simple cycle and a combined cycle gas turbine power plant configuration.

In the schematic diagram for a simple cycle, the conditions for



1.1 Schematic representation of a gas turbine in (a) simple cycle configuration and (b) combined cycle configuration.

© Woodhead Publishing Limited, 2010

https://boilersinfo.com/

Table 1.1 Key differences in requirements for aero engines and heavy industrial gas turbines

Parameter	Aeroengine	IGT
Weight	Very important	Not significant
Operating time (hours)	25 000	> 100 000
– steady state	< 1000	> 100 000
– peak temperature		
Cyclic duty	Severe	Severe
Environment	Non-corrosive	Corrosive
Size	Small	Large

temperature T_n and pressure P_n are noted at key thermodynamic points in the gas turbine, where n represents the following:

1. compressor inlet
2. compressor discharge
3. turbine inlet
4. turbine exhaust.

Despite their common heritage, the aero and heavy industrial gas turbines have significant differences in design and technology. Table 1.1 shows the most notable differences between these technologies.

Owing to the weight constraints the most obvious physical differences will be found in the rotor and casing constructions, but other differences are also notable, particularly in the combustor and turbine sections. The key driver for power generation technology is cost of electricity (COE) and the driver for aircraft engines is specific fuel consumption (SFC). Both parameters are driven by efficiency and lead to higher pressures and temperatures, which challenge the gas turbine designer. While the focus of this chapter is heavy industrial gas turbines, frequent reference to the aircraft industry is made to highlight the synergy between these industries.

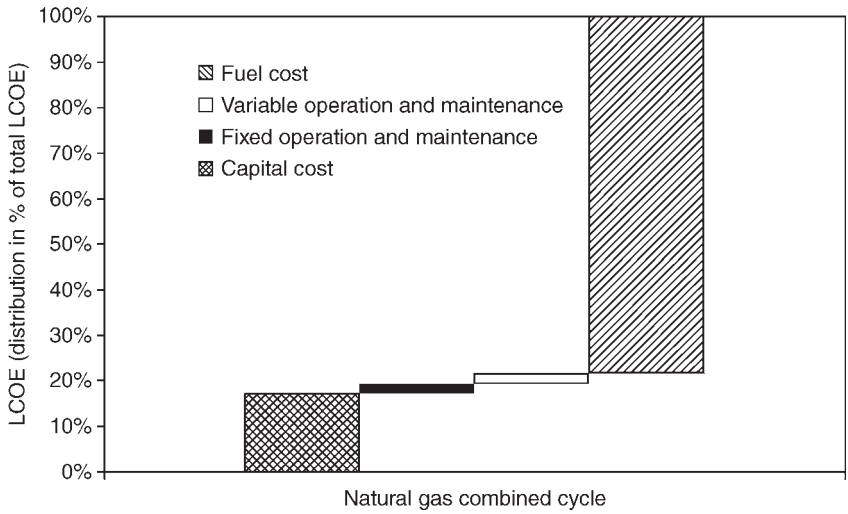
When evaluating the available power generation technologies, COE is levelized over a specified operating period, usually 20 years. This gives the levelized cost of electricity (LCOE) on a per annum basis, and can be expressed as

$$\begin{aligned}\text{LCOE} = {} & \text{fuel cost} + \text{capital cost} + \text{variable maintenance cost} \\ & + \text{fixed maintenance cost}\end{aligned} \quad [1.1]$$

Figure 1.2 shows the LCOE breakdown for a modern gas turbine combined cycle power plant. It can be seen that the major portion of the LCOE is fuel cost, while capital cost makes up most of the remainder.

© Woodhead Publishing Limited, 2010

https://boilersinfo.com/

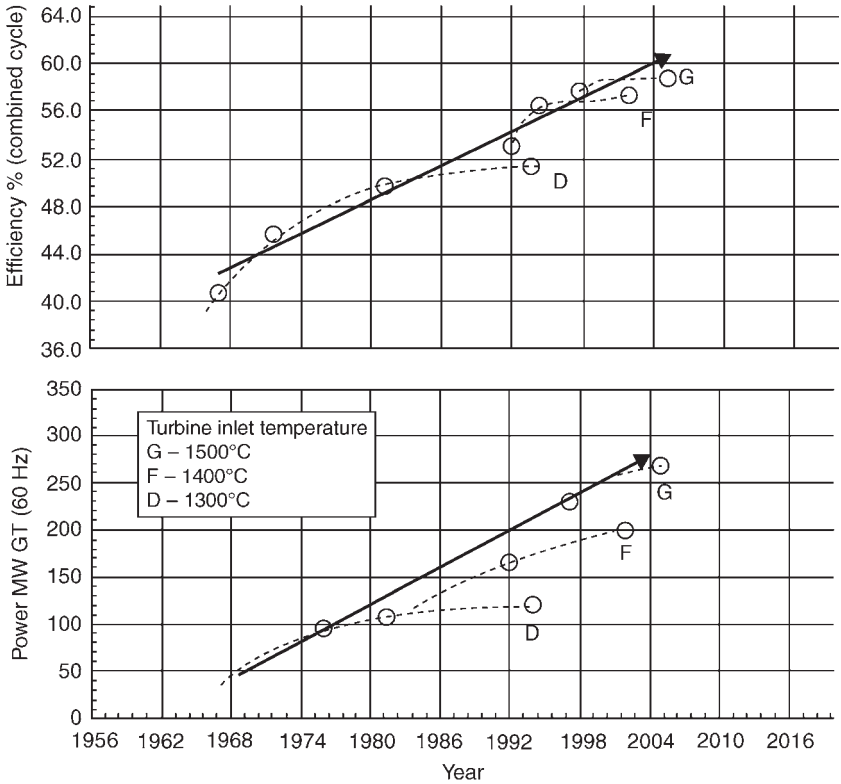


1.2 LOCE for a natural gas combined cycle (NGCC) power plant (source of data US Department of Energy (NETL, 2007)).

With the main contribution to LCOE being fuel cost, natural gas-fired combined cycles must achieve the highest possible cycle efficiency. Over the past decades this increase has been significant, as can be seen in Fig. 1.3. A similar trend for firing temperature (temperature entering the turbine, T_3) and pressure ratio P_2/P_1 could also be derived. As you will see, these advancements have been made possible through improvements in materials and technologies. The second most significant contributor to the COE is capital cost, therefore, an evaluation of total life cycle cost, to compare the efficiency benefit versus additional cost of higher grade materials is necessary. The LCOE distribution shown in Fig. 1.2 is a very simplified view of the total actual operating cost for a gas turbine based power plant, and also assumes a base-load duty cycle, presented later. The importance of availability, reliability and degradation should not be under-stated. Parts replacement costs are high, and frequent maintenance drives up operating cost. Forced outages must be avoided and efficiency has to be maintained at a competitive level over extended operating intervals. Upgraded conditions in the gas turbine tend to increase risk, therefore extensive rig testing and highly instrumented prototypes are manufactured and tested to verify analysis predictions prior to full commercial product release and market acceptance.

Emissions constraints for natural gas combined cycle (NGCC) plants include strict regulations for nitrogen oxides (NO_x) and carbon monoxide (CO). Advanced lean premix combustion systems, constrained by emissions, must be capable of operating with contradicting requirements for high temperature and low NO_x emissions. Furthermore, the emission of

© Woodhead Publishing Limited, 2010



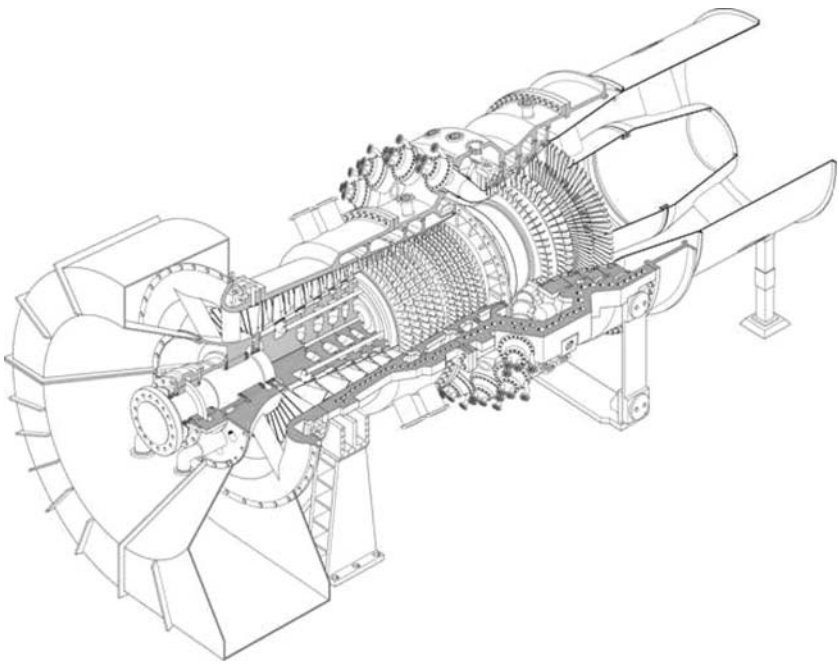
1.3 Trends in output and efficiency (used with permission from Siemens Energy, Inc.).

greenhouse gases like carbon dioxide (CO_2) is an increasing concern in the world today and often influences decisions regarding the deployment of new power generation technology. When comparing fossil fuel technologies, NGCC has the lowest emissions of CO_2 (one-half of the emissions compared to a coal-fired steam power plant). However, integrated gasification combined cycle (IGCC) plants fuelled by coal are currently being designed to capture CO_2 and produce hydrogen-rich syngas (or synthesis gas), which can be burned in gas turbine engines yielding CO_2 emissions almost five times lower than those from a NGCC. The challenges of operating on hydrogen-rich fuels resulting from coal-derived syngas (with CO_2 captured) will be discussed in more detail later in this chapter.

© Woodhead Publishing Limited, 2010

1.2 Development of materials and coatings for gas turbines and turbine components

An advanced industrial gas turbine engine is shown in Fig. 1.4. From left to right the major components of the gas turbine are the compressor section, combustor section and turbine section. The engine shown drives a generator from the compressor (cold end), and employs a can-annular combustion system, where individual transition pieces convey the hot combustion gases to the inlet of the turbine. It is a single-shaft (rotor) engine that operates at 3600 r/min (60 Hz) and is optimized for combined cycle application. A (50 Hz) system operates at 3000 r/min and is approximately 1.2 times the size. The casings are designed with a horizontal split line and multiple vertical joints for maintenance of the individual sections of the engine. The materials for the major components of the gas turbine are subjected to differing operating conditions and criteria, both of which influence material selection.



1.4 Advanced SGT6-6000G industrial gas turbine (used with permission from Siemens Energy, Inc.).

© Woodhead Publishing Limited, 2010

1.2.1 Compressor

Blades and vanes of large industrial gas turbines are made primarily from hardenable stainless steels (martensitic or precipitation hardenable). Examples are 17-4 and AISI 616 (422) SS. These materials are suitable for the size and temperatures seen in large industrial engines. For single-shaft gas turbine engines, the size of the first stage blade is limited by the centrifugal stress at the running speed. This in turn limits the possible flow rate as it defines the annulus size of the compressor inlet. The length of the blade can be increased significantly when a stronger and/or lower density material is introduced, provided the attachment to the rotor is suitable. In areo engines, with large bypass fan blades, composites and fabricated air foils are being used, along with titanium (Ti) alloys, which have much lower density than low-chromium (Cr) steels. The lower density blades also reduce the pull on the rotor disc and attachment, which will be discussed later in this chapter. Owing to the much higher cost of titanium when compared to stainless steels, Ti blades are not common in heavy-duty industrial turbines. Another factor that affects material selection is the pressure ratio, because the compressor discharge temperature is related to pressure ratio. For a compressor using air as a working fluid ($\gamma = 1.4$) the relationship is approximated by

$$T_2 - T_1 = \frac{T_1[(\mathrm{PR})^{0.286} - 1]}{\acute{\eta}c} \qquad [1.2]$$

where $\acute{\eta}c$ is the isentropic efficiency and T_2 is the compressor discharge temperature from Fig. 1.1. At high pressure ratios, the temperatures can exceed the capability of stainless steels and require the use of Ni (nickel)-based alloys, such as Alloy 625 or Alloy 718. Aero engines operating at pressure ratios above 40:1 commonly use these types of materials. Large industrial gas turbines which are optimized for combined cycle application typically operate in a range of 18:1 to 20:1 within the temperature capability of stainless steels. Some manufacturers offer even higher pressure ratio in applications with reheat cycles and closed-loop steam cooling of the turbine. The use of Ni alloys in the compressor has a direct impact on cost not only for the airfoil materials, but also for the rotor and casings. To avoid higher temperatures, and more importantly to achieve high simple cycle efficiency, compressors with inter-cooling can be employed. For combined cycle applications, where heat is recovered from the exhaust gas of the gas turbine, inter-cooling is not currently used because the low-grade heat rejected by the inter-cooler cannot be recovered efficiently in the cycle. Further, inter-cooling lowers the exhaust gas temperature, so there is a net reduction in combined cycle efficiency.

© Woodhead Publishing Limited, 2010

Coatings are used in the compressor section for two primary functions: to decrease airfoil surface roughness, and blade and vane tip operating clearances. Coatings on compressor airfoils are used to reduce friction losses and provide some erosion protection against particle ingestion. This is a low-cost method for gaining aerodynamic efficiency, and the coatings can be reapplied during a repair interval. Abradable and abrasive coatings, particularly in the rear section of the compressor, are used to manage tip clearances. In the case of abradable coatings applied to the casing, the compressor blade tips cut into the coating, thereby allowing the operating clearances to be minimized. Variations in assembly alignment, distortion of cases and transient excursions can be accommodated with this type of coating. Similarly, abrasive coatings applied to the rotor can accommodate these variations, as the tips of the stationary vanes are cut by the rotating disc. Both systems are widely used in aircraft engines and industrial gas turbines.

1.2.2 Combustion system

The two major components of the combustion systems are the combustor and the transition and these components see the highest temperatures in the gas turbine. In today's advanced industrial engines, this temperature is above 1550°C and in the next generation engines could exceed 1700°C. Conversely, since no work is extracted in the combustion system, the mechanical loading on these parts (due to pressure) is low. In addition to the extreme temperature, combustor components are subjected to high-frequency, low-amplitude pressure oscillations, which can lead to high cyclic stress. Acoustic resonance and unsteady heat release (referred to as combustor dynamics) is the source of these pressure oscillations. To combat this loading, the structure could be stiffened, but additional stiffness tends to generate higher transient thermal stress, which can lead to low cycle fatigue. In Fig. 1.4 the mid-section of the engine contains the combustor and transition pieces. The hot sections of the combustor are thin-walled components that can be formed from sheet stock and welded. For advanced combustors, internal cooling passages are manufactured into a layered structure, which can be made prior to forming the final shape. This feature enables the designer to minimize the amount of cooling air consumption, or use steam to cool the components, as in the SGT6-6000G transitions seen in Fig. 1.4. Although the pressure loading is relatively low, creep remains a concern, mainly due to high temperature, but also in areas where pressure is acting on large surfaces with little or no curvature.

Materials for combustors and transitions must be easily formed and welded, exhibit resistance to high-temperature oxidation, have good compatibility with thermal barrier coatings (TBCs) and have excellent

© Woodhead Publishing Limited, 2010

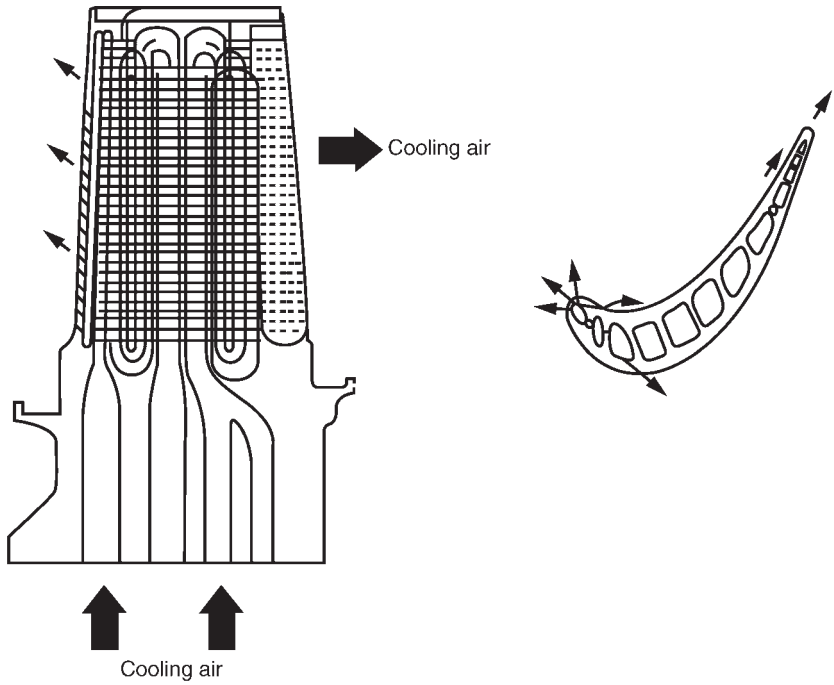
high-cycle and low-cycle fatigue strength. In the presence of combustor dynamics, wear between mating parts must also be considered. Material for the combustor liner and transition piece is typically Ni-based alloy wrought sheet, such as Alloy X, Alloy 617 and Alloy 230. These alloys also contain a high Cr content, which improves oxidation resistance. These alloys have stable, but relatively low yield strength (compared to turbine superalloys) to temperatures over 800°C, high ductility for forming and good fatigue capability in both low-cycle and high-cycle regimes. The designer can trade material capability and cost of the various available alloys to suit the specific application or area of concern, but in general, the aforementioned materials have good formability, weldability and coating compatibility. For advanced transitions with steam cooling, the compatibility with this working fluid at high temperature is another parameter for consideration.

Coatings are applied to combustion systems components to provide an insulation barrier from the hot gas stream and to control wear between mating parts. Thermal barrier coatings, described further in the turbine section, have enabled significant increases in operating temperature. The internal surfaces of the combustors and transitions are coated with a TBC and cooled either by convective cooling through internal channels in the liner, by allowing the cooling air to penetrate the liner through cooling holes that eject into the flow path, or by closed-loop steam cooling. As mentioned earlier, wear between mating components is a concern and gas turbine manufacturers have conducted extensive tests of various material combinations and loading scenarios to quantify the wear characteristics of suitable material combinations. Coatings can also be applied at mating surfaces to protect the base material. Commercially available chromium carbide coatings or T-800 can be applied to the mating surfaces during manufacturing, and reapplied during a repair cycle.

1.2.3 Turbine

The turbine section is subjected to high temperature, aerodynamic and mechanical loading. While the bulk average temperature entering the turbine is lower than the combustor temperature due to the addition of cooling air or heat extraction from steam cooling, the stage 1 vane can be subjected to very high local temperature. The rotating blade shown in Fig. 1.5 is designed with a combination of convective cooling augmented by turbulators in the cooling channels, and film cooling ejected at the leading edge, the trailing edge and the suction side (low-pressure side) of the airfoil. Figure 1.6 shows a historical perspective of turbine airfoil technology and material development over the past 40 years. The step changes in gas temperature with the introduction of cooling technologies and the application of TBCs are notable. Betteridge and Shaw (1987) offer a more

© Woodhead Publishing Limited, 2010

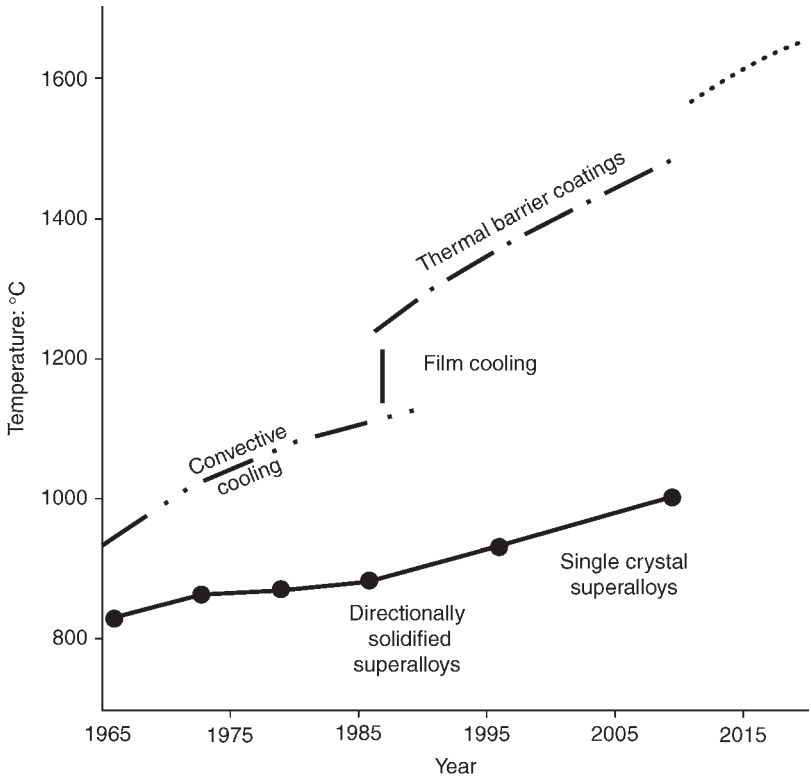


1.5 Cross-section of a cooled rotating turbine blade (used with permission from Siemens Energy, Inc.).

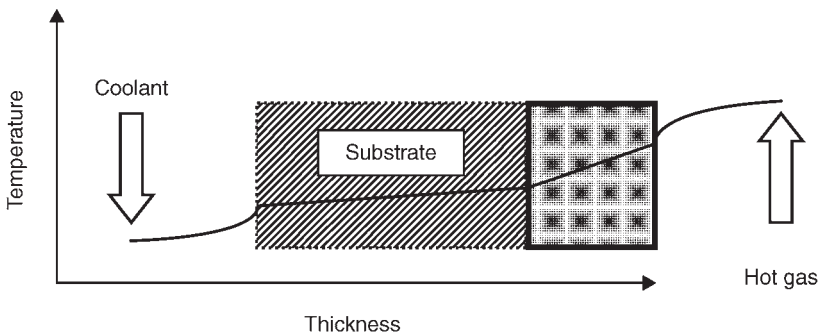
detailed perspective of the superalloy developments, and Scalzo and Bannister (1994) describe the historical advancements in cooling technology for industrial gas turbines in the United States.

The turbine and combustion system are able to operate at temperatures above the incipient melting point of the base metal by using cooling in combination with TBC applied by either plasma spray deposition or electron beam physical vapour deposition (EBPVD). R. L. Jones of the Naval Research Laboratory describes the differences between these processes, in particular, the microstructural differences, which affect the coating performance (Jones, 1996). In both processes a metallic interlayer bond coat is applied between TBC and substrate to (a) provide an oxidation and corrosion resistant layer and (b) provide a compatible material for applying the ceramic coating. The net effect of coating, film cooling and convective cooling can be seen in Fig. 1.7 where the temperature difference between the hot gas path and substrate can reach 600°C. An issue arises when coating is lost from the airfoil surface due to damage or delaminating, commonly referred to as spallation. This exposes the bondcoat and, subsequently, the metallic substrate to local gas path temperature. Coating durability is extremely important for this reason, but if the coating is lost,

© Woodhead Publishing Limited, 2010



1.6 A historical trend of turbine materials and technology (used with permission from Siemens Energy, Inc.).



1.7 Through-thickness temperature gradient for a coated substrate.

© Woodhead Publishing Limited, 2010

the oxidation resistance of the substrate must be adequate to meet part life requirements.

In terms of substrate, superalloys with high Cr content exhibit the best corrosion resistance, while superalloys with high aluminium content offer increased oxidation resistance and improved coating compatibility. In nickel-based superalloys, the higher aluminium concentration also promotes the precipitation of a strengthening second phase known as gamma prime (γ'). Gamma prime is an inter-metallic compound with an ordered crystal structure and a composition based on Ni_3Al. The gamma prime exhibits a yield stress anomaly whereby its strength increases with temperature, and it is this attribute that imparts superalloys with their exceptional high-temperature mechanical properties. Achieving the optimum balance between mechanical properties, environmental resistance and manufacturability is a challenge which attracts significant research and development effort. The metallurgical complexities of Ni-based superalloys are presented by Sims *et al*. (1987). In Fig. 1.6 it can be seen that the introduction of single crystal superalloys has enabled high operating temperature of the substrate. The net effect of allowing higher substrate temperature is the ability to lower cooling air consumption and therefore raise turbine efficiency. This significant performance improvement can offset the additional cost of single crystal alloys, however, producing large industrial gas turbine components (three times larger than aircraft engine parts) with single crystal is difficult. Seth (2000) summarized these challenges stating 'When used for large Utility Gas Turbine parts, the result is very low yield due to distortion and cracking of the core, shell rupture, mold-metal reaction and numerous crystal defects'.

1.2.4 Casings

The casings of large industrial gas turbines are classified as pressure vessels and the design guidelines are in fact very similar to those of steam turbines. Without a weight constraint, however, the casings of large industrial gas turbines are unlike aircraft engines in both construction and materials. To facilitate servicing of the engine gas path, the casings share a common horizontal bolted joint as well as several vertical joints, allowing individual casing sections to be removed independently. This feature also allows the use of different materials based on the temperature and loading of that section of the engine. The coupling of these joints is accomplished with industrial grade bolting systems and Bickford (2007) provides a good overview of various bolted joints and materials. In general two temperature and material classifications can be derived. For low-temperature classification up to about 430°C, a low-alloy steel material like ASTM A193 GR B16 can be used. This material is common in petrochemical and power

© Woodhead Publishing Limited, 2010

applications and the cost is relatively low in comparison to the high-temperature high-performance materials. For operating temperatures above 430°C a 400 series stainless steel or nickel alloy like Alloy 750 or Alloy 718 may be needed to provide necessary strength and resistance to relaxation or creep, but the cost of these materials is significantly higher than that of the low-alloy steel. Furthermore, it is necessary to consider the thermal expansion coefficient difference between the bolting material and the casing material in order to avoid yielding of the flange or bolting during operation.

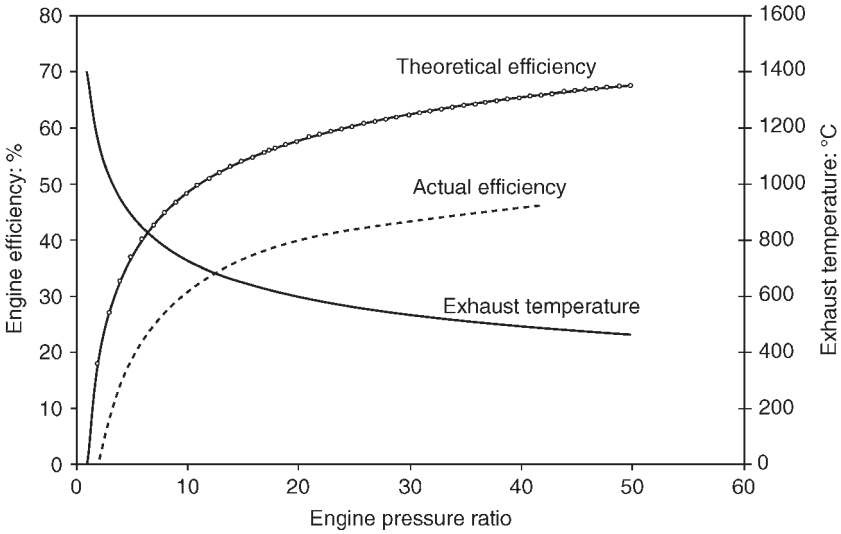
1.2.5 Rotors

A basic trade-off exists when considering rotor materials for advanced high-temperature engines: cost versus cooling air consumption. The lower cost approach and the approach which is commonly used in heavy industrial gas turbines, is forged steel discs either bolted or welded together. Rotor discs are subjected to high stress at the inner diameter, usually corresponding to the lowest temperature, and lower stress at the rim or gas path, which is the region of highest temperature. A significant drop in strength at higher temperature can drive the material selection to Ni-based alloys such as Alloy 706 or Alloy 718 and such a choice is typical in aero engines for the lowest possible weight and highest strength. In heavy industrial gas turbines large discs become challenging to manufacture in these Ni-based materials and the cost associated with the materials can be prohibitive. To address higher temperatures, cooling air can be fed through the rotor to keep the bulk temperature within an allowable range. In gas turbines, however, any air that is used for cooling is a penalty on efficiency and output.

1.3 Higher temperature efficiency operation

This section discusses the challenges of reaching higher temperature and efficiency and the issues facing the gas turbine designer with regard to extending material capabilities, improving aerodynamic efficiency, all while achieving high mechanical integrity. In simple cycle, the gas turbine efficiency is related to pressure ratio by the relationship shown in Fig. 1.8. The difference between the theoretical efficiency and efficiency with losses increases with pressure ratio due to higher loading and inefficiencies in the compressor and turbine airfoils, the increased effect of compressor tip clearances with smaller airfoils (especially in the rear of the compressor), and increasing turbine leakage air due to non-ideal sealing between stationary and rotating parts. The relationship shown is for a constant turbine inlet temperature, selected at 1500°C. In combined cycle applications, there exists an optimum engine pressure ratio for a given turbine inlet temperature. For example, for an inlet temperature of 1400°C, the optimum

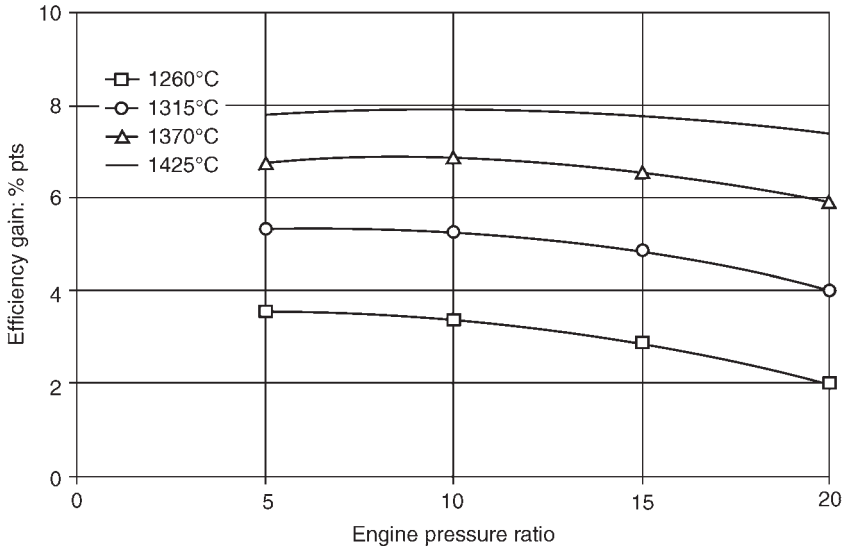
© Woodhead Publishing Limited, 2010



1.8 Gas turbine efficiency versus engine pressure ratio.

pressure ratio is about 17:1, whereas an inlet temperature of 1500°C would lead to a higher pressure ratio of about 20:1. This results from a balance between the gas turbine power and efficiency, and the steam cycle power. Because of the decreasing exhaust temperature with increasing pressure ratio, there is reduced steam turbine output with increased pressure ratio. The inlet conditions to the heat recovery steam generator (Fig. 1.1) define the amount of steam and conditions at which it can be produced. There is, in theory, an optimum design point where this inverse relationship between the gas turbine efficiency and steam turbine power results in the maximum net combined cycle efficiency. The design point of the gas turbine engine is therefore selected to be near this optimum, but also considers a range of potential advancements to the engine frame such that future growth is possible without complete engine redesign. Figure 1.9 shows the effect of increasing turbine inlet temperature and pressure ratio on combined cycle plant efficiency. An engine with reheat and/or inter-cooling will produce differing results. Also, there are limitations to how high the exhaust temperature can be increased. Today's high-temperature combined cycle engines operating at greater than 1500°C and about 20:1 pressure ratio can reach 60% combined cycle efficiency.

© Woodhead Publishing Limited, 2010



1.9 Effect of turbine inlet temperature on combined cycle efficiency (used with Permission from Siemens Energy, Inc.).

1.3.1 Increasing gas turbine pressure ratio

Increasing pressure ratio and increased stage loading capability in the compressor have driven technology and materials advancements to produce high-efficiency gas turbine systems. A trend of decreasing isentropic compressor efficiency is seen when increasing pressure ratio (at constant polytropic efficiency) (Saravanamuttoo *et al.*, 2001, p. 61). To address this, high-efficiency airfoils have been developed to incorporate advanced three-dimensional aerodynamic features mostly adapted from high-pressure-ratio aero engines, where pressure ratios of over 40:1 are successfully deployed. At these high pressure ratios, the leakage of air between rotating and stationary components is more severe. This is more difficult to manage in large industrial gas turbines compared to aero engines because of the scale, where small gaps result in large areas due to large diameters. Also, the large casings and rotors of industrial gas turbines have much slower thermal response compared to the gas path components and often result in minimum clearance conditions for seals and blade tips being limited by transient operation (start up, shut down, etc.). Significant clearance improvements have been enabled by the use of state of the art transient thermal mechanical analysis calibrated to engine measurements, which are capable of accurately calculating the transient interactions between components, thereby allowing for optimization of engine clearances.

© Woodhead Publishing Limited, 2010

1.3.2 Turbine design for high inlet temperature

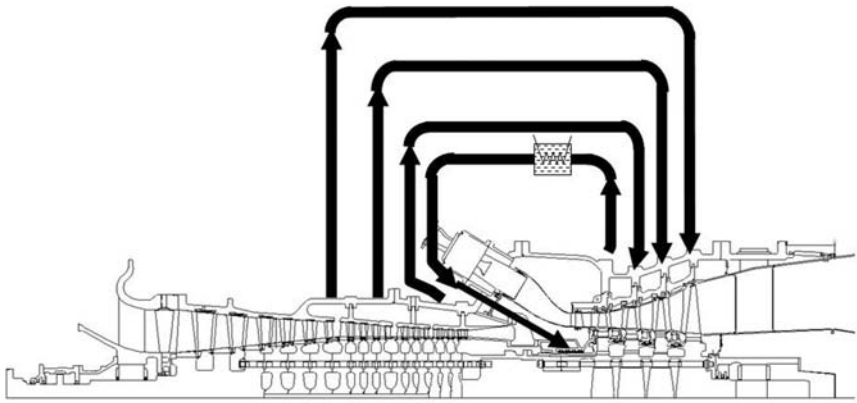
The significant increases in turbine temperatures over the past two decades have been enabled primarily by advancements in coatings, film cooling and materials capability. The two main parameters which influence turbine airfoil design, particularly high-temperature airfoils, are the work extracted by the turbine stage and the Mach number of the flow stream. The work or enthalpy parameter can be plotted against the ratio of axial velocity and tangential velocity (C_a/U) on a single diagram with constant efficiency curves (see Fig. 1.9). Increasing loading at constant flow coefficient will result in lower efficiency and one solution could be to increase the number of stages, thereby reducing the work per stage (Δh), or increase the tangential velocity (U), also referred to as wheel speed. Achieving the desired cycle pressure ratio in the fewest number of stages, however, is a cost benefit for industrial gas turbines, and a necessity to minimize weight in aero engines. Therefore, high-pressure-ratio turbines operate with higher loading, or work extracted, per stage than do lower-pressure-ratio turbines. Industrial turbines, unlike aero engines, are not constrained by size or weight, and can operate with low flow coefficients by allowing large annulus size (C_a is low). Furthermore, high Mach numbers and high velocities lead to increased friction losses and high heat transfer in the turbine stage and high Mach numbers can introduce shock losses.

The optimization of loading distribution throughout the turbine becomes a trade-off between airfoil count, cooling air consumption and number of stages, but the following limitations constrain the design:

- annulus dimensions constrained by centrifugal stress limits of the blades and rotor discs
- number of blades limited by attachment design to the rotor
- the blade length limited by gas bending stress and vibration.

To further complicate the optimization process, the tip clearances and other leakage paths are more critical at high pressure ratio. In particular, if the pressure differential increases across a constant opening or gap, the flow increases and this flow bypasses the stage doing no work. As mentioned earlier, higher work leads to higher heat load on the airfoil. Referring back to Fig. 1.6, the heat transfer coefficient of the hot gas and the gas temperature define the conditions of the gas stream for cooling design. Figure 1.10 shows the turbine cooling system for a modern industrial gas turbine. The supply conditions (compressor extractions) to the turbine are selected to enable safe operation of the gas turbine over a wide range of ambient conditions and part load conditions. The coolant pressure and temperature are defined by the compressor characteristics and the coolant flow is calculated to meet the constraints of the overall system as shown in

© Woodhead Publishing Limited, 2010



1.10 Cooling circuit for a modern industrial gas turbine (used with permission from Siemens Energy, Inc.).

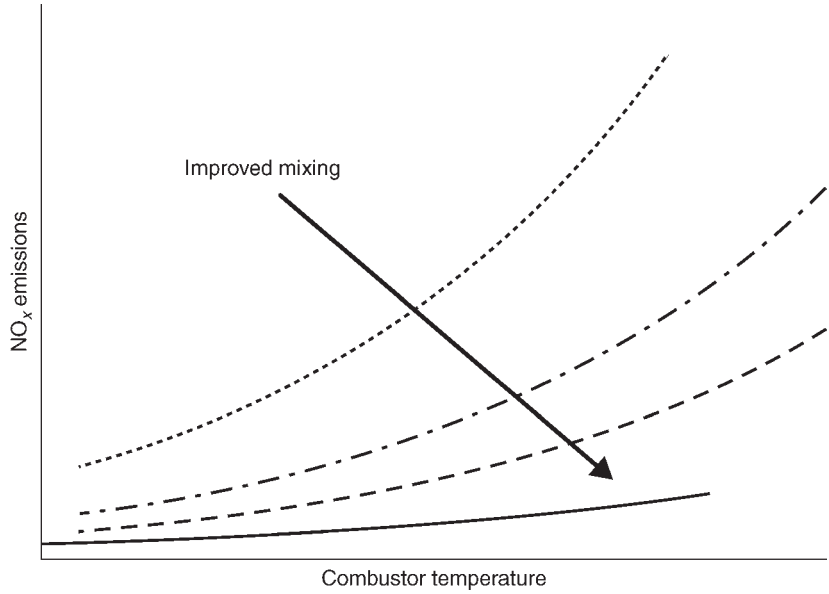
Fig. 1.7. The ribs or turbulators shown in Fig. 1.5 augment internal heat transfer coefficients to take the heat out of the substrate, while the TBC, having very low conductivity, acts as an insulator to limit the heat flow from the hot gas to the substrate. With the numerous combinations possible, optimization between cooling air consumption and aerodynamic efficiency becomes an iterative process that is facilitated by advanced design tools. The use of state-of-the-art simulation tools coupled with multi-variable analysis processes like 'design of experiments' and Monte Carlo allow exploration of a very broad design space and aid in the optimization process. Throughout the design process, the theoretically derived optimum must be concurrently balanced against manufacturing capabilities, constraints and cost to arrive at the best solution.

1.3.3 High-temperature combustion

Environmental constraints on the emissions of harmful gases like NO_x (NO_2, NO) and CO define the envelope of operating temperature for the gas turbine combustor. The most common fuel used in industrial applications is natural gas, however, a wide variety of fuels can be burned in gas turbines including those derived from coal gasification. The relationship of NO_x emissions and combustor temperature is shown in Figure 1.11 for premix style, dry low emissions systems. Leonard and Stegmaier (1993) derived a curve for an ideally premixed combustor which is shown by a solid line in the graph. CO emissions become more limiting at part load, as described later in section 1.5, therefore the following discussion focuses mainly on NO_x emissions at high temperature.

Today's advanced combustion systems can operate with NO_x emissions

© Woodhead Publishing Limited, 2010



1.11 Relationship of NO_x emissions and combustor temperature.

below 10 parts per million (ppm) at F-class temperature (equivalent to 1400°C at the turbine inlet) and 15 ppm for G-class (1500°C inlet). It can be seen that improved mixing can lower NO_x emissions across a wider range of combustor temperatures; however, the challenges associated with this task are multidimensional. Limitations due to combustor flashback and pressure oscillations or dynamics, affect the operability of premix systems at high temperature and lowering emissions at these conditions is the subject of extensive continuing research and development.

The efficiency of the gas turbine combined cycle is highly dependent on the inlet temperature to the turbine and the combustor temperature is limited by emissions. Therefore, the difference between the combustor temperature and the turbine inlet temperature should be minimized. Air cooling of the transition piece and combustor liner, in addition to leakages through seals and gaps, will increase this difference. Steam-cooled transitions were first deployed in the late 1990s to maintain high turbine inlet temperature and low NO_x emissions (Southall and McQuiggan, 1995). For base-loaded combined cycle plants with few starts, this system provided advantages in power output and emissions. The demand for high-cycling, flexible plants has driven the gas turbine designers to develop air-cooled systems and improved premix combustors, which can simultaneously achieve low emissions and high turbine inlet temperature.

Emissions standards vary world-wide and also depend on whether the application is simple cycle or combined cycle. In the USA the

© Woodhead Publishing Limited, 2010

Environmental Protection Agency (EPA) develops and enforces standards for emissions. Here, the low emissions standard for combined cycle power plants often necessitates the use of a selective catalytic reduction (SCR) system. NO_x removal efficiency can reach 95% in state-of-the-art SCR systems. In combined cycle applications, the exhaust from the gas turbine passes through a heat recovery steam generator (HRSG) which utilizes the gas turbine exhaust energy to produce steam and subsequently generate power in a steam turbine power plant. Figure 1.1 shows the schematic representation of a combined cycle power plant. The temperature of the exhaust gas decreases as it flows through the HRSG and provides suitable conditions (lower temperature) for applying SCR technology. As stated earlier, these systems can achieve about 95% reduction efficiency; therefore, gas turbine emissions for combined cycle gas turbines can be as high as 40 ppm and still achieve 2 ppm emissions from the HRSG stack. This reduction of emissions requires significant amounts of ammonia injection and can lead to ammonia carry-over or slip, which is a harmful emission and can lead to excessive degradation of the HRSG, (EPA, 1997; EPA, 2004).

1.4 Design for hydrogen-rich gases

Integrated gasification combined cycle power plants utilize a gasification process using coal or other feedstock that produces a fuel comprising mainly hydrogen and CO. Gas turbines, which were optimized for operation on natural gas fuel, have been adapted to burn high-hydrogen and other synthetic gaseous fuels. By utilizing a combustor capable of operating on syngas fuels and making minor control changes to gas turbine and associated auxiliary systems, industrial gas turbines have been deployed for IGCC. Table 1.2 shows the fuel properties for three sample fuels – a typical natural gas, a coal-derived synthetic gas (syngas) and a hydrogen-rich syngas – alongside pure hydrogen (US DOE, 2004). The hydrogen-rich gas can be the product of 'shifting' CO, which is a major portion of a typical syngas composition to CO_2. The resulting CO_2 in this case is captured and stored to reduce greenhouse gas emissions. Today's IGCC gas turbines inject nitrogen or steam to control NO_x emissions. This process dilutes the fuel, lowers the flame temperature and thereby lowers the emissions of the

Table 1.2 Comparison of heating values for syngas and natural gas

Fuel	Approximate heating value LHV (KJ/kg)
Natural gas	43 000
Syngas (diluted)	5000
High-hydrogen 'shifted' syngas	7500
Pure hydrogen	120 000

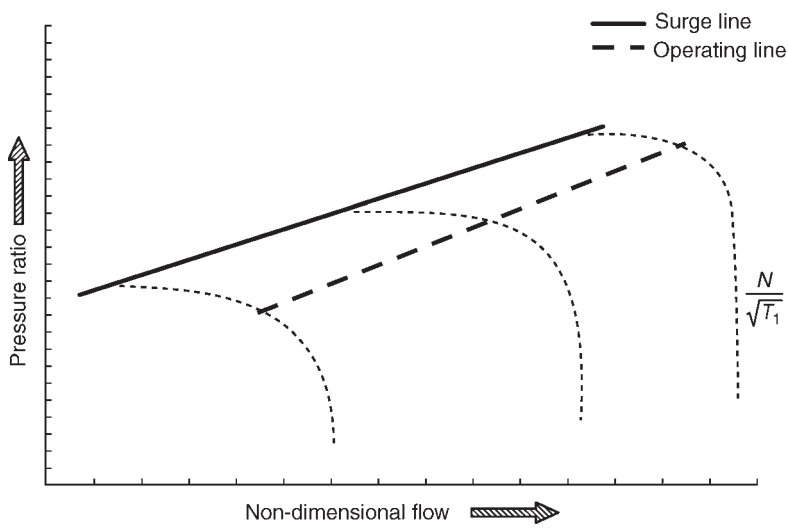
© Woodhead Publishing Limited, 2010

combustion system. From the table, it can be seen that the heating value (kJ/kg) of the diluted syngas fuels is significantly lower than that of natural gas. Therefore, if heat input to the gas turbine is held constant, this affects the fuel mass flow and consequently, the operability of the compressor and combustor. A second observation is the high concentration of hydrogen, especially in the shifted case, which presents a challenge for the combustion system operability and emissions. In addition, a high concentration of H_2O in the combusted fuel, and the potential for contaminants in the fuel stream, have direct implications on all of the hot gas path components and materials.

1.4.1 Compressor operability (surge margin)

For the same heat input, the fuel flow of diluted syngas is greater by a factor of almost 10 when compared to that of natural gas. For a typical natural-gas-fired turbine, the fuel flow is about 2–3% of the engine air flow while it is almost 20% when utilizing diluted syngas. The difference is enough to cause a noticeable imbalance between the turbine and compressor mass flows, which affects the compressor operating characteristics.

Figure 1.12 presents pressure ratio versus the non-dimensional mass flow of an industrial gas turbine compressor. A curve drawn near the inflection points of the speed curves defines the surge line of the compressor, while one operating line established by the turbine is depicted by the dashed line. The difference between the operating line and the surge line is called the surge margin. When a natural gas engine is operated on syngas, the flow through



1.12 Compressor characteristic.

© Woodhead Publishing Limited, 2010

the turbine section increases and the turbine acts as a fixed orifice, which causes the pressure ratio to increase. To maintain the same turbine pressure ratio as for the natural gas engine, the flow to the turbine section must be reduced or the geometry of the turbine vane 1 must be modified to open the throat area and allow higher mass flow. There are three primary mechanisms for reducing the flow to the turbine, adjusting the inlet guide vanes, extracting air from the compressor exit and lowering the fuel dilution.

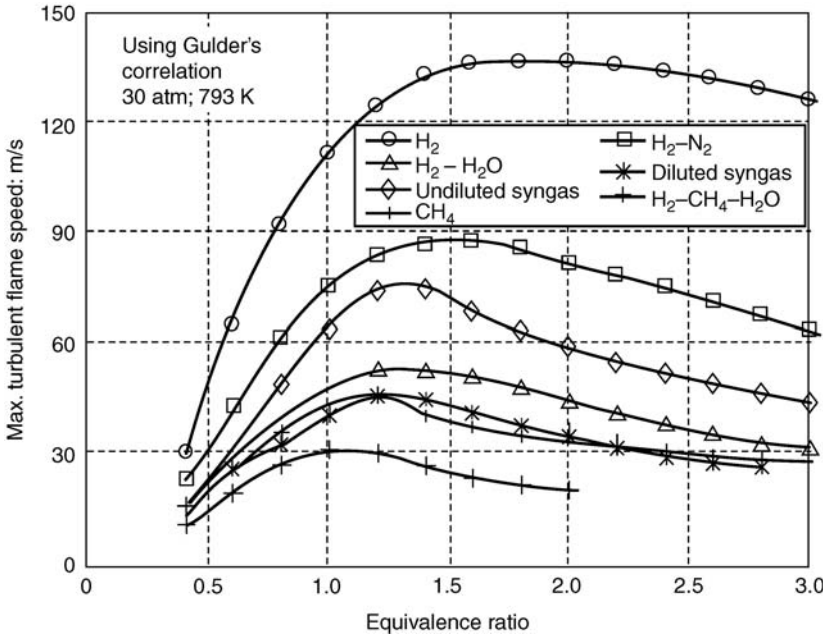
Adjusting the inlet guide vanes lowers the compressor mass flow and consequently lowers the flow to the turbine section. Note, during start up and loading of an industrial gas turbine, the inlet guide vanes and firing temperature are used to control the part load power. For a syngas-fired engine, closing the inlet guide vanes at full power results in constant pressure ratio, but lower compressor flow. From Fig. 1.12 it can be seen that this leads to a reduced surge margin. This condition is exacerbated during a hot day, grid under-frequency event as the compressor operates on a lower speed line, because the operating point is shifted to the left on the graph. Modifications to the compressor are possible to gain surge margin, including the addition of stages to the compressor. This approach, however, is a more drastic change to the engine frame and, therefore, it is often more appealing simply to extract air from the gas turbine.

Air extracted from the gas turbine can be used to supplement the air used in producing oxygen for an IGCC plant which utilizes a cryogenic air separator. In fact, it is possible to supply all of the necessary air from the gas turbine, and some applications of IGCC have been developed to supply a range of extraction amounts to address the potential issue of compressor surge described earlier. There are cases where no extraction is necessary, and this is highly dependent on the fuel composition, which governs the amount of dilution needed to meet NO_x emissions requirements.

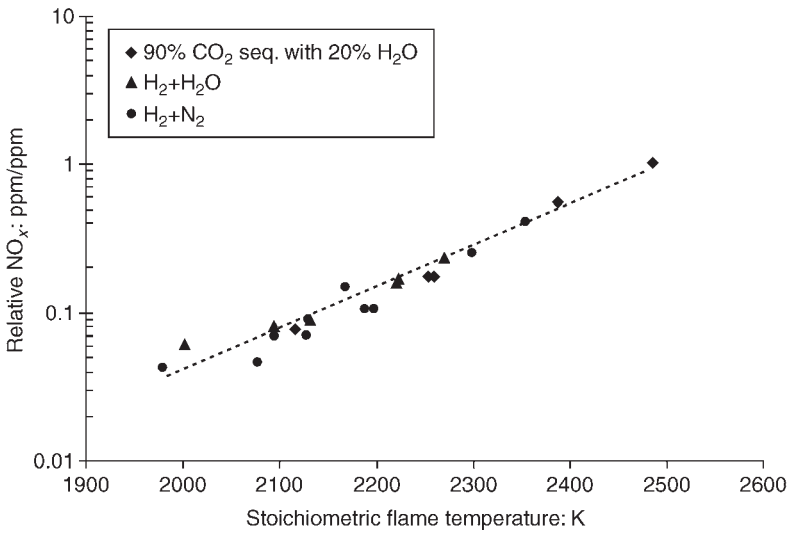
1.4.2 High-hydrogen combustion

Hydrogen is the most challenging fuel for combustion due to its high flame speed, propensity for flashback and higher dilution requirement for NO_x emissions, flame speed and flashback abatement. Figure 1.13 shows the predicted flame speed of various syngas fuels and that of natural gas, where the highest flame speed is found with hydrogen. Combustion systems for IGCC-based gas turbines are currently based on a diffusion flame burner. This combustor has been proven to operate reliably with a variety of synthetic fuels with 15 ppm NO_x emissions (Wu *et al.*, 2007). Until the 1990s, diffusion flame burners were also the primary choice for natural gas applications while the dry low NO_x (DLN) combustors were being deployed and proven. Like the diffusion combustors burning natural gas, the combustor for IGCC applications requires dilution with nitrogen, steam

© Woodhead Publishing Limited, 2010



1.13 Predicted turbulent flame speed for various fuels (used with permission from Siemens Energy, Inc.).



1.14 Correlation of relative NO_x with stoichiometric flame temperature (used with permission from Siemens Energy, Inc.).

© Woodhead Publishing Limited, 2010

or both to achieve acceptable NO_x emissions from the gas turbine. The relative NO_x emissions are exponentially proportional to the flame temperature, as can been seen in Fig. 1.14.

Future developments of combustors for IGCC are targeting premix combustors which can operate at high temperature, with low emissions and require little or no dilution. For example, under sponsorship by the US Department of Energy, research is being conducted to address the challenges of operating a premix style combustor with high hydrogen content in the fuel. Compared to natural gas (over 93% methane), hydrogen has a significantly higher flame speed (Fig. 1.12) and shorter ignition delay time, which can lead to combustor flashback, or flame holding, in addition to the operability limitations due to combustor pressure fluctuations or dynamics.

1.4.3 Turbine design and materials for high hydrogen

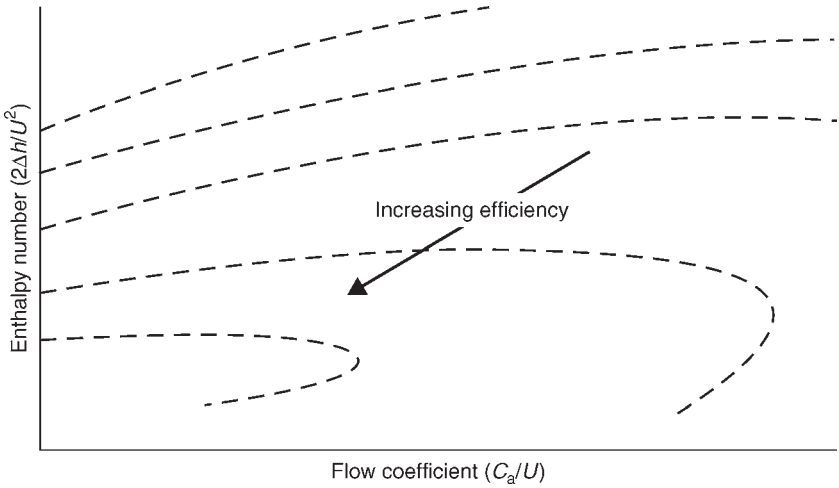
The combustion products from diluted, hydrogen-rich gas are significantly different from those from natural gas combustion and lead to:

- higher heat loads on airfoils
- higher turbine exhaust temperature
- material degradation.

The increased heat loads on the airfoils are caused by high gas path heat transfer coefficients due to higher mass flow, as well as the increased moisture content in the fuel. As a result, natural gas turbines adapted for high-hydrogen operation are de-rated to lower turbine inlet temperatures in order to maintain metal temperatures within allowable limits. Referring to Fig. 1.15, the increased axial velocity due to the higher mass flow would also tend to reduce turbine efficiency. In IGCC applications, particularly with high dilution, the measures taken to manage surge margin, namely reducing compressor flow or extracting air from the compressor exit, can help the turbine section.

In addition to the heat loads imposed by combustion products, contaminants in the fuel stream can cause deposition and erosion of the turbine materials. In IGCC, the products of coal gasification can include heavy metals, sulphur, potassium, sodium and fly ash entrained in the syngas. Sulphur removal in the plant can reduce the concentrations to about 10 ppm, and even lower levels are achievable but with added cost. Despite extensive clean-up processes, some levels of contaminants will be present in the fuel which enters the gas turbine. Particulate or ash deposition has been experimentally studied at Brigham Young University to measure the effects of various parameters including temperature and particle size. The findings of the study showed that there was a threshold temperature in the range

© Woodhead Publishing Limited, 2010



1.15 A turbine enthalpy diagram.

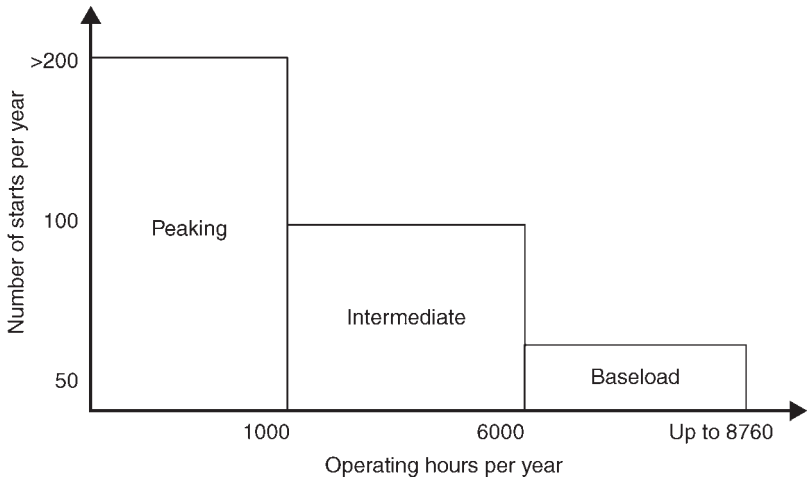
860–960°C where the deposition increased exponentially. Testing under the same programme showed the effect of film cooling was a decreased deposition rate (Crosby *et al.*, 2007). The effect of fuel contaminants is the subject of ongoing research under the sponsorship of the US Department of Energy and in the private sector.

1.5 Design to run at variable generation rates

Gas turbines are a key element in meeting electricity demand during peak periods due to their inherent fast starting and load-following capabilities. Figure 1.16 shows the operating regimes for industrial gas turbines used for power generation. It can be seen that the utility gas turbine can be subjected to a wide range of duty cycles ranging from peaking duty, with frequent starts and stops, through base load operation with a low number of starts. In reality, gas turbine engines are being operated in a combination of these regimes, identified as intermediate duty. An example is the need for additional capacity in the southeast region of the USA in the summer time due to residential and commercial air conditioning. Consequently, the gas turbine design must be capable of high cycling (limited by low cycle fatigue), and extended high-temperature operation (limited by creep). These damage mechanisms are not, however, independent. The combined effects of cyclic and high-temperature operation leads to thermal mechanical fatigue (TMF), a combined creep and fatigue interaction.

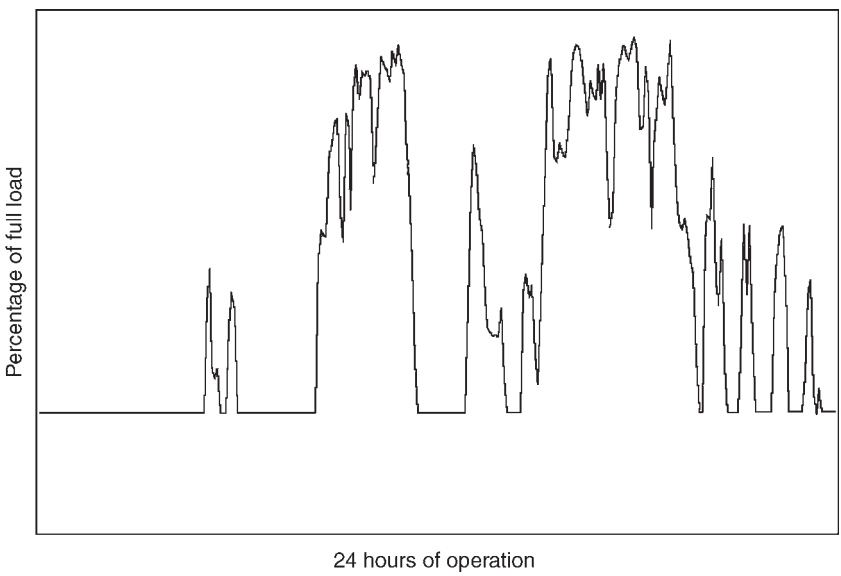
The Electric Power Research Institute showed a steady decline in gas turbine capacity factor (the ratio of actual operating hours versus available operating hours) of over 38% from 1998 to 2004. Largely driven by natural

© Woodhead Publishing Limited, 2010



1.16 Operating regimes based on ISO-3977-2.

gas prices (see Fig. 1.2 for the relative impact on COE), NGCC plants, originally specified as baseload duty, adapted operation to intermediate and even cycling duty. The definition of baseload so far has omitted a very important aspect to the gas turbine engine duty cycle: variable generation rates or load following. Figure 1.17 depicts load following over a 24 hour period. Gas turbine load is modulated to meet the varying demands

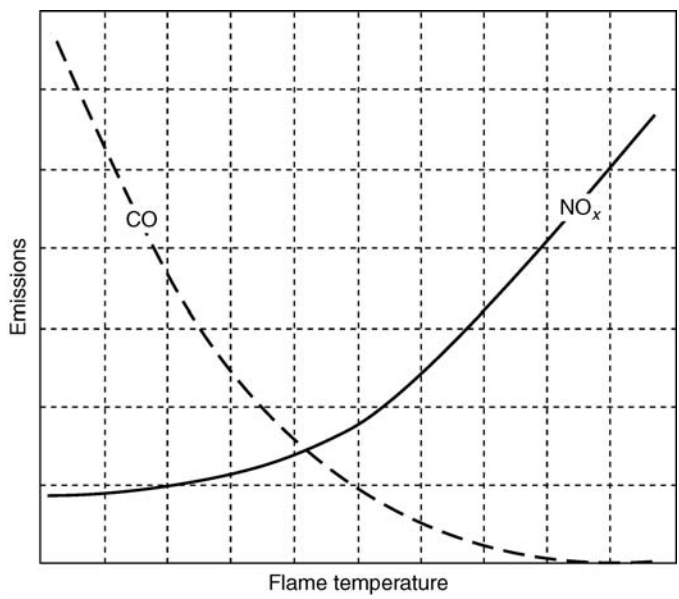


1.17 Operating at variable generation rates – an example of load following.

© Woodhead Publishing Limited, 2010

throughout the day, for example, the low demand for power during the night compared to the high afternoon load in warm climates with air-conditioning load. In the case of load following, the gas turbine combined cycle can be remotely governed by a central dispatch controlling multiple generation facilities to manage capacity and demand. Also, in the figure, there is an apparent minimum load to which the gas turbine output can be lowered. As can be seen from the graph, by keeping the combined cycle plant on-line at low loads, the plant can respond very rapidly to changes in demand, which it cannot do if shut down. There are further complications of cycling combined cycle plants, including a rough estimated cost of $10 000–$15 000 per gas turbine start (Parkinson, 2004), and impacts to HRSG and steam turbine components, that must be considered by an operator to determine if it is more economical overall to keep the plant running at low load overnight, maybe at a loss of revenue, versus the cost of a shut down.

Environmental constraints, such as NO_x and CO emissions, are the limiting factors that define this lower limit of operation, also known as turn down. The inverse relationship of NO_x emissions and CO emissions versus combustor temperature is shown in Fig. 1.18. The gas turbine, by design, controls part-load power by closing the compressor inlet guide vanes to reduce flow, which in turn reduces pressure ratio (see Fig. 1.12), and lowers turbine inlet temperature. The combustor temperature is reduced, and the CO emissions increase (exponentially) to the point where the plant permitted limit is reached. In addition to the emissions issue, the turbine



1.18 NO_x and CO emissions trends.

© Woodhead Publishing Limited, 2010

and compressor operating off the design point have lower efficiency and the gas turbine heat rate is worse at part loads. This situation exacerbates the issue of operating at part load overnight. While many combined cycle plants, particularly in the USA, are equipped with SCR systems, this provides abatement primarily for NO_x emissions. As such, some power plants have also included a separate catalyst of CO abatement.

1.6 Future trends

The gas turbine will continue to be an important part of the power generation technology mix to serve future energy demands. In a carbon constrained world, the gas turbine technology is a necessary element to provide low emissions, base load and peaking capacity, especially for the widely varying and unpredictable generation from renewable energy technologies. In fact, the National Renewable Energy Laboratories (NREL) shows that an almost equal capacity of peaking and combined cycle gas turbine plants is needed for every gigawatt of renewable energy installed capacity. To meet this demand, and remain environmentally compliant, cycling and high efficiency will be key, while economics are achieved with increased output to reduce capital costs on a $/kW basis. Because the main driver for increased combined cycle efficiency is firing temperature, high-temperature-material systems using minimal cooling in the turbine and combustor are needed.

Referring back to Fig. 1.6, it can be seen that a step change in surface temperature capability will facilitate an increase of gas path temperatures beyond 1600°C. To meet this challenge, high-temperature, low-conductivity ceramic coatings are being developed by several manufactures. However, operating temperatures are well above the melting point of the substrate and will require the coatings to be highly reliable. Debonding or spallation of coatings would lead to rapid degradation of the metallic substrate, therefore, a next generation of engine health monitoring and on-line diagnostics will be required to identify coating and material distress before a failure occurs. Ceramic matrix composites (CMC) materials are being introduced into industrial gas turbines to offer high-temperature capability with little cooling required. High CMC cost due to producibility problems is currently a major drawback. Collaborative efforts across military and civil aviation as well as power generation industries are necessary to advance the manufacturing readiness level of CMC and reduce the costs. Developments in superalloys for industrial applications will continue to target increased temperature capability, better compatibility with coating systems, and improved oxidation and corrosion resistance. Manufacturers are utilizing elemental additions to today's superalloys to identify chemistries that will improve these materials.

© Woodhead Publishing Limited, 2010

Producing large single crystal castings for turbine blades and vanes is a significant manufacturing challenge and has limited the deployment of these superalloys into heavy industrial gas turbines, again driven by cost and producibility. To address this, modular components are being investigated to allow the use of more expensive materials only in areas where absolutely needed. A turbine vane segment where a single crystal airfoil is coupled with a conventionally cast shroud is one possible combination. While this solves one manufacturing issue, others could arise including the manufacturing of necessary joints between components and precision tolerances that can tend to drive up costs.

Through the utilization of high-temperature, high-strength materials solutions, gas turbines can reach gas path operating temperatures of over 1700°C. Furthermore, new and novel approaches in sealing and cooling will reduce the consumption of cooling and leakage flow in the hot section of the engine to improve the efficiency further. Advanced aerodynamic flow path optimization will continue to extend the efficiency capability of both compressor and turbine sections. With these improvements a combined cycle efficiency of 65% is within reach. Governments and major original equipment manufacturers (OEMs) are collaborating on research and development in these areas to reach this next level of efficiency for NGCCs and coal-based IGCC with capture. These developments not only seek to reduce fuel consumption, but also to reduce emissions of NO_x, CO and CO_2. The already low emissions from NGCCs will continue to make them an important technology to meet the future energy demands, the movement towards lower CO_2 emissions and the growing renewable energy market.

1.7 Sources of further information

Betteridge, W. and Shaw, S. W. K., 'Overview development of superalloys', *Material Science and Technology*, September 1987, **3**.

Crosby, J. M., Lewis, S., Bons, J. P., Ai, W., and Fletcher, T. H., 'Effects of particle size, gas temperature, and metal temperature on high pressure turbine deposition in land based gas turbines from various synfuels', *ASME Turbo Expo 2007*, Montreal, Canada, GT2007-27531, 2007.

Diakunchak, I., Kiesow, H. J., and McQuiggan, G., 'The history of the Siemens gas turbine', *ASME Turbo Expo 2008,* Berlin, Germany, GT2008-50507, 2008.

Erickson, G. L., 'Superalloy developments for aero and industrial gas turbines,' *Proceedings of ASM 1993 Materials Congress Materials Week '93*, Pittsburgh, Pennsylvania, 17–21 October 1993.

Fuskuizumi, Y., Muyama, A., Shiozaki, S., and Uchida, S., 'Large frame gas turbines, the leading technology of power generation industries', *Mitsubishi Heavy Industries, Ltd Technical Review,* 2004, **41** (5).

Stringer, J. and Viswanthan, R., 'Gas turbine hot-section materials and coatings in

© Woodhead Publishing Limited, 2010

electric applications', *Proceedings of ASM 1993 Materials Congress Materials Week '93*, Pittsburgh, Pennsylvania, 17–21 October 1993.
Seth, B., Superalloys – the utility gas turbine perspective, 2000, *Superalloys 2000: 9th international symposium on superalloys* (eds T.M. Pollock *et al.*), TMS
US Department of Energy, *Gas Turbine Handbook*, see http://www.netl.doe.gov/technologies/coalpower/turbines/refshelf/handbook/TableofContents.html for further information.

1.8 References

Betteridge, W. and Shaw, S. W. K. (1987), 'Overview development of superalloys, *Material Science and Technology*, **3**, September.
Bickford, J. H. (2007), *Introduction to the design and behaviour of bolted joints*, 4th edn, Vol. 1: *Non-Gasketed Joints*, Taylor & Francis.
Crosby, J. M., Lewis, S., Bons, J. P., Ai, W., and Fletcher, T. A. (2007), 'Effects of particle size, gas temperature, and metal temperature on high pressure turbine deposition in land based gas turbines from various synfuels', *ASME Turbo Expo 2007*, Montreal, Canada, GT2007-27531, 2007.
EPA (1997), *EPA 420-F-05-015, Environmental fact sheet*, see http://www.epa.gov/oms/regs/nonroad/aviation/aircr-fr.pdf for further information.
EPA (2004), *National emission standards for hazardous air pollutants for stationary combustion turbines*, see http://www.epa.gov/EPA-AIR/2004/March/Day-05/a4530.htm for further information.
Jones, R. L. (1996), *Thermal barrier coatings. Mettalurgical and ceramic protective coatings*. London, Chapman and Hall.
Leonard, G. and Stegmaier, J. (1993), 'Development of an aeroderivative gas turbine dry low emissions combustion system', *International Gas Turbine and Aero Engine Congress and Exposition*, Cincinnati, Ohio.
National Energy Technology Laboratory, US Department of Energy (2007), *Cost and performance baseline for fossil fuel plants,* DOE/NETL-2007/1281, see www.netl.doe.gov for further information.
Parkinson, G. (2004), 'Capacity utilization of combined cycles in the US', *Power Magazine*, Nov–Dec.
Saravanamuttoo, H., Rogers, G., and Cohen, H. (2001), *Gas turbine theory*, 5th edn, Prentice Hall.
Scalzo, A. J. and Bannister, R. L. (1994), Evolution of heavy duty power generation and industrial combustion turbines in the United States, ASME 94-GT-488.
Seth, B. (2000), Superalloys – the utility gas turbine perspective, *Superalloys 2000: 9th international symposium on superalloys* (eds T. M. Pollock *et al.*), TMS.
Sims, C. T., Stoloff, N. S., and Hegal, W. C. (1987), *Superalloys II,* Wiley-Interscience.
Southall, L. and McQuiggan, G. (1995), 'New 200 MW Class 501G combustion turbine', ASME paper 95-GT-215.
US DOE (2004), *Quality guidelines for energy system studies*, US Department of Energy Office of Systems and Policy Support, see http://www.netl.doe.gov/publications/others/quality_guidelines/main.html for further information.
Wu, J. *et al.* (2007), Advanced gas turbine combustion system development for high hydrogen fuels, ASME GT2007-28337.

© Woodhead Publishing Limited, 2010

2

Gas-fired combined-cycle power plant design and technology

A. D. RAO, University of California, USA

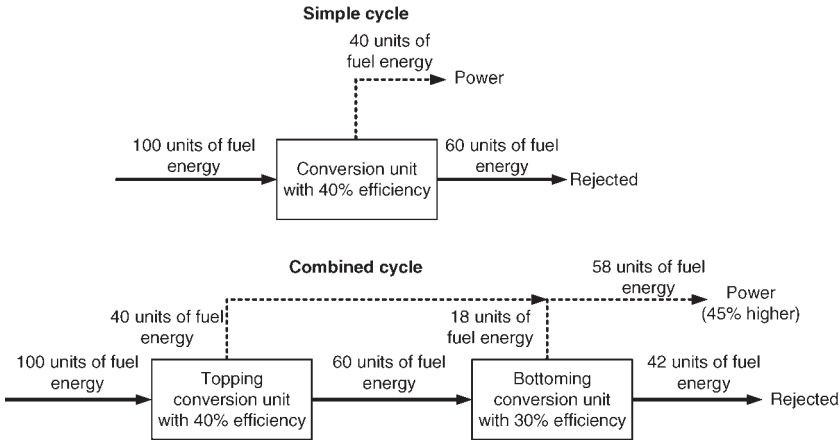
Abstract: A combined cycle consists of combining two power cycles in series to obtain a high overall thermal efficiency, significantly higher than the individual efficiencies of the two cycles making up the combined cycle. In the combined cycle discussed in this chapter, a Brayton cycle or gas turbine is utilized for the topping cycle and a steam Rankine cycle for the bottoming cycle. Combined cycles come in a variety of sizes, depending on the size and number of gas turbines utilized, and may range from less than 10 MW to in excess of 500 MW while using a single gas turbine. In addition to having high thermal efficiencies, outstanding environmental performance, easy start-up and shut-down and low cooling water requirements, combined cycles have significantly lower staffing, capital cost and construction time requirements when compared to boiler based power plants. On the other hand, the clean fuels required by a combined cycle are significantly more expensive when compared to fuels such as coal and biomass that can be directly combusted in a boiler. Included in this chapter are a discussion of types of gas turbines for combined-cycle applications, types of steam cycles in combined-cycle plant, plant design and technology, fuel specifications, control technologies for criteria pollutants as well as for CO_2 emissions, and limitations of gas-fired combined-cycle plants. Future trends for improvements in performance and emissions are also discussed.

Key words: combined cycle, efficiency, gas turbine, HRSG, steam turbine, topping cycle, bottoming cycle, pre-combustion control, post-combustion control, SCR, Wobbe Index.

2.1 Introduction

A combined cycle consists of combining two power cycles in series to obtain a high overall thermal efficiency, significantly higher than the individual efficiencies of the two cycles making up the combined cycle. Figure 2.1

© Woodhead Publishing Limited, 2010



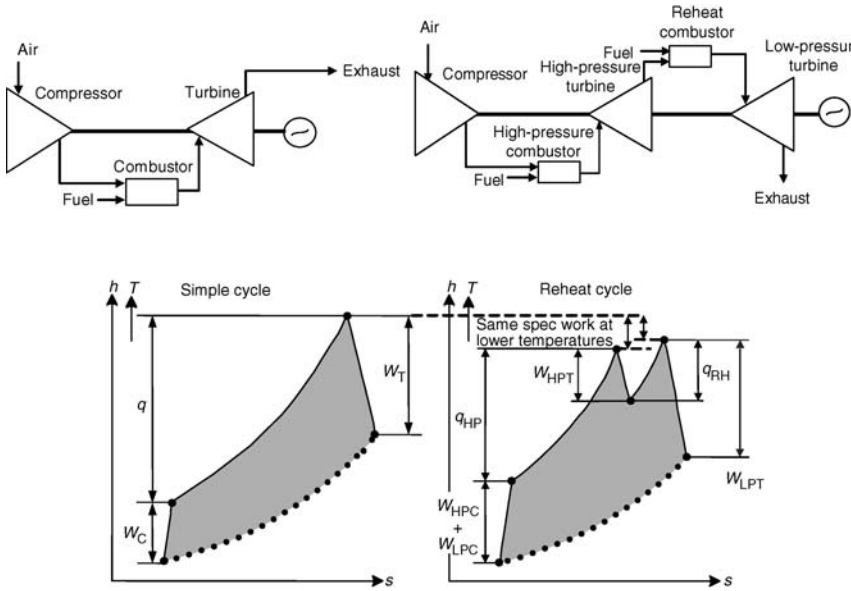
2.1 Efficiency gain of a combined cycle over a simple cycle.

depicts simplified block flow sketches showing the energy flows in a single or 'simple cycle' and in a combined cycle. In the case of a simple cycle with a thermal efficiency of 40%, 40 units of electrical energy are produced when 100 units of fuel energy are supplied while 60 units of energy are rejected (primarily through its exhaust gas). In the case of a combined cycle, by installing a second or 'bottoming' cycle with a thermal efficiency of 30% in series with the previous cycle of 40% efficiency, it can be seen that an additional 18 units of electrical energy are developed from the energy rejected by the 'topping' cycle, resulting in an overall thermal efficiency as high as 58% (neglecting generator, heat and mechanical losses as well as the small change in efficiency of the topping cycle when its exhaust pressure is increased to accommodate the bottoming cycle). In the combined cycle discussed in this chapter, a Brayton cycle or gas turbine is utilized for the topping cycle and a steam Rankine cycle for the bottoming cycle. Combined cycles come in a variety of sizes depending on the size and number of gas turbines utilized. Combined cycle sizes may range from less than 10 MW to in excess of 500 MW when using a single General Electric H class 50 cycle gas turbine.

2.1.1 Types of gas turbines for combined-cycle applications

The optimum pressure ratio for a gas turbine in combined-cycle applications is much lower than that required for peak thermal efficiency of a simple-cycle gas turbine. Most combined-cycle applications employ gas turbines with the basic Brayton cycle configuration, i.e. adiabatic compression and expansion, and near constant pressure heat addition in the combustor (Cengel and Boles, 1998). A number of variations are possible to the

© Woodhead Publishing Limited, 2010



2.2 Gas turbine with and without reheat.

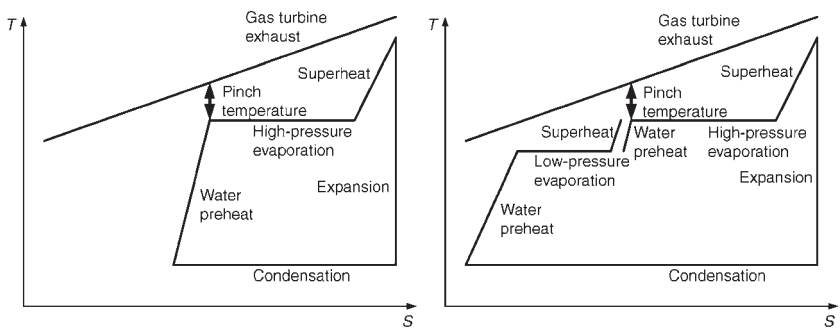
Brayton cycle and the ones most useful in combined-cycle applications are addition of reheat during expansion and intercooling during compression while maintaining very high pressure ratios. Reheat can be used to either increase the cycle efficiency for a given turbine inlet temperature or to achieve a target thermal efficiency while lowering the required turbine inlet temperature. Gas turbines with and without reheat are is depicted in Fig. 2.2 along with the enthalpy (h) and temperature (T) versus entropy (s) diagrams for the case where cycle efficiency is held the same while the turbine inlet temperature is lowered for the reheat cycle. In these diagrams, the heat added in the combustor of the gas turbine without reheat is represented by q while q_{HP} and q_{RH} represent the heat added to the high-pressure (HP) and the reheat combustors of the reheat cycle. W_C and W_T represent the work associated with the compressor and the turbine for the case without reheat, while W_{LPC}, W_{HPC}, W_{LPT} and W_{HPT} represent the work associated with the low-pressure (LP) compressor, the HP compressor, the LP turbine and the HP turbine respectively for the case with reheat. Refer to Cengel and Boles (1998) for more details on the thermodynamic characteristics of such power cycles.

2.1.2 Types of steam cycles in combined-cycle plant

Steam generated in gas turbine exhaust is superheated before it is supplied to a steam turbine for expansion in order to increase the thermal efficiency.

© Woodhead Publishing Limited, 2010

Reheating can also be advantageously used in the steam cycle when exhaust temperature of the gas turbine is high, typically in excess of 550°C. Further improvements in efficiency may be obtained by producing steam at different pressures; a large state-of-the-art combined cycle consists of generating steam at three different pressures in addition to superheating and reheating the steam. Figure 2.3 depicts the temperature (T) versus entropy (s) diagrams for single and dual pressure non-reheat ideal Rankine steam cycles. Refer to Cengel and Boles (1998) for a discussion of the thermodynamic characteristics of various types of Rankine cycles. As can be seen, the amount of heat recovered from gas turbine exhaust and consequently work produced is limited by the 'pinch' temperature (typically 5–10°C depending on value of energy recovered) when steam at a single pressure is generated. By lowering its pressure, more steam may be generated but the efficiency of converting the recovered heat to work is reduced. An optimum pressure exists for a given gas turbine exhaust temperature that maximizes the efficiency. By inclusion of a second lower-pressure steam generator, more heat may be recovered and consequently more work may be produced. A single steam turbine serves both high-pressure steam and lower-pressure steam, the lower-pressure steam after superheating being introduced into the steam turbine at the appropriate stage. In the idealized examples depicted in Fig. 2.3, water entering the evaporator is at its saturation temperature. In practice, however, the economizer is designed to heat up water to a temperature typically below its saturation temperature by 5–10°C ('approach temperature') at the design point, this is to avoid sudden phase change occurring across a level control valve located just upstream of the steam drum, or to avoid steaming within the economizer, especially during part-load operation and start-up as this approach temperature decreases.



2.3 Single and dual pressure ideal steam cycles with zero approach temperature.

© Woodhead Publishing Limited, 2010

2.2 Plant design and technology

2.2.1 Fuel specifications, limits and variability

In addition to natural gas, there is a wide variety of gaseous fuels that can be fired in a gas turbine, such as liquefied natural gas (LNG) after vaporization, gasification derived syngas (or synthesis gas), blast furnace gas, refinery waste gas (Rao *et al.*, 1996), landfill gas and gas from anaerobic sewage treatment plants. Composition of these gases as well as that of natural gas can vary significantly. In order to protect the gas turbine and to be able to burn these fuels efficiently, allowable ranges in composition and contaminants are defined by the original equipment manufacturers for each gas turbine model. Acceptable ranges are also defined for temperature, heating value and a modified Wobbe Index (MWI). MWI is calculated from the volumetric lower heating value (LHV) of the fuel gas, its specific gravity relative to air (SG) and its absolute temperature (T) by equation [2.1]

$$\mathrm{MWI} = \mathrm{LHV}/\sqrt{(\mathrm{SG})(T)} \qquad [2.1]$$

This index is a relative measure of energy entering the combustor for a fixed nozzle pressure drop. Typical allowable variations in this index are $\pm 5\%$.

An issue associated with utilizing a fuel with a heating value that is much lower than what a gas turbine is designed for is that the gas turbine compressor pressure ratio can increase due to a significantly larger mass (associated with the fuel) flowing through the turbine. This can cause compressor surge and damage. Possible solutions could be to close inlet guide vanes to limit the amount of air entering the engine and/or to extract air from compressor discharge if there is use for such pressurized air and if the engine can be modified for this capability. Modifications to the fuel delivery system, including control valve and combustor to burn the fuel efficiently and limit formation of pollutants, may also be required. Fuels with a LHV, as low as approximately $4\,\mathrm{MJ/nm^3}$, are acceptable for some gas turbine models after required modifications are made. If H_2 content of a fuel gas is very high, pre-ignition and flashback can be issues if a pre-mixed combustor designed to limit NO_x formation is utilized. Although typically not present in most fuel gas streams, upper limits also exist for O_2 content to avoid pre-ignition and flashback. Preheating fuel using heat from the bottoming cycle can increase overall combined-cycle efficiency while the upper limit is set by design capabilities of the fuel delivery system, including materials used in the fuel control valve, as well as considerations of pre-ignition and flashback when a pre-mixed combustor is utilized. Lower limit for fuel temperature is typically set by the need to keep fuel gas safely above its dew point and avoid formation of methane (CH_4) and CO_2 hydrates.

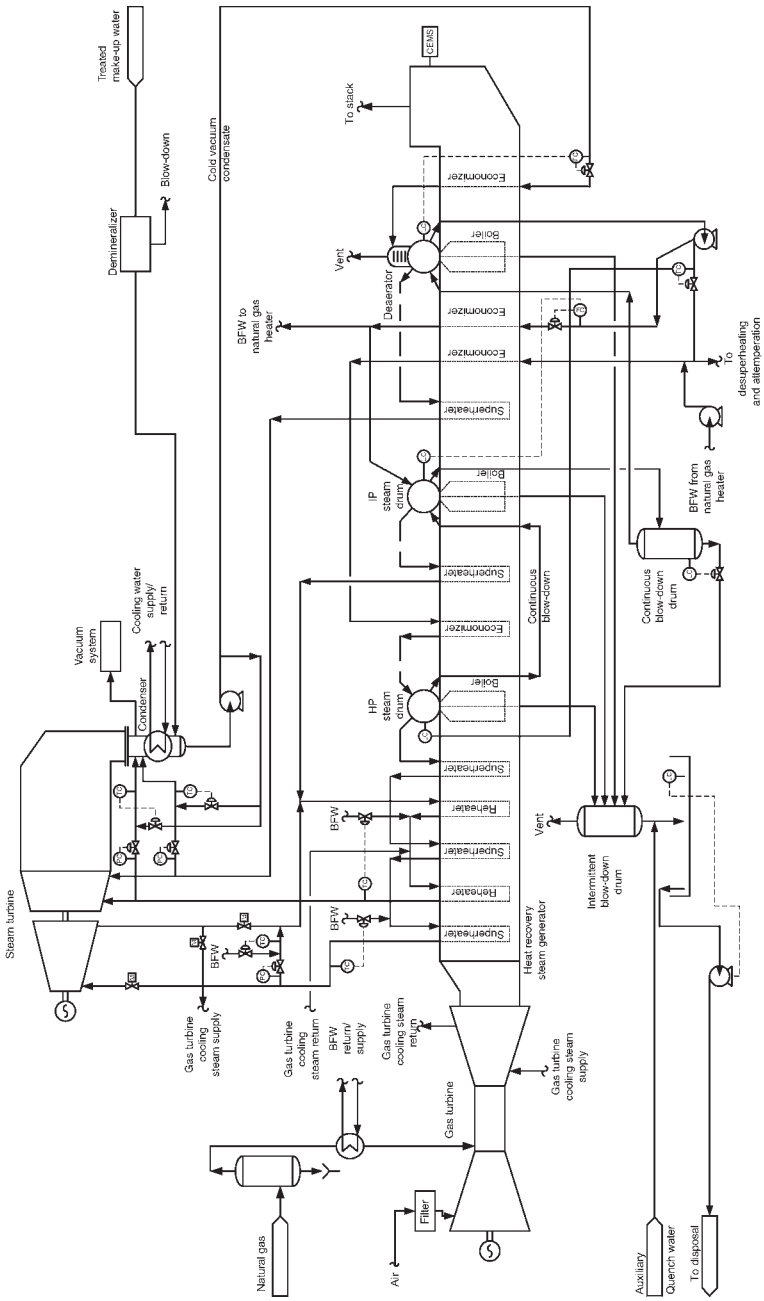
© Woodhead Publishing Limited, 2010

Fuel components such as moisture, as well as higher hydrocarbons, typically set the dew point. Joule–Thompson cooling across any pressure let-down valve should be taken into consideration. Natural gas as well as LNG are generally free of contaminants that can cause corrosion and/or erosion in a gas turbine but the other fuels can contain contaminants. For example, landfill gas, as well as gas from anaerobic sewage treatment plants, can contain siloxanes which can leave silica deposits on turbine blades. An activated carbon bed located upstream of the gas turbine can remove these compounds by adsorption. Stringent limits are specified for lead, vanadium, calcium, magnesium, total alkalis (sodium and potassium), sulfur compounds, as well as particulate loading by size.

2.2.2 Typical plant process description

Figure 2.4 depicts a steam-cooled gas turbine combined cycle (Smith, 2004a) with a triple pressure reheat steam cycle (most gas turbines are air cooled, however, the cooling air being provided by the gas turbine compressor). Ambient air is drawn into the gas turbine air compressor via a filter to remove air-borne particulates, especially those that are larger than 10 microns. Fuel and compressed air are mixed and combusted. Hot gas turbine exhaust flows through a heat recovery steam generator (HRSG). Demineralized make-up boiler feed water (BFW) is sprayed directly into the surface condenser which condenses steam leaving the LP section of a steam turbine at a vacuum. This negative operating pressure of the condenser is set by the temperature of the cooling medium used in the surface condenser. In the case of cooling water supplied by wet cooling towers operating in ambient conditions of 15°C and 60% relative humidity, the corresponding operating pressure is typically 4.4 kPa while maintaining a reasonable temperature rise for the cooling water and a reasonable 'hot-end' temperature difference between the condensing steam and cooling water in the surface condenser. The combined stream of cold vacuum condensate and make-up BFW is drawn from the surface condenser by the vacuum condensate pump and is heated in an economizer within the HRSG and then supplied to an integral de-aerator that also generates LP steam (at about 460 kPa). The de-aerator removes dissolved gases such as O_2 and CO_2 in the feed water, which can cause corrosion. Chemicals are also injected into the water to scavenge the small amounts of remaining O_2. A small amount of steam is vented with the dissolved gases. Excess steam generated in the de-aerator after superheating is fed to the LP section of the steam turbine. Superheating in addition to increasing cycle efficiency also avoids condensation of steam into droplets. Intermediate pressure (IP) BFW is extracted from the main BFW pump and flows through the IP economizer in the HRSG. Saturated IP steam generated (at about 2850 kPa) in the HRSG

© Woodhead Publishing Limited, 2010



2.4 Combined cycle with steam-cooled gas turbine and triple pressure reheat steam cycle.

© Woodhead Publishing Limited, 2010

is combined with steam leaving the HP section of the steam turbine before it is reheated (to about 570°C, depending on the gas turbine exhaust temperature) and fed back to the IP section of the steam turbine. Saturated HP steam generated (at about 17 400 kPa) in the HRSG is superheated (to about 570°C, again depending on the gas turbine exhaust temperature) and fed to the HP section of the steam turbine. The BFW pump supplies water to the attemperators for temperature control of the superheated and reheated steam. In an attemperator, the steam comes into direct contact with water whereby the steam is cooled through the evaporation of the water. Cooling steam required by the gas turbine is provided from the HP steam turbine exhaust. Steam returning from this closed-circuit cooling of the gas turbine is also combined with the IP steam before it is reheated within the HRSG in parallel with the superheater coils. Steam drums of the HRSG are continuously purged to control the amount of build-up of dissolved solids. The continuous blowdown is cascaded from the HP steam drum to the IP steam drum and blowdown from the IP steam drum is routed to a drum where LP steam is recovered. Water discharging from this drum is fed to a second lower-pressure drum and flash steam produced is vented to the atmosphere.

As seen from the above plant process description, the function of an HRSG is to recover heat from the exhaust of a gas turbine to generate steam. The principal mode of heat transfer from gas to water or steam in an HRSG is by convection. The tubes through which water or steam flow are finned to enhance heat transfer surface area. Gas turbine exhaust flowing over the tubes is contained in a casing without any refractory lining because of the significantly lower temperatures as compared to a fired boiler. Since the gas is essentially free of particulates, high gas velocities can be maintained to enhance heat transfer further. However, pressure drop across the HRSG is increased as the velocity is increased, while gas turbine output and efficiency are decreased. This inefficiency manifests itself as higher gas inlet temperature to the HRSG and, since only a portion of this heat is converted to work by the steam cycle, a trade-off exists between overall combined-cycle efficiency and HRSG size, and consequently plant cost. Pressure drop for an HRSG with triple pressure reheat steam cycle is typically 28 mm Hg (mercury) while that for a cycle without reheat is slightly lower, typically 24 mm Hg inclusive of stack losses. Catalysts required for reduction of NO_x and CO emissions can also be housed within the HRSG casing and the corresponding increase in pressure drop should be accounted for.

Steam from the bottoming cycle may be exported in combined heat and power applications. Duct or supplemental firing may be utilized to increase steam production. This consists of combusting fuel gas in duct burners utilizing O_2 contained in the gas turbine exhaust flowing through the

© Woodhead Publishing Limited, 2010

HRSG. Attention should be given to overall system efficiency and emissions as well as impact on tube metallurgy due to the higher gas temperatures. Duct burners may be installed either upstream of the superheater/reheater coils or more downstream within the HRSG, i.e. after the gas has been cooled down somewhat in order to limit temperature rise when a significant degree of duct firing is required.

Tube surface temperatures should always be maintained safely above the acid dew point of the gas to avoid using expensive tube materials such as Teflon®-coated tubes in the lower-temperature sections of the HRSG. Limiting dew point is typically set by H_2SO_4 (sulfuric acid) which is formed when sulfur present in the fuel is oxidized to SO_3 (typically 1–5%) in the gas turbine combustor (Ganapathy, 1989) and combines with water vapour to form H_2SO_4. This dew point temperature (T_{DP} in K) may be estimated from the partial pressures (in atmospheres) of H_2O vapour and SO_3 by equation [2.2] (Pierce, 1977)

$$1000/T_{DP} = 1.7842 + 0.0269 \log P_{H_2O} - 0.1029 \log P_{SO_3} + 0.0329 \log P_{H_2O} \log P_{SO_3} \quad [2.2]$$

Recirculation of heated condensate may be employed to raise tube surface temperature of the condensate heater coil, typically the cold condensate temperature being lower than the acid dew point.

In larger combined-cycle plants where steam is generated at high pressures, demineralized make-up water is required for the steam system. A demineralizer consists of mixed-bed ion exchangers, one in operation mode and one in stand-by mode, filled with cation and anion resins, with internal-type regeneration. This system includes facilities for resin-bed regeneration, chemical storage and neutralization basin.

There are various ways of rejecting heat from the surface condenser depending on site conditions and economic parameters. For example, cooling towers may be utilized where plenty of fresh water is available for use as make-up to the cooling towers. Mechanical draft cooling towers have the advantage of lower capital cost but higher electrical power requirement when compared to natural draft cooling towers. Once-through cooling may be utilized when the plant is located close to a large body of water. When using brackish or sea water for cooling, appropriate materials for the surface condenser (such as titanium (Ti)) should be selected. Air-cooled surface condensers can also be used for 'dry' locations, but plant efficiency is compromised owing to the higher temperature of the cooling medium (air), need for larger temperature approach and correspondingly higher surface condenser operating pressure.

Diversion dampers can be provided upstream of the HRSG to bypass gas turbine exhaust directly to the stack, allowing the gas turbine to operate

© Woodhead Publishing Limited, 2010

when the steam cycle is down. Leakage across this valve is always a concern and such an arrangement is typically avoided; during normal operation the leakage flow is not available for heat recovery, while during maintenance of the steam cycle, leakage of hot gas towards the HRSG is a concern, requiring two dampers in series with a buffer gas maintained in between.

Multiple trains of gas turbines (sometimes as many as four gas turbines) with individual HRSGs may be combined with a single steam turbine in which each of the turbomachineries has its own electrical generator. In a 'single-shaft' design, the gas turbine, steam turbine and a single generator are all arranged on a common shaft.

2.3 Applicable criteria pollutants control technologies

2.3.1 NO_x control

Dry low-NO_x combustors currently offered for natural gas applications consist of pre-mixing fuel with air and burning it under lean conditions to reduce flame temperature and thus formation of NO_x. Values as low as 9 ppm by volume on a dry basis and 'corrected' for 15% (by mole) O_2 content in the flue gas are guaranteed for some of the engines. Environmental emissions standards are becoming more stringent, however, and values as low as 2 ppm are being required in a number of locations in the USA. To approach such stringent emission requirements, a selective catalytic reduction (SCR) unit is essential at the current time. NH_3 (in aqueous form, which is easier to store) is injected upstream of an SCR unit located within the HRSG to react with the NO_x to form N_2 and H_2O. Gas turbine back pressure is increased in order to accommodate pressure drop across the SCR. Pressure drops as low as 4–5 mm Hg are typical and the corresponding impact on overall combined-cycle efficiency is quite small. Optimum location for an SCR unit within an HRSG which uses 3% V_2O_5 (vanadium pentoxide) as the active material in the catalyst is typically in the 300–400°C temperature zone.

2.3.2 CO and volatile organic compounds control

Oxidation catalysts can provide greater than 90% destruction of CO, volatile organic compounds (VOCs), formaldehyde and other toxic compounds. Oxidation catalysts like the SCR unit are housed within an HRSG at an appropriate temperature and are typically formulated with platinum group metals to achieve maximum conversion of the pollutants. Conversion rates increase with temperature and thus it is advantageous to place this catalyst near the HRSG inlet. Typical catalyst life may be 10 years or more of continuous operation. Occasional washing may be required to

© Woodhead Publishing Limited, 2010

maintain catalytic performance. At the end of the effective life of the catalyst, spent catalyst is typically recycled for the precious metal value. Pressure drops as low as 3 mm Hg are typical and the corresponding impact on overall combined-cycle efficiency is quite small.

2.3.3 NH_3 control (selective catalytic reduction (SCR) unit slippage)

NH_3 slippage through the SCR unit can be a cause for concern from an environmental emissions standpoint in certain locations. Catalysts for NH_3 oxidation are under development for installation in the HRSG downstream of the SCR unit to oxidize the NH_3 to elemental N_2. Pressure drop of this additional catalytic unit is expected to be similar to that of an SCR unit.

2.4 CO_2 emissions control technologies

Approximately a third of all the CO_2 emissions due to human activity come from fossil fuel-based power plants, with each power plant capable of emitting several million tonnes of CO_2 annually. These emissions could be reduced substantially by capturing and storing the CO_2. Two basic options are available for CO_2 capture in gas turbine combined-cycle plants: (i) pre-combustion capture, which consists of capture from the fuel before combustion in the gas turbine and (ii) post-combustion capture, which consists of capture from flue gas before it enters the atmosphere. The separated CO_2 may then be sequestered geologically or used for enhanced oil or coal bed methane recovery. Compression of the captured CO_2 to a pressure in the range of 11–15 MPa is typically required, depending on sequestration method employed and distance between the sequestration site and the power plant.

2.4.1 Pre-combustion control

In pre-combustion capture, a fossil fuel such as natural gas is catalytically reformed by the reaction, $CH_4 + H_2O = 3H_2 + CO$, or partially oxidized to form a syngas consisting primarily of a mixture of H_2 and CO. The next step is catalytic shifting of the CO to CO_2 by the reaction, $CO + H_2O = H_2 + CO_2$, followed by heat recovery, syngas cooling and separation of CO_2 from the syngas for sequestration utilizing an absorber column and a stripper column, with a suitable solvent circulating between the two columns. About 85–90% of the CO_2 may be absorbed into the solution in the absorber. Solvent loaded with the CO_2 is regenerated in the stripper using steam, while a high-purity CO_2 stream is released. The pressure at

© Woodhead Publishing Limited, 2010

which the CO_2 is released depends on the type of solvent used. Physical solvents such as mixtures of the dimethyl ethers of polyethylene glycol and chemical solvents such as amine solutions are available and their suitability depends on the syngas pressure; physical solvents such as the glycol are more suitable for higher syngas pressures, typically in excess of 4 MPa. Remaining gas (decarbonized syngas) leaving the absorber, which is now mostly H_2, is combusted (in gas turbines) with reduced CO_2 emissions to the atmosphere (Rao *et al*., 1999). An advantage of this scheme as compared to post-combustion capture is that the CO_2 present in the syngas is available at a high partial pressure, thereby lowering the energy penalty of separating and pressurizing the captured CO_2 stream. The high H_2 content of decarbonized syngas precludes use of current design pre-mixed gas turbine combustors to limit the formation of NO_x, auto-ignition and flash-back being major challenges. Thermal diluent addition is required to the gas in order to reduce NO_x generation when utilizing 'diffusion'-type combustors. Steam may be injected into the gas turbine as thermal diluent, or water vapour may be introduced into the fuel gas by direct contact with hot water in a counter-current column, while recovering low-temperature waste heat. This second method is thermally more efficient when there is a significant amount of low-temperature waste heat available in the plant for the humidification operation.

In partial oxidation plants where O_2 is utilized to generate syngas, N_2 supplied by an elevated pressure air separation unit used to produce the O_2 may also be utilized as a thermal diluent. The choice for relative amounts of the two diluents depends on a number of factors such as amount of low-temperature waste heat available for the humidification operation and amount of excess N_2 available from the air separation unit. It should be noted that the specific heat of the triatomic H_2O molecule is significantly higher than that of the diatomic N_2 molecule on a molar basis and thus relative amounts of diluents required (i.e. H_2O vapour versus N_2) on a volumetric or molar basis for a given amount of syngas are quite different to achieve similar flame temperatures.

Gas turbine pressure ratio increases when firing syngas as it has a much lower calorific value than natural gas. Increase in pressure ratio is dependent upon the amount and nature of diluent added and the degree to which the gas turbine compressor inlet guide vanes are closed. Surge margin available in the compressor could thus constrain the amount of diluent that may be added and the resulting reduction in NO_x emissions, in addition to constraints set by the combustor design with respect to achieving stable combustion while limiting CO emissions. Air extraction from the compressor may be utilized in case of the partial oxidation scheme in order to limit the increase in engine pressure ratio, since the extracted air after cool down and heat recovery can be efficiently used in an elevated

© Woodhead Publishing Limited, 2010

pressure air separation unit. The quantity of air that may be extracted is constrained by the minimum required to flow through the combustor liner.

H_2O vapour content of the working fluid flowing through the turbine section will be significantly higher when firing syngas (with H_2O vapour diluent added) as compared to that when natural gas is directly fired in the gas turbine. Reduction in turbine firing temperature may be required to limit hot gas path temperatures owing to different aero-heat transfer characteristics and life-spans of thermal barrier coatings, as well as the life-spans of any ceramics that may be utilized in future advanced gas turbines. Additional reduction in firing temperature may be required to accommodate higher cooling air temperatures resulting from increase in the engine pressure ratio. In the case of a steam-cooled gas turbine, however, reduction in firing temperature due to the increase in pressure ratio may be less significant because the cooling steam temperature may be maintained independently of the gas turbine pressure ratio, assuming the LP air-cooled stages of the gas turbine do not become limiting. Thus, the choice of diluent to be utilized, i.e. H_2O vapour versus N_2 or their relative amounts, should be included in trade-off and optimization studies. Use of diluents alone with the constraints discussed above cannot reduce NO_x emissions sufficiently to meet the stringent requirement of 2 ppm (by volume on a dry basis) and an SCR is still required.

A previous study (Rao *et. al.*, 1999) has shown catalytic reforming is more efficient than partial oxidation in pre-combustion CO_2 capture plants, the heat rate for the partial oxidation option being about 8% higher while utilizing cryogenic air separation for producing O_2. Compared to a plant without CO_2 capture where natural gas is directly fired in gas turbines, both plant efficiency and cost are significantly compromised with pre-combustion capture of CO_2: an increase of more than 30% in heat rate and a more than doubling of the plant cost on a per kW basis may be expected (Rhudy, 2005).

High-temperature membranes which are under development for separation of H_2 (Roark *et al.*, 2003) should provide some improvement in performance and possibly also cost for the reforming option, while high-temperature ion transport membranes which are under development for air separation (Richards *et al.*, 2001) should provide some improvement in performance and possibly also cost for the partial oxidation option.

2.4.2 Post-combustion control

In post-combustion capture, a fuel such as natural gas is first combusted (in gas turbines) and the CO_2 formed during the combustion process is separated from the flue gas for sequestration. When air is utilized in the combustion process, CO_2 separation may be accomplished utilizing

© Woodhead Publishing Limited, 2010

commercially proven amine solvent processes (Chapel *et al.*, 1999). When nearly pure O_2 is used in the combustion process ('oxy-combustion'), the flue gas is essentially a mixture of CO_2 and H_2O without significant amounts of N_2 , making it easier to separate out a relatively pure CO_2 stream for sequestration while emitting essentially no CO_2 to the atmosphere (Martinez-Frias *et al.*, 2002). Recycle of CO_2 and/or steam to the combustor is required to control turbine firing temperature. An air separation unit is required to supply the required O_2 for combustion.

Amine-based CO_2 capture

The process includes an absorber column and a stripper column with aqueous mono-ethanolamine (MEA) solution with proprietary additives circulating between the two columns. Flue gas leaving the HRSG, after cooling in a direct contact cooler and pressurization in a blower to overcome pressure drop in the downstream equipment, is supplied to the absorber where it comes into contact with the MEA solution. About 85–90% of the CO_2 may be absorbed into the solution. Solvent loaded with the CO_2 is regenerated in the stripper using steam, while a high-purity CO_2 stream is released near atmospheric pressure. This method of CO_2 capture does not impact combined-cycle plant design except for equipment added downstream of the HRSG. Compared to a plant without CO_2 capture, where natural gas is directly fired in gas turbines, both overall plant efficiency and cost are again compromised: an increase of more than 20% in heat rate and a more than doubling of the plant cost on a per kW basis (Rhudy, 2005) may be expected. At the present time, this approach for CO_2 capture appears to have lower penalties than the other approaches discussed in this chapter.

Oxy-combustion

In one variant of this cycle being developed by Clean Energy Systems (Martinez-Frias *et al.*, 2002), a clean fuel such as natural gas and O_2 provided by an air separation unit are supplied to a combustor (derived from rocket engine technology) operating at a pressure in excess of 10 MPa and a temperature of 540–760°C. The combustor exhaust temperature is controlled by injection of recycled water and, in some cases, steam. Combustion products consisting of approximately 90% H_2O vapour, 10% CO_2 by volume and a small amount of O_2 enter a HP turbine. Exhaust from the HP turbine at a pressure of approximately 1 MPa – after reheating to a temperature in excess of 1240°C by combusting additional natural gas with O_2 – enters an IP turbine followed by a LP turbine, which exhausts the gases into a condenser at atmospheric or subatmospheric pressure to condense the H_2O vapour and separate the CO_2. Most of the condensed water after

© Woodhead Publishing Limited, 2010

preheating in the turbine exhaust is re-circulated to the HP combustor. Humid CO_2 exiting the condenser may be treated in a catalytic combustor if the residual O_2 content is excessive. Another variant of the oxycombustion cycle being developed by Graz University of Technology (Sanz *et al.*, 2005) utilizes a single combustor (non-reheat cycle) operating at a more modest pressure of about 4 MPa as compared to Clean Energy System's HP combustor pressure, while the combustor exhaust temperature is controlled by recycled steam and a compressed mixture of CO_2 and H_2O vapour.

2.5 Advantages and limitations of gas-fired combined-cycle plants

In addition to having high thermal efficiencies (60% natural gas LHV basis with a current state-of-the-art combined cycle utilizing a steam-cooled 'H class' gas turbine at an ambient temperature of 15°C), outstanding environmental performance, easy start-up and shut-down and low cooling water requirements, combined cycles have significantly lower staffing, capital cost and construction time requirements when compared to boiler-based power plants. A combined cycle takes approximately one-third of the time it takes to build a pulverized coal plant. On the other hand, the clean fuels required by a combined cycle, such as natural gas, syngas or distillate, are significantly more expensive when compared to fuels such as coal and biomass that can be directly combusted in a boiler. Advantages for a combined cycle include high reliability, smaller plot space requirement and capability for phased construction, i.e. the gas turbine can be installed during the initial phase (when utilizing a non-steam-cooled gas turbine) to generate peak power before the steam cycle is added, at which point the plant can be used for base-loaded power generation. Advanced gas turbines, however, are constructed with 'exotic' materials designed to withstand the extreme operating temperatures necessary to achieve the high efficiency. These materials tend to have relatively low tolerance for thermal cycling and so gas turbine manufacturers severely limit the number of starts per year when warranting performance of gas turbines for such peaking service. Combined cycles have been also used for intermediate-load power generation in some cases and again number of starts per year should be limited, not only owing to the gas turbine limitations but also owing to the HRSG limitations: tubes in the high-temperature sections of the HRSG also cannot tolerate too many thermal cycles.

Natural gas-fired combined-cycle plants can use distillate fuel oil as back-up fuel to address any potential interruption in natural gas supply. However, in recent years this practice has become more uncommon because of additional emissions of sulfur oxides (SO_2 and SO_3) formed from the

© Woodhead Publishing Limited, 2010

sulfur present in fuel oil, as well as possible deactivation of CO oxidation catalyst, and undesirable formation of ammonium salts (ammonium bisulfate, sulfate and bisulfite) by reaction between NH_3 slipping through the SCR with SO_3. The ammonium salts can deposit in lower-temperature sections of the HRSG and reduce heat transfer through HRSG tubes (requiring frequent washes), as well as giving rise to particulate emissions. It may thus be better to ensure natural gas fuel availability by securing firm gas transportation.

Performance of a gas turbine is affected by ambient conditions of temperature, barometric pressure and to a lesser extent humidity. As ambient temperature or humidity increase or barometric pressure decreases (or site elevation increases), the mass flow of air intake to the gas turbine is reduced. This can have a direct impact on performance of a combined cycle. For example, power output can decrease by more than 10% as ambient temperature increases from 15°C to 35°C, and by approximately 20% as site elevation increases from sea level to 1800 m. Gas turbine efficiency is also reduced as ambient temperature increases, because its compressor power is increased. In a combined cycle, the steam bottoming cycle tends to dampen the effect of ambient temperature, however, and its heat rate increases by approximately 3% as ambient temperature increases from 15°C to 35°C. The magnitude of this sensitivity, however, depends on gas turbine exhaust temperature and flow rate (corresponding to a certain ambient temperature) selected for optimizing the steam cycle design. Combined-cycle heat rate may actually show a minimum at the design point ambient temperature, its heat rate increasing at lower temperatures. Effect of air humidity on gas turbine performance depends on the gas turbine firing temperature control scheme used, i.e. whether the exhaust temperature is biased by compressor pressure ratio to the approximate firing temperature. Performance of the steam cycle can also be affected by humidity. Higher humidity can reduce power output, because surface condenser operating pressure is increased as cooling water temperature is increased when cooling towers are utilized for plant heat rejection. Decrease in power output has a direct effect on plant capital cost on a per kW basis, while decrease in efficiency affects plant operating cost on a per kW basis.

Combined-cycle power output can be reduced initially through reducing gas turbine inlet air flow by closing compressor inlet guide vanes; the corresponding overall combined-cycle efficiency is not reduced by a significant amount. Further reductions in power output require a reduction in gas turbine firing temperature, which has a significant effect on overall plant efficiency. Heat rate can increase by nearly 20% as power demand is decreased by 50% of its rating point. Part load operation of the bottoming steam cycle should take into consideration increase in heat transfer surfaces within the HRSG per unit of heat transferred, and reduction in steam

© Woodhead Publishing Limited, 2010

pressures for a floating pressure steam system, which is typically used in combined-cycle applications. For example, steaming in the IP and LP economizers should be avoided, and pipes should be properly sized for the higher steam velocities at the lower pressures (reduction in velocities due to lower mass flow rates having a less pronounced effect).

Like all turbomachinery, gas turbines experience loss in performance with time. Part of this performance degradation is recoverable and is typically associated with compressor fouling; this can be partially fixed by water washing or more fully by mechanical cleaning of compressor blades and vanes. Mechanical cleaning requires opening the unit, resulting in a loss in plant capacity factor. Gas turbines also undergo a non-recoverable loss, which is due mostly to increased clearances in turbine and compressor sections as well as to changes in airfoil contours and surface finish. This loss can only be fixed through replacement of affected parts at required inspection intervals.

2.6 Future trends

Some of the technological advances being made or being investigated to improve the basic Brayton cycle include the following, in addition to changes in the basic cycle configuration such as inclusion of reheat combustion and intercooling (which is justified for very high-pressure-ratio cycles):

- firing temperature of 1700°C or higher, which would require development and use of advanced materials including advanced thermal barrier coatings and turbine cooling techniques
- advanced combustor liner materials (combustion air and combustion products being hotter) due to increases in firing temperature
- high blade metal temperature in the neighbourhood of ~1040°C while limiting coolant amount (this would again require the development and use of advanced materials including advanced thermal barrier coatings)
- pressure gain combustor
- cavity or trapped vortex combustor
- high-pressure-ratio compressor (much higher than 30 to take full advantage of higher firing temperature).

Addition of novel bottoming cycles is yet another approach to improving overall combined-cycle performance. Overall cycle efficiencies utilizing advanced technology gas turbines approaching 65% on natural gas on an LHV basis may be expected in the 2020 to 2025 time frame (Dennis, 2008).

© Woodhead Publishing Limited, 2010

2.6.1 Gas turbine firing temperature, pressure ratio and intercooling

The single most important design parameter that affects gas turbine thermal efficiency is its firing temperature. Thus, increases in firing temperature are required to make substantial increases in thermal efficiency. Current state-of-the-art gas turbines have firing temperatures (rotor inlet temperatures) that are limited to about 1430°C. This increase in firing temperature has been made possible by being able to operate turbine components that come into contact with the hot gases at higher temperatures, while at the same time utilizing closed-circuit steam cooling. In a state-of-the-art air-cooled gas turbine with firing temperature close to 1320°C, as much as 25% of the compressor air may be used for turbine cooling, which results in a large parasitic load of air compression. In air-cooled gas turbines, as the firing temperature is increased, the demand for cooling air is further increased. Closed-circuit steam cooling of the gas turbine provides an efficient way of increasing the firing temperature without having to use a large amount of cooling air. Furthermore, steam with its very large heat capacity is an excellent coolant. Closed-circuit cooling also minimizes momentum and dilution losses in the turbine while the turbine operates as a partial reheater for the steam cycle. Another major advantage with closed-circuit cooling is that the combustor exit temperature and thus the NO_x emissions are reduced for a given firing temperature; the temperature drop between the combustor exit gas and the turbine rotor inlet gas is reduced because the coolant used in the first-stage nozzles of the turbine does not mix with the gases flowing over the stationary vanes. Note that control of NO_x emissions at such high firing temperatures becomes a major challenge. The General Electric and Mitsubishi H class gas turbines as well as the Siemens and Mitsubishi G class gas turbines incorporate steam cooling, although the H class turbines include closed-circuit steam cooling for the rotors of the HP stages. A drawback with closed-circuit cooling, however, is the absence of a cooler protective film over the outside surface of the blades, which is possible with open-circuit 'film cooling'. Some gas turbine designers are taking this film-cooling approach for higher temperature stages of the more advanced engines.

Pressure ratio must also be increased in order to take full advantage of higher firing temperature from an overall thermal efficiency standpoint. Higher pressure ratios are also required to limit turbine exhaust temperature and thermal stresses at the roots of the last-stage turbine blades, which tend to be long in gas turbines for large-scale combined-cycle applications and are uncooled. A research study recently completed for the US Department of Energy (Rao *et. al.*, 2008) showed that for an 8% decrease in combined-cycle heat rate, an increase in firing temperature in excess of 300°C was

© Woodhead Publishing Limited, 2010

required over an H class gas turbine while the pressure ratio had to be increased from 24 to 50. Advanced materials in both the combustor and the turbine are required to withstand the severe environment created by the higher temperatures. Spray intercooling of such a high-pressure-ratio gas turbine compressor can decrease compressor discharge temperature by more than 100°C without decreasing overall combined-cycle efficiency. Reduction in compressor discharge temperature has beneficial impacts on compressor material costs as well as NO_x formation within the combustor.

2.6.2 Reheat gas turbines

As pointed out previously, reheating can be used to reduce firing temperature for a given cycle efficiency, but the pressure ratio required for such a cycle tends to be higher than that required for a simple-cycle gas turbine with higher firing temperature to achieve the same thermal efficiency. Reheat gas turbines have been in commercial operation, as offered by Alstom, and these gas turbines can play a role in achieving higher efficiencies in the future, but as firing temperatures are increased to realize even higher efficiencies, compressor pressure ratio may become the limiting technology.

2.6.3 Materials development

Taking the firing temperature beyond 1430°C poses challenges for the materials in the turbine hot gas path. Conventionally cast nickel-based superalloys are being replaced by directional solidification blades as well as single crystal blades, which provide significant benefits. Single crystal blades have been utilized successfully in advanced turbines but, in addition to this, developments of advanced thermal barrier coatings are being investigated, including extensive use of ceramics. Ceramic coatings provide thermal barrier protection to reduce metal temperatures. These coatings, however, need to be able to withstand an environment containing water vapour at a high partial pressure. Development of ceramic matrix composites for the hot components or sections of the turbine is also under consideration. Ceramic composites employing silicon carbide fibres in a ceramic matrix, such as silicon carbide or alumina, are commercially available, while single crystal oxide fibres are under consideration. Combustor materials for higher firing temperatures that can withstand a combination of creep, pressure loading, high cycle and thermal fatigue are also under investigation.

© Woodhead Publishing Limited, 2010

2.6.4 Combustor developments

Pressure gain combustor

A pressure gain combustor produces an end-state stagnation pressure that is greater than the initial state stagnation pressure. An example of such a system is the constant volume combustion in an ideal spark-ignited engine. Such systems produce a greater available energy in the end state than constant-pressure systems. It has been shown that the heat rate of a simple-cycle gas turbine with a pressure ratio of 10 and a turbine inlet temperature of ~1200°C can be decreased by more than 10% utilizing such a constant-volume combustion system (Gemmen *et al.*, 1994). Pulse combustion which relies on the inherent unsteadiness of resonant chambers can be utilized as a pressure gain combustor. Research continues at General Electric and at NASA for the development of pressure gain combustors. This technology holds promise for making significant improvements in cycle efficiency as long as the friction losses can be managed.

Trapped vortex combustor

The trapped vortex combustor (TVC) has potential for numerous operational advantages over current gas turbine engine combustors (Hsu *et al.*, 1995). These include lower weight, lower pollutant emissions, effective flame stabilization, high combustion efficiency, and operation in the lean-burn modes of combustion. The TVC concept evolved from studies of flame stabilization and is a departure in combustor design, using swirl cups for flame stabilization. Stability in swirl-stabilized combustors is somewhat limited and blow-out can occur under certain operating conditions. On the other hand, TVC maintains a high degree of flame stability because the vortex trapped in a cavity provides a stable recirculation zone that is protected from the main flow in the combustor. A bluff body dome distributes and mixes the hot products from the cavity with the main air flow. Fuel and air are injected into the cavity in such a manner that a vortex is naturally formed. The combustion process in a TVC may be considered as staged, with two pilot zones and one main zone, the pilot zones being formed by cavities incorporated into the liners of the combustor (Burrus *et al.*, 2001). The cavities operate at low power as rich pilot flame zones resulting in low CO and unburned hydrocarbon emissions, as well as providing good ignition and lean blow-out margins. At higher power conditions of greater than 30% power, the additional fuel is staged from cavities into the main stream while the cavities are operated at sub-stoichiometric conditions. An operating range of greater than 40% relative to conventional combustors has been demonstrated in experiments, with

© Woodhead Publishing Limited, 2010

combustion efficiencies greater than 99%. Use of the TVC holds special promise as an alternative option for suppressing NO_x emissions in syngas applications where pre-mixed burners may not be employed.

Catalytic combustor

Lean stable combustion can be obtained by catalytically reacting fuel–air mixtures with a potential for simultaneous reduction in NO_x, CO and unburned hydrocarbons (Smith, 2004b). Catalytic combustion also has the potential for improving lean combustion stability and for reducing combustion-related pressure oscillations. This type of combustor can also play a special role in syngas applications to reduce NO_x emissions.

2.7 Sources of further information

Combined-cycle power plants

Boyce M P (2001), *Handbook for cogeneration and combined cycle power plants*, New York, American Society of Mechanical Engineers.

Fuel gas specifications

General Electric (2002), *Specification for fuel gases for combustion in heavy-duty gas turbines*, Power Systems Bulletin GEI 41040G.

Advanced combined cycles

Bolland O (1991), 'A comparative evaluation of advanced combined-cycle alternatives', *ASME Journal of Engineering for Gas Turbines and Power,* 113, 190–197.

Gas turbine materials

Hannis J, McColvin G, Small C J and Wells J (2007), *Mat UK Energy Materials Review Materials R&D Priorities For Gas Turbine Based Power Generation.*

Schafrik R and Spragu R (2004), 'Gas turbine materials', *Advanced Materials and Processes*, May, 29–33.

2.8 References

Burrus D L, Johnson A W, Roquemore W M and Shouse D T (2001), 'Performance assessment of a prototype trapped vortex combustor for gas turbine application', In *Proceedings of the ASME IGTI Turbo-Expo Conference*, New Orleans.

Cengel Y A and Boles M A (1998), *Thermodynamics: an engineering approach,* New Jersey, WCB McGraw-Hill.

Chapel D G, Mariz C L and Ernest J (1999), 'Recovery of CO_2 from flue gases: commercial trends', presented at the Canadian Society of Chemical Engineers annual meeting, 4–6 October, Saskatoon, Saskatchewan, Canada.

Dennis R A (2008), 'DOE advanced turbine program ceramic material needs for

© Woodhead Publishing Limited, 2010

advanced hydrogen turbines', presented at US Advanced Ceramics Association Spring Meeting, May, Arlington, VA.

Ganapathy V (1989), 'Cold end corrosion: causes and cures', *Hydrocarbon Processing*, 57–59.

Gemmen R S, Richards G A and Janus M C (1994), 'Development of a pressure gain combustor for improved cycle efficiency', In *Proceedings of the ASME Cogen Turbo Power Congress and Exposition*.

Hsu K Y, Gross L P and Trump D D (1995), 'Performance of a trapped vortex combustor', paper no. 95-0810, presented at the AIAA 33rd Aerospace Sciences Meeting and Exhibition, 9–12 January, Reno, Nevada.

Martinez-Frias J, Aceves S, Smith J R and Brandt H (2002), 'Thermodynamic analysis of zero-atmospheric emissions power plan', presented at the ASME International Conference, November New Orleans, Louisiana.

Pierce R R (1977), 'Estimating acid dewpoints in stack gases', *Chemical Engineering*, 11 April, 125–128.

Rao A D, Francuz D J and West E (1996), 'Refinery gas waste heat energy conversion optimization in gas turbines', In *Proceedings of the ASME Joint Power Generation Conference*, October, Houston.

Rao A D, Francuz D J, Scherffius J and West E (1999), *Electricity production and CO_2 capture via partial oxidation of natural gas*, CRE Group Ltd, report by Fluor Daniel Inc.

Rao A D, Francuz D J, Maclay J D, Brouwer J, Verma A, Li M and Samuelsen G S (2008), *Systems analyses of advanced brayton cycles for high efficiency zero emission plants,* US DOE/NETL report, University of California, Irvine.

Rhudy R (2005), *Retrofit of CO_2 capture to natural gas combined-cycle power plants*, prepared by the International Energy Agency Greenhouse Gas Program for EPRI as a technical update.

Richards R E, Armstrong P A, Carolan M F, Stein V E, Cutler R A, Gordon J H and Taylor D M (2001), 'Developments in ITM oxygen technology for integration with advanced power generation systems', In *Proceedings of the 26th International Technical Conference on Coal Utilization and Fuel Processing,* March.

Roark S E, Machay R and Sammells A F (2003), 'Hydrogen separation membranes for vision 21 energy plants', In *Proceedings of the 28th International Technical Conference on Coal Utilization and Fuel Systems*, March, Clearwater, Florida.

Sanz W, Jericha H, Luckel F, Göttlich E and Heitmeir F (2005), 'A further step towards a Graz cycle power plant for CO_2 capture', In *Proceedings of ASME Turbo Expo*, 6–9 June, Reno-Tahoe.

Smith D (2004a), 'H system steams on', *Modern Power Systems*, February, 17–20.

Smith L L (2004b), *Ultra low NO_x catalytic combustion for IGCC power plants*, US DOE topical report by Precision Combustion, Inc.

© Woodhead Publishing Limited, 2010

3

Integrated gasification combined cycle (IGCC) power plant design and technology

Y. ZHU, Pacific Northwest National Laboratory, USA;
H. C. FREY, North Carolina State University, USA

Abstract: The main process areas of integrated gasification combined cycle (IGCC) plants without and with carbon dioxide (CO_2) capture are described. Key factors in IGCC plant design are described for major process areas, including gasification, water–gas shift, gas turbine, CO_2 capture, and other emissions control technologies. The advantages and limitations of coal IGCC plants are discussed. The main development trends of IGCC technologies are reviewed and summarized.

Key words: gasification, combined cycle, gas turbine, water–gas shift (WGS), CO_2 capture

3.1 Introduction: types of integrated gasification combined cycle (IGCC) plants

The global share of coal for power generation was 41% in 2005 and could increase to 46% in 2030 (Energy Information Administration, 2008). With coal remaining a key source for electric power generation, further research and development (R&D) of clean coal technology is required because coal combustion represents a significant source of many air pollutants and carbon dioxide (CO_2). Integrated gasification combined cycle (IGCC) is a promising technology for clean generation of power and co-production of chemicals from coal and other feedstocks including petroleum coke, biomass, and municipal solid wastes. Potential advantages of IGCC systems over conventional (not ultra super critical) pulverized coal (PC) power generation systems include higher thermal efficiency, lower emissions, and greater fuel flexibility (Ratafia-Brown *et al.,* 2002a; Rezaiyan and Cheremisinoff, 2005). However, IGCC plants are more costly than PC plants when no CO_2 capture is required (Klara, 2007). If substantial CO_2

© Woodhead Publishing Limited, 2010

capture is required, IGCC is expected to have significant cost and performance advantages over PC plants (Nexant, 2006; Klara, 2007).

IGCC features the conversion of solid or liquid fuels to a synthesis gas ('syngas') in a gasification step. The syngas can be used as a fuel for a gas turbine combined cycle for electricity generation or as a feedstock for chemical synthesis (e.g. ammonia and methanol, etc.), or both. Gasification technology has been used for gas, chemical, and liquid oil production for more than a century (Rezaiyan and Cheremisinoff, 2005; Breault, 2008). The Cool Water IGCC demonstration project, which is the first modern IGCC commercial-scale system, began operation in 1984 (Breault, 2008). More recently, several coal-fueled IGCC commercial-scale demonstration projects have been developed and are now in operation, including Wabash River, Polk, ELCOGAS, Nuon Power, Vresova, and Nakoso (Wabash River Energy Ltd, 2000; Tampa Electric, 2002; Ratafia-Brown *et al.*, 2002a; Hannemann *et al.*, 2002, 2003; Luby and Susta, 2007; Ishibashi and Shinada 2008; Higman, 2008). The key characteristics of these commercial plants are given in Table 3.1. Several new coal IGCC power plants are in development and are expected to be in service in the near future. The 1200 MW Nuon Magnum IGCC plant in The Netherlands is scheduled to begin operation in 2011 (de Kler, 2007). A 275 MW IGCC power plant with carbon capture, known as the FutureGen plant, could be the first-of-a-kind IGCC plant that includes CO_2 capture, if this project is revived after being cancelled in late 2008 (FutureGen Alliance, 2007).

Two configurations of IGCC plants are now described in more detail. These are the IGCC without CO_2 capture and the IGCC with CO_2 capture.

3.1.1 IGCC without CO_2 capture

Figure 3.1 depicts a conceptual design of an IGCC system without CO_2 capture. In this system, coal or other feedstocks react with a high-purity oxygen or air to produce a syngas rich in carbon monoxide (CO) and hydrogen (H_2) (Rezaiyan and Cheremisinoff, 2005). If high-purity oxygen is required, an air separation unit (ASU) is typically used to produce the oxidant. In a typical entrained-flow high-pressure gasifier (see section 3.2.1, subsection on 'Entrained-flow gasifier'), most minerals in coal ash are melted at high temperature and cooled by water quenching to form a glass-like slag. The sygnas is cooled and sent to a water scrubbing unit to remove particulate matter (PM), ammonia, and other impurities. The syngas is sent to a physical or chemical solvent-based process to remove acid gases, such as hydrogen sulfide (H_2S) and carbonyl sulfide (COS), from the syngas. The separated acid gases are further recovered to produce elemental sulfur or sulfuric acid as a by-product. The clean syngas is sent to a gas turbine combined cycle for power generation. A combined cycle consists of a gas

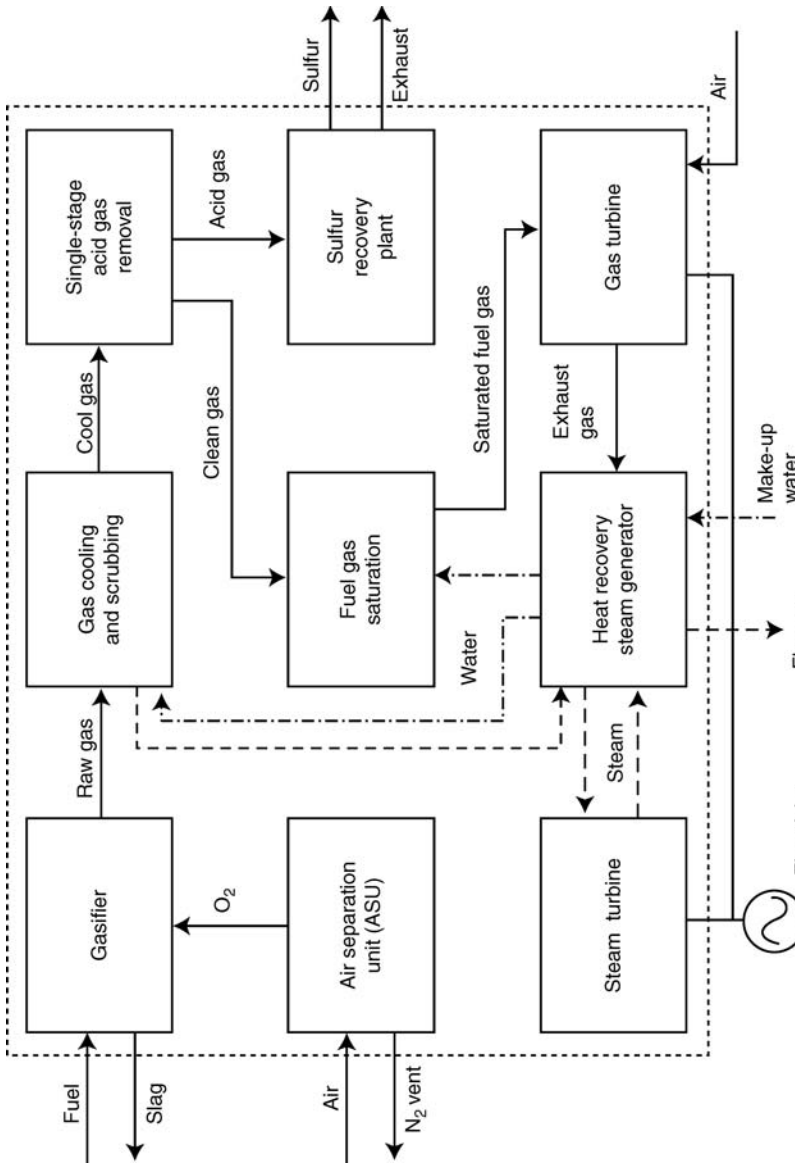
© Woodhead Publishing Limited, 2010

Table 3.1 Major existing commercial and demonstration coal integrated gasification combined cycle (IGCC) power plants

	Existing coal IGCC projects						Demonstration IGCC projects	
Name	Tampa Electric Polk	Wabash River Repowering	Nuon Power Buggenum	ELCOGAS	Sokolovska Uhelna Vresova	Nakoso	Cool Water IGCC	Dow Chemical /Destec LGTI Project
Site	Polk, Florida	West Terre Haute, Indiana.	Buggenum, Netherlands	Puertollano, Spain	Vresova, Czech Republic	Iwaki City, Japan	Daggett, California	Plaquemine, Louisiana
Status	Commercial	Commercial	Commercial	Commercial	Commercial	Demonstration	Demonstration	Demonstration
Years	1996 to present	1995 to present	1994 to present	1997 to present	1996 to present	2007 to present	1984 to 1989	1987 to 1995
Net power output (MWe)	250	262	253	300	400	250	120	160
Efficiency (%) (HHV basis [a])	35.4	39.7	41.4	41.5	n/a	40.5	n/a	n/a
Gasifier type	Entrained-flow (General Electric)	Entrained-flow (Conoco-Phillips E-Gas)	Entrained-flow (Shell)	Entrained-flow (Prenflo)	Moving-bed (Lurgi)	Entrained-flow (Mitsubishi)	Entrained-flow (General Electric)	Entrained-flow (Conoco-Phillips E-Gas)
Oxidant	Oxygen	Oxygen	Oxygen	Oxygen	Oxygen	Air	Oxygen	Oxygen
Feed	Coal slurry feed	Coal slurry feed	Coal slurry feed	Coal dry feed	Lignite dry feed	Coal dry feed	Coal slurry feed	Coal slurry feed
Gas cooling	Radiant water tube and convective fire tube boiler	Vertical fire tube boiler	Water tube boiler	Convective water tube boiler	n/a	Syngas cooler	Radiant water tube and convective fire tube boiler	Downflow fire tube boiler
Particulate removal	Wet scrubbing	Metallic candle filter + wet scrubbing	Cyclone + ceramic candle filter + wet scrubbing	Ceramic candle filter + wet scrubbing	n/a	Candle filter + wet scrubbing	Wet scrubbing	Wet scrubbing
Acid gas removal [b]	MDEA	MDEA	Sulfinol-M	MDEA	Rectisol	MDEA	Selexol	Amine
CO_2 capture	No	No	No	No	No	No	No	No
Sulfur recovery (sulfur by-product)	Sulfuric acid plant (sulfuric acid)	Claus (sulfur)	Claus (sulfur)	Claus (sulfur)	n/a	n/a	Claus (sulfur)	Selectox (sulfur)
NO_x control	N_2 injection	Steam dilution	N_2 injection	N_2 injection	n/a	n/a	Water saturation	Steam dilution
Gas turbine	General Electric (GE) 7FA	GE 7FA	Siemens V94.2	Siemens V94.3	2 x GE 9E	Mitsubishi M701DA	GE 7E	Westinghouse 501

Source: Ratafia-Brown *et al.* (2002a); Tampa Electric (2002); Wabash River Energy Ltd (2000); Hannemann *et al.* (2002); Hannemann *et al.* (2003); Ishibashi and Shinada (2008); Higman (2008); Luby and Susta (2007).
[a] HHV: higher heating value; [b] MDEA: methyl diethanol amine.

© Woodhead Publishing Limited, 2010



3.1 Conceptual diagram of IGCC system without CO_2 capture.

© Woodhead Publishing Limited, 2010

turbine, a heat recovery steam generator (HRSG), and a steam turbine (Brooks, 2000). The gas turbine includes a compressor, a high-pressure combustor, and an expander. The syngas is combusted with compressed air in the combustor at a pressure of 15 bar or higher. The expander recovers rotational energy from the pressurized high-temperature combustor exhaust. The heat from the gas turbine exhaust is recovered in a HRSG to produce high-temperature steam. The HRSG comprises a series of heat exchangers, including a superheater, boilers for various steam pressure levels, and feedwater heaters. The generated steam, usually at two or three pressure levels, is then expanded in a series of steam turbines. Both the gas turbine and steam turbines drive a generator.

3.1.2 IGCC with CO_2 capture

Although IGCC systems with CO_2 capture have not yet been commercially demonstrated, IGCC systems are considered to have advantages in CO_2 capture compared to conventional PC plants because of higher operating pressure and higher concentration of CO_2 in syngas than in flue gas (Ratafia-Brown *et al.,* 2002b). High-pressure syngas has a much smaller volume flow rate than the atmospheric pressure exhaust gas from a PC plant. A recent study estimates that the total plant cost for an IGCC system with CO_2 capture is approximately 15% lower than that of a supercritical PC plant with CO_2 capture (Klara, 2007).

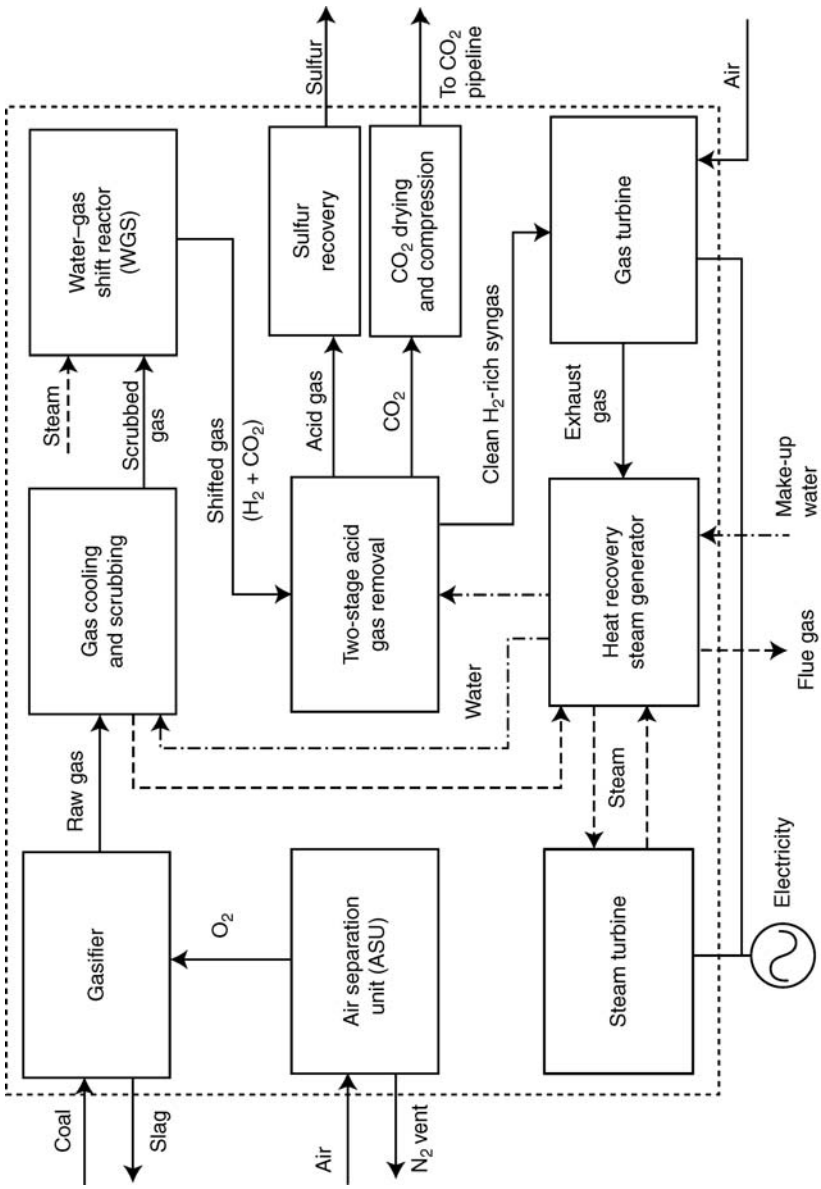
Compared to IGCC plants without CO_2 capture, the major differences of IGCC plants with CO_2 capture (see Fig. 3.2) include: (i) a water–gas shift (WGS) reaction process downstream of gas cooling and scrubbing; (ii) a two-stage acid gas removal process with a sulfur removal stage and a CO_2 capture stage; (iii) a CO_2 drying and compression unit; (iv) a gas turbine modified for firing syngas with high H_2 content; and (v) a steam cycle designed to provide extra steam for WGS reaction if required and to provide steam or water for syngas dilution (Maurstad, 2005; Klara, 2007).

In this system, raw syngas generated from gasification is cooled, and fine particles in the syngas are removed by water scrubbing. The syngas rich in H_2 and CO is sent to a WGS reactor, in which the bulk of CO is converted into CO_2 by reaction with steam (Hiller *et al.,* 2006)

$$CO + H_2O \leftrightarrow CO_2 + H_2 \qquad [3.1]$$

From the WGS reaction, H_2 is produced from steam. Hence, the H_2 to CO ratio of the shifted syngas is very high compared to raw syngas from the gasification. The shifted syngas is sent to a two-stage acid gas removal process, in which the first stage removes sulfur compounds, and the second stage removes CO_2. High-purity CO_2 is separated from the syngas and is ready for compression and sequestration. After acid gas removal, the H_2-

© Woodhead Publishing Limited, 2010



3.2 Conceptual diagram of IGCC system with CO_2 capture.

© Woodhead Publishing Limited, 2010

rich syngas is sent to a gas turbine combined cycle. Dilution nitrogen or steam/water injection to the combustor is typically used to control NO_x emissions by reducing the peak flame temperature.

3.2 IGCC plant design and main processes technologies

The main processes technologies in an IGCC plant are described. The major types of gasifiers and their features are reviewed. The main differences between IGCC systems with CO_2 capture and those without CO_2 capture are also described.

3.2.1 Coal gasification

Coal gasification converts coal into gaseous components via partial oxidation under elevated pressure and temperature. The oxygen consumption of a gasifier is generally 20–70% of the amount required for complete combustion (Rezaiyan and Cheremisinoff, 2005). In gasification, coal particles are heated and devolatilized to produce a variety of species, including char, oil, tars, and gases. The volatiles and char are gasified in solid–gas phase reactions to generate H_2, CO, H_2O, and CO_2. The volatiles also react with oxygen to produce CO, CO_2, H_2, and other gaseous products. The slowest reactions in gasification are heterogeneous carbon–gas reactions (Higman and van der Burgt, 2003; Rezaiyan and Cheremisinoff, 2005).

In a gasification process, reactions include combustion reactions and gasification reactions. The overall reaction can be represented as (Higman and van der Burgt, 2003)

$$C_nH_m + n/2\ O_2 = nCO + m/2\ H_2 \qquad [3.2]$$

where, for coal, n and m are approximately equal.

The combustion reactions involve the oxidation of carbon and hydrogen to CO, CO_2, and water (H_2O), which provide heat for gasification reactions. The gasification reactions mainly include the Boudouard, methanation, and water gas shift reactions

$$C + CO_2 \leftrightarrow 2CO \qquad [3.3]$$

$$C + 2H_2 \leftrightarrow CH_4 \qquad [3.4]$$

$$C + H_2O \leftrightarrow CO + H_2 \qquad [3.5]$$

Three kinds of gasification technologies are generally applied in IGCC systems, including moving-bed, fluidized-bed, and entrained-flow gasifiers.

© Woodhead Publishing Limited, 2010

Table 3.2 Characteristics of major types of gasification technologies

Gasification type	Moving-bed gasifier	Fluidized-bed gasifier	Entrained-flow gasifier
Example	Lurgi, British Gas/ Lurgi (BGL)	Kellogg Rust Westinghouse (KRW), high-temperature Winkler (HTW)	General Electric (GE), Conoco-Phillips E-Gas, Shell, or Prenflo
Temperature (°C)	370–650	800–1050	1250–1600
Pressure (bar)	20–25	20–30	20–85
Oxidant	Oxygen or air	Oxygen or air	Oxygen or air
Fuel particle size (mm)	6–50	6–10	Fine particles, < 0.1
Fuel feed	Dry	Dry	Dry/slurry
Fuel flexibility	Cannot be used to handle fine particles	Reactive, non-caking fuels	Conventional fuel, i.e. coal and oil, and less reactive fuels, e.g. chemical wastes
Syngas	Large amount of methane and heavy hydrocarbon compounds	Some methane and other heavy hydrocarbon compounds	Small amount of methane and no other heavy hydrocarbon compounds
Oxidant consumption	Low	Medium	High
Conversion efficiency	99%	97%	$> 98\%$

Source: Higman and van der Burgt (2003); Rezaiyan and Cheremisinoff (2005); Maurstad (2005); ENEA *et al.* (2005).

The main features of these three kinds of gasifiers are listed in Table 3.2. The details of each type of gasification technology are briefly described.

Entrained-flow gasifier

Entrained-flow gasifiers feature co-current flow of feedstock and oxidant. To ensure efficient mixing and high carbon conversion, solid feedstocks must be finely pulverized. Entrained-flow gasifiers typically use oxygen as an oxidant and operate at temperatures well above ash slagging conditions to assure reasonable carbon conversion and to facilitate ash removal in molten form from the gasifier (Higman and van der Burgt, 2003). To maintain high temperature (about 1250–1600°C), the oxygen-to-fuel ratio is higher than for other kinds of gasifiers. At the high operating temperature, only small amounts of methane are produced and the concentration of other hydrocarbons in the syngas is negligible to zero.

© Woodhead Publishing Limited, 2010

Entrained-flow gasifers can be slurry-feed or dry-feed gasifiers. Slurry-feed gasifiers have higher operating pressure than dry-feed ones because the pressure limit of lock-hoppers used in dry-feed is lower than that of a slurry pump. Thus, slurry-feed enables higher syngas production capacity. However, the water in slurry needs to be evaporated and heated to the operating temperature by using part of the feedstock, which has a penalty on the cold gas efficiency of the process. A slurry-feed entrained-flow gasifier can be single-stage, such as the General Electric (previously Texaco) design, or two-stage, such as the Conoco–Phillips E–Gas design. For a slurry-feed single-stage gasifier, the gasification normally takes place at temperatures between 1250 and 1600°C and at a pressure of about 30 bar (Tampa Electric, 2002; Higman and van der Burgt, 2003). Coal slurry and oxidant are introduced at the top of the gasifier, and syngas rich in H_2 and CO is generated. The hot syngas with molten ash is cooled and sent to a wet scrubbing unit to remove particles. The slag is quenched by water and removed from the bottom of the quench chamber. In a slurry-feed two-stage entrained-flow gasifier, the coal slurry is split into two parts, with one part injected with oxidant to the first stage and the remaining part with slurry only injected to the second stage. The hot syngas from the first stage reacts with the remaining slurry and provides heat for the endothermic reactions in the second stage. The sygnas produced in a two-stage gasifier has relatively higher methane content and thus higher caloric value than the one produced in a single-stage gasifier because of lower temperature in its second stage (Rezaiyan and Cheremisinoff, 2005).

For a slurry-feed single-stage entrained-flow gasifier, two types of raw syngas cooling methods are commercially available, including water quench and syngas cooler (radiant only or radiant and convective coolers). In the water quench design, raw syngas from the gasification zone is cooled and saturated by quenching water. In the syngas cooler design, hot syngas is cooled in a heat exchanger, in which the reduction in sensible heat of syngas is partially recovered by generating high-temperature steam. For example, the Polk plant uses the syngas cooler design (Tampa Electric, 2002). IGCC plants with syngas coolers generally have higher efficiencies than those with water quench. However, the syngas cooler design increases system cost because of the higher equipment cost for steam generation (Frey and Akunuri, 2001; Holt, 2004).

An example of a dry-feed single-stage entrained-flow gasifier is the Shell gasifier. This type of gasifier has higher operating temperature and thus a higher carbon conversion efficiency than a slurry-fed gasifier. However, it has relatively lower operating pressure because of pressure limitations of dry-feed technologies (Higman and van der Burgt, 2003; Maurstad, 2005).

Entrained-flow gasifiers have great fuel flexibility because of high gasification temperature. For low-rank coals with high moisture and ash

© Woodhead Publishing Limited, 2010

content, however, the current entrained-flow gasifiers would have lower efficiency and higher cost than those with bituminous coal as the feedstock (Holt and Todd, 2003). The high-moisture and high-ash coal has lower energy density compared to bituminous coal and thus more oxygen is consumed. For dry-feed gasifiers, the high-moisture coal requires more heat for coal drying.

Fluidized-bed gasifier

In a fluidized-bed gasifier, solid fuel is broken into small pieces and introduced over a gas distributor plate through which oxidant flows upward. Hence, the fuel particles are suspended by the upward-moving oxidant and undergo turbulent movement, including back-mixing. The turbulent mixing promotes a uniform temperature in the fluidized bed. Because fluidized-bed gasifiers would plug if ash were to melt, the bed temperature must be below the ash melting or slagging temperature. Either purified oxygen or air can be used as the oxidant. The feedstock is dried and pyrolysed rapidly to release its volatile matter, which burns and supplies the heat for the endothermic gasification reactions.

The raw syngas flows through a cyclone to remove particles. The removed particles containing char and ash are recycled to the reaction zone. Fluidized-bed gasifiers typically operate at temperatures between 900 and 1050°C, which is below the softening point of ash (Higman and van der Burgt, 2003).

The major advantages of fluidized-bed gasifiers include their fuel flexibility resulting from good mixing of feedstock and oxidant to ensure efficient heat and mass transfer, and their ability to deal with small particles. One disadvantage is the removal of unreacted coal particles together with the ash, which leads to lower carbon conversion efficiency than other gasifiers. The lower operating temperature of fluidized-bed gasifiers leads to higher methane and tar contents in the product gas than that of entrained-flow gasifiers (Holt, 2004). When substantial CO_2 capture is required, high methane content would affect CO_2 capture efficiency because methane cannot be easily converted to CO_2 in the water–gas shift reaction. Fluidized-bed gasifiers are best suited for reactive fuels that do not agglomerate, or 'cake', in the fluidized bed.

The major features of a fluidized-bed gasifier are summarized in Table 3.2. A typical example of a fluidized-bed gasifier is Kellogg Rust Westinghouse (KRW) gasifier, which is used at the Pinon Pine plant (Rezaiyan and Cheremisinoff, 2005).

Moving-bed gasifier

In moving-bed gasifiers, also referred to as a 'fixed-bed' gasifiers, oxidant and steam are introduced in the lower part of the gasifier and flow vertically

© Woodhead Publishing Limited, 2010

upward, while feedstock is introduced at the top of the gasifier. The feedstock is heated by up-flowing hot syngas. Volatile components are driven off from the feedstock in the upper part of the gasifier reactor vessel and are partially gasified. The remaining char moves towards the bottom of the gasifier and is combusted in the bottom zone of the reactor. The heat from the combustion zone provides thermal energy for the endothermic gasification reactions, which occur in the middle portion of the gasifier. A typical outlet gas temperature of a moving-bed gasifier is between 425 and 650°C (Higman and van der Burgt, 2003). At this temperature, heavy hydrocarbon compounds, such as tars and oils, will not be cracked. Therefore, typically a downstream condenser is used to remove heavy hydrocarbon compounds, leading to a process condensate stream that requires treatment. Furthermore, a relatively large amount of methane is produced because of the low syngas outlet temperature.

Moving-bed gasifiers can be slagging or dry ash gasifiers. Examples are the British Gas/Lurgi (BGL) slagging gasifier and the Lurgi dry ash gasifier. The combustion zone temperature in dry ash gasifiers (about 1000°C) is much lower than that in slagging gasifiers (about 2000°C). Therefore, dry ash gasifiers are more suitable for reactive feedstock, such as lignite, rather than bituminous coal. The oxygen consumption of moving-bed gasifiers is lower than that of other types of gasifiers because of efficient heat transfer from counter-current flow and the relatively low operating temperature (delaMora *et al.*, 1985). This kind of gasifier is suitable for handling large particles. Fine particles tend to be entrained with the exiting syngas and can block the syngas flow path (Simbeck *et al.*, 1983; Higman and van der Burgt, 2003).

3.2.2 Water–gas shift (WGS) reaction

To facilitate CO_2 capture from syngas, a key design goal is to convert CO in the raw syngas to CO_2, which can be separated by using effective and proven techniques to produce a CO_2-rich gas. The purified CO_2-rich gas can be compressed and injected to a reservoir for the purpose of sequestration. A WGS reactor is used to convert CO to CO_2 for syngas produced from hydrocarbon feedstocks.

The WGS reaction is exothermic and thus lower temperature favors CO conversion. However, at low temperature, the reaction rate is low. Multiple-stage catalytic high-temperature shift (HTS) and low-temperature shift (LTS) reactors have been investigated, which can achieve high CO conversion efficiency and relatively high reaction rates (Chiesa *et al.*, 2005a; Hiller *et al.*, 2006). The HTS typically operates at temperatures between 300 and 510°C, and the LTS often operates between 180 and 270°C. In a two-stage WGS process of an IGCC system, syngas from the water

© Woodhead Publishing Limited, 2010

scrubbing unit enters the HTS reactor with steam from the steam cycle, where about 85–92% of the CO in syngas is converted. The syngas from the HTS reactor is cooled and sent to a LTS reactor, where the CO conversion can reach up to about 97–98% (Chiesa *et al.*, 2005a). For clean gases with only small quantities of sulfur or hydrocarbons, iron–chromium oxide-based catalysts are often used in the HTS reaction and copper–zinc–aluminum oxide-based catalysts are available for the LTS reaction (Hiller *et al.*, 2006). For syngas from coal gasification, which contains sulfur and hydrocarbons, cobalt–molybdenum-based catalysts are used at temperatures between about 200 and 500°C (Twigg, 1997; Hiller *et al.*, 2006).

Membrane-based WGS reactors are in development (Bracht *et al.,* 1997). In these reactors, the WGS reaction takes place on a membrane containing a catalyst. The produced H_2 permeates selectively through the membrane during the shift reaction process. Therefore, the chemical equilibrium of the shift reaction moves more towards the product side because of the H_2 removal. Design studies have indicated that membrane WGS reactors may be more cost-effective than conventional WGS reactors (Bracht *et al.*, 1997; Amelio *et al.*, 2007). However, membrane WGS reactors have not been commercially applied in IGCC plants and are still in an early development phase.

3.2.3 Gas turbine

High-pressure gaseous fuel, such as syngas from coal gasification, is combusted with air from the gas turbine compressor. The most typical pollutant of concern is NO_x, which is produced when air is heated to a higher temperature and at high pressure. A common technique for preventing NO_x emissions is to reduce peak temperature in the combustor by adding a thermal diluent, such as water, steam or nitrogen (Ratafia-Brown *et al.,* 2002a; Holt, 2003). The current state-of-practice gas turbines used in existing IGCC plants are F class. For example, both the Polk and Wabash River IGCC plants use GE 7FA gas turbines (Wabash River Energy Ltd, 2000; Tampa Electric, 2002). Current F class technology has a simple cycle efficiency ranging from 36 to 38.5% and combined cycle efficiency from 56 to 58% (Lebedev and Kostennikov, 2008).

In IGCC plants without CO_2 capture, the syngas sent to the gas turbine is rich in both CO and H_2. For IGCC plants with substantial CO_2 capture, the fuel for the gas turbine would be syngas rich in H_2.

Hydrogen-rich syngas-fired gas turbine

Removal of CO_2 from syngas leads to about 10% loss in lower heating value (LHV) because CO in the raw syngas is shifted to H_2, and H_2 has a lower

© Woodhead Publishing Limited, 2010

volume basis heating value than CO (Shah *et al.*, 2005). Compared to gas turbines fired with syngas containing both CO and H_2, gas turbines fired with syngas rich in H_2 require more syngas to maintain the nominal output of gas turbine and thus more feedstock is required for the overall system.

Todd and Battista (2000) have reported a gas turbine test with 46–95% H_2 in fuel gas. The test indicated that for an increase in the H_2 content of the syngas, the amount of steam injection needed to maintain a constant NO_x emissions level increased. Hydrogen-rich syngas firing also leads to a higher water content of gas turbine exhaust gas, which leads to higher heat transfer capabilities than the exhaust gas from syngas without CO_2 capture (Chiesa *et al.*, 2005b). However, the high moisture content in exhaust gas resulting from steam injection and hydrogen combustion could significantly shorten turbine bucket or rotating blade life. Siemens has tested its F class machines with H_2 content ranging from 30 to 73% in fuel gas (Brown *et al.*, 2007). The test results showed that their emissions and operation targets could be achieved even when the CO_2 capture was as high as 90%.

NO_x emissions control

Nitrogen oxides formation occurs for any fuel burned with air because of high-temperature reactions involving O_2 and N_2 in the combustion air, and increases with temperature and residence time. Currently, three types of technologies are available for NO_x emissions control in gas turbine operations, namely: (i) improved premixed combustion, such as dry low NO_x (DLN) burner and catalytic combustion; (ii) dilution of combustion gases in the flame, to reduce peak flame temperature, using steam, H_2O, N_2, or a mix; (iii) post-combustion removal, such as selective catalytic reduction (SCR) and Sconox process (Todd and Battista, 2000; Chiesa *et al.,* 2005b).

DLN burners are designed to mix air and fuel before the combustion to achieve a lean and uniform air-to-fuel ratio. The main goal of DLN burners is to avoid hot spots that have poorly mixed fuel-to-air ratios and that lead to localized high peak temperatures, leading to disproportionately high NO_x production. DLN burners operate at fuel lean conditions, in order to limit the peak flame temperature. Catalytic combustors speed up combustion kinetics, thereby enabling fuel to burn at lower temperatures, which in turn reduces the amount of NO_x formation. Although DLN is a common commercially available technology, catalytic combustors are not widely deployed. Syngas fuel for gas turbines has H_2 content varying from 8.6 to 61% (Brun *et al.,* 2002). Klara (2007) indicates that syngas with 90% CO_2 removal could have a H_2 content as high as 90%. There is some concern that DLN and catalytic combustors may not be appropriate for use with fuels that are rich in H_2, since H_2 has a fast reaction rate and there may be

© Woodhead Publishing Limited, 2010

potential for a flame to ignite upstream of the desired combustion zone (Chiesa *et al.,* 2005b).

Fuel dilution is widely used in current IGCC plants for NO_x control, such as N_2 injection in the Polk IGCC and steam dilution in Wabash River IGCC plant (Wabash River Energy Ltd, 2000; Tampa Electric, 2002). The use of thermal diluents is expected to be a practical approach for mitigating NO_x emissions for H_2-rich syngases. Todd and Battista (2000) reported that gas turbine tests with steam and N_2 dilution achieved NO_x emissions below 10 ppm for syngas with 20–90% CO_2 capture. Post-combustion removal options, such as SCR, can be combined with thermal dilution to achieve even lower NO_x emissions levels.

SCR is a widely used technology that has been applied to large gas turbines. SCR is capable of NO_x reduction efficiencies between 70 and 90%. It is considered the most likely post-combustion NO_x control candidate for use with IGCC syngas-fired gas turbine exhaust (Ratafia-Brown *et al.*, 2002a). In the SCR process, ammonia (NH_3) is injected into the exhaust gas and the NO_x selectively reacts in the presence of a catalyst with NH_3 and O_2 to form N_2 and H_2O. The optimum temperature range is 250–427°C (US Environmental Protection Agency, 2003).

3.3 Applicable CO_2 capture technologies

For IGCC systems, pre-combustion CO_2 control schemes are generally considered to be more economical than the post-combustion CO_2 control methods that would be used in PC plants (Holt, 2004; Klara, 2007). For pre-combustion control, CO_2 can be captured by the following methods, including: (i) physical and chemical absorption; (ii) membranes separation; and (iii) cryogenic separation (Murai and Fujioka, 2008). Selection of suitable CO_2 capture technologies depends on many factors, such as CO_2 partial pressure, CO_2 recovery and purity requirements, limitations of capture methods, and costs.

3.3.1 Physical and chemical absorption

Physical and chemical absorption have been extensively investigated for CO_2 capture in IGCC systems (Doctor *et al.,* 1994; Griffiths and Scott, 2003; Klara, 2007). Syngas that has undergone WGS would be sent to a physical or chemical absorption unit to remove CO_2 and other acid gases. In the physical absorption process, CO_2 is removed by dissolving CO_2 in a solvent. The current widely used physical solvents include liquid methanol, such as the Rectisol process, and a glycol solvent (dimethyl ether of polyethylene glycol), such as the Selexol process (Nexant, 2006; Klara, 2007). The glycol solvent process is estimated to be a better option with lower cost for IGCC

© Woodhead Publishing Limited, 2010

systems (Doctor *et al.,* 1994; Breckenridge *et al.*, 2000). The liquid methanol process is complex and needs refrigeration of solvents, which leads to higher cost. Furthermore, the power consumption for refrigeration leads to an energy penalty for the overall system (Korens *et al.*, 2002). The low operating temperature of the liquid methanol process results in a lower solvent circulation rate and lower net power requirement compared to the glycol solvent process. IGCC systems using a two-stage Selexol process for CO_2 capture have been evaluated by Klara (2007). Syngas from the WGS process is cooled and enters the first stage of the Selexol process to remove H_2S, and is then sent to the second stage to remove 95% of the CO_2 in syngas.

In chemical absorption methods, CO_2 is removed by reaction with a solution (Hiller *et al.,* 2006). A typical chemical solvent is methyl diethanol amine (MDEA) (Korens *et al.*, 2002). Chemical solvents have better performance than the physical solvents at low CO_2 partial pressure. Thus, chemical solvents may have a niche for air-blown IGCC plants, in which the CO_2 in syngas is diluted by N_2 and thus has a lower partial pressure than for oxygen-blown systems. The CO_2 partial pressure of the WGS shifted syngas in oxygen-blown IGCC plants is estimated to be 12–20 bar (Klara, 2007). Because the physical solvent solubility is proportional to CO_2 partial pressure (Hiller *et al.*, 2006), physical solvents may have better performance over chemical solvents for CO_2 capture in oxygen-blown IGCC plants. Chemical solvents require a large amount of heat for regeneration, whereas physical solvents can be partly stripped by pressure drop and low heat is needed (Hiller *et al.*, 2006).

3.3.2 Membrane separation

Different kinds of membranes have been used to separate CO_2 from other components of syngas, especially H_2. They include CO_2-selective membranes, such as polyvinylamine with the main permeate being CO_2, and H_2-selective membranes, such as polymer and ceramic membrane with the main permeate being H_2 (Kaldis *et al.*, 2004; Grainger and Hagg, 2008). The driving force for the membrane separation is pressure differential across a permeable membrane. High partial pressure of the permeate component in the syngas favors the separation process. Membrane separation can be used downstream of a WGS reactor and a sulfur removal process. A CO_2-selective membrane used downstream of the WGS and the sulfur removal unit is estimated to be capable of achieving greater than 85% CO_2 recovery at 95% purity (Grainger and Hagg, 2008). The total plant cost of an IGCC system with a CO_2-selective membrane (85% CO_2 recovery) is estimated to be about 15% higher than that with a two-stage Selexol process (90% CO_2 recovery) (Klara, 2007; Grainger and Hagg, 2008). The H_2 loss to the CO_2 product stream is higher in the membrane process than that in a Selexol

© Woodhead Publishing Limited, 2010

process, which leads to lower power output and thus higher cost. For the H_2-selective membrane, the permeated H_2 is produced at near-atmospheric pressure, which requires compression before it is sent to the gas turbine combustor and thus increases the overall power consumption (Kaldis *et al.*, 2004). Membrane technology is still in an early phase of development and is not yet commercialized.

3.3.3 Cryogenic separation

Cryogenic separation involves gas refrigeration so that the CO_2 can be liquefied and separated from other gases. The advantage is that this process produces a liquid CO_2 ready for transportation by pipeline for sequestration. The major disadvantage is the large amount of energy required for refrigeration (Burr and Lyddon, 2008).

3.4 Applicable emissions control technologies

In this section, the main emissions control technologies for coal IGCC plants are introduced, including particulate matter, mercury, and acid gas removal technologies.

3.4.1 Particulate matter removal

In IGCC systems, raw syngas typically has PM consisting of unreacted carbon and fly ash. The PM needs to be removed to avoid erosion or deposition problems for downstream equipment, such as damage to gas turbine blades (Oakey *et al.,* 2004). In Table 3.3, the main PM control methods used in current IGCC systems are listed, including wet scrubbing, cyclones, and candle filters. Wet scrubbing has been commercially used in the Polk plant (Tampa Electric, 2002).

In the wet scrubbing process, syngas contacts with water spray to remove most of the particles, hydrogen chloride (HCl), and NH_3. The syngas from the scrubber is saturated with water. The PM in the blowdown black water settles out, and the remaining water is referred to as gray water. Most of the gray water is recycled to the water scrubber (Tampa Electric, 2002). The PM removal efficiencies of wet scrubbing can reach 99.9% for particles over 2 μm and between 95 and 99% for particles over 1 μm (Rezaiyan and Cheremisinoff, 2005).

Cyclone filters are primarily used for removing bulk PM from gas streams. Syngas with PM enters a cyclone, which forces the PM to separate from the gas flow by centrifugal force. Cyclones have been used with fluidized-bed and entrained-flow gasifiers (Rezaiyan and Cheremisinoff, 2005). The char and other PM captured in cyclones can be recycled to

© Woodhead Publishing Limited, 2010

Table 3.3 Applications and characteristics of particulate matter (PM) removal technologies

Technology	Application in IGCC plants	Development status	Control efficiency	Operational characteristics
Wet scrubber	Tampa Polk Station, Wabash River Repowering, Nuon IGCC, ELCOGAS	Commercial	70 to > 99%	4 to 370°C
Cyclone	Nuon IGCC, ELCOGAS	Commercial	30 to 90% for PM_{10}, and 0 to 40% for $PM_{2.5}$	Ineffective with fine particles capture
Candle filter (ceramic or metallic)	Wabash River Repowering, Nuon IGCC, ELCOGAS	Demonstration	>99.9%	Inlet gas temperature should be 250 to 500°C
High-temperature fabric filter (Baghouse filter)	Some biomass gasification plants	Demonstration	99 to 99.9%	Gas needs to be cooled to below 300°C; tar needs to be removed to prevent tar condensation

Source: Tampa Electric (2002); Wabash River Energy Ltd. (2000); Korens *et al.* (2002); Rezaiyan and Cheremisinoff (2005); Rich *et al.* (2003).

gasifiers to improve carbon conversion. Cyclones are effective at removing larger particles, but ineffective at removing small particles. Therefore, in practice, cyclones are generally combined with other PM control methods, such as candle filters, wet scrubbing, or both (Wabash River Energy Ltd, 2000; Hannemann *et al.,* 2002).

Candle filters have been used for fine particle removal in IGCC plants, such as Wabash River, Buggenum, and ELCOGAS plants (Wabash River Energy Ltd, 2000; Scheibner and Wolters, 2002; Hannemann *et al.*, 2003). Candle filters can remove particles in the range 0.5–100 μm. Their design efficiency is typically greater than 99.9% (Wabash River Energy Ltd, 2000; Korens *et al.*, 2002). A candle filter consists of a filter vessel and porous ceramic or metal tubes ('candle elements') mounted in tube sheets. The syngas flows through the elements and the tubes. Candle filters are cleaned by periodically passing pulsing clean gas to discharge the PM from the outside walls. Candle filters are designed for hot and dry PM removal and thus are typically used with dry syngas cooling. The captured particles can be recycled directly to the gasifier. There is reduced process waste water generation compared to wet scrubbing.

© Woodhead Publishing Limited, 2010

Candle filters use ceramic or sintered metal as materials. Ceramic filters generally have lower availability than metallic filters because of candle breakage (Korens *et al*., 2002). Some IGCC plants have cyclones upstream to reduce the PM load on the candles. Downstream wet scrubbers are usually added as back-up in case candle breakage occurs. The Wabash River plant originally used ceramic candle filters and replaced them with metallic elements to avoid breakage problems (Korens *et al*., 2002).

Other PM control methods include baghouse filters. Baghouse filters have been used in some biomass-fueled gasification plants, but not yet in coal-fueled IGCC plants. Baghouse filters typically require inlet gas temperatures of less than 300°C (Rezaiyan and Cheremisinoff, 2005). This temperature constraint would require cooling of the syngas prior to the filtering, thereby leading to a penalty on plant thermal efficiency.

3.4.2 Mercury removal

Mercury is a hazardous air pollutant for which emission regulations have been developed in recent years. An activated carbon bed has been demonstrated for mercury removal at Eastman Chemical coal-to-chemicals gasification plant in Tennessee for over 20 years, with a removal efficiency of between 90 and 95% (Parsons, 2002; Denton, 2003). In the activated carbon bed, the carbon is impregnated with sulfur at a concentration of between 10 and 15 wt% (Parsons, 2002). Most of the mercury in the syngas is in elemental form. The elemental mercury reacts with the sulfur in the bed to form mercury sulfide (HgS). The HgS on the spent carbon is stable, and the best option currently available is to dispose of it. The spent carbon can also be incinerated and the mercury can be recovered by cooling and condensation. In a design study by Parsons (2002), an activated carbon bed located downstream of syngas cooling and upstream of acid gas removal would operate at a temperature of approximately 38°C, since low temperature is favored for a high level of mercury removal. A disadvantage of activated carbon is that it cannot be regenerated.

3.4.3 Acid gas removal

The principal goal of acid gas removal processes in current IGCC plants is to remove sulfur compounds from syngas. The currently applied sulfur removal technologies for IGCC plants include chemical solvents, physical solvents, or a mixture of both. The principal chemical solvents are aqueous amines, such as MDEA (Korens *et al*., 2002). The widely used physical solvents include methanol used in the Rectisol process and dimethyl ether of polyethylene glycol used in the Selexol processes (Weiss, 1998; Breckenridge *et al*., 2000). A widely used mixed chemical/physical process is Sulfinol,

© Woodhead Publishing Limited, 2010

Table 3.4 Applications and characteristics of acid gas removal technologies

Solvents	Application in IGCC plants	Operation condition	Removal efficiency	Sulfur in cleaned syngas	Comments
MDEA	Polk, Wabash River, ELCOGAS, Nakoso	About 40 to 120°C and ambient to intermediate pressure	> 98%	100 ppmv	COS removal is limited. A COS hydrolysis reactor needs to be used upstream
Selexol	Cool Water	0 to 40°C and > 20 bar	> 99%	10 to 15 ppmv	The COS solubility is low and a COS hydrolysis reactor may be required if high sulfur removal is required
Rectisol	Vresova	−10 to −70°C and > 20 bar	> 99.9%	0.1 ppmv	High solubility of COS and no COS hydrolysis reactor is needed, high cost because of refrigeration requirement
Sulfinol-D and Sulfinol-M	Buggenum	5 to 40°C and > 5 bar	> 98.5%	< 40 ppmv	Higher COS solubility than the amine solvent. An upstream COS hydrolysis unit is likely to be required if deep H_2S removal is required

Source: ENEA *et al.* (2005); Korens *et al.* (2002); Higman and van der Burgt (2003); de Kler (2007); Denton (2003); Breckenridge *et al.* (2000).

which uses a mixture of sulfolane (tetra-hydrothiophene dioxide) and an aqueous amine (Korens *et al.*, 2002). Major applications and characteristics of acid gas removal technologies used in IGCC plants are summarized in Table 3.4.

MDEA is widely used for acid gas removal in IGCC plants, such as Polk, Wabash River, ELCOGAS, and Nakoso (Ratafia-Brown *et al.,* 2002a; Ishibashi and Shinada, 2008). In an MDEA process, syngas and MDEA flow counter-currently in an absorber. Acid gas is removed by forming a loose chemical bond between acid gas components and the MDEA. The rich solvent loaded with acid gases is regenerated in a stripping tower by steam heating to release acid gases. The Polk plant uses a 25–50% water solution of MDEA to remove about 99% of H_2S from the syngas (Tampa Electric, 2002). Both CO_2 and H_2S react with MDEA and thus IGCC plants that

© Woodhead Publishing Limited, 2010

have high CO_2 levels in syngas might not be able to reduce syngas H_2S concentration below 100 ppm (Korens *et al*., 2002). The MDEA process generally has low capital cost compared to physical solvent processes when the syngas pressure is lower than 30 bar and if it is not necessary to achieve very high removal efficiency (Korens *et al*., 2002). However, it requires larger amounts of heat for regeneration as a chemical solvent, which reduces the overall system efficiency.

The Selexol process uses a physical solvent, a mixture of dimethyl ether of polyethylene glycol, to remove acid gases. This process was used in the Cool Water plant (Breckenridge *et al*., 2000; Ratafia-Brown *et al.,* 2002a). Acid gases are absorbed by the solvent at room temperature and at pressures of higher than 34 bar (Breckenridge *et al.,* 2000). The rich solvent is flashed or stripped by steam or clean syngas to release and recover the acid gases in a concentrated side stream. The sulfur level can be reduced to 10–15 ppmv (Korens *et al*., 2002).

The Rectisol is another process using a physical solvent, liquid methanol. Rectisol has been used globally for gas treating and is used in the Vresova coal-fueled IGCC plant (Korens *et al*., 2002; Luby and Susta, 2007). Sulfur and CO_2 compounds are typically absorbed by liquid methanol at approximately -10 to -70^{o}C at pressures higher than 20 bar (ENEA *et al.,* 2005). The acid gases concentration in cleaned syngas can reach very low levels and thus this process is widely used for systems that require high-efficiency sulfur removal (Korens *et al*., 2002).

Compared to chemical solvents, physical solvents have higher loading capacity for acid gas at high acid gas partial pressure, higher selectivity for H_2S and COS over CO_2, more stability, and lower heat requirement for solvent regeneration (Korens *et al*., 2002). The MDEA or amine processes will not remove COS, and the Selexol process has low COS solubility. Therefore, a COS hydrolysis unit, which is used to convert COS to H_2S, is usually used upstream of the amine or Selexol process. The Rectisol process has high COS solubility and thus no COS hydrolysis reactor is needed (ENEA *et al.,* 2005). The major advantages of the Rectisol process include its ability to achieve very high sulfur removal in a single step, use of a readily available solvent, and flexibility in process configuration. However, it is more expensive than the amine or Selexol processes because of its complexity and refrigeration requirements (Korens *et al*., 2002; Denton, 2003).

The Sulfinol process is a combination process that uses a mixture of amines and a physical solvent (sulfolane). The Sulfinol solvents allow higher acid gas loading and lower energy requirement for regeneration than those of pure chemical solvents (Korens *et al*., 2002). Sulfinol-D uses diisopropanolamine (DIPA) and Sulfinol-M uses MDEA. When a high degree of H_2S selective removal is required, Sulfinol-M is used and it can produce a

© Woodhead Publishing Limited, 2010

treated gas with less than 40 ppmv sulfur (Korens *et al.*, 2002). Sulfinol-M has been used in the Buggenum plant (Hannemann *et al.,* 2002). Syngas flows counter-currently with the Sulfinol solvent in an absorber tower. The rich solvent-loaded acid gas enters a regenerator and is heated to discharge the acid gases.

3.4.4 Sulfur recovery and tail gas treatment

In most IGCC plants, the H_2S from the acid gas removal can be converted to elemental sulfur, or recovered as sulfuric acid. A typical elemental sulfur recovery technology is the Claus process, which has been used in Wabash River, Buggenum, and ELCOGAS plants (Wabash River Energy Ltd, 2000; Hannemann *et al.,* 2002; Hannemann *et al.,* 2003). One third of the H_2S in the acid gas stream is converted to sulfur dioxide SO_2 and water vapor in a furnace by partial oxidation with oxygen. The SO_2 reacts with the remaining H_2S to generate elemental sulfur and H_2O. A waste heat boiler is used to recover the heat from the hot exhaust stream to produce high-pressure steam. The sulfur is condensed and low-pressure steam is generated. The condensed sulfur is collected as a molten liquid to obtain high-purity by-product. The off-gas from the condenser goes to several catalytic conversion stages to recover the remaining sulfur. The overall sulfur recovery efficiency is greater than 98% in the Wabash River plant (Wabash River Energy Ltd, 2000). The sulfur recovery efficiencies of a Claus plant decrease with a decrease in the inlet H_2S concentration. If the H_2S content is lower than 15%, it will lead to unstable temperature in the furnace and results in low sulfur recovery efficiencies and high cost (Korens *et al.*, 2002).

A sulfuric acid by-product recovery process is used in the Polk plant (Tampa Electric, 2002). In the sulfuric acid plant, the H_2S is converted to SO_2 in a furnace under a vacuum condition. A waste heat boiler is used to cool the hot gas from the furnace and generate medium-pressure steam. The gas is further cooled and dried. The gas enters three stages of reactors. SO_2 in the gas is oxidized to sulfur trioxide (SO_3). The converted gas enters absorbing towers, where a strong sulfuric acid solution with 98% purity is used as the solvent to absorb SO_3 and the acid purity is increased to 98.5%. The sulfur recovery efficiency is over 99.5% at the Polk plant (Tampa Electric, 2002).

Tail gas treatment (TGT) is generally required when the sulfur recovery requirement is over 99.8%. A widely used TGT process is the Shell Claus off-gas treating (SCOT) process (Korens *et al.*, 2002). This process consists of a catalytic hydrogenation/hydrolysis step and an amine scrubbing unit. The tail gas from the Claus process is treated in a catalytic reactor to reduce the sulfur compounds, such as SO_2 and COS, to H_2S via hydrogenation or hydrolysis. The gas is cooled and enters an amine scrubbing unit. The acid gas-rich solution is regenerated in a stripping column. The treated tail gas

© Woodhead Publishing Limited, 2010

can be compressed and sent, with the clean fuel gas, to the combined cycle unit. The acid gas from the stripper is recycled back to the Claus plant for further conversion of the H_2S.

3.5 Advantages and limitations of coal IGCC plants

The major advantages and limitations of coal IGCC plants are described in this section.

3.5.1 Advantages of coal IGCC plants

The major advantages of IGCC plants include fuel flexibility, and the potential for high efficiency and low emissions (Ratafia-Brown *et al.*, 2002a; Nexant, 2006). If CO_2 capture is required, another potential advantage of IGCC plants is lower cost than PC plants.

The high temperature and high pressure of the gasification process mean that some low-value fuels, including petroleum coke, biomass, and municipal solid wastes, can be converted into syngas by gasification. The feedstock flexibility feature of IGCC reduces the dependence on a specific fuel for power generation and enables diversity of fuel sources.

The thermal efficiencies of IGCC plants range from 39 to 43%, which can be higher than those of conventional PC plants, which range from 35 to 42% (Breault, 2008). IGCC plants may have environmental advantages over conventional subcritical PC plants. For example, in a design study, the emissions of SO_2, NO_x, PM, and volatile organic compounds (VOCs) of an IGCC plant were estimated to be 41%, 67%, 48%, and 57% of the corresponding emissions from a subcritical PC plant, respectively (Nexant, 2006).

In Table 3.5, the performance, emissions, and costs of a generic IGCC plant are compared with a supercritical PC plant, both without and with CO_2 capture. For both cases, without and with CO_2 capture, the IGCC plant has higher efficiency. The IGCC plant also has lower emissions for NO_x, PM, Hg, and CO_2 on a net power output basis than those of the PC plant because of higher net plant efficiency and higher removal efficiencies. The mercury control efficiency for the IGCC plant is assumed to be 95% based on achievable removal efficiency in practice (Klara, 2007). For the bituminous coal fired PC plant, Hg control was assumed to be 90%, which is the mid-point of a range of observed efficiencies from 83.3 to 98% based on Hg co-capture in combination with a fabric filter and a wet flue gas desulfurization (FGD) scrubber (Klara, 2007).

For SO_2 emissions, the IGCC plant without CO_2 capture has a lower emission rate than the PC plant without CO_2 capture. The removal efficiency is assumed to be 99.7% for IGCC. FGD technology may be capable of reaching

© Woodhead Publishing Limited, 2010

Table 3.5 Comparison of generic integrated gasification combined cycle and pulverized coal power plants

Description	Integrated gasification combined cycle[a]		Pulverized coal (PC) power plants[b]	
Pollution control methods:[c]				
Sulfur control	Selexol/MDEA/Sulfinol		Wet FGD	
Nitrogen control	Nitrogen dilution		Low-NO_x burner and SCR	
Particulate control	Water scrubbing		Fabric filter	
Mercury removal	Activated carbon		Fabric filters and FGD	
CO_2 capture	2nd stage of Selexol		Amine	
Performance:[d]	Without CO_2 capture	With CO_2 capture	Without CO_2 capture	With CO_2 capture
Net power output, MWe	633	530	550	546
Efficiency, % HHV	39.5	32.1	39.1	27.2
Raw water usage, gallon/min	3850	4430	5440	10 440
Emissions:[e]				
SO_2 emissions, g/MWh	46.7	46.1	335	Negligible
NO_x emissions, g/MWh	225	234	277	398
Particulate matters (PM), g/MWh	27.9	34.4	51.2	73.9
Hg emissions, g/MWh	0.0022	0.0028	0.0045	0.0065
CO_2 emissions, kg/MWh	778	99	804	115
Cost (2007 US dollars):				
Total plant cost, $/kW	1840	2500	1570	2870
Cost of electricity, $/MWh[f]	78	106	63	115
Cost of CO_2 avoided, $/metric ton[g]		35		73

Note: [a]Entrained-flow gasifier-based IGCC: the data are based on average values from different cases.
[b]Supercritical PC.
[c]MDEA: methyl diethanol amine; Sulfinol: Sulfinol-M, mixture of sulfolane and MDEA; SCR: Selective catalytic reduction; FGD: Flue gas desulfurization.
[d]The design coal is Illinois No. 6: 10.91 wt% ash, 2.82 wt% sulfur, and 30 506 kJ/kg HHV (dry basis); HHV: higher heating value; For CO_2 capture cases, the nominal capture efficiency is assumed to be 90%.
[e]Based on net power output.
[f]The capacity factor is assumed to be 80% for IGCC and 85% for PC plants.
[g]The cost of CO_2 avoided is defined as the difference in the 20-year levelized cost-of-electricity between controlled and uncontrolled like cases, divided by the difference in CO_2 emissions in kg/MW h.
Source: Klara (2007).

over 99% SO_2 removal efficiency. A more reliably achievable SO_2 removal rate of 98% was assumed for the PC plant (Klara, 2007). For the CO_2 capture cases, the amine system used for CO_2 capture in the PC plant is estimated to absorb almost all SO_2, resulting in negligible emissions (Klara, 2007).

© Woodhead Publishing Limited, 2010

Comparing the cases without and with CO_2 capture, the net efficiency decreases about 7% on a relative basis for the IGCC plant, while it decreases about 12 % on a relative basis for PC plants. The IGCC plant uses a two-stage Selexol process for acid gas and CO_2 removal and PC plant uses an amine system for CO_2 removal. The auxiliary energy consumption is larger for the amine process than that for the physical solvent process. For the PC plant, there is higher auxiliary load for CO_2 compression compared to the IGCC plant because of the lower pressure of exhaust gas, compared to syngas, from which CO_2 is captured. The emissions of NO_x, PM, and Hg increase on a g/MW h basis when CO_2 capture is required because of the decrease in plant efficiencies. The SO_2 emission decreases because of additional sulfur removal in the CO_2 removal process.

The raw water usage of an IGCC plant is about 70% that of a supercritical PC plant for the no CO_2 capture case and it is 42% for the CO_2 capture case. IGCC plants use both gas turbines and steam turbines for power generation, whereas PC plants use only steam turbines for all power generation and thus have larger raw water usage for cooling tower water make-up. The biggest water demand for power plants is the cooling tower make-up, which is 84–91% of the total raw water usage for IGCC plants and about 90% for PC plants (Nexant, 2006; Klara, 2007). Other water usages for IGCC plants include slurry water if gasifiers are slurry-feed, PM scrubbing, and boiler make-up. These water usages are a small percentage of the total raw water usage. With CO_2 capture, the average raw water usage for both IGCC and PC plants increases, as shown in Table 3.5. The primary reason for the IGCC plant is the water usage required by the WGS reaction. For the PC plant, the large increase in water usage results from the cooling water demand in the amine process used for CO_2 capture (Klara, 2007).

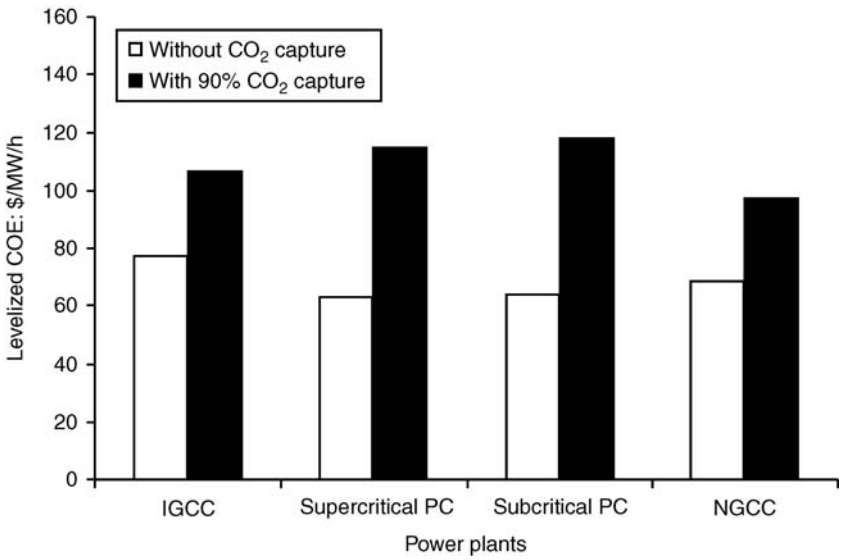
IGCC plants have less solid waste for disposal compared to PC plants (Nexant, 2006). For a non-slagging gasifier-based IGCC plant, fly ash would be captured and recycled to the gasifier to improve carbon conversion and thus less solid waste is produced (Rezaiyan and Cheremisinoff, 2005). For a slagging gasifier-based plant, the largest solid waste generated is slag, which is typically a glass-like material and can be a marketable by-product for cement production as demonstrated in the Tampa plant (Ratafia-Brown *et al.,* 2002a). The measured leaching for slags from moving-bed and entrained-flow gasifiers ranges from <0.001 to about 2 mg/l, while the leachates of the solid residue from a PC combustor range from <0.3 to about 600 mg/l (Pflughoeft-Hassett, 1997; Armesto and Merino, 1999). IGCC slag is less leachable than PC combustion bottom ash and, therefore, is expected to have less harmful environmental impacts when disposed in a landfill.

IGCC plants have cost advantage for Hg control from syngas compared to conventional PC plants because of the higher pressure and thus lower

© Woodhead Publishing Limited, 2010

volume of syngas, which reduces the Hg removal equipment size and cost. The cost of using an activated carbon bed for syngas Hg removal in an IGCC plant is only about 9% of that in a PC plant for flue gas Hg removal (Parsons, 2002).

Although IGCC plants are estimated to have higher cost than PC plants when no CO_2 capture is required, IGCC systems are estimated to have lower cost when CO_2 capture is required, as shown in Table 3.5 (Nexant, 2006; Klara, 2007). The total plant cost of the IGCC plant is estimated to be 87% of a PC plant with CO_2 capture. CO_2 removal in the IGCC plant occurs for the high-pressure syngas prior to combustion. Hence, CO_2 removal takes place for a much higher CO_2 concentration and a lower volumetric flow rate for the syngas in an IGCC system compared to the flue gas from a PC power plant. In Fig. 3.3, the levelized cost of electricity (COE) for IGCC, subcritical and supercritical PC, and natural gas combined cycle (NGCC) are compared. The levelized COE is the cost of a power plant over its lifetime levelized over a 20 year period to an annual payment and then divided by the plant annual energy output to yield a value expressed in $/MW h (Klara, 2007). CO_2 capture systems are estimated to increase the COE by approximately a 35% increase for a typical IGCC system, compared to an 80% increase for a typical PC plant, and a 40% increase for a typical NGCC plant (Klara, 2007).



3.3 Comparison of the estimated levelized cost of electricity (COE) for selected power plants technologies with and without CO_2 capture (IGCC, integrated gasification combined cycle; PC, pulverized coal; NGCC, natural gas combined cycle) (Source: data from Klara (2007)).

© Woodhead Publishing Limited, 2010

3.5.2 Limitations of coal-fueled IGCC plants

The limitations for IGCC technology include high cost when no CO_2 capture is required and low availability depending on the type of gasifier and whether spare gasifiers are included. In addition, because of less commercial experience, IGCC technologies have higher technical and economic risks compared to conventional PC technologies. If CO_2 capture is not needed, the levelized COE for an IGCC plant is estimated to be approximately 20% higher than that for a PC plant and 14% higher than that of an NGCC plant.

Availability refers to the percentage of a period of time for which a unit is in service or available for operation if called upon. The availability of currently operating IGCC plants is around 80%, whereas the availability of subcritical and supercritical PC plants can be greater than 90% (Tampa Electric, 2002; Nexant, 2006). In IGCC plants, the gasification block generally has lower availability than that of the combined cycle (Wabash River Energy Ltd, 2000; Tampa Electric, 2002). An IGCC system with two operating gasification trains and a spare gasification train is estimated to have availability above 90% (Bechtel *et al.,* 2003). Although adding spare equipment leads to an increase in capital cost, Kreutz *et al.* (2005) estimate that the economic benefit of the increase in the achievable capacity factor generally outweighs the increase in capital costs with adding a spare gasifier. For slagging gasifiers, conventional refractory materials lead to a relatively low gasifier availability because of the short life of materials. Improved refractory materials with longer life are being developed and field tested to attempt to improve the availability of slagging gasifiers (Powell, 2007).

3.6 Future trends

3.6.1 Trends in coal gasification

The development trends for coal gasification technologies are summarized with respect to coal feeding and gasification technologies. The trends in coal feeding technologies include the following.

- Pressure increase for dry-feed gasifier: for dry-feed entrained-flow gasifiers, the conventional lock hopper feed technology limits the operating pressure to about 40 bar (Maurstad, 2005). Dry-feed pumps to deliver coal at a higher pressure would enable an increase in dry-feed gasifier pressure and thus have benefits for reducing downstream equipment sizes and costs because of lower volume flow rate of syngas. An example of this technology is the GE Stamet solids feed pump (Parkes *et al.,* 2008).
- Coal/liquid CO_2 slurry-feed: liquid CO_2 has been suggested as a

© Woodhead Publishing Limited, 2010

potential candidate for the coal slurry-feed medium (Clayton *et al.,* 2002; Holt and Todd, 2003). Liquid CO_2 has a much lower heat of vaporization than water and is able to carry more coal per unit mass of fluid. Therefore, the liquid to be evaporated and the required heat for evaporating liquid CO_2 are both less than those for the water–coal slurry feeding. A liquid CO_2–coal slurry could enhance dispersion of coal particles in the gasifier and thus potentially improve the carbon conversion (Parkes *et al.,* 2008). For IGCC with CO_2 capture system, the option of using liquid CO_2–coal slurry may be technically feasible since a source of liquid CO_2 is available. The impacts of using CO_2 for slurry-feed medium on the CO_2 capture cost have not been evaluated.

The development trends in gasification technologies include the following.

- Higher gasification pressure: increasing gasification pressure would reduce the reactor vessel size for a given capacity and improve the performance of physical solvents for CO_2 capture since physical solvent solubility is proportional to CO_2 partial pressure.
- Quench design for CO_2 capture: for CO_2 capture, quench cooling provides an economic way of providing moisture to sygnas for the WGS reaction. It reduces or avoids the need for steam extraction from the steam cycle and also eliminates the need for an expensive syngas cooler. Although quench cooling, compared to use of a heat exchanger for syngas cooling, leads to lower plant efficiency for IGCC plants that do not have carbon capture, it could lead to a slight efficiency advantage for plants with CO_2 capture (Klara, 2007). A high-pressure quench design has been provided by GE in some gasification plants, such as the 70 bar high-pressure GE gasifiers used in the asphalt-fueled ISAB Energy IGCC plant in Italy (Collodi and Brkic, 2003). Shell is offering a commercial partial water quench design for Shell coal gasification (Holt, 2006). ConocoPhillips has indicated that more water would be sent to the second stage of the gasifier for CO_2 capture application (Parkes *et al.,* 2008).
- Material development for the refractory lining of slagging gasifiers: because of thermal fatigue and flow of slag, the refractory lining of slagging gasifiers has a short life, which may be no more than three months. To address this issue, phosphate-modified high-chrome oxide refractory material has been developed with a goal of increasing gasifier availability to 90% (Powell, 2007; Breault, 2008).
- Warm and hot gas clean-up: warm gas clean-up refers to syngas cleaning at temperatures between 250 and 500°C (Higman and van der Burgt, 2003). Hot gas clean-up would be at higher temperatures. Warm or hot gas clean-up could reduce the energy penalty introduced by syngas cooling that is required by current 'cold gas clean-up' acid gas removal

© Woodhead Publishing Limited, 2010

processes, such as scrubbing and solvent-based processes. For example, Research Triangle Institute (RTI) and Eastman have conducted pilot-scale testing of a desulfurization process using ZnO sorbent and operating temperature between 315 and 760°C, a direct sulfur recovery process at 500–600°C, and a multi-contaminant control system to remove NH_3 and other trace metals at 200°C (Gupta *et al.,* 2008).

3.6.2 Trends in CO_2 capture

For CO_2 pre-combustion capture in IGCC plants, trends in technology development mainly include physical solvents, membranes, sorbents, and chemical looping gasification.

- Physical solvents: because of the relatively high CO_2 partial pressure in syngas, physical solvents can be used to separate CO_2 from the syngas. The research and development trends include developing solvents that can operate at higher temperature in order to reduce energy loss associated with syngas cooling, improving selectivity to reduce H_2 losses, and increasing CO_2 recovery pressure (Figueroa *et al.,* 2008).
- Membranes: membrane improvements include better thermal stability at warm temperature, more tolerance to sulfur, and decrease in membrane thickness (Figueroa *et al.,* 2008). Several innovative membranes have been developed, such as the Eltron H_2 membrane, which has been tested at a small scale at 0.68 kg/day H_2 separation (Breault, 2008).
- Sorbents: currently, solid sorbents are under development, which can absorb CO_2 and be regenerated. RTI have developed a lithium silicate-based sorbent for CO_2 removal from syngas at temperatures of 250–500°C and pressures of 20–40 bar. Bench-scale testing of this sorbent has shown a CO_2 removal efficiency of more than 90% at syngas conditions (Figueroa *et al.,* 2008; Gupta *et al.,* 2008).
- Chemical looping gasification: a chemical looping gasification system includes two or three solid particle loops. A loop is used to gasify coal with O_2 supplied by a solid O_2 carrier in the loop. Another loop is used to capture CO_2 by water–gas shift reaction and circulating solids sorbents. The third loop is used to drive off CO_2 for compression and sequestration. Bench and pilot scale testing is being conducted for this technology (Figueroa *et al.*, 2008).

3.6.3 Trends in gas turbine technologies

A common goal in the gas turbine community is to achieve higher efficiencies for gas turbine simple and combined cycles. The typical approaches to increasing gas turbine efficiency are to increase the pressure

© Woodhead Publishing Limited, 2010

Table 3.6 Major specifications of F, G, and H class gas turbines

	F class	G class	H class
Firing temperature (°C)	1250 to 1350	1400 to 1500	1430 to 1500
Exhaust temperature (°C)	580 to 600	590 to > 600	590 to 625
Pressure ratio	15 to 17	18 to 21	19 to 25
Mass flow, kg/s	625 to 650 (50 Hz) 430 to 450 (60 Hz)	750 (50 Hz) 580 (60 Hz)	685 to 820 (50 Hz) 560 (60 Hz)
Turbine blade cooling method	Air cooling	Combined steam–air cooling	Combined steam–air cooling or air cooling
Simple cycle capacity (MW)	230 to 300 (50 Hz) 150 to 185 (60 Hz)	270 to 330 (50 Hz) 250 to 260 (60 Hz)	280 to 350 (50 Hz) 270 (60 Hz)
Simple cycle efficiency (% LHV basis)	35 to 38.5	n/a	n/a
Combined cycle capacity (MW)	340 to 410 (50 Hz) 230 to 280 (60 Hz)	400 to 490 (50 Hz) 370 (60 Hz)	480 to 530 (50 Hz) 400 (60 Hz)
Combined cycle efficiency (% LHV basis)	54 to 58	58 to 59.5	60
NO_x emissions, (ppmv)	9 to 25	25	9 to 25

Note: LHV = lower heating value.
Source: Lebedev and Kostennikov (2008); Matta *et al.* (2000); Grace (2007); Kalyanaraman (2007); Gas Turbine World (2002).

ratio and the turbine inlet temperature. In addition, the use of intercoolers for compressors can enhance efficiency. The limitations to increasing efficiency include trade-offs with the cost and the need for erosion and corrosion-resistant materials that have long life at high temperature. In current practice, state-of-the-art gas turbine technologies include the 'F', 'G', and 'H' classes. The specifications of each of these classes are given in Table 3.6. Gas turbines are typically designed for operation with natural gas, since this is the main market for gas turbine power generation worldwide. Hence, these classes of gas turbines are optimized for natural gas.

F class gas turbines operate at pressure ratios of 15–17 and turbine inlet temperatures as high at 1350°C, and can achieve combined cycle efficiency as high as 58 % (on a lower heating value basis). F class gas turbines use air as the medium for cooling of turbine blades and stators that are in the 'hot gas flow path', which typically is the first and second stages of the expander. With advances in manufacturing methods, these blades can be formed as a single crystal, which enhances their longevity compared to prior generations of gas turbines when operated in a high-temperature environment as part of a rotating machine.

The G and H class gas turbines differ from the F class primarily in that they use more advanced hot gas path cooling designs that include the use of steam,

© Woodhead Publishing Limited, 2010

or combinations of steam and air, rather than only air. Steam–air cooling features a closed-loop steam cooling used for the combustor can and for the turbine stators and rotors that are in the hot gas path of the first two stages of the expander, and air cooling for the other stages (Matta *et al.,* 2000). The improved heat transfer capabilities of steam cooling enable operation at higher turbine inlet temperatures and thus improve the thermal efficiency of gas turbines (Lebedev and Kostennikov, 2008). In addition, these classes have higher pressure ratios than the F class. G and H class gas turbines have about 60% combined cycle efficiency, and a combined cycle capacity of approximately 400 MW (Matta *et al.,* 2000; Grace, 2007; Kalyanaraman, 2007; Lebedev and Kostennikov, 2008). A study by Zhu and Frey (2006) estimated that the net plant efficiency and power output of an IGCC system with an H class gas turbine are 11% and 46% higher on a relative basis than those of an IGCC system with an F class gas turbine, respectively.

The major development trend in turbine blade materials is the use of high-temperature materials and coatings, such as turbine blades composed of single crystal materials. Increased firing temperatures with higher pressure ratio leads to higher efficiency but poses material and coating challenges. To maintain the durability for long-term service, thermal barrier coating, chromium steel for discs, and single crystal materials for blades and vanes could be used to increase the allowable material temperature (Lebedev and Kostennikov, 2008).

3.7 Sources of further information

The US Department of Energy, National Energy Technology Laboratory, Gasification Technologies Program: http://www.netl.doe.gov/technologies/coalpower/gasification/

The International Energy Agency Clean Coal Centre: http://www.iea-coal.org.uk/site/ieacoal_old/home

The International Energy Agency Greenhouse Gas R&D Programme (IEA GHG): http://www.ieagreen.org.uk/aims.html

Gasification Technologies Council: http://www.gasification.org/

3.8 References

Amelio M, Morrone P, Gallucci F and Basile A (2007), 'Integrated gasification gas combined cycle plant with membrane reactors: Technological and economical analysis', *Energy Conversion and Management*, 48(10), 2680–2693 doi:10.1016/j.enconman.2007.04.023.

Armesto L and Merino J L (1999), 'Characterization of some coal combustion solid residues', *Fuel*, 78, 613–618, doi:10.1016/S0016-2361(98)00164-1.

Bechtel, Global Energy, and Nexant (2003), *Gasification Plant Cost and Performance Optimization*, Final report DE-AC26-99FT40342, Prepared for US

© Woodhead Publishing Limited, 2010

Department of Energy, National Energy Technology Laboratory, Pittsburgh, PA, September 2003.

Bracht M, Alderliesten P T, Kloster R, Pruschek R, Haupt G, Xue E, Ross J R H, Koukou M K and Papayannakos N (1997), 'Water gas shift membrane reactor for CO_2 control in IGCC systems: techno-economic feasibility study', *Energy Conversion and Management*, 38 (Suppl.), S159–S164, doi: 10.1016/S0196-8904 (96)00263-4.

Breault R W (2008), 'DOE's gasification program overview', Presented at *Future of Coal in Pennsylvania: A Dialogue*, Clean Air Council, Harrisburg, PA, 24 April 2008.

Breckenridge W, Holiday A, Ong J and Sharp C (2000), 'Use of Selexol process in coke gasification to ammonia project', Presented at *Laurance Reid Gas Conditioning Conference*, Norman, Oklahoma, 27 February–1 March 2000.

Brooks F J (2000), 'GE gas turbine performance characteristics', GER-3567H, GE Power Systems, Schenectady, New York.

Brown P, Fadok J and Chan P (2007), 'Siemens gas turbine H_2 combustion technology for low carbon IGCC', Presented at *2007 Gasification Technologies Conference*, San Francisco, California, USA, 14–17 October 2007.

Brun K, Jones R M and Shilling N Z (2002), 'The IGCC process: from opportunity fuel to clean electric power', Presented at *5th European Gasification Conference*, Noordwijk, The Netherlands, 8–10 April 2002.

Burr B and Lyddon L (2008), 'A comparison of physical solvents for acid gas removal', Presented at *Gas Processors Association 87th Annual Conference*, Grapevine, TX, 2–5 March 2008.

Chiesa P, Consonni S, Kreutz T and Williams R (2005a), 'Co-production of hydrogen, electricity and CO_2 from coal with commercially ready technology. Part A: Performance and emissions', *International Journal of Hydrogen Energy*, 30, 747–767, doi:10.1016/j.ijhydene.2004.08.001.

Chiesa P, Lozza G and Mazzocchi L (2005b), 'Using hydrogen as gas turbine fuel', *Journal of Engineering for Gas Turbines and Power*, 127(1), 73–80, doi:10.1115/ 1.1787513.

Clayton S J, Stiegel G J and Wimer J G (2002), 'US DOE's perspective on long-term market trends and R&D needs in gasification', Presented at *5th European Gasification Conference*, Noordwijk, The Netherlands, 8–10 April 2002.

Collodi G and Brkic D (2003), 'The experience of snamprogetti's four gasification projects for over 3000 MWth', Presented at *2003 Gasification Technologies Conference*, San Francisco, California, 12–15 October 2003.

de Kler R (2007), 'Nuon's Magnum plant: a step towards sustainability,' *Modern Power Systems*, 1 April 2002 (URL: http://www.modernpowersystems.com/ story.asp?sectionCode = 88&story Code = 2045630).

delaMora J A, Grisso J R, Klumpe H W, Musso A, Roszkowski T R, Thompson B H, Lienhard H and Beyer T (1985), *Evaluation of the British Gas Corporation/ Lurgi Slagging Gasifier in Gasification-Combined-Cycle Power Generation*, EPRI AP-3980, Prepared by Ralph M. Parsons Company, British Gas Corporation, and Lurgi GMBH for Electric Power Research Institute, Palo Alto, California.

Denton D L (2003), 'Coal gasification – today's technology of choice and

© Woodhead Publishing Limited, 2010

tomorrow's bright promise', Presented at *AIChE – Eastern Tennessee Section*, 29 October 2003.

Doctor R D, Molburg J C, Thimmapuram P R, Berry G F and Livengood C D (1994), *Gasification Combined Cycle: Carbon Dioxide Recovery, Transport, and Disposal*, ANL/ESD-24, Prepared by Argonne National Laboratory for the United States Department of Energy, Morgantown, West Virginia.

Energy Information Administration (2008), *International Energy Outlook 2008*, DOE/EIA-0484(2008), Ch. 1, World energy demand and economic outlook (URL: http://www.eia.doe.gov/oiaf/ieo/world.html).

ENEA, ISI, and Risø (2005), *Hydrogen Pre-Feasibility Study*, EUR 21512 EN, Final report, Prepared for European Commission, DG Joint Research Centre, Institute for Energy and Institute for Prospective Technological Studies.

Figueroa J D, Fout T, Plasynski S, McIlvried H and Srivastava R D (2008), 'Advances in CO_2 capture technology – The US Department of Energys carbon sequestration program', *International Journal of Greenhouse Gas Control*, 2(1), 9–20, doi:10.1016/S1750-5836(07)00094-1.

Frey H C and Akunuri N V (2001), *Probabilistic Modeling and Evaluation of the Performance, Emissions, and Cost of Texaco Gasifier-based Integrated Gasification Combined Cycle Systems using ASPEN*, Prepared by North Carolina State University for Carnegie Mellon University and US Department of Energy, Pittsburgh, PA.

FutureGen Alliance (2007), FutureGen Fact Sheet, 7 June 2007, (URL: http://www.futuregenalliance.org/publications/fg_factsheet_7_final.pdf).

Gas Turbine World (2002), *Gas Turbine World 2000–2001 Handbook*, Vol. 21, Pequot Publishing, Southport, CT.

Grace D (2007), *Design Evolution, Durability and Reliability of Mitsubishi Heavy Industries Heavy Duty Combustion Turbines*, Pedigree Matrices, Vol. 7, 1012715, Technical Update, Electric Power Research Institute, Palo Alto, California.

Grainger D and Hagg M (2008), 'Techno-economic evaluation of a PVAm CO_2-selective membrane in an IGCC power plant with CO_2 capture', *Fuel*, 87, 14–24, doi:10.1016/j.fuel.2007.03.042.

Griffiths J and Scott S (2003), 'Evaluation of options for adding CO_2 capture to ChevronTexaco IGCC', Presented at *2003 Gasification Technology Conference*, San Francisco, California, USA, 12–15 October 2003.

Gupta R, Turk B, Lesemann M, Schlather J and Denton D. (2008), 'Status of RTI/Eastman warm gas clean-up technology and commercialization plans', Presented at *2008 Gasification Technologies Conference*, Washington, DC, 8 October 2008.

Hannemann F, Schiffers U, Karg J and Kanaar M, (2002), 'V94.2 Buggenum experience and improved concepts for syngas applications', Presented at *2002 Gasification Technologies Conference*, San Francisco, California, USA, 27 – 30 October 2002.

Hannemann F, Koestlin B, Zimmermann G, Morehead H and Peña F G (2003), 'Pushing forward IGCC technology at siemens', Presented at *2003 Gasification Technologies Conference*, San Francisco, California, USA, 12–15 October 2003.

© Woodhead Publishing Limited, 2010

Higman C (2008), 'European coal gasification projects', Presented at *FutureGen Workshop*, Tokyo, Japan, 25 February 2008.

Higman C and van der Burgt M (2003), *Gasification*. Gulf Professional Publishing (Elsevier): New York.

Hiller H, Reimert R, Marschner F, Renner H, Boll W, Supp E, Brejc M, Liebner W, Schaub G, Hochgesand G, Higman C, Kalteier P, Müller W, Kriebel M and Schlicht H (2006), 'Gas production', in *Ullmann's Encyclopedia of Industrial Chemistry*, 7th edition, Wiley–VCH, Weinheim, doi: 10.1002/14356007.a12_169.pub2.

Holt N (2003), 'Operation experience and improvement opportunities for coal-based IGCC plants', *Materials at High Temperatures*, 20(1), 1–6, doi: 10.3184/096034003782749198.

Holt N (2004), 'Gasification process selection – trade-offs and ironies', Presented at *2004 Gasification Technologies Conference*, Washington, DC, 4–6 October 2004.

Holt N (2006), 'IGCC and gasification for a changing marketplace', Presented at *2006 Gasification Technologies Conference*, Washington, DC, 1–4 October 2006.

Holt N and Todd D (2003), 'Summary of recent IGCC studies of CO_2 capture for sequestration', Presented at *2003 Gasification Technologies Conference*, San Francisco, CA, 14 October 2003.

Ishibashi Y and Shinada O (2008), 'First year operation results of CCP's Nakoso 250MW air-blown IGCC demonstration plant', Presented at *2008 Gasification Technologies Conference* Washington, DC, 7 October 2008.

Kaldis S P, Skodras G and Sakellaropoulos G P (2004), 'Energy and capital cost analysis of CO_2 capture in coal IGCC processes via gas separation membranes', *Fuel Processing Technology*, 85, 337–346, doi: 10.1016/S0378-3820(03)00204-2.

Kalyanaraman K (2007), 'At 340 MW, a powerhouse', *Turbomachinery International*, July/August, 26–27.

Klara J M (2007), *Cost and Performance Baseline for Fossil Energy Plants*, Vol. 1, Bituminous Coal and Natural Gas to Electricity, Final report, DOE/NETL-2007/1281, Revision 1.

Korens N, Simbeck D R and Wilhelm D J (2002), *Process Screening Analysis of Alternative Gas Treating and Sulfur Removal for Gasification*, Prepared by SFA Pacific for the US Department of Energy, National Energy Technology Laboratory, Pittsburgh, PA.

Kreutz T, Williams R, Consonni S and Chiesa P (2005), 'Co-production of hydrogen, electricity and CO_2 from coal with commercially ready technology. Part B: Economic analysis', *International Journal of Hydrogen Energy*, 30 (7), 769–784, doi:10.1016/j.ijhydene.2004.08.001.

Lebedev A S and Kostennikov S V (2008), 'Trends in increasing gas-turbine units efficiency', *Thermal Engineering*, 55(6), 461–468, doi: 10.1134/S0040601508060037.

Luby P and Susta M R (2007), 'Exploring the many carbon capture options', *Power*, 151(4), 40–50.

Matta R K, Mercer G D and Tuthill R S (2000), *Power System for the 21st Century –*

© Woodhead Publishing Limited, 2010

'H' Gas Turbine Combined-Cycles, GER-3935B, GE Power Systems, Schenectady, New York.

Maurstad O (2005), *An Overview of Coal based Integrated Gasification Combined Cycle (IGCC) Technology*, MIT LFEE 2005-002 WP, Massachusetts Institute of Technology, Cambridge, MA.

Murai S and Fujioka Y (2008), 'Challenges to the carbon dioxide capture and Storage (CCS) technology', *IEEJ Transactions on Electrical and E*lectronic Engineering, 3(1), 37–42, doi:10.1002/tee.20231.

Nexant (2006), *Environmental Footprints and Costs of Coal-Based Integrated Gasification Combined Cycle and Pulverized Coal Technologies*, EPA-430/R-06/006, Prepared for the US Environmental Protection Agency, Office of Air and Radiation, Washington, DC.

Oakey J, Simms N and Kilgallon P (2004), 'Gas turbines: gas cleaning requirements for biomass-fired systems', *Materials Research*, 7(1), 17–25 doi: 10.1590/S1516-14392004000100004.

Parkes J, Maxson A and Wheeldon J (2008), *Advanced Coal Power Systems with CO_2 Capture: EPRI's Coal Fleet for Tomorrow Vision*, 1016877, Electric Power Research Institute, Palo Alto, CA.

Parsons (2002), *The Cost of Mercury Removal in an IGCC Plant*, Prepared for the US Department of Energy, National Energy Technology Laboratory, Pittsburgh, PA.

Pflughoeft-Hassett D F (1997), *IGCC and PFBC By-Products: Generation, Characteristics, and Management Practices*, Final report, 97-EERC-09-06, Prepared for Environmental Protection Agency, Office of Solid Waste, Arlington, VA.

Powell C (2007), *Improved Refractory Materials for Slagging Gasification Systems, R&D Facts*, The US Department of Energy, Office of Fossil Energy, National Energy Technology Laboratory, Albany, OR.

Ratafia-Brown J A, Manfredo L M, Hoffmann J W and Ramezan M (2002a), *Major Environmental Aspects of Gasification-based Power Generation Technologies*, Final report, prepared by Science Applications International Corporation for Gasification Technologies Program, US Department of Energy, Washington DC.

Ratafia-Brown J A, Manfredo L M, Hoffmann J W, Ramezan M and Stiegel G J (2002b), 'An environmental assessment of IGCC power systems', Presented at *19th Annual Pittsburgh Coal Conference*, Pittsburgh, PA, 23–27 September 2002.

Rezaiyan J and Cheremisinoff N P (2005), *Gasification Technology*, Taylor & Francis Group, Boca Raton, Florida.

Rich J W, Robert H, Choi G N, Hennekes R J, Heydenrich R, Hooper M and Radtke K (2003), 'WMPI–waste coal to clean liquid fuels', Presented at *2003 Gasification Technologies Conference*, San Francisco, California, 12–15 October 2003.

Scheibner B and Wolters C (2002), 'Schumacher hot gas filter long-term operating experience in the Nuon Power Buggenum IGCC power plant', *Proceedings of 5th International Symposium on Gas Cleaning at High Temperature*, 17–20 September 2002.

Shah M, Raybold T, Jamal A, Drnevich R, Bonaquist D and Jones R (2005), 'IGCC:

© Woodhead Publishing Limited, 2010

CO_2 capture ready?', Presented at *2005 Gasification Technologies Conference*, San Francisco, CA, 9–12 October 2005.

Simbeck D R, Dickenson R L, and Oliver E D (1983), *Coal Gasification Systems: A Guide to Status, Applications and Economics,* AP-3109, Prepared by Synthetic Fuel Associates, Inc. for Electric Power Research Institute, Palo Alto, California.

Tampa Electric (2002), *Tampa Electric Polk Power Station Integrated Gasification Combined Cycle Project*, Final technical report, DE-FC-21-91MC27363, Prepared for the US Department of Energy, Office of Fossil Energy, National Energy Technology Laboratory, Morgantown, West Virginia.

Todd D M and Battista R A (2000), 'Demonstrated applicability of hydrogen fuel for gas turbines', *Proceedings of the IChemE Gasification 4 Conference*, Noordwijk, The Netherlands.

Twigg M V (1997), *Catalyst Handbook,* 2nd edition, Manson Publishing, London.

US Environmental Protection Agency (2003), *Air Pollution Technology Fact Sheet, Selective Catalytic Reduction*, EPA-452/F-03-032, U S Environmental Protection Agency, Washington DC.

Wabash River Energy Ltd (2000), *Wabash River Coal Gasification Repowering Project*, Final technical report, Prepared for the US Department of Energy, Office of Fossil Energy, National Energy Technology Laboratory, Morgantown, West Virginia.

Weiss H (1998), 'Rectisol wash for purification of partial oxidation gases', *Gas Separation and Purification,* 2, 171–176.

Zhu Y and Frey H C (2006), 'Uncertainty analysis of integrated gasification combined cycle (IGCC) systems based on frame 7H versus 7F gas turbine', *Journal of Air and Waste Management Association,* 56, 1649–1661.

© Woodhead Publishing Limited, 2010

4

Improving thermal cycle efficiency in advanced power plants: water and steam chemistry and materials performance

B. DOOLEY, Structural Integrity Associates, Inc., USA;
R. SVOBODA, Svoboda Consulting, Switzerland

Abstract: The fundamental need for improved cycle efficiency of steam power plants will require an increase in steam temperatures and pressures from today's upper end of about 300 bar/600°C/620°C up to 378 bar/732°C/760°C. These plants will be equipped with once-through boilers running under stringent water/steam purity requirements, with oxidizing all-volatile treatment (AVT(O)) or oxygenated treatment (OT), condensate polishers and no copper alloys in the system. While the conditions in the lower temperature end are common to current power plants, conditions in the high temperature region, above 600°C, will require additional research.

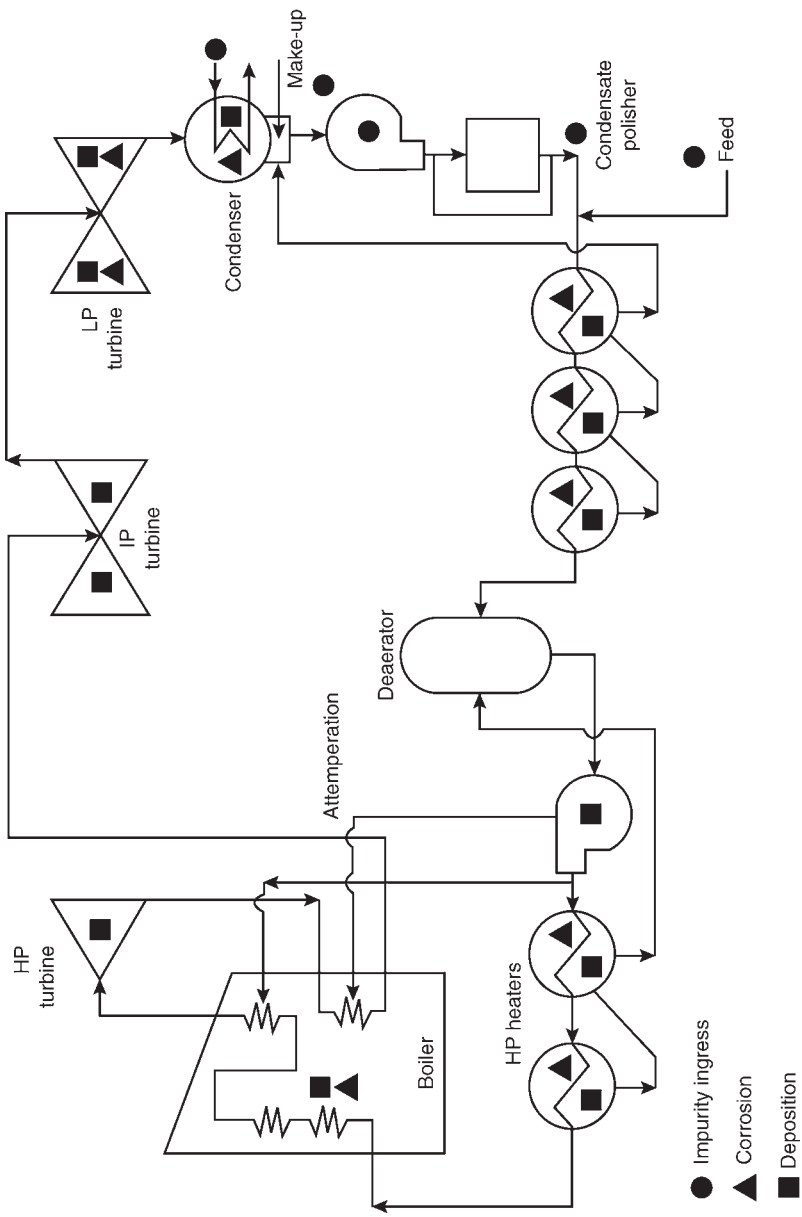
Key words: cycle chemistry, boilers, turbines, ultra-supercritical power plants.

4.1 Introduction

Conventional utility and industrial fossil plants can be divided into two main groups dependent on whether the boiler is a drum-type or once-through. Around the world, the drum-type unit is much more predominant. Supercritical plants, however, operate above the critical pressure of water, that is 22.06 MPa (IAPWS, 2007), thus evaporation will take place without a phase change and no water level equivalent to that in drum boilers will exist. Therefore, supercritical plants will be equipped only with once-through type boilers. Figure 4.1 shows a schematic diagram of a simplified fossil cycle with a once-through boiler, and also indicates the cycle locations where contaminant ingress, corrosion and deposition occur.

The cycle chemistry in any fossil plant has the major influence on the availability and reliability of the key components. For instance, 15 boiler

© Woodhead Publishing Limited, 2010



4.1 Common locations of contaminant ingress, corrosion, and deposition in a thermal cycle with once-through boiler.

© Woodhead Publishing Limited, 2010

tube failure mechanisms are influenced by the plant fluids (Dooley and McNaughton, 2007) with the major mechanisms being: hydrogen damage, caustic gouging, acid phosphate corrosion, corrosion fatigue and pitting. In the steam turbine, seven steam path mechanisms are influenced by the transport of impurities into the steam (McCloskey *et al*., 1999), with the major losses being attributed to L-1 blade failures due to corrosion fatigue and disc cracking due to stress corrosion. Deposition of impurities and oxides on to turbine blade surfaces can also result in marked turbine performance losses. Feedwater system availability and performance losses in many cases can also be attributed to the plant cycle chemistry, with the most dangerous one being flow-accelerated corrosion (Chexal *et al*., 1998).

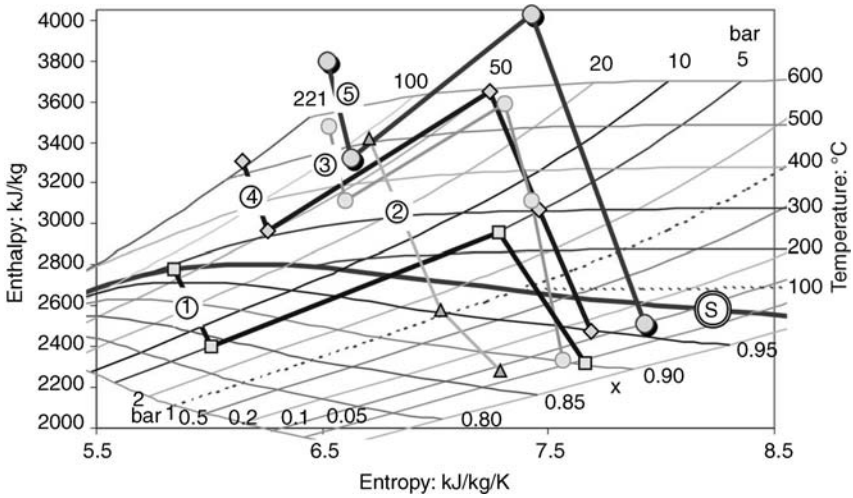
Thus it remains clear that the selection, optimization and maintenance of the treatment regimes establish the conditions for smooth, safe and economic operation of all fossil plants. The owners of plants usually control operation by comparison to guideline and action levels based on the guidance provided by organizations such as the International Association for the Properties of Water and Steam (IAPWS), the International Electrotechnical Commission (IEC), the Vereinigung der Grosskraftwerksbetreiber (VGB), the Electric Power Research Institute (EPRI) and the Central Research Institute of Electric Power Industry (CRIEPI).

4.2 Key characteristics of advanced thermal power cycles

The fundamental need for improved cycle efficiency will require an increase in steam temperatures and pressures. Available materials make cycles with steam conditions of 300 bar/600°C/620°C feasible in today's market. A number of material development programs in Europe and the US will enable higher primary steam temperatures, like the development of a cycle with steam conditions at 375 bar/700°C/720°C, or the US Department of Energy (DOE) program with even 378 bar/732°C/760°C and a predicted plant efficiency of approximately 60%. The boiler water walls will need to be constructed of tubes made of higher strength, corrosion-resistant martensitic steels. The high-pressure boiler outlet headers, piping, and the final stage of the superheater tubes will need to be fabricated of Ni-based alloys (Gabrielli and Schwevers, 2008). The materials of hot steam piping, valves, and the inlet parts of the high pressure (HP) and intermediate pressure (IP) turbines will also require an advancement of materials.

Optimal economy demands high operational flexibility from power plants, which in turn requires that the plants are suitable for a variable load program and two-shift operation (i.e. cycling operation). However, the

© Woodhead Publishing Limited, 2010



4.2 Mollier diagram with the turbine expansion curves for common types of power plants. (S = saturation line; 1 = boiling water reactor; 2 = cycle with no reheat; 3 = drum boiler cycle with reheat; 4 = supercritical once-through boiler cycle with single reheat; 5 = ultra-supercritical plant cycle. The points represent the inlet and outlet of the HP, IP and LP turbines respectively.)

requirement for daily cycling and/or two-shift operation can create undesirable thermal stresses in the steam turbine and boiler pressure parts components. These concerns can be minimized by adopting sliding pressure operation that significantly minimizes temperature differences in the boiler and steam turbine systems.

Figure 4.2 shows the steam expansion path in the turbine of various types of today's power plants on the Mollier diagram, as well as a possible advanced cycle with 378 bar/732°C/760°C cycle. Its steam expansion path has not yet been defined. It could be with a single reheat, as with the other examples, or also with double reheat. For Fig. 4.2, single reheat at a pressure of 80 bar was assumed. It is evident that the steam conditions at the boiler outlet (main steam, reheat steam) will be considerably above today's turbine steam conditions, but will inevitably end in conventional grounds when entering the final parts of expansion, that is in the outlet of the IP turbine and in the LP turbine. This means that the components in the water/steam cycle will on one hand have to deal with the chemistry-related issues that are already relevant to today's power plants, and on the other hand will also have to cope with issues that may come up with higher steam temperatures and pressures.

Materials performance will depend on the combined influence of materials properties, stresses, and chemical environment. The following

© Woodhead Publishing Limited, 2010

considerations will focus on the chemical environment and its consequences in supercritical power plants with a once-through steam generator.

4.3 Volatility, partitioning and solubility

4.3.1 Volatility and partitioning

In drum boiler units, the transfer of chemical species from boiler water to steam, such as conditioning agents and impurities, is on the one hand determined by the mechanical carry over (entrainment of droplets of boiler water into the steam), and on the other hand by its volatility. The quantity that can be dissolved in the boiler water and in steam is determined by the species' solubility. These effects have been described in detail by Dooley *et al*. (2004).

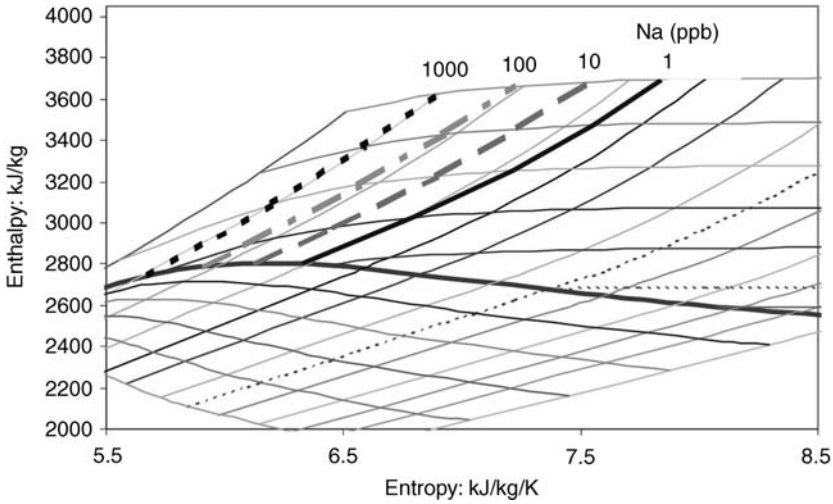
Relations are somewhat simpler with a once-through boiler, especially at supercritical conditions. As there is no phase change of water into steam, all chemical species are fully entrained from feedwater into steam. The key limiting factor will be the species' solubility, which determines under what conditions the species will not continue to stay in water or steam, but will deposit on component surfaces.

4.3.2 Solubility

The solubility of a species depends on its nature. Metal oxides may have a maximum of solubility in water at temperatures between 100 and 300°C, with decreasing solubility with higher temperature. For example, in NH_3 conditioned feedwater at $pH_{25°C} = 9.0$, magnetite has a maximum of solubility around 150°C (Sturla, 1973; Tremaine and LeBlanc, 1980), cupric and cuprous oxide around 250°C and 200°C respectively (Palmer and Bénézeth, 2004).

A wealth of data has been generated in the past 50 years on the solubility of species in steam, but as Harvey and Bellows (1997) point out, very few reliable data are available, particularly at low steam pressures, naming only those for NaCl and silica as being adequate. Figure 4.3 illustrates the solubility of NaCl in steam. It is seen that, with increasing steam pressure, the solubility of NaCl also increases. The background data summarized by Palmer and Bénézeth (2004) indicate that this trend is valid at least up to a steam density of 150 g/l (steam of 378 bar/760°C has a density of 86 g/l). It is therefore expected that such NaCl deposits in the hottest parts of an ultra-supercritical turbine are less likely than in turbines with more moderate steam conditions.

© Woodhead Publishing Limited, 2010



4.3 Solubility of NaCl in steam (Svoboda (2006) with data derived from Harvey and Bellows (1997)).

Generally, it can be said that deposits may develop preferentially in the feedwater train (heaters, valves, etc.), in the boiler, and in the conventional parts of the steam turbine. The turbine may, however, possibly suffer from deposits originating from the new boiler materials that may be transported into the turbine.

4.4 Deposits and corrosion in the thermal cycle of a power plant

This section contains information that also relates to subcritical plants. While evaporation in supercritical plants (no boiling, no phase transition) is different from subcritical plants, steam expansion and condensation are quite similar (Fig. 4.2). Therefore, processes in a supercritical boiler will in some respects differ from subcritical boilers, but effects in the turbine will be basically the same.

4.4.1 Deposits

Precipitation of impurities from the feedwater will occur when their solubility limits are reached, resulting in the deposition of oxides and other insoluble impurities. Deposits in the turbine are a consequence of precipitation from superheated steam once the solubility limits of the impurities are reached, at which point the deposition of mineral particles, acid, and caustic droplets occurs. Deposits may also occur when liquid films containing the impurities re-evaporate at some locations in the turbine.

© Woodhead Publishing Limited, 2010

Deposits in components of the steam water cycle are detrimental because they can result in the following.

- Heat transfer is hindered: this can lead to heat and efficiency losses, and may lead to overheating and failure of boiler tubes.
- Impaired functionality: examples are blocked movement of a valve by deposits on its stem, increased pressure drop across feedwater heaters that pushes the required capacity of the feedwater pumps over its limits, uneven fouling of flow distribution nozzles resulting in uneven water flow distribution in the boiler, and fouling of a steam turbine that reduces its steam swallowing capacity and can lead to reduced turbine output and efficiency.
- Under-deposit corrosion occurs: a special chemical environment may develop between the deposits and the base metal by concentration of impurities. Such effects can, for example, be present under boiling water conditions (which do not occur in supercritical plants), or be caused by electrochemical effects related to crevice corrosion.
- The deposits can be corrosive by themselves: examples are deposits of NaOH that can form a highly concentrated liquid phase at elevated temperatures (Lindsay, 1978) and cause corrosion attack in the HP or IP turbine (Svoboda and Bodmer, 2004), or NaCl deposits that cause pitting corrosion when the turbine is shut down under moist air. This will be discussed in more detail later in this chapter.

4.4.2 Corrosion in the boiler

As there is no phase transition and no boiling with the evaporation of feedwater in supercritical boilers, corrosive impurities will not attain high local concentrations as is the case in the boiling zone of subcritical boilers. The main focus of feedwater chemistry will therefore be the prevention of deposits by keeping the feedwater corrosion products down to very low levels at the economizer inlet.

According to current planning, these supercritical and ultra-supercritical boilers are being designed for sliding pressure operation in order to accommodate needs for a variable load and/or shift operation regime. Therefore, the waterwall tubes will experience all forms of heat transfer conditions from single-phase/supercritical type of heat transfer (no density differences or concentration occurring) to nucleate boiling as in drum boilers, dry-out as well as departure from nucleate boiling (DNB) regions. So all possible types of water-side corrosion mechanisms, as known in subcritical boilers, are possible. Even stress corrosion cracking could possibly be experienced with some of the materials being proposed for high temperature/high strength ferritic waterwall tubing.

© Woodhead Publishing Limited, 2010

The subcritical utility boiler-turbine cycle is subject to two basic types of corrosion damage. One type of corrosion is the general attack on ferritic materials during periods of adverse feedwater conditions such as high oxygen concentration in combination with dissolved contaminants, low pH, etc. This corrosion may take place during system operation as well as during shutdown. The second type of corrosion is caused by acid or alkaline contamination of the boiler water in the presence of deposited products, and occurs during system operation.

Deviations from recommended chemistry limits that result in either depressed or elevated pH values, promote failures of boiler tubing. These types of attack are accelerated by the presence of internal metal oxide deposits that permit soluble contaminants to concentrate during the process of steam generation or nucleate boiling. Supercritical units that do not operate on a sliding pressure mode are generally not susceptible to this corrosion mechanism since high contaminant concentrations are not produced in a single-phase fluid. Also, the presence of condensate polishers in the feedwater system prevents large amounts of soluble contaminants from entering the boiler.

Although there are many variations from a descriptive basis, the majority of these types of failures can be classified into one of the following two categories (Dooley and McNaughton, 2007).

1. Caustic gouging. This type of damage is normally characterized by irregular wastage of the tube metal beneath a porous deposit. It progresses to failure when the tube wall thins to a point where stress rupture occurs locally. In this process, the microstructure of the metal does not change and the tubing retains its ductility.
2. Hydrogen damage. This type of corrosion damage usually occurs beneath a relatively dense deposit. Although some wastage occurs, the tube normally fails by thick-edge fracture before the wall thickness is reduced to the point where stress rupture would occur. Hydrogen, produced in the corrosion reaction, diffuses through the underlying metal, producing decarburization and intergranular microfissuring of the structure. Brittle fracture occurs along the partially separated boundaries, and in many cases, an entire section is blown out from the affected tube.

Ductile attack is more probable when the boiler water contains highly soluble alkaline chemicals such as sodium hydroxide. Hydrogen damage, on the other hand, is more apt to occur when a low pH boiler water environment is produced as a result of condenser leakage (if it bypasses or leaks through the condensate demineralizer) or some other type of system contamination. It is recognized that the successful operation of a utility

© Woodhead Publishing Limited, 2010

once-through boiler unit with respect to water technology is coupled to the proper operation of the condensate demineralizer system.

In addition, of course, all types of boilers, including supercritical boilers are at risk of corrosion during shutdown, when no adequate conservation measures (shutdown or layup) have been taken.

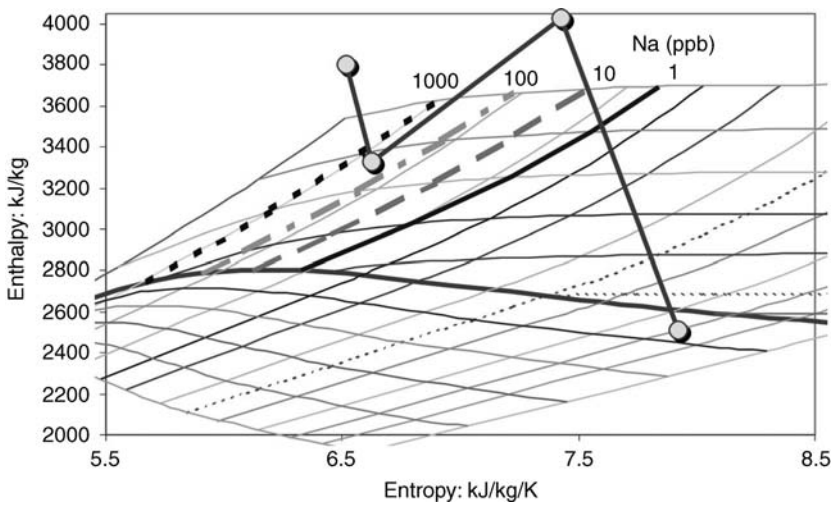
4.4.3 Corrosion in the steam turbine

Corrosion driven by deposits on the turbine surfaces

Once the solubility limit of a substance is surpassed, deposition will take place. This is typically the case when solubility decreases when the steam expands (Fig. 4.4). All dry parts of the steam turbine are affected. As long as these deposits are solid, no corrosion is expected. However, if the turbine is exposed to moist air during shutdown, hygroscopic salts will draw moisture and form a corrosive environment, which can initially cause pits on the turbine surfaces that eventually can cause severe damage to the turbine blades (Fig. 4.5).

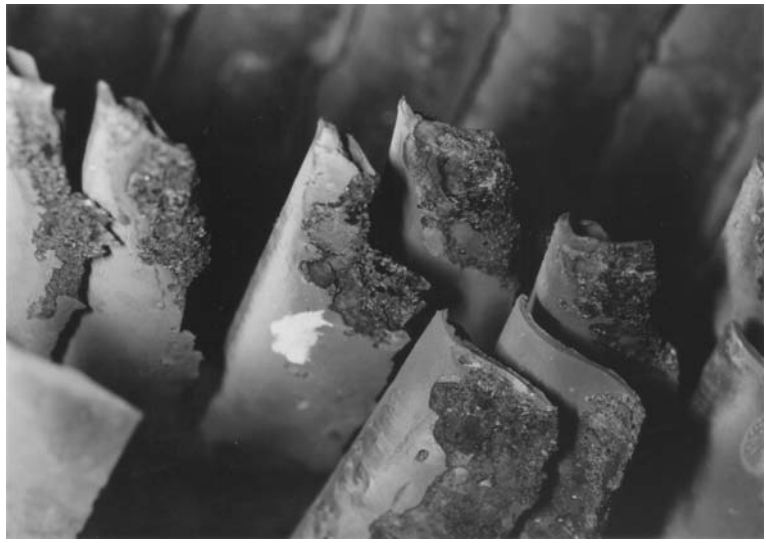
Liquid films in the superheated parts of the steam turbine

Certain species may melt at temperatures in the turbine (NaOH: melting point 323°C), or may already draw water at temperatures well above the



4.4 Expansion curve of a supercritical turbine and the solubility of Na (as NaCl) in the Mollier diagram. It is seen that with a few ppb of Na in steam, NaCl deposits can be expected in the later stages of the IP turbine and in the LP turbine.

© Woodhead Publishing Limited, 2010



4.5 Corrosion damage in a LP turbine. During operation NaCl was deposited from impure steam on to the blade. When the turbine was idle during shutdown, it was exposed to moist air, which together with the NaCl, caused the corrosion attack. This photograph is actually from a drum boiler unit; such attack on turbine blades would, however, be the same with supercritical boilers.

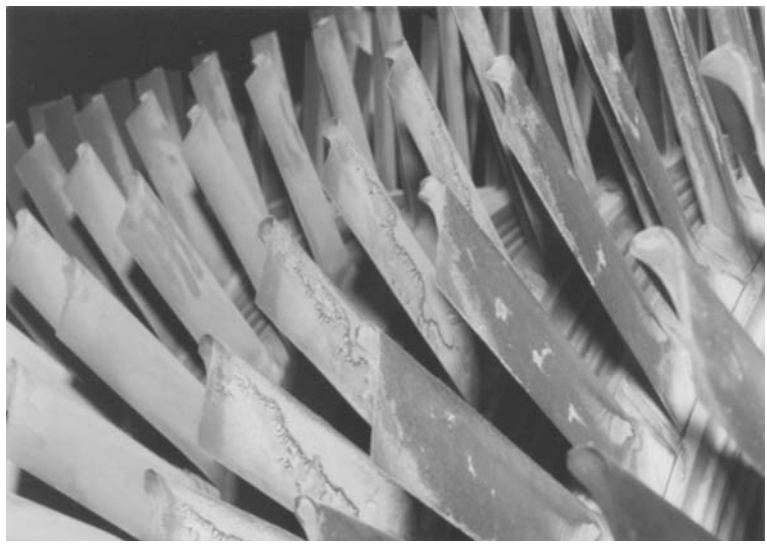
saturation line, causing the formation of an aqueous liquid film far in the still superheated region. An example is NaOH, which may form a highly concentrated (up to 90%) liquid film at steam temperatures above 300°C (Lindsay, 1978). Such a hot solution of NaOH is highly corrosive to certain materials, like austenitic stainless steels, or even to welding joints of unalloyed steel if not heat treated. Figures 4.6 and 4.7 illustrate footprints and effects of such liquid films.

Chemical environment in the phase transition zone

The phase transition zone (PTZ) in the turbine is the boundary between dry (superheated) steam and steam that already contains condensed water droplets (moist steam). It is closely related to the saturation line in the Mollier diagram, Fig. 4.2. Where condensation begins, species will partition into the liquid phase, according to their partitioning coefficients (Palmer *et al.*, 2004). As the quantities of water are still very low, the concentration may be very high, and can be either acidic or caustic, depending on the species' properties. This is similar to the effects responsible for acid rain.

When the turbine is operating, the chemical environment in susceptible

© Woodhead Publishing Limited, 2010



4.6 Deposits on an IP turbine. This figure shows the rotor of an IP turbine in a supercritical plant that had been subject to ingress of NaOH from the condensate polishers. After opening the turbine, the rotor had a thin white coloration, that intensified within the following few days and developed into the sodium carbonate deposit seen in the figure. The structure of the deposit indicates a dried-up liquid film. Condensation of a solid or a liquid would have given a less distinct geometric surface structure. Because of the large centrifugal forces at the turbine rotor, this film must have been very thin and, considering its residues, indicates a high concentration of caustic. It should be mentioned that no damage resulted from this incident (Svoboda and Bodmer, 2004).

locations in the PTZ consists of dynamic liquid films and deposition of salts, oxides, and impurities. There is no oxygen in the liquid films. However, when the turbine shuts down, most organizations do not provide any protective environment, and so the deposits become moist once the surfaces cool down, and cause passivity breakdown. Repetition of the operating/shutdown environments eventually leads to pits and then to microcracks. It is recognized that pitting can possibly also initiate during operation in crevice areas such as blade attachments. Only when the turbine is operating is the loading (cyclic or steady state) sufficient to drive the microcracks into corrosion fatigue or stress corrosion cracks. When the unit is operating again there are liquid films present, which provide the environment for the cracks to propagate. Thus advanced supercritical units must also have facilities to provide shutdown protection for the LP turbine PTZ. This is usually accomplished with dehumidified air.

© Woodhead Publishing Limited, 2010



4.7 Corrosion damage in an HP turbine. This figure shows the casing between the stationary blades near the outlet of a subcritical HP turbine, at approximately 350°C or some 80°C superheat. It can be seen that the unalloyed material had been washed out to more than 1 mm depth, leading to a failure of the seal strips. This shape of attack indicates the presence of a liquid during turbine operation. However, it is not clear if this was a highly concentrated aqueous solution or molten NaOH (Svoboda and Bodmer, 2004).

4.4.4 Corrosion of other components in the water/steam cycle

The other components in the water/steam cycle offer manifold possibilities where corrosion may occur, for example the condenser tubes, feedwater heaters, etc. (see also Fig. 4.1). Heitmann (1997) gave an overview on corrosion in such water/steam cycle components. Basically, there are no special requirements for an ultra-supercritical plant compared to normal supercritical plants plants in this part of the cycle. Additional aspects may, however, arise in relation to higher temperatures in some feedwater heaters, valves, and piping, possibly necessitating special conditions for feedwater treatment or other materials.

4.5 Water and steam chemistry in the thermal cycle with particular emphasis on supercritical and ultra-supercritical plant

The main objectives of water chemistry control are to ensure the long-term integrity of the materials of construction and the successful operation of the

© Woodhead Publishing Limited, 2010

boiler–turbine power cycle. The particular types of chemical treatment may vary depending on many factors such as the variety of materials, operating conditions, system design, etc.

Control of the chemistry in once-through steam generating units is based on the following features (Gabrielli and Schwevers, 2008):

- No phase separating devices (i.e. steam drum) in the system;
- Feedwater, boiler water, and steam are the same fluid stream;
- Sliding pressure operation includes fluid conditions typical of both supercritical and subcritical operation.

The above design considerations require that the concentrations of feedwater contaminants be kept to a minimum and be within allowable turbine steam purity limits (as specified by the steam turbine supplier) as the solubility of contaminants increases with higher steam parameters. Corrosion products transported to the boiler (or superheater/reheater/turbine) from the condensate and feedwater system must also be kept at low enough concentrations to minimize fouling of boiler tube and turbine surfaces, and thus the potential for damage and/or efficiency losses.

For once-through systems, feedwater conditioning to minimize general corrosion and the production of iron oxide can be accomplished with either oxidizing all-volatile treatment (AVT(O)) or oxygenated treatment (OT). Owing to the greater concern for copper transport at supercritical pressures and its impact on turbine performance, feedwater systems in these once-through units consist primarily of ferritic alloys and do not contain copper alloys downstream of the condensate polishers.

Controlling feedwater contaminants to a minimum is critical in once-through units, as there is no mechanism for their removal in the feedwater (downstream of the condensate polishing system) and their aggressive behavior cannot be arrested by the typical feedwater chemical treatments (OT or AVT). Contaminant ingress (from condenser in-leakage, make-up water, etc.) is generally controlled by a condensate polishing system.

The most frequent contributor to boiler waterside corrosion, fouling, and failures has been the accumulation of metal oxide deposits. These deposits form principally on heat transfer surfaces, but can also foul control orifices, which can then cause overheating of waterwall tubes.

A reduction in the amount of debris and metal oxide deposition within the boiler can be successfully accomplished throughout its life cycle by:

- good storage and on-site erection conditions;
- minimum metal oxide concentrations in the boiler feedwater during start-up operations as well as at load conditions;
- adherence to operational water chemistry guidelines;

© Woodhead Publishing Limited, 2010

- adherence to optimum layup procedures that prevent or reduce shutdown corrosion;
- periodic chemical cleanings.

Materials of construction most commonly used in the condensate and feedwater systems of once-through utility cycles are ferritic alloys, stainless steels, and titanium. Copper alloys are not used in feedwater heaters because copper oxides can dissolve in the supercritical fluid resulting in turbine fouling. Carbon and stainless steel tubes are therefore utilized in feedwater heaters and stainless steels and titanium are used for condenser tubes.

4.5.1 All-volatile treatment (AVT)

AVT is defined as the exclusive use of volatile conditioning agents. Volatile chemicals evaporate from the water into the steam in a gaseous form. When steam condenses, the chemicals dissolve into the water. They do not form a solid phase and thus they do not form a scale or deposit on heat transfer surfaces. Common volatile conditioning agents are ammonia, amines, and hydrazine (or hydrazine substitutes); however, reducing agents such as hydrazine would never be considered for use in a supercritical or ultra-supercritical plant.

With AVT, feedwater pH ranges from 8.8 to 9.8. Low-level AVT has a pH between 8.8 and 9.3 (especially in plants with copper alloys), and high-level AVT has a pH between 9.2 and 9.8. Even though high pH AVT provides better corrosion protection of steel, it has disadvantages, including questions of wastewater treatment, chemicals and consumption, and exclusion of ion exchange resin to run in H^+ form.

AVT (R) is defined as AVT that employs a reducing agent such as hydrazine or other oxygen scavengers. This results in a low (highly negative) electrochemical potential (ECP) or oxidation/reduction potential (ORP). Thus the highest possible oxidation state in the oxide layer is magnetite. It has the disadvantage of being more soluble than hematite, and forms thicker and more porous magnetite layers, resulting in a higher iron content in the water. Subsequently, ripples can be formed on waterwall deposits. This is beneficial in plants with copper heat exchangers in the feedwater train because it reduces copper corrosion and therefore the release of copper into the feedwater. In once-through systems, the cycle does not, however, include copper or its alloys. AVT (R) also favors flow-accelerated corrosion (FAC) in the high pressure feedwater system if it contains carbon steel alloys and therefore it is not used as a water treatment regime in the considered type of power plants.

AVT (O) is defined as AVT that does not employ a reducing agent, and therefore the ECP or ORP will be substantially higher (more positive) than

© Woodhead Publishing Limited, 2010

with AVT(R). AVT(O) favors the formation of hematite layers on top of the magnetite, which are less soluble and hence more stable than the magnetite layers that form under AVT(R). As a result, the oxide layer is thinner and denser, and provides a more protective margin against FAC, and minimizes orifice fouling.

4.5.2 Oxygenated treatment (OT)

OT involves adding only ammonia and oxygen to the feedwater to provide more oxidizing power to ensure that all carbon steel surfaces are passivated with hematite. OT will provide a high ECP or ORP that supports the formation of hematite layers, which are less soluble and hence more stable than either the magnetite layers of AVT(R) or the mixed magnetite/hematite layers of AVT(O). As a result, the level of iron oxide in the feedwater is much lower. It gives an excellent protective margin against FAC and minimizes orifice fouling.

As an additional bonus, this treatment has already been successfully used with very low-level AVT, i.e. feedwater pH 8.0–8.5. The related small ammonia concentrations permit a very long life of H^+ mixed beds, and ease wastewater questions. On the other hand, low feedwater pH enhances the risk of FAC in components that contain two-phase water and steam, in cases where they are not made of sufficiently resistant alloyed steel (min. 1.25% Cr). In particular, low pH OT should not be considered for plants with air-cooled condensers (Dooley *et al.*, 2009). Of course, OT can also be applied with higher pH levels up to 9.8.

OT is not without problems. Oxygen, when coupled with anions, will be corrosive. OT therefore requires a strict control of feedwater impurities, which means high performance and reliability of the condensate polishers. Operating guidelines around the world generally agree that a conductivity after cation exchange of <0.15 μS/cm is required.

4.5.3 Chemistry specifications for feedwater and steam

Tables 4.1 and 4.2 give key data on cycle chemistry specifications by VGB (2004) and EPRI (2002, 2005). It has to be acknowledged that there are a number of other such specifications on the same subject, e.g. specifications set up by other organizations or large utilities. These specifications are, however, mostly quite similar, and the specifications mentioned here can be considered as being typical.

It must also be mentioned that such specifications can never be fully condensed into a simple table. The full specifications contain additional data and conditions, as well as a wealth of other information, that also have to be taken into account when applying them in practice.

© Woodhead Publishing Limited, 2010

Table 4.1 VGB specifications for feedwater and steam. Cycle with once-through steam generator and all-ferrous metallurgy (simplified summary). Normal operation limits

Parameter	Unit	All-volatile treatment		Oxygenated treatment	
		Feedwater	Steam	Feedwater	Steam
pH	–	9.2–9.8		8.4–9.8	
Acid conductivity	µS/cm	< 0.20	< 0.20*	< 0.15	< 0.20*
Oxygen	µg/kg	2–100		30–150†	
Silica	µg/kg	< 20	< 20	< 20	< 20
Iron	µg/kg	< 10	< 20	< 10	< 20
Copper	µg/kg		< 3		< 3
Sodium	µg/kg	< 10	< 5	< 10	< 5
Chloride	µg/kg				
Sulfate	µg/kg				
TOC	µg/kg	‡		‡	

* Higher action values may be defined if the increase of acid conductivity can be attributed to CO_2 from air in-leakage and organic decomposition products can be excluded.
† Target values.
‡ To be determined for the specific case.

Table 4.2 EPRI specifications for feedwater and steam. Cycle with once-through steam generator and all-ferrous metallurgy (simplified summary). Normal operation limits

Parameter	Unit	All-volatile treatment		Oxygenated treatment	
		Feedwater	Steam	Feedwater	Steam
pH	–	9.2–9.6		8.0–8.5	
Acid conductivity	µS/cm	≤ 0.20*	≤ 0.20*	≤ 0.15*	≤ 0.15*
Oxygen	µg/kg	≤ 10*		30–150*	
Silica	µg/kg		≤ 10		≤ 10
Iron	µg/kg	≤ 2		≤ 2	
Copper	µg/kg	≤ 2		≤ 2	
Sodium	µg/kg		≤ 2*		≤ 2*
Chloride	µg/kg		≤ 2		≤ 2
Sulfate	µg/kg		≤ 2		≤ 2
TOC	µg/kg		≤ 100		≤ 100

* Core parameters.

© Woodhead Publishing Limited, 2010

4.6 Challenges for future ultra-supercritical power cycles

The following gives an outline of discussions made at the International Association for the Properties of Water and Steam (IAPWS, 2009) on extending the range of available water and steam property data in order to accommodate upcoming needs of the power industry.

The relevant chemical issues in future ultra-supercritical fossil-fired units will depend primarily on the properties of water and water plus additives/impurities under these extreme conditions, as well as the stability of the metal oxide layer formed on the walls of the containment alloy and its interfacial interactions with superheated steam (i.e. its mechanical and chemical stability, and the effect of solutes on the interface). The chemistry will most likely be very different from that experienced in existing supercritical units, and there are virtually no supporting experimental data on the properties of pure water or solutions in steam at these conditions. Even the stability of common alkalizing agents and the effect of impurities are uncertain.

The higher temperature and pressure regime corresponding to ultra-supercritical conditions imposes severe limitations on the currently known materials that can be considered for constructing such plants. A means of calculating these properties of water directly or by extrapolation, as well as ultimately measuring these fundamental properties, must be considered. The behavior of chemicals dissolved in this medium is difficult to predict as it is outside the experience of most chemists and chemical engineers, mainly because the solvent density is also significantly higher than experienced in supercritical units or in supercritical water oxidation applications.

4.6.1 Physical properties and thermodynamic properties of the solutions

The dielectric constant, viscosity, thermal conductivity, surface tension, and the ionic product of water in the ultra-supercritical region of interest for advanced power plants can be calculated or derived from existing data (IAPWS, 2009). Knowledge of the dielectric constant of steam over a range of condition (which include the conditions of ultra-supercritical plant operation) is important, especially for ionic species, because the behavior of dissolved impurities and treatment chemicals will depend strongly on the value of the dielectric constant. Computer simulations at present provide the most promising path for estimating the dielectric constant at these extreme conditions.

A point to be considered is the range/reliability of existing formulations, especially when ions are involved and the problem of extrapolation of

© Woodhead Publishing Limited, 2010

available formulations to higher temperature and higher density of water may be very important. The simulation study by Harvey and Mountain (2003) suggests the possibility of important changes in the hydration of ions at the conditions of operation. Their study extended only to 500°C and gas-like densities ($< 26\,kg/m^3$) and much higher temperatures may lessen ionic hydration, but this effect will be compensated to some extent at higher densities ($86.7\,kg/m^3$ for 760°C/38 MPa).

Consideration of the properties of solutions would be linked to such phenomena as: pH; ionic association of solutes; solubilities of impurities, e.g. Cl^-, SO_4^{2-}, Na^+, SiO_2, Ca^{2+}, CO_2; metal-containing species from the feedwater train and boiler; organic acids (although these would likely be decomposed to give principally CH_4/CO_2); corrosion products; and possible additives (NH_3, O_2).

4.6.2 Transport properties of the solutions

The diffusion of electrolytes and neutral species including O_2 is an important factor affecting corrosion. Very little information is presently available regarding diffusion coefficients at ultra-supercritical conditions. Nuclear magnetic resonance (NMR) spectroscopy could be used to determine diffusion coefficients in bench-scale experiments (Nakahara and Yoshimoto, 1995). The diffusion of O_2 and other neutral species to the walls of the tubes should be especially considered given the flow of steam that is possibly moving at supersonic velocities. It may be possible to carry out laboratory-scale measurements of the transport properties of additives and prototype solutes in the heat-transporting fluid by means of cells fitted with microelectrodes.

One important tool with prospects for a breakthrough in experimental capabilities is electrical conductivity. Currently, these techniques are limited to about 450°C, but they can operate to remarkably low concentrations, below $< 10^{-5}$ molar solute (IAPWS, 2009). Conductance data at extremely low concentrations allow for direct determination of ionic mobilities (limiting values of conductance) without the need for a tenuous extrapolation. Elimination of one variable in the conductance model, coupled with the use of specialized cells for low density steam measurements, would lead to an unprecedented improvement in accuracy. Analysis of the uncertainty inherent in the existing low density conductance data indicates that the high temperature, high dilution flow technique can provide a radical improvement in the values of solute dissociation constants.

Moreover, as these cells offer vastly improved sensitivity at lower pressures and concentrations over the original static design of Franck *et al.* (1962), which was capable of reaching the extreme conditions of 800°C and 400 MPa, it is anticipated that the flow-through cell configuration for

© Woodhead Publishing Limited, 2010

laboratory measurements can be readily adapted to reach 760°C and 40 MPa. In addition to providing accurate data for modeling ultra-supercritical cycle chemistry, experience with the design of the high temperature, low density conductance technique could lead to future development of new power plant chemistry control instruments for monitoring directly the purity of superheated steam.

4.7 Acknowledgement

The contribution of information on existing and currently planned supercritical boilers by F. Gabrielli, Alstom Power Inc. is herewith gratefully acknowledged.

4.8 References

Chexal B, Horowitz J, Jones R, Dooley R B, Wood C, Bouchacourt M, Remy F, Nordmann F and St Paul P (1998), *Flow-accelerated corrosion in power plants*, EPRI Technical Report TR-106611R1, www.epri.com.

Dooley R B, Ball M, Bursik A, Rziha M and Svoboda R (2004), 'Water chemistry in commercial water-steam cycles', In *Aqueous systems at elevated temperatures and pressures: physical chemistry in water, steam and hydrothermal solutions*, Ch. 17, Elsevier, ISBN 0-12-544461-3.

Dooley R B and McNaughton W B (2007), *Boiler and HRSG tube failures: theory and practice*, EPRI, 1012757, www.epri.com.

Dooley R B, Aspden J D, Howell A G and DuPreez F (2009),'Assessing and controlling corrosion in air-cooled condensers', *Power Plant Chem.* 11(5), 264–274.

EPRI (2002), *Cycle chemistry guidelines for fossil plants: all-volatile treatment*: revision 1, Palo Alto, CA, EPRI 1004187, www.epri.com.

EPRI (2005), *Cycle chemistry guidelines for fossil plants: oxygenated treatment*, Palo Alto, CA, EPRI 1004925, www.epri.com.

Franck E U, Savolainen J E and Marshall W L (1962), 'Electrical conductance cell assembly for use with aqueous solutions up to 800°C and 4000 bars,' *Rev. Sci. Instrumn*, 33, 115–117.

Gabrielli F and Schwevers H (2008), 'Design factors and water chemistry practices–supercritical power cycles, 15th int. conf. *Properties of water and steam*, Berlin September 2008.

Harvey A H and Bellows J C (1997), *Evaluation and correlation of steam solubility data for salts and minerals of interest in the power industry*, NIST Technical Note Nr, 1387.

Harvey A H and Mountain R D (2003), 'Molecular dynamics calculation of the diffusivity of sodium chloride in steam', *Ind. Engng. Chem. Res.*, 42, 404.

Heitmann H G (1997), *Praxis der Kraftwerkschemie*, 2nd edition, Essen, Germany, Vulkan-Verlag, ISBN 3-8027-2179-9; English translation: *Handbook of power plant chemistry*, Boca Raton, Florida, CRC Press, 1993, ISBN 0-8493-9303-5.

© Woodhead Publishing Limited, 2010

IAPWS (2007), *Revised release on the IAPWS industrial formulation 1997 for the thermodynamic properties of water and steam*, August 2007, www.iapws.org.

IAPWS (2009), *Thermophysical properties associated with ultra-supercritical coal-fired steam generators*, *Draft for an IAPWS certified research need (ICRN)*, www.iapws.org.

Lindsay W T (1978), 'Physical chemistry in steam turbines', Westinghouse steam-turbine generator technology symposium, Charlotte, USA, October 1978.

McCloskey T, Dooley R B and McNaughton W (1999), *Turbine steam path damage: theory and practice*, EPRI, Technical Report TR-108943, www.epri.com.

Nakahara, M and Yoshimoto Y (1995), 'Hydrophobic slowdown and hydrophilic speedup of water rotation in supercooled aqueous solutions of benzene and phenol,' *J. Phys. Chem.*, 99, 10698.

Palmer D A and Bénézeth P (2004), 'Solubility of copper oxides in water and steam', 14th int. conf. *Properties of water and steam*, Kyoto, Japan, September 2004.

Palmer D A, Simonson J M and Jensen J P (2004), 'Partitioning of electrolytes to steam and their solubilities in steam', In *Aqueous systems at elevated temperatures and pressures: physical chemistry in water, steam and hydrothermal solutions*, Ch. 12, Elsevier, ISBN 0-12-544461-3.

Sturla P (1973), '*Oxidation and deposition phenomena in forced circulating boilers and feedwater treatment*', 5th national feedwater conf., Prague, Czechoslovakia (in French).

Svoboda R and Bodmer M (2004), '*Investigations into the composition of the water phase in steam turbines*', 14th int. conf. *Properties of water and steam*, Kyoto, Japan, September, 2004 (see also Palmer and Bénézeth, 2004).

Svoboda R (2006), '*Chemistry in steam turbines*', ESAA power station chemistry conf., Leura, X. Australia, March 2006, *Power Plant Chem.* 8(5), 270–276.

Tremaine P R and LeBlanc J C (1980), 'The solubility of magnetite and the hydrolysis and oxidation of Fe^{2+} in water to 300°C', *J. Solution Chem.*, 9-6, 415.

VGB (2004), *Guidelines for feedwater, boiler water and steam quality for power plants/ industrial plants*, 2nd edition, VGB-R 450 Le, http://www.vgb.org.

© Woodhead Publishing Limited, 2010

Part II

Gas separation membranes, emissions handling, and instrumentation and control technology for advanced power plants

© Woodhead Publishing Limited, 2010

5

Advanced hydrogen (H_2) gas separation membrane development for power plants

S. J. DOONG, UOP, a Honeywell Company, USA

Abstract: Advanced H_2 membrane technologies have the potential to improve the cost and efficiency of future power plants for H_2 production and/or CO_2 capture. In this chapter, the types of membrane materials used for hydrogen separation are first presented. Membrane engineering issues follow, with focus on membrane system design and performance. Possible integration schemes of H_2 membrane systems in power plants are then discussed. Hydrogen storage and transportation issues are also briefly covered. Finally, future trends and further sources of information are commented upon at the end of the chapter.

Key words: hydrogen separation membrane, inorganic membrane, membrane reactor.

5.1 Introduction

Hydrogen has been touted as the energy carrier of the future. The current interest in hydrogen energy development mainly stems from the resource depletion of oil and gas, the security concern of energy dependence on petroleum imports for Western countries, and environmental issues, especially global warming. Because water is the main product when hydrogen is used as a fuel, hydrogen can be employed for clean energy production by a variety of conventional and new energy generation devices, such as turbine, engine, and fuel cell. While currently there is strong demand for hydrogen in refineries for hydro processing or hydro treating applications, the future demand for hydrogen can be expected to further increase continuously when hydrogen is used in the power industry. When hydrogen usage penetrates into the transportation industry with mass

© Woodhead Publishing Limited, 2010

production of fuel-cell vehicles, a global hydrogen economy will become a reality

Hydrogen can be produced from a variety of sources: water, natural gas, coal, biomass, etc. Commercial production technologies generally exist, but they do not offer cost-effective solutions for widespread use of H_2 in the energy sector. Furthermore, separation of H_2 from other by-products in production processes is always required, especially in thermochemical process for converting fossil fuels. To sustain the future use of fossil fuels in power plants, capture and sequestration of CO_2 has become critically important. Converting fossil fuels to a gas mixture of H_2 and CO_2 prior to combustion is one elegant way to achieve this objective. The CO_2/H_2 mixture can be used directly as a fuel in an oxygen combustion atmosphere or in a fuel-cell device. More conveniently, this high-pressure fuel gas can first be separated to produce a pure CO_2 stream for sequestration and a pure H_2 stream for a fuel source. In a polygeneration power plant, the separated H_2 can also be delivered to power parks or filling stations for distributed power generation or transportation applications. Separation of H_2/CO_2 is one enabling technology for CO_2 capture in future power plants.

Incorporating a CO_2 capture unit in a power plant significantly reduces the energy efficiency and increases the cost of electricity (EPRI and NETL, 2000; Parsons, 2002; Gielen, 2003). This has spurred the development of H_2 separation membranes recently. Conventional H_2 purification techniques include pressure swing adsorption (PSA), polymeric membrane separation, solvent absorption, and cryogenic distillation. In addition to their high costs, all of the above H_2 separation techniques operate at low temperatures ($< 50^{\circ}C$), and are difficult to integrate with modern power plants. In modern power plants such as integrated gasification combined cycle (IGCC), where H_2 containing syngas is generated at very high temperatures, high-temperature hydrogen separation technologies can eliminate the need for cooling the fuel gas and reheating it again for gas turbines. Furthermore, high-temperature separation technologies can combine both chemical reactions and separation in a single step to simplify the process, reduce the cost, and improve the efficiency. There is a strong incentive to develop advanced H_2 separation technologies which are cost effective and operate at higher temperatures ($> 200^{\circ}C$). Membrane separation is one of the areas that has been vigorously pursued by researchers globally to address this aspect of the future H_2 economy.

In this chapter, potential membrane materials used for hydrogen separation are first presented. Membrane engineering issues will follow, with the focus on membrane system design and performance. Possible integration schemes of H_2 membrane systems in power plants are then discussed. Hydrogen storage and transportation issues will also be briefly

© Woodhead Publishing Limited, 2010

covered. The chapter will end with comments on future trends and further sources of information.

5.2 Hydrogen membrane materials

Based on materials used, H_2 membranes can be classified into organic and inorganic membranes. Organic membranes are mainly polymeric. Inorganic membranes can be made of metal, ceramic, or carbon. Based on the transport mechanisms, membranes can be classified into porous and dense membranes. In porous membranes, H_2 diffuses through small pores of the membrane structure. As separation is determined by the molecular size or weight of the gas species, H_2 can diffuse much faster than other larger gas components. Inside the pores of the membrane, the diffusion process can be of the Knudsen type, where the mean free path of the gas molecules is close to the pore diameter. If the pore diameter is made even smaller, the diffusion process can be an activated one, where the gas molecules are strongly interacted by the walls of the pore. If gas is adsorbed on the wall of the pores, surface diffusion can also occur, which helps to facilitate the gas diffusion process. The membrane pore diameters can also be made such that larger gas molecules are too big to enter the membrane pores, a phenomenon called the molecular sieving effect. Almost all porous membranes use molecular sieving or activated diffusion to effect separation as the Knudsen diffusion does not give an acceptable separation factor.

In a dense membrane, H_2 permeates through the bulk of the membrane material via a solution–diffusion mechanism. Essentially, gas molecules first need to dissolve or adsorb on the surface of the membrane. The dissolved or adsorbed gas molecules then diffuse or migrate through the bulk of the membrane, and finally desorb to the permeate side of the membrane. The membrane permeability P can be described as a product of the solubility coefficient S and the diffusivity coefficient D.

$$P = SD \qquad [5.1]$$

The membrane flux F is then related to the permeability by the following equation

$$F = P\Delta p/L \qquad [5.2]$$

where Δp is the partial pressure difference across the membrane for the permeating component and L is the membrane thickness.

In general, porous membranes tend to give higher flux than the dense ones; however, dense membranes can have better selectivity. As the membrane flux increases with the reduction of its thickness, it is desirable to have a very thin membrane. Composite membranes have been developed

© Woodhead Publishing Limited, 2010

to increase the flux by placing a very thin, dense, or active layer on top of a porous support layer to improve the overall membrane strength. Asymmetric membrane can be considered as one type of composite membrane, where the active layer and the porous support layer are made of the same material. Membrane materials can also be combined or mixed to improve their performance. For example, mixed-matrix membranes contain inorganic particles inside the framework of the polymer membrane (Zimmerman *et al.*, 1997; Mahajan and Koros, 2000; Jha and Way, 2008). Cermet membranes contain both ceramic and metallic materials, which will be discussed later. With the above background information, the H_2 membranes will be discussed based on their materials in this section.

5.2.1 Polymeric membrane

The only H_2 membrane technology that has been widely used on a large commercial scale is based on polymeric materials. In the early 1980s, Monsanto commercialized the first hydrogen membrane process – Prism® (MacLean *et al.*, 1986). Since then, polymeric membranes have been used in H_2 recovery from purge streams in ammonia plants and refineries. In syngas plants, it has also been used for adjustment of H_2/carbon monoxide (CO) ratio. The major suppliers are Air Products, Air Liquide, Praxair, UOP, and UBE (Japan).

Polymer membranes are a dense type of polysulfone, polystyrene, cellulose acetate, polyimide, or polyaramade among others (Koros and Fleming, 1993). Separation of H_2 mainly can be attributed to the fast diffusion coefficients of smaller H_2 molecules being transported through the bulk of the membrane. Other gas molecules can still permeate through the membrane, depending on the relative solubility and diffusivity in the polymer material. Therefore, polymeric membranes are rarely used for producing high-purity H_2. While polyimide or polyaramade shows H_2/methane (CH_4) selectivity well above 100, most other polymeric membranes have typical H_2/CH_4 selectivities in the order of 30~70 (Koros and Fleming, 1993; Al-Rabiah *et al.*, 2001; Orme *et al.*, 2003). The maximum operating temperature is about 110°C. The maximum pressure differential across the membrane, depending on the temperature, can be as high as 100 bars at 40°C (Air Products and Chemicals, 1999).

Polymeric membranes are very susceptible to the swelling effect, plasticized owing to the solubility of other larger molecules, such as hydrocarbons or CO_2. Pretreatment of the feed gas before the membrane can be complicated and costly. Pretreatment is also used to prevent condensation of hydrocarbon gas on the membrane surfaces. Because hydrocarbons and other larger molecules are enriched on the feed side of the membrane after H_2 permeation, the dew point of the residue stream can

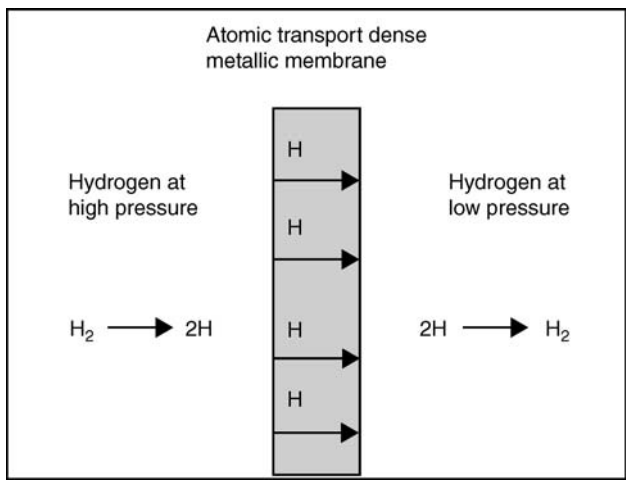
© Woodhead Publishing Limited, 2010

increase. The possibility of condensation is further increased as the membrane temperature drops due to the Joule–Thomson effect when H_2 permeates from the high-pressure feed side to the low-pressure permeate side. Other problems include resistance to certain chemicals such as hydrochloric acid (HCl) and sulfur oxides (SO_x) (Adhikari and Fernando, 2006). The pretreatment issue and the low temperature capability make the polymeric membrane less attractive for applications in the power sector. The low H_2/CO_2 selectivity (< 10) is another disadvantage for power plant application, as the feed gas tends to contain a large amount of CO_2, especially after the water–gas shift reaction. Nevertheless, polymeric membranes have the advantages of low cost, easy fabrication, and plenty of field experience. Research on high-temperature polymeric membranes (to 300°C) has been reported (Costello *et al.*, 1994; Rezac *et al.*, 1995; Pesiri *et al.*, 2003), but these studies have been limited only to laboratory testing.

5.2.2 Metallic membrane

Metal membranes are all of the dense type as well, following the solution–diffusion mechanism with the H_2 molecules first dissolving in the metal framework, dissociating into two atoms, atomic hydrogen transporting through the membrane, and recombining back to molecular H_2, as shown in Fig. 5.1. The H_2 flux, F, across the membrane, with a thickness L, can be described by the following equation

$$F = P\left(p_{\text{feed}}^{n} - p_{\text{perm}}^{n}\right)/L \qquad [5.3]$$



5.1 Atomic hydrogen transport in metal membrane.

© Woodhead Publishing Limited, 2010

where P is the permeability, and p_{feed} and p_{perm} are the hydrogen partial pressure at the feed and permeate side respectively. If n is equal to 0.5, equation [5.3] becomes the famous Siveret's law. A deviation from 0.5 for n indicates the presence of mass transfer resistances other than the metal itself. Except for defects, the metal membrane can produce very high-purity H_2 owing to its high selectivity. This is in marked contrast to the conventional thinking that membrane processes are considered primarily for bulk separation for enriching product, rather than for purification to achieve a high-purity product.

Palladium (Pd) and its alloys are the most common metal membranes for H_2 purification applications. Operating temperatures of the Pd membranes are in the range 300–600°C. At low temperatures, Pd segregates into two phases and becomes brittle during H_2 permeation (Shu *et al.*, 1991). Binary alloys such as with copper (Pd–Cu) and with silver (Pd–Ag) have been used to overcome this problem without sacrifice of H_2 flux (Athayde *et al.*, 1994; McCool *et al.*, 1999; Roa *et al.*, 2002; Tosti *et al.*, 2003; Howard *et al.*, 2004). Alloys have the advantage of reducing the amount of expensive Pd in the membrane. Further, by changing the surface morphology and the electronic structure of metal Pd, alloys exhibit better chemical stability than pure Pd, in terms of the resistance to poisoning by gaseous impurities such as hydrogen sulfide (H_2S), CO, H_2O, etc. (Gao *et al.*, 2004). It is well documented that Pd–Cu alloy shows improved resistance to sulfur (Morreale *et al.*, 2004; Kamakoti *et al.*, 2005; Yang *et al.*, 2008).

In addition to Pd, refractory metals in group IV and V elements such as vanadium (V), niobium (Nb), tantalum (Ta), zirconium (Zr), and titanium (Ti) are all good candidate materials for H_2 separation membranes. In fact their H_2 permeabilities are higher than Pd (Buxbaum and Kinney, 1996). The major issue with these metals is that they can easily form an oxide layer on the surface in the air, rendering them incapable of dissolving or dissociating H_2 molecules. Current practice uses a thin layer of Pd or Pd alloy coated on the surface of the refractory metals to catalyze the dissociation and reassociation of H_2 (Buxbaum and Marker, 1993; Moss *et al.*, 1998; Mundschau *et al.*, 2006). Using this approach, Eltron Research Inc. has reported very high H_2 fluxes, > 280 cc STP/cm^2/min, at 713 K with a partial pressure of hydrogen of 1.37 MPa using a 127 μm thick membrane (Mundschau *et al.*, 2005a, b). These self-supporting membranes are strong enough to sustain high pressure differentials and are able to overcome the H_2-induced embrittlement problem commonly associated with the group IV and V metals (Xie *et al.*, 2006). Development of non-Pd-based metal alloy materials will continue to play a significant role in reducing the cost, increasing the permeability, and improving the durability of H_2 separation membranes (Ozaki *et al.*, 2003; Hashi *et al.*, 2005; Phair and Donelson, 2006; Ryi *et al.*, 2006).

© Woodhead Publishing Limited, 2010

In actual practice using metallic membranes, intermetallic diffusion at high temperatures is one concern that needs to be addressed. Owing to the high cost of Pd metal, it is very desirable to fabricate an ultra-thin membrane, which is then supported by a porous substrate. If metal such as stainless steel is chosen as the support material, Pd and iron (Fe) or chromium (Cr) intermetallic diffusion cannot be avoided. One alternative approach is to use ceramic materials for support. However, ceramics have the drawbacks of difficult fabrication, lower pressure rating, and poor sealing, resulting in de-lamination between the metal and the support. A good compromise is to insert a thin layer of ceramic barrier between the metal membrane and the stainless steel support (Nam and Lee, 2001; Ma *et al*., 2004). Membranes produced by this approach have been shown to be stable after over 6000 hours of continuous testing in the temperature range 350–450°C (Ma, 2008). For Pd-coated V membranes, hydrogen flux decay was also observed owing to intermetallic diffusion, and inserting a layer of porous aluminum oxide has improved the membrane stability (Edlund and McCarthy, 1995).

Among all high-temperature inorganic membranes for H_2 separation, Pd membranes are in the most advanced stage of development. In fact, the Pd membrane system was successfully scaled up to 25 tons per day H_2 capacity in the early 1960s (McBride and McKinley, 1965). Small-scale Pd membranes are commercially available for H_2 purification in the electronic industry. Membrane reactors incorporating Pd have also been considered for H_2 production and CO_2 capture with integration in power generation cycles, although this has only been tested experimentally at laboratory scale (Uemiya, 1991; Tong *et al*., 2006; Barbieri *et al*., 2008; Tosti *et al*., 2008). Cost and stability are still the major barriers for commercialization of metallic membranes in large scale.

5.2.3 Ceramic membrane

Ceramic membranes can be either porous or dense. Porous ceramic membranes are usually amorphous, made of alumina, silica, zirconia, or titania in a form of metal oxide. These materials possess good thermal and chemical stability in harsh operating conditions. In order to separate H_2 efficiently, pore diameters of the membrane must be less than 1 nm (Diniz da Costa *et al*., 2002; Lee and Oyama, 2002). Table 5.1 lists the molecular diameters for several gases. Note that the H_2O molecule is smaller than H_2 and the difference of molecular size between H_2 and CO_2 is relatively small. As in dense membranes, the active layer with small pore size needs to be supported by a thick layer with pore size between 0.5 and 50 μm. An intermediate layer with pore size between 0.005 and 0.5 μm is also used to bridge the support and the active layer (Judkins and Bischoff, 2005).

© Woodhead Publishing Limited, 2010

Table 5.1 Kinetic diameters of gas molecules (Koros and Fleming, 1993)

Gas	Kinetic diameter (nm)
He	0.26
H_2O	0.265
H_2	0.289
CO_2	0.33
Ar	0.34
O_2	0.346
H_2S	0.36
N_2	0.364
CO	0.376
CH_4	0.38
C_2H_4	0.39
Xe	0.396
C_3H_8	0.43

Hydrogen product purity is almost always less than 100% as microporous membranes with uniform pore size and defect-free properties are difficult to fabricate. The improvement of selectivity comes with a reduction of flux for microporous ceramic membranes. As a result, their flux is only comparable to Pd membranes. Two main problems of the amorphous microporous membranes are their tendency to densify at high temperatures and the hydrothermal stability of silica membranes in the presence of steam (Yoshino *et al.*, 2005).

A recent experimental analysis conducted by the US Department of Energy (DOE) showed that the microporous membrane failed to meet the performance target in terms of H_2 product purity and recovery (US DOE, 2007b). This probably was caused by the poor selectivity of the microporous membrane. While this may be a setback for this type of membrane development, it should not deter further research in microporous membrane material and fabrication. One possible application is to use a multi-stage approach, where the microporous membrane is used for bulk removal of CO_2 and other larger contaminants, followed by a highly selective but more expensive Pd or metallic membrane.

Dense ceramic membranes are mainly of the perovskite type, which has the following formula

$$A_{1-x}A'_xB_{1-y}B'_yO_{3-z}$$

where

A is selected from the group consisting of barium (Ba), strontium (Sr), calcium (Ca), magnesium (Mg)

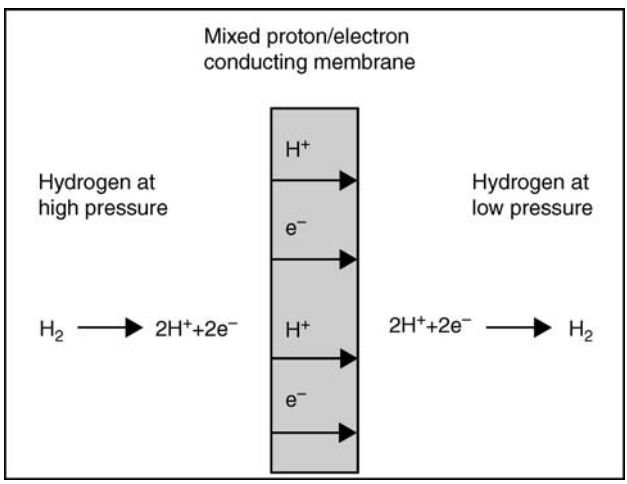
A′ is selected from the Lanthinide series, such as cerium (Ce), praseodymium (Pr), neodymium (Nd), gadolinium (Gd), ytterbium (Yb)

© Woodhead Publishing Limited, 2010

B and B′ are selected from any transition metal, such as cerium (Ce), yttrium (Y), cobalt (Co), (Ti), (V), (Cr)
O is oxygen
x and y are numbers between 0 and 1
z is a number sufficient to neutralize the charge in the mixed metal oxide.

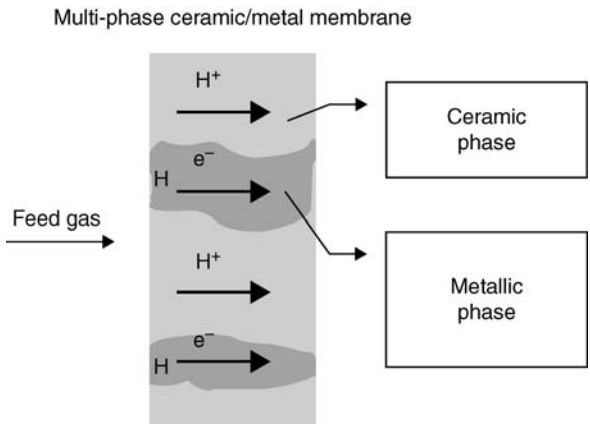
This class of material exhibits mixed protonic–electronic conductivity at high temperatures, 600~1000°C (Iwahara, *et al.*, 1981; Norby and Larring, 2000; Qi and Lin, 2000; White *et al.*, 2001; Hamakawa *et al.*, 2002; Norby, 2007). When a H_2-containing gas mixture is introduced on one side of the membrane, H_2 dissociates into proton (H^+) and electron (e^-) on the surface. The dissociated species are transported through the membrane to its opposite side where the species recombine to form an H_2 molecule, as illustrated in Fig. 5.2. The selectivity of this type of membrane is very high, as only H_2 can permeate through the membrane. However, the H_2 flux currently demonstrated in the lab is very low (Doong *et al.*, 2005). Its unique high-temperature operating range makes it possible to closely couple with the coal or biomass gasifier without further cooling down the syngas. On the other hand, the high-temperature operation makes the robust design of membrane support, module, and housing more challenging. The tolerance to contaminants in the coal-derived syngas is another concern, especially the stability issue in the presence of CO_2. Certain perovskites can be converted to more stable carbonate compounds with CO_2. Dense perovskite membranes are still in an early stage of development.

To increase the H_2 flux of dense ceramic membranes, a hydrogen-permeable metallic material can be incorporated into the dense, mixed



5.2 Mixed proton/electron conducting membrane.

© Woodhead Publishing Limited, 2010



5.3 Multi-phase ceramic/metal membrane.

conducting ceramic phase, as a cermet (Dorris *et al*., 2003; Mundschau, 2005). The transport mechanism is illustrated in Fig. 5.3. The H_2 transport is predominantly carried by the metallic phase, which offers a high flux. Therefore, typical ceramic materials without ion-conducting property such as Al_2O_3, stabilized ZrO_2, can also be used for the ceramic phase (Balachandran *et al*., 2005). With metal encapsulated in the ceramic framework, the shape integrity of the metal phase is no longer an issue. The ceramic/metal composite structure can afford a higher temperature operation (~900°C) than metal membranes. At such a high temperature, it has better tolerance to sulfur compounds in the feed gas (Balachandran *et al*., 2006).

5.2.4 Zeolite membrane

Zeolites are porous crystalline aluminosilicates with their framework consisting of an assemblage of SiO_4 and AlO_4 tetrahedra. The unique feature of uniform pore size distribution distinguishes the zeolites from other amorphous microporous materials. Zeolite membranes typically are prepared by growing polycrystalline zeolite into a continuous film on the surface of a porous support. Gas permeation is based on the diffusion of the gas molecules through the interconnected channels or intracrystalline pores (Lin, 2001). Gas separation could be affected both by the molecular sizes of the gases and by their adsorption properties (Hong *et al*., 2005 ; Kanezashi *et al*., 2008). Therefore, for H_2 separation, high-temperature operation is used to suppress the adsorption of CO_2 and improve the H_2/CO_2 separation factor. Current research on zeolite membranes focuses on tailoring the micropore size and fabricating defect-free membranes (Caro and Noack, 2008).

© Woodhead Publishing Limited, 2010

5.2.5 Carbon molecular sieve membrane

Carbon molecular sieve is another group of materials, similar to zeolite, which possesses a pore size in the range of gas molecular dimensions and a very sharp pore size distribution. It is produced by pyrosis of organic precursors such as polymers, coke, coal, or biomass. Flat, tubular, or hollow-fiber carbon molecular sieve membranes of asymmetrical structure could be fabricated from the precursors of the same geometry (Jones and Koros, 1994; Ismail and David, 2001; Saufi and Ismail, 2004). However, these may have the disadvantage of brittleness and difficulty to handle for scaling up. Alternatively, the membranes could be produced by coating on a porous support of ceramic or stainless steel. Carbon molecular sieve membranes supported on ceramic tubes have been tested in a refinery pilot plant using hydrocracker off-gas for about 100 hours (Liu, 2005). Operating at 220°C, the membranes were stable in the presence of significant H_2S, NH_3, and higher hydrocarbons, presumably owing to low adsorption of these contaminants on carbon at high temperatures. The H_2 flux was quite comparable to the dense Pd membranes. Like any microporous membrane, producing an ultra-high purity of H_2 from a feed containing bulk CO_2 is a challenge for the carbon molecular sieve membrane.

5.3 Membrane system design and performance

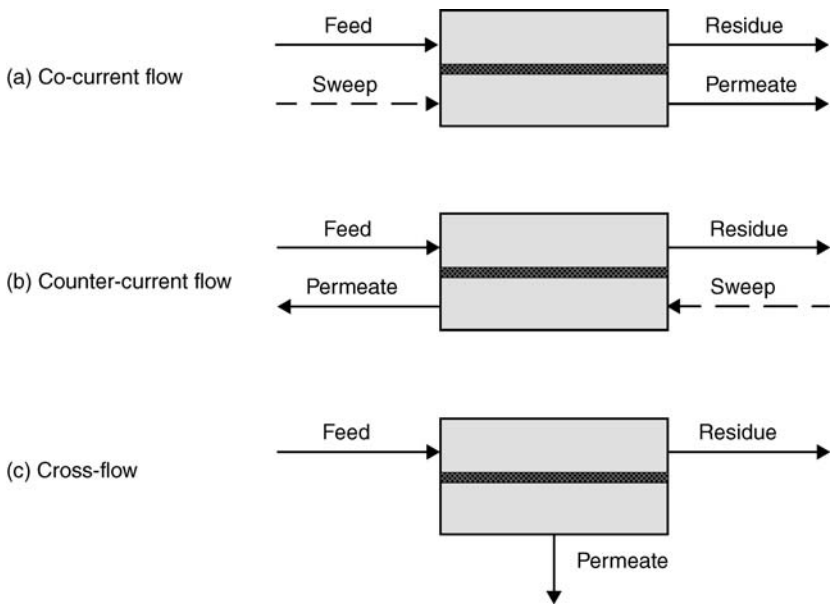
Practical use of the membrane materials for gas separation in process equipment requires that the membrane be packaged in a container called a module. Several types of membrane module exist, which include planar, tubular, hollow-fiber, spiral-wound, and monolith (for inorganic membrane) types. A membrane module, as a mass transfer device, actually resembles a heat exchanger. A planar membrane module, with the sheets of flat membrane parallel to each other and a spacer or flow channel in between is similar to a plate-and-frame heat exchanger. Scale-up of the planar membranes relies on stacking up of multiple modules. A tubular membrane typically has a diameter larger than 5 mm, again resembling a tubular heat exchanger in its basic form. In a hollow-fiber module, the membrane tube diameter is well under 10 mm. It has the highest packing density among all the membrane module types. When a flat membrane system is wrapped around a central pipe for collecting the permeate, it becomes a spiral-wound module. A monolith membrane refers to a honeycomb structure with multiple channels (Thompson, 1991). Ceramic membranes, especially ion-conducting membranes, can be made of this type of structure, primarily based on ceramic processing techniques. Typical packing densities, i.e. membrane surface area per module volume, are 300–500 m^2/m^3 for planar module, 300–1000 m^2/m^3 for tubular module,

© Woodhead Publishing Limited, 2010

600–800 m^2/m^3 for spiral wound, and 6000–15 000 m^2/m^3 for hollow-fiber module (Koros and Fleming, 1993; Kluiters, 2004).

Choice of membrane architectural design depends on many factors, with cost probably being the most important. A vast majority of commercial polymeric membranes are either hollow-fiber or spiral-wound. A plate-and-frame device tends to be used only on a small scale. Commercial H_2 membrane experiences indicate that hollow-fiber may have an edge over the spiral-wound in terms of cost. However, the spiral module has the advantage of lower pressure drop and is less prone to fouling. Inorganic membranes can be tubular, planar, or monolithic configurations. Recent development has also produced hollow-fiber ceramic membranes (Wei *et al.*, 2008). In an early stage of development for inorganic membranes, there is no clear winner with regard to module choice. Planar design is quite popular in the area of fuel-cell stacks and has been adopted by Air Products in their ion transport membrane for oxygen separation from air (Adler *et al.*, 2000; Armstrong *et al.*, 2006). The tubular design has the advantage of fewer sealing points, especially the closed-one-end design, which also adds an additional benefit of free thermal expansion (Gottzmann *et al.*, 2000; Anderson *et al.*, 2008). The design consideration currently focuses on the reliability issues, especially sealing of the membrane materials to the module body.

Based on flow patterns, membrane modules can be divided into three types of operation, co-current, counter-current, and cross-flow, as shown in Fig. 5.4. In co-current configuration, the driving force is initially large and



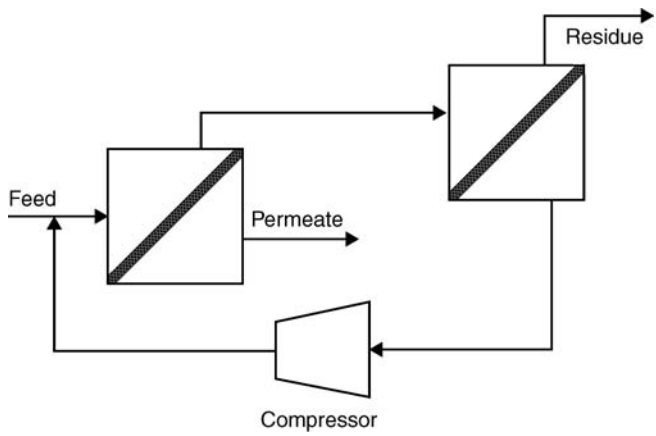
5.4 Different membrane flow patterns.

© Woodhead Publishing Limited, 2010

starts to decrease along the membrane flow path. In the counter-current arrangement, the driving force can be kept relatively constant. Optional use of sweep gas can decrease the partial pressure of the permeating component and increase the driving force. However, the separation of sweep gas from the permeate becomes necessary if the permeate gas is the desirable product, as in the case of the H_2 membrane. For the cross-flow pattern, which is generally seen in spiral-wound or monolithic modules, the driving force also decreases along the membrane feed flow path, but to a lesser extent than the co-current one. Although counter-current is considered the best flow pattern, the differences among the three flow patterns can become quite small, when the membrane used has a superior selectivity or the operating pressure ratio is high (Rautenbach and Dahm, 1987).

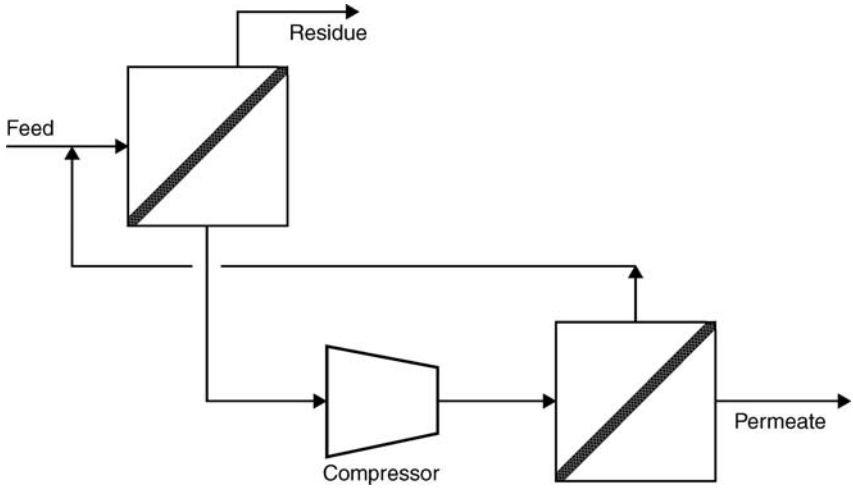
Membrane systems can also be configured into multiple stages to improve the performance, especially for the membranes with poor selectivity, such as porous ceramic membranes or polymeric membranes (Chiappetta *et al.*, 2006). As many options are possible, Figs 5.5 and 5.6 show only the two membrane systems that are the most commonly used. The first one shown in Fig. 5.5 is used to enhance the permeate product recovery or enrich the retentate (residue) product purity. The second one in Fig. 5.6 is used to increase the permeate product purity or the retentate product recovery. The drawback of the multistage membrane arrangements is the requirement for gas recompression. Nevertheless, this offers more process options for industrial applications of membrane systems, as there is no need to employ a high-performance and expensive membrane. Instead, with multistage configurations, engineers can design a cost-effective membrane system.

In evaluating a membrane's performance, the working module and the operating conditions need to be taken into consideration. It has been



5.5 Two-stage membrane arrangement for enhancing residue product purity.

© Woodhead Publishing Limited, 2010



5.6 Two-stage membrane arrangement for enhancing permeate product purity.

recognized that the cost of the membrane material may not account for the majority of the entire module cost, as the active membrane materials used in a module have been progressively decreased through research efforts in improving the flux. The fabrication of the membrane, the membrane support material, the module structure material, and construction can represent a significant portion of the total module cost. In addition to the membrane itself, the failure mode of a module can be attributed to membrane sealing, membrane support, module manifold, interconnect, etc. Membrane performances are strongly affected by the gas contaminants in the feed, the operating temperature and pressure condition, the gas flow distribution inside the module, external mass transfer effects, and temperature distribution, which all demand careful engineering design. The US Department of Energy has listed several performance targets for hydrogen membrane development, as shown in Table 5.2 (US DOE, 2007b).

The current status in Table 5.2 is based on the metallic membranes. Although high flux and low cost are the key parameters, the membrane must also demonstrate its capability of operating in real-life conditions, including high temperature, high pressure differential, in a water–gas shift environment containing CO and steam, and certain degrees of tolerance to sulfur. As can be seen, the challenges are in the area of cost and stability/durability. This would require a complete hydrogen separation system demonstration integrated with actual plant applications such as IGCC to obtain a better assessment of cost, life-time, and other scale-up issues.

© Woodhead Publishing Limited, 2010

Table 5.2 Hydrogen metal membrane separation targets (US DOE, 2007b)

Performance criteria	Units	Current status	2010 target	2015 target
Flux	$m^3/h/m^2$	67	60	90
Cost	$/$m^2$	2100	1000	<1000
Temperature	°C	300–400	200	300
Operating capability	MPa	6.8	2.7	5.4–6.8
Stability/durability	years	0.9	3	5
Sulfur tolerance	ppmv	~20	20	> 100
CO tolerance	–	Yes	Yes	Yes
Hydrogen purity	%	99.999%	99.5%	99.99%

Note: Flux is under 0.68 MPa (100 psi) hydrogen partial pressure differential. Operating capability refers to total pressure differential across the membrane.

5.4 Hydrogen membrane integration with power plant

It is not practical to integrate H_2 membrane processes with conventional steam power plants that burn coal, oil, or natural gas. The discussion in this section will focus on the combined-cycle power plants and future fuel-cell power plants. The integration also includes hydrogen membrane reactor concepts, with both reforming reaction and water–gas shift reaction.

Hydrogen membranes can be integrated with advanced power plants from two perspectives: one is for CO_2 capture the other is for H_2 production. All future power plants will be potentially subjected to government regulations regarding CO_2 emissions; therefore, a cost-effective technology to capture CO_2 such as the H_2 membrane may play a significant role. One advantage of H_2 membranes is that they produce a CO_2-rich stream at high pressure, thus minimizing the requirement for further compression. However, the CO_2 stream may still contain H_2 and other impurities, which would require further treatment (Gary and Tomlinson, 2002; Carbo *et al.*, 2006; Chiesa *et al.*, 2007). The issue of CO_2 capture is the subject of a separate chapter. On the other hand, H_2 production from coal, biomass, and natural gas is an important pathway to realize the concept of the future H_2 economy. During off-peak hours, a power plant can produce H_2, store it, and transport to future H_2 filling stations, or even sell it as a chemical feed stock. The required H_2 purity will be very high in this case. Hydrogen membrane offers an energy-efficient solution to H_2 separation in the future polygeneration power plants.

Regardless of scenario, a shift reactor is almost certainly required for the power plants fed with fossil fuels. The shift reaction is

$$H_2O + CO = H_2 + CO_2 + 41.2\,\text{kJ/mole} \qquad [5.4]$$

A water–gas shift reaction converts CO to CO_2 and generates additional H_2, which without a doubt aids both carbon capture and H_2 production. After the shift reaction, a gas separation unit will be needed to produce a H_2-rich

© Woodhead Publishing Limited, 2010

stream for clean power or H_2 by-product generation and a CO_2-rich stream for sequestration. A simplified flow diagram showing the integration of shift reactor and gas separation with a fossil-fuel power plant is depicted in Fig. 5.7.

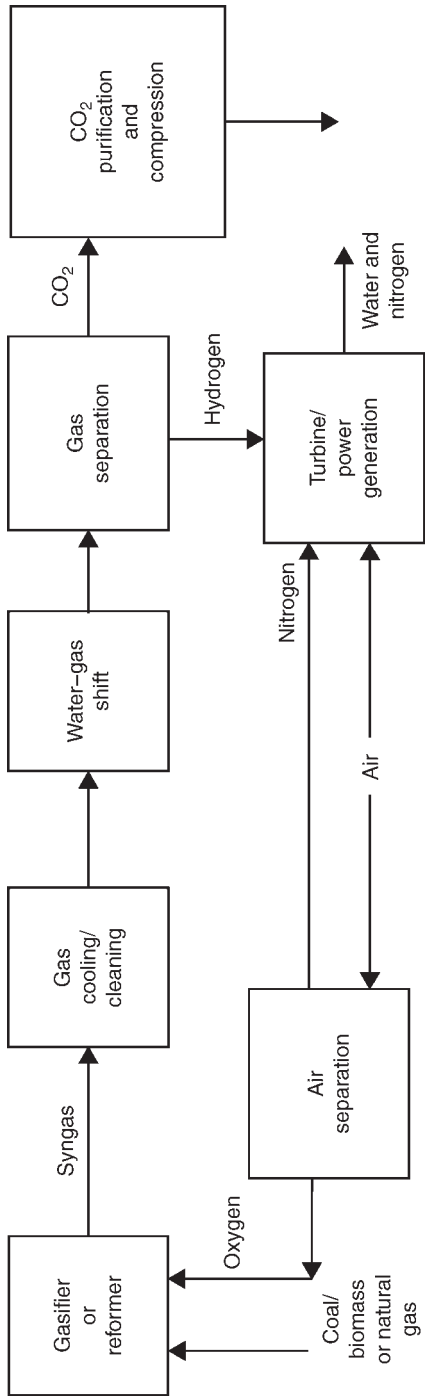
The only current commercial process for CO_2 separation from syngas is a solvent absorption process such as Selexol, Rectisol, or other amine scrubbing processes. For H_2 production, another purification unit such as PSA is required to meet the hydrogen product purity specification. The best integration scheme for the H_2 membranes is to replace both the solvent process and the subsequent PSA process. While commercial polymeric H_2 membrane processes may be used to compete with PSA in this case, they suffer two major disadvantages: low H_2 purity and low operating temperatures. The advanced inorganic membranes such as metallic or dense ceramic membranes can produce very high-purity H_2. Their high operating temperatures allow the hydrogen membranes to be combined with the shift reactor into a membrane reactor, as shown in Fig. 5.8.

The shift reaction typically takes place at 200°C or higher, which matches the operating temperatures of most inorganic H_2 membranes very well. One critical issue that needs to be addressed in the integration scheme is the contaminants in the syngas stream from coal gasification plants. While certain sour-shift catalysts, Co/Mo, are sulfur resistant, most of the inorganic membranes have not been proven for their sulfur tolerance. Thus, a high-temperature gas-cleaning section before the membrane shift reactor is required to remove any contaminant that may be harmful to the catalysts and/or the membrane materials.

Unfortunately, such high-temperature gas clean-up technologies have not been developed commercially. The gas still needs to be cooled down to about ambient temperature, stripped of the sulfur compounds by one of the conventional solvent processes, and heated back up to above 200°C for the membrane shift reactor. This greatly reduces the efficiency of a power plant (Schlather and Turk, 2007). If maximum CO_2 capture or high efficiency of H_2 production is desired, a low-temperature shift reactor to increase the CO conversion will have to be employed. The typical low-temperature shift catalyst Cu/zinc (Zn), which operates below 300°C, is not sulfur tolerant. The syngas will need to be cooled down for sulfur removal before the shift reactor. Even with the development of sulfur-tolerant low-temperature shift catalysts and membrane materials, sulfur compounds are still present in the CO_2-rich stream from the membrane residue and need to be removed. Therefore, development of high-temperature clean-up technologies is crucially important for the shift reactor, with or without simultaneous H_2 separation, to be added to an IGCC power plant.

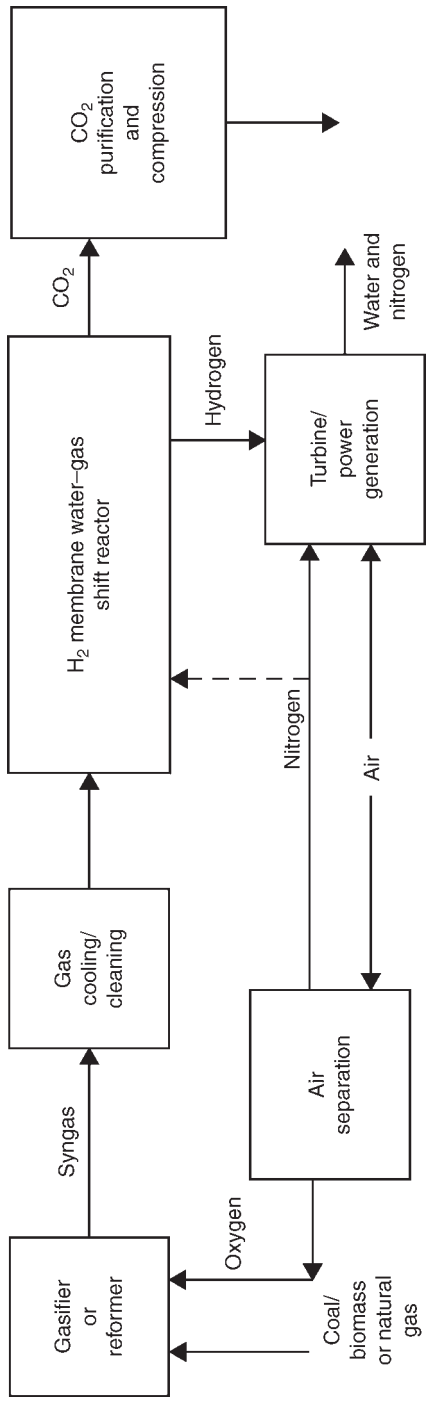
Figures 5.7 and 5.8 assume that turbines are employed for power generation in the power island block. The H_2-rich fuel gas needs to be mixed

© Woodhead Publishing Limited, 2010



5.7 Conceptual diagram for a fossil-fuel power plant with pre-combustion CO_2 capture.

© Woodhead Publishing Limited, 2010



5.8 Conceptual diagram for a fossil-fuel power plant incorporating H_2 membrane shift reactor.

© Woodhead Publishing Limited, 2010

with nitrogen (N_2) to reduce the combustion temperature to within an acceptable range for the turbine blades. Conveniently, the N_2 stream, which is readily available from the front-end air separation plant in the gasification island, can be used as a permeate sweep gas to enhance H_2 permeation for the H_2 membrane. Use of N_2 sweep gas in a counter-current flow pattern (see section 5.3) can potentially increase the H_2 recovery as the driving force can be kept constant throughout the membrane length. This arrangement also overcomes one of the main drawbacks of the membrane separation processes, i.e. low permeate pressure. High-pressure sweep of N_2 can maintain a high pressure on the permeate side of the membrane and avoid expensive recompression of the H_2. However, pure H_2 by-product will not be possible with N_2 sweep in the membrane.

Future power plants will adopt more efficient fuel-cell technologies. Among all fuel cells, the solid oxide fuel cell (SOFC) is probably the most suited to utility power applications, owing to its high-temperature operation (600–1000°C) and less stringent requirement for fuel quality. At the cathode side of the SOFC, oxygen is ionized and transported by the electrolyte to the anode side, where oxygen ions react with H_2 and CO. Unlike turbines, SOFC generates an anode off-gas that is not diluted by the N_2 from air. The CO_2-rich anode exhaust still contains an appreciable amount of H_2 and CO, which needs an after treatment, especially if CO_2 capture is required. Typical treatment options include cryogenic separation, solvent absorption, oxycombustion in a burner, etc. One way to integrate with a H_2 membrane is to use a membrane shift reactor to process the anode off-gas as shown in Fig. 5.9 (Dijkstra and Jansen, 2004; Jansen *et al*., 2004). The permeated H_2 is reacted with the air in the cathode off-gas, which is used as a sweep gas for the membrane reactor.

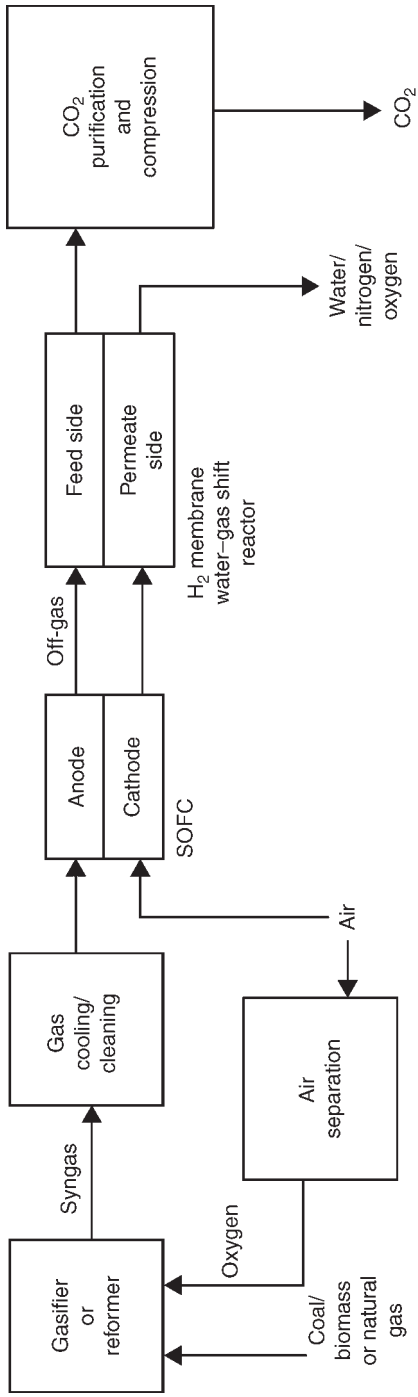
A membrane shift reactor can also be placed before the power island, similar to the arrangement shown in Fig. 5.8. The H_2 permeate stream is sent to the anode side of the fuel cell, and a CO_2-rich stream is captured in the retentate side of the membrane. In the fuel cell, the off-gases from both anode and cathode can be combined in a burner, without any CO_2 in the exhaust gas.

High-temperature membranes have also been proposed to combine with a natural gas reformer to enhance CH_4 conversion and H_2 production (Prabhu *et al*., 2000; Onstot, 2001; Tsura *et al*., 2004). Essentially, a syngas generation reactor is combined with the membrane shift reactor. In addition to the shift reaction, the following two CH_4 conversion reactions take place in the membrane reformer

$$CH_4 + H_2O = CO + 3H_2 - 220\,\text{kJ/mole} \quad [5.5]$$

$$CH_4 + 2H_2O = CO_2 + 4H_2 - 179\,\text{kJ/mole} \quad [5.6]$$

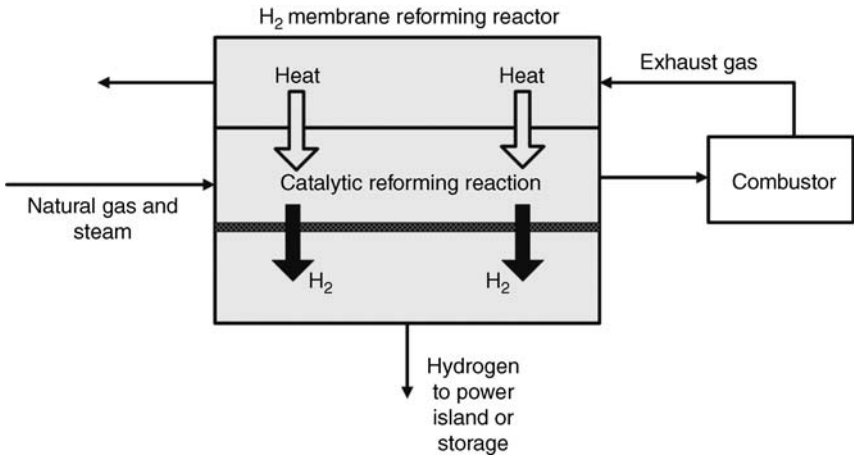
© Woodhead Publishing Limited, 2010



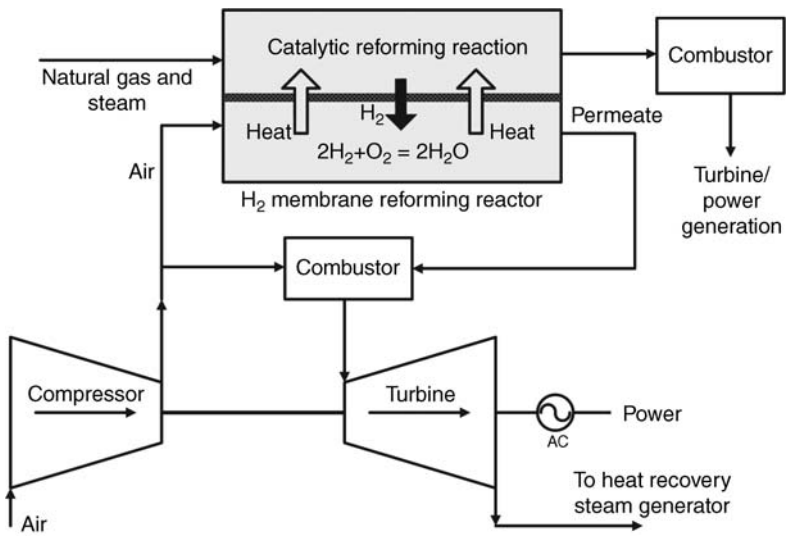
5.9 SOFC power plant incorporating H_2 membrane shift reactor.

© Woodhead Publishing Limited, 2010

If hydrogen is removed while it is being produced in the reformer, the equilibrium will be shifted towards the right-hand sides of the above reactions. As a result, H_2 production and CH_4 conversion will be increased. The H_2 gas in the permeate side can be sent to a gas turbine for power generation or sold as a by-product. The raffinate stream, which contains unconverted CH_4, CO, and H_2 is fed to a burner to supply the heat required for the endothermic reforming reactions, as shown in Fig. 5.10. Another



5.10 Natural gas membrane reformer using hot exhaust gas to supply heat.



5.11 Natural gas membrane reformer using air sweep to supply combustion heat. Adapted from Bredesen *et al.* (2004) and Asen and Andersen (2007).

© Woodhead Publishing Limited, 2010

option is to use air as a sweep gas, where it reacts or burns with the permeated H_2 to generate the combustion heat for the reforming reactions. Figure 5.11 shows one possible layout for this heat-integrated membrane reformer process (Bredesen *et al.*, 2004; Asen *et al.*, 2007). The permeate stream leaving the membrane reformer may still contain H_2 and is burned with part of the air leaving the turbine compressor. The hot exhaust gas then expands through the turbine and eventually enters a heat recovery steam generator.

5.5 Hydrogen storage and transportation

If hydrogen is generated as a by-product in future power plants, it needs to be stored and transported to the point of use. Hydrogen storage systems are also needed at fueling stations or power parks. Further, space-efficient and cost-effective on-board H_2 storage systems will be needed for mobile applications. At present, H_2 can be transported by pipeline or by highway via cylinders, tube trailers, and cryogenic tankers, with a small amount shipped by rail car or barge (US DOE, 2007a). However, these are only limited to a small number of plants for industrial uses. A comprehensive delivery infrastructure for H_2 transportation faces many challenges, mainly in cost and energy efficiency. Even if the technical challenges can be overcome, it would still require massive financial investment to build all the infrastructures.

Hydrogen is an extremely light gas, so it needs to be highly compressed or cooled to liquid form to store and transport the gas effectively. Technologies for compressed H_2 gas and cryogenic H_2 liquid are proven and mature. The compressed H_2 typically reaches 50 to 70 bar, using 6–7% percent of the total energy stored in the H_2 for compression (Wolf, 2003). Much higher pressure, to 700 bar, may be required if a high-pressure H_2 cylinder is to be used for on-board storage. The disadvantage of compressed gas storage is the weight and space required for the tank. On the other hand, the liquefaction of H_2 requires about 30 % of its energy content. However, on a volumetric basis, it can store more energy content than compressed H_2. The boil-off of liquid H_2 is an issue for long-term storage application, and potentially a safety/environmental hazard as well.

One alternative storage/delivery method is to utilize high-energy-density carriers to directly bind the hydrogen atom in a form of chemical compound or feedstock such as natural gas, methanol, ethanol, or other liquids that can be produced, transported, and reformed back to H_2 at the site of use. The other alternative is to use novel materials such as metal hydrides, chemical hydrides, or solid adsorbents to store hydrogen reversibly in either chemisorption or physisorption mode. The novel storage materials are still in a research and development stage, but have received much research

© Woodhead Publishing Limited, 2010

attention recently. While these are mainly directed for on-board application, their future success in improving the volumetric and gravimetric storage efficiency of H_2 will benefit substantially the off-board storage application.

A high-purity H_2 can reduce the cost of H_2 transportation and storage through the reduction of volume without inert or impurities. Proton exchange membrane (PEM) fuel-cell vehicles require very high-quality H_2, down to ppb level of CO and sulfur compounds. Hydrogen produced from a membrane system needs to satisfy these requirements. Alternatively, H_2 can be produced at a low purity, mixed with natural gas, and delivered using the existing pipeline infrastructure. At the site of distribution, H_2 is then separated or purified just prior to dispensing. Membrane can be used for this application, although the cost of this type of separation strategy is not known currently.

In future power plants, H_2 can be produced and stored during the electricity off-peak hours. The ability to store bulk H_2 provides the benefit of peak-shaving for hourly, daily, and seasonal demand variation of electricity. However, the selection of storage will be dictated by economic factors (Taylor *et al*., 1986). At present, H_2 produced centrally as in a fossil fuel power plant most likely will be stored in a steel pressure vessel, which is still quite costly. Development of fiber composite materials for pressure tanks shows promise in reducing the cost (US DOE, 2007c). Hydrogen storage in geologic formations is also an option for bulk H_2 storage, a technology borrowed from natural gas storage under rock caverns (Lindblom, 1985; US DOE, 2007b). Unless H_2 needs to be transported off-site, liquid H_2 storage is not currently a low-cost option. Owing to lack of infrastructure, transportation of H_2 will be more a long-term issue.

5.6 Future trends

Advanced H_2 membrane technologies have the potential to improve the cost and the efficiency of future power plants for H_2 production and/or CO_2 capture. In the near term, the market will be mainly driven by regulations on CO_2 emissions of the power plants, which would require a cost-effective CO_2 capture technology such as H_2 membrane. The notion of central production of H_2 from fossil fuel sources for H_2 filling station applications will be a much longer-term vision. The two somewhat different objectives could affect the process integration schemes for the H_2 membrane systems and ultimately impact the development of the membrane materials. For example, H_2 purity requirement may not be very high if the goal is only to reduce CO_2 emissions of power plants.

High-temperature inorganic membranes will be at the forefront of H_2 membrane material research. The high-temperature capability of inorganic membranes can realize the benefit of process intensification by combining

© Woodhead Publishing Limited, 2010

H_2 separation and chemical reactions such as shift and reforming reactions in a single reactor. Membrane reactor technology not only offers operational simplicity, but it also raises the conversion of reactions and improves the energy efficiency (Drioli, 2004). This unique feature along with the advantages of the membrane reactor is difficult to attain for other separation techniques. However, the conditions encountered in a membrane shift reactor would be quite different from a conventional shift reactor or a H_2 membrane separator. The gas phase is expected to be dominated by CO_2, which may affect the kinetics or even the life span of the catalysts. Membrane selectivity or flux could also be adversely affected in a compositional regime of low H_2. Packaging catalysts in an already complicated membrane module could also add another dimension of complexity and challenge for design engineers. Research into membrane reactor systems, especially integrated with the actual IGCC plant conditions, will receive increasing attention.

Among the inorganic membrane materials for H_2 separation, metallic membranes are projected to reach commercialization first for power plant applications. Research has advanced to non-Pd metal and alloy membranes. The enormous possibilities of alloy constituents and compositions, similar to the polymeric membrane research in the 1980s, will open a new horizon for metal membrane research. Discovery of new surface catalysts of non-Pd type will have a significant benefit in further reducing the membrane cost. Hybrid systems such as the cermet, mixed-matrix membrane are expected to play an increasing role as well.

Improving the membrane stability and durability should be a priority issue for H_2 membranes to be successfully employed in power plants. This would require a robust membrane system design capable of handling coal-derived syngas. Material research should expand beyond the membrane material to include support, sealing, and housing materials. The tolerance of sulfur and other contaminants for the membrane materials and/or shift catalysts needs to be improved. As mentioned earlier, developing gas clean-up technologies operating at temperatures comparable to the membrane shift reactors is an important enabler for the H_2 membranes or the membrane shift reactors to be efficiently integrated in power plants. One novel but ambitious approach is to integrate gas clean-up, shift reaction, and H_2 separation into one step.

Another non-membrane related area that warrants further research is large-scale H_2 storage, which has not received much research attention compared to on-board storage research. Cost-effective H_2 storage adds significant value to power plants in addressing the peak-shaving issue. A system analysis and economic evaluation for an IGCC plant incorporating H_2 membrane and H_2 storage would be a valuable study.

© Woodhead Publishing Limited, 2010

5.7 Sources of further information and advice

There are numerous books and monographs on the subject of membranes. For a general overview of membrane fundamentals and applications, the reader can refer to Mulder (1997) and Baker (2004). For gas separation by polymeric membranes, the latest monograph edited by Freeman *et al*. (2007) provides a good state-of-the-art review. Recently, research on inorganic membrane materials and applications has expanded quite rapidly, especially in the energy and fuel areas. Bose (2008), Mallada and Menendez (2008), Kanellopoulos (2000), Burggraff and Cot (1996), and Hsieh (1996) are excellent references in the field of inorganic membranes. The book by Marcano and Tsotsis (2002) specifically deals with the area of the membrane reactor.

The US Department of Energy (www.energy.gov) has been championing membrane research for many years. Development of novel membranes for separation and purification is included in several key publications: *Hydrogen posture plan* (US DOE and DOT, 2006); *A national vision of America's transition to hydrogen economy–to 2030 and beyond* (US DOE, 2002); *Hydrogen, fuel cells and infrastructure technologies program: Multi-year research, development and demonstration plan* (US DOE, 2007a); and *Hydrogen from coal program* (US DOE, 2007b). The DOE has held annual meetings on merit review and peer evaluation for H_2 projects. Reports and proceedings are available on their website (www.hydrogen.energy.gov/annual_review.html).

The International Energy Association (IEA) has been issuing high-level research reports on a broad range of energy areas. Hydrogen separation research can be found in the greenhouse gas research and development program (www.ieagreen.org.uk) and the hydrogen implementation agreement (www.ieahia.org). The Energy Research Center of the Netherlands (www.ecn.nl/) also supports a strong membrane research program as they focus on pre-combustion CO_2 capture technologies. The North American Membrane Society (www.membranes.org), European Membrane House (www.euromemhouse.com), and European Membrane Society (www.emsoc.eu) regularly organize international conferences on membrane research. Interested readers can go to their websites for lists of conferences and programs.

5.8 References

Adhikari S and Fernando S (2006), 'Hydrogen membrane separation techniques', *Ind. Eng. Chem. Res*., 45, 875–881.

Adler S, Richards R E and Dyer P N (2000), 'Separation of oxygen from oxygen-containing gas', US Patent 6,090,265.

© Woodhead Publishing Limited, 2010

Air Products and Chemicals (1999), 'Advanced prism membrane systems for cost effective gas separations', Prism separators brochure, www.airproducts.com/Products/Equipment/PRISMMembranes/page08.htm.

Al-Rabiah A A, Timmerhaus K D and Noble R D (2001), 'Membrane technology for hydrogen separation in ethylene plants', 6th World Congress of *Chemical engineering*, Melbourne, Australia.

Anderson D H, Evenson IV C R, Harkins T H, Jack D S, Mackay R and Mundschau M V (2008), 'Hydrogen separation using dense composite membranes, Part 2: Process integration and scale-up for H_2 production and CO_2 sequestration', in Bose A, *Inorganic membranes for energy and fuel applications,* New York, Springer, Ch. 9, 241–254, doi:10.1007/978-0-387-34526-0_9.

Armstrong P, Foster T, Bennett D and Stein V (2006), 'ITM oxygen: Scaling up a low cost oxygen supply technology', *Annual Gasification Technologies Conference*, Washington DC, US.

Asen K I and Andersen H S (2007), 'Method for manufacturing a hydrogen and nitrogen containing gas mixture', US Patent 7,163,648.

Athayde A L, Baker R W and Nguyen P (1994), 'Metal composite membranes for hydrogen separation', *J. Membrane Sci.*, 94, 299–311.

Balachandran U, Lee T H, Chen L, Song S J, Picciolo J J and Dorris S E (2005), 'Current status of dense cermet membranes for hydrogen separation', *22nd Annual Pittsburgh Coal Conference,* Pittsburgh, USA.

Balachandran U, Lee T H, Chen L, Song S J, Picciolo J J and Dorris S E (2006), 'Hydrogen separation by dense cermet membranes', *Fuel*, 85, 150–155, doi:10.1016/j,fuel.2005.05.027.

Baker R W (2004), *Membrane technology and applications,* West Sussex, Wiley.

Barbieri G, Brunetti A, Tricoli G and Drioli E (2008), 'An innovative configuration of a Pd-based membrane reactor for the production of pure hydrogen: Experimental analysis of water gas shift', *J. Power Sources*, 182, 160–167, doi:10.1016/j.jpowsour.2008.03.086.

Bose A C (2008), *Inorganic membranes for energy and fuel applications*, New York, Springer.

Bredesen R, Jordal K and Bolland O (2004), 'High-temperature membranes in power generation with CO_2 capture', *Chem. Engng Processing*, 43, 1129–1158.

Burggraff A J and Cot L (1996), *Fundamentals of inorganic membrane science and technology*, Amsterdam, Elsevier.

Buxbaum R E and Kinney A B (1996), 'Hydrogen transport through tubular membranes of palladium-coated tantalum and niobium', *Ind. Engng Chem. Res.*, 35, 530–537.

Buxbaum R E and Marker T L (1993), 'Hydrogen transport through non-porous membranes of palladium-coated niobium, tantalum and vanadium', *J. Membrane Sci.*, 85, 29–38.

Carbo M C, Jansen D, Haije W G and Verkooijen A (2006), 'Advanced membrane reactors for fuel decarbonisation in IGCC: H_2 or CO_2 separation', 5th Annual Conference on *Carbon capture and sequestration*, Alexandria VA, USA.

Caro J and Noack M (2008), 'Zeolite membranes – recent developments and progress', *Microporous Mesoporous Mater.*, 115, 215–233.

Chiappetta G, Clarizia G and Drioli E (2006), 'Design of an integrated membrane

© Woodhead Publishing Limited, 2010

system for a high level hydrogen purification', *Chem. Engng J.* 124, 29–40, doi: 10.1016/j.cej.2006.08.009.

Chiesa P, Kreutz T G and Lozza G G (2007), 'CO_2 sequestration from IGCC power plants by means of metallic membranes', *J. Engng for Gas Turbines and Power*, 129, 123–134, doi: 10.1115/1.2181184.

Costello L M, Walker D R B and Koros W J (1994), 'Analysis of a thermally stable polypyrolone for high temperature membrane-based gas separations', *J. Membrane Sci.* 90, 117–130.

Dijkstra J W and Jansen D (2004), 'Novel concepts for CO_2 capture', *Energy*, 29 1249–1257, doi:10.1016/j.energy.2004.03.084.

Diniz da Costa J C, Lu G Q, Rudolph V and Lin Y S (2002), 'Novel molecular sieve silica (MSS) membranes: characterization and permeation of single-step and two-step sol-gel membranes', *J. Membrane Sci.*, 198, 9–21.

Doong S J, Ong E and Lau F (2005), 'Direct extraction of hydrogen from coal using a membrane reactor integrated with a gasifier' *22nd Annual Pittsburgh Coal Conference*, Pittsburgh, USA.

Dorris S E, Lee T H and Balachandran U (2003), 'Metal/ceramic composites with high hydrogen permeability', US Patent 6,569,226 B1.

Drioli E (2004), 'Membrane reactors', *Chem. Engng Processing*, 43, 1101–1102, doi:10.1016/j.cep.2004.04.002.

Edlund D and McCarthy J (1995), 'The relationship between intermetallic diffusion and flux decline in composite-metal membranes: implications for achieving long membrane lifetime', *J. Membrane Sci.*, 107, 147–153

EPRI and NETL (2000), 'Evaluation of innovative fossil fuel power plants with CO_2 removal', Technical Report 1000316, Palo Alto, EPRI and Pittsburgh. NETL.

Freeman B, Yampolskii Y and Pinnau I (2007), *Materials science of membranes for gas and vapor separation*, West Sussex, Wiley.

Gao H, Lin Y S, Li Y and Zhang B (2004), 'Chemical stability and its improvement of palladium-based metallic membranes', *Ind. Engng Chem. Res.*, 43, 6920–6930, doi:10.1021/ie049722f.

Gary D and Tomlinson G (2002), 'Hydrogen from coal', Mitretek Technical Report, MTR 2002-31, DOE Contract DE-AM26-99FT40465.

Gielen D (2003), 'The future role of CO_2 capture and storage: Results of the IEA–ETP model', International Energy Agency Working Paper, EET/2003/04, Paris.

Gottzmann C F, Prasad R, Schwartz J M, Bergsten V E, White J E, Mazanec T J, Cable T L and Fagley J C (2000), Tube and shell reactor with oxygen selective ion transport ceramic reaction tubes, US Patent 6,139,810.

Hamakawa S, Lin L, Li A and Iglesia E (2002), 'Synthesis and hydrogen permeation properties of membranes based on $SrCeYbO_3$ thin films', *Solid State Ionics*, 48, 71.

Hashi K, Ishikawa K, Matsuda T and Aoki K, (2005), 'Hydrogen permeation characteristics of (V,Ta)-Ti-Ni alloys', *J. Alloys and Compounds*, 404–406, 273–278, doi:10.1016/j.jallcom.2005.02.085.

Hong M, Falconer J L and Noble R D (2005), 'Modification of zeolite membrane for H_2 separation by catalytic cracking of methyldiethoxysilane', *Ind. Engng Chem. Res.*, 44, 4035–4041.

© Woodhead Publishing Limited, 2010

Howard B H, Killmeye R P, Rothenberger K S, Cugini A V, Morreale B D, Enick R M and Bustamante F (2004), 'Hydrogen permeance of palladium–copper alloy membranes over a wide range of temperatures and pressures', *J. Membrane Sci.*, 241, 207–218, doi:10.1016/j.memsci.2004.04.031.

Hsieh H P (1996), *Inorganic membranes for separation and reaction*, Amsterdam, Elsevier

Ismail A F and David L I B (2001), 'A review on the latest development of carbon membranes for gas separation', *J. Membrane Sci.*, 193, 1–18.

Iwahara H, Esaka T, Uchida H and Maeda N (1981), 'Proton conduction in sintered oxides and its application to steam electrolysis for hydrogen production', *Solid State Ionics*, 3/4, 359.

Jansen D, Pex P P A C, Dijkstra J W and Kluiters S C A (2004), 'Membrane reactors; key technology for production of de-carbonized energy carriers', 7th International Conference on *Greenhouse gas control technologies*, Vancouver, Canada.

Jha P and Way J D (2008), 'Carbon dioxide selective mixed-matrix membranes formulation and characterization using rubbery substituted polyphosphazene', *J. Membrane Sci.*, 324, 151–161.

Jones C W and Koros W J (1994), 'Carbon molecular sieve gas separation membranes – I. Preparation and characterization based on polyimide precursors', *Carbon*, 32, 1419–1425.

Judkins R and Bischoff B (2005), 'Scale-up of microporous inorganic hydrogen-separation membrane', *22nd Annual Pittsburgh Coal Conference*, Pittsburgh, USA.

Kamakoti P, Morreale B, Ciocco M, Howard B, Killmeyer P, Cugini A and Sholl D (2005), 'Prediction of hydrogen flux through sulfur-tolerant binary alloy membranes', *Science*, 37, 569–573.

Kanellopoulos N K (2000), *Recent advances in gas separation by microporous ceramic membranes*, Amsterdam, Elsevier.

Kanezashi M, O'Brien-Abraham J, Lin Y S and Suzuki K (2008), 'Gas Permeation through DDR-type zeolite membranes at high temperatures', *AIChE J.*, 54(6), 1478–1486.

Kluiters S C A (2004), 'Status review on membrane systems for hydrogen separation', ECN-C-04-102, Petten, The Netherlands, Energy Center of the Netherlands.

Koros W J and Fleming G K (1993), 'Membrane-based gas separation', *J. Membrane Sci.*, 83, 1–80.

Lee D and Oyama S T (2002), 'Gas permeation characteristics of a hydrogen selective supported silica membrane' *J. Membrane Sci*, 210, 291–306.

Lin Y S (2001), 'Microporous and dense inorganic membranes: current status and prospective', *Separation and Purification Technol.,* 25, 39–55.

Lindblom U E (1985), 'A conceptual design for compressed hydrogen storage in mined caverns', *Int. J. Hydrogen Energy,* 10, 667–675.

Liu P (2005), 'Hydrogen production via a commercially ready inorganic membrane reactor', US DOE Annual Hydrogen Program Review Meeting, Washington DC.

Ma Y H (2008), 'Composite Pd and Pd/alloy membranes', in Bose, A. *Inorganic*

© Woodhead Publishing Limited, 2010

membranes for energy and fuel applications, New York, Springer, Ch. 13, 241–254, doi:10.1007/978-0-387-34526-0_13.

Ma Y H, Akis B C, Ayturk M E, Guazzone F, Engwall E E and Mardilovich I P (2004), 'Characterization of intermetallic diffusion barrier and alloy formation for Pd/Cu and Pd/Ag porous stainless steel composite membranes', *Ind. Engng Chem. Res.*, 43, 2936–2945.

MacLean D L, Bollinger W A, King D E and Narayan R S (1986), 'Gas separation design with membranes; in Li, N. N. and Calo, J. M. *Recent development in separation science*, Vol. IX, Boca Raton, CRC Press, FL, USA, Ch. 12, 227–244.

Mahajan R and Koros W J (2000), 'Factors controlling successful formation of mixed-matrix gas separation materials', *Ind. Engng Chem., Res.*, 39, 2692–2696, doi: 10.1021/ie990799r.

Mallada R and Menendez M (2008), *Inorganic membranes: Synthesis, characterization and applications*, Amsterdam, Elsevier.

Marcano J G S and Tsotsis T T (2002), *Catalytic membrane and membrane reactors*, Weinheim, Wiley-VCH.

McBride R B and McKinley D L (1965), 'A new hydrogen recovery route', *Chem., Engng, Prog.*, 61 (March), 81–85.

McCool B G, Xomeritakis G and Lin Y S (1999), 'Composition control and hydrogen permeation characteristics of sputter deposited palladium–silver membranes', *J. Membrane Sci.*, 161, 67–76.

Morreale B D, Ciocco M V, Howard B H, Killmeyer R P, Cugini A V and Enick R M (2004), 'Effect of hydrogen-sulfide on the hydrogen permeance of palladium–copper alloys at elevated temperatures', *J. Membrane Sci.*, 241, 219–224, doi:10.1016/j.memsci.2004.04.033.

Moss T S, Peachey N M, Snow R C and Dye R C (1998), 'Multilayer metal membranes for hydrogen separation', *Int. J. Hydrogen Energy,* 23, 99–106.

Mulder M (1997), *Basic principles of membrane technology*, Dordrecht, Kluwer.

Mundschau, M. V. (2005), 'Hydrogen transport membranes', US Patent 6,899,744 B2.

Mundschau M V, Xie X, Evenson IV C R and Sammells A F (2005a), 'Membranes for the purification of hydrogen produced from coal-derived water–gas shift mixtures', *22nd Annual Pittsburgh Coal Conference*, Pittsburgh, USA.

Mundschau M V, Xie X and Sammells A F (2005b), 'Hydrogen transport membrane technologies for simultaneous carbon dioxide capture and hydrogen separation in a membrane shift reactor', in Thomas, D. C. and Benson, S. M. *Carbon dioxide capture for storage in deep geologic formation*, Vol. 1, Amsterdam, Elsevier, Ch. 16, 291–306.

Mundschau M V, Xie X, Evenson IV C R and Sammells A F (2006), 'Dense inorganic membranes for production of hydrogen from methane and coal with carbon dioxide sequestration', *Catalysis Today*, 118, 12–23, doi: 10.1016/j.cattod.2006.01.042.

Nam S-E and Lee K-H (2001), 'Hydrogen separation by Pd alloy composite membranes: introduction of diffusion barrier', *J. Membrane Sci.*, 192, 177–185.

Norby T (2007), 'Ceramic proton and mixed proton–electron conductors in

© Woodhead Publishing Limited, 2010

membranes for energy conversion applications', *J. Chem. Engng Jap.*, 40, 1166–1171.

Norby T and Larring Y (2000), 'Mixed hydrogen ion–electronic conductors for hydrogen permeable membranes', *Solid State Ionics*, 136–137, 139–148.

Onstot W J, Minet R G and Tsotsis T T (2001), 'Design aspects of membrane reactors for dry reforming of methane for the production of hydrogen'. *Ind. Engng Chem. Res.*, 40, 242–251.

Orme C J, Stone M L, Benson M T and Peterson E S (2003), 'Testing of polymer membranes for the selective permeability of hydrogen', *Separation Sci. Technol.*, 38, 3225–3238, doi:10.1081/SS-120022595.

Ozaki T, Zhang Y, Komaki M and Nishimura C (2003), 'Hydrogen permeation characteristics of V–Ni–Al alloys', *Int. J. Hydrogen Energy,* 28, 1229–1235.

Parsons (2002), 'Evaluation of fossil fuel power plants with CO_2 recovery', Final Report, DOE Contract No. DE-AM26-99FT40465.

Pesiri D R, Jorgensen B and Dye R C (2003), 'Thermal optimization of polybenzimidazole meniscus membranes for the separation of hydrogen, methane, and carbon dioxide', *J. Membrane Sci.*, 218, 11–18, doi:10.1016/S0376-7388(03)00129-7.

Phair J W and Donelson R (2006), 'Development and design of novel (non-palladium-based) metal membranes for hydrogen separation', *Ind. Engng Chem. Res.*, 45, 5657–5674, doi:10.1021/ie051333d.

Prabhu A K, Liu A, Lovell L G and Oyama S T (2000), 'Modeling of the methane reforming reaction in hydrogen selective membrane reactors', *J. Membrane Sci.*, 177, 83–95.

Qi X and Lin Y S (2000), 'Electrical conduction and hydrogen permeation through mixed proton–electron conducting strontium cerate membranes', *Solid State Ionics*, 130, 149.

Rautenbach R and Dahm W (1987), 'Gas permeation – module design and arrangement', *Chem. Engng Process*, 21, 141–150.

Rezac M E, Koros W J and Miller S J (1995), 'Chemical stability of polyimide membranes at temperature near Tg', *J. Appl. Polymer Sci.*, 58, 165–170, doi:10.1002/app.1995.070580118.

Roa F, Block M J and Way J D (2002), 'The influence of alloy composition on the H_2 flux of composite Pd–Cu membranes', *Desalination*, 147, 411–416.

Ryi S-K, Park J-S, Kim S-H, Cho S-H and Kim D-W (2006), 'The effect of support resistance on the hydrogen permeation behavior in Pd–Cu–Ni ternary alloy membrane deposited on a porous nickel support', *J. Membrane Sci.*, 280, 883–888, doi:10.1016/j.memsci.2006.03.007.

Saufi S M and Ismail A F (2004), 'Fabrication of carbon membranes for gas separation – a review', *Carbon*, 42, 241–259, doi:10.1016/j.carbon.2003.10.022.

Schlather J and Turk B (2007), 'Comparison of a new warm-gas desulfurization process versus traditional scrubbers for a commercial IGCC power plant', *Annual Gasification Technologies Conference*, Washington, DC.

Shu J, Grandjean B P A, van Neste A and Kaliaguine S (1991), 'Catalytic palladium–based membrane reactors: a review', *Can. J. Chem. Engng*, 69, 1036–1060.

Taylor J B, Alderson J E A, Kalyanam K M, Lyle A B and Phillips L A (1986),

© Woodhead Publishing Limited, 2010

'Technical and economic assessment of methods for the storage of large quantities of hydrogen', *Int. J. Hydrogen Energy,* 11, 5–22.

Thompson D F (1991), 'Ceramic honeycomb structures as oxygen separators or concentrators', US Patent 5,034,023.

Tong J, Su L, Kashima Y, Shirai R, Suda H and Matsumura Y (2006), 'Simultaneously depositing Pd–Ag thin membrane on asymmetric porous stainless steel tube and application to produce hydrogen from steam reforming of methane', *Ind. Engng Chem. Res.,* 45, 648–669.

Tosti S, Adrover A, Abasile A, Camilli V, Chiappetta G and Violante V (2003), 'Characterization of thin wall Pd–Ag rolled membranes', *Int. J. Hydrogen Energy,* 28, 105–112.

Tosti S, Basile A, Bettinali L, Borgognoni F, Gallucci F and Rizzello C (2008), 'Design and process study of Pd membrane reactors', *Int. J. Hydrogen Energy,* 33, 5098–5105, doi:10.1016/j.ijhydene.2008.05.031.

Tsura T, Yamaguchi K, Yoshioka T and Asaeda M (2004), 'Methane steam reforming by microporous catalytic membrane reactors', *AIChE J.*, 50(11), 2794–2805.

Uemiya S, Sato N, Ando H and Kikuchi E (1991), 'The water gas shift reaction assisted by a palladium membrane reactor', *Ind. Engng Chem. Res.,* 30, 585–589.

US DOE (2002), *A national vision of America's transition to hydrogen economy–to 2030 and beyond*, Washington DC.

US DOE and DOT (2006), *Hydrogen posture plan: An integrated research, development and demonstration plan*, Washington DC.

US DOE (2007a), *Hydrogen, fuel cells and infrastructure technologies program: Multi-year research, development and demonstration plan*, Washington DC.

US DOE (2007b), *Hydrogen from coal program: Research, development, and demonstration plan*, Washington DC.

US DOE (2007c), 'Low cost, high efficiency, high pressure hydrogen storage', *Ann. Prog. Rep.*, 608–610.

Wei C C, Chen O Y, Liu Y and Li K (2008), 'Ceramic asymmetric hollow fiber membranes–One step fabrication process', *J. Membrane Sci.*, 320, 191–197, doi:10.1016/j.memsci.2008.04.003.

White J H, Schwartz M and Sammells F (2001), 'Solid state proton and electron mediating membrane and use in catalytic membrane reactors', US Patent 6,281,403 B1.

Wolf J (2003), 'Hydrogen infrastructure: from production to the tank. The new developments of the technology', *Linde Technol.*, 2, 20–24.

Xie X, Evenson IV C R, Mundschau M V, Wright H A and Grimmer P J (2006), 'High-pressure operation of dense hydrogen transport membranes for pure hydrogen production and simultaneous CO_2 capture', *23rd Annual Pittsburgh Coal Conference*, Pittsburgh, USA.

Yang J Y, Nishimura C and Komaki M (2008), 'Hydrogen permeation of $Pd_{60}Cu_{40}$ alloy covered V–15Ni composite membrane in mixed gases containing H_2S', *J. Membrane Sci.*, 309, 246–250, doi:10.1016/j.memsci.2007.10.036.

Yoshino Y, Suzuki T, Nair B N, Taguchi H and Itoh N (2005), 'Development of tubular substrates, silica based membranes and membrane modules for

© Woodhead Publishing Limited, 2010

hydrogen separation at high temperature', *J. Membrane Sci.*, 267, 8–17, doi:10.1016/j.memsci.2005.05.020.

Zimmerman C M, Singh A and Koros W J (1997), 'Tailoring mixed matrix composite membranes for gas separations', *J. Membrane Sci.*, 137, 145–154.

© Woodhead Publishing Limited, 2010

6

Advanced carbon dioxide (CO_2) gas separation membrane development for power plants

A. BASILE, Italian National Research Council, Italy;
F. GALLUCCI, University of Twente, The Netherlands;
P. MORRONE, University of Calabria, Italy

Abstract: In this chapter carbon dioxide (CO_2) separation from power plant flue gases through membranes will be discussed. The performances of membrane systems (permeation characteristics, stability, and so on) will be discussed with particular attention to the membrane materials available and membrane modules. An example of membrane design for integration in power plants will be given. Even though membrane systems are not yet applied industrially for such separation, the advances in the field make membranes very attractive for application in the near future. Some consideration of material costs will also be given at the end of the chapter.

Key words: CO_2 separation, membranes, membrane modules, modelling, plant design.

6.1 Introduction

As is well known, the large amount of anthropogenic carbon dioxide (CO_2) emissions is growing rapidly as the world's economy expands. For reducing CO_2 emissions into the atmosphere, three strategies are available (Gessinger, 1997): (i) energy intensity reduction; (ii) carbon intensity reduction; (iii) improvements in the sequestration of CO_2.

The first strategy requires efficient use of energy, whereas the second needs the use of non-fossil fuels, such as hydrogen (H_2) or renewable sources. The last option will be considered in this chapter and is related to the development of technologies for efficiently capturing and sequestering CO_2.

According to Carapellucci and Milazzo (2003) fossil-fuelled power plants are the largest contributor to CO_2 emissions (33–40% of the total CO_2

© Woodhead Publishing Limited, 2010

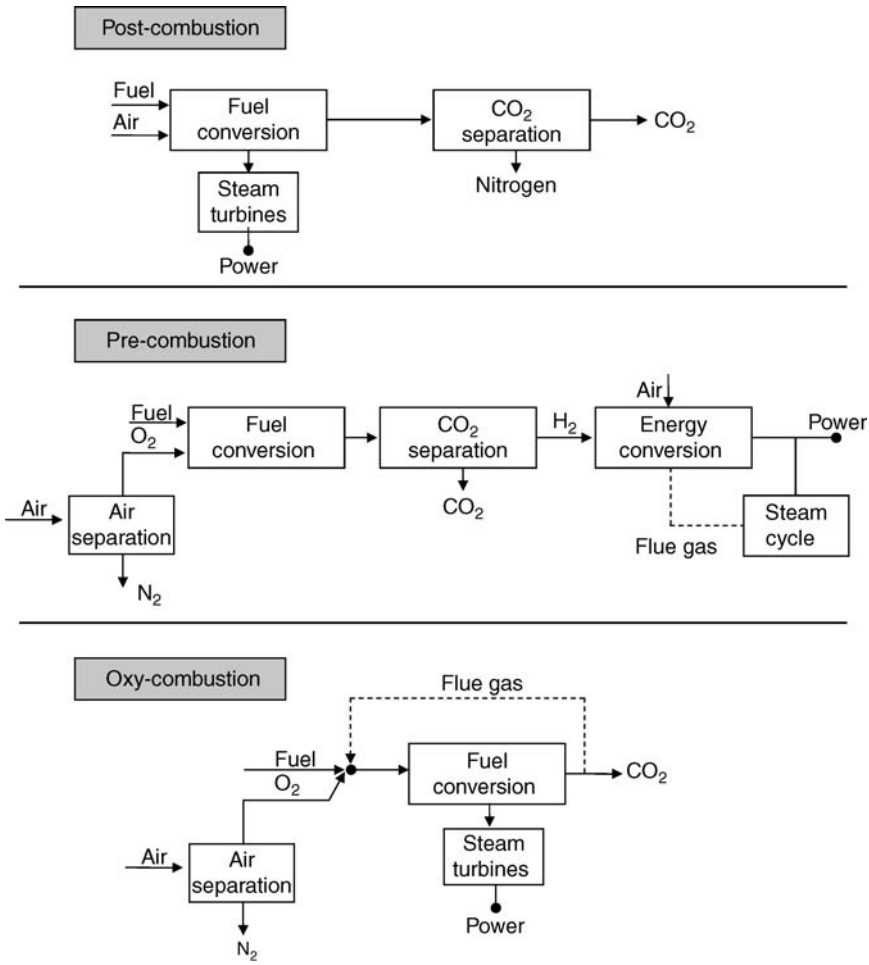
emitted in the atmosphere), so CO_2 must be separated and captured from the flue gas of these point sources before direct sequestration. However, sequestration of CO_2 must be considered a mid-term solution to be used only until H_2 or renewable energy technologies are considered mature enough to be industrially exploited.

Many papers and also many excellent reviews have recently been published on the current status of carbon capture and storage technologies (e.g. Meisen and Shuai; 1997; Chiesa *et al.*, 2005; Figueroa *et al.*, 2008; Gibbins and Chalmers, 2008; Pennline *et al.*, 2008; Yang *et al.*, 2008). In these papers it is clear that CO_2 separation and capture processes can be mainly divided into three technological pathways: post-combustion processes, pre-combustion processes, and oxy-fuel combustion power cycles. There are many emerging technologies under study, such as chemical-looping combustion, that show an interesting reduction in the complexity of the separation of CO_2 from a gas stream (for details see, for example, Rydén and Lyngfelt (2006)), as well as membrane gas separation for CO_2 removal in power generation (Dijkstra and Jansen, 2004; Kaldis *et al.*, 2004; Ho *et al.*, 2006; Mundschau *et al.*, 2006; Tarun *et al.*, 2007).

Each one of these pathways could benefit from integration of membranes into the power plants. To understand better the use of membranes in the three technological pathways, some details regarding the principles of the three main CO_2 capture options are given. Figure 6.1 shows the conceptual scheme of the three main CO_2 capture options.

- *Post-combustion capture*: CO_2 is separated from other flue gas constituents (such as nitrogen (N_2), nitrogen oxide (NO_x) and sulfur dioxide (SO_2)) either originally present in the air or produced during combustion. For combustion, existing power plants use air (composed of almost four-fifths N_2) and produce a flue gas at atmospheric pressure having a CO_2 concentration less than 15%. Thus the driving force for CO_2 capture is low: typically less than 0.15 atm. The main traditional technique used to perform the post-combustion capture is via chemical absorption, for example absorption with monoethanolamine (MEA). This technique, widely used in the natural gas industry for more than 60 years, is able to produce a relatively pure CO_2 gas stream. As a solvent of CO_2, amines are available in three forms (primary, secondary, and tertiary), each one with advantages and disadvantages. In fact, this technology suffers from a number of problems: (i) capital costs are high; (ii) the operation is complex and usually requires full-time supervision; (iii) maintenance is expensive and labour-intensive. The installation of membrane plants using CO_2 selective cellulose acetate membranes began around 1980, mainly at small gas processing plants (less than 6000 N m^3/h, where amine systems are too complex and expensive). So, there is still

© Woodhead Publishing Limited, 2010



6.1 Principles of three main CO_2 capture options.

room for improvements. Research is mainly focused on improving the performance of the membranes by increasing their selectivity and permeability and also decreasing their cost (Falk Paterson *et al.*, 2000).

- *Pre-combustion capture*: for gasification or reforming processes, CO_2 is removed from the fuel before the combustion. In fact, fuels are first converted into a mixture of CO_2 and H_2 via a natural gas reforming process, or into a mixture of CO and H_2 via a coal gasification process followed by the shift reaction. Traditionally, chemical processes (such as MEA absorption) or physical processes (such as pressure swing adsorption) are used to capture CO_2. New technologies are also being studied and these all fall within the process categories of wet scrubbing

© Woodhead Publishing Limited, 2010

Table 6.1 An overview of the three CO_2 separation and capture processes (after Figueroa, 2008)

Process	Type of power plant	CO_2 capture method	Advantages	Disadvantages	Other considerations
Post-combustion	• Natural gas-fired combined cycle • Coal-fired steam power plant • IGCC	Chemical or physical solvents scrubbing Membranes	• Applicable to the majority of existing coal-fired power plants • Retrofit technology option	Flue gas is diluted in CO_2 at ambient pressure resulting in: • low CO_2 partial pressure • CO_2 produced at low pressure compared to sequestration requirements • higher circulation volume required for high capture levels	• Low-temperature process • Production of relatively pure CO_2 stream • Both chemical and physical absorption are mature technologies
Pre-combustion	• Natural gas-fired combined cycle with partial oxidation or with methane steam reforming and subsequent WGS reaction • Oxygen-blown IGCC with WGS reactor	Chemical or physical solvents scrubbing Membranes	Synthesis gas is concentrated in CO_2 at high pressure and so results in: • high CO_2 partial pressure • high driving force for separation • more technologies available for separation	• Applicable mainly to new plants, as only few plants are now in operation • Barriers to commercial application of gasification are common to pre-combustion capture: – availability – cost of equipment – extensive supporting system requirements	• Technology for CO_2 capture similar to post-combustion processes but smaller in size, potentially less expansive than post-combustion processes • IGCC power plants applying this process are more efficient than pulverised-coal-fired plants • Both chemical and physical absorption are mature technologies
Oxy-fuel combustion power cycles	• O_2/CO_2 combustion in natural gas-fired combined cycle with exhaust gas recirculation • O_2/CO_2 combustion of coal with exhaust gas recirculation • Chemical looping combustion	Condensing of water in the exhaust gases, remaining dry gas consists mainly of CO_2.	• Very high CO_2 concentration in flue gas • Retrofit and repowering technology option	• Large cryogenic O_2 production requirement may be cost prohibitive • Cooled CO_2 recycle required to maintain temperatures within limits of combustor materials • Decreased process efficiency • Added auxiliary load	• Oxygen from air separation unit • The exhaust stream is free of N_2, sulfur components, and particulates. Exhaust gas stream is about 90% CO_2 (vol) on a dry basis. Further sequestration of CO_2 is not necessary and CO_2 can be compressed for storage or transportation • The main advantage is the elimination of NO_x control equipment and the CO_2 separation step • Boiler size and SO_2 scrubber are reduced • The technology is not yet considered mature

© Woodhead Publishing Limited, 2010

with physical sorption, chemi- or physisorption with solid sorbents. Membranes can also be applied for this separation (Elwell and Grant, 2006). Except for membranes, all these techniques must be regenerable.

- *Oxy-fuel combustion* power cycles: the fuel is burned in an O_2 stream that contains no (or little) N_2. In fact, O_2 is used as a fuel oxidising agent instead of air. In these plants, the main separation step is O_2 from N_2: pure O_2 is first separated from air and then sent to the energy conversion unit. The combustion takes place in an environment of O_2/CO_2 mixture and the resulting flue gas is a high-purity CO_2 stream. Although some experience with O_2 fuel combustion in the glass, steel, and aluminium industries is well known, the oxy-fuel concept has not yet been applied to large power plants. For example, when pulverised-coal-fired power plants are considered, this option could not be considered to be viable for implementation in the short term. Also, here, membranes can be applied to the separation of O_2 from air, but this type of membrane will not be discussed in this chapter.

Some important aspects of these three processes are summarised in Table 6.1. Pre- and post-combustion processes as well as oxy-fuel combustion power cycles all give a significant reduction in thermal efficiency, and both material and operative costs for a power plant based on these processes would be quite high. Membranes can be applied in all the processes considered.

In this chapter the attention will be largely devoted to a discussion of the different membrane materials available and under investigation for CO_2 separation/capture. Some details regarding the preparation of these membranes and the module design will be given. Furthermore, the performances of membrane separation systems will be discussed and modelling work will also be presented. It has to be pointed out that membranes are currently under study for this separation, but not yet commercially available. On the other hand, advances in membrane performance, as well as the great economic efforts in this field (in terms of research projects, also discussed in the chapter), mean that these membrane systems are expected to be of great importance and wide application in the near future.

For capture based on membrane separation, both polymeric and inorganic membranes can be used to produce clean gas from a mixture gas (from coal gasification or steam methane reforming processes). Inorganic membranes are very attractive for CO_2 removal in integrated gasification combined-cycle (IGCC) power plants as well, owing to their simplicity, flexibility, ability to maintain high CO_2 pressure, and their potential to perform separations at low energy penalties. However, the costs of inorganic membranes are very high and no commercially available gas

© Woodhead Publishing Limited, 2010

separation inorganic membranes are yet present on the market. On the other hand, gas separation using polymeric membranes is today commercially available. Nevertheless, CO_2 capture in large-scale power production still suffers from inadequate performance when polymeric membranes must be used. In fact, syngas is delivered at pressures and temperatures that depend on the type of fuel processor used, and the integration of polymeric membranes requires the cooling of the flue gases because of their lack of high-temperature stability. Moreover, polymeric membranes also show inadequate performance in terms of both permeability and actual selectivities, which are lower because of plasticisation effects (Carapellucci and Milazzo, 2003).

6.2 Performance of membrane system

Gas separation using membranes is a highly attractive energy-efficient technique for CO_2 capture (Basu *et al.*, 2004; Abertz *et al.*, 2006). A membrane is a physical device able to remove selectively one or more components in a mixture while rejecting others. Membrane gas separation shows different advantages over conventional processes and has been well described in many excellent reviews. See, for example, Maier (1998), Koros (2002), and Stern (2002).

The concept of membrane separation was first used in 1748 by Nollet (1748), whereas, in 1831, Mitchell (1831) first reported that different gases permeated through rubber membranes and that the flux of each gas was different. Later, Graham (1861) discovered H_2 penetration through palladium and gas diffusion through ceramic membranes. One century later, Loeb and Sourirajan (1962) developed the first anisotropic membrane.

Initially, membrane separation research was directed mainly towards reverse osmosis, which is extensively covered in the patent literature. In the last 30 years, great progress has been observed in the separation of gases by membrane technology. In fact, the first successful commercialisation of gas separation membranes for hydrogen recovery was realised in 1977 by Monsanto/Permea (Koros, 1991) followed later by Cynara, Separex, and Generon (Spillman, 1989; Koros, 1991). During the 1980s and 1990s, these commercialisations also led to substantial innovations in membrane materials, which improved both gas separation efficiency and membrane lifetime. Finally, membrane gas separation became commercially competitive with existing separation technologies. Membrane separation processes are used today in bulk chemistry as well as the petrochemical industrial sectors.

Membranes offer several advantages such as their small size, simplicity of operation and maintenance, compatibility and diversity, and no production of pollutant by-products. Today, the main membrane separation techniques

© Woodhead Publishing Limited, 2010

are: reverse osmosis, nano-, ultra-, and microfiltration, pervaporation, gas separation, vapour permeation, and electrodialysis. In particular, the 'standard' membrane processes (reverse osmosis, nano-, ultra-, and microfiltration) are now reasonably commonplace in the majority of chemical sectors (Sutherland, 2008). On the other hand, gas separation membranes are used in many industrial processes, such as in the production of air enriched with O_2, separation of CO_2 and water (H_2O) from natural gas, purification of H_2, and so on. Different reviews and books can be found in the literature describing these aspects (Koros, 1991; Osada and Nakagawa, 1992; Paul and Yampol'skii, 1994; Baker, 2002; Basu *et al.*, 2004).

In 1992, studying the application of polymeric membranes for recovering CO_2 from a flue gas of a power plant, Feron *et al.* (1992) and Van Der Sluijs *et al.* (1992) showed that up to 76% of CO_2 removal is achievable and, moreover, that the economic competitiveness of the process depends on the membrane used, in particular, on its selectivity to the gas transport. Before going into details on these aspects, and in order to better understand how a membrane works, a brief description of the principle of gas separation is now presented. A deeper discussion could be found, for example, in O'Stern (2002), Paul and Yampol'skii (1994), and Maier (1998).

In separating one or more gases from a feed mixture and generating a specific gas-rich permeate, a membrane acts as a 'filter' that allows the preferential passage of certain substances. In particular, a membrane will separate gases only if some components of the mixture are able to pass through the membrane more rapidly than others. In other words, the flux of the gas to be separated should be higher with respect to all the others (under the same conditions). The flux of a specific gas through the membrane under a pressure difference is called permeability (P). It is related to both the diffusivity coefficient (D, which measures the mobility of the molecules within the membrane) and solubility coefficient (S, which measures the solubility of gas molecules within the membrane), whereas the ability of the membrane selectively to transport one gas species and not another is called perm-selectivity (α). The relationship between permeability, diffusivity, and solubility for a generic component i is described by

$$P_i = D_i \cdot S_i \qquad [6.1]$$

For ideal gases, the permeability is related to the gas permeation rate (Q_i) through the membrane, the surface area (A) of the membrane, the thickness (l) of the membrane and the driving force for separation, the pressure difference across the membrane (Δp)

$$P_i/l = Q_i/(A \cdot \Delta p) \qquad [6.2]$$

© Woodhead Publishing Limited, 2010

The ideal perm-selectivity (α) of gas i over another gas, j, is defined as

$$\alpha_{i/j} = P_i/P_j \quad [6.3]$$

It should be stressed that it is generally not possible to predict the mass transport behaviour of a mixture starting from single component measurements. Future research on gas and vapour mixture separation is of great importance, because the separation efficiency of the membrane for practical applications is a crucial parameter.

The ideal perm-selectivity is convenient because in the absence of strong interactions between the permeating gases, the permeability coefficients of the pure gases can be used. In the case of mixtures, strong interactions between the permeating components are generally present, and so another parameter is more important for the design of a membrane plant: the separation factor, SF. For a binary mixture it is defined as

$$\mathrm{SF}_{i/j} = (Y_i/Y_j)/(X_i/X_j) \quad [6.4]$$

where Y and X are the molar concentrations in the permeate and feed sides, respectively, and the subscripts i and j refer to the two components in the mixture. During experiments, both X_i and X_j are fixed by the experimental conditions, whereas Y_i and Y_j must be determined by gas chromatography or mass spectrometry. The separation factor is defined to be always > 1 and depends on the experimental conditions, such as pressure difference or the absolute pressure of the supplied gas.

Membranes can be separated into two types: porous and non-porous (or dense) membranes. Porous membranes separate gases based on molecular size by small pores in the membrane. More common for gas separation, membranes used (for example) in natural gas applications are non-porous or asymmetric membranes. These membranes separate on the basis of solubility and diffusivity. For both porous and non-porous membranes there are many possible separation mechanisms, but only five of them are considered the most important for gas separation through membranes: Knudsen diffusion, molecular sieving, surface diffusion, capillary condensation, and solution–diffusion separation (Spillman, 1989; Fritzsche and Kurz, 1990; Paul and Yampol'skii, 1994; Gallucci and Basile, 2009). Among these, molecular sieving and solution–diffusion are the main mechanisms for nearly all gas-separating membranes.

In dense membranes, the gas transport is based on a solution–diffusion mechanism and results in a selective transport of gases and in their separation. In porous membranes, other mechanisms take place. Knudsen separation is based on gas molecules passing through membrane pores small enough to prevent bulk diffusion: the separation is based on the difference in the mean path of the gas molecules due to collisions with the pore walls,

© Woodhead Publishing Limited, 2010

Table 6.2 Molecular weight (Da) and kinetic diameter (Å) of some gases (kinetic diameter can be understood as the diameter of a pore needed to let that specific molecule pass)

Molecule	Molecular weight: Da	Kinetic diameter: Å
H_2	2	2.89
H_2O	18	2.65
N_2	28	3.64
O_2	32	3.46
CO_2	44	3.30

which is related to the molecular weight (see Table 6.2). Specifically, the selectivity for any gas pair is equal to the inverse ratio of the square root of their molecular weight. For example, for CO_2/N_2 separation, Knudsen diffusion predicts a selectivity of 0.8. This type of diffusion process does not provide sufficient separation in most instances, although the technique has been successfully used in the large-scale separation of uranium isotopes.

Molecular sieving separates gas mixtures on the basis of size exclusion and so is potentially useful in separating molecules of different sizes. The diffusion of smaller gases happens at a much faster rate than larger gas molecules and thus CO_2/N_2, selectivity is greater than 1, as CO_2 has a smaller kinetic diameter than N_2. Molecules adsorb to the surface of the pore walls of membranes in surface diffusion (Bredesen *et al.*, 2004). The level of interaction between the adsorbed gases and pore surface determines the rate of surface diffusion. Thus, molecules diffuse along the surface of the pore walls and separation is achieved mainly by the difference in the degree of the interactions for the individual gases. High selectivity can be achieved in cases for which preferential adsorption on one component occurs. Capillary condensation could be considered an extension of surface diffusion: it happens when the vapour pressure becomes low and adsorbed gas undergoes partial condensation within the pores. This condensed component diffuses more rapidly through the pore than gases, generating the separation of the condensable gas.

The polymeric membranes currently used in most commercial applications are solution–diffusion membranes. In fact, very high selectivity can be obtained in dense polymer membranes where the transport mechanism is based on the solution and diffusion of the different gases and vapours of the mixture within the membrane phase. The mechanism consists of three steps: (i) sorption of the mixture components from the feed side according to their solubility coefficient in the polymer matrix; (ii) diffusion of the gases adsorbed within the membrane phase according to their concentration gradients; (iii) desorption of these components from the outer face of the membrane in the permeate phase.

© Woodhead Publishing Limited, 2010

Polymeric solution–diffusion membranes for gas separation are generally described as having four structural levels, each of which influences the performance of the membrane:

- level I: chemical composition of the polymer that forms the selective layer;
- level II: steric relationships in repeat units of the selective polymer;
- level III: morphology of the separating layer of the membrane;
- level IV: the overall membrane structure, including relationships between the separating layer and the rest of the membrane.

Levels I and II involve the chemistry of the polymer and its performance with respect to the gas flux through the membrane. At level III, the membrane can be distinguished as symmetric or asymmetric: it depends on the morphology of the membrane, whether it is the same across its thickness or not. In particular, symmetric membranes have a uniform density across the thickness, while the others do not. Commercial solution–diffusion membranes are of the asymmetric type and possess a porous support layer able to assure resistance to mechanical strength and a very thin layer able to perform the separation of gases.

In addition to these four structural levels, in commercial membranes there are also three higher levels of organisation: (i) the geometry of the membrane, which influences the next organisation level; (ii) the manner in which the membrane is packaged in the membrane module, consisting of the final package where the membranes are assembled into their pressure containment; (iii) the membrane system, consisting of all of the hardware required, along with the permeators in order to achieve a given separation. Some aspects of the membrane geometries and membrane modules will be discussed in a later section of this chapter.

Depending on the operating temperature relative to the glass transition temperature (T_g) of the polymer, polymeric membranes can be of rubbery or glassy form (Plate and Yampol'skii, 1994). A rubbery membrane is an amorphous polymeric material that operates above its T_g under the condition of use: the membrane is usually in thermodynamic equilibrium. In these membranes, the sorption of low molecular weight is typically described by Henry's law for cases in which the sorbed concentrations are low

$$C_D = K_D f \qquad [6.5]$$

where C_D is the concentration of gas in the membrane matrix, K_D is Henry's law constant, and f is the fugacity (a measure of the chemical potential) of the gas considered. For rubbery polymers and low concentrations of penetrant, the diffusion coefficient D_i is typically constant and P_i is

© Woodhead Publishing Limited, 2010

independent of the feed pressure. In the case of the presence of high-activity gases or vapours, deviation from Henry's law sorption is observed. In rubbery membranes, the transport of molecules is typically described by a solution–diffusion mechanism, whereby solution of low molecular weight in rubbery polymers is similar to penetrant sorption into low molecular weight liquids.

A glassy membrane is an amorphous polymeric material that operates below its T_g under the conditions of use: the membrane is far from thermodynamic equilibrium. The polymer chains are packed imperfectly, leading to excess free volume in the form of microscopic voids in the polymeric matrix. Within these voids Langmuir adsorption of gases occurs, which increases the solubility. In contrast to rubbery membranes, glassy membranes are able to discriminate effectively between extremely small differences in the molecular dimensions of common gases (e.g. 0.2 to 0.5 Angstrom). In glassy membranes, the transport of molecules is typically described by the so-called dual-mode model. A part of the gas molecules is absorbed in the polymer matrix, and follows Henry's law, whereas another part is adsorbed into microscopic voids and its concentration, C_H, is described by the following equation

$$C_H = C'_H \cdot b \cdot f/(1 + b \cdot f) \quad [6.6]$$

where C'_H is the maximum adsorption capacity and b is the ratio of rate coefficients of adsorption and desorption.

The total sorption for glassy polymers is then described by the sum of the two components of gas molecules adsorbed in the polymeric matrix (Paul and Yampol'skii, 1994)

$$C = C_D + C_H \quad [6.7]$$

The success of the dual-mode sorption model in describing penentrant sorption in glassy polymers is due to the physical significance that can be related to model parameters.

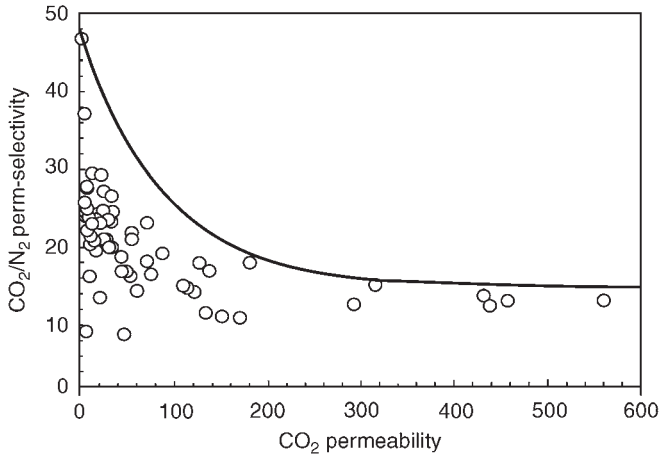
For both glassy and rubbery membranes, the transport properties for gases are almost similar and the relationship between temperature and the transport of small molecules is generally viewed as an activated process, which obeys an Arrhenius relationship

$$P = P_0 \exp(-E_P/RT) \quad [6.8]$$

$$D = D_0 \exp(-E_D/RT) \quad [6.9]$$

$$S = S_0 \exp(-H_S/RT) \quad [6.10]$$

© Woodhead Publishing Limited, 2010



6.2 CO_2/N_2 selectivity versus the CO_2 permeability of polymeric membranes.

where P_0, D_0 and S_0 are the initial conditions, E_P and E_D are the activation energies for permeation and diffusion, respectively, and H_S is the heat of sorption, R is the universal gas constant, and T is the absolute temperature.

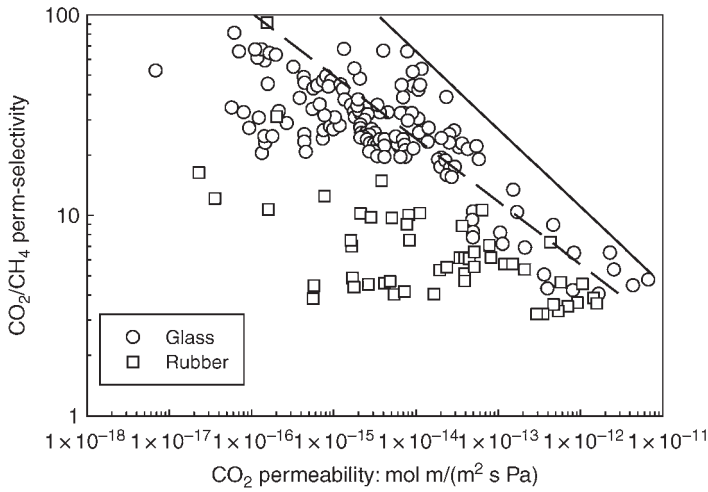
From these equations, it follows that for both glassy and rubbery polymers, an increase in the temperature produces an increase in the permeability and a decrease in the selectivity of a membrane. By contrast, the activation energy is generally smaller in glassy polymer.

It is interesting to observe that there is a trade-off between selectivity and permeability: membranes with a high selectivity show a low permeability, and vice versa. Figure 6.2, in which the ideal CO_2/N_2 selectivity versus fast component CO_2 permeability of polymeric membranes is reported, well illustrates the situation (Powell and Qiao, 2006). Compared to other separations, such as O_2–N_2 and CO_2–CH_4 mixtures (Scholes *et al.*, 2008), CO_2–N_2 mixture appears to be an easer separation.

Robeson (1991) suggested that this trade-off possesses an upper bound. Figure 6.3 shows an example of this upper bound, for a range of glassy and rubbery membranes involved in CO_2/CH_4 separations. Since the paper published by Robeson, only a few examples of polymeric membranes which exceed the upper bound have been published, and overcoming it is the focus of many recently awarded patents in polymeric membranes. In fact, achieving both high CO_2 permeability and high selectivity is desirable.

It should also be said that exceeding the Robeson limit in not a rigid rule. In fact, for example, the polybenzimidazole membrane exceeds the Robeson upper bound for H_2/CO_2 selectivity versus H_2 permeability in the range of temperature 100–400 °C (Berchotold, 2006). Moreover, recently, Koros and

© Woodhead Publishing Limited, 2010



6.3 Comparison of Robeson's curve for CO_2/CH_4 separation by glass (o) and rubber (□) membranes.

Mahajan (2000) suggested the possibility of exceeding the upper bound by using the so-called mixed-matrix membranes.

Apart from permeability and selectivity, other membrane properties are also very important, such as their thermal, chemical, and plasticisation resistance, as well as the aging affects for ensuring continual performance over long time periods. Moreover, cost effectiveness to manufacture as standard membrane modules is also important. Considerable experimental research has been addressed to meeting these aims. An extensive review describing the original polymeric and inorganic membrane patents was recently published by Scholes *et al.* (2008), with particular attention paid to CO_2 separation through polymeric membrane systems for flue gas applications. This review is particularly interesting because it focuses on recent novel approaches in polymeric membranes that achieve separation performance above Robeson's upper bound and therefore are possibly more commercially competitive than present membrane gas separation technologies.

Another important extensive review on polymeric CO_2/N_2 gas separation membranes for the capture of CO_2 from power plant flue gases was recently published by Powell and Qiao (2006). In this review, a chemist's view is adopted, that is the gas permeability properties of dense membranes are seen in the light of their chemical structure. As opposed to this, the already cited paper published by Carapellucci and Milazzo (2003) investigates the engineering aspects of using membranes for CO_2 separation from flue gas. Only a few of the important aspects related to polymeric membranes from these three papers will be considered here.

© Woodhead Publishing Limited, 2010

6.3 CO_2 membrane materials and design

The optimal membrane should exhibit high CO_2 perm-selectivity and high permeability. Also the material resistance is important. The CO_2 separation membranes can be made of different polymers. As previously mentioned, there is always a compromise between the selectivity and the flux depending on the membrane material used. In this section the different membrane materials available will be discussed.

Baker (2002) reported recently, in his excellent review, that the market for membrane acid gas separation systems can be classified into categories:

(a) very small systems (< 5 million scfd (standard cubic feet per day)); these membrane units are very attractive;
(b) small systems (5–40 million scfd), where two-stage membrane systems are used to reduce methane loss; amine and membrane systems are in competition and the choice depends on site-specific factors;
(c) medium to large systems (> 40 million scfd), where membrane systems are generally too expensive to compete with amine plants in this range.

A low-cost alternative to amine plants could also be the combination of membrane systems to remove the bulk of the CO_2 and amine plants to act as polishing systems, but the savings in capital cost are largely offset by the increased complexity of the plant due to the presence of two different separation processes.

It must be concluded that membrane systems at present cannot compete with current amine systems for most CO_2 removal applications. The main problem is related to the relatively low selectivity and permeability of current membranes. For example, under normal operating conditions cellulose acetate membranes show $\alpha_{CO_2/CH_4} = 12–15$, that is quite a low value (reflecting the plasticisation effect by CO_2). Moreover, there are also some issues associated with the post-combustion capture of CO_2 from flue gas that limit the use of membranes:

- the CO_2 concentration is low, and consequently a very large amount of flue gas must be processed;
- flue gas is at high temperature and membranes are easily destroyed, so it is necessary to cool the gas mixture below 100 °C before sending it to the membrane for separation;
- membranes must be chemically resistant to aggressive gases present in the flue gas mixture;
- in order to improve the performance of the membrane it is necessary to improve the pressure difference across the membrane itself, and this requires a significant amount of power.

Polymers studied for CO_2–N_2 membrane separation in different papers

© Woodhead Publishing Limited, 2010

Table 6.3 Performance of polymeric membranes in terms of CO_2 permeance and CO_2/N_2 selectivity. Data adopted from Ho (2006), Powell (2006), and Scholes (2008); (FT = facilitate transport membrane)

Material	CO_2/N_2 selectivity	CO_2 permeance: $m^3 m^{-2} Pa^{-1} s^{-1}$
Polydimethylsiloxane	11.4	3200*
Polydimethylphenilene oxide	19	2750
Poly(4-vinylpyridine)/polyetherimide	20	52
Polyethersulfone	25	665
Polyacrylonitrile with ethylene glycol	28	91
Polysulfone	31	450
Polyimide	43	735
Poly(ethylene oxide)	52	52
Poly(amide-6-b-ethylene oxide)	61	608
Polyvinyl alcohol (cross linked)	170	8278*
Vinyl alcohol / acrylate copolymer – FT	1417	2400*
Polyvinyl alcohol (cross-linked formaldehyde)	1782	338*

* Data are in Barrer.

include many different types, some of which are shown in Table 6.3, where the performance in terms of single gas permeance and CO_2/N_2 selectivity is reported. These membranes could be mainly used for separating post-combustion flue gas mixtures, with CO_2 and N_2 being the main components.

Considering that $P_{CO_2} = S_{CO_2} \cdot D_{CO_2}$ and in order to increase the permeability of CO_2 in a polymeric membrane, the research looks into the increases of CO_2 diffusivity through the polymeric structure or the increases of CO_2 solubility in the membrane matrix (Powell and Qiao, 2006). Another possible aspect to be investigated is the preparation of new membranes, such as mixed-matrix, hybrid, facilitated transport, and membrane contactors.

6.3.1 Mixed-matrix membranes

Membrane separation processes have several advantages over conventional separation techniques, such as, for example, energy saving, space saving, and being easy to scale up. Unfortunately, a membrane capable of combining high flux, high selectivity, and high stability is still not realistic. Nevertheless, mixed-matrix membranes could be the best solution to these problems in the near future. In fact, this new type of membrane, which is able to combine the advantages of polymeric and inorganic membranes, seems to allow a superior performance. As already stated, molecular sieves show high gas transport properties. Nevertheless, there are a lot of problems regarding their processing ability. For this reason, Nomura *et al.* (1997) modified silicalite membranes to incorporate solid particles within a polymeric membrane, obtaining some improvements in the selectivity of the molecular sieve membranes. In fact, as also reported by Powell and Qiao

© Woodhead Publishing Limited, 2010

(2006), the presence of solid particles in a polymeric matrix can modify the permeability under three different effects:

- by acting as molecular sieves (and so altering the permeabilities of the previous polymeric membrane);
- by disrupting the polymeric structure (and so increasing the permeabilities);
- by acting as a barrier (and so reducing the permeabilities).

This new polymer–zeolite research trend includes the following pairs:

- poly(ethylene oxide)–various nanoparticles (Patel *et al*., 2004; Zheng *et al*., 2004);
- polydimethylsiloxane–silicalite (Tantekin-Ersolmaz *et al*., 2000);
- polyamide–carbon molecular sieve (Vu *et al*., 2006);
- polyamide–silica (Kusakabe *et al*., 1996);
- Nafion–zirconium oxide (Apichatachutapan *et al*., 1996);
- HSSZ-13–polyetherimide (Husain and Kotos, 2007);
- acrylonitrile butadiene styrene–activated carbon (Anson *et al*., 2004).

Two interesting paper on these membranes were published by Koros and coworkers in the late 1990s (Zimmerman *et al*., 1997; Mahajan *et al*., 1999), in which more details can be found.

6.3.2 Hybrid membranes

Hybrid membranes offer some advantages with respect to porous inorganic ones. In this case, the surface of a porous inorganic support material is chemically modified in order to have a good affinity with CO_2. For this reason, these membranes should be termed surface-modified inorganic membranes, thus avoiding confusion with mixed-matrix membranes. The working concept of these membranes is quite simple: the porous support has a low resistance to CO_2 flux transport, whereas the chemical modifications are devoted to better controlling the selectivity (Shekhawat *et al*., 2003; Luebke *et al*., 2006).

This new chemical–inorganic support research trend includes the following pairs:

- trichlorosilane–alumina (Luebke *et al*., 2006);
- polyether–silica (Kim *et al*,, 2005);
- organosilane–Vycor glass (Singh *et al*., 2004);
- tetrapropylammonium–silica (Yang *et al*., 2002);
- trimethoxysilane–titania (Abidi *et al*., 2006);
- trimethoxysilaneγ–alumina (Abidi *et al*., 2006);

© Woodhead Publishing Limited, 2010

- aminopropylhydroxysilyl–hexagonal mesoporous silica (Chaffee, 2005; Knowles *et al.*, 2005).

The potential of hybrid membranes for CO_2 capture in an IGCC was evaluated recently by Luebke *et al.* (2006). Unfortunately, in the conclusions the authors stated that despite the high performance of their membranes being attractive, the selectivity was not so good as to be competitive with respect to other processes.

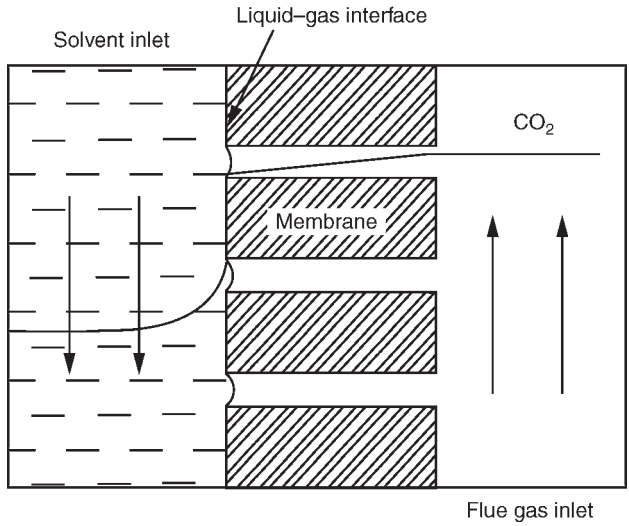
6.3.3 Facilitated transport membranes

The first facilitated transport membranes patent was awarded to General Electricity in 1967 (Scholes *et al.*, 2008). Facilitated transport membranes show high selectivity and high flux (Shekhawat *et al.*, 2003), and are one way to circumvent the Robeson flux/selectivity trade-off. These membranes are obtained by incorporating a carrier (pure water, glycine, etc.) in a membrane able to react with the gas of interest. This reaction is reversible, so the gas at first dissolves in the membrane and then is selectively transported by the carrier by diffusion from one face (feed side) of the membrane to the opposite once (downstream side). Here, the gas is released, while the carrier agent is recovered then diffused back to the feed side. The driving force for gas transportation is the partial pressure difference across the membrane. The carrier increases both the permeability and the selectivity of the membrane. Facilitated transport membranes are in the form of fixed carrier membranes, solvent-swollen polymer membranes, and mobile carrier membranes (Shekhawat *et al.*, 2003). For a comparison of the performance of these membranes with other in terms of CO_2 permeability and CO_2/N_2 selectivity, see Table 6.3. The problems these membranes show, include poor chemical stability of the carriers, evaporation and degradation related to immobilised liquid membranes, and short lifetime (at best a month, as reported in the literature).

6.3.4 Membrane contactors

Membrane contactors are today considered one of the best ways to control CO_2 emissions using membrane technology (Yan *et al.*, 2007). As already stated, among CO_2 separation techniques, such as chemical and physical absorption, solid adsorption, carbon molecular sieve adsorption, cryogenic distillation, and membrane separation, the best established is the method that uses absorption into alkanolamine solutions using conventional contactor equipment (e.g. packed columns or tray columns). Unfortunately, this method is energy-consuming and not easy to operate because of problems caused by foaming, flooding, channelling, and so on.

© Woodhead Publishing Limited, 2010



6.4 CO_2 membrane gas absorption principle.

Membrane gas absorption technology combines membrane separation and chemical absorption technologies. A conceptual schema of a membrane contactor is shown in Fig. 6.4.

The first pioneering work on membrane gas–liquid contactors was performed in 1985 by Qi and Cussler (1985): the separation of the two phases was achieved using a porous polymeric membrane, different from the gas membrane separation process. The latter does not use solvents and strongly depends on the membrane selectivity, while the membranes used in a membrane contactor are generally not selective. The separation role is fulfilled by the absorption liquid. In an ideal situation, in order to minimise the mass transfer resistance, all the pores of the membrane should be completely filled by gas and so the membrane itself does not separate the gases. As a consequence, in these systems the reactive absorption liquids are preferably physical reactive liquids because of their higher absorption rate and capacity. The main advantages of these contactors over conventional column contactors are the reduction in size, operational flexibility, elevated mass transfer rate, and linear scale-up. For example, the membrane surface area of commercial hollow-fibre membrane modules varies in the range 1500–3000 m^2/m^3 of contactor volume (Kumar *et al.*, 2002), whereas in conventional contactors (bubble column, packed, and plate columns) it is in the range 100–800 m^2/m^3. The higher membrane surface area of commercial hollow-fibre membrane modules thereby results in a great size reduction of the contactor.

In Table 6.4 it is quite evident that the membrane contactor offers a much larger contact area per unit volume than other conventional absorbers (Yan

© Woodhead Publishing Limited, 2010

Table 6.4 Specific surface area of some contactors

Contactor	Specific surface area m^2/m^3
Free dispersion column	1–10
Packed column	100~800
Packed/trayed column	10~100
Mechanically agitated column	50~150
Membrane contactor	1500~3000

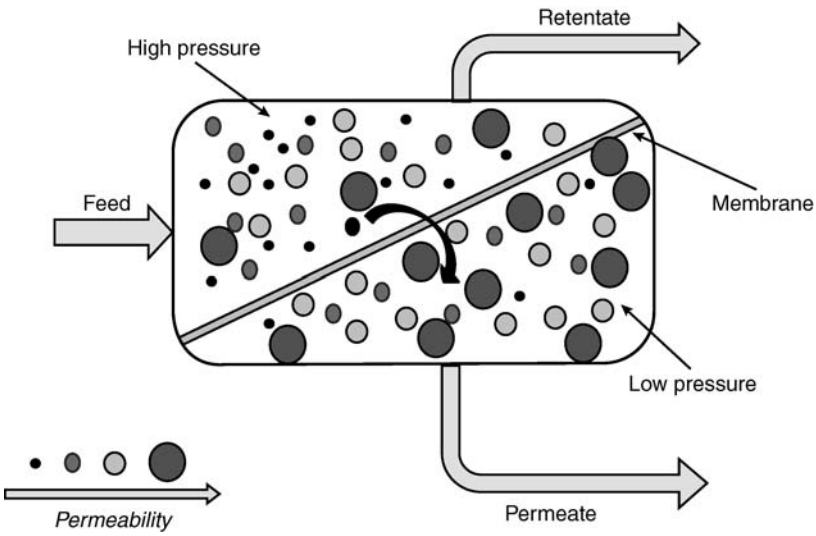
et al., 2007). These advantages over conventional contactors were seen by Gabelman and Hwang (1999) as another interesting potential possibility in the recovery of CO_2 from flue gas, natural gas, and other industrial process gas streams. Of course these membrane contactors must be tested on a larger scale and also long-term stable operations are required. It is important that in long-term operations the pores of the membrane remain completely gas filled (i.e. non-wetted): only in this way can an increase of the overall mass transfer resistance be avoided. To overcome wetting, the development of new absorption liquids for the CO_2 removal using membrane contactors is under study. For example, Kumar *et al.* (2002) studied a new absorption liquid based on the alkaline salts of an amino acid in a single-membrane gas–liquid contactor. The liquid is able to prevent the wetting of commercial polypropylene membranes and the results seem very promising for CO_2 removal. An interesting review of CO_2 absorption using chemical solvents in a hollow-fibre membrane contactor was recently published by Li and Chen (2005).

6.4 Membrane modules

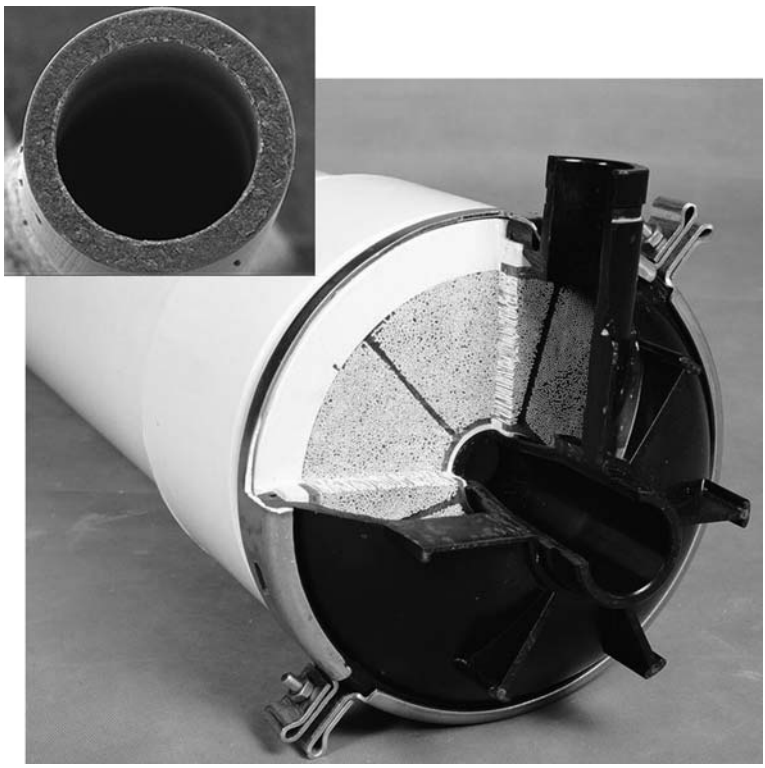
In order to use a membrane in a separation process it must be packed in a proper device, a so-called membrane module. A conceptual scheme of a membrane module is shown in Fig. 6.5. The requirements that a membrane module must meet are low production costs, high packing density, low energy consumption, and good control of concentration polarisation. In the practical applications of a separation processes membrane, the modules are quite different (Westmoreland, 1968; Eckman, 1992; Gunther *et al.*, 1996; Baker, 2000). Stirred batch cells or dead-end filter cells are used in small-scale laboratory applications, whereas two types of configurations are used in large-scale industrial applications: flat (plate-and-frame, spiral-wound, and disc tube modules) and tubular (tubular, capillary, and hollow-fibre modules) configurations. The membrane modules used in gas separations are only the capillary, hollow-fibre, and spiral-wound module; these are shown schematically in Figs 6.6 to 6.8 respectively.

As can be observed, the design of these modules is quite different, as well

© Woodhead Publishing Limited, 2010

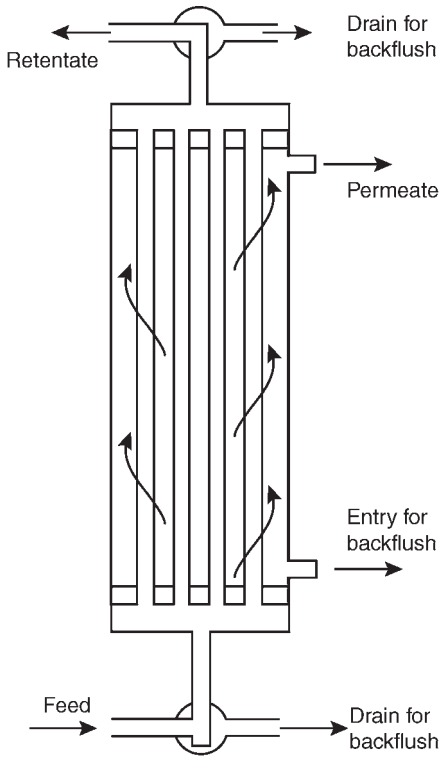


6.5 Conceptual scheme of a membrane module.

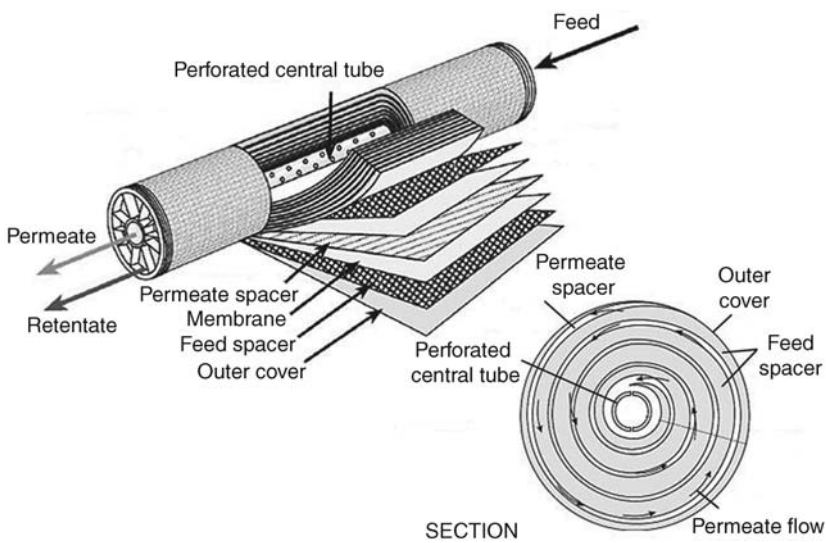


6.6 Capillary module: extruded or spun fibres with membrane on the inside circumference (often also on the outside).

© Woodhead Publishing Limited, 2010



6.7 Hollow fibre module: fine fibres with shell-side feed.



6.8 Spiral-wound module: membrane and permeate channel wound around a permeate pipe.

© Woodhead Publishing Limited, 2010

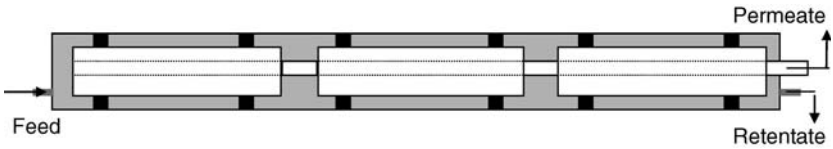
Table 6.5 Membrane equipment configuration

Capillary (Fig. 6.6)	• Cleanable by reversing permeate flow • Well-developed equipment • Low area cost • Low hold-up volume • Pretreatment required to prevent plugging • Intolerant of capillary rupture • Operating power range: 200 W/m^2 • Flux range: 20–50 l/m^{2}h • Energy requirement: 4–10 Wh/l$_{permeate}$
Hollow fibres (Fig. 6.7)	• Low area cost – (best) • Compact – (best) • Low hold-up volume • Well developed • Somewhat tolerant of fibre rupture • High-pressure capability • Sensitive to dirty feed – (worst) • Poor cleanability – (worst) • Energy requirement assuming no power recovery: $4 \times 10^{-3} \frac{\text{Pressure (psi)}}{\text{Conversion}} \cdot \frac{\text{W h}}{\text{litre permeate}}$
Spiral-wound (Fig. 6.8)	• Inexpensive, mature hardware – (best) • Compact, low hold-up • Wide pressure range • High temperature possible • Pretreatment required • Difficult to clean • Operating power range: 20–70 W/m^2 • Flux range: 10–50 l/m^{2}h • Energy requirement: 1–6 W·h/l$_{permeate}$

as their mode of operation, production costs, and the energy requirements (mainly owing to pressure drop inside the membrane module). In Table 6.5 a list of the principal characteristics of some membrane modules is reported.

It should be stated that there is no membrane module able to solve all the problems. Equally, the commercial membrane modules available today are specifically designed for a particular membrane process application.

© Woodhead Publishing Limited, 2010



6.9 Schematic drawing of a spiral-wound membrane installed in multi-module vessel.

6.4.1 Spiral-wound module

The spiral-wound module is a variation of the basic plate-and-frame concept, where the feed gas mixture, pressurised in the module and forced to pass through the membrane surface, selectively permeates the membranes, forming the permeate gas mixture. The configuration of the spiral-wound module is formed by a membrane envelope of spacers and a membrane wound around a porous tube (see Fig. 6.8) The feed gas mixture is sent in the axial direction through the feed channels across the membrane surface. The permeate gas mixture is collected in the central porous tube. Owing to the pressure drop, small spiral-wound modules consist of only one envelope (membrane area 1–2 m^2, membrane channel 2–5 m). Commercial spiral-wound modules have a multi-leaf arrangement with a larger membrane surface and an extended permeate path (membrane area 3–60 m^2, membrane length 1 m, membrane diameter 10–60 cm). Generally, various elements (two to six) are connected in series inside a single pressure vessel, as shown in Fig. 6.9.

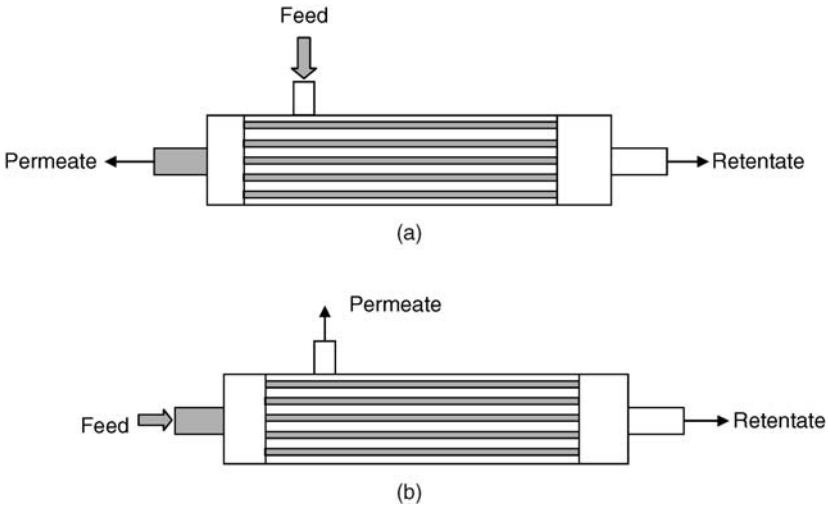
6.4.2 Capillary membrane module

The capillary membrane module (see Fig. 6.6) is formed by a large number of membranes having a capillary dimension, inner diameter 0.2–5 mm. These capillary membranes are placed in a shell tube module and arranged in parallel. The feed gas mixture, sent inside (or outside) the capillary membranes, permeates selectively through the membranes and the permeate gas mixture is then collected in the outside shell tube (or inside the membrane bore). The capillary membrane module provides a very high membrane packing density.

6.4.3 Hollow-fibre membrane modules

In the hollow-fibre membranes (outer diameter 50–100 μm), prepared using the spinning process, the selective layer is on the outside of the fibres (Fig. 6.7). These fibres are installed as a bundle of several thousand fibres. The hollow-fibre modules are formed of two basic geometries: the shell-side feed

© Woodhead Publishing Limited, 2010



6.10 The two types of hollow-fibre modules typically used: (a) shell-side feed; (b) bore-side feed.

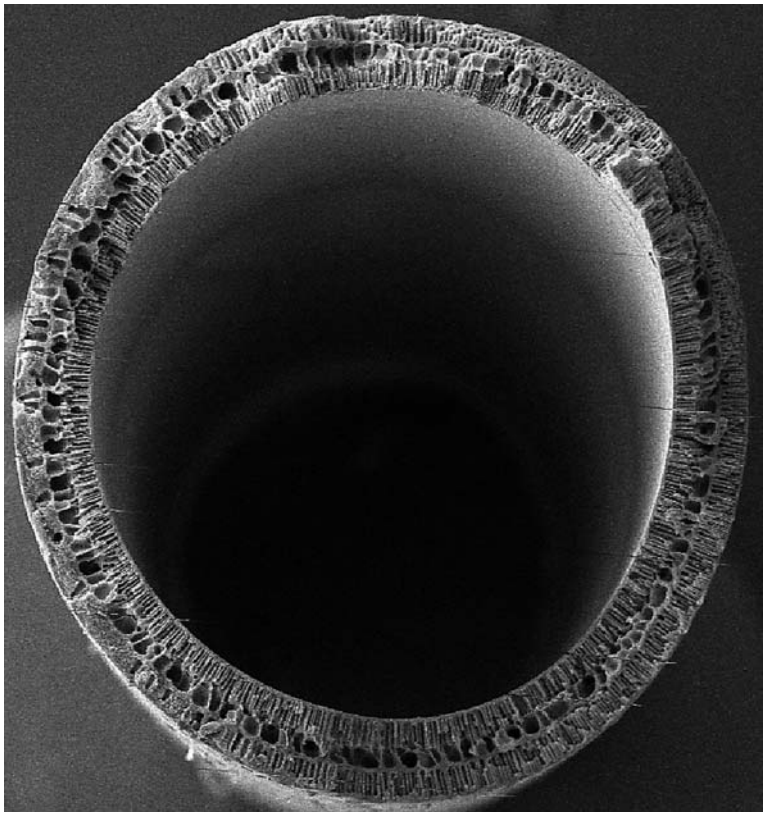
design (Fig. 6.10(a)) and the bore-side feed (Fig. 6.10(b)). In the first case, the system is shell-side pressurised: the feed permeates through the fibre wall and is collected at the open fibre ends. These modules operate at pressures in excess of 100 bar, because this design is easy to realise and, moreover, very large membrane areas can be used. For this reason, the fibres usually have small diameters (typically 50 μm inner diameter and 100–200 μm outer diameter) and thick walls. In the second case the fibres are open at both ends and the feed fluid circulates through the bore of the fibres. To minimise the pressure drop inside the fibres, the diameters are usually larger than those of the fine fibres used in the previous case. A hollow-fibre cross-section is shown in Fig. 6.11.

Hollow-fibre membranes have the highest packing density of all module types available on the market today. Their production is very cost effective. In fact, expensive, sophisticated, and very high-speed automated spinning machine, fibre-handling, and module fabrication equipment is required to produce these modules (Baker, 2000).

6.4.4 Membrane modules comparison

Many factors must be considered in choosing the most suitable module, such as the specific separation to be performed, manufacturing cost, concentration polarisation and fouling (if any), packing density, cleanability, permeate side pressure drop, high-pressure operation, and limitation of type of material. Depending on the membrane processes considered, several types of modules can be used (see Table 6.6).

© Woodhead Publishing Limited, 2010



6.11 Hollow-fibre membrane: cross-section.

With respect to the packing density of the commercially available polymeric membrane modules, the following trend is observed: hollow-fibre > capillary > spiral-wound > plate-and-frame > tubular.

In Table 6.7 the packing density of the commercially available inorganic membrane modules is shown (Baker, 2000). The single plate geometry shows a very low packing density, whereas single tubes typically range between 35 and 280 m^2/m^3. The packing density of most of the inorganic membrane modules of the shell-and-tube type is in the same range as the organic type: 150–300 m^2/m^3. In contrast to organic membranes, no commercial inorganic membranes are yet currently available in the high packing density such as spiral-wound and hollow-fibre membranes. Nevertheless, quite recently, hollow-fibre ceramic and carbon membranes were prepared by Li and co-workers (Liu *et al.*, 2003; Li, 2005; Ismail and Li, 2008). The packing density of these membranes is in the range 500–9000 m^2/m^3, with an area of standard module in the range 50–150 m^2.

Multi-channel monolith modules (with a single element in a module)

© Woodhead Publishing Limited, 2010

Table 6.6 Commercially available membrane modules, their costs, control of concentration polarisation, and applications

Membrane module	Cost	Characteristics	Packing density: m^2/m^3	Control of concentration polarisation	Applications
Plate-and-frame	Medium	Flat sheet membranes	100–200	Good	MF, UF, RO, PV, D, ED
Spiral-wound	Low	Flat sheet	700–1,000	Good	UF, RO, PV, GS
Tubular	Very high	*i.d.* $>$ 5 mm	100–500	Very good	MF, UF, RO, D
Capillary	Low	*i.d.*$<<$ 0.5 mm	500–4 000	Very good	UF, MF, PV, GS, D, SLM
Hollow-fibre	Very low	*i.d.*$<$ 0.5 mm	4 000–30 000	Very poor	RO, GS, PV, D

MF = microfiltration; UF = ultrafiltration; RO = reverse osmosis; PV = pervaporation;
D = dialysis; ED = electrodialysis; GS = gas separation; SLM = supported liquid membrane

Table 6.7 Characteristics of various module types of inorganic membranes (Baker, 2000)

Module type	Packing density: m^2/m^3
Single plate	30–40
Single tube	35–280
Shell-and-tube	120–300
Multi-channel monolith (with a single element)	300–540
Multi-channel monolith (with multiple elements)	100–200

present a packing density in the range 300–540 m^2/m^3. As the number of elements increases in a multi-channel monolith module, the packing density tends to decrease.

It is difficult to quantify correctly the cost of a module because the same module design varies widely depending on the application considered. Generally, the hollow-fibre modules are cheaper than the others, even if these modules must be produced for very high-volume applications in order to justify the expense in developing and building the spinning and module fabrication equipment. In Table 6.8 the module manufacturing cost per square metre of membrane is shown (selling costs are usually two to five times higher than manufacturing ones). High-pressure modules are more expensive than low-pressure or vacuum modules.

Membrane modules with high packing density, that is hollow-fibre or spiral-wound ones, are used for gas separation. In this context, the

© Woodhead Publishing Limited, 2010

Table 6.8 Other parameters for membrane module design (Eckman, 1992)

Parameters	Hollow fine fibres	Capillary fibres	Spiral-wound	Plate and frame	Tubular
Manufacturing cost $/m^2	2–10	5–50	5–50	50–200	50–200
Permeate-side pressure drop	High	Moderate	Moderate	Low	Low
Suitability for high-pressure operation	Yes	No	Yes	Marginal	Marginal

Monsanto hollow-fibre module, equipped with polysulphone–silicone membranes, and also spiral-wound modules (Separex, Grace), equipped with cellulose acetate membranes, started to enjoy great success in the late 1980s (Rautenbach and Albrecht, 1989). Also Dow introduced a fine cellulose acetate hollow-fibre module (packing density of 50 000 m^2/m^3) for gas permeation, which separates very low trans-membrane pressure differences and feed operating pressures around 8–9 bar (Rautenbach and Albrecht, 1989). In these membranes, the flow pattern in the module is not counter-current as in the Monsanto module, but cross-flow (as in reverse osmosis hollow-fibre modules), with the feed flowing radially through the bundle from inside to outside. It is important to stress that the design is advantageous with respect to feed side pressure losses.

A very important factor for the fabrication of a specific module design is the membrane material. During the last few decades the technology to produce high-performance ultra-thin membranes in high packing membrane density has constantly improved. Nowadays, membranes with an active layer of 0.05 μm are produced. As a result of this improvement, concentration polarisation and fouling (not relevant for gas separation) are the two major factors determining system performance. Future research will be addressed at the improvement of fluid flow, to overcome (or at least to reduce) the problem of concentration polarisation, easily cleaned modules, and novel membrane materials.

6.5 Design for power plant integration

The design of CO_2 membrane separation systems to be integrated in power plants is generally curved out by modelling work, which takes into consideration the characteristics of membranes as well as the performances of the power plant. In this section, the model most used will be discussed and an example of membrane design will be given.

Modelling the performance of gas permeation modules is now described.

© Woodhead Publishing Limited, 2010

Simulation models for gas separation membranes have been developed by a number of investigators. For example, recently Corti *et al*. (2004) simulated the CO_2 removal in power generation using membrane technology in which two models were considered: perfect mixing and cross-flow models; whereas Bounaceur *et al*. (2006) performed a membrane module simulation for post-combustion CO_2 capture. Any such permeator model must take into account:

- an equation describing the gas transport across the membrane;
- the mass balance equation for each component of the gas mixture;
- the pressure drops occurring on both sides of the membrane;
- boundary conditions.

There are three important parameters that determine the efficiency of a membrane separation process: the selectivity, the ratio 'pressure feed'/'pressure permeate', and the stage cut (i.e. the ratio of the molar permeate flow to the molar feed flow). In a gas separating module three idealised flow patterns are assumed: (i) perfect mixing of feed and permeate, (ii) co- or counter-current plug flow of feed and permeate, and (iii) cross-flow permeation, with the permeate stream perpendicular to the membrane.

The separation obtained in a single permeation stage can be multiplied several times, if necessary. Many combinations of the several permeation stages are possible (see details, Ho and Sukar, 1992). Generally, the number of stages necessary for achieving a certain enrichment of a gas can be determined by a graphical procedure commonly used in design of distillation columns (Violante *et al*., 1992).

In the following, the three above-mentioned flow patterns are analysed in detail, considering at first a membrane system for the CO_2 separation from a mixture of N_2 (90%) and CO_2 (10%), and afterwards the same procedure extended to a four-component mixture. Details concerning the transport equations as well as the three schemes used can be found in Hwang and Kammermeyer, (1975) and Basile and Gallucci (2009).

As an application of the models illustrated above for a simple one-stage removal plant, let us consider a membrane system for the CO_2 separation from a mixture of N_2 (90%) and CO_2 (10%). A polydimethylsiloxane membrane is considered (Table 6.3), and the pressure ratio is 10. The scope of the numerical simulations is the comparison between the three different flow patterns, complete mixing, co-current, and cross-flow. Special attention will be focused on the calculation of CO_2 permeate concentration as a function of CO_2 recovery ratio (R), defined as follows

$$R = \theta \frac{y_{CO_2}}{x^{in}_{CO_2}} \qquad [6.11]$$

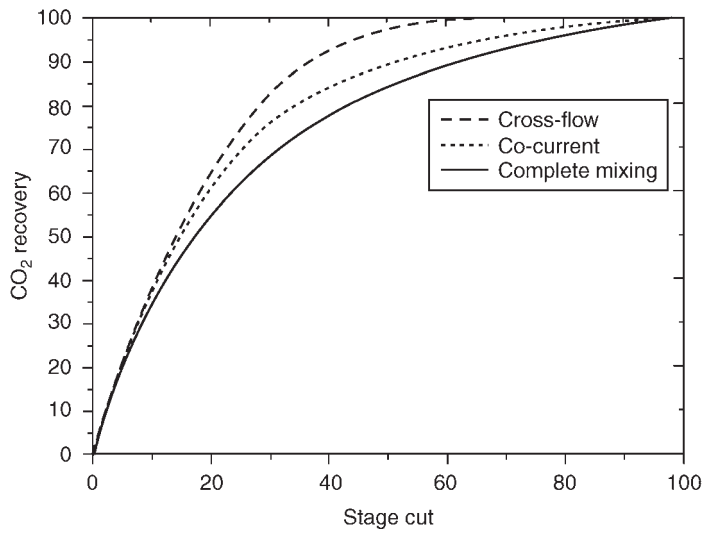
© Woodhead Publishing Limited, 2010

where θ is the stage cut (i.e. the ratio of total permeate flow rate to total feed flow rate), $x_{CO_2}^{in}$ the CO_2 molar concentration in the feed flow, and y_{CO_2} is the molar concentration of CO_2 in the permeate side. In other words, the recovery ratio is the fraction of CO_2 in the feed actually captured in the permeate side.

In general, an increase in θ (and so an increase of the membrane area) is not linear with the recovery of CO_2. For this reason, in a problem like CO_2 capture, it is more useful to use R as an independent variable instead of θ (Corti *et al.*, 2004).

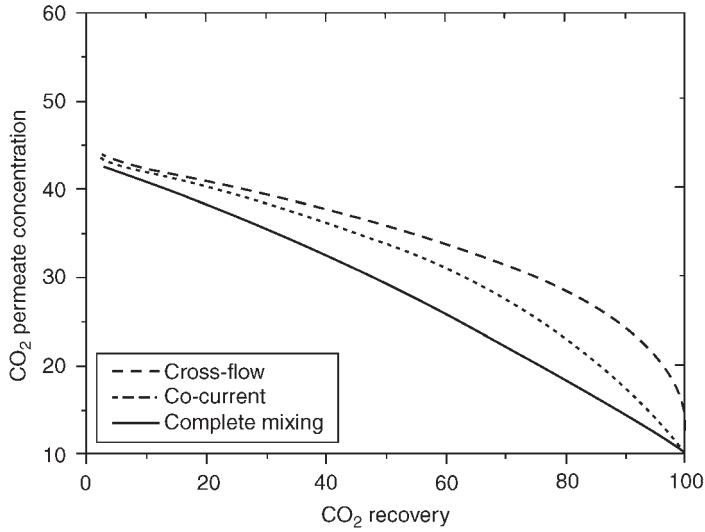
The recovery ratio with respect to the stage cut is depicted in Fig. 6.12 for the three flow modes. A complete CO_2 recovery is reached for values of stage cut less than 100%. For example, even though the recovery approaches 100%, the stage cut is nearly 60% for the cross-flow mode, and so a further increase in membrane area does not provide any rise in effectively recovered CO_2.

Figure 6.13 shows the CO_2 permeate concentration with respect to recovery. It is clear that, with low values of CO_2 recovery, a concentrated permeate product can be obtained, whereas an increase in recovery produces a significant decrease in purity. It is clear that it is not possible to obtain simultaneously high recovery and high purity in a one-stage membrane system. Moreover, it is shown that the cross-flow mode is the most efficient separation technique. As an example, if a 30% CO_2 recovery is considered, the corresponding permeate molar fractions are 39, 38, and 35%, for cross-flow, co-current flow, and complete mixing flow modes respectively.



6.12 CO_2 recovery ratio versus stage cut for three different flow mode patterns: complete mixing, co-current, and cross-flow.

© Woodhead Publishing Limited, 2010



6.13 CO_2 permeate concentration for three flow patterns: complete mixing, co-current, and cross-flow (CO_2 feed concentration 10%).

Several parameters greatly influence the separation performances, such as the pressure ratio, the feed flow rate, the permeability, and the selectivity. In the following, the influence of the feed CO_2 concentration will be estimated. In particular, an increase in the CO_2 feed concentration from 10% to 20% was considered and the effect on CO_2 permeate molar fraction was calculated.

Figure 6.14a shows that, in order to obtain a permeate flow with 40% CO_2 purity, the recovery fraction is 25% for the case of feed concentration 10%. Furthermore, an increase in CO_2 concentration by 5% (Fig. 6.14b) permits a 80% recovery to be obtained with the same value of CO_2 purity (40%). A further increase in CO_2 feed concentration up to 20% permits the recovery to be increased to values higher than 90%. On the other hand, for a fixed value of CO_2 recovery, as an example, 20%, the purity reaches 41%, 50%, and 54% for CO_2 concentrations equal to 10, 15, and 20%, respectively.

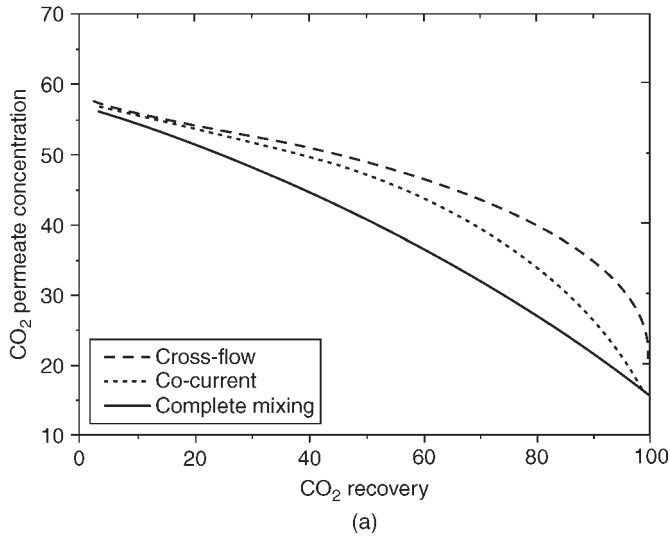
The numerical procedure can be extended for a four-component mixture (CO_2, N_2, CH_4, H_2) in cross-flow and co-current flow mode. The membrane is the same as the previous example, and the properties for the other components are reported in Table 6.9. Moreover, the molar fractions are typical of a syngas obtained by a steam reforming process (Bounaceur *et al.*, 2006).

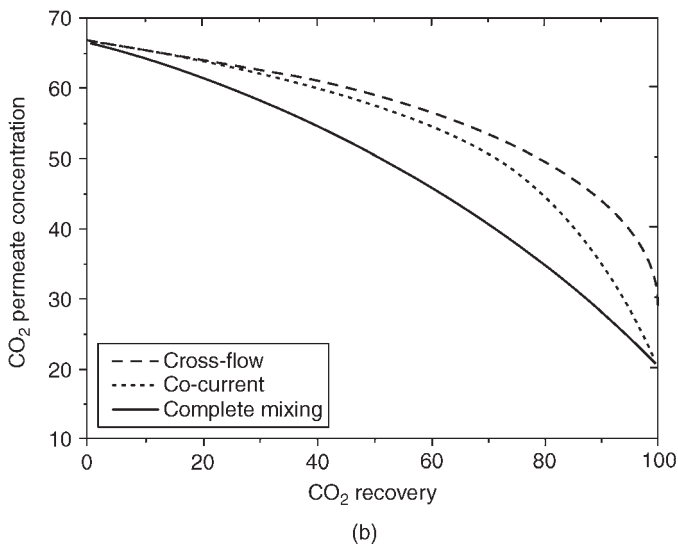
Figure 6.15a shows the permeate concentration of all species with respect to CO_2 recovery fraction. The most permeable gas (CO_2) concentration

© Woodhead Publishing Limited, 2010

Table 6.9 Membrane properties

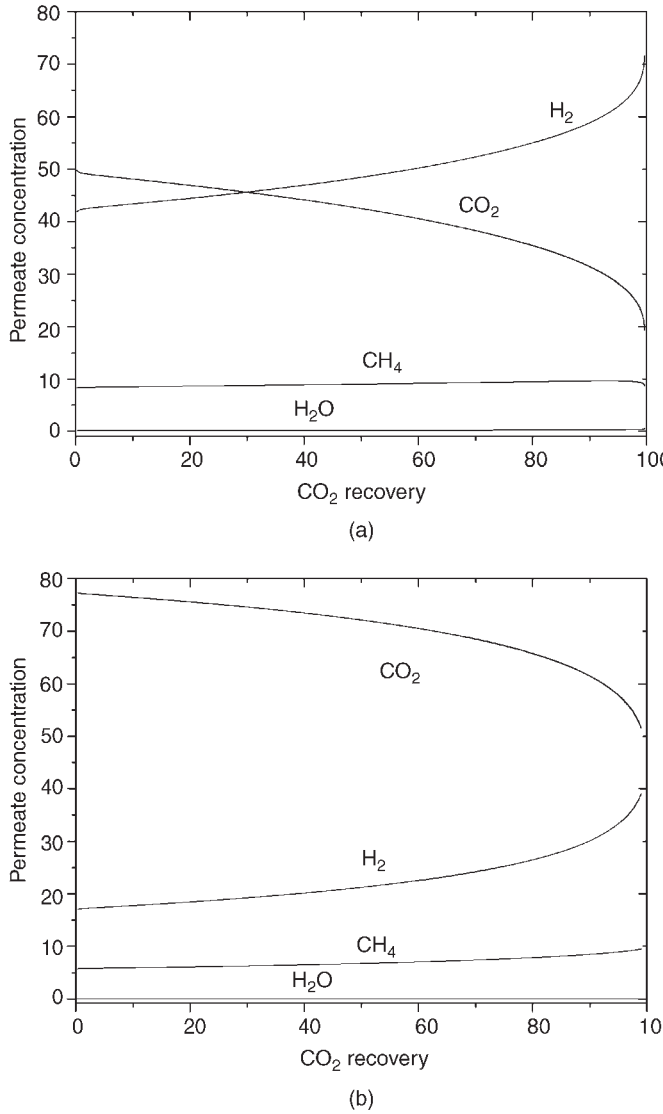
Gas	Permeability: Barrer	Feed concentration: %
H_2O	10	9.1
CO_2	3200	16.4
CH_4	940	7.4
H_2	500	67.1





6.14 CO_2 permeate concentration for three flow patterns: complete mixing, co-current, and cross-flow (CO_2 feed concentration (a), 15% (b) 20%).

© Woodhead Publishing Limited, 2010



6.15 Permeate concentration versus CO_2 recovery fraction for all mixture components in (a) the first and (b) the second stage.

decreases with the increasing of recovery, in a similar way to Fig. 6.13. On the contrary, the permeate concentration of H_2 increases linearly up to the recovery value of 50%, and then increases very rapidly. Moreover, the methane concentration in the permeate side presents a slight increase – from 8 to 9.5% – with the recovery fraction. Finally, the component with the lower permeability (H_2O) has a negligible permeate concentration. In fact, the selectivity of CO_2 with respect to H_2O is very high (320).

© Woodhead Publishing Limited, 2010

Table 6.10 Feed mixture concentration in the second stage

Gas	Feed concentration: %
H_2O	0.2
CO_2	41.3
CH_4	9.1
H_2	49.5

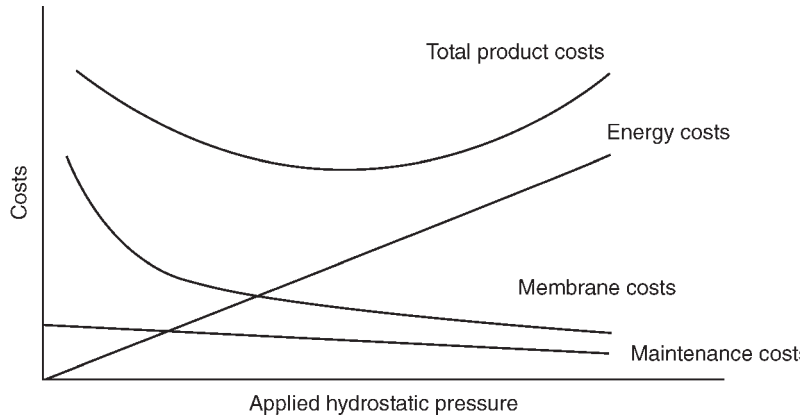
In order to increase the performance of the membrane in terms of purity, a second stage is necessary. In this case, an additional separation is achieved because the permeate stream of a membrane unit is further treated in other membrane units. For example, consider a single stage that guarantees 50% recovery (Fig. 6.15b), which corresponds to a 20% stage cut. Consider a second stage capable of treating the previous permeate flow. The mixture concentration is reported in Table 6.10.

The results show that the second stage increases the performance of the system remarkably. In particular, the CO_2 permeate concentration starts from 77% and decreases very slowly with the recovery, and the difference between the two flow modes, cross- and co-current flow, is less pronounced with respect to the single-stage system. Finally, the single stage permits 41.3% to be obtained with 50% recovery, while the two-stage system gives a CO_2 permeate concentration of nearly 70%, as the figure shows.

6.6 Cost considerations

The cost-effective level of CO_2 capture depends on several plant design factors, also including the plant size. For example, the effect of systematically increasing the CO_2 capture efficiency using currently available amine-based CO_2 capture technology for pulverised-coal-fired plants was recently investigated by Rao and Rubin (2006). In their analysis the authors did not consider membranes as a new potential technology for solving such problems. Conversely, a most recent paper by Favre (2007), trying to answer the question of whether gas permeation membranes can compete with absorption, gives a critical comparison of dense polymeric membrane capture processes versus amine absorption in a post-combustion process. The main conclusions of this simulation work is that the membrane potentially competes with amine absorption in terms of energy requirement (of the compressor) when the CO_2 content in the feed exceeds 20%. Unfortunately, there are no pilot-scale experiments with membranes for post-combustion CO_2 capture available for better verification of these conclusions. On the other hand, a conclusion of pilot plant studies of the CO_2 capture demonstrated that a huge heat-duty reduction can be achieved

© Woodhead Publishing Limited, 2010



6.16 Membrane costs as a function of pressure

when a mixed monoethanolamine (MEA) and methyldiethanolamine (MDEA) aqueous solution is used (Idem *et al.*, 2006).

It should also be considered that the total production costs in membrane processes are the sum of fixed charges associated with repayment of the plant investment cost (including depreciable items such as the membrane modules and non-depreciable items such as land) and of operating costs (energy, membrane replacement, maintenance). In particular, the investment costs are directly proportional to the membrane area, which is directly proportional to the energy requirements (an increase in the feed pressure corresponds to an increase in the energy consumption); whereas the total investment costs of a filtration plant are a function of the membrane properties (as well as of many other design parameters). The relationship of these variables (total production costs, energy costs, membrane costs, and maintenance costs) with respect to the applied feed pressure is schematically reproduced in Fig. 6.16.

As already stated, the quantitative analysis strongly depends on specific application, plant, and location as well as on the characteristics of membranes and modules. For example, one important aspect is the driving force for CO_2 separation: using membranes depends on the partial pressure difference between permeate and retentate sides of the membrane. Therefore, in post-combustion capture, owing to the low driving force as a consequence of the low CO_2 partial pressure in the flue gas, the use of commercial polymeric membranes results in relatively large energy requirements and CO_2 avoidance costs in comparison to chemical absorption. For example, in a natural gas combined cycle (where CO_2 pressure is about 0.04 bar) chemical absorption using amines is considered to be the preferred capture technology (Damen *et al.*, 2006). In post-combustion capture in a natural gas combined cycle, absorption processes

© Woodhead Publishing Limited, 2010

are relatively expensive due to the low CO_2 loading: cryogenic CO_2 separation is considered less attractive than membrane contactors (Idem *et al*., 2006); whereas pre-combustion membranes are only considered in the inorganic form (palladium-based, SiO_2, carbon, zeolite, and perovskite). Even if these membranes show good selectivities, sufficient stability, and lifetime, they still require a greater development effort to be used in such plants. In the pre-combustion capture of integrated gasification combined cycle, inorganic membranes for separating CO_2 and H_2 have also been proposed for improving the energetic and economic performance of the capture process (Damen *et al*., 2006).

The performance (as well as the cost) of membranes affect capture costs, of course. The effect of changing the CO_2 permeability and the CO_2/N_2 selectivity of a commercial poly(phenylene oxide) (initial values: $P_{CO_2} = 72$ Barrer, α_{CO_2/N_2}) was investigated through a model simulation by Ho *et al*. (2006). They found that an increase of the CO_2 permeability reduces the capture cost (in fact, less membrane area is required for the same CO_2 recovery rate). When $\alpha_{CO_2/N_2} = 20$ is increased, the mole fraction of CO_2 in the permeate side increases too, and this higher CO_2 molar fraction corresponds to less compression (i.e. in a smaller compressor that requires less energy), and both capital and operating costs are consequently decreased. Also, the differential pressure across the membrane must be carefully considered. In fact, its increase determines a reduction of the capture costs: a decrease in the feed pressure requires a smaller compressor and so both a reduction in capital costs and a smaller amount of energy. In both the case of feed gas compression, as well as in the case of creation of a vacuum on the permeate side, the work performed is estimated using the equation reported by Favre (2007). The energy consumption of a membrane (to be used in a post-combustion CO_2 capture) has already been estimated using such an equation by Bounaceur *et al*. (2006). They found that the feed compression consumes more energy than the vacuum pumping created in the permeate side. Moreover, increasing the constraints in the recovery and permeate composition requires higher CO_2/N_2 membrane selectivity and also requires more energy. In order to meet the real conditions of a membrane capture process, the same authors also reported the simulation results when a multistage membrane system is considered: multistage compressors are useful especially when the pressure ratio is low. Their main result is that the overall energy consumption decreases by a factor of 4 when the system is switched from a single-stage to five-stage compressions. Nevertheless, in order to have a significant conclusion the effects of more realistic conditions must also be taken into account.

© Woodhead Publishing Limited, 2010

6.7 Sources of further information

The interest of the scientific community in CO_2 capture and sequestration via different technologies is reflected in the enormous number of on-going research projects co-funded by different industrial companies. Just to give a very brief overview of the work in this direction, some projects (in the EU FP6 and FP7 only) are discussed here. Described first below are some projects in the European framework programme FP6 dealing with CO_2 capture and sequestration (information taken from the projects' websites):

CASTOR: A European initiative grouping 30 partners (industries, research institutes, and universities) with the aim to develop and validate innovative technologies for CO_2 capture and storage. The key targets of CASTOR are as reported on the project website:

- a major reduction in post-combustion capture costs, from 50–60 € down to 20–30 € per ton of CO_2 (large volumes of flue gases need to be treated with low CO_2 content and low pressure);
- to advance general acceptance of the overall concept in terms of storage performance (capacity, CO_2 residence time), storage security, and environmental acceptability;
- to start the development of an integrated strategy connecting capture, transport, and storage options for Europe.

This project has focused more on the development of absorption liquids for post-combustion CO_2 capture.

CAPRICE: CAPRICE stands for CO_2 capture using Amine Process International Cooperation and Exchange. TNO, a Dutch organisation, has been running the project since 2007. CAPRICE is funded by the European Union and is scheduled to last two years. It comprises:

- ten research centres (Regina University, Alberta Research Council, International Test Center, Energy Inet, IFP, Trondheim University, Stuttgart University, Tsinghua University, Topchiev Institute of Petrochemical Synthesis, and Salvador University);
- three industrial electricity companies (E-ON, Dong Energy, and Vattenfall).

DeSANNS: The DeSANNS project aims to develop new nanoporous materials for separation by adsorption for H_2 purification and CO_2 capture. The research encompasses two material families:

- periodic mesoporous oxides;
- metal organic frameworks.

© Woodhead Publishing Limited, 2010

Partners are using state-of-the-art technology for material synthesis, molecular modelling, spectroscopic characterisation, and high-pressure adsorption to achieve fundamental understanding of the synthesis–structure–adsorption triangle and thereby optimise adsorbent efficiency in target applications.

CACHET: CACHET is an integrated research project, aimed at developing technologies to reduce greenhouse gas emissions from power stations by 90%. The consortium comprises research institutes, universities, energy businesses, and both engineering and manufacturing companies. CACHET is co-ordinated by BP and funded by the EU, new member states, USA, Canada, China, and Brazil. The overall goal of the CACHET project is to develop innovative technologies that will substantially reduce the cost of CO_2 capture while simultaneously producing H_2 from natural gas fuel. Existing CO_2 capture costs are in the range 50–60 €/t and CACHET will target substantial reduction to 20–30 €/t, with 90% capture rate and CO_2 delivered at pipeline pressure for disposal.

Following a four-year period of extensive assessment, the CO_2 Capture Programme project selected several innovative technologies exhibiting high potential for efficient H_2 production with CO_2 capture, which meet EU cost targets of 20–30 €/ton for CO_2 capture. The most promising technologies are 'hygensys' (advanced steam methane reforming), redox technologies ('one-step reforming', and 'chemical looping reforming'), 'hydrogen membrane reactors for natural gas reforming and water gas shift' and 'sorption-enhanced water gas shift'.

NANOGLOWA: A project based on CO_2 capture through nanostructured membranes, NANOGLOWA brings together universities, power plant operators, industry, and SMEs. Twenty-six organisations from 14 countries throughout Europe joined the NANOGLOWA consortium in order to develop optimal nanostructured membranes and installations for CO_2 capture from power plants. It is claimed that the application of nanostructured membranes for CO_2 capture and separation brings down the energy penalty related to the conventional absorption with amines. The project plan is really devoted to membrane material science, to be then integrated in a separation process. In fact, the project tasks are:

- basic materials;
- membrane development;
- membrane production;
- module development;
- process development;
- diagnostics development;

© Woodhead Publishing Limited, 2010

- power generation.

CO2ReMoVe: CO2ReMoVe is a consortium of industrial, research, and service organisations with experience in CO_2 geological storage. The consortium proposes a range of monitoring techniques, applied over an integrated portfolio of storage sites, which will develop:

- methods for base-line site evaluation;
- new tools to monitor storage and possible well and surface leakage;
- new tools to predict and model long-term storage behaviour and risks;
- a rigorous risk assessment methodology for a variety of sites and time-scales;
- guidelines for best practice for the industry, policy makers, and regulators.

The project results should encourage widespread application of CO_2 geological storage in Europe and neighbouring countries.

COACH: COACH is a coordination project between the EU and China, signed in 2006. The eight Chinese and 12 European industrial firms, research centres, and public-sector organisations working on this project will draft the technical recommendations required to design a coal-fired power plant in China. That plant will include facilities to capture CO_2 and the project will also deal with transport and storage of CO_2 in a mature oil and gas reservoir. Building work is scheduled to begin in 2011, and the capture and storage chain should come on stream in 2015.

Also in the European framework programme 7 there are different projects dealing with CO_2 capture, the biggest are perhaps the projects CAESAR, DECARBit, and CESAR. All these projects see the participations of big research groups along with companies dealing with energy conversion.

CAESAR: This is a project coordinated by ECN (The Netherlands). One of the four pre-combustion CO_2 capture technologies that are being developed in CACHET is the sorption enhanced water–gas shift (SEWGS) process. The SEWGS process produces hot, high-pressure H_2 in a catalytic CO shift reactor with simultaneous adsorption of CO_2 on a high-temperature adsorbent. The system operates in a cyclic manner with steam for adsorbent regeneration. The overall objective of the proposed project CAESAR is the reduction of energy penalty and costs of the SEWGS CO_2 capture process through optimisation of sorbent materials, reactor, and process design. The partners of the project claim that for an optimised SEWGS process CO_2 avoidance cost could be reduced to < 15/ton CO_2.

The emphasis in CACHET was placed on demonstrating the SEWGS process on a larger scale in a continuous, multi-bed SEWGS process

© Woodhead Publishing Limited, 2010

demonstrator. CAESAR goes one step further in taking boundary conditions such as cost and efficiency into account. This presses for better sorbents, reactor, and process design.

DECARBit: The project coordinated by Sintef (Norway) has an overall objective of zero-emission pre-combustion power plants by 2020 with a capture cost of less than 15 €/ton, with the highest feasible capture rate. DECARBit responds to the urgent need for further research and development in advanced pre-combustion capture techniques substantially to reduce emissions of greenhouse gases from fossil fuel power plants. The project aims at accelerating technological development and contributing to the deployment of large-scale carbon capture and storage (CCS) plants.

CESAR: The consortium of the project consists of three research organisations, three universities, one solvent supplier, one membrane producer (SME), three equipment suppliers, two oil and gas companies, and six power generators. The project aims to decrease the cost of CO_2 capture down to 15 €/ton CO_2. CESAR aims at breakthroughs via a combination of fundamental research on advanced separation processes, capture process modelling and integration, and solvent process validation studies. CESAR will use the pilot built in the CASTOR (FP6) project.

The activities and innovations CESAR focuses on are:

- novel (hybrid) solvent systems;
- new high-flux membranes contactors;
- improved modelling and integration studies on system and plant level;
- testing of new solvents and plant modifications in the Esbjerg pilot plant.

In the Esbjerg pilot plant novel technologies are assessed and compared with mainstream techniques to provide a fast track towards further scale-up and demonstration.

6.8 References

Abertz V, Brinkmann T, Dijkstra M (2006),'Developments in membrane research: from material via process design to industrial application', *Adv. Engng Mater.*, 8, 328–358.

Abidi N, Sivadea A, Bourret D, Larbot A, Boutevin B, Guida-Pietrasanta F, Ratsimihety A (2006), 'Surface modification of mesoporous membranes by fluoro-silane coupling reagent for CO_2 separation', *J. Membrane Sci.,* 270, 101–107.

Anson M, Marchese J, Garis E, Ochoa N, Pagliero C (2004), 'ABS copolymer-activated carbon mixed matrix membranes for CO_2/CH_4 separation', *J. Membrane Sci.*, 243, 19–28.

© Woodhead Publishing Limited, 2010

Apichatachutapan W, Moore RB, Mauritz KA (1996), 'Asymmetric nafion/(zirconium oxide) hybrid membranes via in situ sol-gel chemistry', *J. Appl. Polymer Sci.*, 62(2), 417–426.

Baker RW (2000), *Membrane technology and applications*, Ch. 3, ISBN 0-07-135440-9, McGraw-Hill.

Baker RW (2002), 'Future direction of membrane gas separation technology', *Ind. Engng Chem. Res.*, 41, 1393.

Basile A, Gallucci F (2009), *Simulation of membrane reactors*, ISBN: 978-1-60692-425-9, New York, Nova Science Pub.

Basu A, Akhtar J, Rahman M, Islam M (2004), 'A review of separation of gases using membrane systems', *Petrol. Sci. Technol.*, 22, 1343–1368.

Berchotold KA (2006), 'Novel polymeric–metallic composite membrane for CO_2 separation at elevated temperatures', *American Filtration and Separation Society Fall Topical Conference*, Pittsburgh, PA.

Bounaceur R, Lape N, Roizard D, Vallieres C, Favre E (2006), 'Membrane processes for post-combustion carbon dioxide capture: A parametric study', *Energy*, 31, 2556–2570.

Bredesen R, Jordal K, Bolland O (2004), 'High-temperature membranes in power generation with CO_2 capture', *Chem. Engng Processing*, 43, 1129–1158.

Carapellucci R, Milazzo A (2003), 'Membrane systems for CO_2 capture and their integration with gas turbine plants', *Proc. IMechE, Part A, J. Power Energy*, 217, 505.

Chaffee AL (2005), 'Molecular modeling of HMS hybrid materials for CO_2 adsorption', *Fuel Processing Technol.*, 86(14–15), 1473–1486.

Chiesa P, Consonni S, Kreutz T, Williams R (2005), 'Co-production of hydrogen, electricity and CO_2 from coal with commercially ready technology. Part A: Performance and emissions', *Int. J. Hydrogen Energy*, 30, 747–767.

Corti A, Fiaschi D, Lombardi L (2004), 'Carbon dioxide removal in power generation using membrane technology', *Energy*, 29, 2025–2043.

Damen K, van Troost M, Faaij A, Turkenburg W (2006), 'A comparison of electricity and hydrogen production systems with CO_2 capture and storage. Part A: review and selection of promising conversion and capture technologies', *Progr. Energy Combust. Sci.*, 32, 215–246.

Dijkstra JW, Jansen D (2004), 'Novel concepts for CO_2 capture', *Energy*, 29, 1249–1257.

Eckman TJ (1992), 'Hollow fiber cartridge', US Patent 5,169,530.

Elwell LC, Grant WS (2006), 'Technology options for capturing CO_2 – special reports', *Power*, 8, 150.

Falk Paterson O, Dannstrom H, Gronvold M, Stuksrud D, Running O (2000), 'Gas treating using membrane gas/liquid contactors', 5th int. conf. on *Greenhouse gas control technologies*, Cairns, Australia.

Favre E (2007), 'Carbon dioxide recovery from post-combustion processes: can gas permeation membranes compete with absorption?', *J. Membrane Sci.*, 294, 50–59.

Feron P, Jansen A, Klaassen R (1992), *Energy Conversion Managmt*, 33, 421.

Figueroa JD, Fout T, Plasynski S, McIlvried H, Srivastava RD (2008), 'Advances in CO_2 capture technology – The US Department of Energy's carbon sequestration program, *Int. J. Greenhouse Gas Control*, 2, 9–20.

© Woodhead Publishing Limited, 2010

Fritzsche A, Kurz J (1990), 'The separation of gases by membranes', in Porter MC (ed.) *Handbook of industrial membrane technology*, New York, William Andrew Publishing, 559–593.

Gabelman A, Hwang ST (1999), 'Hollow fiber membrane contactors', *J. Membrane Sci.*, 159, 61–106.

Gallucci F., Basile A. (2009), 'Pd-based membranes synthesis and their application in membrane reactors', Gorley G. V., in: *Handbook of membrane research: propernes, performance and applications*, New York, Nova Science Pub, Ch. 1, ISBN 978-1-60741-638-8.

Gessinger G (1997), 'Lower CO_2 emissions through better technology', *Energy Conversion Managmt*, 38(S1), 25–30.

Gibbins J, Chalmers H (2008), 'Carbon capture and storage', *Energy Policy*, 36, 4317–4322.

Graham T (1861), *Phil. Mag.*, 32, 402.

Gunther R, Pershcall B, Reese D, Hapke J (1996), 'Engineering of high pressure reverse osmosis', *J. Membrane Sci.*, 121, 953.

Ho W, Sirkar KK (1992), *Membrane handbook*, New York, Van Nostrand Reinhold.

Ho MT, Allinson G, Wiley DE (2006), 'Comparison of CO_2 separation options for geo-sequestration: are membranes competitive?', *Desalination*, 192, 288–295.

Husain S, Koros WJ (2007), 'Mixed matrix hollow fiber membranes made with modified HSSZ-13 zeolite in polyetherimide polymer matrix for gas separation', *J. Membrane Sci.*, 288, 195–207.

Hwang ST, Kammermeyer K (1975), *Membranes in separation*, New York, Wiley Interscience.

Idem R, Wilson M, Tontiwachuthikul P, Chakma A, Veawab A, Aroonwilas A, Gelowitz D (2006), 'Pilot plant studies of the CO_2 capture performance of acqueous MEA and mixed MEA/MDEA solvents at the university of Regina CO_2 capture technology development plant and the Boundary Dam CO_2 capture demonstration plant', *Ind. Engng Chem. Res.,* 45, 2414–2420.

Ismail AF, Li K (2008), 'From polymeric precursors to hollow fiber carbon and ceramic membranes', in Mallada R and Menendez M (eds) *Inorganic membranes: synthesis, characterization and applications*, Elsevier, Ch. 13, 81–119.

Kaldis SP, Skodras G, Sakellaropoulos GP (2004), 'Energy and capital cost analysis of CO_2 capture in coal IGCC processes via gas separation membranes', *Fuel Processing Technol.,* 85, 337–346.

Kim H, Lim C, Hong S (2005), 'Gas permeation properties of organic–inorganic hybrid membranes prepared from hydroxyl-terminated polyether and 3-isocyanatopropyltriethoxysilane', *J. Sol–Gel Sci. Technol.,* 36(2), 213–221.

Knowles GP, Graham JV, Delaney SW, Chaffee AL (2005), 'Aminopropyl-functionalized mesoporous silicas as CO_2 adsorbents', *Fuel Processing Technol.,* 86, 1435–1448.

Koros W (1991), 'Gas separation', in Baker RW, (ed.) *Membrane separation systems – Recent developments and future directions*, New York, William Andrew Publishing.

Koros W, Mahajan R (2000), 'Pushing the limits on permeabilities for large scale gas separation: which strategies', *J. Membrane Sci.*, 175, 18.

© Woodhead Publishing Limited, 2010

Koros W (2002), 'Gas separation membranes: needs for combined materials science and processing approaches', *Macromol. Symp.,* 188, 13.

Kumar PS, Hogendoorn JA, Feron PHM, Vesteeg GF (2002), 'New absorption liquids for removal of CO_2 from diluite gas streams using membrane contactors', *Chem. Engng Sci.,* 57, 1639–1651.

Kusakabe K, Ichiki K, Hayashi J, Maeda H, Morooka S (1996), 'Preparation and characterization of silica–polyimide composite membranes coated on porous tubes for CO_2 separation', *J. Membrane. Sci.*, 115, 65–75.

Li J-L, Chen BH (2005), 'Review of CO_2 absorption using chemical solvents in hollow fiber membrane contactors', *Separation Purification Technol.*, 41, 109–122.

Li K (2005), 'Hollow fibre ceramic membranes', Proc. XXII European Membrane Society summer school on *Inorganic membranes: Preparation, characterization and applications*, University of Zaragoza, Jaca, Spain, 5–9 September 2005.

Liu S, Li K, Hughes R (2003), 'Preparation of porous aluminium oxide (Al_2O_3) hollow fiber membranes by a combined phase-inversion and sintering method', *Ceramics Int.,* 29, 875–881.

Loeb S, Sourirajan S (1962), 'Seawater demineralization by means of a semipermeable membrane, in Gould RF (ed.) *Saline water conversion – II*, Advances in Chemistry (ACS) Series, Vol. 38, Washington DC, American Chemical Society, Ch. 9, 117–132.

Luebke D, Myers C, Pennline H (2006), 'Hybrid membranes for selective carbon dioxide separation from fuel gas', *Energy & Fuels*, 20(5), 1906–1913.

Mahajan R, Zimmerman CM, Koros WJ (1999), 'Fundamental, practical aspects of mixed matrix gas separation membranes', *ACS Symp. Ser*, 733, 277.

Maier G (1998), 'Gas separation with polymer membranes', *Angew. Chem. Int. Ed.*, 37, 2960.

Meisen A, Shuai X (1997), 'Research and development issues in CO_2 capture', *Energy Conversion Managmt*, 38(S1), 37–42.

Mitchell JV (1831), *J. R. Inst.*, 2(101), 307.

Mundschau MV, Xie X, Evenson CR, Sammells AF (2006), 'Dense inorganic membranes for production of hydrogen from methane and coal with carbon dioxide sequestration', *Catalysis Today*, 118, 12–23.

Nollet JA (1748), *Lecons de physique-experimental*, Paris, Hippolyte–Louis Guerin.

Nomura M, Yamaguci T, Nakao SI (1997), 'Silicalite membranes modified by counterdiffusion CVD technique', *Ind. Engng Chem. Res.*, 36, 4217–4223.

Osada Y, Nakagawa T (1992), *Membrane science and technology*, New York, Marcel Dekker Inc.

Patel N, Miller AC, Spontak RJ (2004), 'Highly CO_2-permeable and selective membranes derived from crosslinked poly(ethylene glycol) and its nanocomposites', *Adv. Functional. Mater.*, 14, 699.

Paul D, Yampol'skii YP (1994), *Polymeric gas separation membranes*, Boca Raton, CRC Press.

Pennline HW, Luebke DR, Jones KL, Myers CR, Morsi BI, Heintz YJ, Ilconich JB (2008), 'Progress in carbon dioxide capture and separation research for gasification-based power generation point sources', *Fuel Processing Technol.*, 89, 897–907.

Plate N., Yampol'skii YP (1994), 'Relationship between structure and transport

© Woodhead Publishing Limited, 2010

properties for high free volume polymeric materials', in *Polymeric gas separation membranes*, Baton Rouge, CRC Press, 115–208.

Powell CE, Qiao GG (2006), 'Polymeric CO_2/N_2 gas separation membranes for the capture of carbon dioxide from power plant flue gases', *J. Membrane Sci*., 279, 1–49.

Qi Z, Cussler EL (1985), 'Microporous hollow fibers for gas absorption, I. Mass transfer in the liquid', *J. Membrane Sci*., 23, 321–333.

Rao AB, Rubin ES (2006), 'Identifying cost-effective CO_2 control levels for amine-based capture systems', *Ind. Engng Chem. Res.,* 45, 2421–2429.

Rautenbach R., Albrecht R. (1989), *Membrane processes*, Wiley.

Robeson L (1991), 'Correlation of separation factor versus permeability for polymeric membranes', *J. Membrane Sci*., 62, 165.

Rydén M, Lyngfelt A (2006), 'Using steam reforming to produce hydrogen with carbon dioxide capture by chemical-looping combustion', *Int. J. Hydrogen Energy*, 31, 1271–1283.

Scholes CA, Kentish SE, Stevens GW (2008), 'Carbon dioxide separation through polymeric membrane systems for flue gas applications', *Recent Patents on Chem. Engng*, 1, 52–66.

Shekhawat D, Luebke DR, Pennline HW (2003), 'A review of carbon dioxide selective membranes – A topical report'. National Energy Technology Laboratory, United States Department of Energy.

Singh RP, Way JD, McCarley KC (2004), 'Development of a model surface flow membrane by modification of porous Vycor glass with a fluorosilane', *Ind. Engng Chem. Res*, 43(12),
3033–3040.

Spillman R (1989), 'Economics of gas separation by membranes', *Chem. Engng Prog*ress, 85, 41.

Stern S (2002), 'Polymers for gas separation: the next decade', *J. Membrane Sci*., 94, 1.

Sutherland K (2008), 'Bulk chemical industry: membrane separation processes in the bulk chemicals industry', *Filtration and Separation*, 12–14.

Tantekin-Ersolmaz SB, Atalay-Oral C, Tatlier M, Erdem-Senatalar A, Schoemanb B, Sterte J (2000), 'Effect of zeolite particle size on the performance of polymer-zeolite mixed matrix membranes', *J. Membrane Sci*., 175, 285–288.

Tarun CB, Croiset E, Douglas PL, Gupta M, Chowdhury MHM (2007), 'Techno-economic study of CO_2 capture from natural gas based hydrogen plants', *Int. J. Greenhouse Gas Control*, 1, 55–61.

Van Der Sluijs J, Hendriks C, Blok K (1992), *Energy Conversion Managmt*., 33, 429.

Violante V, Drioli E, Basile A (1992), 'Metodi di ingegneria nei processi di separazione dei gas mediante membrane', *La Chimica e L'Industria*, 74, 11–21.

Vu DQ, Koros WJ, Miller SJ (2003), 'Effect of condensable impurity in CO_2/CH_4 gas feeds on performance of mixed matrix membranes using carbon molecular sieves', *J. Membrane Sci*., 221, 233–239.

Westmoreland JC (1968), 'Spiral wrapped reverse osmosis membrane cell', US Patent 3,367,504.

Yan S-P, Fang M-X, Zhang W-F, Wang S-Y, Xu Z-K, Luo Z-Y, Cen K-F (2007), 'Experimental study on the separation of CO_2 from flue gas using hollow fiber

© Woodhead Publishing Limited, 2010

membrane contactors without wetting', *Fuel Processing Technol.*, 88(5), 501–511.

Yang H, Xu Z, Fan M, Gupta R, Slimane RB, Bland AE, Wright I (2008), 'Progress in carbon dioxide separation and capture: A review', *J. Envir. Sci.*, 20, 14–27.

Yang SM, Lee YE, Hyun SH, Lee CH (2002), 'Organic-templating approach to synthesis of nanoporous silica composite membranes (I): TPA-templating and CO_2 separation', *J. Mater Sci.*, 37(12), 2519–2525.

Zheng Z, Xu X, Fan X, Lau WM, Kwok RWM (2004), 'Ultrathin polymer film formation by collision-induced cross-linking of adsorbed organic molecules with hyperthermal protons', *J. Am. Chem. Soc.*, 126, 123–136.

Zimmerman CM, Singh A, Koros WJ (1997), 'Tailoring mixed matrix composite membranes for gas separations', *J. Membrane Sci.*, 137, 145.

© Woodhead Publishing Limited, 2010

7

Advanced flue gas cleaning systems for sulfur oxides (SO_x), nitrogen oxides (NO_x) and mercury emissions control in power plants

S. FALCONE MILLER and B. G. MILLER,
The Pennsylvania State University, USA

Abstract: This chapter discusses current and future control technologies for sulfur oxides, nitrogen oxides, and mercury in the power generation sector. Current control technologies addressed focus on flue gas desulfurization technologies for sulfur oxides, selective catalytic reduction, selective non-catalytic reduction, and hybrid technologies for nitrogen oxides, as well as powdered activated carbon injection for mercury control. Future control technologies for nitrogen oxides and mercury capture are discussed.

Key words: flue gas desulfurization, selective catalytic reduction, selective non-catalytic reduction, powdered activated carbon, sulfur dioxide, nitrogen oxides, mercury.

7.1 Introduction

Coal combustion generates several pollutants including acid gases, specifically sulfur dioxide (SO_2), sulfur trioxide (SO_3), hydrogen chloride (HCl), hydrogen fluoride (HF), and oxides of nitrogen, particulate matter, and mercury. Particulate matter control is discussed in Chapter 8 and control of acid gases, specifically SO_2 and NO_x, and mercury are discussed in this chapter.

Acid gases cause widespread damage when they precipitate as acid rain or when they form weak acidic solutions with moisture at ground level. These effects include damage to soil productivity, damage to vegetation and aquatic life, and damage to manmade structures (Miller and Tillman, 2008). Consequently, SO_2 and NO_x emission standards have been introduced in many countries on a national and regional basis. International standards and bilateral agreements have also been implemented by several countries

© Woodhead Publishing Limited, 2010

(Soud, 2000; Wu, 2002; Rubin *et al*., 2004; Miller, 2005). Major landmark SO_2 regulations include: the Clean Air Act Amendments of 1970, 1977, and 1990 in the United States; the Stationary Emissions Standards of 1970 in Japan; the 1983 SO_2 Emissions Regulations of the Federal Republic of Germany; and the United Nations Economic Commission for Europe's (UNECE) Convention on Long-Range Transboundary Air Pollution (LRTAP), which came into force in 1983. Since the mid-1980s, SO_2 emissions regulations have been implemented in most other industrialized nations and many developing countries. Similarly, major landmark NO_x regulations include the UNECE LRTAP and the Clean Air Act Amendments of 1970, 1977, and 1990. These have been followed by more stringent NO_x regulations in countries throughout the world.

Mercury exists in three forms in coal-derived flue gas: elemental (Hg^o), oxidized (Hg^{2+}) and condensed on ash particles (Hg_p). In the natural environment, mercury can go through a series of chemical transformations to convert it to a highly toxic form, methylmercury (CH_3Hg), which enters the food chain, particularly in aquatic organisms, and bioaccumulates (EPA, 1997a). Mercury exposure results in neurological disorders. Legislation to control mercury from coal-fired power plants is in various stages of implementation. In the United States, the US Environmental Protection Agency (EPA) announced the Clean Air Mercury Rule in 2005; however, in 2008 the District of Columbia Circuit Court vacated the rule on the grounds that it did not meet the stipulations of the 1990 Clean Air Act Amendments. EPA is currently re-evaluating options for further mercury legislation, but many states have passed mercury emissions legislation that is more stringent than that outlined in the Clean Air Mercury Rule. Internationally, legislation for addressing mercury emissions from power plants is contained in the UNECE LRTAP on Heavy Metals, which was adopted in 1998 and went into effect in 2005.

In the utility sector, the reduction of SO_2 emissions is achieved by utilizing lower-sulfur fuels (by blending a low-sulfur coal with the parent/design high-sulfur coal, completely switching to a lower-sulfur coal, or coal cleaning to remove pyritic sulfur) or installing a flue gas desulfurization (FGD) system. Depending upon the application, cost, and efficiencies required, FGD systems available are wet scrubbers, spray dryer-absorbers (or semi-dry systems), and dry injection systems. These are discussed in section 7.2.

Technologies to control NO_x emissions from coal-fired power plants can be divided into two groups: (i) combustion modifications where the NO_x production is reduced during the combustion process, and (ii) flue gas treatment, which removes the NO_x from the flue gas following its formation. Post-combustion technologies of significance include selective catalytic reduction (SCR), selective non-catalytic reduction (SNCR) and hybrid systems, which are discussed in sections 7.3, 7.4, and 7.5, respectively.

© Woodhead Publishing Limited, 2010

Many research organizations, federal agencies, technology vendors, and utilities are actively involved in the process of identifying, developing, and demonstrating cost-effective mercury control technologies for the electric utility industry. Approaches for controlling mercury include coal treatment/combustion modifications, sorbent injection, and FGD enhancement/oxidation (Feeley, 2006). To date, the use of activated carbon injection (ACI) has shown the most promise as a near-term mercury control strategy and this technology is discussed in section 7.6. The US Department of Energy (DOE) and others are conducting field tests of a number of alternative approaches to enhance ACI mercury-capture performance for both bituminous and low-rank coal applications, including the use of chemically-treated powdered activated carbons (PACs) that compensate for low chlorine concentrations in the flue gas.

Future trends will be discussed in section 7.7, which will focus on NO_x and mercury control technologies because strategies for SO_2 are considered mature. Technologies to enhance mercury capture in wet FGD systems will be discussed. Novel mercury control concepts will be introduced.

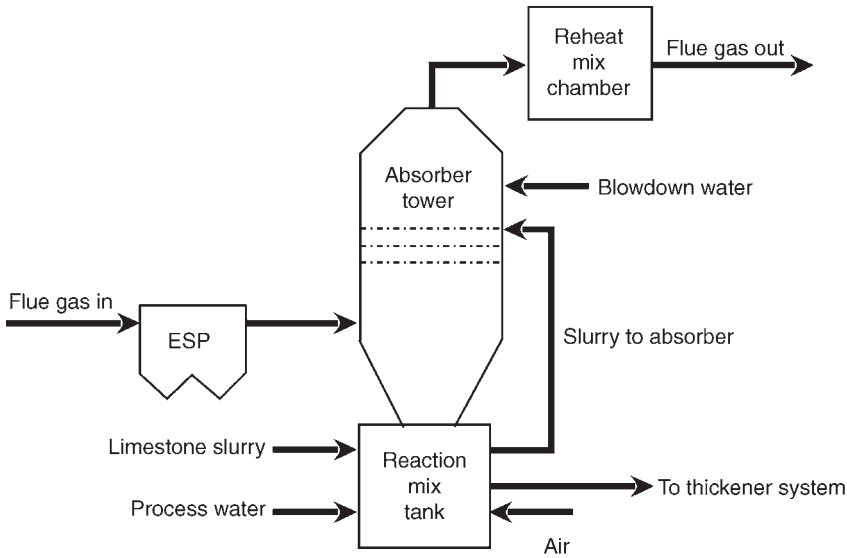
7.2 Flue gas desulfurization (FGD)

A variety of SO_2 control technologies are in use and others are in various stages of development. Commercialized processes include wet, semi-dry (slurry spray with drying), and completely dry processes, which are discussed in this section. The wet FGD scrubber is the dominant worldwide technology for the control of SO_2 from utility power plants, with approximately 85% of the installed capacity, although the dry FGD systems are also used for selected lower-sulfur applications (Kitto and Stultz, 2005).

7.2.1 Wet flue gas desulfurization technology

Wet scrubbers are the most common FGD method currently in use and include a variety of processes, the use of many sorbents, and are manufactured by a large number of companies. The sorbents used by wet scrubbers include calcium-, magnesium-, potassium-, or sodium-based sorbents, ammonia, or seawater. Currently, there are no commercial potassium-based scrubbers in use and only a limited number of ammonia or seawater systems in use or being demonstrated. The calcium-based scrubbers are by far the most popular for power generation and this technology is discussed in this section.

© Woodhead Publishing Limited, 2010



7.1 Schematic diagram of generic wet scrubber system components.

Limestone and lime-based scrubbers

Wet scrubbing with limestone and lime are the most popular commercial FGD systems. The inherent simplicity, the availability of an inexpensive sorbent (limestone), production of a usable by-product (gypsum), reliability, availability, and the high removal efficiencies obtained (which can be as high as 99%) are the main reasons for this popularity. Capital costs are typically higher than other technologies, such as sorbent injection systems; however, the technology is known for its low operating costs as the sorbent is widely available and the system is cost effective.

Figure 7.1 is a generic schematic diagram showing the major components and layout utilized for a wet scrubber system. Note that the limestone storage, pulverizer, and feed slurry storage tank to produce the limestone slurry are not shown in Fig. 7.1. The reaction tank in this system has to be sized to provide sufficient time for sulfur components to precipitate and for the dissolution of additives to occur.

In a limestone/lime wet scrubber, the flue gas is scrubbed with a 5–15% (by weight) slurry of calcium sulfite/sulfate salts along with calcium hydroxide ($Ca(OH_2)$) or limestone ($CaCO_3$). Calcium hydroxide is formed by slaking lime (CaO) in water according to the reaction

$$CaO(s) + H_2O(l) \rightarrow Ca(OH)_2(s) + \text{heat} \qquad [7.1]$$

In the limestone and lime wet scrubbers, the slurry containing the sulfite/sulfate salts and the newly added limestone or calcium hydroxide are

© Woodhead Publishing Limited, 2010

pumped to a spray tower absorber and sprayed into it. The sulfur dioxide is absorbed into the droplets of slurry and a series of reactions occur in the slurry. The reactions between the calcium and the absorbed sulfur dioxide create the compounds calcium sulfite hemihydrate ($CaSO_4 \cdot \frac{1}{2}H_2O$) and calcium sulfate dihydrate ($CaSO_4 \cdot 2H_2O$). Both of these compounds have low solubility in water and precipitate from the solution. This enhances the absorption of sulfur dioxide and further dissolution of the limestone or hydrated lime.

The reactions occurring in the scrubbers are complex. Simplified overall reactions for limestone- and lime-based scrubbers are

$$SO_2(g) + CaCO_2(s) + \tfrac{1}{2}H_2O(l) \rightarrow CaSO_3 \cdot \tfrac{1}{2}H_2O(s) + CO_2(g) \quad [7.2]$$

for a limestone scrubber and

$$SO_2(g) + Ca(OH)_2(s) + H_2O\ (l) \rightarrow CaSO_3 \cdot \tfrac{1}{2}H_2O(s) + \tfrac{3}{2}H_2O(l) \quad [7.3]$$

for a lime scrubber.

The calcium sulfite hemihydrate can be converted to the calcium sulfate dihydrate with the addition of oxygen by the reaction

$$CaSO_3 \cdot \tfrac{1}{2}H_2O(s) + \tfrac{3}{2}H_2O(l) + \tfrac{1}{2}O_2(g) \leftrightarrow CaSO_4 \cdot 2H_2O(s) \quad [7.4]$$

The actual reactions that occur, however, are much more complex and include a combination of gas–liquid, solid–liquid, and liquid–liquid ionic reactions. In the limestone scrubber, the following reactions describe the process. In the gas–liquid contact zone of the absorber (see Fig. 7.1 for a typical schematic diagram of a limestone scrubber system), sulfur dioxide dissolves into the aqueous state

$$SO_2(g) \leftrightarrow SO_2(l) \quad [7.5]$$

and is hydrolyzed to form ions of hydrogen and bisulfate

$$SO_2(l) + H_2O(l) \leftrightarrow HSO_3^- + H^+ \quad [7.6]$$

The limestone dissolves in the absorber liquid forming ions of calcium and bicarbonate

$$CaCO_3(s) + H^+ \leftrightarrow Ca^{++} + HCO_3^- \quad [7.7]$$

which is followed by acid–base neutralization

$$HCO_3^- + H^+ \leftrightarrow CO_2(l) + H_2O\ (l) \quad [7.8]$$

© Woodhead Publishing Limited, 2010

stripping of the CO_2 from the slurry

$$CO_2(l) \leftrightarrow CO_2(g) \quad [7.9]$$

and dissolution of the calcium sulfite hemihydrate

$$CaSO_3 \cdot \tfrac{1}{2}H_2O(s) \leftrightarrow Ca^{++} + HSO_3^- + \tfrac{1}{2}H_2O(l) \quad [7.10]$$

In the reaction tank of a scrubber system, the solid limestone is dissolved into the aqueous state (reaction [7.7]), acid–base neutralization occurs (reaction [7.8]), the CO_2 is stripped out (reaction [7.9]), and the calcium sulfite hemihydrate is precipitated by the reaction

$$Ca^{++} + HSO_3^- + \tfrac{1}{2}H_2O(l) \leftrightarrow CaSO_3 \cdot \tfrac{1}{2}H_2O(s) + H^+ \quad [7.11]$$

The dissolution of the calcium sulfite in the gas–liquid contact zone in the absorber is necessary in order to minimize scaling of the calcium sulfite hemihydrate in the absorber (Wark *et al.*, 1998). The equilibrium pH for calcium sulfite is ≈6.3 at a CO_2 partial pressure of 0.12 atmospheres, which is the typical concentration of CO_2 in flue gas. Typically the pH is maintained below this level to keep the calcium sulfite hemihydrate from dissolving (i.e. keep reaction [7.10] from proceeding to the right).

The slurry returning from the absorber to the reaction tank can have a pH as low as 3.5, which is increased to 5.2 to 6.2 by the addition of freshly prepared limestone slurry into the tank (Wark *et al.*, 1998). The pH in the reaction tank must be maintained at a pH that is less than the equilibrium pH of calcium carbonate in water, which is 7.8 at 77°F.

The reaction equations for the lime scrubber are similar to those for the limestone scrubber, with the exception that the following reactions are substituted for reactions [7.7] and [7.8], respectively (Stultz and Kitto, 1992)

$$Ca(OH)_2(s) + H^+ \leftrightarrow CaOH^+ + H_2O(l) \quad [7.12]$$

$$CaOH^+ + H^+ \leftrightarrow Ca^{++} + H_2O(l) \quad [7.13]$$

Limestone scrubbing with forced oxidation (LSFO) is one of the most popular systems in the commercial market. A limestone slurry is used in an open spray tower with in-situ oxidation to remove SO_2 and form a gypsum sludge. The major advantages of this process, relative to a conventional limestone FGD system (where the product is calcium sulfite rather than calcium sulfate (gypsum)), are easier dewatering of the sludge, more economical disposal of the scrubber product solids, and decreased scaling on the tower walls. LSFO is capable of greater than 90% SO_2 removal (Radcliffe, 1991).

In the LSFO system, the hot flue gas exits the particulate control device,

© Woodhead Publishing Limited, 2010

usually an electrostatic precipitator (ESP), and enters a spray tower where it comes into contact with a sprayed dilute limestone slurry. The SO_2 in the flue gas reacts with the limestone in the slurry via the reactions listed earlier to form the calcium sulfite hemihydrate. Compressed air is bubbled through the slurry, which causes this sulfite to be naturally oxidized and hydrated to form calcium sulfate dihydrate. The calcium sulfate can be first dewatered using a thickener or hydrocyclones then further dewatered using a rotary drum filter. The gypsum is then transported to a landfill for disposal. The formation of the calcium sulfate crystals in a recirculation tank slurry also helps to reduce the chance of scaling.

The absorbing reagent, limestone, is normally fed to the open spray tower in an aqueous slurry at a molar feed rate of 1.1 moles of $CaCO_3$/mole of SO_2 removed. This process is capable of removing more than 90% of the SO_2 present in the inlet flue gas. The advantages of LSFO systems are (Radcliffe, 1991) as follows.

- There is a lower scaling potential on tower internal surfaces owing to the presence of gypsum seed crystals and reduced calcium sulfate saturation levels. This in turn allows a greater reliability of the system.
- The gypsum product is filtered more easily than the calcium sulfite ($CaSO_3$) produced with conventional limestone systems.
- There is a lower chemical oxygen demand in the final disposed product.
- The final product can be safely and easily disposed in a landfill.
- The forced oxidation allows the limestone utilization to be greater than conventional systems.
- The raw material (limestone) used as an absorbent is low in cost.
- LSFO is an easier retrofit than natural oxidation systems since the process uses smaller dewatering equipment.

A disadvantage of this system is the high energy demand due to the relatively higher liquid-to-gas ratio necessary to achieve the required SO_2 removal efficiencies.

Materials of construction

In the operation of wet scrubbers, two major problems that are encountered are corrosion and wet–dry interface scaling; these problems can be minimized by use of special construction materials and limited recycling of scrubber solutions. As the level of dissolved solids in the lime/limestone slurry increases, scaling potential also increases. If excess scaling is experienced, large pressure drops of the gas can cause a shutdown.

The slurry pH of the recirculated slurry is typically between 5 and 6 in the recirculation tank of a limestone system. The pH in the spray zone and on the tray can be as low as 3.5 to 4. Chloride concentrations are usually

© Woodhead Publishing Limited, 2010

Table 7.1 Some alloy materials for wet FGD service (Kitto and Stultz, 2005)

Alloy	Cr: wt.%	Mo: wt%	Ni: wt%	Ni: wt%	Max. Cl: ppm
316L	16.0	2.0	10.0	0	10 000
20	19.0	2.0	32.0	0	12 000
317L	18.0	3.0	11.0	0	15 000
825	19.5	2.5	38.0	0	15 000
317LM	18.0	4.0	13.5	0	18 000
317LMN	17.0	4.0	13.5	0.1	20 000
904L	19.0	4.0	23.0	0	20 000
2205	22.0	3.0	4.5	0.14	30 000
255	24.0	2.9	4.5	0.1	45 000
G	21.0	5.5	36.0	0	50 000
254-SMO	19.5	6.0	17.5	0.18	55 000
AL-6XN	20.0	6.0	23.5	0.18	55 000
625	20.0	8.0	58.0	0	55 000
C-22	20.0	12.5	50.0	0	100 000
C-276	14.5	15.0	51.0	0	100 000

designed at 20 000 ppm by weight but can be as high as 100 000 ppm when seawater is used as make-up water. Alloy construction (see Table 7.1) has been the most popular selection for absorber materials in the US (Kitto and Stultz, 2005). Rubber-lined, carbon steel scrubber modules are popular in Europe.

The industry has used a number of different alloys for the absorber shell, tray, and internal supports. Rubber linings, flake-glass linings, and ceramic tile systems have also been used. The material selection on any project is dependent on the process chemistry and the cost–benefit analysis of the material from a lifecycle perspective.

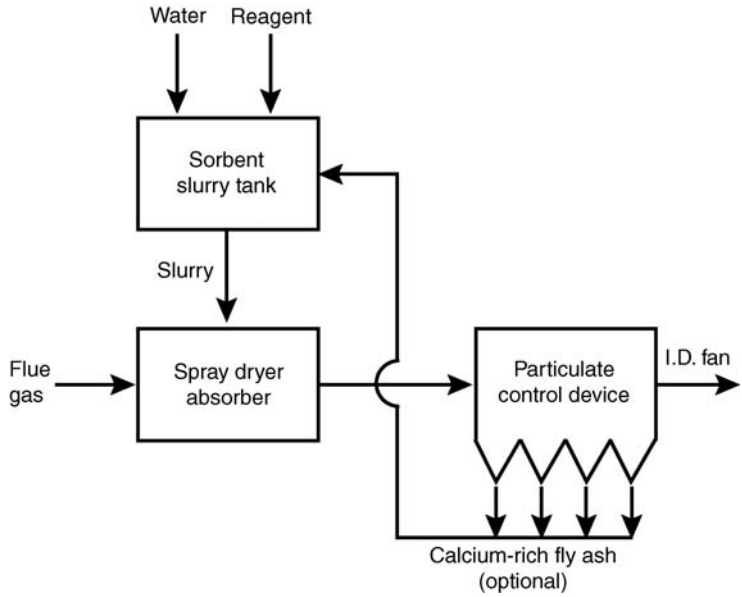
7.2.2 Dry flue gas desulfurization technology

Dry FGD technology includes lime or limestone spray drying, dry sorbent injection including furnace, economizer, duct, and hybrid methods, and circulating fluidized-bed scrubbers. These processes are characterized by dry waste products that are generally easier to dispose than waste products from wet scrubbers. All dry FGD processes are throw-away types.

Spray dry scrubbers

Spray dry scrubbers are the second most widely used method to control SO_2 emissions in utility coal-fired power plants. Wet scrubbing requires considerable equipment, and alternatives to wet scrubbing were developed including spray dry scrubbers. Lime (CaO) is usually the sorbent used in the spray drying process, but hydrated lime ($Ca(OH)_2$) is also used. This

© Woodhead Publishing Limited, 2010



7.2 Typical spray dryer absorber and particulate control system components.

technology is also known as semi-dry flue gas desulfurization and is generally used for sources that burn low- to medium-sulfur coal. This process has been used in both retrofit applications and new installations on units burning low-sulfur coal (Wark *et al*., 1998; Srivastava *et al*., 2000). An example of a typical spray dryer absorber and particulate control system is shown in Fig. 7.2.

In this process, the hot flue gas exits the boiler air heater and enters a reactor vessel. A slurry consisting of lime and recycled solids is atomized/sprayed into the absorber. The slurry is formed by the reaction presented previously

$$CaO(s) + H_2O(l) \rightarrow Ca(OH)_2(s) + \text{heat} \qquad [7.1]$$

The SO_2 in the flue gas is absorbed into the slurry and reacts with the lime and fly ash alkali to form calcium salts

$$Ca(OH)_2(s) + SO_2(g) \rightarrow CaSO_3 \cdot \tfrac{1}{2}H_2O(s) + \tfrac{1}{2}H_2O(v) \qquad [7.14]$$

$$Ca(OH)_2(s) + SO_3(g) + H_2O(\nu) \rightarrow CaSO_4 \cdot 2H_2O(s) \qquad [7.15]$$

The scrubbed gas then passes through a particulate control device downstream of the spray drier. Some of the collected reaction product, which contains some unreacted lime, and fly ash are recycled to the slurry

© Woodhead Publishing Limited, 2010

feed system while the rest is sent to a landfill for disposal. Factors affecting the absorption chemistry include the flue gas temperature, SO_2 concentration in the flue gas, and the size of the atomized slurry droplets. Spray dryers can typically achieve SO_2 removal efficiencies ranging from 70 to 95%.

The lime spray dryer process offers a few advantages over the LSFO process (Radcliffe, 1991).

- Only a small alkaline stream of scrubbing slurry must be pumped into the spray dryer. This stream contacts the gas entering the dryer instead of the walls of the system. This prevents corrosion of the walls and pipes in the absorber system.
- The pH of the slurry and dry solids is high, allowing for the use of mild steel materials rather than expensive alloys.
- The product from the spray dryer is a dry solid that is handled by conventional dry fly ash particulate removal and handling systems, which eliminates the need for dewatering solids handling equipment and reduces associated maintenance and operating requirements.
- Overall power requirements are decreased because less pumping power is required.
- The gas exiting the absorber is not saturated and does not require reheat, thereby capital costs and steam consumption are reduced.

There are some disadvantages of the lime spray dryer compared to the LSFO system (Radcliffe, 1991).

- A major product of the lime spray dryer process is calcium sulfite, as only 25% or less oxidizes to calcium sulfate.
- The solids handling equipment for the particulate removal device has to have a greater capacity than conventional fly ash removal applications.
- Fresh water is required in the lime slaking process, which can represent approximately half of the system's water requirement. This differs from the wet scrubbers where cooling tower water can be used for limestone grinding circuits and most other make-up water applications.
- The lime spray dryer process requires a higher reagent feed ratio than a conventional system to achieve high removal efficiencies. Approximately 1.5 moles CaO/mole of SO_2 removed are needed for 90% removal efficiency.
- Lime is also more expensive than limestone, therefore the operating cost is increased.
- A higher inlet flue gas temperature is needed when a higher-sulfur coal is used, which in turn reduces the overall boiler efficiency.

© Woodhead Publishing Limited, 2010

Other sorbent injection processes

A number of dry injection processes have been developed to provide moderate SO_2 removal, which are easily retrofitted to existing facilities and are low capital cost. There are five basic processes. Two are associated with the furnace – furnace sorbent injection and convective pass (economizer) injection – and three are associated with injection into the ductwork downstream of the air heater – in-duct injection, in-duct spray drying (discussed in the preceding section), and hybrid systems. Combinations of these processes are also available. Sorbents include calcium- and sodium-based compounds; however, the use of calcium-based sorbents is more prevalent. Furnace injection has been used in some small plants using low-sulfur coals. Hybrid systems may combine furnace and duct sorbent injection or introduce a humidification step to improve removal efficiency. These systems can achieve as high as 70% removal and are commercially available (Soud, 2000). Process schematic diagrams for dry injection SO_2 control technologies are illustrated in Fig. 7.3.

Figure 7.4 is a representation of the level of SO_2 removal that the dry calcium-based sorbent injection processes achieve and the temperature regimes in which they operate (Rhudy *et al.*, 1986). The peak at approximately 2200°F represents furnace sorbent injection, the peak at about 1000°F is convective pass/economizer injection, and the peak at the low temperature represents all of the processes downstream of the air heater.

Furnace sorbent injection

Furnace sorbent injection (FSI) is the simplest dry sorbent process. In this process, illustrated in Fig. 7.3a, pulverized sorbents, most often calcium hydroxide and sometimes limestone, are injected into the upper part of the furnace to react with the SO_2 in the flue gas. The sorbents are distributed over the entire cross-section of the upper furnace where the temperature is in the range 1400 to 2400°F and the residence time for the reactions is 1–2 s. The sorbents decompose and become porous solids with high surface area. At temperatures higher than ≈2300°F, dead-burning or sintering is experienced.

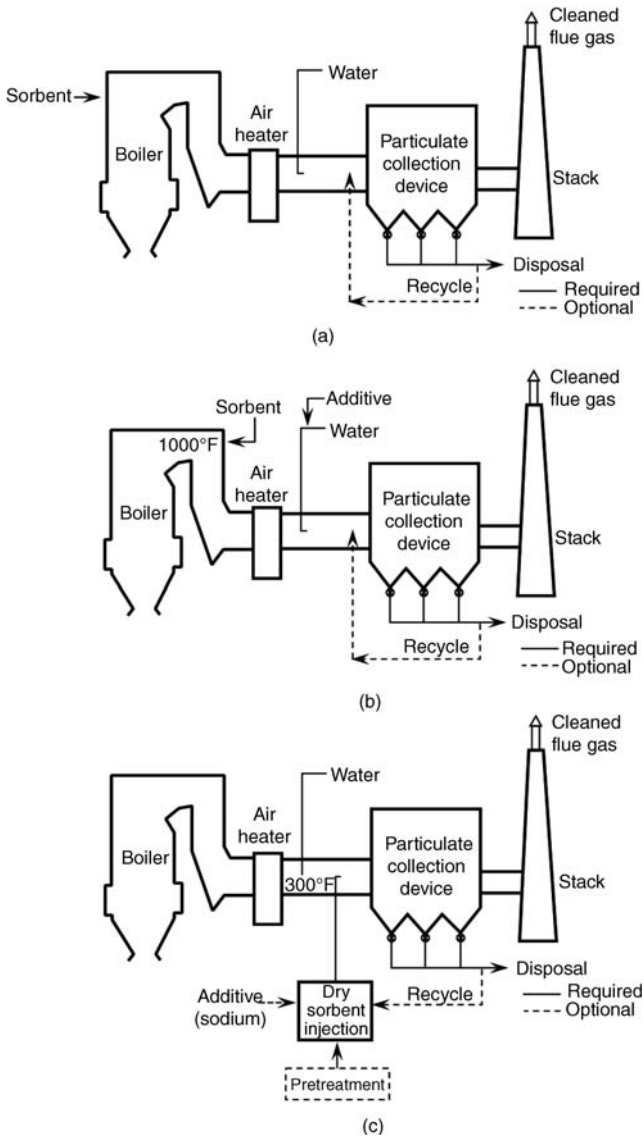
When limestone is used as the sorbent, it is rapidly calcined to quicklime when it enters the furnace

$$CaCO_3(s) + \text{heat} \rightarrow CaO(s) + CO_2(g) \quad [7.16]$$

Sulfur dioxide diffuses to the particle surface and heterogeneously reacts with the CaO to form calcium sulfate

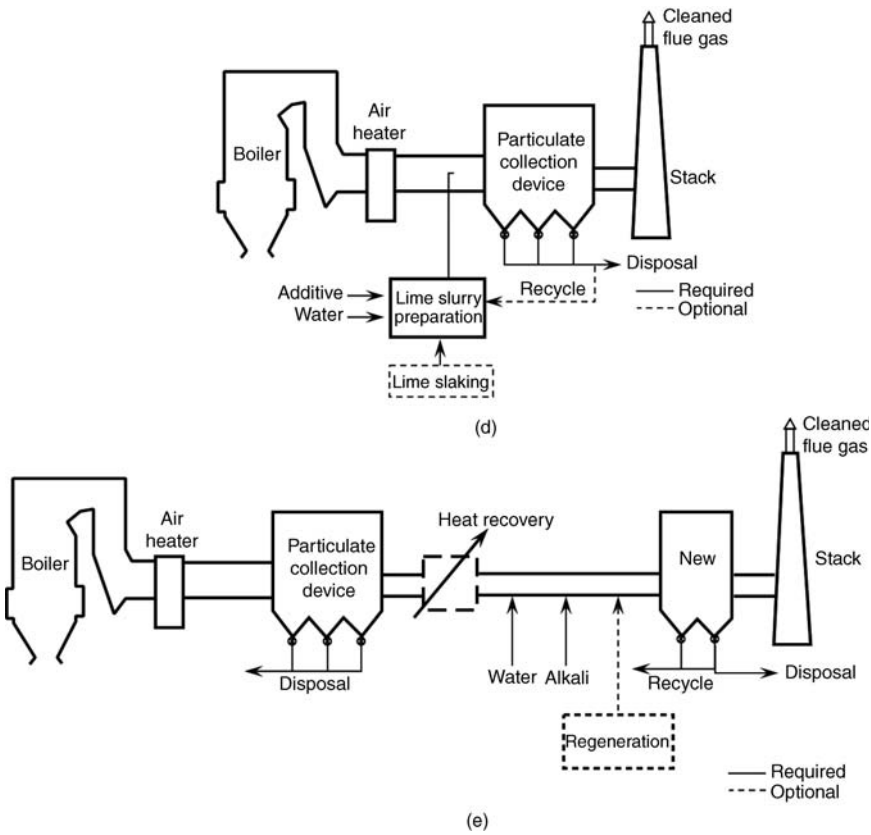
$$CaO(s) + SO_2(g) + \tfrac{1}{2}O_2(g) \rightarrow CaSO_4(s) \quad [7.17]$$

© Woodhead Publishing Limited, 2010



7.3 Simplified process schematic diagrams for dry injection SO_2 control technologies: (a) furnace sorbent injection; (b) economizer injection; (c) duct sorbent injection: dry sorbent injection; (d) duct sorbent injection: duct spray drying; (e) hybrid system (source: adapted from Rhudy, *et al*. (1986)).

© Woodhead Publishing Limited, 2010



7.3 (continued)

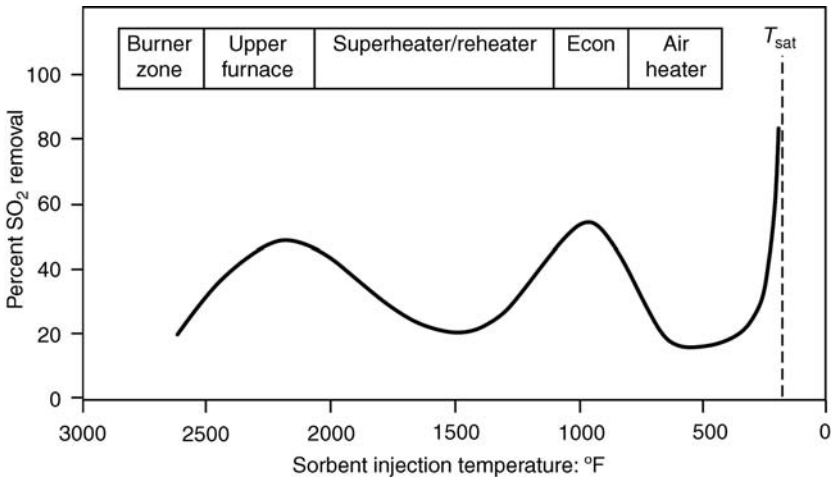
Sulfur trioxide, although present at a significantly lower concentration than SO_2, is also captured using calcium-based sorbents

$$CaO(s) + SO_3(g) \rightarrow CaSO_4(s) \qquad [7.18]$$

Approximately 15–40% SO_2 removal can be achieved using a Ca/S molar ratio of 2.0 in the flue gas. The optimum temperature for injecting limestone is ≈1900–2100°F.

The calcium sulfate that is formed travels through the rest of the boiler flue gas system and is ultimately collected in the existing particulate control device with the fly ash and unreacted sorbent. Some concerns exist regarding increased tube deposits as a result of injecting solids into the boiler and the extent of calcium deposition is influenced by overall ash chemistry, ash loading, and boiler system design.

© Woodhead Publishing Limited, 2010



7.4 SO_2 capture regimes for hydrated calcitic lime at a Ca/S molar ratio of 2.0 (source: adapted from Rhudy, *et al.* (1986)).

The following overall reactions occur when using hydrated lime as the sorbent:

$$Ca(OH)_2(s) + \text{heat} \rightarrow CaO\ (s) + H_2O(v) \quad [7.19]$$

$$CaO(s) + SO_2(g) + \tfrac{1}{2}O_2(g) \rightarrow CaSO_4(s) \quad [7.17]$$

$$CaO(s) + SO_3(g) \rightarrow CaSO_4(s) \quad [7.18]$$

Approximately 50–80% SO_2 removal can be achieved using hydrated lime at a Ca/S molar ratio of 2.0. The hydrate is injected at very nearly the same temperature window as limestone and the optimum range is 2100–2300°F.

There are several advantages of the FSI system (Radcliffe, 1991). One advantage is the simplicity of the process. The dry reagent is injected directly into the flow path of the flue gas in the furnace and a separate absorption vessel is not required. The injection of lime in a dry form allows for a less complex reagent handling system. This in turn lowers operating labor and maintenance costs, and eliminates the problems of plugging, scaling, and corrosion found in slurry handling. There are lower power requirements since less equipment is needed. Steam is not required for reheat, whereas most LSFO systems require some form of reheat to prevent corrosion of downstream equipment. The sludge dewatering system is eliminated since the FSI process produces a dry solid, which can be removed by conventional fly ash removal systems.

© Woodhead Publishing Limited, 2010

The FSI process has a few disadvantages when compared to the LSFO process (Radcliffe, 1991). One major disadvantage is that the process only removes up to 40 and 80% SO_2 when using limestone and hydrated lime, respectively, at Ca/S molar ratios of 2.0, whereas the LSFO process can remove more than 90% SO_2 using 1.05 to 1.1 moles CaO/mole SO_2 removed. Hence, more sorbent is needed in the FSI process, and lime, which works better than limestone, is more expensive than limestone. There is a potential for solids deposition and boiler convective pass fouling, which occurs during the humidification step through the impact of solid droplets on to surfaces. Also, there is a potential for corrosion at the point of humidification, the ESP, the downstream ductwork, and the stack. The efficiency of an ESP can be reduced by increased particulate loading and changes in the ash resistivity. This can, in turn, lead to the installation of additional particulate collection devices. Sintering of the sorbent is a concern if it is injected at too high a temperature (e.g. $> 2300^{\circ}$F for hydrated lime). Multiple injection ports in the furnace wall may be needed to ensure proper mixing and to follow boiler load swings and hence shifting temperature zones. Hydration of the free lime in the product may be required. Lime is very reactive when exposed to water and can pose a safety hazard for disposal areas.

Economizer injection

In an economizer injection process (shown in Fig. 7.3b), hydrated lime is injected into the flue gas stream near the economizer inlet where the temperature is between 950 and 1050°F. This process is not commercially used at the present time, but has been extensively studied because it was found that the reaction rate and extent of sulfur capture (see Fig. 7.4) are comparable to FSI. However, the economizer temperatures are too low for dehydration of the hydrated lime (only about 10% of the hydrated lime forms quicklime) and the hydrate reacts directly with the SO_2 to form calcium sulfite

$$Ca(OH)_2(s) + SO_2(g) \rightarrow CaSO_3(s) + H_2O(v) \quad [7.20]$$

This process is best suited for older units in need of a retrofit process and can be used for low-to high-sulfur coals. The advantages and disadvantages of this system are similar to the FSI process (but will not be discussed in detail, since this process is not presently being used in the power industry) with the notable exception that there is no reactive CaO contained in the waste.

© Woodhead Publishing Limited, 2010

Duct sorbent injection: dry sorbent injection

Dry sorbent injection (DSI), also referred to as in-duct dry injection, is illustrated in Fig. 7.3c. Hydrated lime is the sorbent typically used in this process, especially for power generation facilities. However sodium-based sorbents have been tested extensively, including full-scale utility demonstrations, and are used in industrial systems such as municipal and medical waste incinerators for acid gas control.

When using hydrated lime in this process, it is injected either upstream or downstream of a flue gas humidification zone. In this zone, the flue gas is humidified to within 20°F of the adiabatic saturation temperature by injecting water into the duct downstream of the air preheater (Radcliffe, 1991). The SO_2 in the flue gas reacts with the calcium hydroxide to form calcium sulfate and calcium sulfite

$$Ca(OH)_2(s) + SO_2(g) + \tfrac{1}{2}O_2(g) + H_2O\ (v) \rightarrow CaSO_4 \cdot 2H_2O(s) \quad [7.21]$$

$$Ca(OH)_2(s) + SO_2(g) \rightarrow CaSO_3 \cdot \tfrac{1}{2}H_2O(s) + \tfrac{1}{2}H_2O(v) \quad [7.14]$$

The water droplets are vaporized before they strike the surface of the wall or enter the particulate control device. The unused sorbent, along with the products and fly ash, are all collected in the particulate control device. About half of the collected material is shipped to a landfill while the other half is recycled for injection with the fresh sorbent into the ducts (Radcliffe, 1991).

The DSI system offers many of the same advantages and disadvantages that other dry systems offer (Radcliffe, 1991). The process is less complex (i.e. no slurry recycle and handling, no dewatering system, fewer pumps, and no reactor vessel) than a wet system, specifically LSFO. The humidification water and hydrated lime are injected directly into the existing flue gas path. No separate SO_2 absorption vessel is necessary. The handling of the reagent is simpler than in wet systems. The costs for DSI systems are less than in wet systems since there is less equipment to install and, since there is less equipment, operating and maintenance costs are reduced. The waste product is free of reactive lime so that no special handling is required.

Some of the problems encountered by the DSI system and its disadvantages, as compared to the LSFO system, are common to other dry processes. Sulfur dioxide removal efficiencies are lower (as is calcium utilization) than wet systems and range from 30 to 70% for a Ca/S ratio of 2.0. Quicklime is more expensive than limestone. When an ESP is used for particulate control, there is the potential for reduced efficiency due to increased fly ash resisitivity and dust loading in the flue gas. Additional

© Woodhead Publishing Limited, 2010

collection devices may be required. A sufficient length of ductwork is necessary to ensure a residence time of 1–2 s in a straight, unrestricted path. Plugging of the duct can occur if the residence time is insufficient for droplet vaporization, leading to increased system pressure drop.

Hybrid systems

Hybrid sorbent injection processes are typically a combination of FSI and DSI systems with the goal of achieving greater SO_2 removal and sorbent utilization (Soud, 2000). Various types of configurations have been tested including injecting secondary sorbents, such as sodium compounds into the ductwork or humidifying the flue gas in a specially designed vessel. Humidification reactivates the unreacted CaO and can increase the SO_2 removal efficiency. Advantages of hybrid processes include high SO_2 removal, low capital and operating costs, less space necessary thereby lending to easy retrofit, easy operation and maintenance, and no waste water treatment (Soud, 2000).

In some hybrid systems, a new baghouse is installed downstream of an existing particulate removal device (generally an ESP). The existing ESP continues to remove the ash, which can be either sold or disposed. Sulfur dioxide removal is accomplished in a manner similar to in-duct injection, with the sorbent injection upstream of the new baghouse (Rhudy *et al.*, 1986).

The potential advantages of this system include the possibility for toxic substances control since a baghouse is the last control device (this is further discussed in Chapter 8 and section 7.6), easier waste disposal, the potential for sorbent regeneration, separate ash and product streams, and more efficient recycle without ash present (Rhudy *et al.*, 1986). The major issue is the high capital cost of adding a baghouse, although the concept of adding one with a high air-to-cloth ratio (3–5 acfm/ft^2) can minimize this cost.

7.3 Selective catalytic reduction (SCR)

Selective catalytic reduction (SCR) of NO_x using ammonia (NH_3) as the reducing gas was patented in the US by Englehard Corporation in 1957 (DOE, 1997) and has been used commercially in Japan since 1980, in Germany since 1986, and in the US starting in the 1990s. This technology can achieve NO_x reductions in excess of 90% and is now widely used in commercial applications worldwide.

© Woodhead Publishing Limited, 2010

7.3.1 Process description

The SCR process uses a catalyst at approximately 570–750°F to facilitate a heterogeneous reaction between NO_x and an injected reagent, vaporized ammonia, to produce nitrogen and water vapor. Ammonia chemisorbs on to the active sites on the catalyst. The NO_x in the flue gas reacts with the adsorbed ammonia to produce nitrogen and water vapor. The principal reactions are (EPA, 1997b)

$$4NO + 4NH_3 + O_2 \rightarrow 4N_2 + 6H_2O \quad [7.22]$$

$$2NO_2 + 4NH_3 + O_2 \rightarrow 3N_2 + 6H_2O \quad [7.23]$$

A small fraction of the sulfur dioxide is oxidized to sulfur trioxide over the SCR catalyst. In addition, side reactions may produce the undesirable by-products ammonium sulfate ($(NH_4)_2SO_4$) and ammonium bisulfate (NH_4HSO_4), which can cause plugging and corrosion of downstream equipment. These side reactions are (DOE, 1997)

$$SO_2 + \tfrac{1}{2}O_2 \rightarrow SO_3 \quad [7.24]$$

$$2NH_3 + SO_3 + H_2O \rightarrow (NH_4)_2SO_4 \quad [7.25]$$

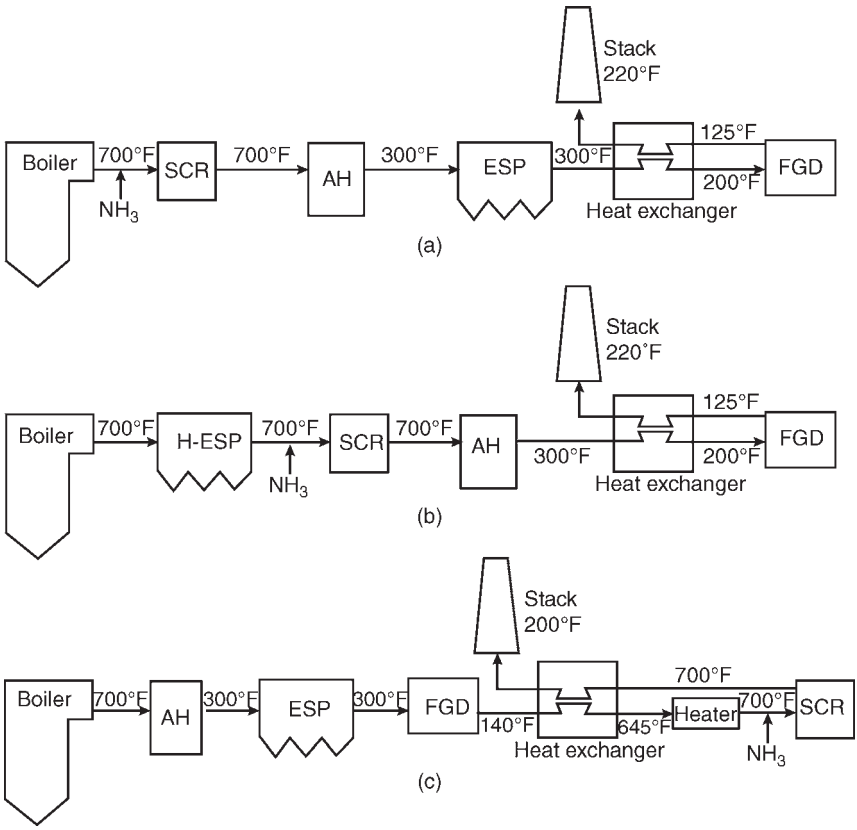
$$NH_3 + SO_3 + H_2O \rightarrow NH_4HSO_4 \quad [7.26]$$

There are three SCR system configurations for coal-fired boilers and they are known as high-dust, low-dust, and tail-end systems. These are shown schematically in Fig. 7.5 (EPA, 1997b). In a high-dust configuration, the SCR reactor is placed upstream of the particulate removal device between the economizer and the air preheater. This configuration (also referred to as hot side, high dust) is the most commonly used, particularly with dry-bottom boilers (Wu, 2002) and is the principal type planned for the installations in the US (McIlvaine *et al*., 2003). In this configuration, the catalyst is exposed to the fly ash and chemical compounds present in the flue gas that have the potential to degrade the catalyst by ash erosion and chemical reactions (i.e. poisoning). However, these can be addressed by proper design as evidenced by the extensive use of this configuration.

In a low-dust installation, the SCR reactor is located downstream of the particulate removal device. This configuration (also referred to as hot side, low dust) reduces the degradation of the catalyst by fly ash erosion. However, this configuration requires a costly hot-side ESP or a flue gas reheating system to maintain the optimum operating temperature.

In tail-end systems (also referred to as cold side, low dust), the SCR

© Woodhead Publishing Limited, 2010



7.5 SCR configurations with typical system temperatures: (a) high-dust system; (b) low-dust system; (c) tail-end system.

reactor is installed downstream of the FGD unit. It may be used mainly in wet-bottom boilers and also on retrofit installations with space limitations (Wu, 2002). However, this configuration is typically more expensive than the high-dust configuration due to flue gas reheating requirements. This configuration does have the advantage of longer catalyst life and use of more active catalyst formulations to reduce overall catalyst cost.

There are several issues that need to be considered in the design and operation of SCR systems, including coal characteristics, catalyst and reagent selections, process conditions, ammonia injection, catalyst cleaning and regeneration, low-load operation, and process optimization (Wu, 2002). Coals with high sulfur in combination with significant quantities of alkaline metals, alkaline earth metals, arsenic, or phosphorus in the ash can severely deactivate a catalyst and reduce its service life. In addition, the SO_3 can react with residual ammonia resulting in ammonium sulfate deposition in the air preheater and loss of performance.

© Woodhead Publishing Limited, 2010

7.3.2 SCR configuration and catalyst composition

The two leading geometries of SCR catalysts are honeycomb and plate (DOE, 1997). The honeycomb form usually is an extruded ceramic with the catalyst either incorporated throughout the structure (homogenous) or coated on the substrate. In the plate geometry, the support material is generally coated with catalyst. Plate-type catalysts have lower pressure drops and are less susceptible to plugging and fouling than the honeycomb types; however, plate-type configurations are significantly larger and more expensive. Honeycomb configurations are significantly smaller than plate types, but have higher pressure drops and plug much more easily.

SCR catalysts were primarily developed by the Japanese as early as 1977. SCR catalysts for utility applications are manufactured from various ceramic materials used as a carrier, such as titanium oxide, and active catalytic components are oxides of base metals such as vanadium (V_2O_5) and tungsten (WO_3).

7.3.3 SCR operation

For optimum SCR performance, the reagent must be well mixed with the flue gas and in direct proportion to the amount of NO_x reaching the catalyst. Anhydrous ammonia has been commonly used as reagent, accounting for over 90% of current world SCR applications (Wu, 2002). It dominates planned installations in the US, although numerous aqueous systems will be installed. Recently, urea-based processes are being developed to address utilizing anhydrous ammonia, which is a hazardous and toxic chemical. When urea ($CO(NH_2)_2$) is used, it produces ammonia, which is the active reducing agent, by the following reactions

$$NH_2 - CO - NH_2 \rightarrow NH_3 + HNCO \quad [7.27]$$

$$HNCO + H_2O \rightarrow NH_3 + CO_2 \quad [7.28]$$

During the operation of the SCR, the catalyst is deactivated by fly ash plugging, catalyst poisoning, and/or the formation of binding layers. The most common method of catalyst cleaning has been the installation of steam soot blowers, although acoustic cleaners have been successfully tested. Once the catalyst has been severely deactivated, it is conventional practice to add additional catalyst or replace it; however, several regeneration techniques have evolved over the last few years providing extended service life for catalysts (Wu, 2002).

Low-load boiler operation can be problematic with SCR operation, specifically with high-sulfur coals. There is a minimum temperature below

© Woodhead Publishing Limited, 2010

which the SCR should not be operated; therefore, system modifications such as economizer bypass to raise the SCR temperature during low-load operation may be required (Wu, 2002).

7.4 Selective non-catalytic reduction (SNCR)

Selective non-catalytic reduction (SNCR) is a proven, commercially-available technology that has been applied since 1974 (Wu, 2002). The SNCR process involves injecting nitrogen-containing chemicals into the upper furnace or convective pass of a boiler within a specific temperature window without the use of an expensive catalyst. There are different chemicals which can be used that selectively react with NO in the presence of oxygen to form molecular nitrogen and water, but the two most common are ammonia and urea. Other chemicals that have been tested in research include amines, amides, amine salts, and cyanuric acid. In recent years, urea-based reagents such as dry urea, molten urea, or urea solution have been increasingly used, replacing ammonia at many plants because anhydrous ammonia is the most toxic and requires strict transportation, storage, and handling procedures (Wu, 2002). The main reactions when using ammonia or urea are, respectively

$$4NO + 4NH_3 + O_2 \rightarrow 4N_2 + 6H_2O \quad [7.29]$$

$$4NO + 2CO\ (NH_2)_2 + O_2 \rightarrow 4N_2 + 2CO_2 + 6H_2O \quad [7.30]$$

A critical issue is finding an injection location with the proper temperature window for all operating conditions and boiler loads. The chemicals then need to be adequately mixed with the flue gases to ensure maximum NO_x reduction without producing too much ammonia. Ammonia slip from an SNCR can affect downstream equipment by forming ammonium sulfates.

The temperature window varies for most of the reducing chemicals used but generally is between 1650–2100°F. Ammonia can be formed below the temperature window and the reducing chemicals can actually form more NO_x above the temperature window. Ammonia has a lower operating temperature than urea, 1560–1920°F compared to 1830–2100°F, respectively.

Enhancers such as hydrogen, carbon monoxide, hydrogen peroxide (H_2O_2), ethane (C_2H_6), light alkanes, and alcohols have been used in combination with urea to reduce the temperature window (Lodder and Lefers, 1985). Several processes use proprietary additives with urea in order to reduce NO_x emissions (Ciarlante and Zoccola, 2001).

The efficiency of reagent utilization is significantly less with SNCR than with SCR. In commercial SNCR systems, the utilization efficiency is

© Woodhead Publishing Limited, 2010

typically between 20 and 60%; consequently, usually three to four times as much reagent is required with SNCR to achieve NO_x reduction similar to that of SCR. SNCR processes typically achieve 20–50% NO_x reduction with stoichiometric ratios of 1.0–2.0.

The major operational impacts of SNCR include air preheater fouling, ash contamination, N_2O emissions, and minor increases in heat rate. A major plant impact of SNCR is on the air preheater, where residual ammonia reacts with the SO_3 in the flue gas to form ammonium sulfate and bisulfate (see reactions [7.26] through [7.28]) causing plugging and downstream corrosion. High levels of ammonia slip can contaminate the fly ash and reduce its sale or disposal. Significant quantities of N_2O can be formed when the reagent is injected into areas of the boiler which are below the SNCR optimum operating temperature range. Urea injection tends to produce a higher level of N_2O compared to ammonia. The unit heat rate is increased slightly due to the latent heat losses from vaporization of injected liquids and/or increased power requirements for high-energy injection systems. The overall efficiency and power losses normally range from 0.3 to 0.8% (Wu, 2002).

7.5 Hybrid SNCR/SCR

SCR generally represents a relatively high capital requirement whereas SNCR has a high reagent cost. A hybrid SNCR/SCR system balances these costs over the life cycle for a specific NO_x reduction level, provides improvements in reagent utilization, and increases overall NO_x reduction (Wu, 2002). However, there is limited experience with these hybrid systems as full-scale power plant operation to date has only been in demonstrations. They are discussed here because they have demonstrated NO_x reductions as high as 60–70%.

In a hybrid SNCR/SCR system, the SNCR operates at lower temperatures than stand-alone SNCRs, resulting in greater NO_x reduction but also higher ammonia slip. The residual ammonia feeds a smaller-sized SCR reactor, which removes the ammonia slip and decreases NO_x emissions further. The SCR component may achieve only 10–30% NO_x reduction with reagent utilization as high as 60–80% (Wu, 2002). Hybrid SNCR/SCR systems can be installed in different configurations including (Wu, 2002):

- SNCR with conventional reactor-housed SCR;
- SNCR with in-duct SCR, which uses catalysts in existing or expanded flue gas ductwork;
- SNCR with catalyzed air preheater, where catalytically active heat transfer elements are used;
- SNCR with a combination of in-duct SCR and catalyzed air heater.

© Woodhead Publishing Limited, 2010

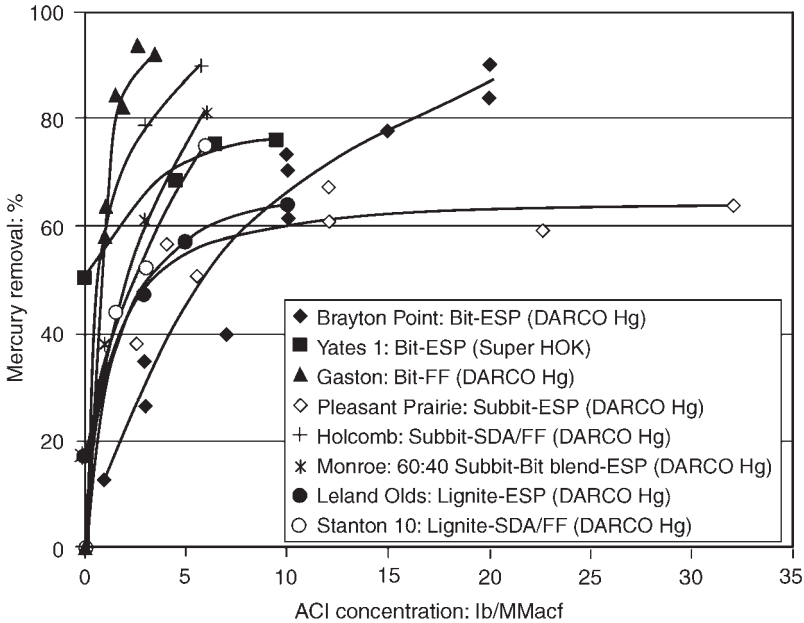
7.6 Activated carbon injection systems

To date, ACI has shown the most promise as a near-term mercury control technology, although continuous long-term operation is required to determine the effect on plant operations. In a typical configuration, PAC is injected downstream of the power plant's air heater and upstream of the particulate control device – either an ESP or a fabric filter. The PAC adsorbs the mercury from the combustion flue gas and is subsequently captured along with the fly ash in the particulate control device. A variation of this concept is the TOXECON^{TM} process (discussed in more detail in Chapter 8) where, a separate baghouse is installed after the primary particulate collector (especially when it is a hot-side ESP) and air heater and PAC is injected prior to the TOXECON^{TM} unit (i.e. TOXECON I^{TM}). This concept allows for separate treatment or disposal of fly ash collected in the primary particulate control device. A variation of the process is the injection of PAC into a downstream ESP collection field to eliminate the requirement of a retrofit fabric filter and allow for potential sorbent recycling (i.e. TOXECON II^{TM} configuration).

The performance of PAC in capturing mercury is influenced by the flue gas characteristics, which are determined by factors such as coal type, air pollution control device configuration, and additions to the flue gas including SO_3 for flue gas conditioning (Sjostrom *et al.*, 2007). Research has shown that HCl and sulfur species (i.e. SO_2 and SO_3) in the flue gas significantly impact the adsorption capacity of fly ash and activated carbon for mercury. Specifically, the following findings have been reported (Feeley, 2006).

- HCl and H_2SO_4 accumulate on the surface on the carbon.
- HCl increases the mercury removal effectiveness of activated carbon and fly ash for mercury, particularly as the flue gas concentration increases from 1 to 10 ppm. The relative enhancement in mercury removal performance is not as great above 10 ppm HCl. Other strong Brønsted acids such as the hydrogen halides – HCl, HBr, or HI – should have a similar effect. Halogens such as chlorine (Cl_2) and bromine (Br_2) should also be effective at enhancing mercury removal effectiveness, but this may be the result of the halogens reacting directly with mercury rather than the halides, thereby promoting the effectiveness of the activated carbon.
- SO_2 and SO_3 reduce the equilibrium capacity of activated carbon and fly ash for mercury. Activated carbon catalyzes SO_2 to H_2SO_4 in the flue gas. Because the concentration of SO_2 is much higher than mercury in the flue gas, the overall adsorption capacity of mercury is likely to be

© Woodhead Publishing Limited, 2010



7.6 Mercury removal as a function of activated carbon injection concentration. Note: legend lists power plant name: coal rank-APCD configuration (PAC type).

dependent on the SO_2 and SO_3 concentrations in the gas, as these form H_2SO_4 on the surface of the carbon.

Figure 7.6 illustrates some results from conventional PAC injection tests performed through numerous DOE test programs (Feeley, 2006; Feeley and Jones, 2008). Conventional PAC injection was the focus of initial field testing and serves as the benchmark for all field PAC injection tests. This work showed that a maximum of approximately 65% mercury capture could be achieved when firing a sub-bituminous coal in a power plant using an ESP.

The conventional PAC testing was followed by work with chemically-treated PACs, which were developed for low-rank coal applications following the low mercury capture results in the initial testing. Some results from the chemically-treated PAC testing are shown in Fig. 7.7 (Feeley, 2006; Feeley and Jones, 2008). With PAC injection at 1 lb/MMacf (million actual cubic feet of flue gas), mercury removal ranges from 70 to 95% for low-rank coals.

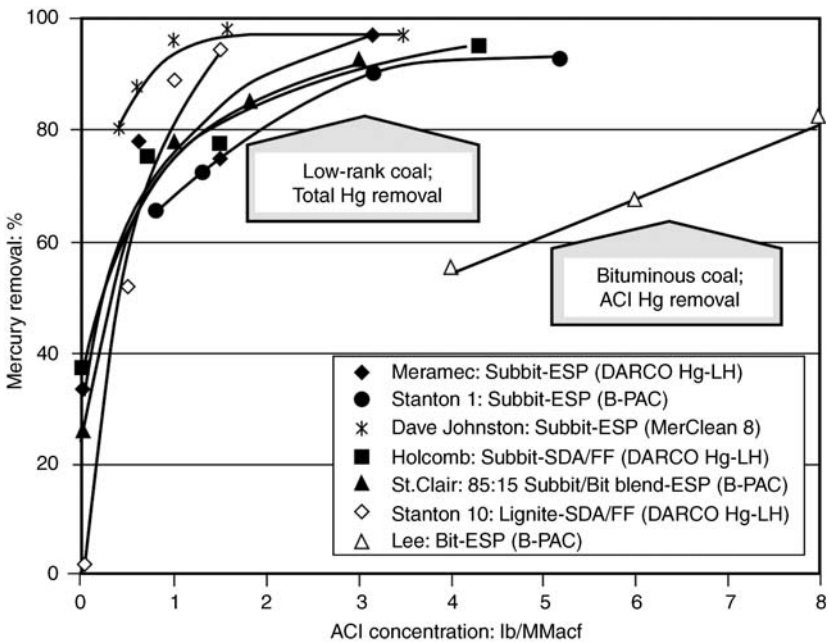
Results from testing using the TOXECON™ technology are given in Table 7.2 (fabric filter configuration) and Fig. 7.8 (ESP configuration) (Sjostrom *et al.*, 2007). In the fabric filter configuration, mercury removals

© Woodhead Publishing Limited, 2010

Table 7.2 Demonstrated mercury removal at 2 or 5 lb/MMacf (modified from Sjonstrom *et al.*, 2007)[a]

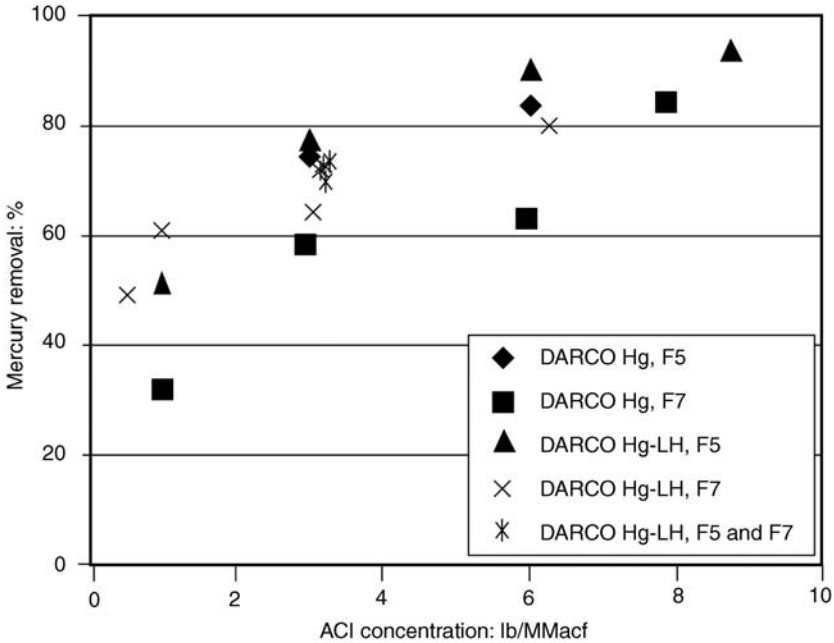
Control device	ESP (5 lb/MMacf)	ESP with SO_3[b] (5 lb/MMacf)	TOXECON™ (2 lb/MMacf)	SDA + FF (2 lb/MMacf)
Low S, very low Cl (Powder River Basin sub-bituminous coal or North Dakota lignite)	78–95% with brominated PAC	40–91% with brominated PAC	70–90%	90–95% with brominated PAC
Low S, > 50 ppm Cl (Some Texas lignites)	78–95%	40–91%	70–90%	90–95% with brominated PAC
Low S, bituminous coal	55–75%	40–91%	ND	ND
Low S, bituminous coal with SCR	15–70%	NA	ND	ND
Low S, bituminous coal	< 15%	NA	NA	NA

[a] ESP = electrostatic precipitator; SDA = spray dryer absorber; FF = fabric filter; NA = not available; ND = not applicable or configuration unlikely.
[b] SO_3 from SO_3 injection.



7.7 Mercury removal as a function of chemically-treated activated carbon injection concentration. Note: legend lists power plant name: coal rank-APCD configuration (PAC type).

© Woodhead Publishing Limited, 2010



7.8 Mercury removal as a function of activated carbon injection concentration using the TOXECON II™ configuration at the Independence Station. Note: DARCO Hg is a conventional PAC whereas DARCO Hg-LH is a brominated PAC.

of 70–90% have been achieved using low-rank coals, while removal efficiencies of 50–90% are expected when using low-sulfur bituminous coals. From Fig. 7.8, 50–80% mercury reduction was achieved when injecting chemically-treated PAC at 4–5 lb/MMacf into the next-to-last ESP field (i.e. F5) and the last ESP field (i.e. F7).

The improved mercury capture efficiency of the advanced chemically-treated sorbent injection systems has given US coal-fired power plant operators the confidence to begin deploying the technology. As of April 2008, nearly 90 full-scale ACI systems have been ordered by US coal-fired power generators (Feeley and Jones, 2008). These contracts include both new and retrofit installations. The ACI systems have the potential to remove more than 90% of the mercury in many applications.

7.7 Future trends

Scrubbing technologies for SO_2 capture are considered mature. Although there are on-going activities to optimize systems, as with any technology,

© Woodhead Publishing Limited, 2010

there are no major near-term technology changes expected; therefore, this section will focus on future trends for NO_x and mercury control.

7.7.1 NO_x control

NO_x control research and development currently underway can be grouped into five areas (Lani, *et al*., 2008)

- next-generation low-NO_x burners;
- rich reagent injection/advanced layered technology approach;
- oxygen-enhanced combustion;
- novel enhanced combustion;
- SCR optimization.

Next-generation low-NO_x burners

Low-NO_x burner (LNB) technology, which is not a post-combustion NO_x control strategy and hence was not discussed in this chapter, is proven and readily available for the utility power industry. However, there is work underway in the development of the next-generation LNB that is based on the second and third generation of commercially-available LNB, but enhanced to achieve a NO_x emission rate of less than 0.15 lb NO_x/MM Btu (per million Btu heat input). Work is focused on low-NO_x firing systems for tangentially-fired boilers and integrating LNB and SNCR for wall-fired boilers.

Rich reagent injection/advanced layered technology approach

Another technology under development is rich reagent injection (RRI), which uses a nitrogen-containing additive such as ammonia or urea to non-catalytically reduce NO_x in the lower furnace – similar to SNCR. This technology is being focused on cyclone-fired boilers, which produce relatively high, uncontrolled NO_x emissions. Combining RRI with overfire air (OFA) technology and SNCR, is known as the advanced layered technology approach (ALTA).

Oxygen-enhanced combustion

Replacing a small fraction – less than 10% – of combustion air with pure oxygen can enhance the NO_x reduction available with LNB and OFA. The oxygen-enhanced combustion reduces NO_x formation due to the creation of a more fuel-rich condition and increased flame temperature at the burner, which drives the combustion reactions toward formation of molecular

© Woodhead Publishing Limited, 2010

nitrogen (N_2) rather than NO_x. This technology is being applied in pulverized-coal-fired boilers, cyclone-fired boilers, and fluidized-bed combustion boilers.

Novel enhanced combustion

Novel enhanced combustion technologies are also under development. These include technologies such as methane de-NO_x and dense phase reburn (DPR). The methane De-NO_x technology combines several NO_x reduction strategies into an integrated system, including a novel burner design using natural gas-fired coal preheating and internal and external combustion staging in the primary and secondary combustion zones. In the DPR system, micronized coal, at a particle size of 80% minus 45 μm, is injected in the dense phase into the furnace while controlling the stoichiometry from the bottom to the top of the furnace.

SCR optimization

While SCR has proven to be an effective NO_x control technology, catalyst deactivation and blockage requires a comprehensive catalyst management program to guide the addition and replacement of catalyst. Hence, work is underway to obtain in-situ SCR catalyst deactivation measurements.

7.7.2 Mercury capture

FGD systems

Although PAC injection has shown the most promise as a near-term mercury control technology, testing is underway to enhance mercury capture for plants equipped with wet FGD systems. These FGD-related technologies include: (i) coal and flue gas chemical additives with fixed-bed catalysts to increase levels of oxidized mercury in the flue gas; and (ii) wet FGD chemical additives to promote mercury capture and prevent re-emission of previously captured mercury from the FGD absorber vessel. There is much interest in these activities as the use of FGD systems at coal-fired power plants is expected to increase significantly over the next 15 years. Wet FGD systems, especially those associated with bituminous coal-fired power plants equipped with SCR systems, appear to be good candidates for capturing mercury. With the projected increase in wet FGD systems for bituminous coal-fired power plants, the co-benefit of capturing mercury with SO_2 can be realized. Research is currently underway to evaluate technologies that facilitate mercury oxidation and to ensure that captured

© Woodhead Publishing Limited, 2010

mercury is not re-emitted from FGD systems. Research to date is encouraging.

Innovative techniques

Innovative techniques for mercury control that could eventually replace and/or augment the more mature technologies discussed above are currently being explored (Feeley and Jones, 2008). These technologies include MerCAP™ (an adsorption process using a fixed structure in the flue gas with sorbent regeneration and mercury recovery), utilizing partially gasified coal for mercury removal, a low-temperature mercury capture process using unburned carbon in the fly ash, pre-combustion mercury removal using thermal treatment, and new sorbent development.

7.8 Sources of further information

Sources of other information include:

- US Department of Energy, National Energy Technology website where coal power systems can be found: http//www.netl.doe.gov/
- US Department of Environmental Protection website: http//www.epa.gov/
- International Energy Agency website: http//www.iea.org

7.9 References

Ciarlante V and Zoccola M (2001), 'Conectiv Energy successfully using SNCR for NO_x control', *Power Engineering*, 105(6), 61–62.

DOE (1997), *Clean coal technology, control of nitrogen oxide emissions: selective catalytic reduction (SCR), topical report number 9*, Washington, DC, US Department of Energy, US Governmental Printing Office.

EPA (1997a), *Mercury study report to Congress*, Washington, DC, US Environmental Protection Agency, Office of Air Quality Planning and Standards, US Governmental Printing Office.

EPA (1997b), *Performance of selective catalytic reduction on coal-fired steam generating units*, Washington, DC, US Environmental Protection Agency, Office of Air and Radiation, US Government Printing Office.

Feeley T (2006), 'US DOE's Hg control technology RD&D program – Significant progress but more work to be done', Proceedings of Conference on *Mercury as a global pollutant, Mercury 2006*.

Feeley T and Jones A (2008), *An update on DOE/NETL's mercury control technology field testing program*, DOE White Paper, www.netl.doe.gov/technologies/coalpower/ewr/mercury/index.html.

Kitto J and Stultz S (eds) (2005), *Steam, its generation and use,* 41st edition, Barberton, Ohio, The Babcock and Wilcox Company.

Lani B, Feeley T, Miller C, Carney B and Murphy J (2008), 'DOE/NETL's NO_x

© Woodhead Publishing Limited, 2010

emissions control RD&D program – bringing advanced technology to the marketplace', *NO_x RD&D Overview*, April Issue, www.netl.doe.gov.

Lodder P and Lefers J (1985), 'Effect of natural gas, C_2H_6, and CO on the homogenous gas phase reduction of NO_x by NH_3', *Chemical Engineering Journal*, 30(3), 161.

McIlvaine R, Weiler H and Ellison W (2003), 'SCR operating experience of German powerplant owners as applied to challenging, US, high-sulfur service', *Proceedings of the EPRI–DOE–EPA combined power plant air pollution control MEGA symposium*.

Miller B (2005), *Coal energy systems*, Oxford, Elsevier.

Miller B and Tillman D (eds) (2008), *Combustion engineering issues for solid fuel systems*, Burlington, Massachusetts, Academic Press.

Radcliffe P (1991), *Economic evaluation of flue gas desulfurization systems*, Palo Alto, California, Electric Power Research Institute.

Rhudy R, McElroy M and Offen G (1986), 'Status of calcium-based dry sorbent injection SO_2 control, Proceedings of the 10th Symposium on *Flue gas desulfurization*, pp. 9-69–9-84.

Rubin E, Sonia Y, Hounshell D and Taylor M (2004), 'Experience curves for power plant emission control technologies', *International Journal of Energy Technology and Policy*, 2(1/2).

Sjostrom S, Campbell T, Bustard J and Stewart R (2007), 'Activated carbon injection for mercury control: overview', Proceedings of the 32nd International Technical Conference on *Coal utilization and fuel systems*.

Soud H (2000), *Developments in FGD*, London, IEA Coal Research.

Srivastava R, Singer C and Jozewicz W (2000), 'SO_2 scrubbing technologies: a review', *Proceedings of the AWMA 2000 annual conference and exhibition*.

Stultz S and Kitto J (eds) (1992), *Steam: its generation and use,* 40th edition, Barberton, Ohio, The Babcock & Wilcox Company.

Wark K, Warner C and Davis W (1998), *Air pollution its origin and control,* 3rd edition, Menlo Park, California, Addison Welsey Longman, Inc.

Wu Z (2002), *NO_x control for pulverized coal fired power stations*, London, IEA Coal Research.

© Woodhead Publishing Limited, 2010

8

Advanced flue gas dedusting systems and filters for ash and particulate emissions control in power plants

B. G. MILLER, The Pennsylvania State University, USA

Abstract: This chapter discusses current and future control technologies for particulates and ash in the power generation sector. Current control technologies addressed include atmospheric pressure systems, which are primarily electrostatic precipitators (mostly dry but to a lesser extent wet) and baghouses, as they are the technology of choice in the power industry. Hybrid systems under development and demonstration are presented. Future control technologies are discussed including pressurized systems such as ceramic and metal filters. Discussions focus on operating principles, designs, and materials of construction.

Key words: particulate control, electrostatic precipitators, baghouses, bag filters, ceramic filters, metallic filters, fine particulate matter, $PM_{2.5}$, PM_{10}

8.1 Introduction

Emissions standards for particulate matter were first introduced in Japan, the US, and Western European nations in the early to mid-1900s. The following decades found many countries also setting standards for particulate emissions including those in Asia, Eastern Europe, Australia, and India. The importance of utilizing coal in an environmentally friendly manner for power generation has led to the introduction or proposal of particulate emissions standards in more than 40 nations (Zhu, 2003). In recent years, there has been increasing concern for control of fine particulate matter and existing particulate emissions standards have progressively become more stringent over the years and the most stringent measures are associated with wealthy countries such as Japan and those in North America and Western Europe (Zhu, 2003).

There are a number of technologies for separating particulate matter from

© Woodhead Publishing Limited, 2010

flue gases generated during coal combustion and these include mechanical/inertial collection (cyclones/multiclones), fabric filtration (baghouses), electrostatic precipitation, wet scrubbers (mainly venturi scrubbers), and hot-gas filtration. However, for large volumes of flue gas such as those typically found in the current power industry (e.g. using atmospheric pressure systems), along with the requirements of adequate collection efficiency of fine particles (particles with aerodynamic diameters smaller than 2.5 and 10 μm and referred to as $PM_{2.5}$ and PM_{10}, respectively) and cost-effective particulate removal, electrostatic precipitators (ESPs) and fabric filters are currently the particulate control devices of choice. Cyclones require low capital investment but they exhibit inadequate collection efficiency of fine particles. Wet (venturi) scrubbing requires wastewater treatment systems, has high energy consumption, and is typically not cost effective for large volumes of flue gas. Particulate matter removal via wet scrubbing is performed, however, when combined with sulfur dioxide capture. Hot-gas particulate filtration, which consists of several control concepts used for high-temperature, high-pressure combustion systems (e.g. pressurized fluidized-bed combustion and integrated gasification combined cycle (IGCC)) is in various stages of development from pilot scale to commercial. Consequently, ESPs and fabric filters, which are the primary control technologies for pulverized-coal-fired power plants, will be the focus of this chapter.

Future trends will be discussed and include hybrid (i.e. combinations of ESPs and fabric filters) and multipollutant systems under development and demonstration. These near- and mid-term particulate control technologies are performed under atmospheric (or near-atmospheric) pressure and especially focus on fine particulate matter (i.e. $PM_{2.5}$) because these particles can cause localized plume opacity, visibility impairment, and have been linked to adverse health impacts. These particles can be categorized as primary particulates (pieces of mineral matter and unburned carbon that are entrained in the flue gas along with trace metals), fine acid aerosols (that are created by the reaction of SO_3 and water vapor), and secondary particulates (those formed in the atmosphere by chemical reactions involving NO_x and SO_2). Future power generation technologies are being developed, as discussed in Chapter 3, that are performed under pressure for gains in system efficiency and to address future carbon management legislation. Particulate matter control in pressured systems, which are considered mid- to longer-term technologies (because these technologies are either not readily deployed, have limited deployment or, in some cases, are not readily accepted at this time), are based on ceramic and metal filter technology and are discussed in section 8.5 as well.

© Woodhead Publishing Limited, 2010

8.2 Materials, design, and development for particulate control

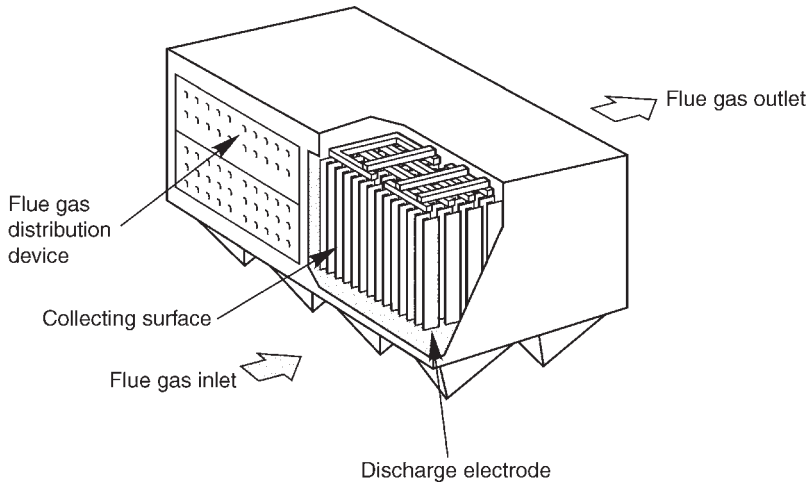
Electrostatic precipitators and fabric filters are currently the technologies of choice for coal-fired power generation facilities as they can meet current and pending legislation particulate matter levels while cleaning large volumes of flue gas, achieve very high collection efficiencies, and remove fine particles. When operating properly, ESPs and baghouses can achieve overall collection efficiencies of 99.9% of primary particulates (over 99% control of PM_{10} and 95% control of $PM_{2.5}$). The primary particulate matter collection devices used in the power generation industry – ESPs and fabric filters (baghouses) – are discussed in this section. Prior to the 1990s, the technology of choice for large coal-fired power plants was the dry ESP, with fabric filters a distant second. Today the preference is for fabric filters (pulse jet type) for the reasons that will be discussed below (Kitto and Stultz, 2005).

8.3 Electrostatic precipitators (ESPs)

Electrostatic precipitators are the most common industrial devices for particulate control, with an estimated 70% share of the total particulate control market (Zhu, 2003). Particulate and aerosol collection by electrostatic precipitation is based on the mutual attraction between particles of one electrical charge and a collection electrode of opposite polarity. The advantages of this technology are the ability to handle large gas volumes (ESPs have been built for volumetric flow rates up to 113 270 m^3/min (4 000 000 ft^3/min)), achieve high collection efficiencies (which vary from 99 to 99.9%), maintain low pressure drops (0.1–0.5 in of water column), collect fine particles (0.5–200 μm), and operate at high gas temperatures (gas temperatures up to 650°C (1200°F)). In addition, the energy expended in separating particles from the gas stream acts solely on the particles and not on the gas stream. Figure 8.1 is a generalized schematic diagram of an ESP (modified from Kitto and Stultz (2005) and Soud and Mitchell (1997)).

Dry ESPs have been used in the control of particulate emissions from coal-fired boilers used for steam generation for about 60 years (Davis, 2000). Initially, all ESPs were installed downstream of the air preheaters at temperatures of 130–180°C (270–350°F), and are referred to as cold-side ESPs. ESPs have been installed upstream of air preheaters where the temperature is in the range 315–400°C (600–750°F) (i.e. hot-side ESPs) as a result of using low-sulfur fuels with lower fly ash resistivity. Wet ESPs (WESPs), a subclass of ESPs, which are discussed separately later, have not historically been used for utility or industrial boiler emissions control when firing coal, oil, or gas (Kitto and Stultz, 2005). However, with the emergence

© Woodhead Publishing Limited, 2010



8.1 Generalized schematic diagram of an ESP (modified from Kitto and Stultz (2005) and Soud and Mitchell (1997)).

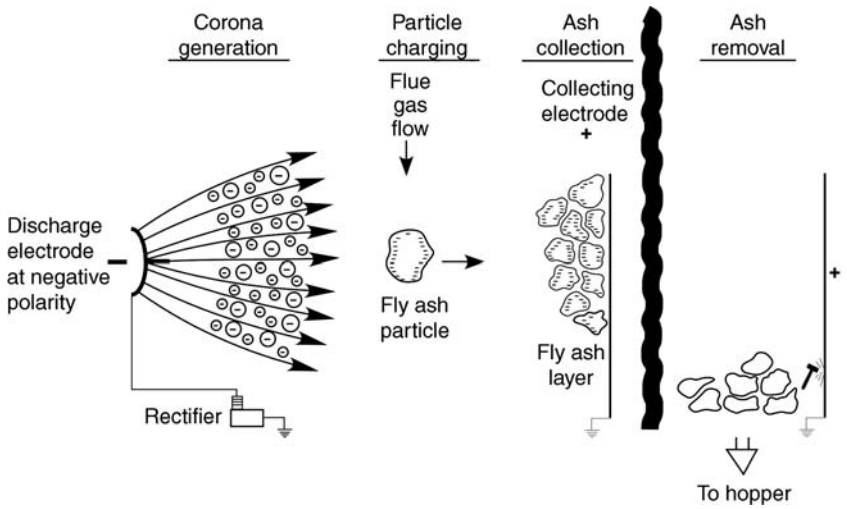
of more stringent emissions control requirements in reducing both fine particles and overall emissions, use of non-traditional fuels, and the interactions of other emissions control equipment, there has been renewed interest in the use of WESPs to control selected emissions, especially sulfuric acid mist and fine dry particles.

8.3.1 Operating principles

There are several basic geometries used in the design of ESPs, but the common design used in the power generation industry is the plate-and-wire configuration. In this design, the ESP consists of a large hopper-bottomed box containing rows of plates, forming passages through which the flue gas flows. Centrally located in each passage are electrodes energized with high-voltage (45–70 kV), negative-polarity, direct current (d.c.) provided by a transformer rectifier set (Elliot, 1989). Power supplied by the transformer rectifier is usually in the range 0.2–0.6 W/m^3 of flue gas treated. The flow is usually horizontal and the passageways are typically 150–200 mm (8–10 in) wide. The height of a plate varies from 5.5 to 12.2 m (18 to 40 ft) with a length of 7.6 to 9.1 m (25 to 30 ft). The ESP is designed to reduce the flue gas flow from 15.2–18.3 m/s (50–60 ft/s) to less than 3.3 m/s (10 ft/s) as it enters the ESP, so the particles can be effectively collected. Experience has shown that flow velocities of 0.9–1.5 m/s (3–5 ft/s) are optimum in order to avoid ash re-entrainment (Davis, 2000).

Electrostatic precipitation consists of three steps: (i) charging the particles to be collected via a high-voltage electric discharge; (ii) collecting the

© Woodhead Publishing Limited, 2010



8.2 Basic concept of charging and collecting particles in an ESP (modified from Soud and Mitchell (1997)).

particles on the surface of an oppositely charged collection surface; and (iii) cleaning the collection surface. These are illustrated in Fig. 8.2 (modified from Soud and Mitchell (1997)).

8.3.2 Particle charging

The electrodes discharge electrons into the flue gas stream, ionizing the gas molecules. These gas molecules, with electrons attached, form negative ions. The gas is heavily ionized in the vicinity of the electrodes resulting in a visible blue corona effect. The fine particles are then charged through collisions with the negatively-charged gas ions resulting in the particles becoming negatively charged. The amount of charge that can be placed on a particle is proportional to the surface area of the particle, with the larger particles requiring less energy for charging and being more readily precipitated than the smaller ones. The charging mechanism for particles greater than 2 μm in diameter is by field charging, which is collision between the corona ions and the particles (Zhu, 2003). As particle size decreases, the charging mechanism changes to diffusion charging, that is as the ions pass near the particles they induce a charge on them. For extremely small particles, below 0.1 μm, Brownian motion assists in both charging and migration, which results in improved capture of smaller particles. Dry ESPs typically have a minimum collection efficiency with particles in the 0.5–1.0 μm size range.

© Woodhead Publishing Limited, 2010

8.3.3 Particle collection

Under the large electrostatic force, the negatively charged ash particles migrate out of the gas stream toward the grounded plates, that is the collecting electrodes, where they collect forming an ash layer. The speed at which the migration of the ash particles takes place is known as the migration or drift velocity. This velocity depends upon the electrical force on the charged particle as well as the drag force developed as the particle attempts to move perpendicular to the main gas flow toward the collecting electrode (Wark *et al.*, 1998). The drift velocity, w, is defined as

$$w = \frac{2.95 \times 10^{-12} p E_c E_p d_p}{\mu_g} K_c \qquad [8.1]$$

where w is in metres per second, p is the dielectric constant for the particles (which typically lies between 1.50 and 2.40), E_c is the strength of the charging field (V/m), E_p is the collecting field strength (V/m), d_p is the particle diameter (μm), K_c is the Cunningham correction factor for particles with a diameter less than roughly 5 μm (dimensionless), and μ_g is the gas viscosity (kg/m s).

The Cunningham correction factor in equation [8.1] is defined as (Wark, *et al.*, 1998)

$$K_c = 1 + \frac{2\lambda}{d_p}\left[1.257 + 0.400e^{\left(-0.55 d_p/\lambda\right)}\right] \qquad [8.2]$$

where λ is the mean free path of the molecules in the gas phase. This quantity is given by

$$\lambda = \frac{\mu_g}{0.499 \rho_g u_m} \qquad [8.3]$$

where u_m is the mean molecular speed (m/s) and p_g is the gas density (kg/m^3). From the kinetic theory of gases, u_m is given by

$$u_m = \left[\frac{8 R_u T}{\pi M}\right] \qquad [8.4]$$

where M is the molecular weight of the gas, T is temperature (K), and R_u is the universal gas constant (8.31×10^3 m^2/s^2 mole °K).

The drift velocity is used to determine collection efficiency using the Deutsch–Anderson equation

$$\eta = 1 - e^{\left(-\frac{wA}{Q}\right)} \qquad [8.5]$$

where w is the drift velocity, A is the area of collection electrodes, and Q is

© Woodhead Publishing Limited, 2010

the volumetric flow rate. The units of w, A, and Q must be consistent since the factor wA/Q is dimensionless.

The ratio, A/Q, is often referred to as the specific collection area (SCA) and is the most fundamental ESP size descriptor (Elliot, 1989). Collection efficiency increases as SCA and w increase. The value of w increases rapidly as the voltage applied to the emitting electrode is increased; however, the voltage cannot be increased above that level at which an electric short circuit, or arc, is formed between the electrode and ground.

8.3.4 Ash removal

The collecting plates are periodically cleaned to release the layer into the ash hoppers as an agglomerated mass by a mechanical (rapping) system in a dry ESP or by water washing in the case of a WESP. The hopper system must be adequately designed to minimize ash re-entrainment into the gas stream until the hopper is emptied. The strength of the electric field and ash bonding on the plates, mass gas flow, and the striking energy must be matched to ensure that ash is not re-entrained into the gas stream (Miller and Tillman, 2008). The ideal situation is where the electric field holding the ash layer that is directly adjacent to the plate is of such strength that the strike energy just breaks this bond and gravity dislodges the particulate matter into the ash hopper.

8.3.5 Collection efficiency

Fly ash collection will never achieve 100%; however, when multiple fields or bus sections are integrated, the process can approach 100%. By rule of thumb, the inlet bus section will collect 80% of the ash delivered at its face. All fields after the inlet field will collect 70% of the ash (Miller and Tillman, 2008). The efficiencies of multiple field precipitators are illustrated in Table 8.1.

Table 8.1 Precipitator efficiency by the number of fields

Number of fields	Amount of ash collected: %	Amount of ash bypassing field: %	Overall efficiency: %
1	80.00	20.00	80.00
2	14.00	6.00	94.00
3	4.20	1.80	98.20
4	1.26	0.54	99.46
5	0.38	0.16	99.84
6	0.11	0.05	99.95

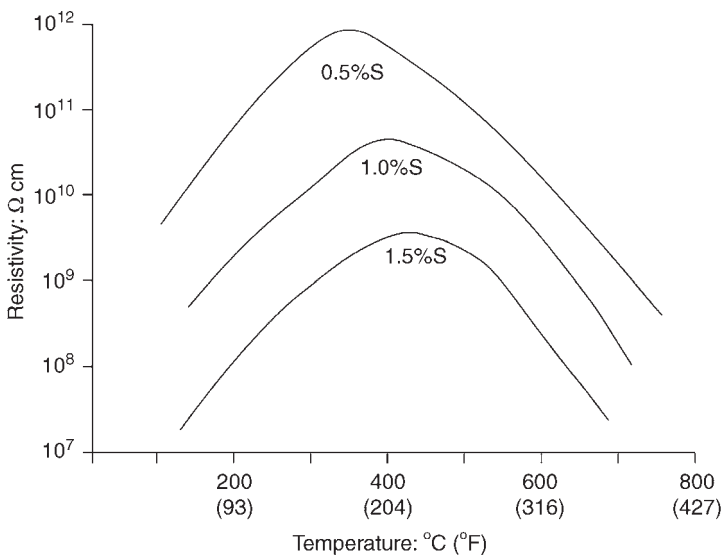
© Woodhead Publishing Limited, 2010

8.3.6 Factors that affect ESP performance

There are several factors that affect ESP performance and are considered when sizing precipitators. Of these, resisitivity is the most important parameter and is often the source of most malfunctions (Miller and Tillman, 2008). Resisitivity is an inverse measure, in Ω cm, of a particle's ability to accept and hold a charge. Lower resistivity indicates improved ability to accept a charge and be collected in an ESP.

Resistivity is dependent on the flue gas temperature and chemistry, and the chemical composition of the ash itself. Electrostatic precipitation is most effective in collecting dust in the resistivity range 10^4–10^{10} Ω cm (Wark *et al.*, 1998). In general, resistivities above 10^{11} Ω cm are considered to be a problem because the maximum operating field strength is limited by the fly ash resistivity. Back corona, the migration of positive ions generated in the fly ash layer towards the emitting electrodes, which neutralize the negatively-charged particles, will result if the ash resistivity is greater than 10^{12} Ω cm. If the fly ash resistivity is below 2×10^{10} Ω cm, it is not considered to be a problem because the maximum operating field strength is limited by factors other than resistivity.

Figure 8.3 is a curve showing the relationship between temperature and resistivity defined by the sulfur content for a family of coals. Two very important relationships are illustrated in this graph. The first is the impact that chemistry has on collection. As sulfur in the coal increases (and hence



8.3 The effect of temperature on resistivity based on coal sulfur content.

© Woodhead Publishing Limited, 2010

SO_2/SO_3 concentration in the flue gas increases), the resisitivity decreases. The second impact is the shape of the curve as temperature changes. The fly ash collectability can be affected by temperature swings in the flue gas.

An example of the effect of ash composition on fly ash resistivity is shown in Fig. 8.4 where resistivity is plotted as a function of temperature for four US lignite (two from North Dakota) and sub-bituminous samples (two from the Powder River Basin) (modified from Miller (2005)). The differences in fly ash resisitivity can be attributed to variations in ash composition. The low-resisitivity fly ashes were produced from coals that contained higher levels of sodium in the coal ash. Higher sodium levels result in lower resistivity. Similarly, higher concentrations of iron also lower resisitvity. Higher levels of calcium and magnesium, however, have the opposite effect on resistivity.

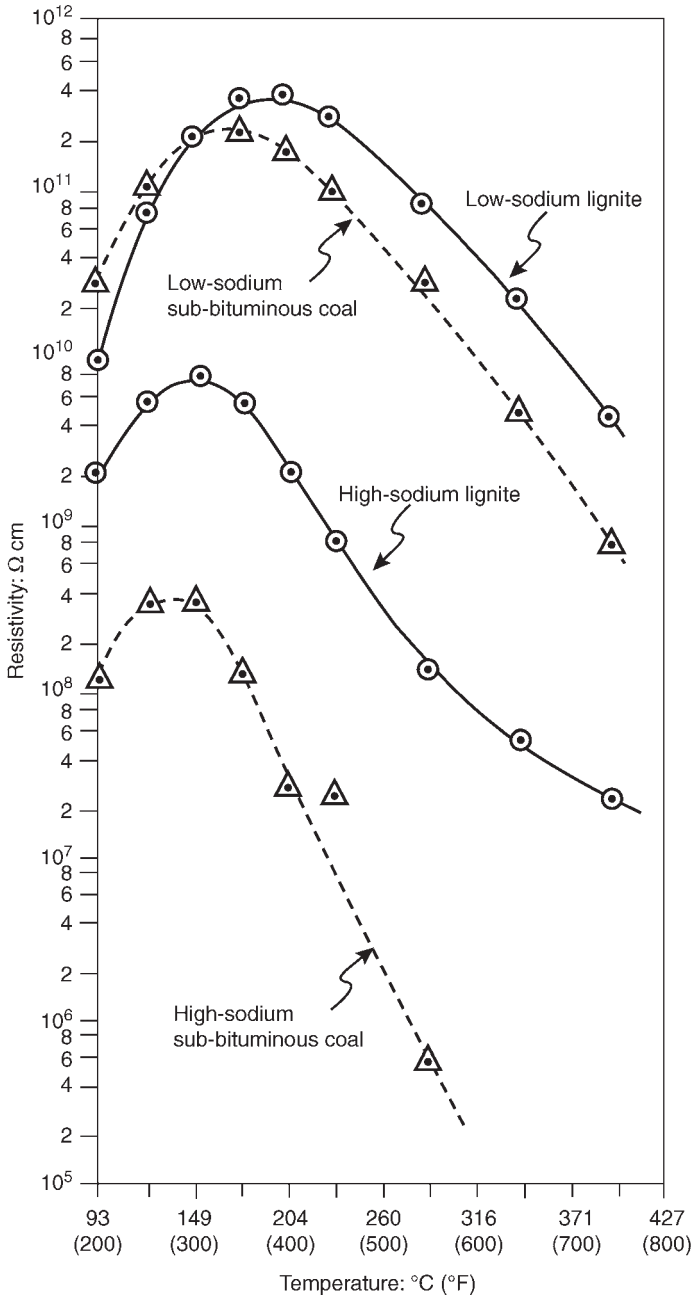
Particle size also affects ESP performance. An ESP is less efficient for smaller particles, that is less than 2 μm, than for larger ones. Therefore, ESP applications with a high percentage of particles less than 2 μm will require more collection surface and/or lower gas velocities.

The dome-shaped curves shown in Figs 8.3 and 8.4 are typical of fly ashes. The shape of the curves is due to a change in the mechanism of conduction through the bulk layer of particles as the temperature is varied (Wark *et al.*, 1998). The predominant mechanism below 150°C (300°F) is surface conduction, where the electric charges are carried in a surface film adsorbed on the particle. As the temperature is increased above 150°C (300°F), the phenomenon of adsorption becomes less effective and the predominant mechanism is volume or intrinsic conduction. Volume conduction involves passage of electric charge through the particles.

The three primary mechanical deficiencies in operating units are gas sneakage, fly ash reentrainment, and flue gas distribution (Elliot, 1989). Flue gas sneakage, that is flue gas that is by-passing the effective region of the ESP, increases the outlet dust loading. Re-entrainment occurs when individual dust particles are not collected in the hoppers but are caught up in the gas stream, increasing the dust loading to the ESP and resulting in higher outlet dust loadings. Non-uniform flue gas distribution throughout the entire cross-section of the ESP decreases the collection ability of the unit.

There are many additional factors that can affect the performance of an ESP, including the quality and type of fuel. Changes in coal and ash composition, grindability, and the burner/boiler system are important. Fly ash resistivity increases with decreasing sulfur content, an issue that must be considered when switching to lower-sulfur coals. Moisture content and ash composition affect resistivity, as discussed earlier. Changes in coal grindability can affect pulverizer performance by altering particle size distribution, which in turn can affect combustion performance and ESP

© Woodhead Publishing Limited, 2010



8.4 Illustration of the effect of ash composition on fly ash resistivity for coals from the same geographical location (modified from Miller (2005)).

© Woodhead Publishing Limited, 2010

performance. Modifications to the boiler system can affect temperatures or combustion performance and thereby affect ESP performance.

8.3.7 Performance enhancement

A change in fuel, a boiler upgrade, a change in emissions regulation, or deterioration in performance may require a precipitator performance upgrade. Enhancement techniques include flue gas conditioning, additional collection surface, improved/modified gas flow distribution, additional sections, wide plate spacing, additional rapping, control upgrades, internal replacements, or modified energization techniques (Elliot, 1989; Kitto and Stultz, 2005; Miller and Tillman, 2008). These enhancements are primarily required owing to difficulties in collecting high-resistivity fly ash and fine particles.

A primary approach to achieving electrical resistivities in the desired range is the addition of conditioning agents to the flue gas stream. This technique is applied commercially to both hot-side and cold-side ESPs. Conditioning modifies the electrical resistivity of the fly ash and/or its physical characteristic by changing the surface electrical conductivity of the dust layer deposited on the collecting plates, increasing the space charge on the gas between the electrodes, and/or increasing dust cohesiveness to enlarge particles and reduce rapping re-entrainment losses (Elliot, 1989).

The most common conditioning agents are sulfur trioxide (SO_3), ammonia (NH_3), compounds related to them, and sodium compounds. Sulfur trioxide is most widely applied for cold-side ESPs, where as sodium compounds are used for hot-side ESPs. Results vary between coal and system, but the injection of 10–20 ppm of SO_3 can reduce the resisitivity to a value that will permit good collection efficiencies. In select cases, SO_3 injection of 30–40 ppm has resulted in reductions of fly ash resisitivity of two to three orders of magnitude (e.g. from 10^{11} to $\approx 10^8$ Ω cm) (Wark *et al.*, 1998). Disadvantages of SO_3 injection systems include the possibility of plume color degradation. Disadvantages for sodium compounds are the potential problems with increased deposition and interference from certain fuel constituents, which affects the economics of the injection. Combined SO_3–NH_3 conditioning is used, with the SO_3 adjusting the resisitivity downward while the NH_3 modifies the space–charge effect, improves agglomeration, and reduces rapping re-entrainment losses (Elliot, 1989).

8.3.8 Wet ESPs

Dry ESPs have been successfully used for many years in utility applications for coarse and fine particulate removal. Dry ESPs can achieve 99 + % collection efficiency for particles 1–10 μm in size. However, dry ESPs: (i)

© Woodhead Publishing Limited, 2010

cannot remove toxic gases and vapors that are in a vapor state at 204°C (400°F); (ii) cannot efficiently collect very small fly ash particles; (iii) cannot handle moist or sticky particulate that would stick to the collection surface; (iv) require much space for multiple fields due to re-entrainment of particles; and (v) rely on mechanical collection methods to clean the plates, which require maintenance and periodic shutdowns (Buckley and Ray, 2003).

Wet electrostatic precipitators (WESPs) address these issues and are a viable technology to collect finer particulates than conventional technology, while also collecting aerosols. The use of WESPs has mainly been in small, industrial-type settings, as opposed to utility power plants, where they are used to control acid mists, submicron particulate (as small as 0.01 μm with 99.9% removal), mercury, metals, and dioxins/furans as the final polishing device within a multipollutant control system (Buckley and Ray, 2003). However, with proposed changes in the current emissions regulations that require the control of a multitude of pollutants, which comprise submicron particles, mists, and metals, there has been an increased interest in WESPs. When integrated with upstream air pollution control equipment, such as a selective catalytic reactor (SCR), dry ESP, and wet scrubber, multiple pollutants can be removed with the WESP acting as the final polishing device.

Wet ESPs operate in the same three-step process as dry ESPs – charging, collecting, and cleaning the particles from the collecting electrode (Altman *et al.*, 2001). However, cleaning of the collecting electrode is performed by washing the collection surface with liquid, rather than by mechanically rapping the collection plates. WESPs continually wet the collection surface and create a dilute slurry that flows down the collecting wall to a recycle tank, never allowing a layer of particulate cake to build up (Altman *et al.*, 2001). As a result, captured particulate is never re-entrained. Also, when firing low-sulfur coal, which produces a high-resisitivity dust, the electrical field does not deteriorate and power levels within a WESP can be dramatically higher than in a dry ESP – 2000 W/28.3 std m^3/min (1000 scfm) versus 100–500 W/28.3 std m^3/min (1000 scfm), respectively.

8.3.9 Materials of construction

Materials for the dry precipitator enclosure and internals are normally carbon steel, ASTM A-36 or equivalent, because gas constituents are non-corrosive at normal operating gas and casing temperatures (Kitto and Stultz, 2005). As in any industry, special conditions may warrant an upgrade in some component materials. In the WESP, the moist corrosive atmosphere requires careful selection of material in critical areas. Materials that have been used include 6% Mo stainless steel, 304 L stainless steel, and alloy 904 L stainless steel (Staehle *et al.*, 2003).

© Woodhead Publishing Limited, 2010

8.4 Fabric filters

Historically, ESPs have been the principal control technology for fly ash emissions in the electric power industry. However, as particulate control regulations have become more stringent, ESPs have become larger and more expensive. Also, increased use of low-sulfur coal has resulted in the formation of fly ash with higher electric resistivity that is more difficult to collect. Consequently, ESP size and cost have increased to maintain high collection efficiency (Bustard *et al.*, 1988). As a result, interest in fabric filters has increased. However, prior to about 1970, the development and use of fabric filters was limited because of two crucial factors: material availability and bag chemical resistance. The availability of materials limited installations to temperatures below 120°C (250°F), and the chemical resistance characteristics of the bags reduced fabric filtration. As advancements were made, the interest in fabric filters increased as a result of successful installations on large coal-fired boilers that proved to have good operation and high collection efficiencies of particulate matter. Fabric filter technology has an extremely high collection efficiency (i.e. 99.9–99.99 + %), is capable of filtering large volumes of flue gas, and its size and efficiency are relatively independent of the type of coal burned (Bustard *et al.*, 1988).

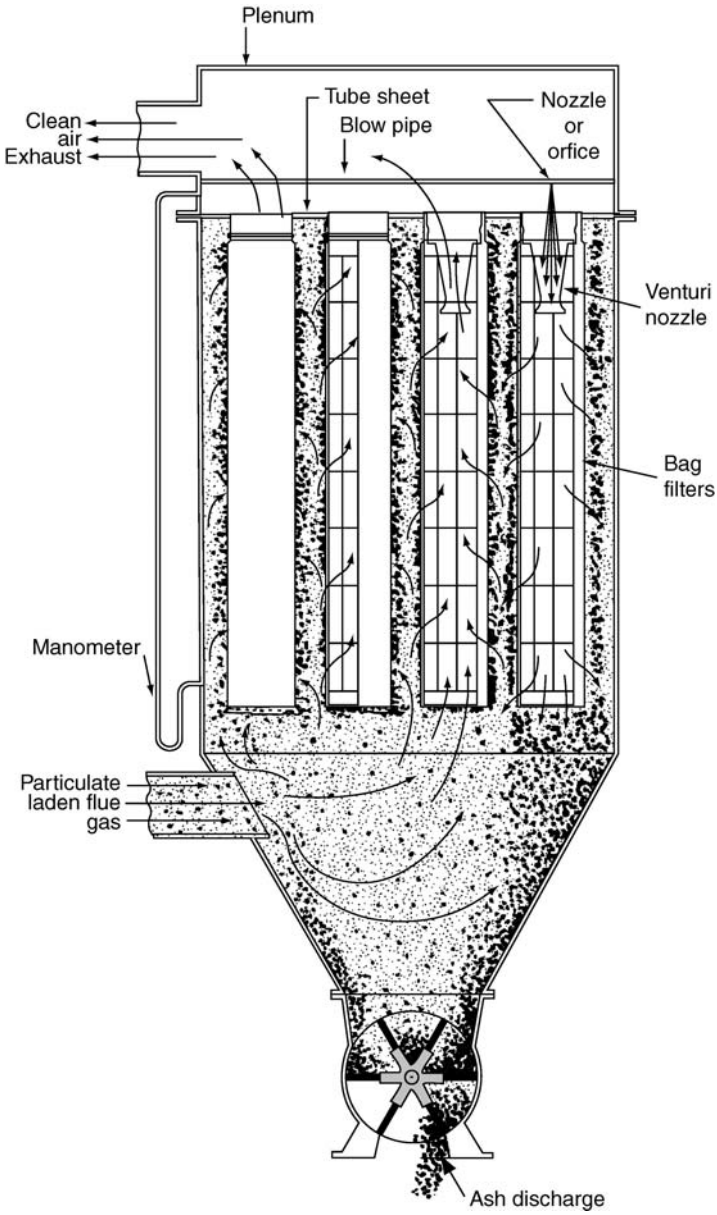
Fabric filters remove particles from a gas stream by passing them through a porous fabric. Particles form a porous cake on the surface of the fabric and it is this cake that does the filtration. Fabric filter systems are referred to as 'baghouses' since the fabric is usually configured in cylindrical bags. These baghouses are typically located downstream of the air preheater and operate in the temperature range 120–180°C (250–360°F).

Advantages of fabric filters include: high collection efficiency over a broad range of particle sizes; flexibility in design provided by the availability of various cleaning methods and filter media; wide range of volumetric capacities in a single installation; reasonable operating pressure drops and power requirements; and ability to handle a variety of solid materials (Wark *et al.*, 1998). Disadvantages of baghouses include large footprints whereby space factors may prohibit consideration of baghouses; possibility of an explosion or fires if sparks are present in the vicinity of a baghouse; and hydroscopic materials usually cannot be handled, owing to cloth cleaning problems.

8.4.1 Operating principles

Baghouses remove particles from the flue gas within compartments arranged in parallel flow paths, with each compartment containing several hundred large, tube-shaped filter bags. Figure 8.5 is an example of air flow in a typical pulse-jet baghouse (modified from Mikropul Environmental

© Woodhead Publishing Limited, 2010



8.5 Generalized schematic diagram of a baghouse (modified from Mikropul Environmental Systems (1989)).

Systems, 1989). A baghouse on a 500 MW coal-fired unit may be required to handle in excess of 0.06 Mm^3/min (2 million ft^3/min) of flue gas at temperatures of 120–180°C (250–350°F) and will consist of many compart-

© Woodhead Publishing Limited, 2010

ments. From an inlet manifold, the dirty flue gas, with typical dust loadings from 0.1 to 10 grains/ft^3 of gas (0.23–23 gs/m^3), enters hopper inlet ducts that route it into individual compartment hoppers. From each hopper, the gas flows upward through the bags where the fly ash is deposited. The clean gas is drawn into an outlet manifold, which carries it out of the baghouse to an outlet duct. Periodic operation requires shutdown of portions of the baghouse at regular intervals for cleaning. Cleaning is accomplished in a variety of ways, including mechanical vibration or shaking, pulse jets of air, and reverse gas flow.

The two fundamental parameters in sizing and operating baghouses are the air-to-cloth (A/C) ratio and pressure drop across the filters. Other important factors that affect the performance of the fabric filter include the flue gas temperature, dew point, and moisture content, and particle size distribution and composition of the fly ash (Soud, 1995).

The A/C ratio, which is a fundamental fabric filter descriptor denoting the ratio of the volumetric flue gas flow (m^3/min (ft^3/min)) to the amount of filtering surface area (m^2 (ft^2)), is reported in units of m/min (ft/min) (Elliot, 1989). For fabric filters, it has been generally observed that the overall collection efficiency is enhanced as the A/C ratio, that is superficial filtration velocity, decreases. Factors to be considered with the A/C ratio include type of filter fabric, type of coal and firing method, fly ash properties, duty cycle of the boiler, inlet fly ash loading, and cleaning method (Soud, 1995).

Pressure drop is a measure of the energy required to move the flue gas through the baghouse. Factors affecting pressure drop are boiler type (which influences the fly ash particle size), filtration media, fly ash properties, and flue gas composition (Soud, 1995).

As the filter cake accumulates on the supporting fabric, the removal efficiency typically increases; however, the resistance to flow also increases. For a clean filter cloth, the pressure drop is about 0.12 kPa (0.5 inches water column (WC)) and the removal efficiency is low. After sufficient filter cake build-up, the pressure drop can increase to 0.50–0.75 kPa (2–3 ins WC) with the removal efficiency 99 + % (Wark *et al.*, 1998). When the pressure drop reaches 1.25–1.49 kPa (5–6 ins WC), it is usually necessary to clean the filters.

The pressure drop for both the cleaned filter and the dust cake, ΔP_T , may be represented by Darcy's equation

$$\Delta P_T = \Delta P_R + \Delta P_C = \frac{\mu_g x_R V}{K_R} + \frac{\mu_g K_C V}{K_C} \qquad [8.6]$$

where ΔP_R is the conditioned residual pressure drop, ΔP_C is the dust cake pressure drop, K_R and K_C are the filter and dust cake permeabilities, respectively, V is the superficial velocity, μ_g is the gas viscosity, and x_R and

© Woodhead Publishing Limited, 2010

x_C are the filter and dust cake thicknesses, respectively. The permeabilities K_R and K_C are difficult quantities to predict with direct measurements since they are functions of the properties of the filter and dust such as porosity, pore size distribution, and particle size distribution. Therefore, in practice ΔP_R is usually measured after the bags are cleaned and ΔP_C is determined using the equation

$$\Delta P_C = K_2 C_i V^2 t \qquad [8.7]$$

where C_i is the dust loading and, along with V, is assumed constant during the filtration cycle, t is the filtration time, and K_2, the dust resistance coefficient is estimated from

$$K_2 = \frac{0.00304}{(d_{g,mass})^{1.1}} \left(\frac{\mu_g}{\mu_{g,70°/F}}\right) \left(\frac{2600}{\rho_p}\right) \left(\frac{V}{0.0152}\right)^{0.6} \qquad [8.8]$$

where d_g is the geometric mass median diameter (m), μ_g is the gas viscosity (kg/m s), ρ_p is the particle density (kg/m^3), and V is the superficial velocity (m/s).

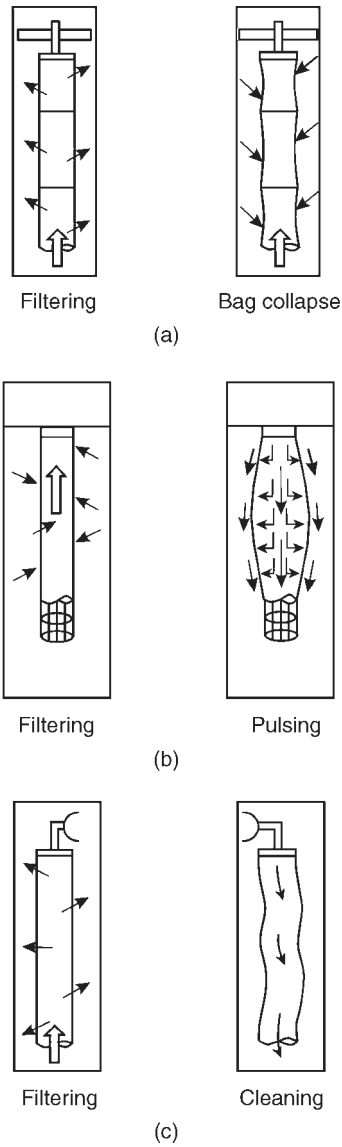
8.4.2 Specific designs

There are three basic types of baghouses – reverse-gas, shake-deflate, and pulse-jet. They are distinguished by the cleaning mechanisms and by their A/C ratio. The two most common baghouse designs are the reverse-gas and pulse-jet types.

Reverse-gas fabric filters are generally the most conservative design of the fabric filter types. The filter typically operates at low A/C ratio ranging from 0.46 to 1.07 m/min (1.5–3.5 ft/min) (Soud, 1995; Wark *et al.*, 1998). Fly ash collection is on the inside of the bags as the flue gas flow is from the inside of the bags to the outside. Reverse-gas baghouses use off-line cleaning where compartments are isolated and cleaning air is passed from the outside of the bags to the inside, causing the bags partially to collapse to release the collected ash. The dislodged ash falls into the hopper. A simplified schematic diagram showing the cleaning cycle is given in Fig. 8.6 (modified from Soud and Mitchell (1997)).

Shake-deflate baghouses are another low A/C type system (0.61–1.22 m/min (2–4 ft/min)) and they collect dust on the inside of the bags, similar to the reverse-gas systems (Wark *et al.*, 1998). With shake-deflate cleaning, a small quantity of filtered gas is forced backward through the compartment being cleaned, which is done off-line. The reversed filtered gas relaxes the bags but does not completely collapse them. As the gas is flowing, or immediately after it is shut off, the tops of the bags are mechanically shaken

© Woodhead Publishing Limited, 2010



8.6 Simplified schematic diagrams of baghouse cleaning mechanisms (modified from Soud and Mitchell (1997)): (a) reverse-gas; (b) pulse-jet; (c) shake-deflate.

for 5–20 s at frequencies ranging from 1 to 4 Hz and at amplitudes of 19–50 mm (0.75–2 inches) (Bustard *et al.*, 1988). A simplified schematic diagram showing the cleaning cycle is illustrated in Fig. 8.6.

In pulse-jet fabric filters, the flue gas flow is from the outside of the bag inward. The A/C ratio is higher than reverse-air units and is typically 0.91–

© Woodhead Publishing Limited, 2010

1.22 m/min (3–4 ft/min) allowing for a more compact installation, but the ratio can vary from 0.61 to 1.52 m/min (2–5 ft/min) (Wark *et al.*, 1998). Cleaning is performed with a high-pressure burst of air into the open end of the bag. Pulse-jet systems require metal cages on the inside of the bags to prevent bag collapse. Bag cleaning can be performed on-line by pulsing selected bags while the remaining bags continue to filter the flue gas. A simplified schematic diagram showing the cleaning cycle is given in Fig. 8.6.

8.4.3 Performance enhancement

The most recognized method to enhance fabric filter performance is the application of sonic energy. Virtually all reverse-gas baghouses have included sonic horns (Elliot, 1989). With this method, low-frequency (<250–300 Hz), high-sound-pressure (0.07–0.15 kPa (0.3–0.6 ins WC)) pneumatic horns are sounded simultaneously with the normal reverse-gas flow to add energy to the cleaning process. Gas conditioning has been explored for improving filter performance, although this is not done commercially (Elliot, 1989).

8.4.4 Materials of construction

Exotic materials are not used for constructing a fabric filter system, because the system is typically operated above the acid dewpoint temperature and the fly ash is dry. The enclosure or casing of the baghouse is typically carbon steel ASTM A-36 or equivalent under normal coal-fired boiler operation. Similarly, hoppers, dampers, and ducting are of carbon steel construction. Cages are normally of carbon steel construction and may include coatings such as pregalvanized coated wire. Stainless steel cages are used in some applications.

8.4.5 Filtration fabrics

Proper filter media selection is critical to maximize particulate collection efficiency, bag cleaning, and extended filter life, and to lower operating costs. There has been substantial research and development on bags and their materials to lengthen their operating life and to select bags for various applications. Fabric filters are made from woven, felted, and knitted materials with filter weights that generally range from as low as 169 g/m^2 (5 oz/yd^2) to as high as 848 g/m^2 (25 oz/yd^2). Filtration media are selected depending on the type of baghouse, their efficiency in capturing particles, system operating temperature, physical and chemical nature of the fly ash and flue gas, durability for a long bag life, and the cost of the fabric. Currently there is a tendency towards using needle felts or polytetrafluoro-

© Woodhead Publishing Limited, 2010

ethylene (PTFE) membranes on woven glass, owing to their ability to withstand higher temperatures (during system upsets which result in temperature excursions) and improve bag performance. To protect bags against chemical attack, the fabrics are usually coated with other materials such as Teflon, silicone, graphite, and GORE-TEX®.

The most common bag material in coal-fired utility units with reverse-gas fabric filters or shake-deflate filters is woven fiberglass (Kitto and Stultz, 2005). A summary of fiberglass fabrics characteristics is provided in Table 8.2. Typical bag size is 305 mm (12 in) diameter with a length of 9.1–11.0 m (30–36 ft).

Table 8.2 Fabric filter media characteristics (modified from Miller (2005))

Glass
Glass fabrics offer outstanding performance in high heat applications. In general, by using a proprietary finish they become resistant to acids, except by hydrofluoric and hot phosphoric in their most concentrated forms. They are attached by strong alkalis at room temperature and weak alkalis at higher temperatures. Glass is vulnerable to damage caused by abrasion and flex. However, the proprietary finishes can lubricate the fibers and reduce the internal abrasion caused by flexing. Maximum operating temperature is 260°C (500°F)
Polyphenylene sulfide (PPS)
Polyphenylene sulfide fibers offer excellent resistance to acids, good to excellent resistance to alkalis, have excellent stability and flexibility, and provide excellent filtration efficiency. Maximum operating temperature is 190°C (375°F)
Acrylic
The resistance of homopolymer acrylic fibers is excellent in organic solvents, good in oxidizing agents and mineral and organic acids, and fair in alkalis. They dissolve in sulfuric acid concentrations. Maximum operating temperature is 127°C (260°F)
Polyester
Polyester fabrics offer good resistance to most acids, oxidizing agents, and organic solvents. Concentrated sulfuric and nitric acids are the exception. Polyesters are dissolved by alkalis at high concentrations. Maximum operating temperature is 132°C (270°F)
Polypropylene
Polypropylene fabrics offer good tensile strength and abrasion resistance. They perform well in organic and mineral acids, solvents, and alkalis. Polypropylene is attacked by nitric and chlorosulfonic acids, and sodium and potassium hydroxide at high temperatures and concentrations. Maximum operating temperature is 93°C (200°F)
Nomex®
Nomex® fabrics resist attack by mild acids, mild alkalis, and most hydrocarbons. Resistance to sulfur oxides above the acid dew point at temperatures above 150°F is better than polyester. Flex resistance of Nomex® is excellent. Maximum continuous operating temperature is 204°C (400°F)
P-84®
P-84® fabrics resist common organic solvents and avoid high pH levels. They provide good acid resistance. P-84® offers superior collection efficiency due to irregular fiber structure. Maximum operating temperature is 260°C (500°F)

© Woodhead Publishing Limited, 2010

The most common bag material in coal-fired utility units with pulse-jet fabric filters is polyphenylene sulfide (PPS) needled felt. In addition to PPS, fiberglass, acrylic, polyester, polypropylene, Nomex®, P84®, special high-temperature fiberglass media, membrane-covered media, and ceramic are used in various applications. A summary of selected filter media characteristics is provided in Table 8.2. Typical bag size is 127 or 152 mm (5 or 6 in) diameter round or oval with a length of 3–8 m (10–26 ft).

8.5 Future trends

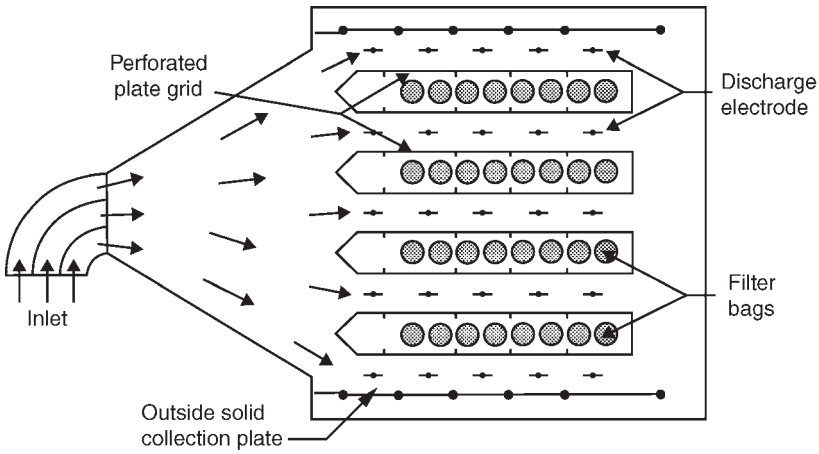
Future trends include the development and demonstration of hybrid systems, which are combinations of ESPs and fabric filters, and multi-pollutant control systems. Many of these systems are considered near- to mid-term technologies in terms of commercialization and deployment. In addition, filtering systems are under development for pressurized power systems, which include ceramic and metal filters. These filtering systems are considered longer-term technologies in their commercialization because the power systems are not being readily deployed at this time.

8.5.1 Near- to mid-term technologies

Hybrid systems

While ESPs can remove over 99% of particulates, baghouses are much better at capturing the very small particles. Hybrid collection systems have been developed to enhance primary $PM_{2.5}$ capture at low costs. One of these technologies, COHPAC® (compact hybrid particulate technology), was developed by the Electric Power Research Institute (EPRI), as a means of improving particulate removal capability of ageing or undersized ESPs at a reasonable cost (Miller *et al.*, 1997). The COHPAC® involves the installation of a pulse-jet baghouse downstream of the ESP or retrofitted into the last field of an ESP. Since the pulse-jet collector is operating as a polisher for achieving lower particulate emissions, the low dust loading to the baghouse allows the filter to be operated at higher A/C ratios (2.44–6.10 m/min (8–20 ft/min)) without increasing the pressure drop. This system allows for the ability to retrofit existing units and achieve high efficiencies at relatively low cost. COHPAC® can be installed either in a separate casing (COHPAC I®) located after the ESP, or within the last one or two fields of the ESP casing (COHPAC II®). COHPAC® has demonstrated low outlet emissions levels (47.9 g/GJ (<0.1 lb/MM Btu)) in full-scale power plant operation and is a promising technology for polishing particulate emissions; it is expected to help utilities in meeting more stringent particulate emissions standards.

© Woodhead Publishing Limited, 2010



8.7 Schematic diagram of the advanced hybrid particulate collector (DOE, 2001).

Another hybrid system under development is the advanced hybrid particulate collector (AHPC™), which is being developed by the University of North Dakota Energy and Environmental Research Center (EERC). The AHPC™ is unique because, instead of placing the ESP and fabric filter in series, the filter bags are placed directly between ESP collection plates (Gebert *et al.*, 2002). A schematic diagram of the AHPC™ is shown in Fig. 8.7 (DOE, 2001). The collection plates are perforated with 45% open area to allow dust to reach the bags; however, because the particles become charged before they pass through the plates, over 90% of the particulate mass is collected on the plates before it ever reaches the bags. The low dust loading to the bags allows them to be operated at high filtration velocity (i.e. a smaller device as 65–75% fewer bags are needed) and to be cleaned without the normal concern for dust re-entrainment. When pulses of air are used to clean the filter bag, the dislodged particles are injected into the ESP fields, where they have another opportunity to be collected on the plates. Because these bags will not need to be cleaned as often as in typical baghouse operation, they are expected to have excellent performance over a long operating life, thereby leading to lower operating costs. Particulate capture efficiencies of greater than 99.99% have been achieved in a 2.5 MW (255 m^3/min (9000 acfm)) slipstream demonstration (DOE, 2003). The AHPC™ technology is expected to increase fine particulate ($PM_{2.5}$) collection efficiency by one or two orders of magnitude (i.e. 99.99 – 99.999%)

© Woodhead Publishing Limited, 2010

Multipollutant control systems

The concept of controlling/removing more than one pollutant from a single control device has been of interest to the coal-fired industry for many years. Initially, technologies to control simultaneously NO_x and SO_2, particulate matter and NO_x, or all three pollutants were developed and tested at various scales. Several of these technologies are discussed in Chapter 7. Two multipollutant technologies, where the primary focus is to remove particulates, are briefly discussed here.

With the interest in removing mercury from flue gas, powdered activated carbon (PAC) injection has shown the most promise as a near-term mercury control technology. In a typical configuration, PAC is injected downstream of the power plant's air heater and upstream of the particulate control device (PCD) – either an ESP or baghouse. The PAC adsorbs the mercury from the combustion flue gas and is subsequently captured along with the particulate matter in the PCD. A variation of this concept is the TOXECON™ process in which a separate baghouse is installed after the primary collector and air heater, and PAC is injected prior to the TOXECON™ unit (i.e. TOXECON I™) (DOE, 2008a). This concept allows for the separate treatment or disposal of fly ash collected in the primary PCD. A variation of this process (TOXECON II™) is the injection of the PAC into the downstream ESP collection field to eliminate the requirement of a retrofit fabric filter and allow for potential sorbent recycling.

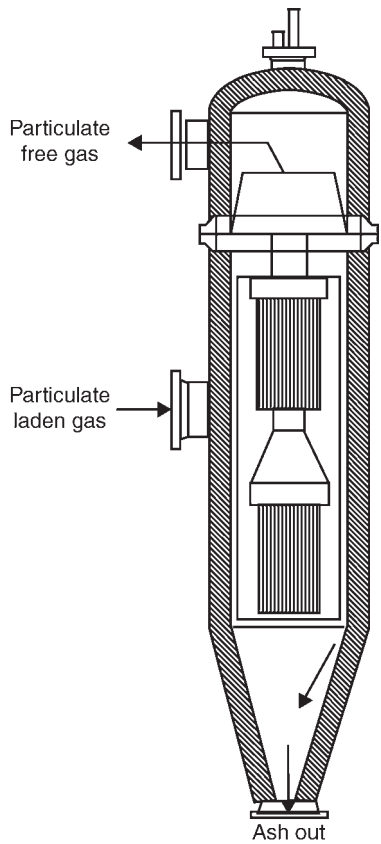
As previously discussed, multiple pollutants can be removed with a WESP. Variations of WESP technology are being developed. One of these, wet membrane ESPs, is being developed as a lower cost technology to reduce $PM_{2.5}$, SO_3, and Hg^{2+} emissions (Caine and Shah, 2006). Wet membrane ESPs use polypropylene or other chemically resistant material as the collecting electrode instead of high-alloy stainless steel to reduce the cost of materials of construction. Another concept is to add a wet ESP field after the dry ESP to collect multiple pollutants within the same footprint of the existing dry ESP. While the dry ESP section will remove PM_{10} with high efficiency ($> 90\%$), the wet ESP last field can remove $PM_{2.5}$, SO_3, and toxic metals with high efficiency ($> 90\%$), while providing some trim control (20–50%) of SO_2 and other gases in addition to removal of mercury.

8.5.2 Mid- to long-term technologies

As a key component in advanced coal-based power applications, such as pressurized fluidized-bed combustion (PFBC) or IGCC plants, hot gas filtration systems protect the downstream gas turbine components from particulate fouling and erosion, cleaning the process gas to meet emissions

© Woodhead Publishing Limited, 2010

requirements. In IGCC systems, the hot gas particulate filter must operate in reducing gas conditions (i.e. in the presence of H_2, CH_4, CO), high system pressure (1.0–2.4 MPa (150–350 psi)) and at operating temperatures usually determined by the method of sulfur removal, that is in bed, external, or by cold gas scrubbing. Typically, these temperatures range around 950°C (1650°F) (in bed), 480–650°C (900–1200°F) (external) and 260–540 °C (500–1000°F) (cold scrubbing). In gasification applications, cold scrubbing of the fuel gas has been demonstrated as effective in cleaning the fuel gas to meet turbine and environmental requirements. However, with this process, plant energy efficiency is reduced, and higher capital costs are incurred. Incorporating a hot particulate filter upstream of the scrubbing unit reduces heat exchanger costs and provides for dry ash handling (partial hot gas cleaning). For bubbling bed PFBC applications, the hot gas filter must operate at temperatures of 860°C (1580°F) and system pressures of 1.2 MPa (175 psia).



8.8 Schematic diagram of a hot-gas filtration vessel (modified from Yongue *et al.* (2007)).

© Woodhead Publishing Limited, 2010



8.9 Photograph of the internals of a hot-gas filtration vessel (DOE, 2008b).

For these commercial-scale systems, multiple filter vessels are required. Thus, the filter design should be modular for scaling. A schematic diagram of a filter vessel is shown in Fig. 8.8 (modified from Yongue *et al.* (2007)) with a photograph of a vessel internals provided in Fig. 8.9 (DOE, 2008b).

Ceramic and metal filters are used in many industrial applications including incinerators, metal smelters, chemical processes, oil refining, and mineral processing. Much development work has been directed towards using these filters in advanced power generation.

Initially, development work in the late 1980s and 1990s focused on ceramic filters for the high-temperature applications. However, they had a history of breaking due to thermal stresses from thermal transients in the

© Woodhead Publishing Limited, 2010

Table 8.3 Examples of materials of composition for various filter media (modified from Pall (2006))

Operating temperature	Chloride-bearing	Sulfur-bearing	Caustic	Oxidizing atmosphere	Reducing atmosphere
1000°C	Ceramic		Ceramic		
900°C	Hastelloy X			Hastelloy X	
800°C		Iron aluminide		Iron aluminide	Iron aluminide
750°C				Ceramic	Ceramic
700°C					Hastelloy X
650°C		310SC	Nickel 201	310SC	310SC
600°C					Ceramic
550°C	Inconel 600			Inconel 600	
500°C	C-276				
420°C		316L		316L	316L
300°C			Nickel 200		
250°C	Alloy 20	Alloy 20	316L		
125°C	C-22				

process, which resulted in developers exploring other options. Then when PFBC technology progressed slowly, the interest in using high-temperature ceramic filters in power generation decreased. These issues, coupled with more moderate IGCC temperatures, resulted in industry exhibiting interest in metallic filters for power generation with significant developmental work beginning in the early 1990s (Alvin, 2004). Consequently, metallic filters are becoming the filter of choice for these applications, although ceramics, which exhibit a wider range of corrosion resistance than many of their metallic counterparts, are still the filter of choice for temperatures above 500–650°C (1100–1200°F) because of sulfidation attack on most metal filters. Table 8.3 lists some materials of construction for different atmospheres and temperatures (modified from Pall Corporation (2006)).

8.6 Sources of further information

Sources of other information include:

- US Department of Energy National Energy Technology Laboratory website where coal power systems can be found: http://www.netl.doe.gov/
- International Energy Agency website: http://www.iea.org

© Woodhead Publishing Limited, 2010

8.7 References

Altman R, Offen G, Buckley W, and Ray I (2001), 'Wet electrostatic precipitation demonstrating promise for fine particulate control, part I', *Power Engineering*, 105(1), 37–39.

Alvin M (2004), *Metal filters for pressurized fluid bed combustion (PFBC) applications*, final report, DOE/NETL contract no. DE-AC26-98FT40002.

Buckley W and Ray I (2003), 'Application of wet electrostatic precipitation technology in the utility industry for $PM_{2.5}$ control', *Proceedings of the EPRI-DOE-EPA combined power plant air pollution control MEGA symposium*.

Bustard C, Cushing K, Pontius D, Smith W, and Carr R (1988), *Fabric filters for the electric utility industry, Vol. 1: general concepts*, Palo Alto, California, Electric Power Research Institute.

Caine J and Shah H (2006), 'Membrane WESP – A lower cost technology to reduce $PM_{2.5}$, SO_3, and Hg^{+2} emissions, *Proceedings of the 2006 environmental control conference*.

Davis W (ed.) (2000), *Air pollution engineering manual*, 2nd edition, New York, Wiley.

DOE (US Department of Energy) (2001), *Advanced hybrid particulate collector fact sheet*, Washington, DC, Office of Fossil Energy.

DOE (US Department of Energy) (2003), *Demonstration of a full-scale retrofit of the advanced hybrid particulate collector (AHPC) collector fact sheet*, Washington, DC, Office of Fossil Energy.

DOE (US Department of Energy) (2008a), *Mercury control projects, topical report number 26*, Washington, DC Office of Fossil Energy.

DOE (US Department of Energy) (2008b), http://www.netl.doe.gov/technologies/coalpower/ gasification.

Elliot T (ed.) (1989), *Standard handbook of powerplant engineering*, New York, McGraw-Hill Publishing Company.

Gebert R, Rinschler C, Davis D, Leibacher U, Studer P, Eckert W, Swanson W, Endrizzi J, Hrdlicka T, Miller S, Jones M, Zhuang Y, and Collings M (2002), 'Commercialization of the advanced hybrid filter technology', Conference on *Air quality III: mercury, trace elements, and particulate matter*, Grand Forks, North Dakota, University of North Dakota.

Kitto J and Stultz S (eds) (2005), *Steam, its generation and use*, Barberton, Ohio, The Babcock and Wilcox Company.

Mikropul Environmental Systems (1989), *Mikro-Pulsaire® filtration products*, Morris Plains, New Jersey, Mikropul Environmental Systems.

Miller B (2005), *Coal energy systems*, Oxford, Elsevier.

Miller B and Tillman D (eds) (2008) *Combustion engineering issues for solid fuel systems*, Burlington, Massachusetts, Academic Press.

Miller R, Harrison W, Prater D, and Chang R (1997), 'Alabama Power Company E. C. Gaston 272 MW electric steam plant – unit no. 3 enhanced COHPAC I installation', *Proceedings of the EPRI-DOE-EPA combined utility air pollution control symposium: The MEGA symposium, Vol. III: Particulates and air toxics*.

Pall Corporation (2006), Pall gas solid separation systems, advanced metal and ceramic filter systems for critical gas solid separation processes, New York, Pall Corporation.

© Woodhead Publishing Limited, 2010

Soud H (1995), Developments in particulate control for coal combustion, London, IEA Coal Research.

Soud H and Mitchell S (1997), *Particulate control handbook for coal-fired plants*, London, IEA Coal Research.

Staehle R, Triscori R, Ross G, Kumar K, and Pasternak E (2003), The past, present and future of wet electrostatic precipitators in power plant applications', *Proceedings of the EPRI-DOE-EPA combined power plant air pollution control MEGA symposium*.

Wark K, Warner C, and Davis W (1998), *Air pollution its origin and control,* 3rd edition, Menlo Park, California, Addison Welsey Longman, Inc.

Yongue R, Guan X, Dahlin R, and Landham E (2007), 'Update on hot gas filtration testing at the power systems development facility', 32nd International Technical Conference on *Coal utilization and fuel systems*, Washington, DC, Coal and Slurry Technology Association.

Zhu Q (2003), *Developments in particulate control*, London, IEA Clean Coal Centre.

© Woodhead Publishing Limited, 2010

9

Advanced sensors for combustion monitoring in power plants: towards smart high-density sensor networks

M. YU and A.K. GUPTA, University of Maryland, USA;
M. BRYDEN, Iowa State University, USA

Abstract: Future advanced combustors and power plants will require a large number of sensors that can provide detailed information for better monitoring and control of the various on-going processes within the system. Traditional sensors are large and expensive for providing comprehensive spatial, temporal, and volume information in a process. There are some inherent barriers to develop new micro- and nano-scale sensors. The use as well as the interpretation of data from a large array of micro- and nano-scale sensors in a power plant operation is another barrier. This chapter addresses various sensor needs, as well as suggesting various sensing strategies. Issues and algorithms that must be considered for the use of a high-density sensor network in future advanced combustors and power plant systems, are also discussed.

Key words: sensor networks, micro/nano sensors, power plant monitoring and control, volume distributed combustion process control.

9.1 Introduction

The new generation of advanced power plants are challenged owing to the on-going needs for significantly more efficiency and reducing pollutants emission, including carbon emissions. This requires new equipment design, new plant configurations, and new instrumentation. Future advanced power plants and processes will require a large number of sensors that can provide detailed information on the various on-going processes within the system. These sensors can be of the same type or different types located at different positions in the power plant. With more sensors, one can obtain comprehensive information, which then must be processed on-line to

© Woodhead Publishing Limited, 2010

control the process. In contrast, with one or few sensors, not much of the detailed information can be captured in the system. The traditional intrusive and non-intrusive sensors are large and expensive as a means of providing comprehensive spatial, temporal, and volume information in a process. Advances in photonics, micro/nano electronics, materials science, and micro-electromechanical systems (MEMS) have led to dramatic improvements in the design of micro- and nano-scale sensors. A revolution in sensing and control is rapidly approaching. It is expected that in a decade, the sensors will be dramatically smaller, less expensive, capable of surviving harsher, more challenging environments and smarter, if progress matches our past experiences in the case of personal computers. These micro-sensors will be able to provide comprehensive information on the various on-going processes occurring in complex situations. However, there are still some inherent barriers to building micro- and nano-scale sensors. In addition, the use as well as the interpretation of data from a large array of micro-scale and nano-scale sensors in a power plant operation are further barriers. Micro- and nano-scale sensors will be fundamentally different from the currently used sensors in power plants and processes. In a similar way to the current sensors, the micro- or nano-scale sensors will be able to provide detailed information on one location, but because they are inexpensive, it is possible to have many to finely tune and control the process in real time from the volume distributed information. Thus the availability of many inputs will pose the challenge of determining the real conditions and how to use the vast amount of information obtained from the sensors.

There are many responses to this coming data flood. A first reaction to this revolution in sensing technology is that more data are good for detailed modeling and model development to evaluate the performance behavior of power plants or processes. However, there are significant challenges in interacting with these micro-sensors and controlling a new generation of power plant. Thus, the coming flood of data will challenge the current data-handling and data-processing capabilities, and change how sensors are used to control power plants and processes. Based on the potential rewards and the significant challenges, it is important to consider research and development efforts for the design and selection of new types of sensors and to develop algorithms and methodologies on how to use them in future devices. Currently, very little is known regarding how to determine the number of sensors that must be used to provide adequate and effective information in a power plant, except that more may be better. Many of the sensors of such types are still under development. Furthermore, it is not known what should be the critical locations for these sensors to provide representative information. Also, it is not known if special features (e.g. multiple functions for a single sensor, on-board processing, and decision-making tools) will substantially improve a plant or process performance.

© Woodhead Publishing Limited, 2010

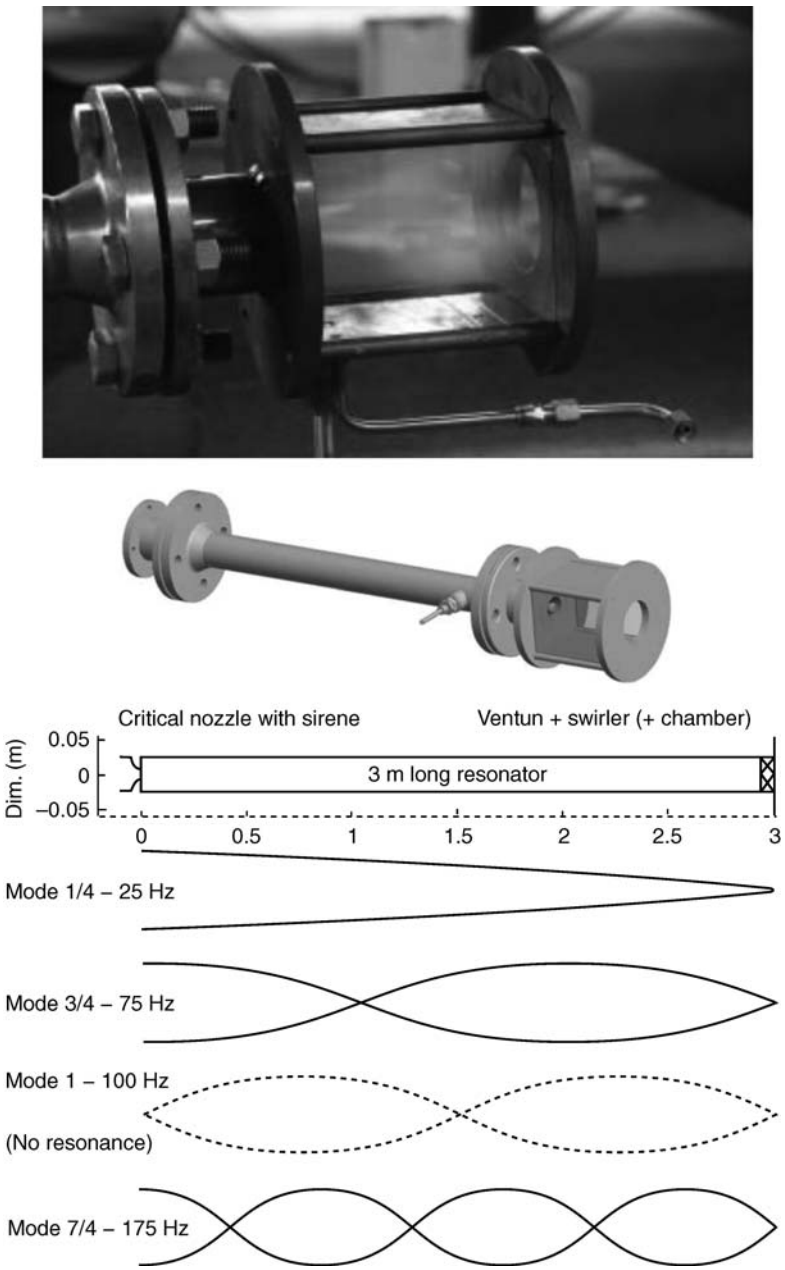
A starting place to resolve the above questions lies in linking sensors to physics-based models that resolve data on the same length and time scales as the sensors. There are a couple of approaches to accomplish this. One approach could be to compare the inputs from the sensors directly with a physics-based model running in real-time mimicking the plant or process behavior. There are several challenges to this approach. The current high-fidelity models are slow and it is not clear how deviations among the data from the many sensors and the model predictions would be handled. Another approach is to have a hierarchical sensor network including leader sensor arrays and micro-scale and nano-scale sensors as swarms or small groups rather than as individual sensors that work together to handle discrete tasks in the sensing and control network. This can be thought of as a holistic or cellular approach to sensors and control. Just as there are many cells in the human body that perform important functions but are not individually directed by the brain, these sensors will need to perform their tasks without continuous direct intervention and reporting. To accomplish this, interactions for these sensors will need to be based on self-organization of complex adaptive systems with limited external direction.

In this chapter, efforts have been focused on developing a new strategy for a high-density sensor network as well as on developing the potential methodologies that can be used so that the network can provide some detailed insights into the combustion, power plant or process operation for further technology advancement. Built upon current progress,[1–3] the various needs for sensors, their relative positions within, at or around the combustor walls or plants, as well the different issues and algorithms considered for use of high-density sensor networks in advanced combustors and power plant systems are discussed.

9.2 Combustion behavior

The combustion behavior is very complex in almost all practical combustion and power plant systems. The combustor performance is dictated by many functions that a process must incorporate and also relies on the outcome of many on-going complex processes in the system. In Fig. 9.1, an experimental combustion test rig is used to examine combustion instability that incorporates pressure waves to affect the combustor performance inside the combustion zone and on into the combustion tunnel. Clearly if one or two sensors are used in the combustion zone or the combustion tunnel, their numerical values will be erroneous because the local value of a given parameter will not reveal the actual representative behavior that occurs in the combustor. Thus, when considering a practical combustion system, there are complex challenges in determining local flow, pressure, chemical

© Woodhead Publishing Limited, 2010



9.1 An experimental combustor with various modes of pressure waves inside the tube.

© Woodhead Publishing Limited, 2010

composition and thermal signatures, and their interactions to seek optimum performance of the system.

9.3 Sensor considerations

The combustor facility must be able to operate over a wide range of conditions for the different sensors under consideration. To control the operation performance effectively, the main problem lies in the determination of the actual conditions within the combustor. Sensors are critical elements for combustion control and combustion monitoring in order to achieve enhanced efficiency and robust performance of the combustion system.

9.3.1 State-of-the-art sensors for combustion monitoring

Optical absorption and emission sensors

Diode-laser-based-absorption sensors have been well demonstrated for in-situ measurements in the flame region or in the exhaust gases of major combustion species, such as water (H_2O), carbon dioxide (CO_2), and oxygen (O_2), gas temperature, velocity, and pressure.[4,5] The light is provided by diode lasers and the detection system includes optical isolators, fibers, and photodetectors. Taking advantage of fiber components for wavelength division multiplexing, multiple lasers may be combined into common signal and reference fibers. However, weak absorption strength in the visible-near-infrared (IR) range requires advanced detection schemes, such as frequency or wavelength modulation and balanced ratiometric detection. Also, the absorption database in near-IR is incomplete, especially for CO_2, in particular under high-temperature and high-pressure conditions. Furthermore, flow turbulence or mechanical vibrations can introduce instabilities in the transmitted radiation and this can degrade the sensor performance.

The light emitted by the flame can also be used to monitor and control the combustion. In this case, information can be gathered from ultraviolet (UV) to IR wavelengths to detect combustion products and temperature. The basic light emission processes, which include chemiluminescence, black body emission, and IR emission, have been demonstrated.[4,5] However, the method allows only line-of-sight detection and provides mainly qualitative information with little spatial resolution, so that volume distributed information is not obtained. This information is critical for seeking local and global performance.

© Woodhead Publishing Limited, 2010

Solid state gas sensors

Gas species monitoring is mainly achieved with semiconductor sensors.[4] These probes use a semiconducting material to detect a particular species. Materials employed are mainly metal oxides, such as zirconium, titanium, and tin oxides doped with other oxides. The corresponding sensors are often designated as ceramic gas sensors. The principle of these sensors relies on the change of the semiconductor resistance or change of voltage or current across the semiconductor with respect to the presence of the probed species. Solid state gas sensors provide useful information concerning the combustion process, but they have some disadvantages. Gas sensors are operated downstream of the process, which induces a time lag between combustion and the corresponding probe measurements. This delay affects the control algorithm stability and design. Also, these sensors have a slow time response and only provide global information about combustion process. Thus, they cannot be used to monitor transient properties.

It is important to point out that both the spatial and temporal resolutions are essential for combustion control. The performance parameters need to be measured in terms of global emissions of the combustion process. In this aspect, the current optical sensors based on line-of-sight methods might lead to low accuracy for evaluating highly non-homogenous flow. In this case, solid state gas sensors exposed to combustion products in the exhaust stream need to be used to evaluate the global performance. However, owing to the time lag of the gas transport, these sensors cannot provide real-time information to provide enough temporal resolution for the desired combustion control. Therefore, as the revolution in sensing and control is rapidly progressing, it is timely to explore high-density, high-performance sensors that can fulfill the requirements of the combustion process of an advanced power plant with zero or near-zero emissions and ultimate high efficiency.

9.3.2 Exploration of novel micro-scale and nano-scale sensors

State observation and performance estimation are central issues in combustion control. Current sensors can barely provide integral information of the entire combustor with adequate precision, high spatial resolution, and bandwidth. Novel micro-scale and nano-scale sensors with improved performance are rapidly developing and starting to play more important roles in many applications, so it is expected that they will also have greater impact on combustion process monitoring, as fuels and energy continue to be of increasing importance.

The high-density sensor networks envisioned for power plants involve a

© Woodhead Publishing Limited, 2010

diverse variety of heterogeneous sensors, including novel micro-scale and nano-scale sensors for pressure, flow, and temperature, and various gas species concentration measurements. The heterogeneous sensor system can provide both complementary and competitive information about a combustion system. Complementary information refers to the measurements of different characteristics of the combustion process, whereas competitive information refers to the measurements of the same characteristic but from different sensor units. Such a heterogeneous sensor system can provide a more reliable view and a higher confidence level of the operational status of advanced combustion unit and power plant system.

To realize an effective, high-density, heterogeneous sensor system, the following two fundamental questions need to be answered: (i) what are the desired parameters to be measured and (ii) what types of sensors need to be used? The first question has been addressed in the literature.[6–10] Some of these parameters include fuel concentration, fuel-to-air ratio, temperature, pressure, flow dynamics and residual gas concentration.[6] The hostile conditions prevailing in combustors mean that the selected sensors should be able to withstand exposure to such an environment. In addition, the selection of the size of the sensor needs to be based on the spatial variations in the flow structure and the sensors needs to provide timely responses to monitor relatively fast transient processes. In the following sections, some possible sensors are discussed to shed some light on the second question.

Fiber optic sensors

Fiber optic sensors have been proven to be successful for measurements in harsh environments;[11–13] these sensors possess the advantages of light weight and high sensitivity, they are not susceptible to electromagnetic interference (EMI), they have remote sensing capabilities, and are multiplexible.[14] Many of these sensors are made intrinsically within the optical fibers, and thus the diameter sizes of these sensors are on the order of micro-scale.[15–21] Fiber optic sensors have been demonstrated to provide measurement of temperature, pressure, gas concentration and other key parameters to monitor details of the combustion process.[15–17]

Among various kinds of fiber optic sensors, fiber Bragg grating (FBG) sensors are good candidates for combustion process monitoring. A fiber optic Bragg grating sensor consists of an optical fiber with a periodic perturbation of the refractive index at the core of the fiber. For a well-written fiber optic Bragg grating sensor, the reflection (and transmission) characteristics of the fiber include a reflection peak at the Bragg wavelength (and a transmission dip at the same wavelength). Owing to the physical relationship between the optical properties of the fiber and an applied strain or temperature field, these sensors are appealing for strain and temperature

© Woodhead Publishing Limited, 2010

sensing. The relationship describing the shift in the Bragg wavelength due to the applied temperature and strain fields can be expressed in terms of a linear equation. The coefficients in this equation may be obtained as Pockel constants.[18] From the earliest stage of their development, fiber Bragg gratings have been considered as excellent sensor elements, suitable for measuring static and dynamic pressure fields. They also offer excellent multiplexing capabilities, which is definitely a good feature for a high-density sensor network. However, in hostile combustion environments, there are physical challenges associated with temperature that must be overcome so that they can be used over a prolonged time.

Another type of fiber optical sensor that can possibly be used in a combusion environment is the Fabry–Perot sensor. A Fabry–Perot cavity formed between two fiber end faces or between a fiber tip and a diaphragm mirror is a good solution for temperature and pressure sensing, but at the expense of spatial resolution. These sensors are typically more sensitive than FBG sensors. For a highly noisy combustion process, these sensors are expected to provide better performance for pressure sensing.

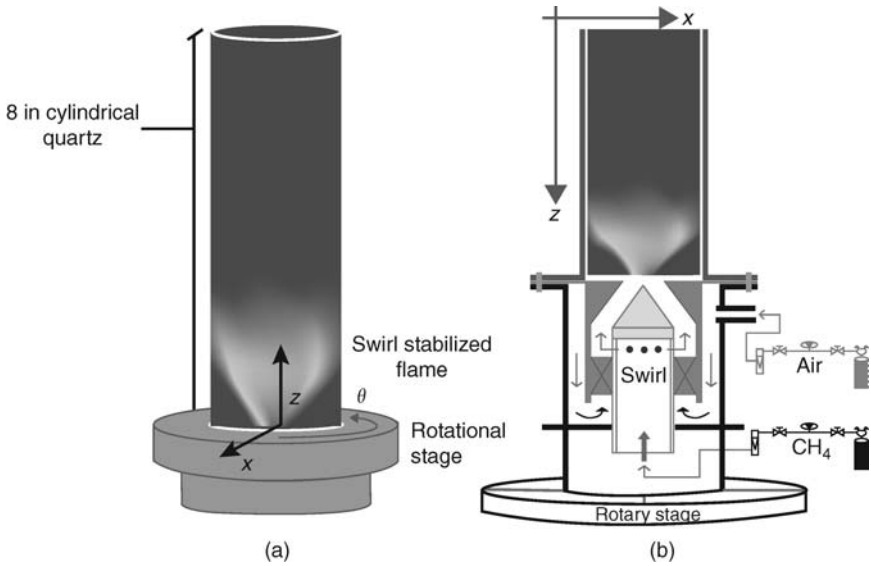
Nano-scale gas sensors

Recently, many different nano-scale structures have been proven to have gas sensing capabilities.[19,20] By taking advantage of these nano-scale sensor techniques, distributed semi-conducting nano-scale sensors can be developed to measure the concentration of O_2, carbon monoxide (CO), and H_2O via the conductance readings from each sensor. Although these species are not adequate for seeking details on the combustion process, they do provide some insights on the combustion process. A challenge in deploying a large number of nano-scale sensors is how to read the sensor data and access each sensor.

9.4 Sensor response

To determine information on quantifying the number and location of sensors that adequately describe the exact performance of a practical combustion system is not trivial. The approach taken here is to tackle this challenge by initially selecting the available sensor(s) that can be used to describe the fate of on-going phenomena inside a practical combustor, and then provide information of the fate of combustor performance using information from single and multiple sensors. Acoustic pressure, including that of combustion noise, has been chosen as the initial representative signature parameter. To achieve fundamental understanding of the influence of the sensor location on the sensor readings, acoustic measurements have

© Woodhead Publishing Limited, 2010



9.2 Schematic diagram of the University of Maryland (UMD) test combustor and (b) detailed view of the UMD test stand.

been carried out at different vertical locations and radial locations immediately outside a test combustor.

The University of Maryland (UMD) 50 kW premixed test combustor, shown in Figs 9.2a and 9.2b, features many of the key characteristics associated with practical combustors and is used here for the experimental test program. The combustor possesses several of the key elements that are of critical importance to simulate the behavior of many practical combustion systems used in the power industry. The combustion chamber is 210 mm long and 55 mm inside diameter. A quartz tube, located downstream of the combustor, provides full optical access to the combustor region. The combustion in these tests occurred at atmospheric pressure under semi-confined condition. The premixed condition was achieved by injecting methane fuel 100 mm upstream of the combustor inlet in order to assure good mixing between the fuel and air. The flame was stabilized using six swirl vanes, which could be given any desired swirl strength using 30, 45, or 60° swirl vane angle to the main flow direction.

Initial efforts involved using a single sensor to determine the extent of spatial variations at different positions downstream of the combustor, as well as its angular variation at any given axial position downstream from the flame-anchoring location in the combustor. Sound pressure measurements were measured using a piezoelectric microphone sensor coupled to a spectrum analyzer. The analyzer recorded the signal from the microphone and performed fast Fourier transform (FFT) on the signal to convert to the

© Woodhead Publishing Limited, 2010

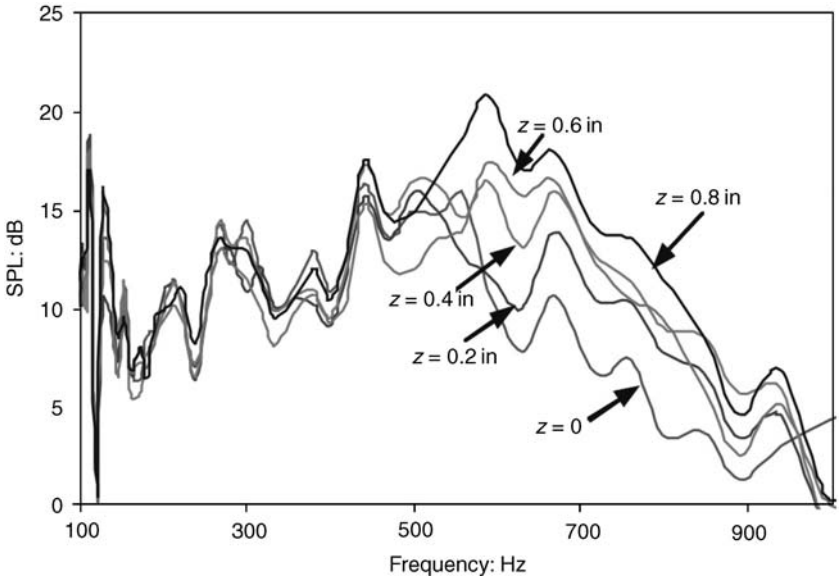
frequency domain. The accuracy of the system was ± 1.5 dB with frequency discrimination of ± 1%. The frequency range was measured from 20 to 20 000 Hz. The sound spectrum analysis was averaged over 10 s to obtain a mean value of the results. The goal here was to assure that there were indeed spatial and temporal variations in sound pressure levels around the combustor. A traversing mechanism was assembled to allow the microphone to be positioned at any desired axial and/or angular location relative to the fixed combustor. The arrangement provided 0.01 in (0.25 mm) vertical resolution and 1° angular resolution.

The acoustic waves generated from the combustor mainly lie in the frequency range 200 Hz–1 kHz. Low frequencies are associated with the combustion roar (200–500 Hz) while the higher frequencies are associated with some modes of acoustic coupling, including the standing waves in the flow ducts. In order to determine how the combustion-generated acoustic waves are related to the microphone's vertical location variation, the focus is initially on the near-field acoustic signatures downstream from the combustor exit. The vertical location of the microphone was therefore limited to within 1 in (i.e. $z < 1$ in) of the burner exit. The radial distance of the microphone from the combustor was fixed at 1 in (25.4 mm). The sound levels were recorded, starting from a vertical position of $z = 0$ to the combustor downstream location in increments of 0.025 in (0.635 mm). Sound pressure levels of only air flow, as well as the background noise associated with the exhaust fan operation and other noise sources, were also recorded as reference sound pressure levels.

Differential sound pressure levels (SPLs) were determined by subtracting the air flow sound level from the total sound pressure level when the combustor was ignited. Since combustion noise was the initial focus here, only the sound spectra over the frequency range 100 Hz–1 kHz are shown. Some representative spectra of differential SPLs are shown in Fig. 9.3; these show over 10 dB SPL variation at around 600 Hz for the microphone locations at $z = 0$ and $z = 0.8$ in. In Fig. 9.3, the differential SPLs spectra are plotted as a function of the sensor vertical positions at different frequencies. Large variations in SPL can be observed as the microphone's vertical location is changed from $z = 0$ to $z = 0.9$ in. In addition, as the microphone height is increased, the SPL does not increase or decrease monotonously. Instead, the SPL fluctuates and the peaks and valleys occur at some fixed positions (e.g. $z = 0.575$ in, $z = 0.6125$ in, and $z = 0.85$ in), even at different frequencies.

The circumferential variation (i.e. angular variation, θ, see Fig. 9.2) of the acoustic signatures from the microphone with respect to the fixed combustor was also examined from 0° to 90° in increments of 10° intervals. The microphone was placed parallel to the combustor wall and was fixed at the vertical location of $z = 0.85$ in. The combustor was set up on a rotational

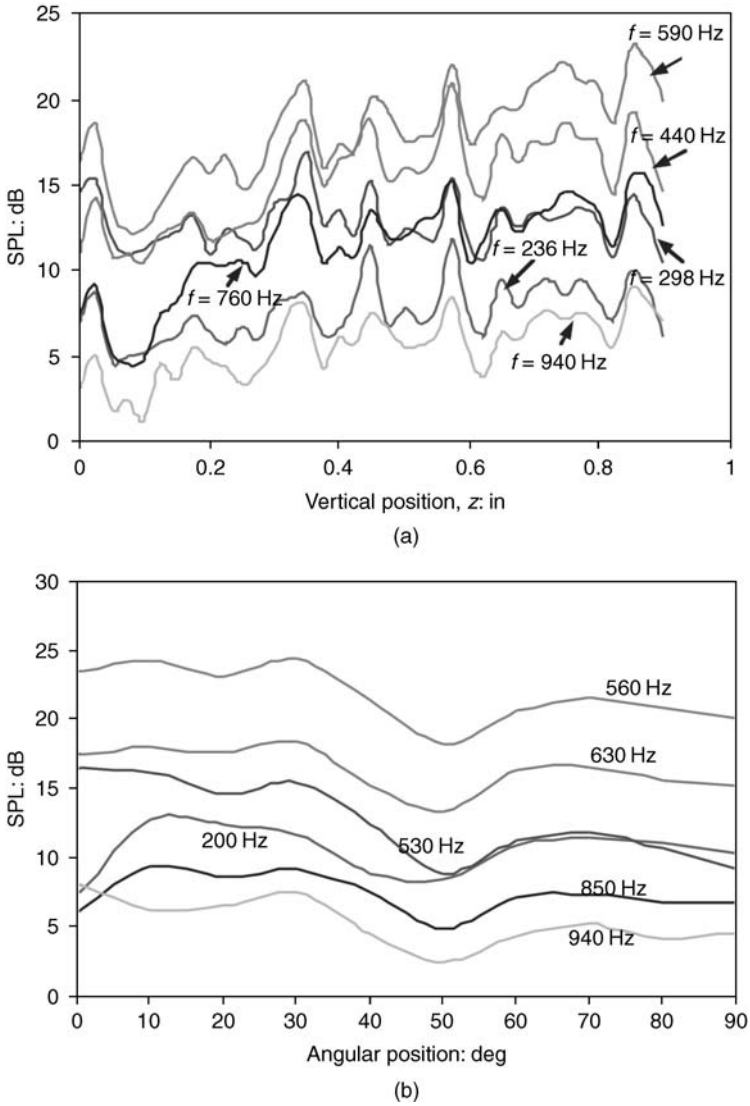
© Woodhead Publishing Limited, 2010



9.3 Spectra of differential SPLs measured at different locations along the vertical axis (*z*).

stage to allow any desired angular position change. As the relative tangential position between the combustor and the microphone was changed, noticeable difference in the SPL spectra were observed, that is the flame exhibited angular variation in the acoustic signatures. The maximum relative SPL variation observed over the 90° angular range was about 8 dB. The differential SPLs with respect to angular positions at different frequencies are illustrated in Fig. 9.4. It can be seen that the SPL variation with respect to angular positions (Fig. 9.4b) is less compared to the data obtained from changing the vertical locations (Fig. 9.4a). This demonstrates that, in order to obtain detailed information for understanding acoustic signatures generated from a combustion process, the incorporation of multiple sensors is necessary; these may, for example, be placed around the combustor, or both axially along the combustor and circumferentially around the combustor with a defined degree of compactness. The extent of compactness of the sensors can be determined from the details of the resolution required to provide the details and accuracy required. Of course, the multi-sensor arrangement will be complex, more costly and may even pose challenges with regard to processing the data, because simple mean value determination from the sensor network array will be erroneous.

© Woodhead Publishing Limited, 2010



9.4 Differential SPL variation versus (a) vertical locations at different frequencies and (b) angular locations (for vertical position $z = 0.85$ in).

9.5 Vision of smart sensor networks

Sensor networks constitute the platform of a broad range of applications related to environment monitoring, inventory tracking and health care. It is envisaged that in the near future, very large-scale networks consisting of a large number of sensor nodes that have a wide range of capabilities will be deployed for various applications, including combustors in advanced power

© Woodhead Publishing Limited, 2010

plants. Although such sensor networks are expected to be a supporting technology for high-performance and high-efficiency power plants or processes of the future, there are many challenges involved in deploying such sensor networks in power plants. First of all, it is necessary to determine how an overall network architecture should be developed that can effectively accommodate the heterogeneity of a large number of sensors. Since it is important to have global control of all the sensors in the network, it is anticipated that a number of subsystems will need to be formed, and each subsystem should be able to handle self-organization of complex adaptive systems with limited external direction. The underlying question is how these subsystems should be defined and how the sensors in each subsystem interact with each other. Moreover, a more difficult problem is related to sensor coverage and placement. The goal here is to determine how many sensors are sufficient and where the sensors should be placed to ensure a defined degree of convergence and confidence.

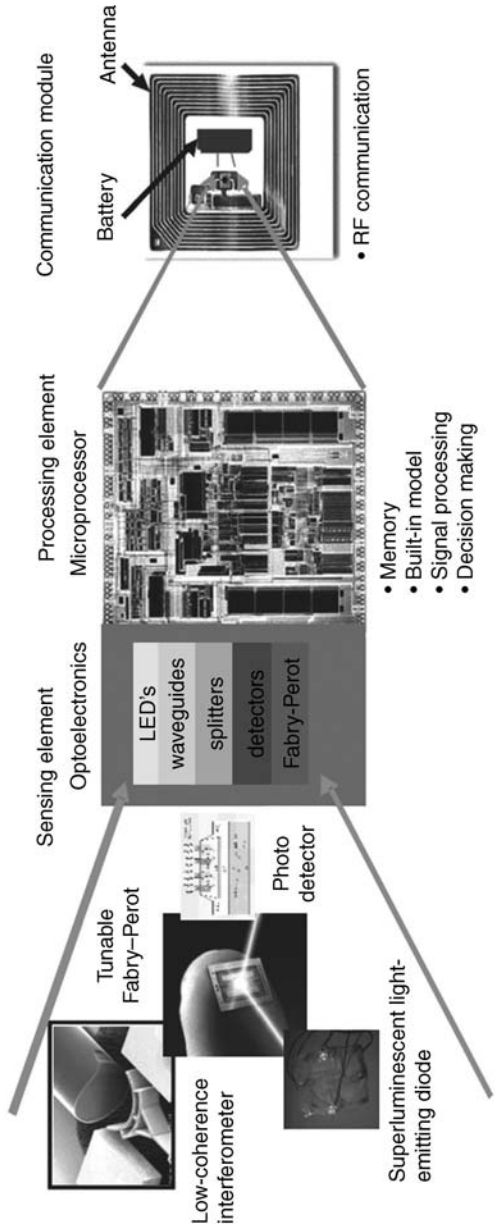
9.5.1 Smart multi-functional sensor platform

Owing to the superior performance of fiber optic sensors in harsh environments and their multiplexing capabilities, fiber optic sensors become the first choice for future smart sensor networks in power plant and process monitoring. The envisioned smart multi-functional sensor system platform (shown in Fig. 9.5) combines micro-opto-electromechanical system (MOEMS) sensing elements, a processing module and a wireless communication module, and uses this sensor platform to realize sensor networks for combustion and power plant monitoring and control.

The multi-functional MOEMS sensing elements feature an integrated differential low-coherence interferometer with multiple sensing interferometers, serving as multiple sensors. Owing to the sensor multiplexing technique, the multiple sensors can be designed in different configurations to fulfill different sensing needs. By using optical fibers as waveguides, the MOEMS sensor platform can support multiple remote fiber optic sensors. Micro-scale Fabry–Perot based pressure, gas and temperature sensors can be developed for combustion monitoring. Owing to the remote sensing capabilities of fiber optic sensors, distributed measurements can be realized in harsh combustion environments. In this way, only the sensor arrays are located in the high-temperature combustor environments, while the MOEMS chip can be located outside the combustor. For example, the fiber optic sensors fabricated using single crystal sapphire fibers are expected to survive at high temperatures, greater than 2000°C.

The processing module features a microprocessor or microcontroller, which enables built-in intelligence for carrying out sensor signal processing, complex modeling and decision making. Depending on the requirements of

© Woodhead Publishing Limited, 2010



9.5 Envisioned smart MOEMS multi-functional sensor platform for combustion and power plant monitoring.

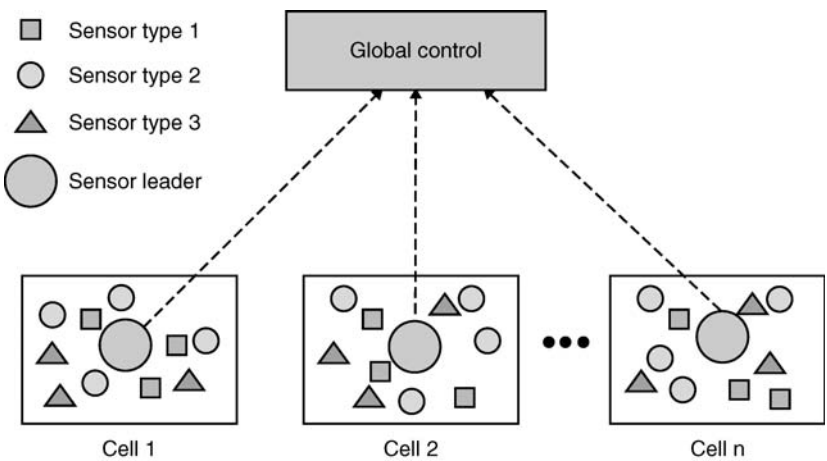
© Woodhead Publishing Limited, 2010

signal conditioning and the required accuracy, the sensor signal processing module will either be implemented by using purely analog circuitry or using a 'drop-in-core' microcontroller or microprocessor with analog-to-digital and digital-to-analog converters.

The wireless communication module will provide an interface, which will facilitate the exchange of sensor data and critical information with the outside world. Each fully integrated MOEMS sensor platform can be equipped with an RF wireless local area network module that will facilitate communication in an ad hoc manner with other nearby sensors or with a peer. Such communication enables the delivery of reliable sensor data to the networks.

9.5.2 Hierarchical network structure

The sensors under consideration in this work are heterogeneous in terms of various aspects including sensing, computing and communicating. The integrated hierarchical framework planned here will accommodate such heterogeneity and render principles for the design and deployment of sensor networks, which includes global control layer, sensor leader layer and the underlying heterogeneous sensor arrays. In this framework, as illustrated in Fig. 9.6, sensor notes are logically organized into different cells (clusters) according to the model mimicking plant behavior. Each cell typically includes sensors that possess different capabilities. In fact, the first principle that is identified for deploying sensor networks is that all the cells in a power plant should in general collaborate. This is usually a commonly agreed upon principle. Typically, a group of sensors residing at the same cell work



9.6 Schematic diagram of the hierarchical network structure.

© Woodhead Publishing Limited, 2010

together for some monitoring tasks and the data acquired from these sensors are delivered to the sensor leader in the cell.

After a set of sensors has been selected as a cell, the second principle identified is as follows: the monitoring task should be tackled only by the sensors in the cell (to the maximum possible extent), and the solution should not assume dependency or seek outside help from sensors in the other cells. This 'independent' rule matches practical applications well, and it greatly simplifies the design problem. Thus, simply put, sensor networks cannot simply be designed and deployed by considering all the possible resources at all times.

Now, given the set of (possibly heterogeneous) sensors, the next principle can be stated as follows: the problem should be solved by the sensors in a distributed manner; no centralized algorithm should be dependent on other external parameters. To enable distributed computation, communications (and therefore coordination) between sensors in a cell are needed. Distributed algorithms inherently possess better scalability and security properties, since they can provide efficient communication protocols and distributed algorithms that solve the incoming coverage determination and sensor placement problems. At the cell level, local sensing and control is organized by the sensor leader, which is essentially a processor with computational and communication capabilities. In the case of fiber optic sensors, a cell itself can be an independent fiber optic system with multiplexed sensors and a central processor.

On finishing the self-organization, sensing and control in each cell, the sensor leader can report the information to a global control station. The global control is optional but may be valuable to maintain the overall system integrity.

9.5.3 Sensor coverage problem

There has been a growing interest in studying the numerous issues of sensor networks. One of the fundamental issues that arises in sensor networks is coverage. The sensor coverage problem has received increased attention recently, as it has been considerably driven by recent advances in affordable and efficient integrated electronic devices. Owing to the large variety of sensors and applications, coverage is subject to a wide range of interpretations. In general, coverage can be considered as the measure of quality of service (QoS) of a sensor network. Furthermore, coverage formulations can try to find weak points in a sensor field and suggest future deployment or reconfiguration schemes for improving the overall QoS.

The coverage problem of sensor networks can be posed in different ways. One way would be to determine the achievable coverage level in an area where sensors have already been deployed. This is the classical coverage

© Woodhead Publishing Limited, 2010

determination problem. On the other hand, it is possible to ask how the sensors should be organized in a given area so that some coverage level can be guaranteed. This formulation is the coverage-constrained sensor placement or deployment problem. Sensor placement directly influences resource management and the type of back-end processing and exploitation that must be carried out with sensed data in distributed sensor networks.

Here, a general sensor coverage determination problem is considered.[21] Given a set of sensors deployed in a target area (area of a cell), it is necessary to determine if the area is sufficiently k-covered, which represents that every point in the area is covered by at least k sensors (same types of sensors or heterogeneous sensors), where k is a predefined constant. Applications requiring $k > 1$ may occur in situations where stronger monitoring is necessary, such as locations with large spatial or temporal gradient. This also occurs when multiple sensors are required to detect an event. Enforcing $k \geq 2$ is also necessary for fault-tolerant purposes. A fundamental question is how many sensors are enough. This question should be addressed by using an available combustion model that can provide information on the condition of each zone in the combustor. The principle here is that for certain critical locations, redundancy is necessary and thus $k > 1$ needs to be satisfied. Ideally, based on the combustion model prediction, the targeted coverage level of each cell in the combustor can be determined.

The second fundamental question to be addressed is how one can carry out effective sensor placement to realize the targeted coverage level. This is a somewhat more difficult problem. There are several attempts to solve this problem with graphic solution for some ideal geometry region. The coverage algorithms developed by Li and Yu[21] can be used here to determine whether a sensor network is k-covered. The solution can be easily translated to a distributed algorithm where each sensor only needs to collect local information to make its decision. Instead of determining the coverage of each location, the approach tries to look at how the perimeter of each sensor's sensing range is covered, thus leading to an efficient polynomial time algorithm. As long as the perimeters of sensors are sufficiently covered, the whole area is sufficiently covered. A difficult problem of sensor coverage and placement in a three-dimensional area of a combustor will now be tackled.

9.6 Sensor information processing

9.6.1 Computational sensor calibration model

The first step here will be to use a computational sensor calibration model to calibrate simultaneously all of the sensors used in the distributed sensor system. Usually, raw sensor output data are imperfect. Such calibrations

© Woodhead Publishing Limited, 2010

will 'remove' some errors embedded in the sensor output and provide more accurate measurements. The basic idea is to provide accurate estimates of 'true' parameter values from the sensor outputs. Thus the initial goal is to find a good mapping from raw reading of the sensors to determine their magnitude that will assist in control algorithm development procedure between the sensor inputs and output units. In order to achieve this, with a given known set of sensor input–output data points (a training sample), a statistical multi-dimensional function can been 'trained' that renders optimal estimates of sensor inputs according to some performance criteria, for example, maximum likelihood (ML) or minimum mean square error (MMSE). The trained model can then be applied to future output signals from the sensor and provide reliable estimated sensor input. As a result, the computational calibration model enables the sensors to endure some adverse effects in the face of uncertainties, non-linearities and cross-talk between sensors.

9.6.2 Data aggregation

With readings from each group of the localized sensors in the distributed network sensor system, preliminary data processing must first be carried out; for example, filtering and aggregating, to derive 'information' from raw readings. Then, the problem must be solved of how the usefulness may be determined of each kind of information extracted in order to achieve the desired parameters in combustion process control for each cell (sensor group). To solve this problem, in general, one needs to be equipped with some model that renders the dependence relationship between the desired parameters and the sensor readings. With such models, some information value of the metrics can be derived, from which different kinds of information can be compared and the most needed information then subsequently transported. For example, Bayesian belief networks models (which can be interpreted as generalizations of hidden Markov models) capture well the dependency structure between various kinds of propositions; notions from information theory, such as information entropy and mutual information, can be exploited to help determine information value. With such information, different kinds of sensor readings will play different roles and will be treated differently for achieving the desired parameters.

9.7 Conclusions

The sample results obtained from a practical combustor using a single sensor have shown that the combustor possesses significant spatial variation. A single sensor is inadequate to provide detailed information from the combustor, in particular when there are large-scale temporal and

© Woodhead Publishing Limited, 2010

spatial variations. The peak signal is located downstream of the combustor and has been found to depend on geometry and operational parameters. The results clearly identify the need for a multi-sensor network placed around the combustor for seeking detailed information that can allow for better control to achieve higher efficiency and improved performance.

A smart sensor network framework for advanced combustion systems in future power plants has been presented, which is aimed at providing a detailed database for future code developments and model validation. A systematic development procedure has been outlined here to determine the sensor type development with multi-function capability, as well as the future means to process the large body of data. The specific focus was on spatial and temporal resolution of the various parameters at all regions of the combustion zone, including the upstream region of the combustion zone, the combustion zone itself and the post-combustion zone. The envisioned sensor network includes a large number of heterogeneous nano-scale or micro-scale sensors, organized by a multi-functional on-chip sensor platform. Optical sensors, such as fiber optic sensors, can perform an important role for on-line monitoring of the detailed processes. The manner in which a hierarchical sensor network can be realized has also been presented.

9.8 Acknowledgements

This research is supported by the US Department of Energy (DoE) and is gratefully acknowledged. The authors would also like to thank Bob Romanasky and Susan Maley for their help and support.

9.9 References

1 Yu M., Bryden K. and Gupta A. K., 'Developing a program to examine the application of high density sensor networks for power plant application', The 31st International Technical Conference on *Coal utilization and fuel systems*, May 2006.

2 Yu M., Bryden K. and Gupta A. K., 'Sensor response and their interpretation in a practical combustor', The 32nd International Technical Conference on *Coal utilization and fuel systems*, June 2007.

3 Yu M., Bryden K. and Gupta A. K., 'Sensor response and sensor network development for practical combustors', *ICCCN 2007*, Hawaii, August 2007.

4 Docquier N. and Candel S., Combustion control and sensors: a review', *Progr. Energy Combust. Sci.*, 2002, 28, 107–150.

5 Allen M. G., 'Diode laser absorption sensors for gas-dynamic and combustion flows', *Measmt Sci. Technol.*, 1998, 9, 545–562.

6 Gupta A. K. and Lilley D. G., *Flowfield modeling and diagnostics*, Tunbridge Wells, Kent, Abacus Press, 1985.

© Woodhead Publishing Limited, 2010

7 Tsuji H., Gupta A. K., Hasegawa T., Katsuki K., Kishimoto K. and Morita M., *High temperature air combustion – from energy conservation to pollution reduction*, Boca Raton, CRC Press, 2003.
8 Bassuk D. D., Gupta A. K. and Magrab E. B., 'On-line monitoring of gaseous flames for air–fuel ratio control', *27th Intersociety Energy Conversion Engineering Conference*, San Diego, CA, 3–7 August 1992, paper no. 92-9226.
9 Gupta A. K., Ramavajjala M., Chomiak J. and Marchionna N., 'Burner geometry effects on combustion and emission characteristics using a variable geometry swirl combustor', *J. Propulsion and Power*, 1991, 7 (4), 473–480.
10 Richards, G., '*The changing energy picture: The role for advanced sensors and control*', paper presented at the 2005 AFRC Annual Meeting, Atlanta, GA, September 2005.
11 Zhang Y. B., Pickrell G. R., Qi B., Safaai-Jazi A. and Wang A., 'Single-crystal sapphire-based optical high-temperature sensor for harsh environments', *Opt. Engng*, 2004, 43 (1), 157–164.
12 Berkovic G., Rotter S., Shafir E., Scandale W. and Todesco E., 'Wavelength-modulated fiber optic sensor for high precision displacement measurement', *Rev. Scient. Instrums*, 2002, 73 (10), 3687–3691.
13 LopezHiguera J. M., Morante M. A. and Cobo A., 'Simple low-frequency optical fiber accelerometer with large rotating machine monitoring applications', *J. Lightwave Technol.*, 1997, 15 (7), 1120–1130.
14 Yu M. and Balachandran B., 'Acoustic measurements using a fiber optic sensor system', *J. Intell. Mater. Systems Struct,* 2003, 14 (7), 409–414.
15 Bae T., Atkins R. A., Taylor H. F. and Gibler W. N., 'Interferometric fiber-optic sensor embedded in a spark plug for in-cylinder pressure measurement in engines', *Appl. Opt.*, 2003, 42 (6), 1003–1007.
16 Boiarski A. A., Pilate G., Fink T. and Nilsson N., 'Temperature measurements in power plant equipment using distributed fiber optic sensing', *IEEE Trans. Power Delivery*, 1995, 10 (4), 1771–1778.
17 Lee K. Y., Velas J. P. and Kim B. H., 'Development of an intelligent monitoring system with high temperature distributed fiber-optic sensor for fossil-fuel power plants', IEEE Power Engineering Society General Meeting, ieeexplore.ieee.org.
18 Steenkiste V. and Springer G., '*Strain and temperature measurement with fiber optic sensors*', New York, Technomic, 1997.
19 Varghese O. K., Kichambre P. D., Gong D., Ong K. G., Dickey E. C. and Grimes C. A., 'Gas sensing characteristics of multi-wall carbon nanotubes', *Sensors and Actuators B*, 2001, 81, 32–41.
20 Schechter I., Ben-Chorin M. and Kux A., 'Gas sensing properties of porous silicon, *Analyt. Chem.*, 1995, 67, 3727–3732.
21 Li J. H. and Yu M., 'Sensor coverage problems in wireless ad hoc sensor networks,' *Int. J. Sensor Networks*, 2007, 2, (3/4), 218–227.

© Woodhead Publishing Limited, 2010

10

Advanced monitoring and process control technology for coal-fired power plants

Y. YAN, University of Kent, UK

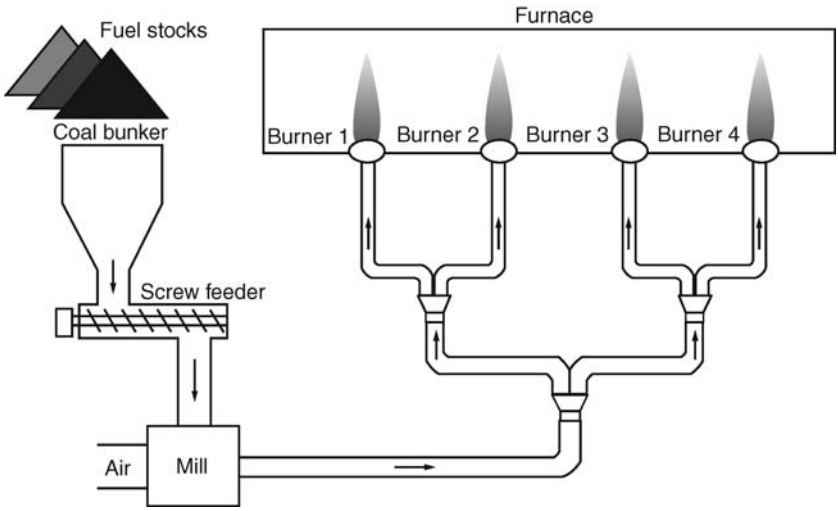
Abstract: To meet increasingly stringent standards on combustion efficiency and pollutant emissions and to maintain fuel flexibility, advanced monitoring and control technologies have become highly desirable in the power generation industry. This chapter describes the current state in the development of such technologies for the optimised operation of coal-fired power stations. Monitoring issues that are covered are concerned with the operation of fuel bunkers, pulverising mills, pulverised fuel injection systems, and furnaces. Other issues such as on-line particle sizing, flame stability monitoring, on-line fuel tracking, and flame imaging are also included. Recent advances in control techniques for the optimisation of pulverising mills, pulverised fuel splitting control, and furnace and boiler operations are described.

Key words: monitoring and measurement, pulverised fuel flow, particle size measurement, flame imaging, pulverising mill control.

10.1 Introduction

Coal-fired power stations are burning an increasingly varied range of fuels and fuel blends, including sub-bituminous and lower volatile coals and biomass of varying composition and combustion properties, under tight economic and environmental constraints. Since existing coal-fired plants are not designed to burn such a diverse range of fuels, the power generation industry has to overcome a range of technological problems such as poor combustion efficiency, increased pollutant emissions and other operational issues such as poor flame stability and slagging and fouling. The recent trend in operating power plants in variable load in response to changes in electricity demand has exacerbated the aforesaid problems. To meet the increasingly stringent standards on combustion efficiency, pollutant emissions and renewables obligations and to maintain fuel flexibility,

© Woodhead Publishing Limited, 2010



10.1 Typical fuel supply and distribution system in a coal-fired power plant.

advanced monitoring and control techniques have become highly desirable in the power generation industry.

In electrical power generation solids fuel is supplied from a bunker into a pulverising mill and the pulverised fuel is then pneumatically conveyed towards the furnace by splitting a larger fuel pipe into smaller ones through bifurcations and/or trifurcations. The fuel distribution network feeds a matrix of burners on a wall-fired or a tangentially fired furnace. Each power generation unit at a coal-fired power station can have typically 20, 24 or 32 or 48 burners. A simplified example of the fuel supply and distribution system is illustrated in Fig. 10.1.

Advanced sensors and process control techniques to permit on-line measurement and subsequent control of the fuel/air flows in individual pipes, the flames of individual burners, and the optimised operation of fuel bunkers and pulverising mills have been regarded as a priority technological development by many leading power generation organisations and government departments (CRF/BCURA, 2004). This trend is further enhanced by the increasingly stringent emissions legislation, better plant maintainability, increased fuel flexibility and the progressive implementation of the carbon capture and storage strategy (APGTF, 2009). The successful development of advanced sensors and control systems will lead to increased fuel flexibility and better control of emissions, which will ultimately improve plant economical performance and viability. For instance, better monitoring and control of the combustion process will result in low carbon levels in ash, allowing ash residue to be used in cement manufacture (because of a low

© Woodhead Publishing Limited, 2010

and controlled carbon content), thereby giving revenue instead of disposal costs.

This chapter describes the current state in the development of monitoring and control technologies for applications in coal-fired power stations. Monitoring issues that are covered in this chapter are concerned with fuel bunkers, pulverising mills, pulverised fuel injection systems, and furnaces. Other measurement issues such as on-line particle size measurement, flame stability monitoring, on-line fuel tracking, and flame imaging are also included. Control techniques associated with pulverising mills, pulverised fuel splitting, and furnace and boiler operations are described and discussed. The monitoring and control techniques are aimed not only to achieve the optimisation of existing plants but also to provide a useful reference for the specification and design of efficient new-build installations. Some topics such as continuous level monitoring of fly ash and continuous emissions monitoring, although very relevant to the scope of this chapter, are excluded because of length restrictions. Many of the measurement and monitoring techniques described in this chapter are at the stage of being trialled on power stations but are not yet established practice.

10.2 Advanced sensors for on-line monitoring and measurement

The coal- and biomass-fired combustion system can be divided into a number of individual processes that are interconnected to each other from fuel supply to emission stacks. Each process requires on-line monitoring and measurement for different reasons. This section highlights the problems that require monitoring and measurement, and the solutions that are available or proposed to resolve them. The topics that are covered in this section include the monitoring of fuel bunkers, pulverising mill, fuel flow rate and particle size distribution, on-line fuel tracking, flame detection, flame stability monitoring, and flame imaging.

10.2.1 Fuel bunker monitoring

It is essential to measure continuously the level of fuel in bunkers and blending silos that feed the pulverising mills and burners. Unreliable levels of fuel in the bunkers can potentially interrupt electricity generation and cause disruption in service. Maintaining a constant supply of fuel in the bunkers has proven to be a challenge. It is therefore desirable to install fuel bunker monitors for continuous level monitoring. The bunkers are often filled by a tripper car system, which moves along a railcar track dispensing the fuel into bunkers. Continuous level measurement of the fuel levels in the

© Woodhead Publishing Limited, 2010

bunkers allows the automated control of the tripper car system. However, the environment in which the monitors operate is very hostile, including dusty atmosphere above the solids fuel surface, wide variations of ambient temperature and humidity (from hot and humid summers to cold winters), and a variety of solid fuel materials within the bunkers.

Several types of fuel bunker monitor have been developed in recent years. They operate on different sensing principles such as radar, ultrasonic, laser, acoustic, capacitance, and load cells. Monitors operating on radar principles use a frequency-modulated continuous wave (FMCW) that can transmit through the dusty atmosphere and be reflected by the fuel surface. This type of monitor is able to provide reliable echo profiles of the fuel in the bunker. For instance, the 24 GHz FMCW SITRANS LR460 monitor (Siemens, 2009) has a small stainless steel horn antenna which requires a mounted opening of only 10 cm and can measure very difficult solids materials within bunkers at ranges of up to 100 m. The ultrasonic continuous level monitor uses a transmitter to generate an ultrasonic pulse and measures the time it takes for a reflected signal to return to a receiver (Koeneman and Sholette, 2006). There are several laser-based fuel level monitors on the market. This type of monitor is often termed TDR (time domain reflectometry). It is claimed that such laser-based monitors have superior dust penetration characteristics and are complete eyesafe, requiring no special permit or safety precautions (Optech, 2006). Some manufacturers claim their TDR coal bunker monitors have outperformed ultrasonic level meters (Endress + Hauser, 2009).

10.2.2 Pulverising mill monitoring

Coal is fed into a pulverising mill where it is ground into a fine powder to allow pneumatic transportation and efficient combustion. Coal-fired power stations in some countries, such as those in the UK, are obliged to vary their electricity output in response to demand, which results in regular mill start-ups and shut-downs. In many cases, pulverising mills are shut down and then restarted before they have cooled adequately, which creates a potential fire hazard within the mill. Mill fires could occur if the coal stops flowing in the mill and the static deposit is heated for a period of time. The problem is pronounced with the co-milling of biomass and coal owing to the higher volatile contents in biomass. Meanwhile, since biomass is often fibrous and non-friable, it is uneconomical to attempt to grind biomass to the same size as coal. The behaviours of coal and biomass blends during milling are not well understood. Actual monitoring data on the milling of blends of coal with biomass and alternative fuels will allow the development and validation of mill performance models. There is therefore a pressing need to continuously monitor and optimise the milling process. It appears that

© Woodhead Publishing Limited, 2010

limited research has been undertaken in this area compared to bunkers, boilers, generators, and other plant components.

Traditionally, an on/off sensor is mounted on the top of the mill to indicate a high level of fuel in the mill (Koeneman and Sholette, 2006). A high-level indication prompts the operator to manage the fuel feed into the mill and reduces blockage and back-ups. The on/off sensor uses commonly a radio frequency (RF) signal. A change in RF admittance indicates the presence of fuel or even the quantity of fuel in contact with the sensor (Koeneman and Sholette, 2006).

In recent years continuous detection of the coal level in a pulverising mill has been studied to improve its operational efficiency and reduce downtime. In the majority of cases vibration sensors (accelerometers) or acoustic emission sensors (microphones) are employed to monitor the operational conditions of the mill and infer the level of fuel in the mill. A single or two accelerometers are normally mounted on the bearing housing to pick up the vibration from the mill shaft (Behera *et al.*, 2007; Su *et al.*, 2008). Multiple microphones are mounted on both sides of the mill with respect of its axis (Bhaumik *et al.*, 2006). Since the signals from both types of sensor are susceptible to contamination by strong background vibration or acoustic noise, a range of signal processing methods have been employed to extract useful information. These include frequency domain analysis, wavelet transform, Hilbert transform, and neural network (Yu *et al.*, 2004; Bhaumik *et al.*, 2006; Kang *et al.*, 2006; Zhang and Trulen, 2006; Behera *et al.*, 2007; Su *et al.*, 2008). Signals from acoustic and vibration sensors are often combined with other mill operating parameters such as pressure difference, drive current, and inlet/outlet temperature (Zhang and Trulen, 2006; Su *et al.*, 2008) to estimate the level of fuel and the operational condition of the mill.

Data modelling techniques have long been applied to extract useful information on milling performance by analysing archived databases (which represent the history of the mills) available at power plants. Mathematical modelling has also been combined with mill data modelling techniques to enhance the real-time performance of the models. For instance, a multi-segment non-linear mathematical model for vertical spindle mills can be developed by analysing the engineering and physical processes such as heat, energy, and mass flow balances (Wei *et al.*, 2006; 2007). All the variables and parameters in the model have clear engineering and physical meanings so the model provides a transparent view of milling processes which is understandable by plant engineers.

© Woodhead Publishing Limited, 2010

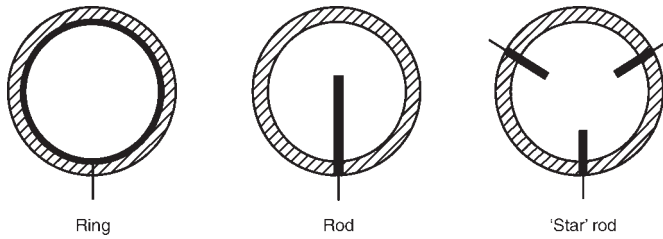
10.2.3 Pulverised fuel flow metering

It is well known that poor pulverised fuel distribution between the feed pipes towards the furnace has resulted in a range of operational problems. These include burners operating off design specification either fuel rich or lean, heavily loaded fuel pipes surging or even plugging, uneven and accelerated wear on conveying pipelines, and flame impingement on furnace walls causing wall corrosion. Despite the use of matched outlet pipes and riffle devices, uneven distribution of pulverised coal inevitably occurs. The mass flow rate and velocity of fuel particles in each feed pipe are known to be crucial parameters influencing the operation of fuel injection systems, combustion efficiency, and pollutant emissions (Yan, 2001; 2002). These parameters should be measured and subsequently controlled to achieve fully balanced and optimal fuel supply to the furnace. The fluid flow in a pneumatic pipeline is essentially a solids–gas two-phase mixture. In the case of co-firing coal with biomass the flow becomes a coal–biomass–air three-phase mixture. However, it is the mass flow rate and velocity of the solids phase that are of primary interest to the plant operators. Fuel particles in the distribution pipework are normally very dilute. For instance, if fuel particles are conveyed in a feed pipe of 20 in (508 mm) in diameter at an estimated mass flow rate of 10 tons/h with a velocity of 25 m/s, then the mass concentration of the fuel is 0.6 kg/m^3, which is equivalent to a volumetric concentration of around 0.1% across the pipe section (Yan, 2002). This dilute dispersal of fuel particles in a large duct poses a difficult flow measurement problem.

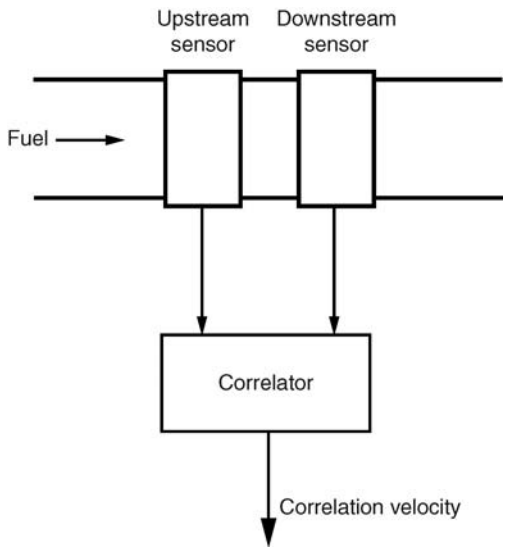
Substantial effort has been put into the development of pulverised fuel flowmeters in the past two decades (Yan, 1996). In addition to thermal, electrical, and acoustical methods, almost all regions across the electromagnetic spectrum, from gamma rays to microwaves, have been applied to develop suitable devices for this application. Among the proposed techniques electrostatic, microwave, and optical types are relatively more developed. Demonstration trials of such meters have been conducted on coal-fired power stations in the UK, USA, Germany, and China (Yan, 2002; Cai *et al.*, 2005). Figure 10.2 shows the different types of electrostatic sensors that have been used to measure the velocity of pulverised fuel. A pair of sensors is normally used to derive particle velocity through correlation signal processing (Fig. 10.3). The large size of the fuel feed pipes, particularly those greater than 500 mm in diameter, makes non-intrusive spool-piece flow sensors less attractive because of their potential difficulties in installation and high capital costs. For such large pipe sizes, sensors based on intrusive probes offer certain advantages and flexibility over spool-pieces (Yan, 2002; Cai *et al.*, 2005; Krabicka and Yan, 2009).

Despite substantial effort in developing pulverised fuel flow sensors using

© Woodhead Publishing Limited, 2010



10.2 Different electrostatic sensors for the velocity measurement of pulverised fuel.



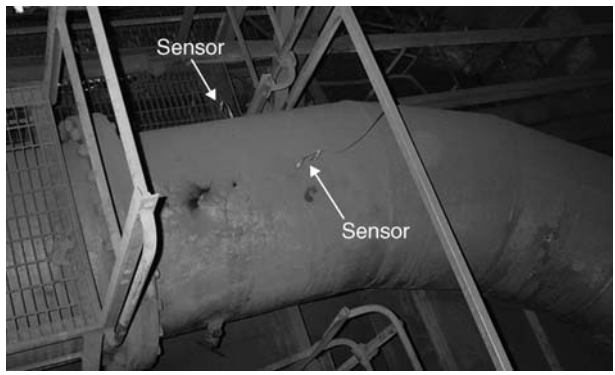
10.3 Principle of cross-correlation velocity measurement.

a range of sensing techniques, progress that has been made is limited. If there is anything that is relatively more successful, it is the correlation-based fuel particle velocity measurement. Few of the proposed techniques are capable of providing absolute concentration measurement and hence absolute mass flow rate measurement (Yan, 2002).

10.2.4 On-line particle sizing

On-line measurement and optimisation of coal fineness and size distribution have the potential to reduce carbon-in-ash levels and NO_x emissions (Miller *et al.*, 2000). The coal fineness and size distribution are dependent primarily upon the performance of the pulverising mill and the fuel properties. Most

© Woodhead Publishing Limited, 2010



10.4 Electrostatic particle fineness sensors under test (Malmgren *et al.*, 2003)

particle sizing techniques currently being used in laboratories are unsuitable for on-line applications (Malmgren *et al.*, 2003). In recent years a number of techniques have been proposed for on-line monitoring of coal fineness and size distribution. These include methods based upon electrostatic, acoustic, optical, and imaging methods. However, progress made in on-line particle sizing is very limited in comparison with other areas of research in combustion instrumentation.

The use of electrostatic sensors for the detection of particle size has generated some interest in both industry and academe in recent years. Two electrostatic sensors mounted mutually perpendicular to one another right after a bend on the mill outlet pipe (Fig. 10.4) have been used to determine mill outlet particle size (Miller *et al.*, 2000). The natural particle segregation in the pipe bend provides the basis for particle fineness detection. The on-line indication of 'fineness', that is percentage of particles greater than 159 μm, is achieved with limited reference data obtained through rotorprobe sampling. Although test data have shown a crude agreement with the classifier speed, the effectiveness of the approach is not yet established.

Zhang and Yan (2003) have studied the possibility of deriving median particle size using an electrostatic mesh sensing grid. The sensing grid has been tested on a small-scale laboratory test rig. In the algorithm developed the ratio between the powers of two sub-sequences derived from the electrostatic signal is used as a particle size indicator.

Trials of acoustic techniques for particle sizing have been undertaken at Longannet Power Station in Scotland (Pattinson and Miller, 1997). Similar work has also been performed by RWE npower in co-operation with Process Analysis and Automation Ltd (Malmgren *et al.*, 2003). In both cases the system comprised acoustic transducers installed on the mill door, mill outlet, and a burner pipe. Power spectra of the acoustic signals were found

© Woodhead Publishing Limited, 2010

to change with the mill coal flow rate and the mill product particle size distribution. However, direct quantitative relationships between the spectra obtained and the particle size distribution were not reported.

Cai *et al*. (2005) applied the light transmission fluctuation method to measure the mean size of pulverised coal. A light beam produced from a diode laser beam was used to traverse through the particle flow before reaching an optical fibre and a photodetector. The mean particle size was derived from the voltage signal from the photodetector. An intrusive probe made of ceramics was used to house the optical components and ensure resistance to abrasive erosion by the fuel particles.

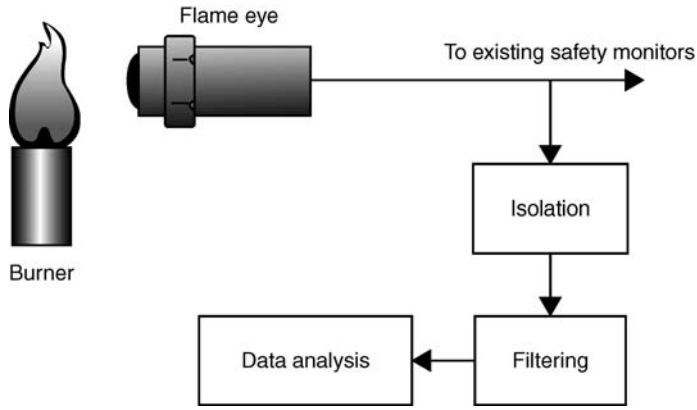
Digital imaging techniques have been applied to measure the size distribution of pulverised fuel (Carter and Yan, 2007). A low-cost charge coupled device (CCD) camera is used to capture the images of particulate flow field, which is illuminated by a low-cost laser sheet generator. The particle size distribution is then determined by processing the images. Results obtained on an industrial-scale combustion test facility demonstrated that the system is capable of measuring particle size distribution, which is consistent with reference data from a laser-scattering-based particle size analyser (Chinnayya *et al*., 2009).

10.2.5 Flame stability monitoring

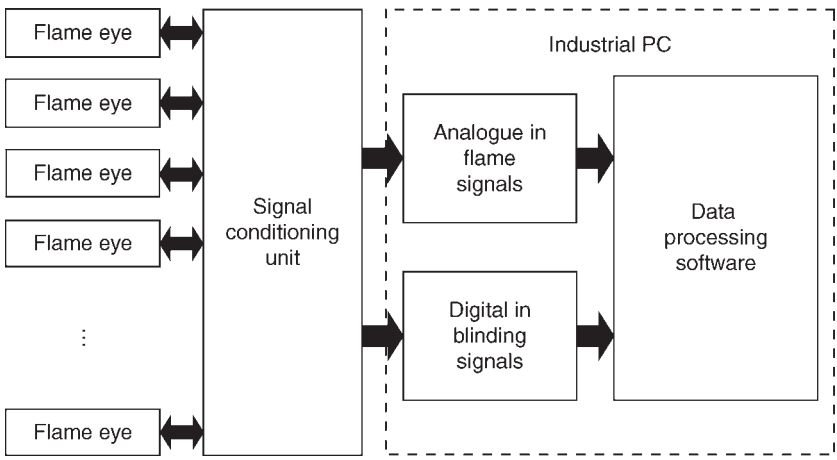
Existing power plants monitor the brightness or intensity of flames in the interests of safety through the use of photo sensors built into optical detectors called 'flame eyes'. The detectors use this information to indicate flame 'present' or 'extinguished', allowing automatic shut-down of fuel feed mechanisms in the absence of a flame. In the past few years some development work has been undertaken to measure the stability of a flame through advanced flame monitoring. This is achieved by 'tapping' the signal from an existing flame eye and processing the resulting data as an analogue signal using a dedicated signal processing system (Carter *et al*., 2009). The basic principle of flame stability monitoring is illustrated in Fig. 10.5. Through analysis of the flame signal the flame intensity and oscillation frequency are measured. The flame stability is indicated by the degree of fluctuations of the measured flame intensity and oscillation frequency.

The flame stability monitoring system described above has been used to obtain immediate, quantified information about the combustion conditions of all the burners of the same unit on a coal-fired power station. Figure 10.6 shows the structure of the system hardware. Owing to the safety critical nature of its operation, each flame eye undertakes an independent periodic 'self-check'. Since the flame eye does not output a valid flame signal during the self-check period, a 'blinding signal' from the flame eye is fed to the system so that the software suspends data acquisition and processing

© Woodhead Publishing Limited, 2010



10.5 'Flame eye'-based flame stability monitoring.



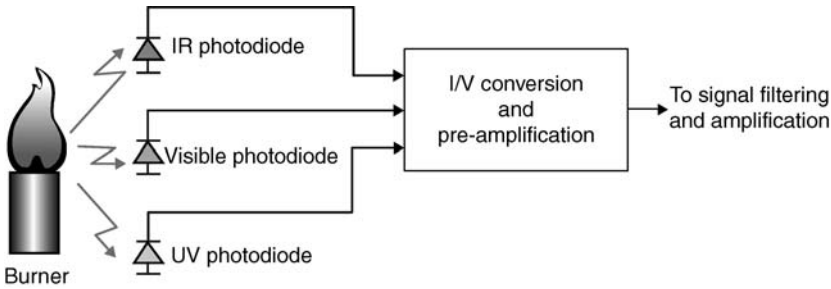
10.6 Structure of a multi-channel flame stability monitoring system.

temporarily. The software displays the flame stability information for all the burners on the top layer of the user interface and for groups of three burners of the same mill on the second layer.

10.2.6 On-line fuel tracking

Many power stations store fuel on large stock piles and it comes from a diverse range of sources, with varying type and quality, including sub-bituminous coals and biomass. It is important to know which fuels are located at specific points in the coal-handling system from the stockyard to the burners, however, the logistical problems involved in keeping track of fuel on the stock piles are often insurmountable. Without an effective fuel-

© Woodhead Publishing Limited, 2010



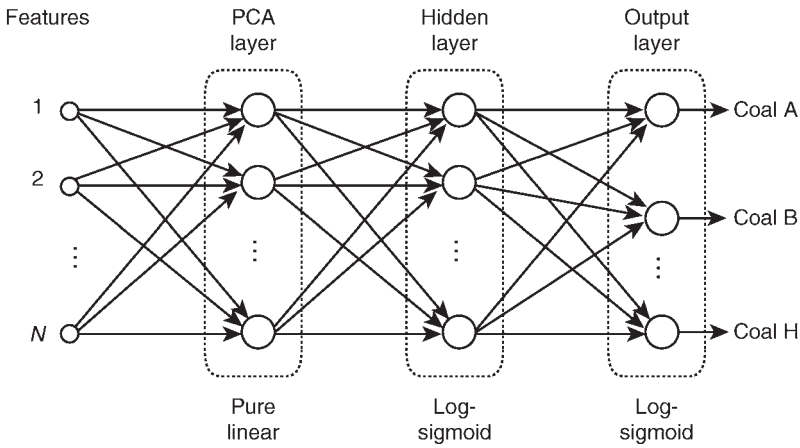
10.7 Basic sensing arrangement of the fuel-tracking monitor.

tracking system, the mills and burners may be inappropriately set, and this has serious safety implications and may prevent an appropriate mix of fuels being burned to meet new CO_2 targets. If the type of fuel being fired is known in real time, the plant engineers can use combustion optimisation software packages to configure the plant for best possible efficiency and minimum emissions.

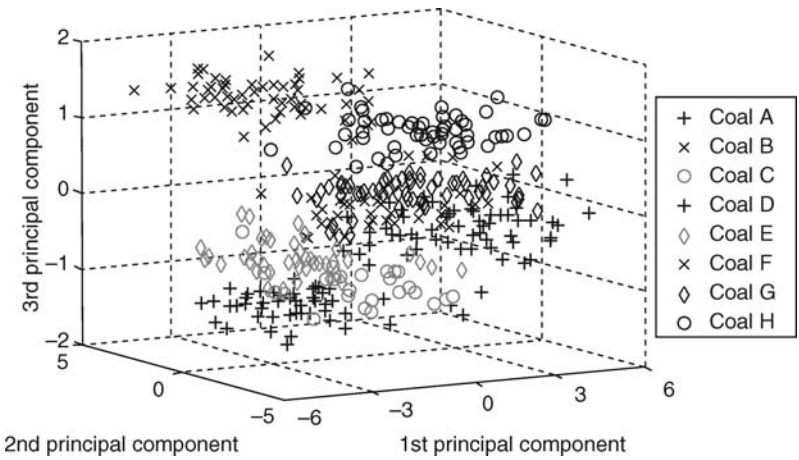
Some on-line coal analysers and coal-tracking systems operating on radiometric, microwave, or passive tagging techniques have been proposed. However, these systems are very expensive and require complex installations. Recent research has demonstrated that on-line fuel tracking can be achieved through advanced flame monitoring (Xu *et al.,* 2004; 2005). Three different wavelength bands of light generated by the flame are received. The basic sensing arrangement of the fuel-tracking monitor is illustrated in Fig. 10.7. The monitor is designed to extract as much information about the combustion flame as possible. It has the same installation specifications as the traditional flame eye (section 10.2.5) so that it can be easily fitted to the existing sight tube that is normally mounted to prevent the monitor from excessive thermal radiation from the flame and provide mechanical support for the monitor.

Once the signals are available from the fuel-tracking monitor, various parameters are derived through digital signal processing (Xu *et al*., 2004; 2005). The first step is to extract the 'features' that will be used to train a fuel-tracking neural network. These features cover both time and frequency domains. Wavelet analysis of the signals is also undertaken and certain signal features, such as the number of zero crossings, are considered. In the time domain, the direct current (d.c.) level and alternating current (a.c.) level are calculated and in the frequency domain quantitative flicker frequency and normalised a.c. power of the flame signal are used. An illustrative neural network for fuel tracking of eight different fuels is shown in Fig. 10.8. The principal component analysis (PCA) layer which isolates the most important features in each case makes the network faster and easier to train as well as enhancing tracking reliability (Xu *et al*., 2005). To illustrate the role of PCA

© Woodhead Publishing Limited, 2010



10.8 Basic neural network for on-line fuel tracking.



10.9 Three-dimensional plot of the first three principal components.

in the classification of flame features according to fuel type, a three-dimensional (3D) plot of the first three principal components is given in Fig. 10.9. It is clear that there are eight different clusters in spite of a certain degree of overlap between them.

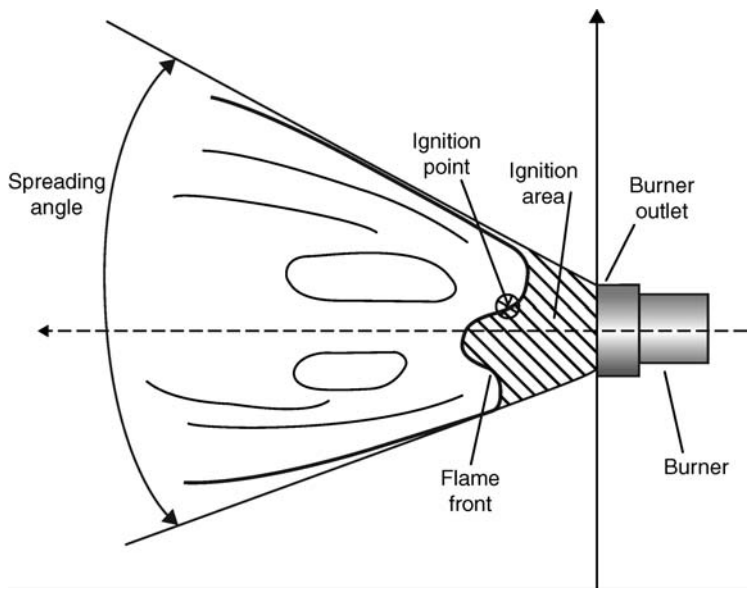
It is important to note that it is unnecessary to train the network to identify individual fuels (e.g. the specific mine from which it is extracted) but rather what group the fuel falls into in regard to its combustion properties. It is thus not necessary for the system to have 'seen' the particular fuel before, so long as it falls into a trained type grouping.

© Woodhead Publishing Limited, 2010

10.2.7 Flame imaging

A conventional flame detector uses a single infrared or ultraviolet photodetector and is limited to a single-point detection of the flame owing to the fundamental line-of-sight sensing arrangement. Digital imaging techniques are an extension of the conventional optical detection approach and are capable of providing two-dimensional (2D) information of a flame field. With the advent of high-performance and low-cost imaging devices in recent years, the application of digital imaging techniques to advanced monitoring and characterisation of combustion flames is becoming increasingly widespread. A range of measurements can be derived from 2D images of the flame when a side view of the flame is available (Lu *et al.*, 2004). These include spreading angle, ignition point and ignition area with respect to the burner outlet, brightness, uniformity, oscillation frequency, temperature distribution, and soot concentration. Some of the parameters are more important than others, depending on the purpose of the measurement and the camera installation arrangement.

When the root region of the flame is optically accessible, as shown in Fig. 10.10, ignition points, which form the flame front where fuel particles become ignited, can be identified readily through image processing. A stable flame requires a steady flame front at which the heat lost and heat release of the fuel are well balanced at the ignition temperature of the fuel. The ignition area is a measure of the normalised area encompassed between the



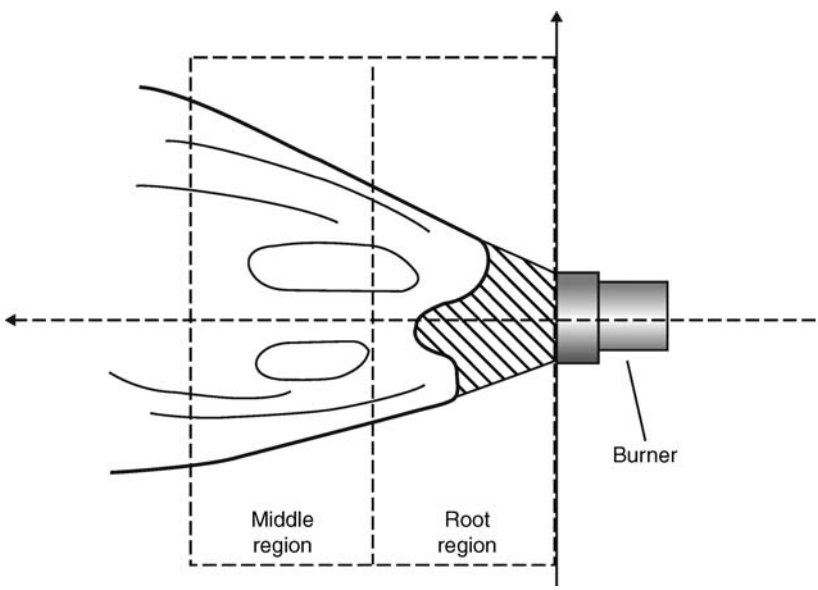
10.10 Definitions of some of the flame parameters.

© Woodhead Publishing Limited, 2010

burner outlet, flame front, and the spreading angle (Fig. 10.10), which gives the integrated information of flame ignitability (Lu *et al.*, 2004).

Another important flame parameter is the oscillation frequency (sometimes referred to as flame flicker), which is a good indication of flame stability and internal structural variability. To quantify this parameter, a random signal is reconstructed by adding and normalising all the grey levels of the individual pixels (corresponding to the radiation intensities of various points) in an area of interest in a flame image and then repeating this process for a series of consecutive flame images (Huang *et al.*, 1999; Lu *et al.*, 2006). The oscillation frequency is defined as the power-density-weighted average frequency in the frequency domain. Although the oscillation frequency of any part of a flame can be studied in principle using this method, the root region and middle region of the flame field are of primary interest to combustion engineers (Fig. 10.11). The root region encompasses essentially the area where the flame front fluctuates (normally from the burner outlet to the maximum possible ignition point). The ignition point and oscillation frequency as outlined above have been used to study flame stability and other characteristics of complex combustion processes such as co-firing biomass with coal (Lu *et al.*, 2008; Molcan *et al.*, 2009) and oxycoal combustion.

Flame temperature and its distribution provide fundamental information on the combustion process, including coal devolatilisation, radiative heat transfer, pollutant formation, and the cause of combustion problems such as slagging and fouling (CRF/BCURA, 2004). Digital imaging is an effective

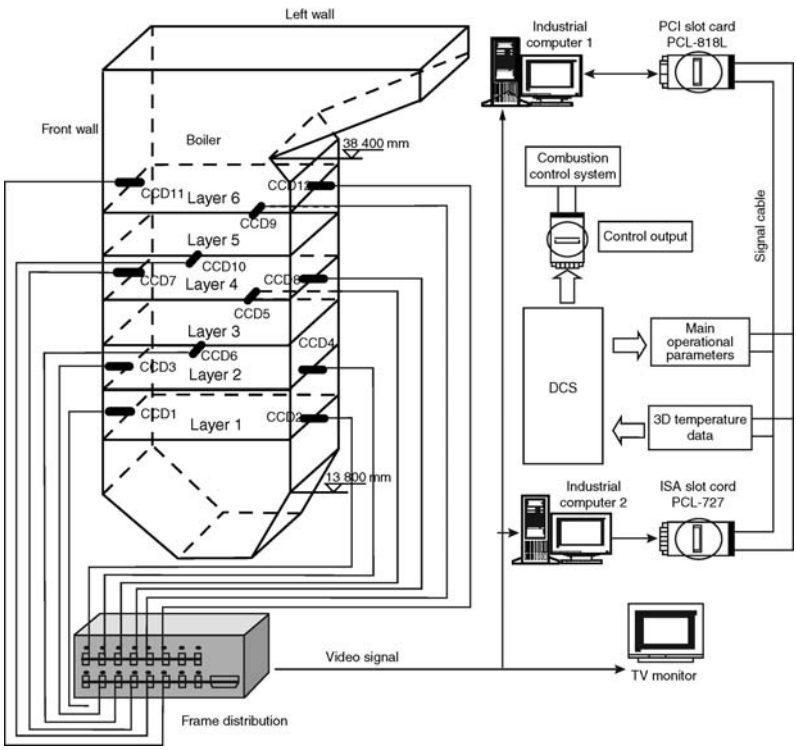


10.11 Definitions of root and middle regions of the flame field.

© Woodhead Publishing Limited, 2010

tool for the measurement of flame temperature and its distribution, which is very difficult to measure using other techniques. Several research groups are working actively to develop imaging-based flame temperature monitoring systems in recent years (Jiang *et al*., 2002; Lu and Yan, 2006; Wang *et al*., 2010). In most cases two-colour or multi-colour pyrometric techniques are applied to determine the flame temperature and its distribution. Apart from flame temperature, there have been attempts to extract other information using advanced signal and image processing algorithms. For example, Sbarbaro *et al*. (2003) used PCA and generalized Hebbian learning to extract the meaningful components from flame images. It was found that some principal components of a flame image from the blue channel are related to fuel and air flow rates.

In addition to the 2D flame imaging work, there have been extensive activities to measure 3D temperature distribution across a flame field. Multiple cameras are normally installed on the furnace walls (Luo and Zhou, 2007; Gilabert *et al*., 2009). For instance, a total of 12 CCD cameras are installed on a power plant furnace to obtain 3D temperature of the flame field (Luo and Zhou, 2007), as shown in Fig. 10.12. The temperature



10.12 Installation of 12 CCD cameras for the measurement of 3D flame temperature (Luo and Zhou, 2007).

© Woodhead Publishing Limited, 2010

distribution is derived by reconstructing the 3D flame field from the 2D flame images using tomographic and pyrometric techniques. Apart from flame temperature distribution, other 3D characteristics such as luminosity distribution, volume, surface area, orientation, and circularity can also be derived through the use of reconstruction algorithms (Bheemul *et al*., 2002; Gilabert *et al*., 2007). It must be said that the 3D flame imaging systems have indeed provided information that would otherwise be impossible to obtain using 2D systems. However, the use of multiple cameras on power plant furnaces can be costly and sometimes prohibitive owing to high capital cost and regular maintenance requirements.

10.3 Advanced control

Because of the inherent complexity and interaction of a larger number of physical and chemical processes in coal/biomass combustion, conventional control techniques are often not effective or inapplicable. Current practice and development of advanced control techniques for improved operation of coal/biomass combustion processes are based on neural network, fuzzy logic, and expert systems. The targeted variables to be controlled and optimised are associated with basic plant equipment such as pulverising mills, pneumatic conveyers, and boilers.

10.3.1 Pulverising mill control

The pulverising mill is notoriously difficult to control because of its complex physical operation, long time delay, and the impracticality of installing conventional process sensors. It is also difficult to develop a mathematical model of the mill for control purposes partly because of the wide coal grindability and variable particle size distributions. Good progress in developing advanced control systems has been made in recent years with three typical examples being given as follows.

Fukayama *et al*. (2004) developed an adaptive state estimator/model for the advanced control of a coal mill. The model considers particle size distribution in the form of a parametric description and coal grindability. The variables to be controlled are the fuel flow through the mill and particle size distribution at the mill outlet. The differential pressure and motor current of the mill (both depend on coal grindability) are the inputs to the control system. The system has been tested on a pilot plant and on a 1000 MW power station.

An expert control system using acoustic signatures from the mill has been developed (Bhaumik *et al*., 2006). The control system relies on a 'knowledge base' which is derived from a set of acoustic signatures under different operational conditions of the mill. A neural network is incorporated to

© Woodhead Publishing Limited, 2010

represent pulverising characteristics of the mill and resulting particle size distribution.

A multi-variable control system for the optimisation of a ball-mill coal-pulveriser has been proposed (Zhou *et al.*, 2003). The system is based on a three-neural decoupling control mechanism and is able to cope with long delay and strong coupling in the system. The method has been tested on a full-scale plant.

10.3.2 Fuel splitting control

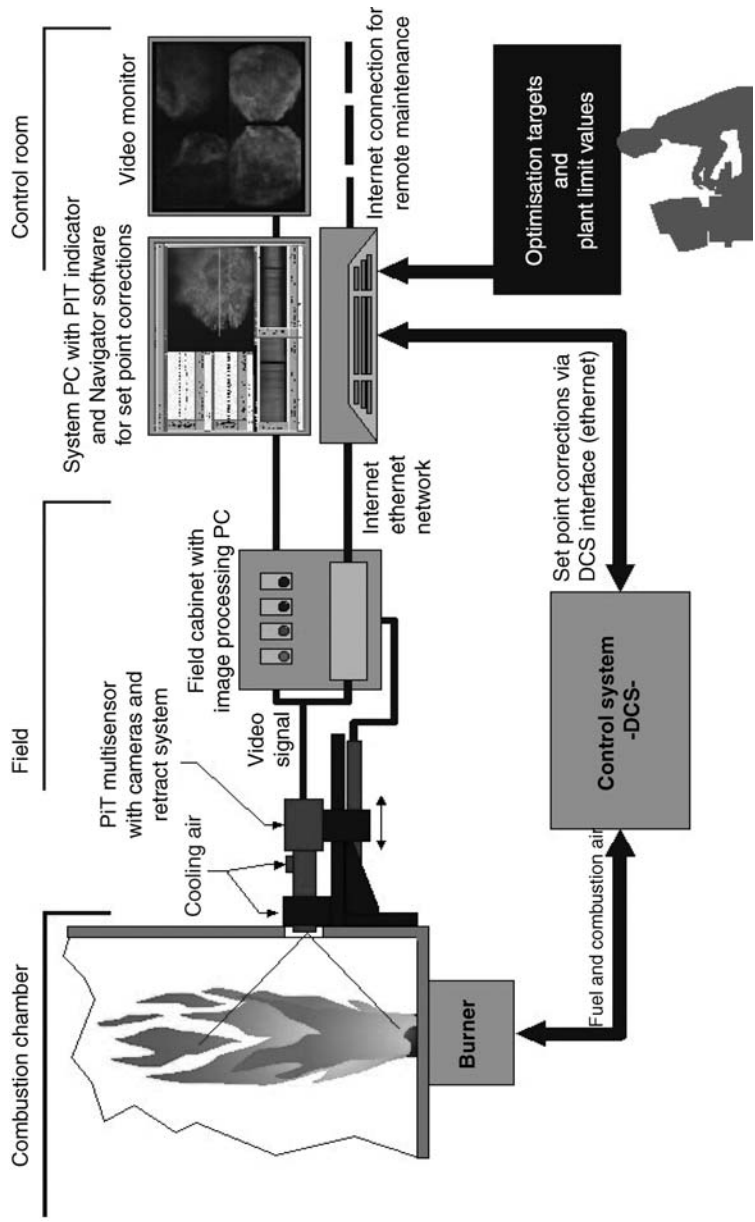
Without reliable control actuators, the benefits to be gained through the installation of pulverised fuel flow meters are limited. In comparison with pulverised fuel flow metering, splitting control of pulverised coal is embryonic. An earlier review has indicated that several industrial organisations in the USA and Denmark have attempted to develop control devices such as adjustable bifurcators/trifurcators and variable-orifice dampers (DTI, 2001). However, plant tests have shown that these devices have only had very limited success to date. Experimental tests were conducted on a small-scale test rig (pipe diameter 40 mm) on which a butterfly valve was used as an actuator (DTI, 2002). Some fundamental research was undertaken on a laboratory rig, where air was injected either upstream or downstream of the splitter to deflect the flow (Bradley, 1990).

10.3.3 Furnace and boiler control

There are significant control problems that should be resolved on the furnace and boiler level. For example, the development of a coordinated control strategy for the control of the main steam pressure and power output of a boiler–turbine system has been reported (Li *et al.*, 2005). The boiler–turbine system is a very complex process which is multivariable, non-linear, and slowly time-varying with large settling time. There also exist strong couplings between the main steam pressure control loop and the power output control loop. The control strategy is implemented in two levels: a basic control level and a supervision level. Conventional proportional–integral–derivative (PID) controllers are used in the basic level to perform basic control functions while the decoupling between the two control loops can be realised in the higher level. Fuzzy reasoning and autotuning techniques are incorporated in the control system.

Another example is the use of flame imaging results for the control and optimisation of coal-fired furnaces (Kiehn and Schmidt, 2009). The closed-loop control system aims to optimise the air/fuel ratio and its distribution on each burner level. It is based on flame imaging sensors and combustion process models that are established through self-learning neural nets.

© Woodhead Publishing Limited, 2010



10.13 Imaging and neural net based combustion control system (Kiehn and Schmidt, 2009).

© Woodhead Publishing Limited, 2010

Multiple imaging sensors are installed on the furnace walls in order to acquire unique information directly from the combustion chamber about ignition, burning and burn out behaviours. All combustion-related data are read from the control system permanently and on-line via an interface (Fig. 10.13). The PiT Indicator/Navigator (Fig 10.13) then correlates these data with the information from the imaging sensors. The control system has been applied at several power stations not only to improve combustion efficiency but also to reduce the content of unburned carbon in the fly ash so that it is saleable to the building industry.

10.4 Future trends

Despite a range of developments and advances that have been made in the areas as described in sections 10.2 and 10.3, a range of issues remain to be resolved. The following trends in future development are expected.

Previous and existing work in the area of pulverising mill monitoring focuses either on the use of acoustic emission or vibration sensors incorporating signal processing algorithms or on data modelling techniques. Both techniques should be combined to improve the performance of the monitoring system. Other sensors for the monitoring of other mill parameters should be integrated in the system, including the mill load, inlet primary air flow rate, differential pressure of the primary air, inlet and outlet temperatures, and particle size distribution at the mill outlet. Apart from the desired fuel level in the mill, the system should also be able to predict pocket fires, particularly in the co-milling of biomass and coal and during mill start-ups and shut-downs as well as an indication of the overall operating condition of the mill. Once the improved monitoring of a pulverising mill is achieved, more effective control and optimised operation of the mill is expected.

Plant data exist for mill settings for different bituminous coals and for blends with low proportions of sub-bituminous coals and biomass. Optimal milling conditions should be identified by analysing the data and fingerprinting milling characteristics. This is especially important for higher levels of sub-bituminous coal and biomass utilisation, where moisture and volatile contents and higher intrinsic reactivities can result in serious operational problems. Meanwhile, computational fluid dynamics (CFD) modelling techniques should be applied to simulate the fuel and air flow within the mill, taking account of the volatile components released from the fuel. The CFD modelling results together with a comprehensive graphical description of the conditions inside the mill concerning both gas and solid phases will enable the engineers to pinpoint possible scenarios that could lead to a fire or faulty condition of the mill.

Currently, there are few devices and systems that can provide absolute

© Woodhead Publishing Limited, 2010

measurement of pulverised fuel flow rate and size distribution. A number of prototypes have been installed on coal-fired power stations but few have met the requirements of the plant operators. The increasing trend towards co-combustion of biomass with coal in recent years will mean that flow rate determination and particle size distribution measurement are likely to be more challenging in view of the complex nature of the coal–biomass–air three-phase mixture. Flow sensors operating on electrostatic, microwave, and optical principles have shown their fundamental limitations for the measurement of pulverised fuel concentration and particle size distribution. However, further development in these areas is expected to continue. Additionally, a combination of multi-modal sensing techniques making full use of their individual advantages should be explored. Other methods such as those based on differential pressure and capacitance tomography for absolute concentration measurement are likely to be very difficult.

A pulverised fuel flowmeter should normally provide the operator with a set of measurements including coal velocity, mass flow rate, fineness and/or particle size distribution. The installation of multiple flow meters on all burner pipes will result in an enormous amount of data. How such data should be analysed and effectively used for the overall optimisation of the entire plant needs to be investigated. More importantly, the feasibility of feeding the data to the control system for automatic control and optimisation of the plant needs further study. Additionally, relationships between the coal mass flow rate, velocity, fuel/air ratio and resulting flame quality, combustion efficiency, and emissions should be identified.

There are still no proven control devices that can adjust the splitting of coal between individual pipes. The absence of such devices will limit the applicability and market potential of the pulverised fuel flowmeters. It is recognised that the split control of fuel particles is an inherently complex subject, particularly in full-scale power station pipes. The dynamic behaviour of fuel particles of different sizes in a large-scale pipe is not well understood and significant fundamental research through coherent experimental and CFD modelling is therefore needed. For instance, the complex interaction between the mass flow rate and the velocity of fuel in the pipe entails sophisticated control algorithms as well as unconventional measurement strategies. Meanwhile, the performance of such a measurement and control system will likely have an impact on the stability of flames and overall performance of the plant.

Some plant engineers are experiencing problems with flame eyes, particularly at lower loads where the burners are stable but the flame eyes indicate differently. The problems are compounded by the fact that some burners are opposed wall firing, so flame eyes can be confused by the flames from the opposite side of the boiler. This issue becomes more significant with the installation of over-firing air systems at some power stations. In the

© Woodhead Publishing Limited, 2010

case of oxyfuel combustion, reliable flame detection is crucial as the properties of an oxyfuel flame can differ significantly from those of an air-fired flame in terms of shape, temperature distribution, and flame stability, particularly when the flue gas recycle ratio varies or the grade of coal changes. Imaging devices may be incorporated in existing flame eyes so that they are able to provide extra information such as flame temperature, oscillation frequency, and on-line fuel tracking, as well as performing the conventional flame eye functions. An integrated data fusion and management system will be required to acquire and process the data from all the flame eyes on the same unit. Such comprehensive data will enable power engineers to assess or predict burner conditions, plant equipment wear, and other more complex plant configurations.

Further development in digital imaging based flame monitoring is expected. In addition to flame temperature distribution in a full-scale furnace where multiple cameras are installed, additional information about the flame field will be extracted from flame images through advanced image processing and pattern recognition. This additional information may include ignition patterns, oscillation frequency distribution, fuel/air balance between burners, and even concentrations of free radicals such as OH*, CH*, and CN*. The flame imaging data will provide ample information for the validation of CFD models of the flames and furnaces, leading to optimised design and operation of coal-fired plant firing a diverse range of fuels under variable load conditions.

10.5 Sources of further information

Selected professional bodies, industrial organisations and research groups that are relevant to monitoring and control of coal/biomass combustion processes are listed below for further information. Other relevant literature can be found in the reference list.

Advanced Power Generation Technology Forum (APG-TF), URL: http://www.apgtf-uk.com/

Coal Research Forum, URL: http://www.coalresearchforum.org/

IEA Clean Coal Centre, URL: http://www.iea-coal.org.uk/site/ieacoal/home

British Flame: URL: http://www.britishflame.org.uk/

The Institute of Measurement and Control, URL: http://www.instmc.org.uk/

Optech, Canada, URL: http://www.optech.ca

Endress + Hauser, URL: http://www.us.endress.com

Siemens Milltronics Process Instruments Inc., URL: http://www.siemens.com/level

© Woodhead Publishing Limited, 2010

Powitec, Germany, URL: http://www.powitec.de/englisch/

PCME Limited, UK, URL: http://www.pcme.co.uk/

Greenbank Group, UK, URL: http://www.greenbankgroup.com/tero-p-flow.asp

Instrumentation, Control and Embedded Systems Research Group, University of Kent, UK, URL: http://www.eda.kent.ac.uk/research/default.aspx

The Wolfson Centre for Bulk Solids Handling Technology, University of Greenwich, UK URL: http://www.gre.ac.uk/wolfsoncentre

Department of Neuroinformatics and Cognitive Robotics, Technical University of Ilmenau, Germany, URL: http://www.tu-ilmenau.de/fakia/4189+M52087573ab0.0.html

State Key Laboratory of Clean Energy Utilisation, Zhejiang University, People's Republic of China, URL: http://www.ceu.zju.edu.cn/web_en/ceee/w_ceee07_aleaders.htm

State Key Laboratory of Coal Combustion, Huazhong University of Science and Technology, People's Republic of China, URL: http://www.hust.edu.cn/english/research/organ/coal.htm

10.6 References

APGTF (2009), *Cleaner fossil power generation in the 21st century – a technology strategy for carbon capture and storage*, UK Advanced Power Generation Technology Forum.

Behera B, Mishra B K and Murty C V R (2007), 'Experimental analysis of charge dynamics in tumbling mills by vibration signature technique', *Minerals Engineering*, 20, 84–91.

Bhaumik A, Sil J, Maity S and Das T S (2006), 'Designing an intelligent expert control system using acoustic signature for grinding mill operation', IEEE International Conference on *Industrial technology*, Mumbai, India, 15–17 December 2006, 500–505.

Bheemul H C, Lu G and Yan Y (2002), 'Three-dimensional visualization and quantitative characterization of gaseous flames', *Measurement Science and Technology*, 13, 1643–1650.

Bradley M S A (1990), 'Prediction of pressures losses in pneumatic conveying pipelines', PhD thesis, University of Greenwich, London, UK.

Cai X S, Li J F, Ouyang X, Zhao Z J and Su M X (2005), 'In-line measurement of pneumatically conveyed particles by a light transmission fluctuation method', *Flow Measurement and Instrumentation*, 16, 315–320.

Carter R M and Yan Y (2007), 'On-line non-intrusive particle size measurement of pulverised fuel through digital imaging', *Chinese Journal of Scientific Instruments*, 28, 1942–1946.

Carter R M, Krabicka J, Yan Y and Cornwell S (2009), 'An integrated instrumentation system for combustion plant optimisation', *Proceedings of International Instrumentation and Measurement Technology Conference*, Singapore, 5–7 May 2009, 780–784.

© Woodhead Publishing Limited, 2010

Chinnayya A, Chtab A, Shao J Q, Carter R M, Yan Y and Caillat S (2009), 'Characterization of pneumatic transportation of pulverised coal in a horizontal pipeline through measurement and computational modelling', *Fuel*, 88, 2348–2356.

CRF/BCURA (2004), *Coal research needs in the UK*, Cheltenham, UK: Coal Research Forum/British Coal Utilisation Research Association.

DTI (2001), 'Technology status review of PF flow measurement and control methods for utility boilers', Technology Status Report 014, DTI/Pub URN 01/560.

DTI (2002), 'Pulverised fuel measurement with split control', Clean Coal Technology Programme, Project Summary 330.

Endress + Hauser (2009). FMP 40 TDR level measurement in coal bunkers. Available from: http://www.us.endress.com (accessed 10 August 2009).

Fukayama Y, Hirasawa K, Shimohira K and Kanemoto H (2004), 'An adaptive state estimator for pulverizer control using moments of particle size distribution', *IEEE Transactions on Control Systems Technology*, 12, 797–810.

Gilabert G, Lu G and Yan Y (2007), 'Three-dimensional tomographic reconstruction of the luminosity distribution of a combustion flame', *IEEE Transactions on Instrumentation and Measurement*, 56, 1300–1306.

Gilabert G, Lu G and Yan Y (2009), 'Three-dimensional monitoring of combustion flames using digital imaging and tomographic reconstruction techniques', International Symposium on *What where when multi-dimensional advances for industrial process monitoring*, Leeds, UK, 23–24 June 2009.

Huang Y P, Yan Y, Lu G and Reed A R (1999), 'On-line flicker measurement of gaseous flames by imaging processing and spectral analysis', *Measurement Science and Technology*, 10, 726–733.

Jiang F, Liu S, Lu G, Yan Y, Wang H, Song Y, Ma R, and Pan Z (2002), 'Flame temperature measurement using the two-colour method', *Chinese Journal of Electrical Engineering*, 22, 133–137.

Kang E S, Guo Y G, Du Y Y and Zhao L H. (2006), 'Acoustic vibration signal processing and analysis in ball mill', Proceedings of the 6th World Congress on *Intelligent control and automation*, Dalian, China, 21–23 June 2006, 6690–6693.

Kiehn D and Schmidt D (2009), Performance contracting for a combustion optimizer, based on neural networks in a coal-fired power plant. Available from: http://www.powitec.de/englisch (accessed 23 August 2009).

Koeneman D and Sholette W (2006), 'Level measurement solutions for coal handling applications', *Power Engineering*, 110, 44–48.

Krabicka J and Yan Y (2009), 'Finite-element modeling of electrostatic sensors for the flow measurement of particles in pneumatic pipelines', *IEEE Transactions on Instrumentation and Measurement*, 58, 2730–2736.

Li S Y, Liu H B, Cai W J, Soh Y C and Xie L H (2005), 'A new coordinated control strategy for boiler–turbine system of coal-fired power plant', *IEEE Transactions on Control Systems Technology*, 13, 943–954.

Lu G and Yan Y (2006), 'Temperature profiling of pulverised coal flames using multi-colour pyrometric and digital imaging techniques', *IEEE Transactions on Instrumentation and Measurement*, 55, 1303–1308.

Lu G, Yan Y and Colechin M (2004), 'A digital imaging based multi-functional flame monitoring system', *IEEE Transactions on Instrumentation and Measurement*, 53, 1152–1158.

© Woodhead Publishing Limited, 2010

Lu G, Yan Y, Colechin M and Hill R (2006), 'Monitoring of oscillatory characteristics of pulverised coal flames through image processing and spectral analysis', *IEEE Transactions on Instrumentation and Measurement*, 55, 286–231.

Lu G, Yan Y, Cornwell S, Whitehouse M and Riley G (2008), 'Impact of co-firing coal and biomass on flame characteristics and stability', *Fuel*, 87, 1133–1140.

Luo Z X and Zhou H C (2007), 'A combustion-monitoring system with 3-D temperature reconstruction based on flame-image processing technique', *IEEE Transactions on Instrumentation and Measurement*, 56, 1877–1882.

Malmgren A, Oluwande G and Riley G (2003), 'Multiphase flow in coal-fired power plant', DTI/Pub URN 03/1635, Report No. Coal R252, Cleaner Fossil Fuels Programme, Department of Trade and Industry.

Miller D, Baimbridge P and Eyre D (2000), 'Pulverised fuel flow measurement and control methods for utility boilers', Report No. Coal R201, DTI/Pub URN 00/1445.

Molcan P, Lu G, Le Bris T, Yan Y, Taupin B and Caillat S (2009), 'Characterisation of biomass and coal co-firing on a 3 MWth combustion test facility using flame imaging and gas/ash sampling techniques', *Fuel*, 88, 2328–2334.

Optech (2006). Product application note – complete coal bunker automation scheme. Available from: http://www.optech.ca (accessed 10 August 2009).

Pattinson M and Miller D (1997), 'The future', IMechE Seminar on *Real-time analysis of bulk materials in the power, minerals and cement industrials*, London, 29 April 1997.

Sbarbaro D, Farias O and Zawadsky A (2003), 'Real-time monitoring and characterization of flames by principal-component analysis', *Combustion and Flame*, 132, 591–595.

Siemens Milltronics Process Instruments Inc. (2009), Measuring pulverized coal in bunkers. Available from: http://www.siemens.com/level (accessed 10 August 2009).

Su Z G, Wang P H, Yu X J and Lv Z Z (2008), 'Experimental investigation of vibration signal of an industrial tubular ball mill: monitoring and diagnosing', *Minerals Engineering*, 21, 699–710.

Wang F, Yan J H, Cen K F, Huang Q X, Liu D, Chi Y and Ni M J (2010), 'Simultaneous measurements of two-dimensional temperature and particle concentration distribution from the image of the pulverized coal flame', *Fuel*, 89(1), 202–211.

Wei J L, Wang J H and Wu Q H (2006), 'Multi-segment pulverised coal mill model and on-line implementation for condition monitoring', *International Journal of Modelling, Identification and Control*, 1, 206–214.

Wei J L, Wang J H and Wu Q H (2007), 'Development of a multi-segment coal mill model using an evolutionary computation technique', *IEEE Transactions on Energy Conversion*, 22, 718–727.

Xu L, Yan Y, Cornwell C and Riley G (2004), 'On-line fuel identification using digital signal processing and fuzzy inference techniques', *IEEE Transactions on Instrumentation and Measurement*, 53, 1316–1320.

Xu L, Yan Y, Cornwell S and Riley G (2005), 'On-line fuel tracking by combining principal component analysis and neural network techniques', *IEEE Transactions on Instrumentation and Measurement*, 54, 1640–1645.

© Woodhead Publishing Limited, 2010

Yan Y (1996), 'Mass flow measurement of bulk solids in pneumatic pipelines', *Measurement Science and Technology*, 7, 1687–1706.

Yan Y (2001), 'Guide to the flow measurement of particulate solids in pipelines – Part I: fundamentals and principles', *Powder Handling and Processing*, 13, 343–352.

Yan Y (2002), 'Guide to the flow measurement of particulate solids in pipelines – Part II: Utilisation in pneumatic conveying and emission monitoring', *Powder Handling and Processing*, 14, 12–21.

Yu X Y, Tang L P, Jia H Y and Zhang J (2004), 'Coal level detection system of coal mill based on Hilbert transform and spectrum correlation', Proceedings of the 2004 China–Japan Joint Meeting on *Microwaves*, Harbin, China, 5–6 August 2004, 455–458.

Zhang G Q and Thulen P C (2006), 'Coal pulverizer monitoring and analysis – a case study', *Proceedings of the ASME Power Conference*, Atlanta, USA, 2–4 May 2006, 169–176.

Zhang J Q and Yan Y (2003), 'On-line continuous measurement of particle size using electrostatic sensors', *Powder Technology*, 135–136, 164–168.

Zhou H, Zhong M H, Zhang L M and Wang Q Z (2003), 'Neural intellectual decoupling control strategy of the middle-storage coal-pulverizing system in power plant', Proceedings of the 6th International Conference on *Electronic measurement and instruments*, Taiyuan, People's Republic of China, 18–21 August 2003, 1–3, 2213–2217.

© Woodhead Publishing Limited, 2010

Part III

Improving the fuel flexibility, environmental impact and generation performance of advanced power plants

© Woodhead Publishing Limited, 2010

11

Low-rank coal properties, upgrading and utilization for improving fuel flexibility of advanced power plants

T. DLOUHÝ, Czech Technical University in Prague, Czech Republic

Abstract: This chapter provides a general overview of relatively new but not commonly used techniques of low-rank coal preparation and upgrading. Options such as washing, drying and briquetting are discussed. All the processes contribute to the increase in heating value of the coal and improve the fuel consistency, resulting in more efficient and controllable combustion.

Key words: coal upgrading, coal preparation, coal drying, coal briquetting.

11.1 Introduction

Coal as a fuel for power plants will play an important role in the near and far future as there are very large coal supplies all over the world, but the quality of coal will vary considerably and gradual deterioration is expected. Upgrading brings a number of beneficial effects, reducing most of the problems associated with lower-quality coal utilization. Washing results in reductions in the amounts of mineral matter present, including a proportion of trace elements and sulphur. Drying reduces the moisture content, and hence increases the heating value. Briquetting improves the combustion characteristics and facilitates the inclusion of additives which will capture the sulphur present. All the processes contribute to the increase in heating value of the coal and improve the fuel consistency, resulting in more efficient and controllable combustion. This chapter provides a general overview of relatively new but not commonly used techniques of low-rank coal preparation and upgrading.

© Woodhead Publishing Limited, 2010

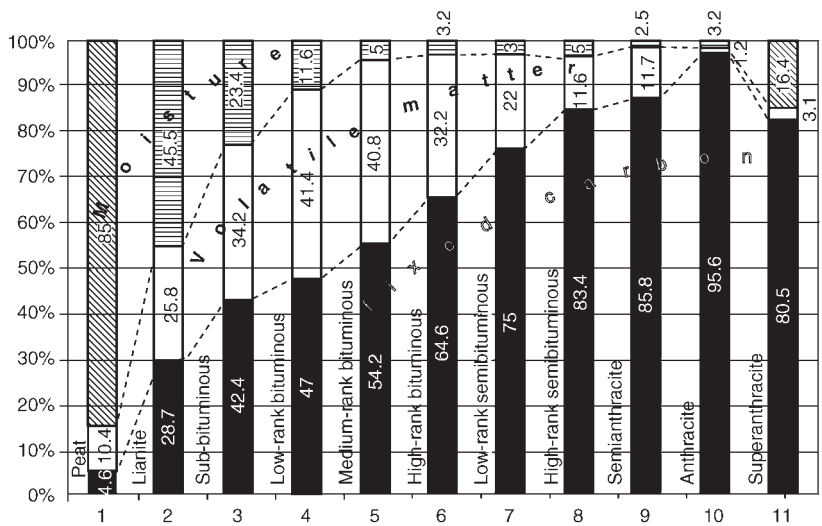
11.2 Properties of low-rank coal

The different types of coal can be classified according to the intrinsic chemical and physical properties of the coal itself due to variation in its origin, constitution, and degree of metamorphism. The various ranks of coal, beginning with the youngest, are peat, lignite, sub-bituminous, semibituminous, semianthracite, anthracite, and superanthracite. Different terminologies are used in different parts of the world. Sub-bituminous and bituminous coal are sometimes considered to cover a broad range of hard coals. Use of both lignite and brown coal for the same rank of coal is quite common.

The various ranks of coal depend upon how much volatile matter, moisture, and oxygen was excluded from the lignite during metamorphism. The distinguishing characteristics of various grades of coal on an ash-free basis by Campbell (Gaffert, 1950) are shown in Fig. 11.1.

The chart shows how the moisture content varies from a maximum with peat to a relatively small percentage with anthracite. Volatile matter has a maximum with low-rank bituminous coal. The percentage of fixed carbon increases steadily from peat to anthracite by grades of metamorphism and accounts principally for the increase in heating value.

In general, coals with high moisture and low heating value are classified as low-rank coal. Lignites, together with some of the lower-rank sub-bituminous coals, are included in this common group. Lignites are brown in colour and frequently show a distinct woody structure. Newly mined lignites usually have a high moisture content and upon exposure disintegrate

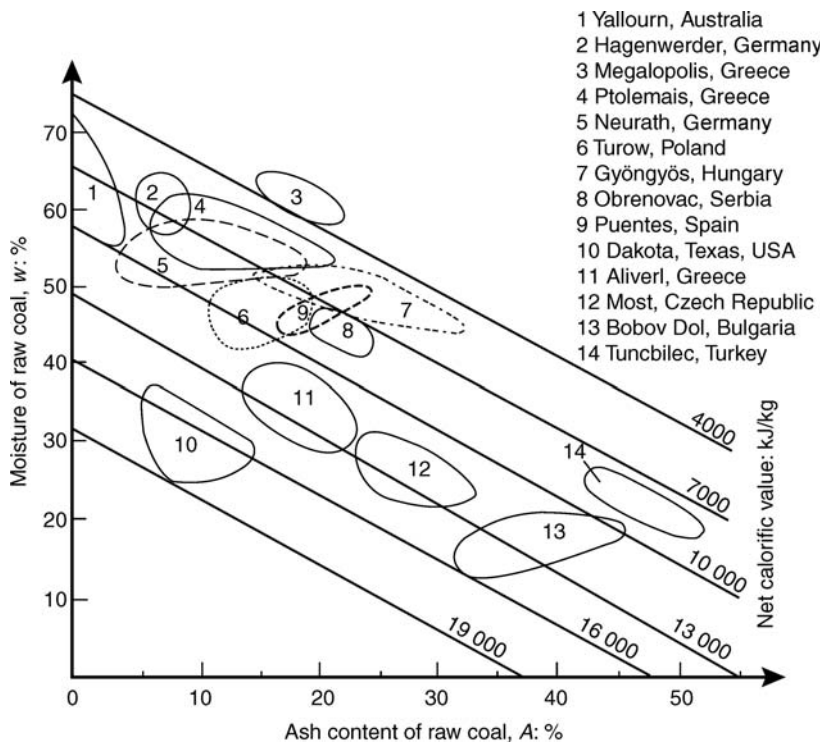


11.1 Chemical composition of various grades of coal (except ash).

© Woodhead Publishing Limited, 2010

rapidly. They burn with a long yellow flame, which has less tendency to smoke than that from bituminous coal. Lignites can be pulverized and burned when the moisture is reduced to about 28% or lower. Sub-bituminous coals are black with shiny surfaces and a laminar structure. They do not coke, but burn freely with a decided tendency to crumble in the fire. They are comparatively soft and pulverize easily, burning with a long yellow flame.

The low-rank coals have moisture contents in the range 30–70% and are rich in oxygen. The ash content of low-rank coals varies very widely, with most falling within the range 5–50%. The result of the moisture and ash content is that the lower heating value (LHV) of the coal is generally in the range 4–18 MJ/kg, considerably below that for most bituminous coals. Figure 11.2 (Hill *et al.*, 1989) shows properties of low-rank coals from different countries.



11.2 Relative moisture and ash contents and calorific value of various low-rank coals.

© Woodhead Publishing Limited, 2010

11.3 Influence on design and efficiency of boilers

High moisture in low-rank coal complicates boiler design. An increased mass flow rate of all substances affects boiler size and the capacity of auxiliary equipment. A considerable difference in the flow rate and heat capacity between flue gas and combustion air resulting from the high moisture content in the coal means that a technical limit is approached as to the extraction of heat from the gas in the air heater. This technical limit is due to the approach of the hot air temperature at the outlet of the air preheater to the inlet flue gas temperature, that is, the 'pinch point' effect. In addition, the combination of a high moisture content in the flue gas, sulphur dioxide (SO_2) and chloride (Cl) content results in a high acid dew point, necessitating high metal temperatures if corrosion rates are to be manageable. As a result, the final flue gas temperatures for low-rank coal boilers are significantly above those for black-coal-fired-boilers. Hence there are two effects of the high moisture content in coal:

- greater heat loss due to the increased flue gas flow;
- additional heat loss due to the necessarily higher final flue gas temperature at which low-rank coal boilers must operate.

The maximum thermal efficiency achievable is some 1.5–4 % lower than that for an equivalent hard coal because of the water content (Dlouhy and Kolovratnik, 2004). Measures for utilization of flue gas waste heat have to be applied if high efficiency is required. A feed water heating arrangement (where flue gas is used directly for heating the condensate and feed water) such as a regenerative feed water preheater has been developed and applied in recent German and Czech lignite-fired power plants. A closed-cycle heat exchange system between the flue gas and the condensate is used involving very low temperature differentials and corrosion resistant material (Dlouhy *et al.*, 2007). However, this is a system that would not be economic for most lower-cost low-rank coals.

11.4 Low-rank coal preparation

Preparation is the most widely used method of pre-combustion treatment of coal. Raw coal needs to be prepared properly for safe, economical, and efficient use in coal combustion systems. Coal preparation differs according to the combustion technique used. If combustion is to be carried out on grates, then normally there is only limited fuel preparation needed. Fluidized-bed combustion needs most coals to be crushed. Depending on the fuel properties, maximum grain sizes of between 3 and 20 mm are desired. In all coal pulverizing systems, coal is dried, ground, classified, and then transported to the boilers. Excepting crushing and pulverization, the

© Woodhead Publishing Limited, 2010

first step of coal pre-treatment can be performed in plants for coal cleaning and classification, which are usually located close to a mine.

Coal cleaning, which is often described as preparation for particular markets, is performed in order to reduce the amount of mineral matter and/or sulphur. Two methods, based on either wet or dry processes, can be used.

Coal washing is a common term for all water-based processes. The objective of the operations is to recover the maximum amount of organic matter from the raw material coming from a coal mine. Washing operations are carried out mainly on bituminous and anthracitic coals. Roughly half the bituminous coals mined worldwide are washed.

Low-rank coals have high moisture contents, and the most important aspect of upgrading is usually drying. Most low-rank coal is run-of-mine material. Selective mining is carried out in some places to improve the quality of low-rank coals. Less than 15% of worldwide production of lignite and sub-bituminous coal is washed or dried (Couch, 2002).

The mineral matter content of coals as mined can range from 5 to 50% and affects the heating value of the coal and its deposition characteristics in a boiler. It can thus affect heat loss from the system and boiler efficiency. The size, distribution, and nature of the mineral matter through the run-of-mine coal can vary widely and depend both on the occurrence in the coal seam and on the mining method.

Coal in most preparation plants is crushed to eliminate large particles of coal. Crushing is followed by screening to produce different sized cuts for treatment. Washing operations are generally carried out within three distinct size ranges: for coarse coal a size from 150 to 10 mm, for intermediate from 10 to 0.5 mm (500 μm), and for fine, below 500 μm in size. Removal of loose shale from the coal and separation of particles with high mineral matter content are the most basic priorities of washing. A difference in relative density is utilized to separate particles with different proportions of mineral matter. If lower relative density is used then the cleaner coal particles will classify as a 'clean coal' stream. Simple washing plants with one separator (a jig or a dense medium drum) for a wide range of particle sizes tend to reject more usable carbon than multi-stage plants where each size range is optimally separated. Various separation units and their potential applications are described by Couch (1991).

For areas where water is in short supply or where severe winter conditions preclude the transport of wet coal, and for some lower rank coals which tend to form slime during wet processing, dry separation methods have been developed. Dry methods are based on differences in physical properties between particles such as density, lustrousness, magnetic conductivity, electric conductivity, and frictional coefficients. For intermediate particle sizes, fluidization methods using air as the medium are generally suitable. For fine coal, electrostatic methods are more applicable. Air-based processes

© Woodhead Publishing Limited, 2010

tend only to work well for fairly narrow size ranges and also involve dust removal before the air is exhausted. An air-based method utilizing dense–medium fluidized bed (ADMFB), which has been developed recently in China, is described by Chen and Yang (1997).

11.5 Technologies of low-rank coal upgrading

In general, coal upgrading involves drying, liquefaction, gasification, briquetting or coking. Drying and briquetting are the most widely used methods for upgrading of a low-rank coal.

The high moisture content and resultant low heating value of low-rank coal affect boiler efficiency and transportation costs. Upgrading technologies increase the calorific value of a low-rank coal by removing water. Dewatering or drying are the processes used for this purpose. Moisture removal can be accomplished through the use of four different technologies – three are thermal and one is non-thermal:

- direct heat by saturated steam;
- indirect heat utilizing waste heat or recirculated flue gas;
- briquetting using simultaneous heat and pressure action;
- electromagnetic radiation similar to that used in a microwave.

Upgrading increases coal energy density, enhances power plant efficiency, and reduces the emission of regulated substances.

11.5.1 Low-rank coal drying

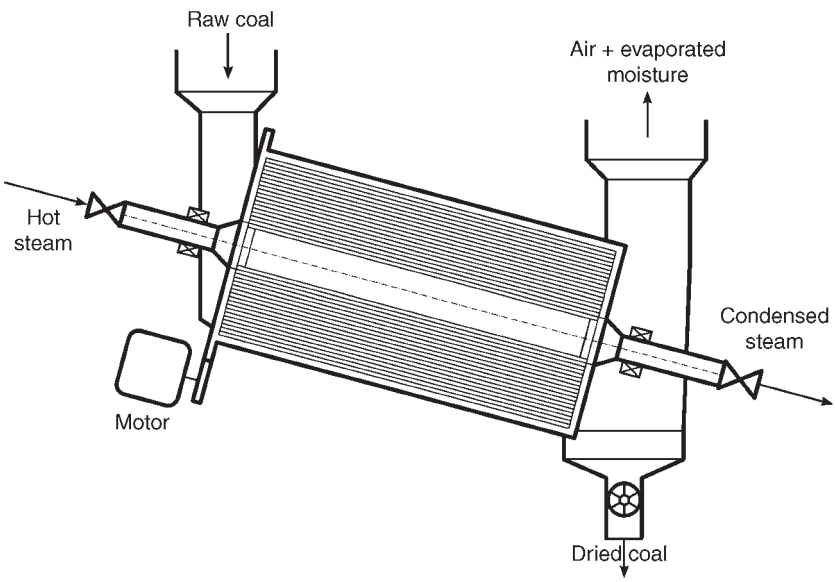
Coal preparation for pulverized coal (PC) combustion always includes drying, which must be very intensive, especially if moist lignite is used. Lignite pulverization is aided by the presence of hot flue gases (with temperature up to 1000°C), which are extracted from the boiler through recirculation ducting. The lignite is fed from the bunkers through horizontal, closed feeders to vertical flue gas recirculation ducts and falls to the lignite mill. A fan mill, with either a fan impeller or with a series of impact blades located in front of the fan impeller, is used for lignite pulverization. The mill must achieve three objectives: to pulverize, dry, and then distribute the fuel to the combustion chamber. The lignite particles are typically reduced to less than 90 m in size (approximately 60% through a 70-mesh screen). The flue gas heat reduces the lignite moisture content down to 5–15%, in other words, to the required level for optimum combustion conditions. The fan enhances turbulent mixing and increases the relative and absolute velocity of the particles and the gas. The disadvantages of this simple drying method consist in the feeding of lignite dust into the boiler together with drying flue gas and all the water vapour formed. Drying

© Woodhead Publishing Limited, 2010

therefore contributes only to the reduction of an ignition and burnout period of lignite particles, but an increase in boiler efficiency and the reduction of boiler size is negligible. When lignite of extremely high moisture content is used as the fuel, an additional step prior to feeding it into the combustion chamber is necessary for more effective removal of lignite moisture. For this purpose, after the mills, a stream rich in lignite and moisture is directed to specially designed electrostatic precipitators, where the dry lignite particles are separated and then fed to the lower boiler burners. From the lignite electrostatic precipitators, the mixture of flue gases and moisture is directed via induced-draft fans to the stack or to the flue gas desulphurizer (FGD). If the lignite is dried externally, a much smaller boiler can be used.

If flue gas is used for drying, heat from the calorific value of coal is consumed for moisture evaporation. The utilization of external heat for drying is more effective. A number of both classic and advanced methods utilizing external heat for coal drying are available.

The tubular dryer is among the techniques with the most industrial-scale experience. It has been widely used in Australia, Germany, and India in connection with lignite/brown coal briquetting. The plant consists, typically, of an inclined rotating shell with a tube heat exchanger (see Fig. 11.3). The shell is heated by low-pressure (waste) steam at 0.4–0.5 MPa and at 160°C, which condenses inside the inter-tube space. Brown coal with a particle size of less than 10 mm enters the tubes with a diameter of 100 mm on the upper



11.3 Steam tubular dryer.

© Woodhead Publishing Limited, 2010

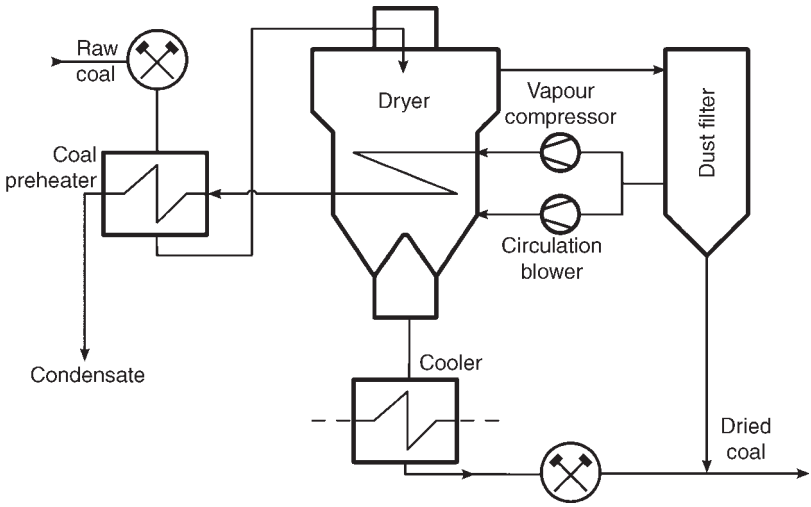
side of the shell, passes through the tubes, and is dried to a 12–15% moisture content. On the lower side of the shell, the dried coal is collected for subsequent use and air with the evaporated moisture is blown out through an electrostatic precipitator, where fine coal particles are separated.

It is possible to increase the drying intensity by using a fluidized-bed dryer instead of a tubular one. The method utilizing a fluidized-bed dryer (known as WTA or 'Wirbelschicht-Trocknung mit interner Abwarmenutzung' in German) has been demonstrated on a pilot scale in Germany (Klutz *et al.*, 1996). The energy required for drying is supplied via heat exchangers that are integrated in the fluidized bed and heated with low-pressure steam. Fluidization is achieved by a partial recirculation of vapour. Drying is carried out in almost pure steam, which is slightly superheated. At constant pressure, an equilibrium between the steam temperature and the residual moisture of the dried lignite is reached. The required moisture content in the dried coal can be adjusted and maintained constant by controlling the fluidized-bed temperature. For a system temperature of approximately 110°C a residual moisture content of some 12% was reached for German Rhenish coal with an inlet moisture up to 60% (Elsen *et al.*, 2001). Lignite drying in a steam atmosphere which is not diluted by air or flue gas enables the utilization of evaporated coal water in an energetically efficient way. Two vapour utilization concepts have been developed for industrial use:

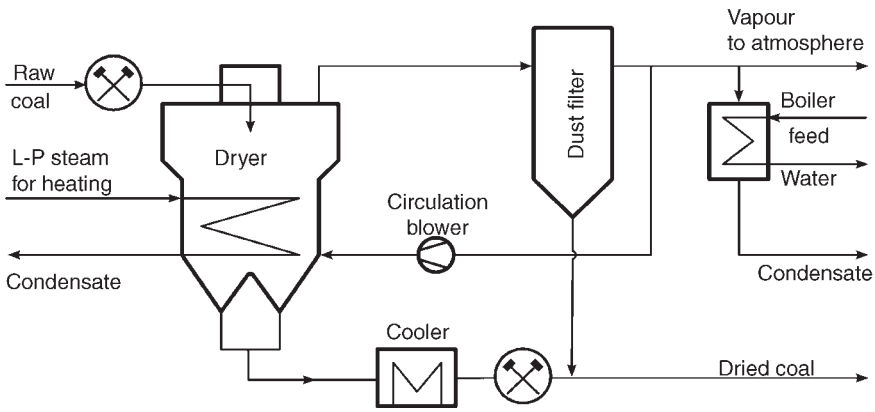
- vapour recompression as an open heat pump process for the heating of a dryer;
- vapour condensation in an external heat exchanger for the preheating of boiler feed water in a power plant.

The WTA drying process has been developed for two different input grain sizes. The coarse-grain variant with particles between 0 and 6 mm is employed where the dried coal must have a specific minimum grain size, for example, for gasification in the high-temperature Winkler (HTW) process or for coke production from lignite. For all other applications, the fine-grain variant with particle size up to 2 mm is usually the more attractive option in technical and economic terms. The fine-grain WTA process can be used as a pre-drying stage in conventional power plants with PC boilers. The fine-grain WTA variant with upstream fine milling and integrated mechanical vapour compression is shown in Fig. 11.4. Following cleaning in an electrostatic precipitator, the vapour obtained from evaporated coal water is divided into two flows. The main flow is passed through a steam compressor where its temperature and pressure are raised to around 150°C and 0.4–0.5 MPa. Compression allows for use of the vapour for the indirect heating of fluidized lignite through heat exchange tubes in the dryer where the vapour condenses. Condensate produced is used to preheat the raw lignite coming from the mill to about 65 to 70°C. The rest of the cleaned vapour is

© Woodhead Publishing Limited, 2010



11.4 WTA variant with integrated mechanical vapour compression.

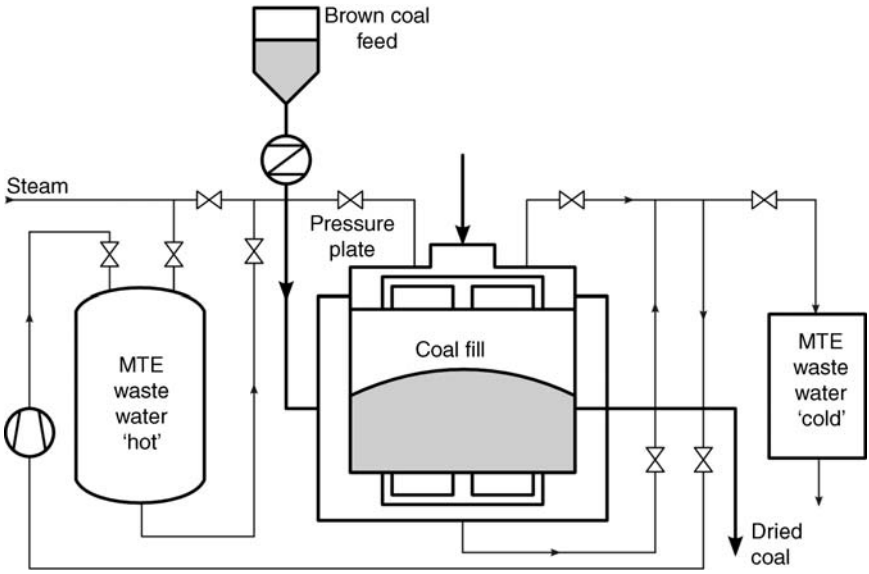


11.5 WTA variant with external heating.

recirculated and employed for fluidizing the bed. If required, the dried coal is cooled and milled to a grain size which is suitable for following use. Figure 11.5 shows the fine-grain WTA variant without a vapour compressor. Heat for drying is obtained from external low pressure (waste) steam. Vapour from the drier is used for boiler feed water preheating in terms of the water–steam cycle in the power plant.

The WTA coarse-grain dryer with integrated vapour compression and coal preheating has been thoroughly tried and tested on a pilot plant with capacity of 53 t/h in Frechen. A fine-grain dryer utilizing vapour condensation with a raw coal input of approximately 210 t/h is under construction in Niederaussem.

© Woodhead Publishing Limited, 2010



11.6 Schematic diagram of MTE dewatering.

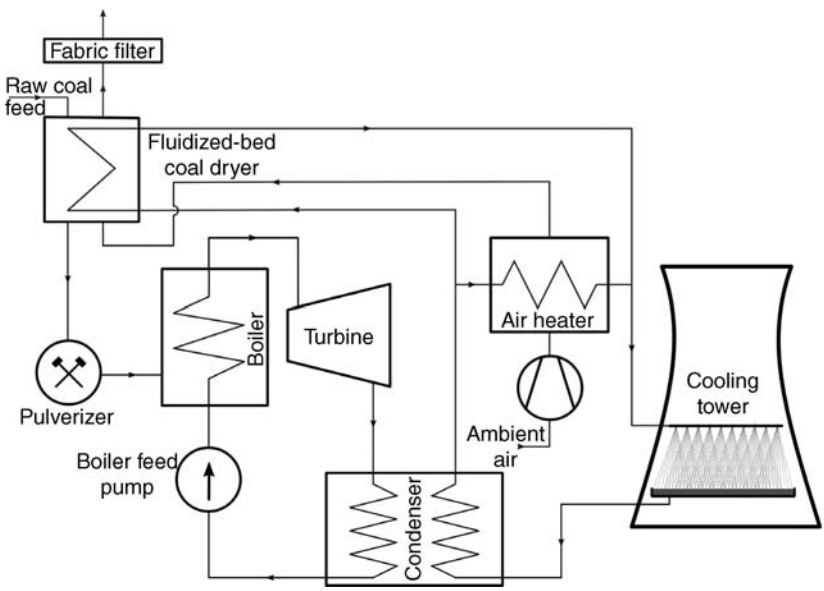
Another method involving mechanical–thermal dewatering is available but has been tried out only on a smaller scale. The main principle of this method, which is also called MTE (or 'Mechanisch–Thermische Entwasserung' in German) is based on the fact that much of the water content is not strongly bound to the coal. The MTE process (Fig. 11.6) combines the mechanical press dewatering concept with the use of elevated temperatures in the range 150–180 °C. Such temperatures enable dewatering at substantially lower mechanical pressures and residence times. The raw coal comes to the pressure chamber where it is slightly pre-pressurized by a press stamp. Hot water is distributed evenly on its surface by sprinklers. Saturated steam is introduced into the chamber and the hot water flows through the coal releasing nearly all its heat content. Water leaving the chamber at around ambient temperature is collected in a cold water tank for following utilization in the cooling system of a power plant. The process is repeated, using pressures up to 6 MPa. The potential of the MTE dewatering was recognized both for German moist lignite (Elsen, 1999) and Australian Victorian brown coal (Chun-Zhu, 2004). Laboratory studies have shown that the percentage of water removal depends on the pressure used and increases approximately linearly as a function of temperature.

A low-temperature lignite drying system utilizing waste heat from a power plant has been developed at Great River Energy's Coal Creek Station in Underwood, North Dakota (USA). The lignite, with a typical moisture of up to 40%, comes from the Falkirk mine. The principle is applicable for

© Woodhead Publishing Limited, 2010

lignite and sub-bituminous coal-fired power plants, which are cooled by evaporative cooling towers. Heat recovered from cooling water can work to dry high-moisture lignite before it is fed to the pulverizers. Circulating cooling water leaving the condenser is utilized to preheat the air used for drying the coal. The temperature of the circulating water leaving the condenser is usually about 49°C and can be used to produce an air stream at approximately 43°C, which is fed into a fluidized-bed coal dryer. Approximately a quarter of coal moisture is removed from lignite during drying. Its water content decreases from 38% to 29.8% and higher heating value improves by 14% from 14.4 MJ/kg to 16.4 MJ/kg. The moist air from the dryer is then discharged and the dried coal is fed back into the power generation process. Among other benefits, coal drying by waste heat reduces cooling tower make-up water requirements and also provides heat rate and emissions benefits. A variation of coal drying could be accomplished by both warm air passing through the dryer, and a flow of hot circulating cooling water, passing through a heat exchanger located in the dryer (see Fig. 11.7). A higher temperature of drying air can be achieved if hot flue gas from the boiler or extracted steam from the turbine cycle is used to supplement the thermal energy obtained from the circulating cooling water. Great River has been testing an in-situ 75 t/h prototype since January 2006. Design and installation of four commercial-scale demonstration dryers is currently underway.

The drying technique utilizing electromagnetic energy was developed by



11.7 Low-temperature lignite drying system.

© Woodhead Publishing Limited, 2010

CoalTek (USA) to reduce the moisture in low-rank coals prior to being burned. The process uses highly controlled electromagnetic, 'microwave' energy to reduce the moisture in low-rank coals. Unique, desired end-characteristics of the coal, including MJ/kg and sulphur content, can be programmed into the process to create a 'designed' coal that meets the specific needs of an individual generation facility or boiler. Processed coal can be an alternative to installing expensive scrubbers at plants needing to come into compliance with SO_2 emission limits. The first commercial processing facility was opened in Calvert City (KY, USA) in 2006 and began shipping its processed coal to industrial customers in the mid-west the same year. The plant's initial capacity of 120 000 t/year was expanded in 2008. The company anticipates substantial growth at other facilities in 2009 and beyond.

Fuels Management, Inc. (FMI) has developed a technology for the enhancement of low-rank coal by using established fluid-bed reactor hardware and patented technology to lower the moisture content, significantly increase the calorific value, and reduce mercury content. Coal is dried in a fluidized-bed reactor with oxidizing environment, which is a key element in promoting stability. The process operates at low temperature (315°C) and no outside source of heat is required as 6–8% of the feedstock coal is burned in the process. The finished product is stable with 0.5% moisture. A commercial demonstration plant has been running since 2009. This unit provides 20 000 t/year of product for test burns and commercial design optimization.

A pre-combustion refinement process for low-rank coal upgrading using heat and pressure has been developed by Evergreen Energy Inc. The resulting product, still a solid fuel, has a moisture content between 8 and 12% compared to approximately 30% in the raw feedstock, and is branded and sold as K-Fuel. This process improves the heat value by approximately 30%. With the K-Fuel process, raw coal enters a large vessel that subjects it to higher temperatures and pressures, much like a pressure cooker. Under these conditions the porous structure of coal collapses and the heated water is squeezed out, producing fuel with a much lower moisture content. At the same time, the heat and pressure force some of the coal's tar to its surface. This coats and seals the outside of the coal and helps prevent it from reabsorbing the lost moisture. The amount of energy used in the process to remove water is about half of what it would take to evaporate the same amount of water in a coal boiler during combustion. A 750 000 t/year K-Fuel processing plant has been built in Gillette (Wyoming, USA). The plant produces refined coal and ships it to customers for test burns as well as on a commercial basis.

© Woodhead Publishing Limited, 2010

11.5.2 Briquetting

Mechanized mining often increases the content of fines in the coal and the proportion of the size fractions suitable for industrial and domestic use decreases. Briquettes or pellets can provide a satisfactory substitute fuel, using the excess fine coal. Briquetting is a traditional form of coal upgrading for domestic use, however, its importance for industrial use is growing. Coal briquettes have been used in the past as smokeless fuels in countries such as Germany, the UK, and the USA on a considerable scale. Furthermore, briquettes can replace sized coal in industrial boilers and in the coal gas furnaces used in chemical production, machinery, and glass industries. Briquettes have also been used on a substantial scale in moving bed gasifiers, where the content of fine coal in coal has to be minimized.

Briquettes are produced by hot pressing from pre-dried coal. They consist of partially carbonized coal. During the briquetting process, some (or most) of the volatile matter is removed from the coal and the product burns smokelessly.

Whitehead (1997) summarized the advantages and disadvantages of various methods of agglomeration technology.

- Mixer agglomeration: this is the simplest and cheapest technique providing the weakest product, simple binders (e.g. water) can be used, conversion of dust to crumb-size product, possible application to condition coals for nearby use.
- Disk pelletizers (or drums): this is a simple and the next cheapest concept, producing relatively weak pellets with a diameter of 5–80 mm.
- Roll press: this is a relatively expensive method needing good binders, a uniform product size with an ovoid or pillow-shaped briquetter; it is the only method used in Western Europe to make smokeless briquettes for domestic use.
- Extrusion: this is a relatively expensive method, needing no binder, with typically a brick-shaped product, and problematic product strength; a traditional method for briquetting both peat and brown coal.

The choice of technology for a particular application depends on the nature of coal used and the required product characteristics, including its handling ability and strength. All the processes are coal-specific in application. Successful development depends both on extensive testing and on assessment work, including evaluation of representative coal properties over the following 10 or 15 years. Economic criteria like the differential between coal cost and product value or binder availability and cost have to be taken into account as well. Briquettes can be made from fine coal, which provides a very low-cost raw material, or from some low-rank coals. In

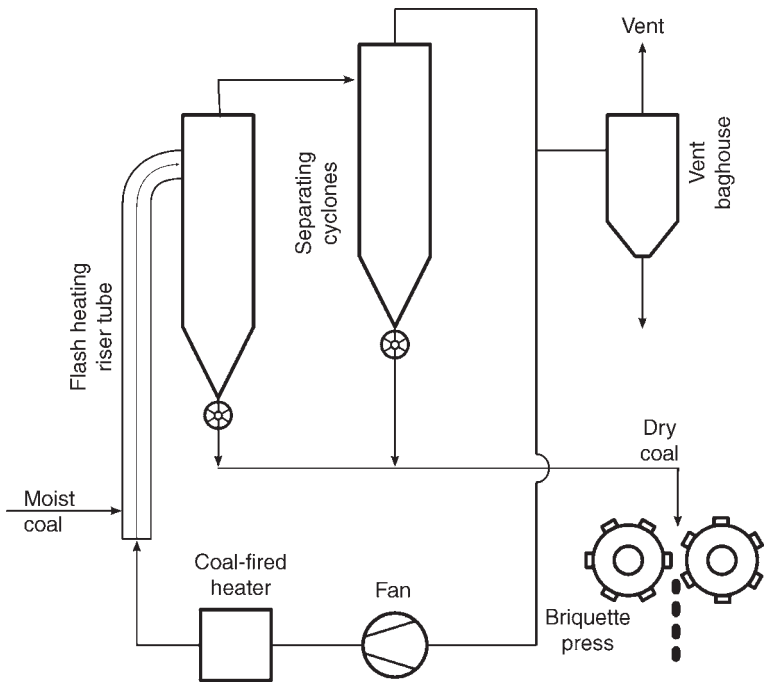
© Woodhead Publishing Limited, 2010

addition, the briquettes can be made with limestone as an additive for sulphur capture and reduction of SO_2 emission during combustion.

For briquetting, coal with very little moisture is required. If moist lignite is used, it must be dried to a water content of around 15%. In general, tubular steam dryers or flue gas dryers are used in briquetting plants. In contrast, pelletizing is possible for a fine coal containing up to 30% of water (Conkle and Raghavan, 1992).

Briquetted and pelletized coal is produced on a limited scale in various places, but large-scale applications have been limited because the processes are relatively expensive. In Australia, binderless briquettes are used in power stations to maintain combustion stability when the as-mined brown coal is of poor quality. In China, large quantities of briquettes are used both domestically and industrially, and production totals more than 50 Mt/year. So-called honeycomb briquettes are widely used.

For slightly larger-scale use, briquettes burn more efficiently, and the use of briquettes is likely to grow. A solution to larger-scale upgrading of low-energy black or brown coals is offered by White Energy Company, which is the exclusive worldwide license holder of the patented White Coal technology (WCT). The process (see Fig. 11.8) upgrades low-rank coals by reducing the moisture and agglomerating undersize coal into physically



11.8 Schematic diagram of WCT briquetting plant.

© Woodhead Publishing Limited, 2010

and chemically stable binderless briquettes that can be handled, transported, and utilized like normal coal. The process involves the crushing and drying of low-rank coals resulting in removal of the coal water content. Hot drying gases are produced through the separate combustion of a small proportion of the coal. Compaction then generates close bonding between the dried coal particles and eliminates nearly all voids. This forms high-density, higher-energy-content briquettes with very low permeability, which is a key factor in providing stability against spontaneous combustion. The briquetting process is a purely mechanical procedure involving material distribution, compaction, cooling, and storage. The product is in a form that can be handled, stored, and transported as conveniently and safely as normal coal. The process requires none of the binders that are normally used to briquette coal, which substantially reduces production costs. Binderless briquetting utilizes natural bonding mechanisms of coal. The ability to generate close bonding between the coal particles (i.e. the application of the compaction force in such a way as to cause the particles to come into intimate contact and establish bonding between them) makes the WCT process different from and more successful than past briquetting attempts.

The process has been developed to a commercially viable stage. It is capable of producing low moisture, physically and chemically stable briquettes from sub-bituminous coal at large scale and with attractive economics. The WCT product has an energy content 50–100% higher than the raw coal from which it is derived.

To date, over 20 000 t of coal have been upgraded in testing programs. A 90 000 t/annum WCT development plant was built in Australia and the process has proven to operate successfully. Coal samples from China, the USA, Australia, Indonesia, and South Africa have all been successfully upgraded. A fully featured demonstration plant has been in operation since the end of 2007. Further research and development around plant scale-up and design will be conducted, as well as work with different types of coals.

11.6 Utilization of low-rank coal in advanced power plants

In most cases, low-rank coals are utilized as received in PC or fluidized-bed boilers. High moisture content in low-rank coals results in fuel-handling problems, increases in mass rate (tonnage) of all substances including emissions, and it affects the efficiency of boiler and heat rates of a power plant. A low calorific value of the coals precludes long-distance transport because of high costs. Utilization of low-rank coal is therefore limited to a close region of the seam.

New benchmarks for lignite-fired power plants set two Neurath blocks F

© Woodhead Publishing Limited, 2010

and G with a gross capacity of 1100 MW referred to respectively as BoA 2 and 3 (Elsen and Fleischmann, 2008). The units use the BoA ('Braunkohlekraftwerk mit optimierter Anlagentechnik' in German) package of advanced optimised lignite technologies with significant improvements to the individual parts of the plant and process steps first employed at Niederaussem. High net efficiency of the power plant of over 43% (LHV) is ascribed to the steam conditions (600/605°C); the steam turbine technology; the nine-stage feed water preheating system; the maximization of waste heat recovery from flue gas and a minimization of auxiliary power needs. Raw lignite with a high moisture content (48–60%) is provided from the opencast mining sites of Garzweiler and Hambach. The lignite is dried using hot flue gases taken from the furnace. The WTA drying principle has not been utilized owing to lack of experience on a large-scale power plant (Smith, 2006). However, the WTA demonstration facility with capacity of 210 t/h has been built next to the Niederaussem BoA unit and commissioning has just begun in 2009. The facility is expected to demonstrate that the WTA system in continuous operation is both technically and economically viable. An overall increase of up to 2.5 percentage points on net thermal efficiency is expected from utilizing the WTA drying technique in future lignite-fired power plants (Stamatelopoulos, 2007). WTA technology is also being proposed as part of a major retrofit planned for the Hazelwood power plant in Australia (Rich *et al.*, 2007).

Upgrading brings a number of beneficial effects, reducing most of the problems concerning low-rank coal utilization. Washing results in reductions in the amounts of mineral matter present, including a proportion of trace elements and sulphur, although there may be a small increase in moisture content. Drying reduces the moisture content, and hence increases the heating value. Briquetting improves the combustion characteristics and facilitates the inclusion of additives, which will capture the sulphur present. All the processes contribute to the increase in heating value of the coal and improve the fuel consistency, resulting in more efficient and controllable combustion.

The effect of coal pre-drying on unit operation was demonstrated by a coal test burn at Coal Creek Unit 2 in October 2001 (Levy, 2005). The lignite was pre-dried by an outdoor stockpile coal-drying system. On average, the coal moisture was reduced by 6.1%, from 37.5 to 31.4%. Analysis of boiler efficiency and net unit heat rate showed that with pre-dried coal, the improvement in boiler efficiency was approximately 2.6%, and the improvement in net unit heat rate was 2.7 to 2.8%. The test data also showed the fuel flow rate was reduced by 10.8% and the flue gas flow rate was reduced by 4%. The combination of lower coal flow rate and better grindability contributed to reducing mill power consumption by approximately 17%. Fan power was reduced by 3.8% owing to lower air and flue

© Woodhead Publishing Limited, 2010

Table 11.1 Effect of utilization of dried lignite in Coal Creek power plant

Parameter	Units	Coal dryer out of service	Coal dryer in service	Change	Units of change
Gross power output	MW	590	589	NC	
Throttle steam temperature	°C	532	531	NC	
Reheat steam temperature	°C	539	539	NC	
SHT spray flow	tonne/h	23.6	20.9	−2.7	tonne/h
Input coal moisture	TM%	36.8	36.8		
Dried coal moisture	TM%		28.6		
Dried coal	% of total	0	14.62		
Total coal flow rate	tonne/h	441	432	−2.02	%
Stack flow rate	m^3/h	2.763×10^6	2.737×10^6	−0.96	%
Specific pulverizer work	J/kg	9.458	9.017	−4.65	%
Total pulverizer power	kW	4.206	4.057	−3.53	%
NO_x mass emissions	kg/h	667	610	−8.52	%
SO_x mass emissions	kg/h	1675	1641	−2.00	%
APH gas exit temperature	°C	188	183	−5	°C
Stack temperature	°C	84	82	−2	°C

gas flow rates. The average reduction in total auxiliary power was approximately 3.8%.

Sarunac (2006) evaluated the effect of utilization of dried lignite in the Coal Creek lignite-fired unit with capacity of 600 MW. Results are summarized in Table 11.1. The benefits resulting from an application of coal drying fell into seven main categories:

- reduced fuel costs;
- reduced ash disposal costs;
- avoided costs of emissions control;
- reduced station service power for the forced draft and induced draft fans and for coal pulverizing (but, in some cases, the power requirements for coal drying could increase station service power);
- water savings;
- reduced mill maintenance costs;
- reduced lost generation due to mill outages.

11.7 Future trends in coal upgrading

Low-rank coals are one of the largest energy resources for power and heat generation in the USA, Russia, Central Europe, and much of the Pacific Rim. Coal-based generation is expected to grow by 25%, supplying 46% of a larger total electricity demand by 2020. Recently, a number of advanced methods for coal upgrading have been developed and published. Some of them are designed for a wide range of applications including coal drying before combustion or briquetting; other ones are suitable only for

© Woodhead Publishing Limited, 2010

gasification or liquefaction processes. New promising methods of low-rank coal upgrading are introduced in the following examples.

A low-rank coal upgrading technology adapting a slurry dewatering technology for brown coal liquefaction (Japan Coal Energy Centre, 2009) is under development in Japan: it is known as the UBC process. This process consists of three stages: slurry preparation/dewatering, solid–liquid separation/solvent recovery, and briquetting. At the first stage, moist low-rank coal is, after pulverizing, mixed with recycled oil then laced with heavy oil (such as asphalt), and heated in a shell-and-tube-type evaporator. Vapour recovered from the coal moisture is pressurized and sent to the shell side of the evaporator to utilize the waste heat in the dewatering stage. During that time, laced heavy oil is effectively adsorbed on to the porous surface of the coal, thus preventing spontaneous combustion. At the stage of solid–liquid separation, the solvent is recovered from the dewatered slurry by the decanter; the solvent remaining in the pores of upgraded coal is also recovered by the steam tubular dryer. Solvent separated during both processes is recycled to the slurry preparation tank. Upgraded coal obtained from the UBC process is still in a powdery state, so briquetting is a convenient preparation for transportation over longer distances. A demonstration plant with a capacity of 5 t/day (raw coal-base) has been built in Cirebon of the Java Barat province in Indonesia and promoters hope for early commercialization.

The Nu-Fuel process developed by Confluence Coal Combustion LLC (Man, 2009) is another means of upgrading low-rank coals. The Nu-Fuel process involves mild thermal treatment, using heat applied externally to a retort. This treatment reduces the moisture content of the coal to any desired level and also converts the complex hydrocarbon molecules in the raw fuel into simpler compounds capable of rapid combustion. The retort is maintained at about 215°C, a temperature well below the point at which pyrolysis of the coal occurs. The retort contents are subjected to a controlled atmosphere consisting of combustion flue gas that flows countercurrent to the coal being treated. Carbon dioxide (CO_2) contained in the blanketing gas is absorbed into the pores of the treated coal, replacing the water driven off. Carbon-to-carbon bonding also takes place on the surface of the coal. The result is that reabsorption of moisture is essentially avoided. The treated fuels have many other improved combustion characteristics, including extremely rapid combustion in a boiler, easy ignition, and stable flames at very low temperatures. The increased reactivity of Nu-Fuel products also makes them potentially superior feedstocks for gasification. The Nu-Fuel process has been thoroughly investigated in bench-scale tests and in a 1 t/day pilot plant. The next phase is to demonstrate the process on a commercial scale.

The future utilization of low-rank coal faces both challenges and

© Woodhead Publishing Limited, 2010

opportunities, including preparation and upgrading, more efficient combustion, and gasification technologies. Efficiency improvements should bring the economic benefits mentioned above and should also be accompanied by a reduction in CO_2 emissions, and possibly by other parallel effects such as a reduction in the amount of NO_x and SO_2 formed.

11.8 Sources of further information

The following books dealing with the low-rank coal utilization and upgrading are recommended:

- Gordon Couch: *Coal upgrading to reduce CO_2 emissions*. CCC/67, London, 2002. The report includes a review of the methods available, and a country by country review of the potential for additional upgrading. The impact of coal upgrading on the thermal efficiency of coal use is discussed, and the countries where there could be the greatest impact are identified.
- Heinz Termuehlen and Werner Emsperger: *Clean and efficient coal-fired power plants*, ASME Press, NY, 2003. This book presents the evolution toward advanced coal-fired power plants. Advanced power plants with an efficiency level of 45% are today commercially available and even more efficient plants are in their development phase.
- Tadeusz Kundra and Arun S. Mujumdar: *Advanced drying technologies*, Marcel Dekker Inc., NY, 2002. The book offers classification and selection criteria for new and advanced drying systems and compares conventional dryers to novel technologies, including modified fluid bed, superheated steam, and impinging stream dryers.

Information about recent technologies and research projects is available on the following web sites:

- www.fe.doe.gov/fred/feprograms.jsp?prog = Clean + Coal + Technology – pages of the Department of Energy's Office of Fossil Energy. The Department typically manages more than 500 active research and development projects spanning a wide range of coal, petroleum, and natural gas topics.
- www.nextgenenergy.org/ – pages of The NextGen Energy Council (NextGen), a non-profit organization comprising a wide variety of energy and technology leaders, state legislators and energy industry experts.
- http://www.lignite.com/ – pages of the Lignite Energy Council, which maintains a viable lignite coal industry and enhances development of US lignite coal resources for use in generating electricity, synthetic natural gas, and valuable by-products.

© Woodhead Publishing Limited, 2010

- http://www.iea-coal.org.uk/site/ieacoal/home – pages of IEA Clean Coal Centre, which provides unbiased information on the sustainable use of coal worldwide.
- www.nedo.go.jp/sekitan/cct/ – contains a survey of clean coal technologies in Japan.
- http://www.power.alstom.com/home/ – pages of Alstom, a global leader in the world of power generation setting the benchmark for innovative and environmentally friendly technologies.
- http://www.rwe.com/web/cms/en/8/rwe/ – pages of RWE, one of Europe's largest power companies involving the most recent technologies for lignite utilization.
- www.whiteenergyco.com – pages of White Energy Company Limited, a public company based in Sydney and focused on the commercialization of coal-upgrading technologies.

11.9 Acknowledgement

This chapter was prepared with the support of the Research Centre 1M0605 financed by the Ministry of Education, Youth and Sports (MEYS) of the Czech Republic.

11.10 References

Chen Q R and Yang Y (1997), 'Current situation and development of dry beneficiation of coal technology', Proceedings of the 14th annual Pittsburgh coal conference: *Clean coal technology and coal utilisation*, Pittsburgh, 23–27 September 1997, University of Pittsburgh.

Chun-Zhu L (2004), *Advances in the science of Victorian brown coal*, Elsevier.

Conkle H N and Raghavan J K (1992), Reconstitution of fine coal, *Coal Preparation*, 11(1–2), 67–76.

Couch G R (1991), *Advanced coal cleaning technology*, IEACR/44, London, IEA Coal Research.

Couch G R (2002), *Coal upgrading to reduce CO_2 emissions*, London, IEA Clean Coal Centre.

Dlouhy T and Kolovratnik M (2004), Influence of coal composition on boiler efficiency (in Czech), Proceedings of international workshop on *Combustion and environment 2004*, Ostrava, 15–16 November, 2004, TU Ostrava, Czech Republic.

Dlouhy T, Kolovratnik M and Hrdlicka F (2007), Design of new Czech brown coal fired power plants, Proceeding of 32nd international technical conference on *Coal utilization and fuel systems*, Clearwater, FL, 10–15 June 2007, Coal Technology Association.

Elsen R and Fleischmann M (2008), 'Neurath F and G set new benchmarks', *Modern Power Systems*, June 2008, 23–30.

© Woodhead Publishing Limited, 2010

Elsen R (1999), 'Wirkunsgradsteigerung durch effiziente Braunkohletrocknung', *BWK*, 51 (5/6), 78–84.

Elsen R, Blumenthal U, Götte Ch, Kamm J and Von Kossak T (2001), 'Palnung und Bau der Pilot-Trocknungsanlage Nederaussem', *VGB Kraftwerkstechnik*, 81 (6), 68–72.

Gaffert G A (1950), *Steam power stations*, Shangiai, Chiao Dah Book Service.

Hill J O, Ma S and Heng S (1989), 'Thermal analysis of Australian coals', *Journal of Thermal Analysis*, 35, 2009–2024.

Japan Coal Energy Centre (2009), 'Low-rank coal upgrading technology (UBC process)', Japan Coal Energy Center, the Institute of Applied Energy, available from: http://www.nedo.go.jp/sekitan/cct/eng_pdf/2_3d2.pdf (accessed 30 January 2009).

Klutz H J, Klöcker K J and Lambertz J (1996), 'Das WTA – Verfahren als Vortrocknungsstufe für moderne Kraftwerkskonzepte auf Basis Braunkohle', *VGB Kraftwerkstechnik*, 76(3), 224–229.

Levy E (2005), Use of coal drying to reduce water consumed in pulverized coal power plants, Lehigh University Energy Research Center, available from: http://www.osti.gov/bridge/servlets/purl/862095-9GniWa/862095.pdf (accessed 12 March 2009).

Man A N, 'Upgrading coals using the NU-Fuel process', Confluence Coal Combustion, Pittsburgh, available from: http://confluencecoal.com/resources/Microsoft_Word__nu_fuel_paper_0205.pdf (accessed 2 February 2009).

Rich G, Hayes B and Heinz G (2007), 'Hazelwood 2030', *Modern Power Systems*, December 2007, 22–29.

Sarunac N, Bullinger C and Ness M (2006), 'Coal Creek prototype fluidized bed coal dryer', Proceeding of 31st international technical conference on *Coal utilization and fuel systems*, Coal Technology Association, Clearwater, FL, 21–25 May 2006.

Smith D (2006), 'RWE to built BoA 2 and 3 without WTA', *Modern Power Systems*, April 2006, 11–15.

Stamatelopoulos G N (2007), 'WTA offers big efficiency gain', *Modern Power Systems*, December 2007, 17–21.

Whitehead J (1997), 'Briquetting coal to enhance value', Conference on *Additional value of coal*, Rotterdam, 25–26 June 1997, London, CoalTrans.

© Woodhead Publishing Limited, 2010

12

Biomass resources, fuel preparation and utilization for improving the fuel flexibility of advanced power plants

L. ROSENDAHL, Aalborg University, Denmark

Abstract: This chapter addresses aspects of using biomass rather than biomass fuels. The concept of CO_2 neutrality is discussed, followed by classification of biomasses relevant for power plant use. A brief discussion of conversion technologies is given, as it applies to choice of fuels, followed by issues of biomass resource availability. The chapter also contains chemical and physical characteristics of a variety of biomasses and biomass mixes, as well as a discussion of pretreatment and fuel preparation technologies.

Key words: biomass, fuel, CO_2 neutral, chemical composition, physical characteristics, classification.

12.1 Introduction

In a carbon-constrained world, it is necessary to consider carefully the advantages and disadvantages of using fossil fuels and subsequently remove carbon dioxide (CO_2) from the flue gasses, versus those of replacing all or some of the fossil fuel with biomass, thus negating the necessity for such removal facilities. In the context of power plants, the most cost-efficient approach to this in the short term (probably some 10–15 years, considering the life expectancy of the majority of the existing world's fossil fuel power plants) is by implementation of some measure of co-firing on existing fossil fuel power plants, where typically solid biomass and fossil fuel are co-combusted in the plant. Several such installations currently exist, mainly in Northern Europe, the USA and in Australia (IEA, 2007a). In the medium to long term, the concept of multi-fuel plants is likely to become dominant, where the firing equipment is designed for flexibility, such that the choice of

© Woodhead Publishing Limited, 2010

fuel, within limits, can be adapted to availability, cost and other relevant factors.

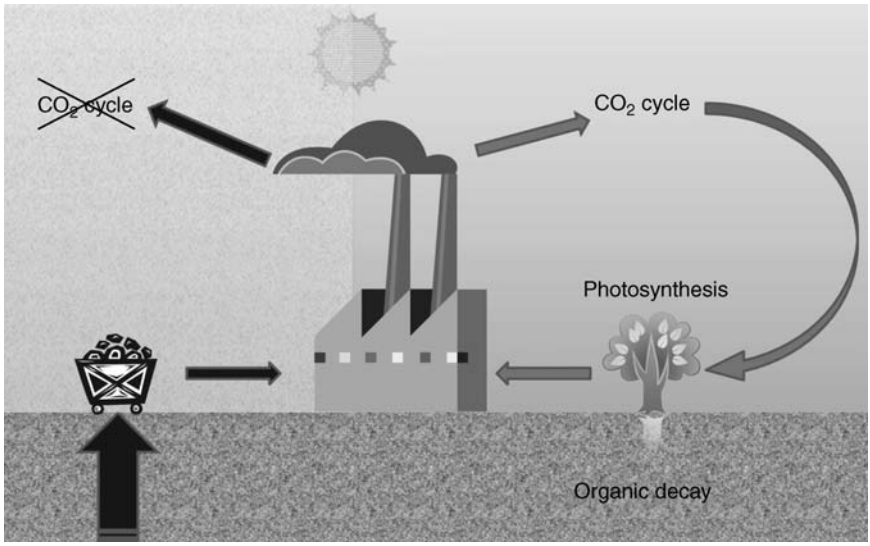
Using biomass as a fuel to produce heat is not a new idea brought about in response to concerns about CO_2 and green house gasses in the latter decades of the 20th century. Indeed, long before mankind realized that the Earth harboured enormous energy resources in terms of fossil material in the form of coal, oil and gas and created an energy system heavily reliant on these, biomass, mainly wood and grasses, was the fuel of choice.

However, in the context of the 21st century, using biomass for energy purposes is as far removed from those early uses as can possibly be imagined. Granted, the process of combustion or gasification is the same, but the logistics, the preparation and the energy intensity of the process is on a completely different scale. Our understanding of these processes, and indeed other processes involving the conversion of biomass, as well as the consequences of utilizing these processes, has also increased to a level where we are able to minimize the environmental impact at the same time as maximizing the energy output.

The renewed interest in biomass as a primary energy source stems from two very different concerns. One is, of course, climate concerns, and the scientific consensus that there exists a link between releasing increasing amounts of fossil carbon into the atmosphere and global warming. The other, more political, concern, is the regionality of the world's energy reserves in terms of primarily oil and gas. These are in the vast majority located in regions of the world which might be characterized as politically unstable, and there is a global desire to lessen national dependencies on these fuels and rather build up an energy system that relies on local resources, such as wind, solar and biomass. Leaving aside the political aspects for the purpose of this chapter, and focusing on biomass, it is the concept of local availability combined with potential CO_2 neutrality that drives the implementation of biomass in the energy sector. CO_2 neutrality, indicated in Fig. 12.1, refers to the balance between the CO_2 absorbed by the biomass through photosynthesis, as it grows, and the CO_2 emitted as it is utilized in some conversion system. In an ideal world, these are identical, and consequently there is no net increase of the carbon content of the atmosphere, contrary to fossil-based CO_2, which represents a net increase as the carbon source has been 'out of circulation' for millions of years. True CO_2 neutrality is only achieved, however, if the entire process of cultivation, harvesting, processing and transportation is based on renewables, and through life cycle analysis (LCA) it becomes evident that most biomass utilization is not truly CO_2 neutral. In general, however, the displacement of fossil CO_2 is orders of magnitude greater than that emitted in order to bring the biomass fuel to the power station.

Setting aside the conversion process, there is also the consideration that

© Woodhead Publishing Limited, 2010



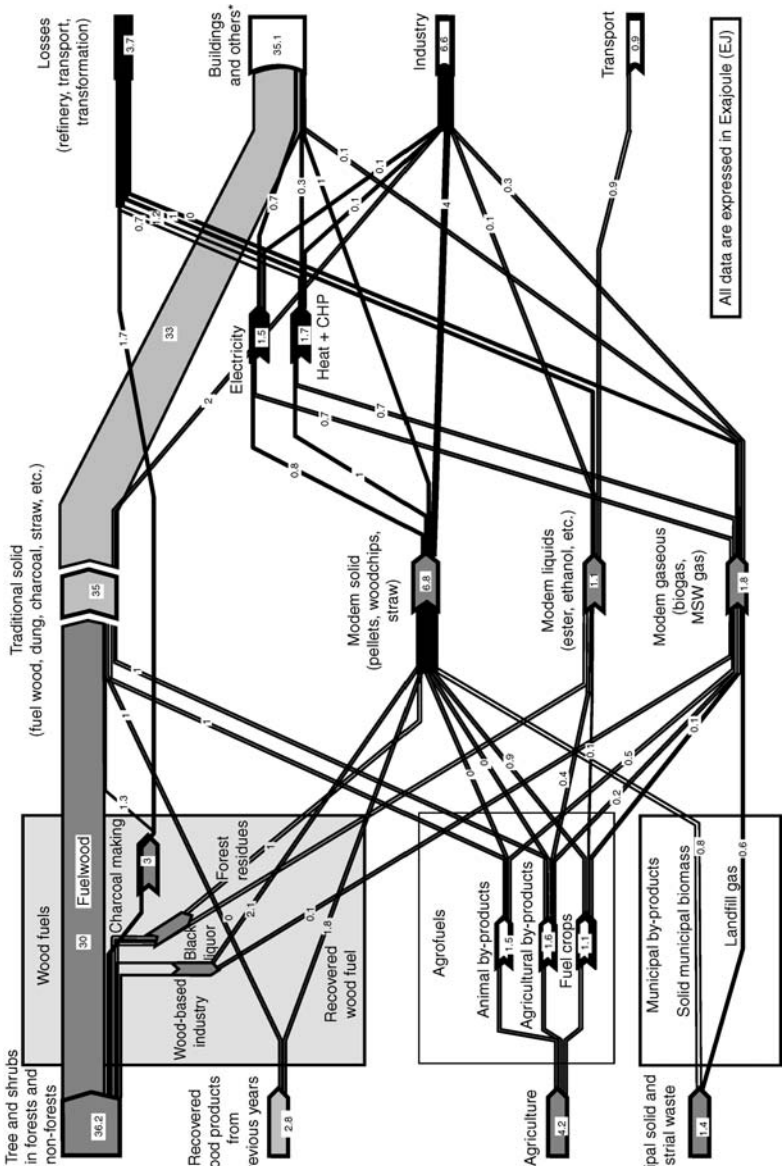
12.1 Simple sketch of atmospheric CO_2 increase due to use of fossil fuels (left) and CO_2 neutral use of biomass (right).

biomass is the main source of food, fodder and fibre. Given the projected growth of the world population it is unlikely that energy will always be the number one priority in terms of available hectares for energy crops.

Biomass can be classified in several ways, according to growth cycle, fibrous structure, aquatic or terrestrial, and primary energy yield. Biomasses can also be classified in a more historical setting based on use in the energy sector, as traditional biomasses and new biomasses. To the former category belong the 'pure' biomasses such as lightly prepared wood, straw, grasses, and to the latter belong the different organic waste streams from agricultural, industrial and domestic biomass use. As can be seen in Fig. 12.2, in 2004 by far the main biomass use came from the traditional biomasses. It can also be seen that this mostly went to heating, and only a small fraction of biomasses went through a pretreatment process allowing it to be used for electricity generation. However, this picture is undergoing tremendous change, with more and more biomass undergoing some sort of pretreatment, allowing it to be transported to and used in either a modern electricity-generating power station, as mono-fuel or as a co-firing fuel together with a fossil fuel, or for production of a liquid biofuel. Furthermore, it is certain that the two smaller contributors, agriculture and municipal solid and industrial waste, will claim a significant part of the growth of the market for biomass for energy, mainly through exploitation of a greater number of waste streams than is currently the case.

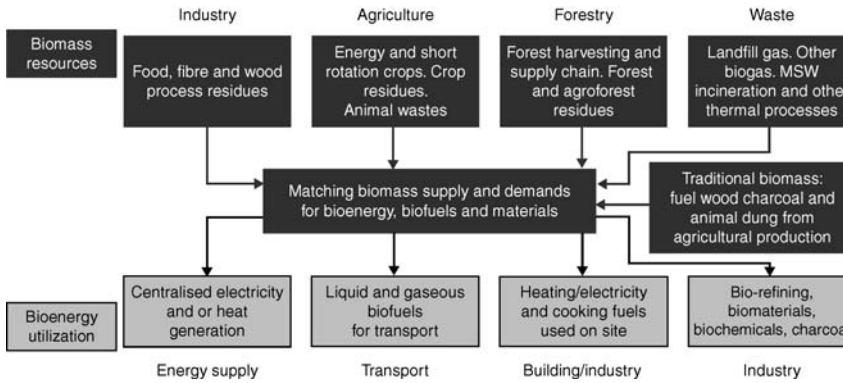
This is indicated in Fig. 12.3, where a wide range of biomasses supplement

© Woodhead Publishing Limited, 2010



12.2 World biomass energy flows (EJ/year) in 2004. For comparison, total primary energy amounted to approximately 470EJ in 2004 (IPCC, 2007).

© Woodhead Publishing Limited, 2010



12.3 Biomass conversion paths from resource to product (Sims, 2007).

the traditional supplies. In the future, selecting the right combination of biomass and conversion technology will also include the product step, where energy in different forms will have to compete with other utilizations of biomass products. The challenges facing the use of biomass in a resource-constrained and CO_2 conscious world can be summarized as follows:

- scarcity of traditional pure biomasses and land for energy purposes;
- identifying new biomasses, including functional biomass mixes;
- optimizing fuel preparation techniques for minimum energy use, maximum homogeneity and transportability, as well as compliance with existing fuel handling equipment at power plants;
- fuel flexibility at the individual plant;
- developing processes which allow for extraction of various nutrients (e.g. phosphorous) to be recycled;
- developing combinations of processes which allow for extraction of various valuable by-products.

These issues will be addressed in the following sections.

12.2 Biomass types and conversion technologies

As mentioned previously, there are many ways to classify biomasses. One often used classification is the four-type classification (McKendry, 2002):

- woody plants;
- herbaceous and grassy;
- aquatic;
- manures.

Woody biomasses are characterized by plants having stems that are covered with bark, and which survive over several years. The stems consist mainly of

© Woodhead Publishing Limited, 2010

lignin and cellulose, and have a vascular system to transport water and nutrients from the roots to the rest of the plant. Woody biomass is available in different forms, as chips, sawdust, pellets, forestry residue and logs. As such, wood can be a by-product or a dedicated energy crop, typically short rotation coppice (SRC) such as willow. Herbaceous and grassy biomasses are plants that have stems and leaves, but die at the end of the growing season. Annual herbaceous plants die completely, and new plants grow from seeds, whereas biennial (for example carrots and parsnip) and perennial (for example grasses) plants leave a part of the plant surviving underground, from which a new stem grows at the beginning of the next growing season. Aquatic biomasses are, for example, algae (Ross *et al.*, 2008) and seaweed, and are naturally characterized by a high degree of moisture. Finally, manure is a by-product primarily from cattle and pig farming.

To a more broad definition of biomass can also be added the following categories:

- municipal solid waste (MSW);
- sewage sludge;
- animal fats.

MSW is in many countries defined as a biomass, and is utilized for heat and power production to varying degrees in different countries, or is disposed of by land filling. One result of landfills is landfill gas, which is a methane-dominated gas emitted through the decomposition of the organic fraction of MSW, and this also represents a biomass resource if captured. An important subcategory of MSW is refuse-derived fuels (RDF), which are based on paper and plastic residues, primarily (Petrou and Pappis, 2009). Sewage sludge is the result of waste water treatment plants, and contains organic material from households, industries and rain water. Animal fats are by-products from meat processing.

12.2.1 Classification of conversion technologies

Biomass conversion technologies are normally classified as 1st, 2nd, or 3rd generation, according to the type of feedstock. First generation technologies take biomass feedstock which could otherwise be used as food, that is primary biomasses. Examples are use of starch and sugars from wheat or maize to produce bioethanol or other bio-alcohols, or rape seeds which are pressed to produce oils or bio-diesel. Use of grains or seeds in direct thermal conversion would also represent 1st generation use. These biomasses could also be used in human or animal food chains, and energy production thus takes place at the potential cost of influencing food supplies and prices.

Second generation technologies, on the other hand, use the fractions of biomass which are not used in either human or animal foodstuffs. Examples

© Woodhead Publishing Limited, 2010

of these are lignocellulosic biomass (straw, waste wood), animal fats resulting from meat processing, MSW and sewage sludge, thus secondary biomass that has already been utilized for a purpose. Typically, for a technology to be able to utilize 2nd generation biomass feedstock, a higher degree of pretreatment is necessary in order to access and process the organic material. This is particularly true for the use of the lignocellulosic biomass for bio-alcohol production, as the biomass primarily consists of lignocellulose, where the carbohydrates are tightly bound to the lignin (Lin and Tanaka, 2006).

Third generation technologies are those utilizing algae for energy production, either directly or by conversion to a liquid biofuel. Algae have spurred considerable interest owing to their high growth rates, high sugar or oil contents, and the fact that they represent a completely new resource, which is not in competition with food production for land. However, whereas 1st generation technologies are already in commercial operation, and 2nd generation technologies either in demonstration or close to commercialization at this time, 3rd generation technologies are still in the future.

It is important to realize that a technology can be either 1st, 2nd, or 3rd generation, depending on the feed stock, but that a conversion technology will often be optimized toward a specific biomass. This also means that the biomass classification and the technology classification overlap to some extent, as wood and herbaceous biomass as well as animal fats can consist of primary biomasses as well as residual biomasses.

For energy purposes, biomasses are also often classified according to their water content, as this is generally decisive in terms of the conversion technology chosen to process the biomass. Thus, high-moisture biomasses such as algae, manure or sewage sludge would not be suited for processes such as gasification or combustion without prior drying, but instead would be appropriate in technologies where high water content is an advantage.

12.2.2 Available biomass resources

For large-scale utilization of biomass it is important to estimate the availability of biomass resources. This is a formidable task, as several factors – technical, political, climatical, demographical – all influence the result. Various estimates and forecasts exist, both on the use of renewable energy based on biomass and on the distribution of this on different types of biomasses. For example, IEA (2007b) indicate a ten-fold increase in biofuels and at least a quadrupling of electricity generation based on biomass in 2030. Parikka (2004) provides data on potential compared to land use in 2004, and shows that for most regions of the world (except Asia), only a small fraction of the potential is actually utilized (see Table 12.1).

© Woodhead Publishing Limited, 2010

Table 12.1 Biomass energy potentials and usage in 2004 (Parrika 2004)

Biomass potential	EJ/year
Woody biomass	41.6
Energy crops	37.4
Straw	17.2
Other	7.6
Total potential	103.8
Usage in 2004	39.7

Other estimates (e.g. Hoogwijk *et al.*, 2003), factor in radically changed land use, where additional acreage is utilized. This of course indicates much higher potentials of various biomasses with consideration of land use, food production and population increase. For example, of the order of 1000 EJ/year could be based on energy crops if land use was to be optimized. It is clear, as the authors also state, that such numbers are associated with considerable uncertainty.

12.2.3 Residual biomass resources

As mentioned initially, residual (or waste) resources represent a significant potential. The benefits are at least two-fold: not only does the residual resource serve as feedstock for products much in demand such as electricity and liquid fuels, but using this resource rather than primary resources also serves to mitigate the problem of handling society's waste streams. Finding good use for some of these can be extremely difficult, and often they end up being landfilled or deposited in other ways. In some situations the amounts of residuals produced serve as a limiting factor on other activities, as is the case for manure and animal farming.

To date, there have been some studies on the use of residual resources for energy. In Denmark, for example, it is estimated that there are approximately 400 000 tons of dry matter available annually in the form of residual biomass from industrial processes (Nikolaisen, 2009), comprising potato waste, beet waste, pea pods and plants, coffee waste, cigar and cigarette waste, olive stones, shea nut waste, mash from beer brewing, grain screen waste, carrageenan and pectin. Characteristic of these residues are that they often have a high water content and thus require drying before being used as power plant fuels. However, they are a cheap resource, and the chemical diversity of these residues can be turned into an advantage by appropriate mixing. Furthermore, although this study is based on Danish conditions, the types of industrial processes producing these residues are internationally abundant, and thus the same types of residues are likely to be available in most areas of the world.

© Woodhead Publishing Limited, 2010

12.3 Chemical constituents in biomass fuels

Before any biomass can be considered for use as a fuel in large-scale primary energy production, the chemical properties of the biomass must be scrutinized. Not only should there be sufficient carbon and hydrogen for a significant energy yield during the selected conversion process, but also the mineral composition and inorganics such as alkali metals are important, as they impact on operation of the plant using a particular type of fuel.

In the following, typical compositions of different biomasses are given. For the primary biomasses such as woody and herbaceous types, there are several factors influencing the content of specific compounds and materials, including soil conditions, fertilization strategy and amount of precipitation. Furthermore, for herbaceous biomasses, leaching due to rainfall after harvesting can drastically reduce the content of some chemical species, mainly chlorine and potassium. This is often indicated by the straw turning grey.

In general, it is the herbaceous biomasses, as well as the residual biomasses such as MSW, sludge and manure, that pose problems in terms of composition, rather than the woody biomasses – with the exception of bark. The European Committee for Standardization has published guidelines for maximum contents of nitrogen: <0.6% DM (dry matter); chlorine: <0.1% DM; and sulphur: <0.1% DM (Obernberger *et al.*, 2006). These guidelines indicate maximum levels for unproblematic firing of biomasses in combustion systems, and are based on operational issues as well as emission levels.

The contents of alkali metals in biomasses pose significant problems with pulverized fuel (PF) firing in existing power plants, as the combination of increased alkali contents and lower ash softening temperatures gives rise to potential slagging and fouling problems, as well as possible corrosion of heat transfer tubes. There are techniques directed at mitigating this, which are discussed later in this chapter.

Also in other conversion technologies these properties of biomasses can be considered negative, and a significant part of the technology design is dedicated to extracting the components which are considered harmful. Furthermore, a growing concern regarding the recyclability of nutrients is beginning to manifest itself. This has two major drivers. One is the possibility of reducing the need for artificial fertilizers (NPK), the production of which is a very energy-intensive chemical process, and the other is the realization that nutrients, especially phosphorus, are a limited resource.

© Woodhead Publishing Limited, 2010

Table 12.2 Composition, heating values and ash properties of selected woody biomasses (DM: dry matter; DAF: dry ash free; LHV: lower heating value; T_soft: softening temperature; T_hemi: hemisphere temperature)

	Kaltschmitt and Hartmann (2001)			Obernberger *et al.* (2006)			Serup *et al.* (2002)				
Biomass	Spruce w/bark	Beech w/bark	Willow w/bark	Willow w/bark	Coniferous w/bark	Deciduous w/bark	Spruce	Beech	Pine	Avg. wood (calc.)	Std. dev. (%)
C % DAF	50.10	48.14	48.06	49.00	54.00	55.00	50.90	49.30	51.00	50.61	6.00
H	6.34	6.23	6.22	6.20	6.10	6.10	5.80	5.80	6.10	6.10	1.48
O	43.46	45.43	45.20	44.00	40.00	40.00	41.30	43.90	42.30	42.84	5.71
N	0.131	0.221	0.551	0.500	0.500	0.300	0.39	0.22	0.10	0.32	53.66
S	0.015	0.015	0.046	0.050	0.100	0.100	0.06	0.04	0.02	0.05	77.31
Si % DM	–	–	–	–	0.200	1.000	–	–	–	–	–
K	0.131	0.151	0.265	0.300	0.200	0.200	–	–	–	0.182	35.65
Ca	0.704	0.291	0.694	0.500	0.500	1.500	–	–	–	0.563	74.78
Mg	0.080	0.040	0.051	0.050	0.100	0.050	–	–	–	0.057	40.37
P	0.030	0.040	0.092	0.080	0.040	0.040	–	–	–	0.054	47.20
Cl % DM	0.005	0.006	0.004	0.030	0.020	0.020	0.030	0.010	0.01	0.015	71.36
Volatiles DM	82.90	84.00	80.30	–	–	–	80.00	83.80	81.80	82.13	2.31
Ash DM	0.60	0.50	2.00	2.00	4.00	5.00	1.50	0.70	0.50	1.87	97.24
LHV DM	18.80	18.40	18.40	–	–	–	19.70	18.70	19.40	18.90	1.22
T_soft (C)	1426	–	1283	–	–	–	–	–	–	–	–
T_hemi (C)	1600	–	–	–	–	–	–	–	–	–	–

12.3.1 Woody biomasses

Data for woody biomasses are given in Table 12.2. The two last columns represent an average and standard deviation based on the data reported in the table, and should be considered as a guideline only in terms of the fuel properties.

12.3.2 Herbaceous biomasses

Data for herbaceous biomasses are given in Tables 12.3 and 12.4. The two last columns in each table represent an average and standard deviation based on the data reported in the table, and should be considered as a guideline only in terms of the fuel properties.

12.3.3 MSW

Data for MSW are given in Table 12.5. Due to the different nature of MSW compared to the previous biomasses, the data in the tables differ from those.

© Woodhead Publishing Limited, 2010

Table 12.3 Herbaceous biomasses: agricultural straws (DM: dry matter; DAF: dry ash free; AR: as received; LHV: lower heating value; T_soft: softening temperature; T_hemi: hemisphere temperature)

	Kaltschmitt and Hartmann (2001)					Obernberg *et al.* (2006)	Nikolaisen *et al.* (1998)			
Biomass	Rye	Wheat	Triticale	Corn	Hemp	Straw mix (wheat, rye, barley)	Wheat (grey)	Wheat (yellow)	Avg. straw (calc.)	Std. dev. (%)
C % DAF	48.95	48.36	46.65	48.98	48.42	49	43.00	42.00	48.39	1.86
H	6.30	6.15	6.27	5.68	6.20	6.3	5.20	5.00	6.15	3.87
O	44.22	44.96	46.55	44.69	44.64	43	38.00	37.00	44.68	2.57
N	0.58	0.51	0.45	0.70	0.78	0.5	0.41	0.35	0.58	21.87
S	0.09	0.09	0.06	0.13	0.11	0.1	0.13	0.16	0.09	24.09
Si % DM	–	–	–	–	–	1	–	–	–	–
K	1.76	1.07	1.12	–	1.62	1	–	–	1.09	32.04
Ca	0.38	0.33	0.33	–	1.41	0.400	–	–	0.47	99.14
Mg	0.06	0.11	0.05	–	0.21	0.07	–	–	0.08	76.99
P	0.16	0.11	0.09	–	0.26	0.1	–	–	0.12	61.26
Cl % DM	0.40	0.19	0.27	0.35	0.20	0.4	0.20	0.75	0.30	31.62
Water	–	–	–	–	–	–	10–20	10–20	–	–
Volatiles DM	76.4	77.00	75.20	76.80	81.40	–	>70	>70	77.36	3.06
Ash DM	4.8	5.70	5.90	6.70	4.80	5.00	3.00	4.00	5.48	13.81
LHV DM	17.4	17.20	17.10	17.70	17.00	–	–	–	17.28	1.61
LHV DAF	–	–	–	–	–	–	18.7	18.2	18.45	–
LHV AR	–	–	–	–	–	–	15	14.4	14.7	–
T_soft (C)	1002	998	911	1050	1336	–	950–1100	800–1000	–	–
T_hemi (C)	1147	1246	1125	1120	1420	–	–	–	–	–

Table 12.4 Herbaceous biomasses: grasses (DM: dry matter: DAF: dry ash free; AR: as received; LHV: lower heating value; T_soft: softening temperature; T_hemi: hemisphere temperature)

	Kaltschmitt and Hartmann (2001)			Obernberger *et al.* (2006)		
Biomass	Miscanthus	Tall fescue	Rye grass	Miscanthus	Avg. grass (calc.)	Std. dev. (%)
C % DAF	49.43	45.25	50.55	49	48.56	5.76
H	6.45	6.89	6.14	6.4	6.47	5.78
O	43.39	46.99	41.78	44	44.04	6.07
N	0.76	0.95	1.47	0.7	0.97	37.86
S	0.16	0.15	–	0.2	0.13	1.71
K	0.75	2.12	–	0.7	0.89	108.64
Ca	0.17	0.42	–	0.2	0.20	90.02
Mg	0.06	0.19	–	0.06	0.08	113.20
P	0.07	0.19	–	0.07	0.08	97.21
Cl % DM	0.22	0.50	–	0.2	0.23	86.08
Volatiles DM	77.60	72.00	74.80	–	74.80	3.74
Volatiles AR	–	–	–	–	0.00	–
Ash DM	3.90	8.50	8.80	4	6.30	43.12
Ash AR	–	–	–	–	0.00	–
LHV DM	17.60	16.40	16.50	–	16.83	3.96
T_soft (C)	973	869	–	–	–	–
T_hemi (C)	1097	1197	–	–	–	–

© Woodhead Publishing Limited, 2010

Table 12.5 Municipal solid waste composition based on data from five Danish cities (Hansen *et al.*, 2007), average values (geographically and periodically) (DM: dry matter; EDOM: enzyme degradable organic matter; LHV: lower heating value)

	Based on DM
Ash (%)	11.8
Fat (%)	13.9
Protein (%)	14.9
Fibres (%)	18.6
EDOM(%)	78.8
K (%)	0.9
P (%)	0.4
N (%)	2.5
C (%)	48.0
H (%)	7.1
S (%)	0.2
Cl (%)	0.6
LHV (MJ)	20.1
Plastic (%)	6.0
Other (%)	0.6

Table 12.6 Residual biomasses, all data as received (EFB: empty fruit bunch (Nikolaisen *et al.*, 2005)

Biomass	Pectin	Grain screening waste	Mash	EFB	Shea chips	Carrageenan	Oliven	Cigar waste	Cigarette waste	Coffee	Avg. residual (calc)	Std. dev. (%)
C % AR	42.30	39.90	44.50	43.80	43.30	39.20	42.90	29.50	34.60	43.70	44.86	4.82
H	5.50	5.20	6.00	5.70	4.60	5.00	4.80	3.60	4.30	5.70	5.60	9.01
O	38.00	34.10	31.60	37.20	31.60	33.60	27.30	20.70	27.80	30.90	34.76	7.85
N	0.900	1.100	2.900	1.300	2.300	0.300	1.10	2.40	2.30	2.20	1.87	51.35
S	0.090	0.150	0.220	0.130	0.240	0.690	0.13	0.39	0.30	0.14	0.28	80.26
Cl	0.030	0.250	0.010	0.350	0.070	0.260	0.24	0.900	1.000	0.39	0.389	36.67
H2O	12.000	10.300	11.400	7.000	13.000	8.600	15.50	10.400	9.100	11.30	12.067	18.58
K2O	5.100	18.000	1.800	31.000	51.000	6.300	36.00	11.00	23.00	33.00	8.300	229.82
CaO	32.000	7.800	8.600	8.300	4.700	31.000	11.00	17.00	16.00	8.80	16.133	77.80
MgO	1.300	2.600	8.800	3.400	5.900	7.400	7.10	4.90	5.40	6.00	4.233	69.24
P2O5	10.000	5.800	33.000	8.800	7.700	1.400	4.900	2.30	3.00	7.30	16.267	68.45
Ash AR	1.20	9.00	3.30	4.60	4.80	8.60	8.10	32.10	20.60	5.70	4.50	89.69
LHV AR	15.77	14.65	17.68	16.64	15.75	14.32	16.40	10.81	12.67	16.97	16.03	9.56

12.3.4 Residual resources

It should be noted that for the residual biomasses given in Table 12.6, large variation in the individual components exists even within the same biomass. This of course also means that using data for 'average residues', the last two columns of Table 12.6, should only be done with caution. It should also be noted that all biomass residues in Table 12.6 have been subject to drying, hence the low water content.

© Woodhead Publishing Limited, 2010

Table 12.7 Wood chip classifications (Serup *et al.*, 2002). Fine chips are for domestic use, medium to coarse for large power plants, air spout chips and chips suited for gasifiers. Hole size refers to the classifier opening for the different sizes

Designation	Hole size (mm)	Fine (%)	Medium	Coarse	Air spout	Gasifier
Dust	3.15	<10	<8	<8	>2	<4
Small	3.15–8	<35	<30	<20	>5	<8
Medium	8–16	–	–	–	>60	<25
Large	16–45	<60	–	–		
Extra large	45–63	<2.5	<6	–	<15	>60
Overlarge	>63	<0.25	<0.6	<3	<3	
Overlong 10	100–200	<1.5	<3	<6	<4.5	<6
Overlong 20	>200	0	<0.5	<1.5	<0.8	<1.5

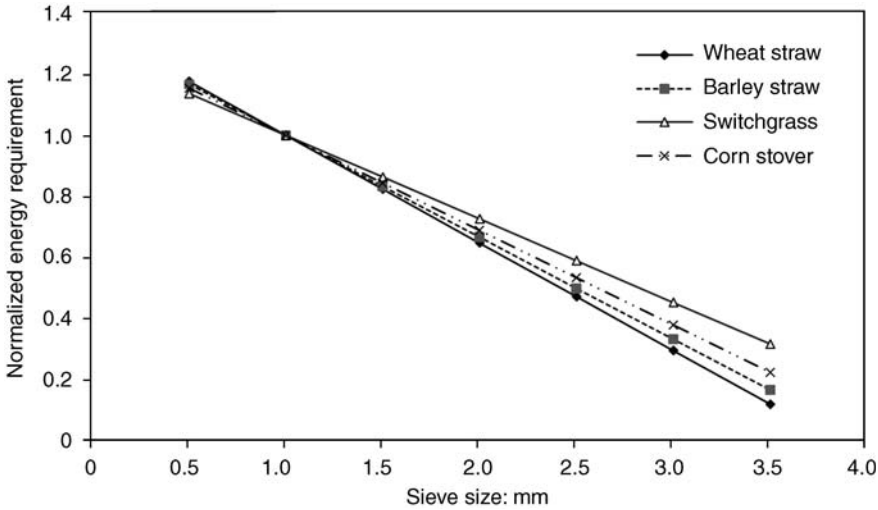
12.4 Physical preparation of biomass fuels

One of the key issues regarding suitability, apart from chemical composition, is the ability of the biomass to be broken down into pieces of a size and nature that allows them to be used as feedstock. This is not so important for the manures and algae, as the individual parts are of the order of millimetres and smaller. For woody and herbaceous biomasses as well as for different kinds of wastes, the optimum physical form of the feedstock, and perhaps even more so, the energy required to obtain this, is decisive in planning and designing a power station or biofuel conversion plant for a specific feedstock.

For herbaceous biomass and MSW, a traditional approach has been to use a shredder or another type of coarse homogenizer, and to fire the resulting feedstock in a grate-fired boiler. These units are quite insensitive to feedstock particle size, as the residence time is at least of the order of minutes. For wood chips, spreader–stokers are popular devices, where the pieces of biomass are introduced into the boiler through a spout, after which they heat up and initiate some of the conversion processes in suspension, before landing on a grate and finalizing their burnout. The European wood chip classification for different energy plants is given in Table 12.7.

However, for high-efficiency utilization of biomass in power production, units operating by suspension firing of pulverized fuel are best suited both in terms of cost of implementation and operational issues. Co-firing up to 5–10% biomass to a fossil fuel boiler causes no noticeable derating of the plant (IEA, 2007a), but does place demands on the biomass in terms of physical properties such as grindability, density, water content and chemical constituents.

© Woodhead Publishing Limited, 2010



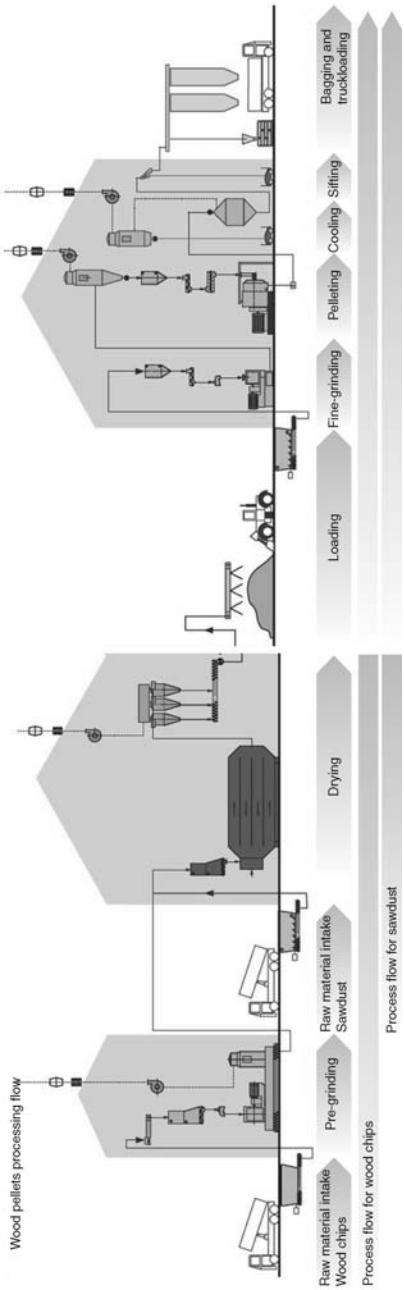
12.4 Energy consumption (normalized for consumption corresponding to 1 mm particle size) for comminution of different biomasses (from Rosendahl *et al.*, (2007)).

Mani *et al*. (2004) characterized the grinding properties of a number of biomasses for PF firing in terms of energy requirements. Based on their results, a cut-off size of approximately 1 mm was identified. In Fig. 12.4 the specific energy requirement as a function of sieve size is shown, indicating that for all the biomasses investigated, a linear correlation between size and energy cost exists.

A current trend in biomass fuels is to pelletize the raw resource, for example wood, waste wood or herbaceous material such as straw or bark. This has several advantages, particularly in terms of introducing biomass as co-firing or stand-alone fuel at large, PF power stations. These include enhancement of fuel homogeneity, increased energy density due to higher density, low water content, greater transportability within highly urbanized regions and the ability to mix the biomass with additives or other biomasses to obtain certain properties, so-called functional fuels**.** The main disadvantage, of course, is that just as grinding is an energy-consuming process, so is pelletizing. However, the higher efficiency of a PF unit compared to a dedicated biomass unit (grate-fired or spreader–stoker) and the higher energy density for transportation normally justifies this.

An example of a pelletizing plant is shown in Fig. 12.5. Depending on the raw material, a pregrinding is necessary in order to be able first to pelletize the biomass, and subsequently grind it to a dust of an acceptable size for a power station. Then, the ground biomass is dried in order to bring the biomass to a water content level of approximately 10%. After that, the actual

© Woodhead Publishing Limited, 2010



12.5 Example of a wood pellet plant (courtesy of Andritz Sprout A/S).

© Woodhead Publishing Limited, 2010

Table 12.8 Energy and costs for pellet production, 100 000 ton per annum plant (data from Anditz Sprout A/S *Woodpelleting - complete processing systems*, Technical Report 245 GB)

Input	Raw material	Virgin softwoods, sawdust or wood chips
	Ingoing material dimensions	25–40 × 10 mm
	Ingoing moisture content	45–50%
	Density	250–300 kg/m^3
Output	Pellet sizes	6–10 mm (dia)
	Pellet standards	CEN/TS 15103 CEN/TS 15210 CEN/TS 14961
Energy and cost	Energy for drying (MW h/t water evaporating)	1.0
	Electrical energy (kW h/t pellets produced)	80.0
	Oil/gas energy input (kW h/t pellets produced)	35.0
	Operational costs – wear parts (€/t pellets produced)	3.5
	Maintenance costs (€/t pellets produced)€	1.0
	Operation of contractor machinery (€/t pellets produced)	1.0
	Additional costs (€/t pellets produced)	1.50

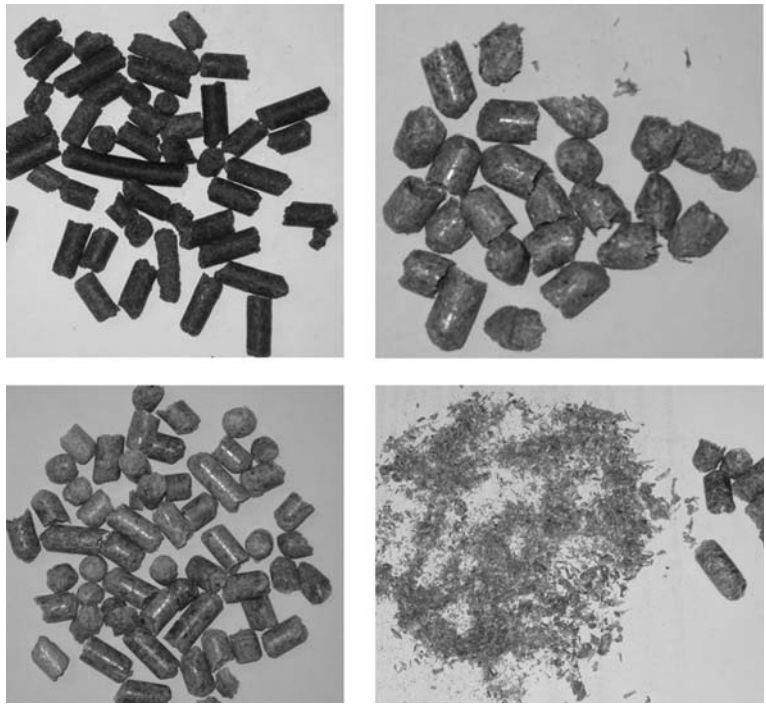
Table 12.9 Size distribution of Danish wheat straw fired at Studstrup Power Station, Unit 1, Denmark (Rosendahl *et al.*, 2007)

Size	Description	Length range (mm)	Fraction of total mass (%)
$<$6 mm	Powder, small straw pieces	0.3–6	20.2
$>$6 mm	Nodes: solid pieces	6–180	10.9
	Heads: whisk-like, hollow	6–140	4.2
	Straw: hollow, near-cylindrical	6–60	64.7

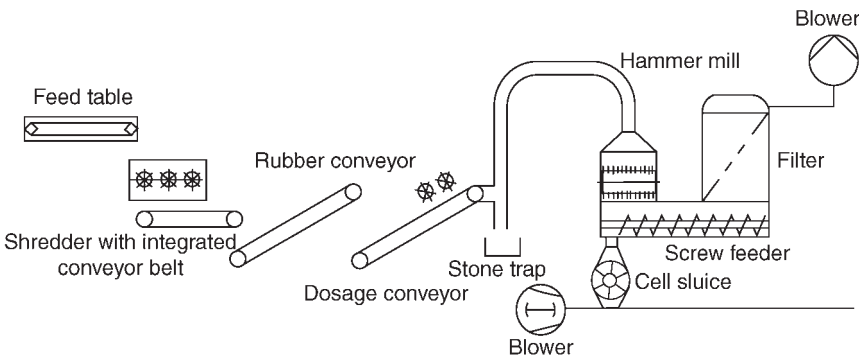
pelletizing process takes place, which is typically carried out using a steam pelletizer. Before packing for shipment, the pellets are cooled and sifted. The energy cost of such a process depends to a large extent on the amount of energy required for drying, as this process step typically consumes about ten times the energy required for the actual pressing step. This is illustrated in Table 12.8, which gives data for a commercially available pelletizing plant. Different types of biomass pellets are shown in Fig. 12.6.

As an aside to PF firing based on pelletized biomass, it should of course also be mentioned that there are PF power plants in continuous operation, co-firing biomass which is not initially pelletized. An example of the pretreatment system of such a plant is shown in Fig. 12.7, and the resulting

© Woodhead Publishing Limited, 2010



12.6 Types of pellets: clockwise from top right are straw pellets; ground straw pellets; wood pellets; and rape seed pellets.



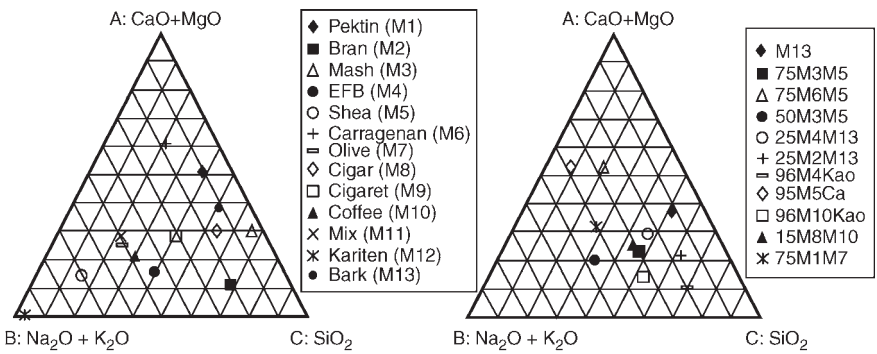
12.7 Preprocessing system Studstrup Power Station, Unit 1, Denmark. (from Rosendahl *et al.* (2007)). Although a PF unit, this system is a shredding system, resulting in quite large particles.

size distribution in Table 12.9. Clearly, this approach gives rise to very inhomogeneous and large particles, but allows the plant to operate with low pretreatment costs.

© Woodhead Publishing Limited, 2010

12.5 Functional biomass mixes

Regardless of the biomass, there are challenges associated with using it as a fuel for large-scale power production. These can stem from both physical and chemical characteristics of the fuel, including too low energy density, slagging and fouling issues, high water content, high lignin content and a multitude of other issues. One possible solution is the use of what can be termed functional biomasses or biomass mixes. The concept is based on identification of the different physical and chemical properties of the individual biomasses, and the problems or challenges associated with them. Once these are known, a functional biomass can be designed by mixing several feedstocks in appropriate amounts to achieve a chemically and physically acceptable fuel. The chemical properties can be obtained by mixing, and if the production of functional fuels is combined with a pelletizing process, biomass pellets can be produced with properties tailored to the specific use. In Denmark, this approach has been investigated from a fuel design and pellet production standpoint (Nikolaisen *et al*., 2005), as well as from an application standpoint (Larsen, 2005; Theis *et al*., 2006a; 2006b). Nikolaisen *et al*. (2005) investigated mixes of residual biomasses primarily based on considerations of ash content and components in order to mitigate deposit formation; the mixes were pelletized and tested in a laboratory-scale combustor. It was found that mixing 96% coffee with 4% kaolinite (96M4Kao) gave very good pellet properties (low dust, low energy consumption), which was also the case for 15% cigar waste and 85% coffee (15M8M10), and 75% carrageenan with 25% shea chips (75M6M5). In terms of chemical composition, the first functional mix kaolinite is added in order to improve ash properties toward lower deposit propensity, whereas the second mixes an alkali-rich residue with a sulphur-rich residue, and the last mix combines two alkali-rich biomass residues. The significant change in ash properties relevant for deposits can be visualized as shown in Fig. 12.8.



12.8 Visualization of changes in ash properties through functional mixing. Left: raw feedstock; right: functional mixes (Nikolaisen *et al.*, 2005).

© Woodhead Publishing Limited, 2010

The results presented above indicate that there is a significant potential in exploring functional mixing in order to enhance biomass properties. This process need not be restricted to residual biomasses, but can be applied across the entire spectrum of biomasses, primary as well as secondary. Owing to their high water content, several residual biomasses are well suited for rapid mixing. One of the key issues, however, is this mixing process, which needs to be associated with some form of physical processing of the biomass, for example pelletizing. This ensures that the chemical constituents of the individual feedstocks and possible other additives such as kaolinite are in close contact, and are released simultaneously in close proximity to each other, to ensure that chemical reactions can take place.

12.6 Summary

Biomass is destined to play a significant role in large-scale power production for several decades to come. There are several reasons for this: first, in many of its forms it represents a fuel for which conversion technologies already exist, needing only relatively minor modifications; second, it is a renewable and local resource; and third, by implementing new conversion technologies, biomass can supply not only heat and electrical power, but also biofuels. By timely consideration and a combination of political will and technical innovativeness, biomass has the potential to play a significant role in CO_2 emission reduction and provide a smooth transition to a fossil-fuel-free world. Most readily available are the co-firing technologies, where existing fossil-fuel-based power plants are retrofitted to use a solid or liquid biomass, thus replacing fossil fuel by biomass. With careful consideration of fuel properties and pretreatment requirements, it is possible to operate such plants with biomass fractions up to some 10% by energy.

There are several challenges to be met in order to accomplish implementation of biomass in the power sector, but the vast increase in research and development activities targeted at biomass use for energy represents an important step in rising to meet these challenges. As new technologies are developed, and existing technologies perfected, political will and investors are crucial in order to deploy large-scale biomass use at a pace fast enough to be able to make a difference.

12.7 References

Hansen, T. L., Cour Jansen, J. I., Spliid, H., Davidsson, & Christensen, T. H. (2007), Composition of source-sorted municipal organic waste collected in Danish cities', *Waste Management*, 27 (4), 510–518.

Hoogwijk, M., Faaij, A., van den Broek, R., Berndes, G., Gielen, D. and Turkenburg, W. (2003), 'Exploration of the ranges of the global potential of biomass for energy', *Biomass and Bioenergy,* 25 (2), 119–133.

© Woodhead Publishing Limited, 2010

IEA (2007a), *Biomass for power generation and CHP*, Paris, France, International Energy Agency (IEA).

IEA (2007b), *Renewables in global energy supply*, Paris, France, International Energy Agency.

IPCC (2007), *Climate change 2007: Mitigation*, Contribution of Working Group III to the Fourth Assessment Report of the Intergovernmental Panel on Climate Change, Figure 4.14. Cambridge: Cambridge University Press.

Kaltschmitt, M. and Hartmann, H. (2001), *Energie aus Biomasse – Grundlagen, Techniken und Verfahren, Berlin: Springer-Verlag*.

Larsen, E. (2005), *Halmtilsatsfyring i naturgasfyret kraftværkskedel*. PSO-ELTRA Project 3149, Energinet.dk.

Lin, Y. and Tanaka, S. (2006), 'Ethanol fermentation from biomass resources: current state and prospects', *Applied Microbiology and Biotechnology,* 69, 627.

Mani, S., Tabil, L. G. and Sokhansanj, S. (2004), 'Grinding performance and physical properties of wheat and barley straws, corn stover and switchgrass', *Biomass and Bioenergy,* 27 (4), 339–352.

McKendry, P. (2002), 'Energy production from biomass (part 1): overview of biomass', *Bioresource Technology,* 83 (1), 37–46.

Nikolaisen, L. (2009), Personal communication, Danish Technological Institute, Århus, Denmark.

Nikolaisen, L., Busk, J., Hjuler, K., Jensen, P. A., Jensen, T. K. and Bloch, L. (2005), *CO_2-neutrale brændslers anvendelighed i kraftværkskedler* (*Applicability of CO_2 neutral fuels in power stations*). PSO Project 5075, Technical Report, Danish Technological Institute.

Obernberger, I., Brunner, T. and Bärnthaler, G. (2006), 'Chemical properties of solid biofuels—significance and impact', *Biomass and Bioenergy*, 30 (11), 973–982.

Parikka, M. (2004), 'Global biomass fuel resources', *Biomass and Bioenergy*, 27 (6), 613–620.

Petrou, E. C. and Pappis, C. P. (2009), 'Biofuels: a survey on pros and cons', *Energy and Fuels*, 23, 1055.

Rosendahl, L. A., Yin, C., Kær, S. K., Friborg, K. and Overgaard, P. (2007), 'Physical characterization of biomass fuels prepared for suspension firing in utility boilers for CFD modelling', *Biomass and Bioenergy*, 31 (5), 318–325.

Ross, A. B., Jones, J. M., Kubacki, M. L. and Bridgeman, T. (2008), 'Classification of macroalgae as fuel and its thermochemical behaviour', *Bioresource Technology,* 99 (14), 6494–6504.

Serup, H., Falster, H., Gamborg, C., Gundersen, P., Hansen, L., Heding, N., Jakobsen, H. H., Kofman, P., Nikolaisen, L. and Thomsen, I. M. (2002), *Wood for energy production. Technology – environment – economy*, Center for Biomass Technology.

Sims, R. E. H. (2007), *Bioenergy project development and biomass supply*, IEA Good Practice Guidelines, International Energy Agency, Paris.

Theis, M., Skrifvars, B., Hupa, M. and Tran, H. (2006a), 'Fouling tendency of ash resulting from burning mixtures of biofuels. Part 1: Deposition rates', *Fuel*, 85 (7–8), 1125–1130.

Theis, M., Skrifvars, B., Zevenhoven, M., Hupa, M. and Tran, H. (2006b), 'Fouling tendency of ash resulting from burning mixtures of biofuels. Part 2: Deposit chemistry', *Fuel*, 85 (14-15), 1992–2001.

© Woodhead Publishing Limited, 2010

13

Development and integration of underground coal gasification (UCG) for improving the environmental impact of advanced power plants

M. GREEN, UCG Engineering Ltd, UK

Abstract: This chapter discusses the process of underground coal gasification from the basic operating principles through to the criteria for geological site selection and the options for syngas utilisation. It reviews how UCG has developed in recent years in coal-producing countries. The application of directional drilling and completion from the oil and gas industry has provided an opportunity for UCG in deeper coal seams. Environmental, regulatory and licensing issues for UCG are examined and the importance of UCG with combined CO_2 capture and storage as a viable and proven option for future power generation is discussed.

Key words: underground coal gasification, directional drilling, UCG, site selection, UCG–CCS, in-situ gasification, UCG future trends, Australia, Europe, Asia, India, USA, IGCC, IPPC, CO_2 capture and storage.

13.1 Introduction

Coal gasification is the conversion of coal to a gas which can be used for heating and power generation. It is a well-established process, and is normally conducted in a high-temperature surface reactor with mined coal, with oxygen/steam as the conversion agents. Another form of gasification is underground coal gasification (UCG) where the same process is taken into the underground coal seam, oxidants are injected through boreholes, and the product gas is brought to the surface for processing and utilisation.

Underground coal gasification is conceptually attractive because no mining or coal transportation is required and the expensive surface reactor is eliminated; the surrounding strata act as the containing vessel. UCG can exploit coal seams which cannot be reached by conventional mining, thereby

© Woodhead Publishing Limited, 2010

extending a country's indigenous coal reserves and providing an additional level of fuel flexibility for the power generation sector. It also eliminates sending men underground and offers an alternative to conventional coal mining. This alternative is safer, more environmentally attractive and, like oil and gas extraction, is efficient in the use of production manpower. The full-scale adoption of UCG technology has the potential to vastly increase useable coal reserves (McCracken, 2008). The technology is applicable to offshore coal resources (DTI, 2006) as well as onshore.

Evidence that coal can be combusted underground comes from the many coal fires, some lasting thousands of years (Wolf, 2006), that have occurred naturally throughout the world. To harness the process, however, and provide a consistent gas of good calorific value from an in-situ coal seam, requires considerable knowledge of the processes involved, and a method of control which ensures that the conversion process, from coal to gas, travels smoothly and efficiently through the seam. UCG requires a thorough understanding of the geology, the chemical kinetics of the reactions and the transport of fluids into and out of the gasification zone. UCG has a long history of development involving some 50 or so trials (Burton *et al.,* 2007) since the 1930s. Large-scale plant for co-fired UCG power generation was constructed by the Soviet Union in the 1970s and at least one is still operating today in Uzbekistan.

The era of low-cost natural gas in the 1990s brought to an end most UCG development, with the notable exception of Europe and China, discussed later. Since 2000, there has been a significant revival of interest in UCG in the major coal-producing countries for reasons of security of supply, the reduced cost of gas production and the ready application of syngas in combined-cycle power generation (integrated gasification combined cycle (IGCC)).

The commercial interest in UCG as a clean coal technology today is being maintained because the process can satisfy all the current environmental requirements, including low carbon emissions. One of the key issues is groundwater protection but equally important are the emissions of sulphur dioxides, nitrogen oxides, particulates, heavy metals like mercury, which are now the subject of strict emission standards in most industrial countries. In addition, the world is closer to regulating carbon emissions for larger power generation sources, with carbon dioxide (CO_2) capture and storage (CCS) of fossil fuels as one of the principal routes for carbon reduction (Oxburgh, 2009) in the medium term. UCG as a gasification process is well suited to pre-combustion capture of CO_2, and local storage in the vicinity of the gasified area may be possible in some circumstances.

© Woodhead Publishing Limited, 2010

13.2 Brief history of UCG

Underground coal gasification has been the subject of intense research and field trials since the Second World War in the former Soviet Union (FSU), Asia, Europe and, not least, in the USA, where the development programme in the 1970s and 1980s extended to 32 separate tests, and a large supporting programme. The US investigation (Friedmann, 2008) led eventually to new control techniques such as moveable injection, and the undertaking of commercial designs for the production of chemicals and synthetic natural gas (SNG). Although UCG was considered to be technically proven in the early 1990s, it could not compete with low-price natural gas and interest diminished in the USA. Meanwhile the European UCG programme, initiated to find an alternative to mining, investigated the feasibility of UCG in the deep and thinner coal seams of Europe.

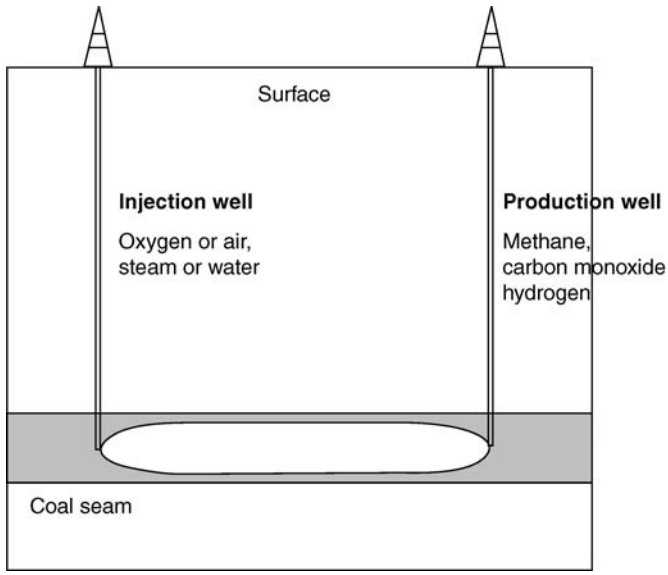
Underground coal gasification development has largely been concerned (Green, 2007) with enhancing the connection between boreholes in coal, controlling the underground process, and scaling up the process to commercial-sized operations. These are not trivial problems, and are hampered by the fact that, in general, tests can only be made at full scale in real coal seams. Trials are expensive and the results are often difficult to assess at the depths and conditions of UCG.

A consortium, supported by the European Commission (EU), adopted the moveable injection system and oxygen firing of UCG and extended it to much deeper coal seams by carrying out two trials at 550 m and 860 m depth. The study showed (DTI, 1999) that UCG in deeper seams is feasible, environmental impact at the surface is eliminated and the higher operating pressure results in greater methane production. The UK Government, which was a partner in the European trial, undertook an in-depth study of the feasibility of UCG for the UK (1999–2004), and supported a feasibility study of UCG under the Firth of Forth, Scotland (DTI, 2006). This prospect has now been granted (March 2009) the first provisional licence for UCG in the UK, and is now under commercial development.

Other UCG activities have been the long-standing Chinese studies of UCG (Liang, 2003), the new field trials in South Africa by Eskom (Varley, 2008) and Sasol (Brand, 2008), and the growing interest by the Australian mining sector in developing UCG (see final section on developments in 2008).

It is estimated that 15–20 billion cubic metres of UCG syngas, worldwide, has been produced to date, equivalent to 12–15 million tonnes of coal and sufficient to power a large city for one year. The largest UCG-based power station at present is 100 MW.

© Woodhead Publishing Limited, 2010



13.1 Basic configuration for the UCG.

13.3 The UCG process

13.3.1 Basic principles

Underground coal gasification works by constructing vertical wells into a coal seam to supply the injection gases oxygen (O_2) and water (H_2O), and to discharge a mixture of production gases, carbon monoxide (CO), hydrogen (H_2), methane (CH_4), and carbon dioxide to surface. While the principle is simple, control of the gasification process has been at the heart of UCG development over many years.

The basic concept (Fig. 13.1) has two boreholes, one for the injection of oxidants and the other for the removal of the product gas. The oxidants react with the coal in a set of gasification and pyrolysis reactions to form the main gasification products and a variety of minor constituents. The underground coal seam is sealed from the surface by impermeable strata of typically clay or mudstone.

Post-gasification investigation of the European UCG trial (Green, 1999) has shown that UCG cavities develop around the injection point and spread upwards to the coal seam roof under strong buoyancy forces. The process then grows in the axial and radial directions to form a pear-shaped cavity.

As the cavity develops, the litho-static pressure of the overlying strata imposes stress and deformation on the growing cavity. Once a certain volume has been attained, fissures form and caving takes place. The deeper the coal seam for gasification, the more likely that the roof will cave. Roof

© Woodhead Publishing Limited, 2010

collapse aids the lateral growth of the cavity, and provided it takes place in a controlled manner, the effects are beneficial to UCG.

13.3.2 Kinetics of the gasification reactions

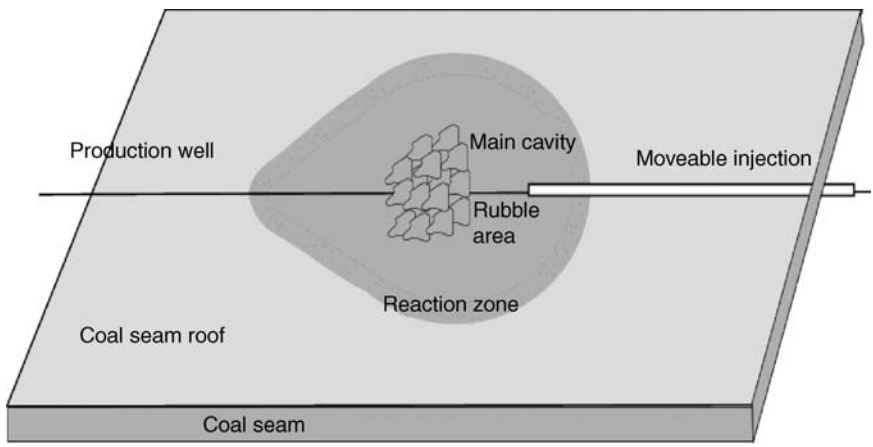
The chemical processes of coal gasification are complex. The reactions take place at the surface of the coal and in the gaseous phase. They include pyrolysis, partial oxidation and hydrogenation.

The heterogeneous nature of the cavity results in considerable temperature variation. At the gasification zone itself, temperatures in excess of 1000°C are observed, as a result of the highly exothermic reactions of combustion. In other parts of the cavity, the endothermic reactions produce rapid cooling. Both tar formation and reactions favoured by low temperature are encouraged in these regions of the cavity (Fig. 13.2).

The reactions with the new coal solid surface take place mostly at the circumference of the cavity, and further reactions continue in the gas phase both in the central area and in the neck of the cavity as the gases pass towards the production well. The ash and char collect as rubble in the centre and a set of zones of decreasing temperature are created where drying, pyrolysis and gasification reactions in the solid and gaseous phase take place (Fig. 13 3).

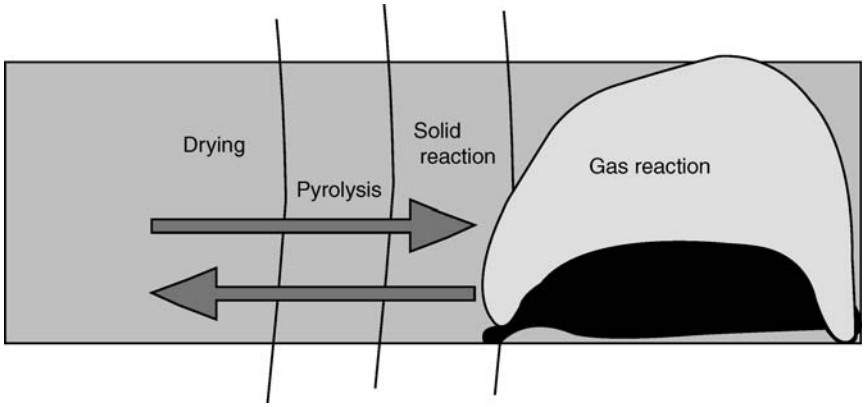
The four basic reactions (Higman and Van der Burgt, 2003) of gasification involving the solid carbon are

$C + O_2 \leftrightarrow CO_2$	(combustion reaction)	− 394 MJ/kmol
$C + CO_2 \leftrightarrow 2CO$	(Boudouard reaction)	+120 MJ/kmol
$C + H_2O \leftrightarrow H_2 + CO$	(water–gas shift reaction)	+125 MJ/kmole
$C + 2H_2 \leftrightarrow CH_4$	(hydrogenation reaction)	− 67 MJ/kmole



13.2 Typical UCG cavity shape.

© Woodhead Publishing Limited, 2010



13.3 Close-up of the reaction zone, perpendicular to the main direction of flow.

The negative sign indicates an exothermic reaction and conversely for endothermic reactions.

Away from the surface of the carbon, the reactions with free oxygen are essentially complete under gasification conditions, and the syngas reaches equilibrium by two further gaseous reactions

$$CO + H_2O \leftrightarrow H_2 + CO_2 \quad \text{(shift reaction)} \quad -41\ \text{MJ/kmol}$$
$$CH_4 + H_2O \leftrightarrow 3H_2 + CO_2 \quad \text{(steam reforming reaction)} \quad +206\ \text{MJ/kmol}$$

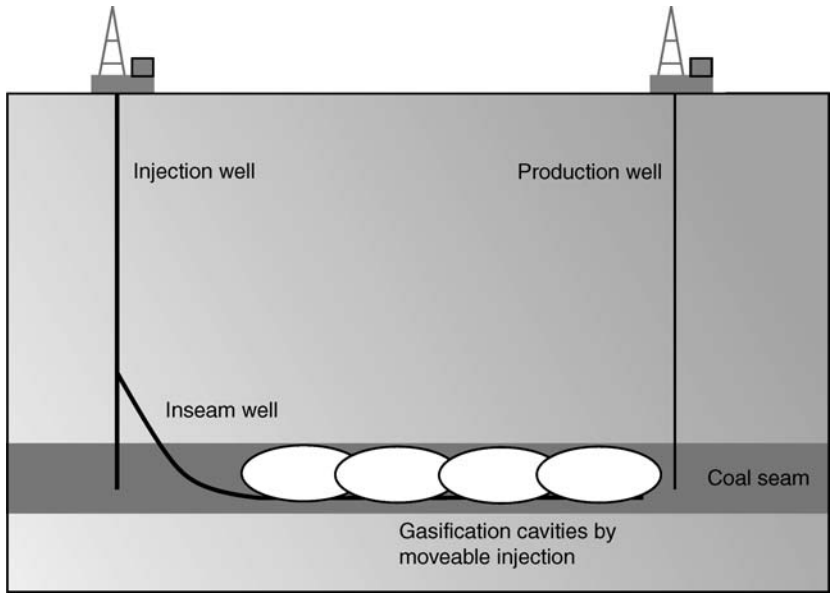
All the above reactions are temperature and pressure dependent.

In the real cavity, other reactions are taking place leading to the formation of intermediate products such as tar, and the pyrolysis process in front of the gasification front produces its own unique combination of gases. Furthermore, the equilibrium conditions are not being reached for the slower reactions, so kinetic modelling provides only a direction for the gasification process in these cases.

Most coals can be gasified in situ but transport of the gases between the inlet and outlet boreholes controls the reaction. Coal can vary considerably in its resistance to flow, even in the same coal seam. Three methods of control broadly described as the FSU, Chinese and Europe/America methods have now evolved.

- The FSU technique uses vertical wells and high-pressure air fraccing or reversed combustion to open up an internal pathway in the coal. The vertical wells can act as both injection and production wells and when gasification between them is complete, a second pair is initiated.
- The Chinese method relies on man-built galleries in the coal seam to act as the gasification channels. Boreholes are constructed into the gallery to provide communicate for the injection and product gases with the

© Woodhead Publishing Limited, 2010



13.4 Directional drilling and moveable injection (CRIP) from USA and European trials.

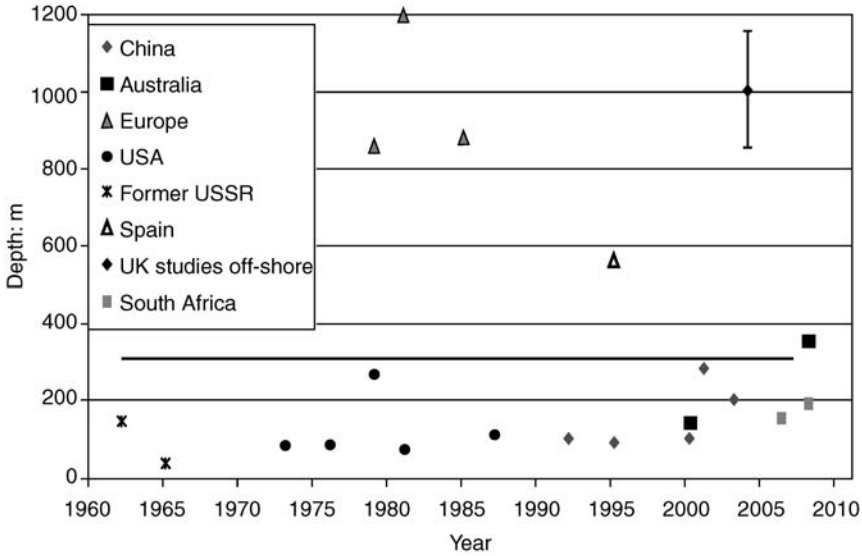
surface. The Chinese tests (Liang and Shimada, 2008) are mostly designed for hydrogen production and operate on alternating air and steam, although the most recent experiments have also included oxygen and steam injection. Seventeen field trials have been started in China since 1986.

- The directionally drilled method developed in Europe/America (Fig. 13.4) creates dedicated long inseam boreholes at a precise horizon in coal seams and links these accurately to a production well which connects to the surface. The drilling and completion technology (DTI, 2005) is adapted from oil and gas production. A moveable injection tube (controlled retraction injection point) (CRIP) is slid into the inseam borehole to position the point of injection. Directional drilling and moveable injection was first used in the final US trials (late 1980s) and taken to greater coal-seam depth in the European trials (1988–1998).

The directionally drilled arrangement was first tested in shallow coal at the Centralia experiment in California, USA (Cena *et al.*, 1984) and at the Rocky Mountain trial (Thorsness *et al.*, 1988) in Wyoming, USA where over 14 000 tonnes of coal were gasified. It was further developed in deeper coal at the European UCG trials in Belgium (860 m depth) and Spain (550 m depth).

The three techniques have been tested extensively in field trials and all

© Woodhead Publishing Limited, 2010



13.5 Depth of UCG field trial 1960–2008.

three approaches are available as technical options for new commercial projects. The choice of configuration depends on the location, depth of the coal seam, the geological conditions, local drilling costs and the use to which the product gas will be put. The trials outside Europe have generally taken place in shallow coal seams (Fig. 13.5), whereas recent European trials in Belgium and Spain have operated at pressures > 50 bar. Apart from the environmental benefits, discussed in the following section, high-pressure operation favours the formation of methane and improving the calorific value of the product gas. There is also evidence that wider cavities are produced as the depth of the coal seam increases.

13.3.3 Oxygen versus air-blown UCG

Oxygen for the gasification process can be supplied as air, enriched air or oxygen. The simpler alternative of air-blown gasification produces a syngas high in nitrogen and a calorific value in the range 3–5 MJ/m^3, which is suitable for combustion and gas turbine operation. The use of enriched air or pure oxygen produces a gas of higher calorific value, typically 9–13 MJ/m^3 (approximately one third that of natural gas) which is more suitable for transportation and the processing of syngas to hydrogen, synthetic natural gas and hydrocarbons, and the capture of CO_2 for CCS. Higher oxygen content will raise the reaction temperatures at the coal surface, and earlier work on UCG from the Soviet era (Kreynin, 2009) suggests that enriched air also aids the growth of the gasification cavity. The disadvantage of air-

© Woodhead Publishing Limited, 2010

blown gasification arises from the huge increase in gas volume which has to be compressed, transported to the coal seam and brought back to the surface without contributing to the energy conversion process in any way.

Oxygen firing is generally required when operating at higher pressure in deep seams, to avoid the high compression requirements prior to injection. It is noteworthy that the majority of the trials that have used directional drilling and moveable injection have been oxygen fired.

Oxygen is currently produced by a cryogenic air separation unit (ASU), which places a higher overhead on the electric demand of the plant. UCG in deep high-pressure coal seams provides the opportunity for the recovery of energy by turbine expansion in the product stream, thereby offsetting to a large extent the electrical demand of the ASU.

The US trials concluded that oxygen firing is the better choice, even for shallow seams, whereas the FSU community, which includes the new commercial companies based on Chinchilla (Peters, 2008; Blindermann, 2009), tend to advocate air-blown systems because of the lower overall cost of power generation.

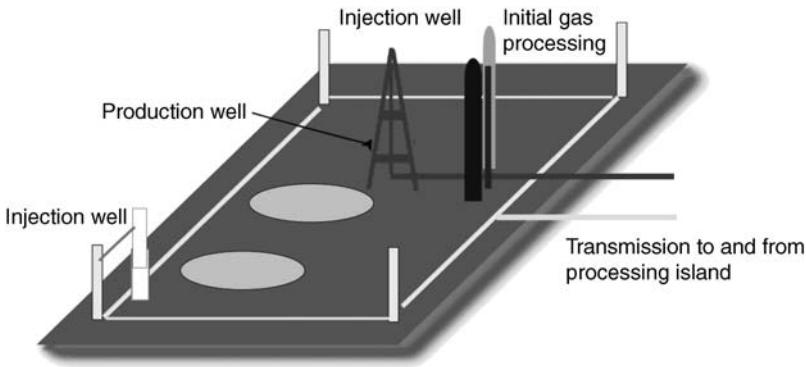
13.3.4 Modelling

A wide range of tools can be used to provide insights into the underground process. Examples include the packed bed cavity models from India (Khadse *et al*., 2006), the risk analysis techniques from the USA, (Burton, *et al*., 2007), and the computational fluid dynamic modelling from Australia (Perkins and Sahajwalla, 2006). In addition, many attempts have been made to model the reaction and flow characteristics of the cavity, and the literature on modelling is extensive, see section 13.10.

Computer models for rock mechanics are used for analysing the stresses in the overlying strata. These powerful tools are widely employed for oil and gas exploration and their use for UCG sites could save time and aborted effort on unsuitable sites.

Practical UCG projects need, above all, a good understanding of the state of cavity development in order to make the right assessment and control decisions for the process. On-line tools, based on gas composition, product flow rates and injection conditions can provide instantaneous mass balances and an assessment of the progress of the gasification process. They can also give a measure of the water ingress into the well and gas escapes from the cavity, which are an essential part of the environmental monitoring process. Much of this supporting technology was developed in the European trial (Green, 1999)

© Woodhead Publishing Limited, 2010



13.6 Possible layout of a UCG outstation built around a single production well.

13.3.5 Commercial-scale operation

The step up from pilot operations to larger-scale UCG operations has been achieved in at least two former Soviet schemes, in Siberia and Uzbekistan, one of which is still running after 40 years. The regulatory regime employed at the time, however, bears little relation to the more exacting environmental requirements of today. UCG in most coal-producing countries will have to meet strict groundwater and emission conditions (Sury, 2004). A key stage in the scale-up to commercial operation is the construction and management of a large number of well pairs operating simultaneously; around 30 UCG channels are required to support a 300 MWe UCG power station.

The layout of a directionally drilled UCG outstation, producing around 100 MW of thermal power, is proposed in Fig. 13 6. A larger UCG project would have a number of these stations, each connected to a processing island for syngas cleaning, power generation or liquid fuel manufacture.

13.4 Criteria for siting and geology

The underground part of UCG requires a multi-disciplinary approach to assess the geological structure, hydrogeology and coal characteristics of the UCG target site. The site will need to be evaluated with a combination of exploratory core drilling, seismic surveys, preferably three-dimensional, and the use of a suitable software package to correlate the exploratory data and identify suitable coal locations. The programme should be designed to identify geological structure at coal seam depth to a resolution of at least coal seam thickness. The total tonnage of coal must be sufficient to meet the output requirements for the project lifetime. In the past, UCG sites have tended to rely on existing mining data, supplemented where necessary with

© Woodhead Publishing Limited, 2010

additional boreholes and seismic, and these continue to offer the least cost opportunity.

A thorough understanding of the coal seam characteristics is a pre-requirement of the design and construction of UCG process wells. It is also important to have good knowledge of the adjacent strata to ensure well bore and environmental integrity, and provide the necessary information for the environmental impact assessment (EIA). The exploration programme, which is necessary and costly, may result in site rejection as the evaluation process unfolds.

13.4.1 Selection criteria for UCG target sites

General rules for target sites are difficult to establish because suitability for UCG depends on factors such as coal type, the characteristics of the strata between coal seam and surface, and not least the regulatory requirements for ground water.

A study initiated under the UK Clean Coal Programme to examine the suitability of on-shore coals (Jones, 2004) used the following generic selection criteria for UCG:

- coal seam > 2 m thick;
- depth between 600 and 1200 m;
- the availability of good density borehole data;
- stand off of > 500 m from abandoned mine workings, license areas;
- vertical separation > 100 m from major aquifers.

The above generic criteria, which are specific to the resource study of UCG in the UK, do not rule out UCG at greater proximity to aquifers or the surface where the geology permits. Every site will require a detailed geological and hydrogeological risk assessment.

13.4.2 Depth of coal seams for UCG

The minimum depth for UCG is a matter of debate. Most trials in the past have been conducted in relatively shallow coal, e.g Chinchilla, Rocky Mountain and the Chinese tests, without any reported adverse environmental impact, although monitoring in the earlier trials was patchy. Cases where contaminant spread has been observed, such as Hoe Creek, USA, are attributed as much to the lack of pressure control during operations as to the site itself (Sury, 2004).

Depth, which is also related to the hydrostatic pressure, will determine the operating pressure of the gasifier and will be a major component of the drilling cost. Gas quality is generally improved with higher operating

© Woodhead Publishing Limited, 2010

pressure. The seam must have a sufficient head of water above it to maintain sealing with prolonged operation.

13.4.3 Coal characteristics

The literature reviews of UCG (Burton *et al.*, 2007; Couch (IEA), 2009) show that all coals from lignite to anthracite have been successfully gasified in situ, and that coal type and rank are a second-order effect. Nevertheless, consideration of the chemical processes involved suggest that the more reactive sub-bituminous coals are preferred, and the experience from surface gasification indicates (Higman and Van der Burgt, 2003) that gasification behaviour is influenced by factors such as rank, swelling, ash and moisture, volatile matter and methane content.

The permeability of the coal and whether it swells or contracts with temperature is cited (EWG, 1989) as an important issue. Ideally a coal is required which shrinks during dehydration and pyrolysis, and coals to be avoided are those which swell significantly on heating. This fact points to a preference for low-rank coals, i.e. sub-bituminous or lignite and coals with a limited tendency to coke. Hard coals are thought to work because the rectangular cleat system brings added directional permeability, which enhances gas flow.

Moisture content is an essential element of the water–gas reactions of gasification. The presence of in-situ water at the reaction face should be an advantage over water which is carried to the well with the oxidants by injection. Too much water initially, however, will make the wet coal difficult to ignite and there is evidence that ignition of the UCG process in the past has caused serious difficulties. A high rate of water influx into the cavity from adjacent seams is generally undesirable, as found for example in the Spanish trial (DTI, 1999).

13.4.4 Structure and physical properties of the coal

Tectonic effects create faulting, folding and volcanic intrusions, which lead to dipping and discontinuities in the seam. These create pathways for the entry of ground water and the dispersal of contaminants from the cavity.

A dipping seam can be a substantial advantage in the presence of excess water because it allows drainage of water and tars away from the gas channels. A steeply dipping seam acts as a chimney for the hot and buoyant product gases and assists the spread of the cavity. Soviet and early US trials favoured sites with steeply dipping seams, i.e. $> 60^{\circ}$, and developed special well configurations for them (Singleton and Pilcher, 2007). Seams with high gradient, however, are the result of exceptional geological disturbance and are relatively rare.

© Woodhead Publishing Limited, 2010

Seam thickness controls the amount of coal that can be extracted from a single seam and it will influence the heat loss from the seam to surrounding material. Coals of 1 m thick have been gasified in Soviet tests, but 1.5–2 m is generally regarded as the minimum requirement.

Maximum thickness is more difficult to assess as the roof itself has a role in arresting the tendency to burn vertically and the roof encourages lateral growth. Most trials have taken place in coals up to about 10 m thick. Greater seam thicknesses have been considered in recent feasibility studies, where gasification in layers has been proposed, but no trials have yet been undertaken in the very thick lignite and sub-bituminous seams which exist widely in China, India and Eastern Europe.

Thicker seams also often contain intercalations or dirt bands, which could cut off the vertical progress of the gasification process unless they readily collapse under the heat and pressure of the process. Typically half a metre would be the maximum thickness of dirt band that the gasification process could tolerate, although local geological factors may influence the acceptable value.

The roof strata above the coal seam ideally need to collapse progressively, as in long-wall mining. This ensures that large caverns are avoided so the gas can intimately mix and react with the coal surfaces. On the other hand, large-scale roof collapse can result in blockage of the gasifier void itself. The roof strata should contain impermeable layers of, say, mudstones or clay to limit water ingress and the dispersal of gases and liquid contaminants. A further factor is the integrity of wells which pass through the roof. They need to be positioned to avoid placing them in the collapsing area.

13.5 Drilling technologies and well construction for UCG

The exploration and production of oil and gas has stimulated the development of drilling and completion technology. The drilling of lateral boreholes over distances of several kilometres in very deep wells, the use of completion tubulars for sour and high-temperature gas and the technology for steering have all advanced rapidly.

Coal seams pose a range of additional technical challenges, compared with oil and gas extraction, as listed below.

- Coal is frequently much weaker than the strata of most oil and gas reservoirs.
- The precision requirements for drilling in a narrow seam are more onerous than most oil and gas projects, but depth and the operating pressure will be lower.
- Downhole casing equipment will be exposed, in the case of UCG, to an

© Woodhead Publishing Limited, 2010

aggressive chemical and thermal environment that is greater than most sour gas operations.
- The financial cost margin available for coal drilling is likely to be lower than that for oil and gas exploration.

Specialist companies working on smaller development budgets rather than the major oil companies or their service providers have largely pioneered the introduction of directional drilling for coal exploration, detection of igneous intrusions, gas safety relief and coal bed methane (CBM).

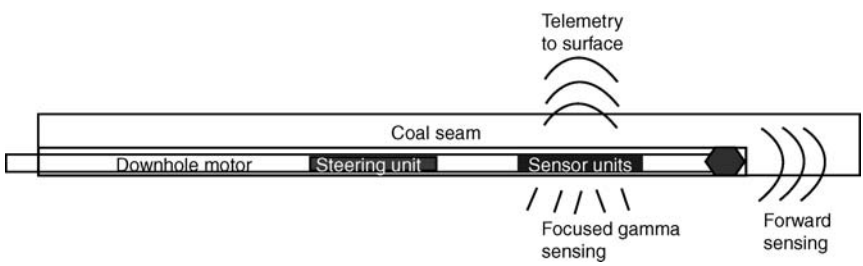
13.5.1 Directional drilling in coal

Inseam directional drilling is becoming the preferred method of accessing and opening up the coal seam for exploration, gas drainage, and UCG. The wells, whether drilled from the surface or an underground mining gallery, have in common a long-reach inseam section which has to follow the seam. For UCG, this well should be as close as possible to the bottom boundary, so that as much of the seam as possible is gasified. The entry point to the coal seam needs special consideration to avoid significant fluid losses.

The mechanical strength of coal is generally much weaker than other geological structures, and coal is unable to support very large pressure gradients without collapse. The key to success in coal drilling is continuously to monitor and control the annular pressure behind the drill bit (DTI, 2005). Water-based drilling fluids are strongly preferred on environmental grounds.

13.5.2 Steering in coal

Steerable bottom hole assemblies (BHA) consisting of a down hole motor, drill bit, and a telemetry package (Fig. 7), are used for the build-up and in-seam sections of the well, and specialist drillers would usually supply and operate the equipment as a separate service.



13.7 Downhole assembly for directional drilling in coal (copyright ©, DTI, 2005).

© Woodhead Publishing Limited, 2010

A recent development is the placing of focused gamma sensors on the BHA to detect the coal seam boundary (Muir, 2008) and to provide continuous signals to follow the coal seam. Bottom hole drilling assemblies can have sensors that look ahead of the drilling bit to identify, in advance, faults and areas of unacceptable structure. This provides geological steering of the well, and is a considerable simplification over the conventional measure-while-drilling (MWD) system for seam location.

Another important requirement for UCG is the ability to intersect wells within the coal seam in order to complete the flow circuit between injection and production wells. Homing devices have been developed for hydrocarbon exploration, to enable wells to be intersected or approached (DTI, 2005). Well-to-well ranging tools can be used to detect a nearby well through magnetic interference. In the active homing systems, a strong magnetic field is generated in one well, which is detected in the other.

13.5.3 Underground engineering of the process wells

The detailed underground engineering design of the wells is the key to the successful operation of the UCG process. The wells are constructed from a series of tubulars that are designed to bring the injection gases to the coal seam, and remove the hot, wet and possibly sour product gases to the surface.

The wells for injection are steel lined to accept coiled tubing, which passes through the central liner and acts as the moveable injection device or CRIP. The coiled tubing is driven into the well by a chain-driven injector head located above the wellhead (DTI, 1999).

The production well must be designed to cope with the hot and corrosive product gas of the UCG process. Material selection of the liners should be consistent with temperature, pressure and the requirement to resist corrosion at the well bottom.

The inseam drilling method requires more expensive hardware for completion, and drilling costs are higher, but the number of process wells from the surface is very much reduced. Furthermore, the method is suitable for deeper coal seams, which has important environmental advantages. Deep coal, both on and off shore, is also accessed, which would otherwise not be mined.

13.6 Integration with power plant

Pre-combustion gas processing is available to prevent the unwanted contaminants reaching the atmosphere, including CO_2 capture. UCG syngas can be cleaned for power generation or for further chemical conversion into energy carriers such as hydrogen, methanol and synthetic natural gas.

© Woodhead Publishing Limited, 2010

13.6.1 Power generation

Syngas is a flexible fuel for power generation. The simplest use of UCG syngas for power generation is to combust the gas in a thermal plant to raise steam for power generation. An example is the Angren power station, Uzbekistan, where UCG has been supplying steam for a 100 MW turbine and generator for many years (Yerostigaz, 2008).

Efficiencies of thermal plant have been gradually increasing, but the process is limited by steam pressure and temperature. Supercritical plant, i.e. steam plant that can operate at higher temperatures and pressures, is providing much of the improvement and ultra-critical plant is under development.

An alternative and arguably more efficient method of power generation is to use the product gas directly in a combined cycle, as in a natural gas power plant. The gas turbine, however, is relatively intolerant to small changes in gas composition. Maintaining the output and quality of the gas from a multi-channel UCG project will require good process control.

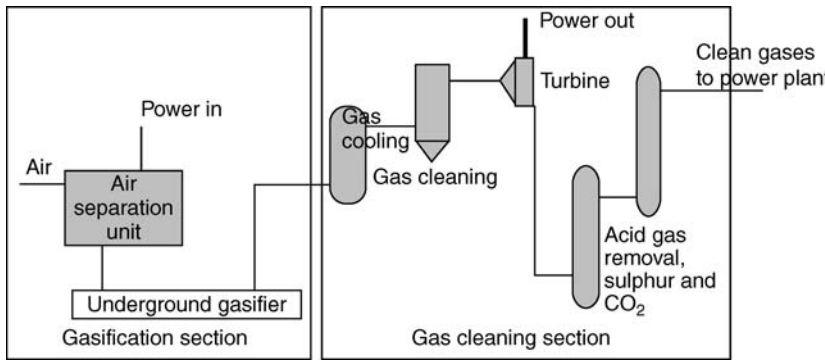
The most efficient option is to burn the gas in a dedicated combined-cycle gas turbine (CCGT), modified for the syngas composition. Some degradation of power is expected on syngas, compared with natural gas, but efficiencies for operation are expected (Beath *et al*., 2004) to be around 45% for modified plant and perhaps higher for plant designed specifically for UCG syngas. The combustor of the turbine would need to be dual fired with natural gas for start up and possible co-firing operation.

Gas turbines have been successfully tested (Kelsall, 2004) on low to medium calorific value gases down to about 4 MJ/m^3, which is representative of air-blown gasification. 500 000 hours of operating experience on IGCC gases has been reported by General Electric (GE) (Jones, 2004) over the full range of hydrogen content up to 90%, with acceptable NO_x emissions. GE has also collaborated with the UCG project at Chinchilla, to test a simulated air-blown UCG product gas for operation on gas turbines of 45 MW and 177 MW output (Blindermann and Jones, 2002).

Industrial gas engines are an alternative method of power generation for smaller-scale UCG projects. Industrial engines usually have electronic control of air-to-gas ratio lambda control, and are more tolerant to the variations in gas quality. A gas engine of 750 kW was installed at Erzhaung UCG trial site, in China (Liang and Shimada, 2008).

Oxy-firing of UCG gas as a method of CO_2 capture could also be used for power generation, where low or zero CO_2 emissions are required. The possibility of a supercritical thermal plant raising steam from oxygen-fired UCG gas is a promising avenue of further research (Hesselmann, 2009) for UCG–CCS.

© Woodhead Publishing Limited, 2010



13.8 Basic flow chart for UCG gasification and clean-up.

13.6.2 Surface plant for gas processing and cleaning

The raw UCG gas mixture leaving the production well contains combustible gases, excess water in the vapour or liquid phase, particulates and minor contaminants in solid, liquid and gaseous form. The gases are hot and leave at a pressure close to that in the underground cavity in the coal seam, which ranges from 1–10 MPa, depending on the depth of the seam.

The flow chart in Fig. 13.8 outlines the gas cleaning section for UCG. It consists of a cooling and washing vessel to condense the water and tars, a solid separation process to eliminate carry-over of char and ash, and an expansion turbine to reduce pressure and, if required, generate power from the expansion of the high-pressure gas.

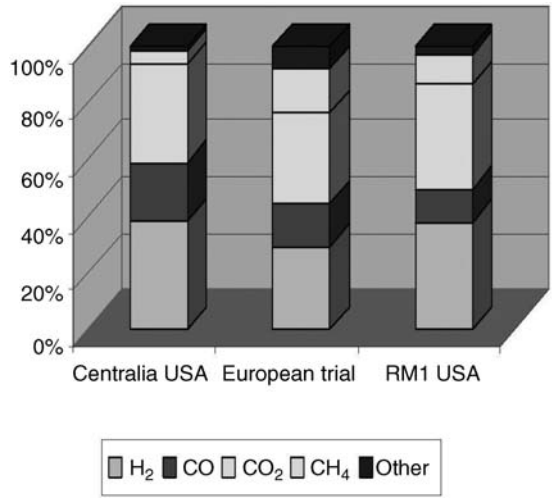
The stream is then ready for the removal of any hydrogen sulphide (H_2S) and minor contaminants. The processes of acid gas removal use either physical adsorption (Selexol) or chemical absorption (proprietary amine solutions) to transfer the gases to a liquid stream, which are then regenerated by pressure or temperature swing. A Claus plant converts the H_2S to elemental sulphur. These processes, which are widely used in gas treatment plants, will need to be tailored to the high pressure and CO_2 content of the UCG product gas.

The injection gases are supplied with an air separation unit (ASU), as in surface gasification reactors. The ASU is a heavy user of power or process steam and the separation results in oxygen purity, often above that required for the UCG process. An alternative is the ion transport membranes (ITM) that are being developed by oxygen suppliers (Allam *et al.*, 2002).

13.6.3 Total and partial CO_2 capture from the product gas

Measured compositions for dry, clean syngas from three trials are shown in Fig. 13.9. UCG is fairly unique as a gasification process in producing CO_2

© Woodhead Publishing Limited, 2010



13.9 Gas composition of dry syngas from oxygen-fired UCG.

and methane as well as the carbon monoxide and hydrogen found in surface gasification. This occurs because lower temperatures and higher pressures in parts of the UCG cavity favour the formation of methane. UCG offers the possibility for both total and partial capture of the CO_2 as follows.

Total CO_2 capture (i.e. > 90% removal)

The three options for the production of a CO_2 stream from UCG syngas are:

- pre-combustion capture of the CO_2 by absorption (Selexol or amines) from the syngas leaving a hydrogen stream for power generation in gas turbines or fuel cells;
- post-combustion capture in the flue gases using a chemical separation process (amine based);
- oxy-firing of the product gas in a boiler or gas turbine producing only CO_2 and water in the flue gas.

These three methods of CO_2 separation are topics of intense study by the power industry (Farley, 2008), and each is being evaluated for power generation. UCG plant can adopt any of these technologies in dedicated plant or as a co-firing option with other fuels.

Partial CO_2 capture

The composition of syngas suggests CO_2 capture in stages. The first would be the removal of just the CO_2 component of the product gas. The second

© Woodhead Publishing Limited, 2010

Table 13.1 Syngas composition for three stages of CO_2 capture

Constituent	Dry UCG, no capture	CO_2 capture only	Shift + CO_2 capture	Reform + Shift + CO_2 capture
CO_2(%)	34.8	5.0	7.3	6.1
CO(%)	16.5	24.0	0.0	0.0
H_2(%)	31.7	46.3	68.6	93.9
CH_4	17.0	24.7	24.1	0.0
Calorific value (MJ/m^3)	10.9	16.9	16.0	10.1
Gas densities (kg/m^3)	1.04	0.62	0.38	0.20
CO_2 emissions (t/MW h)	0.89	0.52	0.32	0.11

would be the shift conversion of CO to H_2 and the third is partial oxidation or steam reforming of the methane. Table 13.1 (Green, 2007) shows the gas composition that would be achieved at each stage, together with its calorific value and gas density.

The ability to provide both pure hydrogen and hydrogen–methane mixtures with low carbon content are attractive utilisation options for UCG syngas. Estimates by the Lawrence Livermore laboratory (Friedmann, 2008) have shown that the cost of capture of just the CO_2 in the UCG product gas, that is the first column in Table 13.1, would have an energy overhead of about 6%, compared with 10–12% for full CO_2 capture. The resulting gas mixture has a carbon content approaching natural gas and about half the calorific value. This is a better gas for transmission and easier to combust in a gas turbine than pure hydrogen.

Further treatment of the gas by the shift and reforming reactions will progressively reduce the carbon content of the gas. Ultimately, the product gas can be lowered to an almost zero emissions fuel of 94% hydrogen.

13.7 Environmental issues and benefits

The potential environmental impacts of a UCG process are visual and acoustic, and include air emissions, groundwater effects and subsidence. The inherent environmental benefits of UCG are the simplicity of surface plant, the absence of coal storage and transportation requirement, and the ability to remove minor polluting constituents such as SO_x, particulates and heavy metals from the production syngas. UCG also avoids completely the safety issues and the associated support equipment required to send men underground.

Underground coal gasification also scores well in life cycle analysis (Beath *et al.*, 2004) because the energy requirements for drilling are relatively small compared with reactor construction. In addition, the large-scale transporta-

© Woodhead Publishing Limited, 2010

tion of coal and ash are avoided and there are virtually no leaks of methane (as in coal mines or with pipelines) to the atmosphere.

13.7.1 Hydrology and ground water contamination

The gasification cavity is a source of minor gaseous and liquid pollutants and can pose an environmental risk to groundwater from the migration of contaminants beyond the immediate reactor zone. Contaminant risk and product gas quality need to be integrated in prediction models to assess the environmental and economic constraints of potential UCG sites. Except for the early US tests in shallow coal seams, all recent UCG trials have shown no detectable effect on groundwater concentrations in surrounding boreholes.

A UCG project site with the appropriate operational controls should present a very low risk to groundwater, but a full analysis of the groundwater risks and hydrogeological modelling of the site will need to be undertaken for every UCG site. Monitoring of groundwater, throughout operations, and a suitable mitigation response to pollution break-out should also be drawn up as part of the environmental approval in most countries.

The surface plant will have a significant requirement for temporary storage of contaminated water streams. Control of spillages and the use of best practice in the processing of effluent waters will be an important part of site management.

The coal seams used for UCG are usually located well below the water table and the process can be envisaged as taking place in a bubble made up of the connecting pathways in the coal and adjacent seams. The pressure of the UCG process needs to balance the hydrostatic pressure of the coal seam to avoid gas escape or contaminant flow outwards. Water is also essential to the operation of the gasifier. Where insufficient head of water exists above the gasifier, or low permeability in the aquifer prevents water movement, the region above the cavity would dry, possibly resulting in gas losses. Ingress of water is more difficult to control by pressure balance and highly permeable strata in contact with the coal should be avoided.

The traditional emissions of concern are the oxides of sulphur and nitrogen, particulates and heavy metals like mercury. Air emissions controls are already stringent in most countries and the technology of mitigation has been well developed.

13.7.2 Regulatory requirements

The authorisation process for UCG projects varies significantly by country, but the EU has one of the most comprehensive regimes for project approval. It requires a UCG project to obtain a permit under the Integrated Pollution

© Woodhead Publishing Limited, 2010

Prevention and Control (IPPC) regulations to demonstrate that the project has met all the safety and environmental requirements of gasification plant. The permit covers ground and surface water protection as required under the European Groundwater Directive (EGD). The Large Combustion Plant Directive (LCPD) will also apply in most cases.

Strict controls are imposed in many countries on the by-products of combustion produced underground. Most require prediction models to address the close interdependence between combustion control and contaminant fate and transport.

The US Environmental Protection Agency (US EPA) has published (EPA, 1999) requirements for UCG wells which prohibit injection of contaminants and calls for assessments of the effect of UCG on drinking water. The European Groundwater Directive, although not specifically written with UCG in mind, is likely to require that the groundwater surrounding the process is declared permanently unsuitable for other purposes like irrigation or animal consumption, and that the hydrogeology surrounding the process is monitored and modelled.

13.7.3 Licensing requirements

The licensing of UCG, which varies by country, has been one of the greatest causes of uncertainty for UCG projects to date. Most existing license regimes allow access for exploration and production of coal under a national coal mining act or they give authority to extract gas and oil from reservoirs under hydrocarbon legislation. Where the two acts exist, side by side, some authorities are proposing that licensing under both types of legislation will be required. The UK, however, which has both Mining and Petroleum Acts, has recently decided that the production of syngas from coal does not require a petroleum license and UCG will be licensed solely by the UK Coal Authority.

The USA takes the position that the licensing of coal covers all types of energy extraction from coal, and UCG is considered to be no different to conventional or open-cast mining. India, by contrast, has developed a special licensing regime for UCG for designated coal blocks specifically for exploitation by UCG. Other countries such as China, South Africa and Canada appear to have approved UCG trials without major difficulty, although the details of the licensing process have not been well publicised. Queensland, Australia, has overlapping coal and gas tenements (licensing areas) which are currently (2008) causing some difficulty.

© Woodhead Publishing Limited, 2010

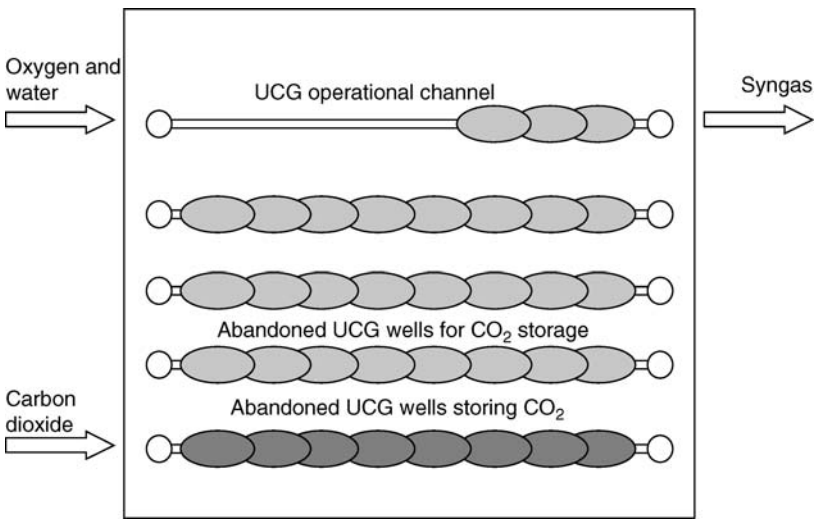
13.7.4 Storage of CO_2 in the vicinity of the UCG process

Underground coal gasification–CCS creates voids in the coal and a highly stressed area above it. Under the right conditions, these voids could be suitable for permanent CO_2 storage. Possible storage receptors for CO_2 are the deeper coal seams in the vicinity of the UCG process and the use of the abandoned cavity and surrounding stressed area.

The UCG gasification process (Fig. 13.10), as it moves through the coal seam, creates voids in the coal seam and stressed areas above, as the cavities are abandoned. After a suitable time during which the gasification cavity returns to equilibrium, areas of high permeability in the coal seam and directly above it are created. The stressed areas (Fig. 13.11), have the potential to store large quantities CO_2 in the dense phase, provided the seam lies at a depth (typically > 700 m) at which supercritical CO_2 can be maintained in its condensed and highly compact form. The gas can also displace methane in virgin coal seams in the process known as enhanced coal bed methane (ECBM) or in nearby saline aquifers, if they exist.

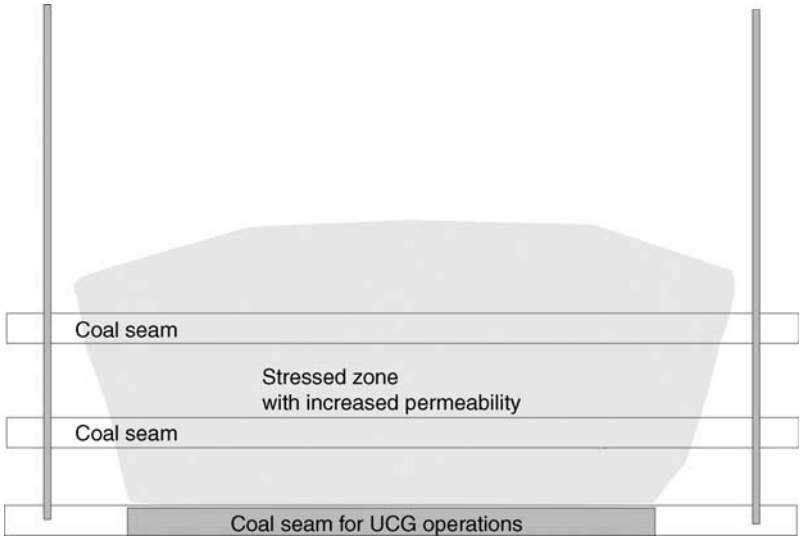
To quote Professor Paul Younger of Newcastle University (Younger, 2008)

> . . . we can use our long-standing knowledge of the response of incumbent strata to longwall coal mining to predict substantial increases in permeability in and immediately above the voids created by gasification. These will still be overlain by low permeability strata forming good 'cap rocks' higher up in the sequence. We are absolutely sure this (UCG–CCS) works. As these engineered zones of high permeability will already be connected to surface power plants by the wells



13.10 Potential sequestration of CO_2 into abandoned UCG cavities.

© Woodhead Publishing Limited, 2010



13.11 Stressed strata above a UCG cavity.

and pipelines used to produce synthesis gas during gasification, they seem to me ideal candidates for permanent sequestration of a large proportion of the carbon dioxide arising.

Laboratory studies have been started at Aachen University (Kempkal *et al.*, 2009) to investigate the storage capacity of coals and chars from in-situ conversion.

An alternative approach for UCG–CCS is under examination in a new EU project led by the Central Mining Institute, Poland to direct the underground reactions towards hydrogen by chemically fixing the carbon in the operating cavity (Rogut and Stein, 2008). The project, which has partners from Poland, Czech Republic, UK, The Netherlands and Germany, will report its findings in 2010.

13.8 Future trends

Underground coal gasification has an opportunity to fill a growing gap in projected coal usage, estimated by the International Energy Agency (Topper, 2008) to be 55% between 2005 and 2030. This represents an increase of 2500–3000 million tonnes per year above the current world production level of about 5000 million tonnes per year. In spite of renewables, nuclear options and the presence of still large supplies of natural gas around the world, coal will remain a source of large-scale energy to the world's economies until the 2050s and well beyond if CCS becomes an effective large-scale solution to carbon emissions from fossil fuels. Coal is in

© Woodhead Publishing Limited, 2010

plentiful supply; the European reserve alone is 130 billion tonnes and the US equivalent, which is the largest in the world, is 240 billion tonnes. Total coal resource of the planet range from 6000 billion tonnes to a recent estimate of 18 000 billion tonnes (Couch (IEA), 2009).

The USA is committed to exploiting coal as a security alternative to Middle Eastern oil. Europe, concerned at its growing dependence on imported oil and gas, is also trying to decrease its dependency on external energy sources. The Council of Energy Ministers has recently confirmed (March 2008) that 'it is necessary to promote environmentally compatible development of the EU's indigenous fossil fuel resources and their efficient and sustainable use through application of advanced technologies' (European Commission, 2009).

The security-of-supply benefits of coal are generally accepted, but the conversion route for power generation, that is IGCC or supercritical thermal plant, is less clear cut. For mined and imported coal, both types of coal plant are being installed in broadly similar numbers, and both are capable of similar plant efficiencies. UCG has the potential advantage of a substantially lower cost of electricity (COE), but is considered by investors to be of higher risk until proven by more extensive commercial operations.

Another question, particularly for the UK and Europe, is whether indigenous coal, in spite of the vast resources that still exist in the EU countries, should be extracted again in large quantities, because of the high CO_2 emissions of coal and the perceived environmental disadvantages of coal and coal mining. Here the benefits of UCG–CCS come into their own, because no coal or ash handling is required at the surface, the network of UCG process wells are temporary and non-intrusive, and local CO_2 capture and storage shows considerable potential.

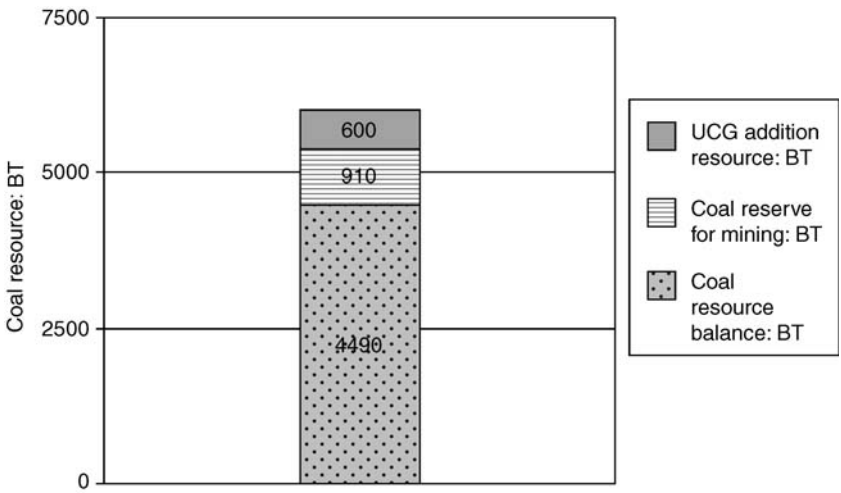
13.8.1 Coal resources for UCG

Calculations of the likely additional coal reserve that UCG would provide based on conservative assumptions for the discount factors of coal resources have suggested that the current declared world coal reserve of around 826 billion tonnes (BP Statistics, 2009) would increase by an additional 491 billion tonnes or 56% with UCG (Fig. 13.12). Coal deposits classed as unmineable in deep seams, near shore and in large lignite deposits, are more likely to be economic with UCG technology. Table 13.2 illustrates the UCG potential in billions of tonnes (BT, column 2) for the major coal-producing countries of the world, assuming that that its UCG reserve is increased by 56% in each case (in practice the increase will vary from country to country). The increase is also expressed as equivalent natural gas in trillions of cubic metres (TCM, column 3) and compared with its current gas reserve (column 4).

© Woodhead Publishing Limited, 2010

Table 13.2 Comparison of existing and additional coal and gas reserves with UCG

	Current proven coal reserves (BP Statistics, 2007)(BT), column 1	Estimated available coal reserve for UCG (from above) (BT), column 2	Potential gas reserves from UCG (as natural gas) (TCM), column 3	Current natural gas reserve 2006 (TCM), column 4
Australia	78.5	44.0	13.2	2.5
China	114.5	64.1	19.2	2.4
Russian Fed.	157.0	87.9	26.3	47.8
India	92.4	51.8	15.5	1.1
USA	246.6	138.1	41.4	5.5
South Africa	48.8	27.3	8.2	0.0
Europe and Asia (excluding Russia)	130.0	72.8	21.8	6.0
Total (coal countries)	867.8	486.0	145.6	65.2



13.12 Estimated UCG share of world coal resources.

The gas reserves of countries like India, Australia and Europe would benefit considerably by the greater conversion of coal to UCG syngas. The breakdown by country in Table 13.2 puts the USA as the greatest beneficiary of UCG, having the potential to increase its equivalent natural gas reserves by a factor of 8.5. Europe and Eurasia combined are in second place and Russia third. China, India and Australia, which have relatively little natural gas, would also find that their gas reserves quadruple with UCG.

© Woodhead Publishing Limited, 2010

13.8.2 Current UCG developments in 2009

Underground coal gasification feasibility studies and demonstrations are underway throughout the world. The lead countries in UCG over the past 5 years have been China, Australia and the UK, but newcomers, such as South Africa, India and Eastern Europe are challenging this position. Furthermore, the USA is now back as an active participant in UCG research and commercialisation. Most of these studies are in the hands of large mining or power companies, who are funding the projects from in-house or other private resources. These studies are confirming that the unit energy cost for UCG is now substantially below the alternatives of natural gas or surface gasification (Beath *et al*., 2004; DTI, 2005; Burton *et al*., 2007).

13.8.3 Asia and South Africa

One of the larger independent companies working on UCG is Xinao Group, China, which has constructed a UCG demonstration plant for methanol production in Inner Mongolia, and has produced its first test results in 2007 using Chinese technology. The company is drawing up plans for a similar plant in Liaoning province that will be 15 times larger to produce 300 000 metric tonnes of methanol per year, for conversion into dimethyl ether, a substitute for diesel fuel (UCG Partnership, 2008). China co-ordinates its UCG programme through the Centre for UCG Research, China University of Mining and Technology. They list 17 trials in mining companies (Liang and Shimada, 2008) and are mostly concerned with the production of hydrogen and the use of roadways as linking structures. A new joint venture between Mongolian mining interests and the Australian company Clean Global Energy project to supply syngas to local power stations has also been announced (Energy Business Review, 2009).

The Indian UCG programme has been led to date by a partnership of two state-run companies, the Oil and Natural Gas Corporation (ONGC) and Coal of India (CIL). UCG became a government priority in 2007, and a number of large Indian companies are undertaking a bidding process for the allocation of UCG coal blocks.

Another newcomer is South Africa, where coal represents 68% of primary energy (Mabadi, 2008) and UCG offers an opportunity to expand the much-needed power capacity. Eskom, the state power company, estimates (Varley, 2008) that 45 billion tonnes of coal, currently considered unmineable in South Africa, may be suitable for UCG. The latest tests in the Majuba coal field are using directional drilling to improve access to the coal field and the trial has been flaring UCG gas since January 2007.

A UCG-fired power generation plant unit of 350 MWe capacity is scheduled to be in operation by 2012. Sasol have also announced (Brand,

© Woodhead Publishing Limited, 2010

2008) the start of a major trial in coal adjacent to the Secunda coal-to-liquids (CTL) plants, with a view to evaluating UCG syngas as a possible fuel for hydrocarbon production in the Fischer Tropsch plant. Sasol, however, at the end of 2009 temporarily suspended the project for economic reasons.

13.8.4 Australia

In Australia, recent efforts began as a small UCG trial at Chinchilla, Queensland in 2000. This has now grown into a major Australian company (Peters, 2008) embarked on the development and production of diesel fuel from UCG. It is planning to build further UCG CTL plants in China, Vietnam and Wyoming. Several other UCG development projects have started in Australia on the strength of this CTL development, and one of these, which is the result of collaboration between CSIRO and a private mining company, has already completed pilot-scale gas production (Davies and Mallet, 2009). Another Australian Company is developing UCG-based power generation at the Kingaroy Power Station, Queensland (Walker, 2009)

13.8.5 Europe

Finally Europe, which was the source of one industrial revolution based on coal, is poised to be the location for another, namely the exploitation of off-shore coal by UCG. Europe has large quantities of off-shore coal in the North Sea (Norway and the UK) in the Mediterranean Sea (Italy) and the Black Sea (Bulgaria and Romania). The on-going UCG activities in Europe include various feasibility studies which are underway in Hungary, Bulgaria and Poland, and the European Commission (EC) is supporting the €3.2 million study of hydrogen production from underground coal, Hydrogen Underground Energy Europe (HUGE) (Rogut and Stein, 2008; Rogut, 2009), described above.

The UK has several on-going regional UCG projects. In Scotland, the coal under the Firth of Forth is a potentially large target for UCG, and a feasibility study has been completed of the geology and well layout, which involves long-reach drilling from the shore to construct the process boreholes (DTI, 2006). Energy Wales has also completed a review of UCG (Sapsford *et al*., 2009) and the University of Newcastle is investigating the potential for UCG in the North-East (Roddy, 2008).

13.9 Conclusion and future trends

Underground coal gasification has made major strides since about 2005. Until then, UCG was seen as an unconventional coal exploitation technology and a longer-term prospect for clean energy when combined

© Woodhead Publishing Limited, 2010

with CCS. The world is beginning to recognise that modern UCG, which is largely based on the technology of the oil and gas industry, is a viable option and available now for large-scale syngas production from coal. Production costs of UCG syngas are highly competitive against the soaring world price of natural gas. Indigenous coal suitable for UCG is often positioned close to where the energy is required.

The 50 field trials undertaken to date have proved that the process works in a wide range of coal types and seam characteristics. Large-scale UCG schemes constructed in a previous era (1980) in the FSU, show that the process can operate at power station scale (> 100 MW).

A suitable coal seam for UCG offers the potential for high return on investment with the right project and careful site selection. The risks are in the areas of coal seam geology, hydrogeology, environmental impact, and in some countries, regulatory uncertainty. The current stock of feasibility studies and demonstration projects leading to first commercial projects is demonstrating that these risks are manageable. Commercial success for the current projects would be the beginning of a major expansion of UCG projects around the world. First commercial movers are currently China and Australia. Recent developments in Wyoming, USA, by BP and the European activity in the UK and Eastern Europe will see Europe and the USA also move ahead in 2009.

In short, the world has recognised that UCG technology, based on technology from the oil and gas industry, actually works, the underground risks are manageable, and there are strong incentives to make the leap from proven pilot trials to commercial schemes. UCG also offers potential new routes to CCS, which are likely to be cheaper and easier to manage. At the beginning of 2010, a total of 11 conditional licenses for offshore UCG in UK territorial waters had been issued.

13.10 Sources of further information

The literature on UCG stretches back to the major UCG research programmes of the 1980s, and vast numbers of publications from that era were published. The proceedings of the annual US conferences, the UCG Symposia (1976–1989) are one important source of information on the early US programme. Publications on UCG virtually ended after 1990 when the US programme ended.

The UK initiative on UCG (1999–2004) produced a series of publications under the DTI publication series, most of which can still be located on the website of the UK Department of Energy and Climate Change (DECC), see http://www.decc.gov.uk/en/content/cms/publications/publications.aspx. A summary document, entitled *The feasibility of UCG in the UK* (DTI, 2004) is available.

© Woodhead Publishing Limited, 2010

Sources of academic literature on UCG can be found in the *Journal of Fuel and Energy*; this contains publication of UCG modelling work by the University of New South Wales and the Indian Institute of Technology. The International Pittsburgh Coal Conference 1999, and 2003–2008, is another valuable source of papers and presentations, particularly the 2008 conference, which held three sessions and a tutorial on UCG.

Finally, the UCG Partnership has hosted four international conferences, held annually since 2005. Members have access to all the presentations on the website at www.ucgp.com.

13.11 Glossary

ASU	air separation unit
BHA	bottom hole assembly
CBM	coal bed methane
CCGT	combined-cycle gas turbine
CCS	CO_2 capture and storage
COE	cost of electricity
CRIP	controlled retractable injection point
CTL	coal to liquids
ECBM	enhanced coal bed methane
EGD	European Groundwater Directive
EIA	environmental impact assessment
EPA	Environmental Protection Agency
EU	European Union
EWG	European Working Group on UCG in Europe
FSU	former Soviet Union
IEA	International Energy Agency
IGCC	integrated gasification combined cycle
IPPC	integrated pollution prevention and control
ITM	ion transport membranes
LCPD	large Combustion Plant Directive
MWD	measure while drilling
SNG	synthetic natural gas
SYNGAS	synthetic gas, and for UCG the product gas of the process
TCM	trillions of cubic metres
UCG	underground coal gasification
UCG-CCS	UCG with CO_2 capture and storage
US EPA	US Environmental Protection Agency

© Woodhead Publishing Limited, 2010

13.12 References

Allam R J, Foster E P and Stein V E (2002), 'Improving gasification economics through ITM oxygen integration', 5th Gasification IChemE Conference, Noordwijk, The Netherlands, April 2002.

Beath A, Craig S, Littleboy A, Rusty M and Mallett C (2004), 'Underground coal gasification: evaluating environmental barriers', CSIRO Exploration and Mining Report. P2004/5.

Blindermann M (2009), 'Ten years of application of the exergy UCG technology', 9th European Gasification Conference, Dusseldorf, March 2009.

Blindermann M S and Jones R M (2002), 'The Chinchilla IGCC project to date. Underground coal gasification and environment', Gasification Technologies Conference, San Francisco, USA, October 2002.

BP Statistics (2009), *BP statistical review of world energy*, BP, June 2009.

Brand J (2008), 'UCG Pilot Study in Secunda, South Africa', Pittsburgh Coal Conference, 2008.

Burton E, Friedmann J and Upadhye R (2007), 'Best Practice in underground coal gasification', Lawrence Livermore National Laboratories, contract no. w-7405-Eng-48, available from https://co2.llnl.gov/pdf/BestPracticesinUCG-draft.pdf.

Cena R, Hill R, Stephens D and Thorsness C (1984), 'The Centralia partial seam CRIP underground coal gasification experiment', Paper to American Institute of Chemical Engineers, November 1984.

Couch G (IEA) (2009), *Underground coal gasification*, CCC/151, see http://www.iea-coal.irg.uk/site/ieacoal/publications/newsletter/current-issue-a/underground-coal-gasification.

Davies B and Mallet C (2009), 'RM1 to Bloodwood Creek', 4th International UCG Partnership Conference, London, February 2009.

DTI (1999), Underground coal gasification – Joint European field trial in Spain project summary, DTI report no 017 1999.

DTI (2004), 'Review of the feasibility of underground coal gasification in the UK', DTI/PUB URN 04/1643..URN 04/1643

DTI (2005), 'Directional drilling in coal', DTI Technology Status Report TSW 024, DTI/Pub URN 05/657.

DTI (2006), 'The feasibility of UCG under the Firth of Forth', Project Summary 382, DTI Publication, URN 06/885.

Energy Business Review (2009), 'CGE enters into $400m coal gasification agreement in Mongolia', *Energy Business Review*, 2 November 2009.

EWG (1989), 'European Working Group. Future Development of UCG in Europe', A comprehensive report to CEC, April 1989.

EPA (1999), 'Class V in-situ fossil fuel recovery wells', US Environmental Protection Agency Report, EPA/816-R-99-014m, September 1999.

European Commission (2009), Council Conclusions on 'Second Strategic Energy Review – An EU energy security and solidarity action plan', Brussels, February 2009.

Farley M (2008), 'A clean future for coal fired power', BCURA Coal Science Lecture, Royal Institution, London,13 October 2008.

Friedman J (2008), 'North American prospects for UCG in a carbon constrained

© Woodhead Publishing Limited, 2010

world', 25th International Pittsburgh Coal Conference, Session 26, October 2008.
Green M (1999), 'UCG first trial in the framework of a community collaboration', Final technical Report, March 1999.
Green M (2007), 'Underground coal gasification – A clean indigenous energy option', *Energy World*, April, P16.
Hesselmann G (2009), 'Oxy-fuel combustion', 9th APGTF Workshop on *Carbon abatement technologies – development and implementation of future UK Strategy*, London, 11–12th February 2009.
Higman C and Van der Burgt M (2003), '*Gasification*', Elsevier Science, ISBN 0-7506-7707-4, 2003.
Jones N, Holloway S, Creedy D and Durucan S (2004), 'UK coal resource for new exploitation technologies', DTI/Pub URN 04/1879 COALR271, November 2004.
Jones R M and Shilling N Z (2004), 'Impact of gas turbine fuel flexibility on IGCC growth', 6th European Gasification Conference, Brighton, May 2004, paper 31.
Kempkal T, Schlüter R, Aeckersberg R, Tian H and Krooss B (2009), 'Carbon dioxide storage in in situ converted coal seams – experimental studies', UCG Partnership Conference, London, February 2009.
Kelsall G (2004), 'Industrial gas turbine combustion system for biogas applications', 6th European Gasification Conference, Brighton, May 2004, paper 021.
Khadse A, Mahajani S, Qayyumi M and Aghalayam P (2006), 'Reactor model for the underground coal gasification channel, *Internation Journal of Chemical Reactor Engineering*, 4, A37.
Kreynin E V (2009), 'Can the underground gasification of coal seams be the industry technology? The Russian experience', 4th UCG partnership International Conference, London, February 2009.
Liang J (2003), 'Overview of the Chinese programme on UCG', DTI Workshop on UCG, China University of Mining and Technology, October 2003.
Liang J and Shimada S (2008), 'UCG Activities in China', Pittsburgh Coal Conference, 2008.
Mabadi M (2008), 'Mobilizing Africa into green economy', 3rd UCG Partnership International Conference, London, February 2008.
McCracken R (2008), 'Mining without mines: UCG', *Energy Economist*, P16, 31, March.
Muir G (2008), 'Drilling sideways for coal bed methane', Presentation to Geo-Drilling 2008, April 2008.
Oxburgh R (2009), 'CCS: Where are we today?', *Carbon Capture Journal*, January, 8.
Perkins G and Sahajwalla V (2006), 'Numerical study of the effects of operating conditions and coal properties on cavity growth in underground coal gasification', *Journal of Energy and Fuels*, 20(2), 596–608.
Peters J (2008), 'Chinchilla project from start to liquid, 3rd International UCG Partnership Conference, London, February 2008.
Roddy D (2008), 'Linking UCG to CCS and the downstream implications', 3rd International UCG, Partnership Conference, London, February 2008.
Rogut J and Stein M (2008), 'Hydrogen oriented underground coal gasification for

© Woodhead Publishing Limited, 2010

Europe', 25th International Pittsburgh Coal Conference, Session 26, October 2008.
Rogut J (2009), 'HUGE project – the innovative content of UCG', 4th International UCG Partnership Conference, London, February 2009.
Sapsford D, Turner M, Brabham P, Griffiths A, Marsh R and Williams K (2009), 'The potential for underground coal gasification in Wales', 4th International UCG Partnership Conference, London, February 2009.
Singleton A and Pilcher R (2007), 'The commercialization of ISE's steeply dipping bed UCG technology', 2nd International UCG Partnership Conference, London, February 2007.
Sury M (2004), 'Review of environmental issues of underground coal gasification', DTI project report, COAL R272, DTI/PUB URN 04/1880.
Thorsness C, Hill R and Britten J (1988), 'Execution and performance of the CRIP process during the Rocky Mountain 1 UCG field test', 14th Annual Underground Coal Gasification Symposium 1988.
Topper J (2008), 'Keynote address by MD IEA Clean Coal Centre to CoalGen Europe 08, Warsaw, July 2008.
UCG Partnership (2008), *Newsletter of the UCG Partnership*, No. 10, October 2008.
Varley J (2008), 'Majuba plans air blown IGCC – but not as we know it', *Modern Power Systems*, January 2008, 23.
Walker L (2009), 'The new power for Australia – cleaner coal', Paper presented to the International Conference on UCG, London, March 2009.
Wolf K H (2006), *The interaction between underground coal fires and their roof rocks*, Doctoral thesis, Delft, ISBN-10: 90-9020939-5.
Yerostigaz (2008), 'Underground coal gasification in the Republic of Uzbekistan', available from http://www.lincenergy.com.au/yerostigaz.php.
Younger P (2008), Letter to the Geological Society, 27th March 2008.

© Woodhead Publishing Limited, 2010

14

Development and application of carbon dioxide (CO_2) storage for improving the environmental impact of advanced power plants

B. Mc PHERSON, The University of Utah, USA

Abstract: This chapter reviews geological storage of power plant CO_2 emissions, including how emissions are captured, and the energy penalty imposed by that capture and subsequent injection for storage. Basic concepts of CO_2 flow and transport are outlined, and the geologic 'trapping mechanisms' that hold CO_2 in place within rock formations are defined. Storage site options are compared, including deep saline formations, hydrocarbon reservoirs and coal seams, and associated site selection criteria. Monitoring technologies and protocols are also discussed. Alternatives to geologic carbon storage are presented, as well as obstacles that must be overcome for any carbon abatement to be embraced by industry.

Key words: CO_2, carbon sequestration, climate change, global warming.

14.1 Introduction

Anthropogenic carbon dioxide (CO_2) is considered by many to be a major contributor to global warming. Sequestration of power-plant-generated CO_2 by injection into deep saline groundwater aquifers and hydrocarbon reservoirs is under testing as a possible alternative for the reduction of excessive CO_2 in the atmosphere. The purpose of this chapter is to introduce fundamental concepts associated with storage of CO_2 emissions underground, also known as geologic carbon sequestration. The concept is to capture CO_2 emissions from power plants and other point sources and store or sequester them deep underground, just as nature has stored natural gas and other fluids for millions of years. Fundamental topics of interest in sequestration research have concerned not just scientific and technical aspects, but practical concerns such as safety issues, economic feasibility,

© Woodhead Publishing Limited, 2010

and assessments of CO_2 storage capacity globally and in specified regions. Section 14.13 of this chapter, entitled 'Sources of further information and advice,' summarizes many appropriate references on these topics.

The chapter begins with a general discussion about power plant emissions, how emissions are captured, and the energy penalty imposed by that capture and subsequent injection for storage. Basic concepts of CO_2 flow and transport are outlined, and the geologic 'trapping mechanisms' that hold CO_2 in place within sequestration rock formations are defined. The chapter then compares storage site options among deep saline reservoirs, oil and gas reservoirs, and coal seams, including site selection criteria. Monitoring technologies and protocols are also discussed. The chapter concludes with some details about alternatives to geologic carbon storage, as well as obstacles that must be overcome for any carbon abatement to be embraced by industry.

14.2 Premise: capture and sequestration of CO_2 from power plants

The first step in the process of geological sequestration is the capture of CO_2, which is perhaps one of the most difficult aspects because of the high cost of separation. Electric power plants fed by 'fossil fuels' such as coal emit flue gases that typically contain up to 15% or more CO_2, and this CO_2 must be chemically separated from the remainder of the flue gas composition, commonly nitrogen, water vapor, nitrogen oxides (NO_x), sulfur dioxide (SO_2), mercury and particulates. Of course, the raw flue gas could be injected, but in the USA such injection would most likely fall under the most strict regulations associated with hazardous waste. For regulation of injection and storage of pure CO_2, the US Environmental Protection Agency recently (in 2008) proposed formal regulatory requirements, and the proposed rule was still under consideration when this chapter was written.

Power plant emissions of CO_2 may be separated and captured either before or after fuel combustion. Separation after combustion is more straightforward than pre-combustion capture. The most general separation procedure is an amine-based 'filter' that absorbs the CO_2 from the raw flue gas passed through it. The CO_2-laden amine compound will release nearly pure CO_2 if heated to higher temperatures, and typically at least some of the amine can be used again (recycled). While this is fairly simple in concept, a critical limitation is that such amine 'scrubbers' may also absorb some H_2S from the flue gases, and even trace amounts of H_2S in the separated CO_2 must be factored into regulatory constraints. If pure oxygen is used in the combustion process rather than air, also known as 'oxy-combustion', much

© Woodhead Publishing Limited, 2010

less flue gas is produced, and that flue gas is especially enriched with respect to CO_2 and can greatly simplify the separation process.

Another form of separation is that from synthetic gas, or 'syngas', produced by pre-combustion reaction of coal with steam and oxygen under high pressure, called 'coal gasification'. While both coal gasification and oxy-combustion processes simplify separation and reduce associated costs, both require a large capital investment relative to traditional pulverized coal power plants. Rubin (2008) reviews CO_2 capture and transport issues in detail.

After separation and capture, in most cases it is best to raise the temperature and pressure of the CO_2 to match reservoir conditions for injection. For deep reservoirs, this will require compression of the CO_2 from atmospheric conditions to 2000 psi or more. One upside of this compression is that the density of the CO_2 is increased to supercritical or liquid, providing for more storage capacity. One downside is that such compression requires power, ultimately resulting in a parasitic energy load on the power plant and, of course, associated CO_2 emissions. Adding this power requirement on top of the power required for separation, power plants that utilize carbon capture and storage (CCS) technologies may require up to 40% more energy than equivalent plants without CCS, depending on the specific technologies used. For example, a typical integrated gasification combined-cycle (IGCC) plant without carbon capture and storage (CCS) is estimated to maintain around 37% net operating efficiency, while an IGCC plant with CCS is estimated to maintain a reduced efficiency of around 32%. A comprehensive review of plant efficiency related to CCS is beyond the scope of this chapter, inasmuch as it includes a huge number of different technology permutations. However, the reader is referred to Beer (2007) for a detailed discussion of electric power generation efficiency related to CCS and other environmental factors.

14.3 Fundamentals of subsurface CO_2 flow and transport

Ideally, injected CO_2 will migrate from injection wells through a geologic formation to remote storage reservoir sites, and remain isolated from the atmosphere in perpetuity. The primary processes of CO_2 sequestration may be considered as analogous to 'freeways and parking lots' – it is essential to consider the properties affecting CO_2 transport along geological flow paths (freeways) and the storage potential in specific geologic reservoirs (parking lots). At issue are the geologic, hydrologic, and geochemical controls of CO_2 transport and storage.

With respect to flow and transport specifically, CO_2 may migrate through

© Woodhead Publishing Limited, 2010

Table 14.1 CO_2 transport properties/parameters and selected references

Parameters	Selected reference
Mobility ratio	Lindeberg and van der Meer, 1996
Relative permeability	Parker *et al.*, 1987
Capillary pressure	Parker *et al.*, 1987
Viscosity/density/enthalpy	Weir *et al.*, 1996
Damkohler number	Ingebritsen and Sanford, 1998
Peclet number	Ingebritsen and Sanford, 1998
Dilution index	Kitanidis, 1994

rock formations in three different forms: (i) in solution in groundwater ($GW/CO_2^{solution}$); (ii) as a separate gas phase (CO_2^{gas}); or (iii) as a separate supercritical phase ($CO_2^{supercrit}$), which exhibits properties of both gases and liquids. CO_2 in solution may coexist with either CO_2^{gas} or $CO_2^{supercrit}$, which occur as separate phases that depend on pressure and temperature conditions. The three different forms of CO_2 respond to pressure and temperature in different ways. However, analogous behavior by oil and natural gas provide some insight.

$GW/CO_2^{solution}$ behaves much like groundwater without CO_2 – a single-phase flow and coupled dissolved component analysis could be used for this type of CO_2 transport alone. This $GW/CO_2^{solution}$ is more dense than normal groundwater, and will sink and travel along the bottom of an aquifer. Its viscosity is not much different than normal groundwater and thus its mobility will be similar, for example its mobility ratio (Table 14.1) will be similar.

CO_2^{gas}, coexisting with groundwater or $GW/CO_2^{solution}$, is a true multiphase system, similar to natural gas found in aquifers. Likewise, supercritical CO_2 exists as a separate phase. Important properties associated with CO_2 transport are listed in Table 14.1.

Two processes that set CO_2 transport apart from other types of transport are gravity segregation and viscous fingering. Both of these processes are caused by differences in properties between groundwater and CO_2: gravity segregation is caused by density contrasts, and therefore buoyancy differences, while viscous fingering is caused by contrasts in viscosity and mobility. Some insight to these processes is gained from petroleum migration studies and previous CO_2 transport studies (Tchelepi, 1994; Lindeberg and van der Meer, 1996; McPherson and Bredehoeft, 1999; Han and McPherson, 2009).

Several groups have simulated regional scale flow and transport of CO_2, including van der Meer (1992; 1993; 1996), Gunter *et al.* (1996), Lindeberg and van der Meer (1996), and Han and McPherson (2009). Results discussed by Lindeberg and van der Meer (1996) and by Han and McPherson (2009)

© Woodhead Publishing Limited, 2010

suggest that gravity segregation is successfully modeled at the regional scale. Viscous fingering is only successfully modeled using high-resolution grids. Together, viscous, gravity and capillary forces act together to create channels of preferred flow in higher permeability materials, sometimes with large by-passed zones in between (Orr, 2004). Detailed studies of and bibliographies related to viscous fingering may be found in van der Meer (1992; 1993; 1996) and Gunter *et al.* (1996).

14.3.1 Effects of rock fractures on flowpath

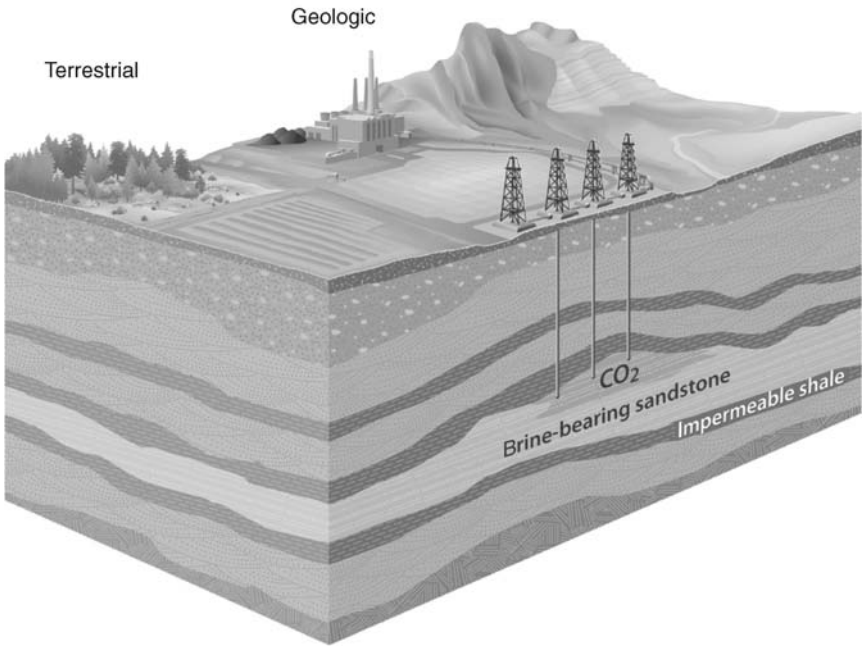
Ideally, the flow path in sedimentary basins would be fractured, maximizing velocity and minimizing the potential for mineral precipitation and associated permeability reduction. On the other hand, the intended storage area of an aquifer, ideally, would trap CO_2 by such mineral precipitation. Transport of CO_2 along the preferred flow paths would be relatively quick, especially when the paths are composed of open fractures, with much slower transfer of CO_2 from these paths to the surrounding by-passed zones (Orr, 2004). Additionally, if the material around the preferred flow paths is composed of much finer pores, supercritical CO_2 will have difficulty penetrating the tighter porous rock matrix where storage will take place, especially because capillary forces may limit penetration. If the CO_2 is dissolved in groundwater, diffusion will be the primary mechanism for transfer to the surrounding country rock if the permeability contrast is not large. Thus, the time-scales for mineral precipitation will be very different in the fast paths and the by-passed zones because the supply of reactants will be controlled by different processes (Gaus *et al.*, 2008).

14.4 Fundamentals of subsurface CO_2 storage

Subsurface storage of liquids and gases has become very common. Perhaps the most common form of storage is natural gas storage (NGS). For NGS, natural gas is injected in the subsurface when demand is least and stored until demand is higher and demand exceeds that available from surface facilities. The storage medium target is typically a geologic rock layer that is highly porous and capped by a low-permeability seal layer such as mudstone, shale or salt (Fig. 14.1). The USA uses nearly 400 NGS facilities in the lower 48 states. Another traditional storage concept is 'aquifer storage and recovery' (ASR), a practice much like NGS, but potable water supplies are stored in subsurface reservoirs until prolonged dry weather conditions warrant tapping those reservoirs.

Both NGS and ASR are temporary storage methods. An example of a permanent storage application is injection and storage of salt water (brines) produced in oil and gas fields; typically, the excess brine produced with oil

© Woodhead Publishing Limited, 2010



14.1 General or 'traditional' fluid storage in the subsurface: injection in porous rock layers immediately below low-permeability seal layers. Also indicated is terrestrial sequestration at the earth's surface.

and gas is re-injected into non-hydrocarbon-bearing formations in the same field. Because the water is not potable and is not fit for irrigation, injection in the deep subsurface is common.

Injection and sequestration of CO_2 in subsurface reservoirs is similar to produced water storage in that it is intended to be permanent, but it is fairly distinct because of CO_2 properties – lower values of density and viscosity create a propensity for CO_2 to migrate towards the surface. Therefore, extra care must be exercised to minimize migration from the intended storage zone and the associated risks. Target rock formations for geologic carbon sequestration include deep saline formations, unmineable coal seams, oil fields and natural gas fields.

When CO_2 moves into the intended storage area or reservoir, the same transport processes discussed above are applicable. As CO_2 migrates through an aquifer, whether in the intended storage area or in the flowpath to that area, various trapping mechanisms may occur, as summarized next.

© Woodhead Publishing Limited, 2010

14.4.1 Aqueous or solubility trapping

Aqueous trapping refers to the trapping of CO_2 by forming a groundwater plus CO_2 solution, leading to carbonic acid and dissociated ions (Gaus *et al.*, 2008). Solubility is controlled by salinity and pressure/temperature conditions.

14.4.2 Hydrodynamic or stratigraphic trapping

Orr (2004) and Koide *et al.* (1995) discuss what is called hydrodynamic trapping: CO_2 moving into zones of high storage (porosity) and permeability, surrounded and trapped by zones of low permeability that restrict CO_2 escape.

14.4.3 Chemical or mineral trapping

This type of trapping refers to the formation of mineral precipitates by reaction between rock and CO_2. It offers the greatest potential for increasing CO_2 sequestration capacity while also immobilizing CO_2 for longer timescales (Gaus *et al.*, 2008). The most fundamental aspect of this mechanism is the formation of carbonic acid when groundwater and CO_2 mix. This acid groundwater dissolves carbonates and silicates, producing bicarbonate ions that tend to neutralize acidity. When the groundwater subsequently becomes more alkaline, calcium carbonate may precipitate, reducing pore space and permeability. Carbonate precipitation consumes bicarbonate ions, rendering the groundwater more acidic, and so on.

The most fundamental reactions are

$$CO_2(g) + H_2O = H_2CO_3, \qquad \text{or carbonic acid formation, and}$$

$$H_2CO_3 = H^+ + HCO_3^-, \qquad \text{or bicarbonate ion formation.}$$

Carbonic acid will dissolve carbonate minerals

$$CO_2 + H_2O + CaCO_3 \rightarrow Ca^{++} + 2HCO_3^-$$

as well as silicate minerals (Berner and Lasaga, 1989)

$$2CO_2 + H_2O + CaSiO_3 \rightarrow Ca^{++} + 2HCO_3^- + SiO_2$$

While these examples are the most basic, they are the building blocks needed to evaluate the fundamental processes such as 'reaction potential'. Some other simple reactions that are common and also extremely important in terms of permeability could also be examined. For instance, dissolution of some aluminosilicates will produce carbonate precipitation and perme-

© Woodhead Publishing Limited, 2010

ability-reducing clays. Gaus *et al.* (2008), Fyfe *et al.* (1996) and Siefritz (1990) all summarize the reactions pertinent to the CO_2 sequestration problem. Among key goals for specific sites is to identify the most important reactions for the flow rates, pressure/temperature conditions, and lithologies present for those sites and for other regional scale aquifers, categorically.

14.4.4 Residual gas or phase trapping

A fluid system is called 'multi-phase' when at least two distinct liquid phases are in place, especially water or brine with a non-aqueous liquid such as oil and water or CO_2 and water. When these distinct fluids come into contact, cohesive forces act on molecules at the interface between the phases. It is typical for an imbalance in the cohesive forces to exist, resulting in surface tension at the interface. This surface tension may cause the interface to contract to as small an area as possible. Such interfacial surface tension may trap CO_2 in pores, especially if fluid saturations are low. The threshold saturation at which CO_2 becomes trapped in this manner is called the 'irreducible saturation' of CO_2, and is a key concept for defining 'residual gas trapping.' The amount of CO_2 that can be trapped by this mechanism is a function of the rock's pore network geometry, pressure, temperature and other fluid properties.

14.5 Enhanced oil/gas and coalbed methane recovery

Carbon dioxide has been injected for enhanced oil recovery (EOR) since the 1950s. For example, the first carbonated water floods were tested as early as 1951, and slugs of pure CO_2 for oil displacement were tested as early as 1963. CO_2 flooding for EOR (CO_2-EOR) is proven to extend the life of mature oilfields, and is reported to be profitable in the vast majority of projects. In the USA, oil that is potentially producible by CO_2-EOR methods is estimated to be at least approximately 200 billion barrels (32 billion m^3) of 350 billion barrels (56 billion m^3) remaining in US oil reserves. The Permian Basin of New Mexico and Texas is most active in terms of CO_2-EOR, yielding about 80% of oil produced by the method in the USA, roughly 180 000 barrels of oil per day. At least nine other states maintain active CO_2-EOR projects or are planning them: California, Colorado, Kansas, Louisiana, Michigan, Mississippi, Oklahoma, Utah and Wyoming. With the possibility of exploiting CO_2-EOR, great economic incentives are unfolding to make CO_2-EOR a standard component of carbon sequestration efforts.

Regarding fundamentals about CO_2-enhanced petroleum recovery, Van der Meer (1992) discusses scales of CO_2 transport and the different processes that apply: (i) microscopic or pore scale, dominated by molecular diffusion

© Woodhead Publishing Limited, 2010

and dispersion; (ii) macrascopic or well scale, dominated by mechanical mixing processes; and (iii) the megascopic or aquifer scale, dominated by gravity segregation and viscous fingering.

14.6 CO_2 storage in deep saline formations

An economically sound approach to CO_2 sequestration is to identify storage sites as close as possible to CO_2 point sources such as fossil fuel power plants. Subsurface saline groundwater aquifers are highly sought after candidates because they ostensibly possess the greatest capacity compared to other sinks (National Energy Technology Laboratory, 2008). Such saline aquifers exist throughout great portions of the continents, improving the chance that the CO_2 sources are near the storage sites and minimizing costs of engineering and transport. These formations tend to be deep (1–5 km or more), and thus increase the costs of compression and injection. However, in most cases many risks are reduced, including risk of leakage to the surface, simply because the storage zone is farther from the surface.

14.7 Comparison of storage options: oil/gas versus coal versus deep saline

According to the National Energy Technology Laboratory (2008), the potential CO_2 storage capacity of North American oil and gas reservoirs is at least 140 billion tons, the minimum storage capacity of unmineable coal seams is over 180 billion tonnes, and the minimum capacity of deep saline rock formations is over 3600 billion metric tonnes. Thus, consideration of potential capacity alone suggests that deep saline formations are a clear choice for CO_2 storage. In addition to these differences in forecasted capacities, the three options also pose quite different technical challenges and benefits.

With respect to unmineable coal seams, these formations are desirable for CO_2 storage because coals absorb CO_2 to varying degrees, trapping the CO_2 even more effectively than other rock types in general. However, accompanying such adsorption can be shrinking or swelling of the coal, ultimately affecting both the injectivity (ability to inject) and ultimate capacity. Also, coal cleats (cleavage or fractures) pose complications because of the sometimes unpredictable flow pathways they create. On the other hand, these coals often hold methane (natural gas) in place, and if this methane can be produced and effectively replaced by CO_2, the added value can be very lucrative.

With respect to deliberate storage of CO_2 in oil and gas fields, many offer the benefits of surface infrastructure for CO_2 delivery and injection,

© Woodhead Publishing Limited, 2010

providing clear practical benefits. Enhanced oil and gas recovery can add great value for the producer, while still providing net CO_2 storage. Also, many of these fields are located in or near communities that are accustomed to such industry operations and thus public support tends to be strong. On the other hand, a risk often cited is abandoned wells that may or may not be plugged effectively and thus offer a leakage pathway to the surface.

Research on CO_2-EOR and CO_2-enhanced gas recovery (CO_2-EGR) continues in earnest today, and new research on deliberate geologic CO_2 storage in tandem with such hydrocarbon recovery is expanding rapidly. A goal of most field operators is to re-produce and recycle as much CO_2 as possible. However, in most cases of CO_2-enhanced recovery, as much as 50% or more of CO_2 injected is left behind and sequestered. Another factor to consider is that produced hydrocarbons will emit more CO_2 when combusted. Thus, one specific research topic associated with enhanced oil or gas recovery and concomitant sequestration is the 'penalty' or net reduction of sequestration associated with CO_2 emitted from the enhanced oil or gas produced and its subsequent combustion.

With respect to storage in deep saline formations compared to oil/gas/coal formations, the saline reservoirs tend to be deeper and thus fewer wells penetrate these formations, at least in general. This leads to reduced leakage risks due to abandoned wells; risk of leakage to the surface is also reduced because of the greater distance between the storage zone and the surface. The greater extent and aggregate thickness of these saline formations also leads to the much higher storage capacity forecasted by the National Energy Technology Laboratory (2008). However, greater depths translate to higher costs of both injection and monitoring, in general.

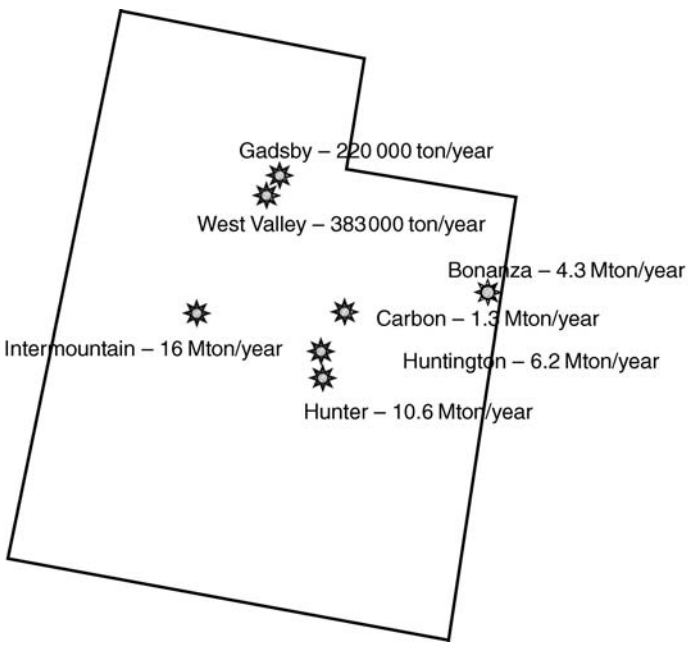
Perhaps the most compelling geologic CO_2 storage option is injection and sequestration in deep saline formations directly underneath active oil and gas fields. This option offers the advantages of both deep saline and oil/gas reservoirs. Additionally, if CO_2 were to leak from a deep saline formation into an oil reservoir above, not only would the oil in the reservoir absorb that CO_2 (solubility of CO_2 in oil is over 30 times greater than CO_2 solubility in brine), but the active production stream would serve as a monitoring tool in addition, to complement of other monitoring technologies. Other advantages of this particular paradigm are discussed by Han and McPherson (2009).

14.8 General site selection criteria

Selecting a site appropriate for geologic sequestration requires consideration of several issues, as listed below.

© Woodhead Publishing Limited, 2010

- Depth of the target formation – deeper formations are better for storage, in general, because they are farther away from the surface.
- Degree of 'stacking' in stacked system – 'stacking' refers to alternating layers of reservoir layers and seal layers; if multiple 'stacks' exist, then any leakage from one reservoir will affect the next reservoir in the stack.
- Vertical and lateral distance of underground sources of drinking water (USDWs) – the farther away from USDWs the better, to minimize risks.
- Presence of existing (natural) CO_2 – if natural CO_2 is already in place within a rock formation, it is more likely that the formation will also hold newly-injected anthropogenic CO_2.
- Mitigation options – sites that maximize mitigation options, such as additional land availability for siting new injection or production wells (to control reservoir pressure, for example), are preferred.
- Land availability for adequate design and distribution of injection, monitoring and mitigation wells is also a key design requirement.
- Surface features and population – location away from major population centers and other critical surface features, such as National Parks, is preferred.
- Storage capacity – higher storage capacity is better. As a specific example, consider that the sum of CO_2 emissions from coal-fired power plants in Utah (Fig. 14.2) is approximately 40 000 000 tons per year. The



14.2 Distribution of major coal-fired power plants in Utah and their respective annual CO_2 emissions.

© Woodhead Publishing Limited, 2010

Carbon sequestration atlas of the United States and Canada by the National Energy Technology Laboratory (2008) indicates that the estimated total subsurface storage capacity of all candidate rock formations in Utah is around 2 000 000 000 tons, suggesting that the equivalent capacity in Utah is 50 years of its emissions (2 000 000 000 tons divided by 40 000 000 tons/year). More storage capacity, thus, translates to more years of emissions equivalent.

The last aspect in this list, storage capacity, is one of the most important criteria for site selection. This topic is also one of the most critical areas of interest to CO_2 emitters and other stakeholders subject to evolving CO_2 sequestration policy and regulatory frameworks. The following section discusses this topic in a more general context.

14.9 Emissions versus potential subsurface storage capacity

Perhaps one of the first exercises undertaken by the scientific community was to evaluate the overall capacity of different forms of CO_2 storage, including geologic sequestration. Specifically, several agencies and organizations, including the International Energy Agency, the US Department of Energy and its National Energy Technology Laboratory, the US Geological Survey, and many other organizations and individuals, have either independently or collaboratively estimated subsurface storage capacity at national and international scales. One recent example for North America is the *Carbon sequestration atlas of the United States and Canada* assembled and published by the National Energy Technology Laboratory (2008) and the US Department of Energy. This atlas includes a summary of the total emissions of CO_2 per year in North America, and an estimate of the total potential CO_2 subsurface storage capacity for North America. The reported minimum total emissions of just stationary CO_2 sources in North America is approximately 3.6 billion tonnes of CO_2 per year, and the total storage capacity approaches 4000 billion tons. Dividing the total potential storage capacity by the current emissions rate suggests that over 1000 years equivalent of current North American CO_2 emissions could be injected and stored in its subsurface. Of course, this estimate applies only if emissions rates do not change and if required infrastructure is installed for all sources. However, the storage capacity estimated is a minimum value, and thus this estimate of capacity in emission-years equivalent is perhaps conservative regardless.

© Woodhead Publishing Limited, 2010

14.10 Sealing and monitoring to ensure CO_2 containment

Some key goals of monitoring CO_2 storage sites are to ensure CO_2 containment, confirm efficacy of trapping mechanisms, and verify storage capacity and associated carbon credits if applicable. Monitoring survey design, deployment, frequency and associated storage reservoir simulation are intended to evaluate how well a specific sequestration project meets or exceeds performance targets stipulated by national and international guidelines. Additional monitoring goals are to track CO_2 well injectivity, verify abandoned well veracity, and to assist with risk assessment and mitigation. Baseline monitoring activities are usually designed to elucidate the geologic, hydrogeochemical, isotopic and other physical conditions prior to injection. Such baseline data are then compared to results of repeat and continuous monitoring surveys conducted after injection to forecast the ultimate fate of CO_2 in the subsurface for different conditions.

As described in a recent report published by the National Energy Technology Laboratory (2009), monitoring technologies vary in spatial coverage as well as spatial and temporal resolution. Among the most common direct monitoring technologies are CO_2 soil flux measurements, water chemical composition sampling and analyses, isotopic tracers in groundwater and in injected CO_2, and mineral composition analysis of rock surfaces exposed to the injection stream. Among the most common indirect monitoring technologies to detect changes in fluid composition and distribution in the subsurface are seismic imaging, electrical conductivity surveys, electromagnetic surveys, and gravity surveys. A combination of technologies is typically applied at an injection site.

At the time this chapter was written, the US government was seeking to clarify rules and regulations associated with monitoring of CO_2 storage sites. Specifically, the US Environmental Protection Agency recently proposed a set of rules for underground injection control associated with subsurface sequestration ('Class VI Injection Well'). While these new rules are still under consideration, a primary objective is to regulate containment of CO_2 and this requires 50 years of post-injection monitoring.

14.11 Alternatives to geologic storage

Other forms of sequestration include terrestrial sequestration, defined as CO_2 absorbed by vegetation and soils (e.g. surface depicted in Fig. 14.1), and mineralization, generally defined as engineered chemical combinations of CO_2 with salts and other substances (cations) to form solid-state minerals. Mineralization is fairly simple in concept: combine CO_2 with cations such as Ca^{2+} and Mg^{2+} to create carbonate minerals. Such cations

© Woodhead Publishing Limited, 2010

are readily available in seawater or oilfield brines, but the chemical reactions that create such minerals are extremely slow. Catalysts are possible (Bond *et al*., 1999), but tend to be very expensive. Terrestrial sequestration methods may effectively 'buy time' (McCarl and Sands, 2007) until the development of new technologies makes larger offsets in CO_2 emissions possible.

A form of sequestration not discussed in detail in this chapter is oceanic sequestration; the majority of anthropogenic CO_2 emissions are actually removed from the atmosphere naturally through uptake by the oceans, but the rate of that uptake is far exceeded by the emissions rate. Some authors have suggested injection of CO_2 in the deep ocean to augment its natural uptake (Ohsumi, 1995; Haugan and Alendal, 2005), but deterrents to this include negative impacts of ocean acidification caused by CO_2 dissolution in seawater (Canadell *et al*. 2007).

14.12 Future trends

The future of sequestration is far from certain at this time. For commercial, large-scale geologic storage to be carried out by industry, it may be necessary to impose laws that require sequestration, and to create financial incentives to facilitate it, or both.

In recent years, many organizations have estimated the cost of commercial-scale geologic sequestration. These estimates range from US $5 to US $80 per ton, depending on whether capture costs are included. Also factoring into these estimates are many other variables, including efficiency of capture, cost of fuel (natural gas, coal), cost of steel, engineering costs, compression costs, and others. Such high costs will preclude commercial geologic sequestration without financial incentives. Otherwise, the cost of electricity would likely increase two-fold or more; past history suggests that such rate hikes lead to widespread objections by rate-payers.

The Federal American Recovery and Reinvestment Act (ARRA) was signed into law on 17 February 2009, and includes many provisions intended to incentivize commercial sequestration, including sequestration tax credits, qualified energy conservation bonds, and new research funding to support sequestration proliferation specifically. The IRS Sequestration Tax Credit would include $20/ton for 'qualified carbon dioxide' captured at qualified facilities and sequestered in deep saline formations, or $10/ton for 'qualified carbon dioxide' used as tertiary injectant in enhanced oil or gas recovery operations. However, these credits are limited in that they 'sunset' or end at the limit of 75 million tons of CO_2 captured and injected.

The US Department of Energy is also disbursing several billion dollars of funding for research, development and field demonstration work, including over $1.5 billion alone for demonstrations of capture and sequestration associated with large-scale industrial CO_2 sources. Finally, energy con-

© Woodhead Publishing Limited, 2010

Table 14.2 Selected studies of CO_2, for enhanced oil recovery, and studies of technical and practical aspects of geologic sequestration of CO_2, including modeling of flow and transport processes

Topic	References
• Fundamentals of CO_2 sequestration and its relationship to climate change	Lackner, 2003 Pacala and Socolow, 2004
• First carbonated water floods	Martin, 1951 Saxon *et al.*, 1951
• Slugs of pure CO_2 for oil displacement	Holm, 1963
• CO_2 sequestration in reservoirs, including enhanced oil/gas recovery	Gunter *et al.*, 1997 DeMontigy *et al.*, 1997 Koide *et al.*, 1993 Orr, 2004
• Economic feasibility of CO_2	Hendriks and Blok, 1995
• Sequestration	Gunter *et al.*, 1996 Bergman *et al.*, 1997 Holt and Lindeberg, 1997
• Safety concerns	van der Burgt *et al.*, 1992 Holloway, 1997a; 1997b
• Potential global CO_2 storage	Hendriks and Blok, 1993 Hendriks and Blok, 1995
• Potential CO_2 storage by region	Bergman *et al.*, 1997 van der Meer, 1992 Holloway and Savage, 1993 Krom *et al.*, 1993
• CO_2 rapping mechanisms	Bachu *et al.*, 1994 Koide *et al.*, 1995
• Modeling of fundamental CO_2 flow and transport processes in aquifers	Weir *et al.*, 1996 van der Meer, 1992; 1996 Holt *et al.*, 1995 Law and Bachu, 1996 Doughty and process, 2004
• Vertical flow and escape through seals	Lindeberg, 1997; Gunter *et al.*, 1993
• Vertical convection; Rayleigh number analysis	Lindeberg and Wessel-Berg 1997
• Simulation of geochemical processes, e.g. precipitation and dissolution	Gunter *et al.*, 1993; Gunter *et al.*, 1996
• Natural geologic CO_2 sources and storage reservoirs	Pearce *et al.*, 1996

servation bonds are also now available as part of the ARRA, with over $2.4billion allocated for use within 3 years (2009–2012).

At the time this chapter was written, over 30 geologic CO_2 sequestration field tests were at various stages of design and deployment in the USA. An additional 25 or more are on-going or slated for deployment soon in other countries. These do not include new demonstrations associated with recent new ARRA (stimulus) funding, which promises many more large-scale

© Woodhead Publishing Limited, 2010

projects. While research and development appears to be keeping up with the schedule of demonstration and deployment, issues of liability for sequestration, pore- and CO_2-ownership, regulatory frameworks and federal versus state jurisdiction are still not definitive. While such legal and regulatory barriers are significant, thus are all being addressed at the state and national levels. Perhaps the most significant barrier to commercial sequestration as a greenhouse gas management approach is financial – incentives are needed to overcome the raw costs of capturing, injecting and monitoring CO_2 in the ground.

14.13 Sources of further information and advice

For further information about carbon capture and geologic storage, readers are referred to the many published works summarized in Table 14.2.

Some key online resources include:

http://www.ieagreen.org.uk/ccs.html
http://energy.er.usgs.gov/health_environment/CO_2_sequestration/
http://www.fossil.energy.gov/sequestration/overview.html

14.14 References

Bachu, S,, Gunter, W. D. and Perkins, E. H. (1994), 'Aquifer disposal of CO_2: Hydrodynamic and mineral trapping', *Energy Conservation and Management* 35: 269–279.

Beer, J. M. (2007), 'High efficiency electric power generation: The environmental role', *Progress in Energy and Combustion Science* 33(2): 107–134, DOI: 10.1016/j.pecs.2006.08.002.

Bergman, P. D., Winter, E. M. and Chen, Z-Y. (1997), 'Disposal of power plant CO_2 in depleted oil and gas reservoirs in Texas', *Energy Conversion and Management*, S211–S216 (Elsevier Science).

Berner, R. A. and Lasaga, A. C. (1989), *Scientific American*, March, 54–61.

Bond, G. M., Egeland, G., Brandvold, D. K., Medina, M. G. and Simsek, F. A. (1999), 'Enzymatic catalysis and CO_2 sequestration', *World Resource Review*, 11, Woodridge, IL.

Canadell, J. G., Le Quere, C., Raupach, M. R., Field, C. B., Buitenhuis, E. T., Ciais, P. T., Conway, J., Gillett, N. P., Houghton, R. A. and Marland, G. (2007), 'Contributions to accelerating atmospheric CO_2 growth from economic activity, carbon intensity, and efficiency of natural sink', *Proceedings of the National Academy of Science USA* 104, 18–866–18–870.

deMontigny, D., Kritpiphat, W., Gelowitz, D. and Tontiwachwuthikul, P. (1997), 'Simultaneous production of electricity, steam, and CO_2 from small gas-fired cogeneration plants for enhanced oil recovery', *Energy Conversion and Management*, S223–S228 (Elsevier Science).

Doughty, C. and Pruess, K. (2004), Modeling supercritical carbon dioxide injection

© Woodhead Publishing Limited, 2010

in heterogeneous porous media', *Vadose Zone Journal* 3: 837–847 (Soil Science Society of America).

Fyfe, W. S., Leveille, R., Zang, W. and Chen, Y. (1996), 'Is CO_2 disposal possible? Capture, utilization and disposal of CO_2', *American Chemistry Society Division of Fuel Chemistry* 41(4): 1433–1435.

Gaus, I., Audigane, P., Andre, L., Lions, J., Jaquemet, N., Durst, P., Czernichowski-Lauriol, I. and Azaroual, M. (2008), 'Geochemical and solute transport modelling for CO_2 storage, what to expect from it?' *International Journal of Greenhouse Gas Control* 2: 605–625.

Gunter, W. D., Perkins, E. H. and McCann, T. J. (1993), Aquifer disposal of CO_2-rich gases: Reaction design for added capacity', *Energy Conversion and Management* 941–948 (Pergamon Press).

Gunter, W. D., Bachu, S., Law, D. H.-S., Marwaha, V., Drysdale, D. L., MacDonald, D. E. and Mccann, T. J. (1996), 'Technical and economic feasibility of CO_2 disposal in aquifers within the Alberta sedimentary basin, Canada', *Energy Conversion and Management*, 1135–1142 (Elsevier Science).

Gunter, W. D., Gentzis, T., Rottenfusser, B. A. and Richardson, R. J. H. (1997), 'Deep coalbed methane in Alberta, Canada: A fuel resource with the potential of zero greenhouse gas emissions', *Energy Conversion and Management*, S217–S222 (Elsevier Science).

Han, W. S. and McPherson, B. J. (2009), 'Optimizing geologic CO_2 sequestration by injection in deep saline formations below oil reservoirs', *Energy Conversion and Management* 50(10): 2570–2582, DOI:10.1016/j.enconman.2009.06.008.

Haugan, P. M. and Alendal, G. (2005), 'Turbulent diffusion and transport from a CO_2 lake in the deep ocean', *Journal of Geophysical Research – Oceans* 110, C09S14, doi:10.1029/2004JC002583.

Hendriks, C. A. and Blok, K. (1993), 'Underground storage of carbon dioxide', *Energy Conversion and Management*, 949–957 (Pergamon Press).

Hendriks, C. and Blok, K. (1995), Underground storage of carbon dioxide', *Energy Conversion and Management*, 539–542 (Elsevier Science).

Holloway, S. and Savage, D. (1993), 'The potential for aquifer disposal of carbon dioxide in the UK', *Energy Conversion and Management*, 925–932 (Pergamon Press).

Holloway, S. (1997a), 'Safety of the underground disposal of carbon dioxide', *Energy Conversion and Management*, S241–S245 (Elsevier Science).

Holloway, S. (1997b), 'An overview of the underground disposal of carbon dioxide', *Energy Conversion and Management*, S193-S198 (Elsevier Science).

Holm, L. W. (1963), 'CO_2 requirements in CO_2 slug and carbonated water oil recovery processes', *Production Monthly*, September.

Holt, T., Jensen, J.-I. and Lindeberg, E. (1995), 'Underground storage of CO_2 in aquifers and oil reservoirs, *Energy Conversion and Management*, 535–538 (Elsevier Science).

Holt, T. and Lindeberg, E. (1997), Gas power with CO_2 deposition located on abandoned platforms, *Energy Conversion and Management*, S247–S252 (Elsevier Science).

Ingebritsen, S. E. and Sanford, W. E. (1998), *Groundwater in geologic processes* (Cambridge: Cambridge Press).

© Woodhead Publishing Limited, 2010

Kitanidis, P. K. (1994), 'The concept of the dilution index', *Water Resources Research* 30(7): 2011–2026.

Koide, H. G., Tazaki, Y., Noguchi, Y., Iijima, M., Ito, K. and Shindo, Y. (1993), 'Carbon dioxide injection into useless aquifers and recovery of natural gas dissolved in fossil water', *Energy Conversion and Management*, 921–924 (Pergamon Press).

Koide, H., Takahashi, M. and Tsukamoto, H. (1995), 'Self-trapping mechanisms of carbon dioxide in the aquifer disposal', *Energy Conversion and Management*, 505–508 (Elsevier Science).

Krom, T. D., Jacobsen, F. L. and Ipsen, K. H. (1993), 'Aquifer based carbon dioxide disposal in Denmark', *Energy Conversion and Management*, 933–940 (Pergamon Press).

Lackner, K. S. (2003), Climate change: A guide to CO_2 sequestration', *Science* 300 (5626): 1677–1678.

Law, D. H.-S. and Bachu, S. (1996), 'Hydrogeological and numerical analysis of CO_2 disposal in deep aquifers in the Alberta sedimentary basin', *Energy Conversion and Management*, 167–1174 (Elsevier Science).

Lindeberg, E. (1997), 'Escape of CO_2 from aquifers', *Energy Conversion and Management*, S235–S240 (Elsevier Science).

Lindeberg, E. and van der Meer, L. G. H. (1996), 'Area 4, reservoir modeling and enhanced oil recovery', Chapter 6 in Holloway, S., ed., *The underground disposal of carbon dioxide*, Final Report of Joule II Project No. CT92-0031 (British Geological Survey).

Lindeberg, E. and Wessel-Berg, D. (1997), 'Vertical convection in an aquifer column under a gas cap of CO_2', *Energy Conversion and Management*, S229–S234 (Elsevier Science).

Martin, J. W. (1951), 'Additional oil production through flooding with carbonated water', *Production Monthly*, July.

McCarl, B. A. and Sands, R. D. (2007), 'Competitiveness of terrestrial greenhouse gas offsets: are they a bridge to the future?', *Climatic Change* 80: 109–126.

McPherson, B. J. O. L. and Bredehoeft, J. D. (2001), 'Overpressures in the Unita Basin, Utah: Analysis using a three-dimensional basin evolution model', *Water Resources Research* 37: 857–871.

National Energy Technology Laboratory (2009), 'Monitoring, verification, and accounting of CO_2 stored in deep geologic formations', US Department of Energy Report #DOE/NETL-311/081508, 132 pp., Pittsburgh, PA.

National Energy Technology Laboratory, (2008), *Carbon sequestration atlas of United States and Canada*, 142 pp., Washington, DC.

Ohsumi, T. (1995), 'CO_2 storage options in the deep-sea', *Marine Technology Society Journal* 29: 58–66.

Orr, F. M. Jr. (2004), *Storage of carbon dioxide in geologic formations*, Distinguished Author Series (Society of Petroleum Engineers).

Pacala, S. and Socolow, R. (2004), 'Stabilization wedges: Solving the climate problem for the next 50 years with current technologies', *Science* 305(5686): 968–972.

Parker, J. C., Lenhard, R. J. and Kuppusamy, T. (1987), 'A parametric model for constitutive properties governing multiphase flow in porous media', *Water Resources Research* 23(4): 618–624.

© Woodhead Publishing Limited, 2010

Pearce, J. M., Holloway, S., Wacker, H., Nelis, M. K., Rochelle, C. and Bateman, K. (1996), 'Natural occurrences as analogues for the geological disposal of carbon dioxide', *Energy Conversion and Management,* 1123–1128 (Elsevier Science).

Rubin, E. S. (2008), 'CO_2 capture and transport', *Elements* 4: 311–317.

Saxon, J., Breston, J. N., and MacFarlane, R. M. (1951), 'Laboratory tests with carbon dioxide and carbonated water as flooding mediums', *Production Monthly*, November.

Siefritz, W. (1990), 'CO_2 disposal by means of silicates', *Nature*, 345–486.

Tchelepi, H. A. (1994), *Viscous fingering, gravity segregation, and permeability heterogeneity in two-dimensional and three-dimensional flow*, PhD Dissertation, Stanford University.

van der Burgt, M. J., Cantle, J. and Boutkan, V. K. (1992), 'Carbon dioxide disposal from coal-based IGCCs in depleted gas fields', *Energy Conversion and Management*, 603–610 (Pergamon Press).

van der Meer, L. G. H. (1992), 'Investigations regarding the storage of carbon dioxide in aquifers in the Netherlands', *Energy Conversion and Management*, 611–618 (Pergamon Press).

van der Meer, L. G. H. (1993), 'The conditions limiting CO_2 storage in aquifers', *Energy Conversion and Management*, 959–966 (Pergamon Press).

van der Meer, L. G. H. (1996), 'Computer modelling of underground CO_2 storage', *Energy Conversion and Management*, 1155–1160 (Elsevier Science).

Weir, G. J., White, S. P. and Kissling, W. M. (1996), 'Reservoir storage and containment of greenhouse gases', *Transport in Porous Media*, 37–60 (Netherlands: Kluwer Academic Publishers).

© Woodhead Publishing Limited, 2010

15

Advanced technologies for syngas and hydrogen (H_2) production from fossil-fuel feedstocks in power plants

P. CHIESA, Politecnico di Milano, Italy

Abstract: This chapter is devoted to production of hydrogen from fossil primary fuels, in particular natural gas and coal. It describes the basic processes commonly adopted, presents in detail the components that accomplish them, and finally reports the mass and thermal balances of two relevant cases. Expected advancements in the technology and application of techniques to remove carbon dioxide for long-term sequestration are also discussed.

Key words: hydrogen production, methane steam reforming, coal gasification, syngas conversion.

15.1 Introduction

This chapter is devoted to hydrogen production from fossil feedstock. Technologies for syngas production are conceptually divided into two categories: gasification usually refers to syngas production systems from solids and heavy liquid fuels. Reforming designates processes used for conversion of gas and light liquids. Since this chapter gives emphasis to hydrogen production also for decentralized power generation, more prominence is given to the second category, considering that gasification represents an economically viable option only on a very large scale. Technologies adopted to produce syngas from the initial charge are examined first. Then the analysis focuses on the processes used for syngas conversion and hydrogen purification.

15.2 Syngas production from gas and light liquids

15.2.1 Charge purification

Since catalysts involved in the whole hydrogen production process may be

© Woodhead Publishing Limited, 2010

poisoned by sulfur in concentration as low as 10 ppb, it is necessary to eliminate hydrogen sulfide (H_2S) and other sulfur compounds contained in primary fuel. Such a treatment is usually required for any kind of charge including natural gas, whose distribution specifications usually set a limit on H_2S of about 50 ppm (71 mg/Nm^3 as total sulfur). Desulfurization is usually carried out in a two-stage process operating in the 350–400°C temperature range. Since the following zinc oxide bed is not very effective in capturing organic sulfur compounds at its normal working temperatures, they are first converted to H_2S. Hydrogenation reactions like the one involving carbonyl sulfide (COS)

$$COS + H_2 \leftrightarrow CO + H_2S \qquad [15.1]$$

occur in a catalytic bed composed of cobalt and molybdenum oxides on an activated alumina base, located in a separate vessel or placed as top layer in the zinc oxide bed. If not present in sufficient concentration, hydrogen has to be added to the charge to reach a 2% minimum concentration in the gas stream (or a hydrogen partial pressure of at least 0.7 bar) in order to drive the reactions at a satisfactory rate.[1] In this process attention should be given to olefins included in the charge that are hydrogenated through a highly exothermic reaction, which may significantly affect the operating temperature of the bed.

In the zinc oxide adsorption bed, H_2S reacts according to the following reaction

$$ZnO + H_2S \leftrightarrow ZnS + H_2O \qquad [15.2]$$

At the operating temperature of the process, reaction equilibrium is closely approached and, since the K_p constant p_{H_2O}/p_{H_2S} is in the range 10^5–10^6, an effective sulfur abatement can be achieved.

15.2.2 Reforming reactions

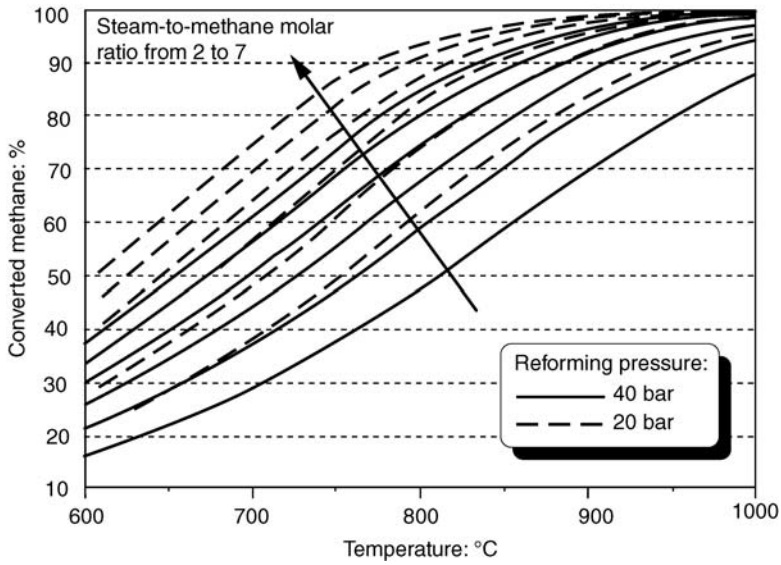
Steam reforming is a reaction able to convert light hydrocarbons to carbon monoxide (CO) and hydrogen according to the reaction

$$C_nH_m + n \cdot H_2O \leftrightarrow n \cdot CO + (n + m/2) \cdot H_2 \qquad [15.3]$$

The process is widely used to produce synthesis gas from natural gas, liquified petroleum gas (LPG) and other light liquids, often in combination with partial oxidation. Since the reforming reaction is highly endothermic (for instance, methane steam reforming reaction)

$$CH_4 + H_2O \leftrightarrow CO + 3 \cdot H_2 \qquad [15.4]$$

© Woodhead Publishing Limited, 2010



15.1 Fraction of methane (CH_4) converted in a steam reforming process at equilibrium, as a function of pressure, temperature and steam-to-methane molar ratio.

presents a standard reaction enthalpy ΔH_0 at 25°C of 206 kJ/kmol$_{CH_4}$ and the number of moles of products is greater than the one of reactants, elevated temperatures and low pressures favor a high degree of conversion. Usually the reaction takes place with a large steam addition compared to stochiometry to enhance methane conversion according to the proportion shown in Fig. 15.1. Products of the steam reforming process are essentially CO and hydrogen (H_2), along with carbon dioxide (CO_2) which is formed by the water gas shift (WGS) reaction

$$CO + H_2O \leftrightarrow CO_2 + H_2 \qquad [15.5]$$

which can be considered at equilibrium at the usual operating conditions.

15.2.3 Adiabatic pre-reforming

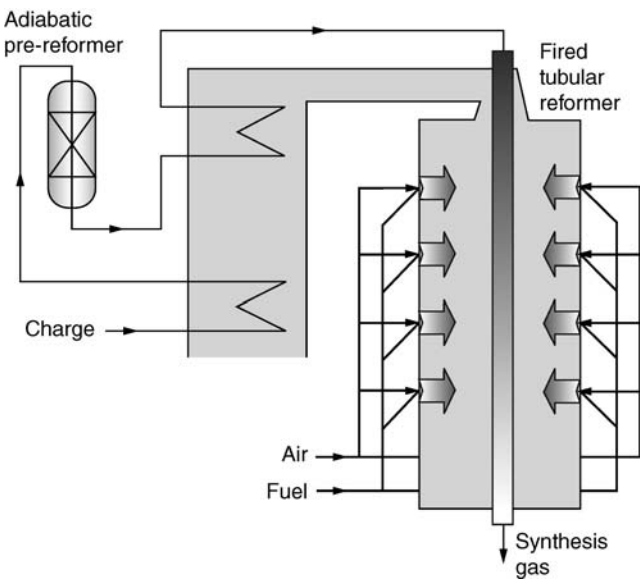
The industrial process often adopts an adiabatic pre-reforming step where a nickel-based catalyst decomposes complex hydrocarbons according to equation [15.3] to avoid cracking in the actual reformer and feeds it with an uniform stream independently of the composition of the primary fuel. Pre-reformer operating temperature is set according to pressure and charge composition in order to respect strict limits about catalyst deactivation and carbon deposit. Since endothermic reforming reactions are balanced by exothermic WGS and methanation (inverse of methane steam reforming,

© Woodhead Publishing Limited, 2010

equation [15.4]) reactions, the overall process leads to a temperature increase of the stream with heavy fuels and usually a decrease with natural gas. Accordingly, the charge is fed to the pre-reformer at temperatures in the 350–550°C range.

15.2.4 Fired tubular reformers (FTR)

The most common process for hydrogen production relies on direct flame tubular steam reformers (FTR) arranged according to the flow scheme sketched in Fig. 15.2. They are essentially composed of a furnace whose burners radiate on tubes filled with nickel-based catalyst to provide the heat required to sustain the endothermic reaction. This is the generally the most competitive technology for plant capacity up to approximately 250 000 Nm^3 of H_2 per hour.[2] Different configurations of the furnace are adopted in the industrial practice aiming to improve heat flux and temperature control along the tube length. To achieve a high methane conversion, temperature at the reformer exit is kept in the 870–920°C range. This highly stresses tubes to creep and requires adoption of high-alloy materials capable of tolerating wall temperatures up to 1050°C.[3] The preferred materials for tubes are austenitic steels 25 Cr–35 Ni with addition of low percentage of Nb (<2%) and Ti (<1%) that promote the formation of precipitates and reduce creep of material grains. In a standard configuration, tube diameter is in the 100–



15.2 Adiabatic pre-reformer and fired tubular reformer for hydrogen production plant.

© Woodhead Publishing Limited, 2010

180 mm range, thickness varies from 8 to 20 mm and the heated section is 10–14 m long.[4]

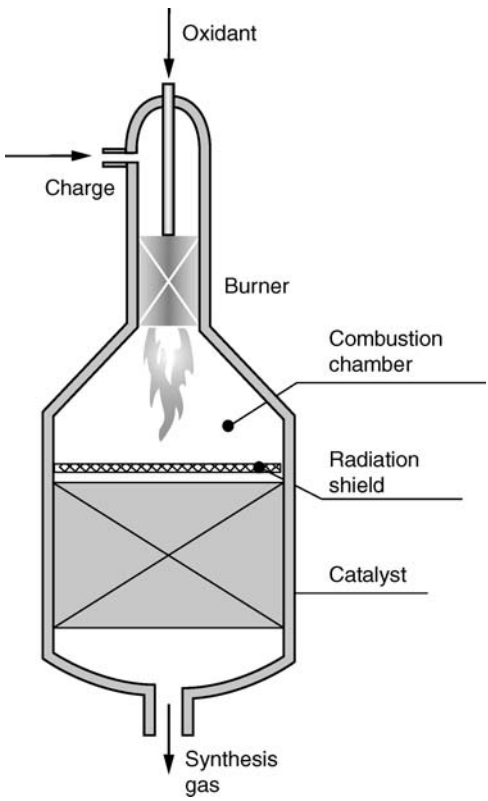
15.2.5 Autothermal reformers (ATR)

Autothermal reforming is a process that combines the reactions (equation [15.4] and equation [15.5]) usually occurring in a FTR process, with the exothermic combustion reactions

$$CH_4 + 3/2O_2 \leftrightarrow CO + 2\ H_2O \qquad [15.6]$$

$$CO + 1/2O_2 \leftrightarrow CO_2 \qquad [15.7]$$

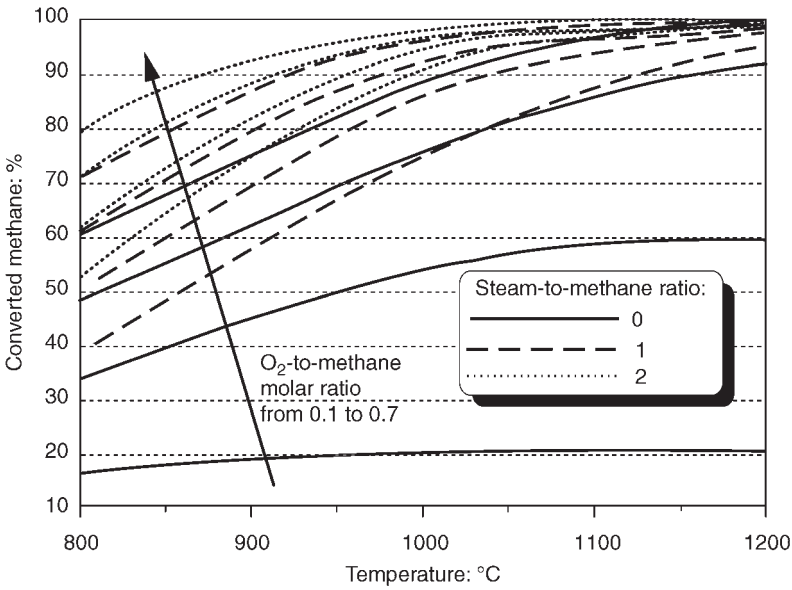
that provide the heat necessary to sustain the endothermic reforming reaction. The whole process is therefore adiabatic and can be carried out in a compact vessel coated with multiple layers of refractory materials, which is consequently cheaper than a FTR reactor. On the other hand, the ATR



15.3 Schematic diagram of an ATR reactor.

© Woodhead Publishing Limited, 2010

process for H_2 production requires pure O_2 as oxidant to avoid syngas contamination with N_2 that would lead to a cost increase in the following purification section. Pure oxygen is provided by cryogenic air separation units that may constitute up to 40% of the plant investment[3] and since they present a sharp scale economy up to 90 000 Nm^3/h, it makes the ATR technology convenient for plants with H_2 output greater than 250 000 Nm^3/h. In ammonia plants, where air is used as oxidant, ATR may compete also at lower sizes. In an ATR reactor (Fig. 15.3) homogeneous and heterogeneous reactions are carried out in series as the stream proceeds progressively from a combustion zone, where a turbulent diffusive flame oxidizes the charge promoting the faster combustion reaction, to a thermal zone where slower reactions (i.e. CO oxidation and pyrolysis of higher hydrocarbons) occur. In the following catalytic zone the final conversion of hydrocarbons is carried out mainly through steam reforming and WGS reactions. Figure 15.4 shows the methane conversion achieved at equilibrium as a function of different charge compositions. In industrial practice the syngas outlet temperature from an ATR is in the range 900–1100°C with an oxygen/hydrocarbon ratio in the range 0.55–0.6. Such a rich combustion may promote soot formation in the reactor that should be absolutely avoided. In normal operation of ATR reactors, soot formation is inhibited by correct design of the burner, steam addition and the action of the catalyst in converting soot precursors.



15.4 Fraction of methane converted in an autothermal reforming process at equilibrium at 40 bar as a function of temperature, steam and O_2-to-methane molar ratio. Diagram accounts only for gaseous phase equilibrium, neglecting any carbon formation.

© Woodhead Publishing Limited, 2010

15.2.6 Heat exchange steam reformers (HESR)

This kind of technology differs from the FTR simply because heat required to sustain the reaction is provided by convection rather than radiation. Since the mass and thermal balance on the catalyst side of a HESR is the same as in the FTR case, in principle any hydrogen plant can be designed according to this technology. In fact, HESR is adopted only for small-scale plants (below 10 000 Nm^3/h hydrogen) where heat is released by combustion of a fuel stream, or in combination with the previous two technologies in order to enhance heat recovery and improve the thermal efficiency of the process. Figure 15.5a shows an arrangement where a FTR operates in series with a HESR working as a gas-heated pre-reformer. Alternatively the HESR can be placed in series with an ATR to form the two-stage configuration shown in Fig. 15.5b. Different configurations can be also devised by placing two reactors in parallel, arranged as two inlets–one outlet (Fig. 15.6a) or two inlets–two outlets (Fig. 15.6b). In the latter case the two reactors can operate with different steam-to-carbon ratio and produce streams with different composition.

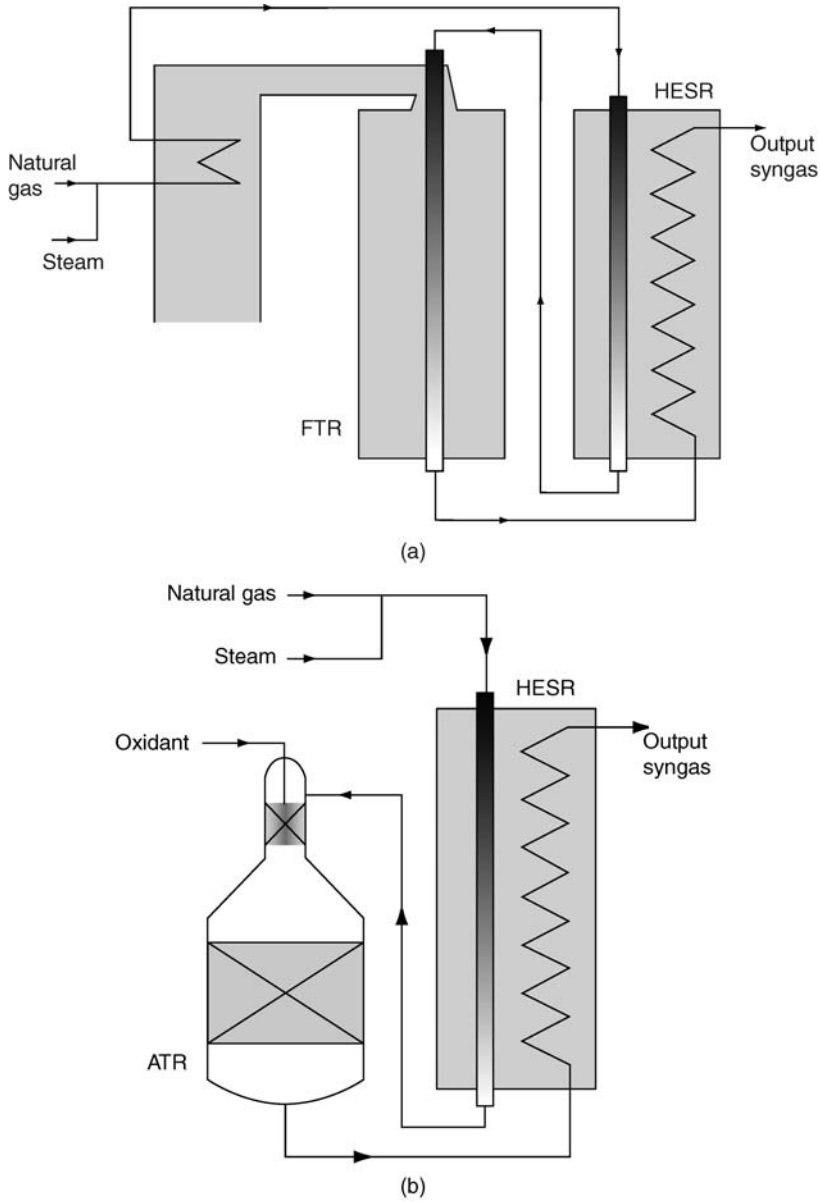
15.2.7 Advanced technologies

Working principles of the catalytic partial oxidation (CPO) are actually the same as the ATR, with the difference that all the reactions occur in heterogeneous phase. Therefore, a CPO reactor does not have the typical burners of the ATR technology and, after the reactants (hydrocarbons, oxidant and optionally steam) have been carefully mixed, the charge is directly sent to the catalytic zone where the following reactions take place at the same time: partial and complete combustion, methane steam reforming, water gas shift. Catalysts used for CPO are usually based on noble metals (Pt, Pd, Rh, Ir)[5] and allow very short contact time (in the range 0.1–10 ms), which results in high space velocity and the possibility to design very compact reactors – the main advantage sought by developing this technology.

Membrane reactors can be arranged according to different operating concepts depending on the chemical species permeated through the membrane. According to Bredesen *et al.*,[6] high-temperature membrane technologies applicable to hydrogen reforming can be summarized as follows:

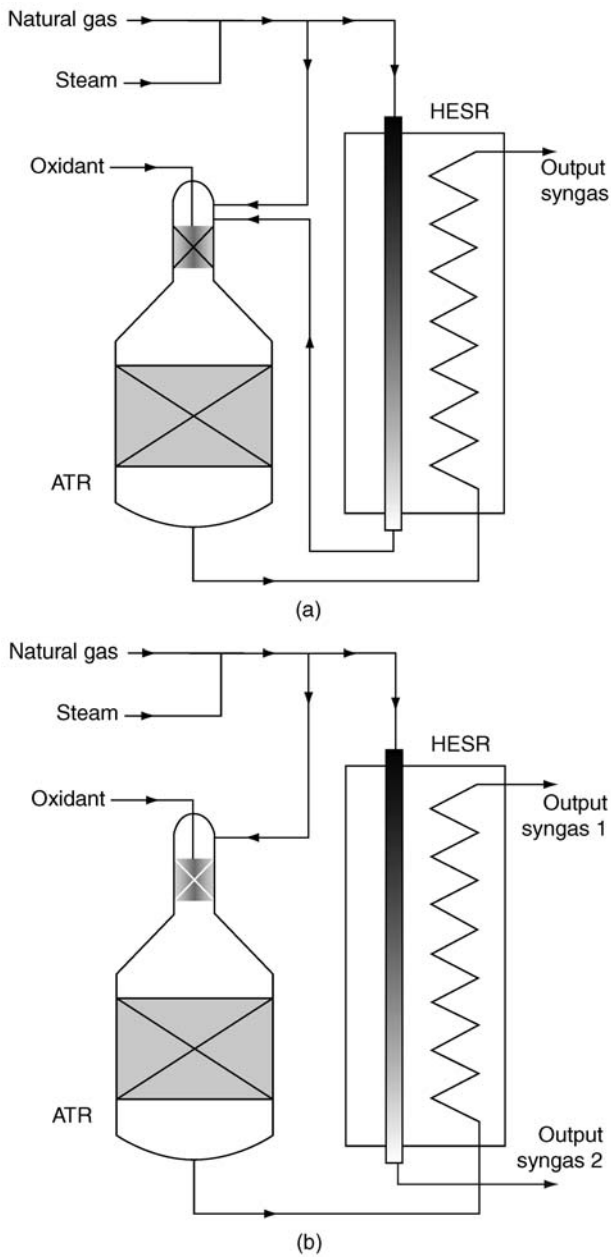
- dense palladium-based membranes for H_2 separation operating in the range 450–500°C;
- microporous membranes for H_2 separation, currently suffering from stability against sintering at temperatures over 400°C, particularly in water vapor containing atmospheres;

© Woodhead Publishing Limited, 2010



15.5 Series arrangements of different reformers: (a) HESR + FTR reactors; (b) HESR + ATR reactors.

© Woodhead Publishing Limited, 2010



15.6 Parallel arrangements of HESR + ATR reactors: (a) two inlet–one outlet configuration; (b) two inlets–two outlets configuration.

© Woodhead Publishing Limited, 2010

- dense electrolytes and mixed conducting (ionic and electronic) membranes for O_2 or H_2 separation operating in the range 700–900°C.

Most relevant applications of all these membranes have asymmetric structure consisting of a thin filtering layer placed over a metallic or ceramic support that affords the required mechanical strength.

A key point of the technology is that continuous hydrogen extraction from a reformer promotes the conversion to products of the steam reforming and WGS reactions. It means that a hydrogen separation membrane reactor allows a methane conversion efficiency that would require much higher operating temperature or steam addition in a conventional reformer. Given that partial pressure difference is the driving force for gas permeation through the membrane, hydrogen is collected on the permeate side usually at low pressure and the following compression may be energetically expensive. This problem does not apply if hydrogen is directly used in fuel cells, reciprocating engines or boilers. On the other hand, dense membranes ideally have infinite selectivity and permit the separation of pure hydrogen so that substantial benefits can be achieved by getting rid of the WGS reactors and purification unit usually included in a hydrogen production process (see section 15.3). The result is a much more compact layout that could fit even in transport vehicles.

Finally, the development of oxygen transport membranes would be extremely beneficial to extend ATR technology also to small-scale plants, because it allows the avoidance of air separation units.

15.2.8 Operational problems occurring in reformer reactors

The main problems related to operations in reformers can be divided into three categories.

- *Metal dusting* afflicts all the configurations that adopt a heat exchanger with process gas and it is caused by metal carburization when the metal comes into contact with a stream rich in carbon, especially in the temperature range between 400 and 800°C. In stainless steels and nickel-based alloys, this phenomenon brings about breaking of the protecting layer of oxides, transfer of carbon in the metal alloy and formation of carbides that eventually leads to matrix disintegration. Since material loss may occur quickly and cause extremely serious damage to the equipment, it is necessary to preserve the reactor from such a risk by careful design that avoids as much as possible operation in the dangerous temperature range, by a correct choice of the materials, and by application of coatings and surface treatments.
- *Catalyst deactivation* is mainly caused by sintering and poisoning. To increase the active surface area and enhance its activity, the reforming

© Woodhead Publishing Limited, 2010

catalyst is usually deposited in small particles on a ceramic support. Sintering essentially involves migration of nickel particles on the support surface and their subsequent coalescence, leading to a net active area loss. Poisoning is essentially due to sulfur contained in the treated stream that is chemisorbed on the catalyst surface, reducing its activity. Also alkaline metals and silica present deactivating effects. Since catalyst deactivation is usually a progressive event, the effects can be prevented by increasing the catalyst volume of the reactor.

- *Carbon deposition* is associated with different phenomena occurring in different conditions and leading to different effects. Deposition of carbon whisker is favored by low steam-to-carbon ratios and high temperatures and results in mechanical disintegration of the catalyst, leading to a reduction in the activity and an increase in the pressure loss. Thermal cracking of higher hydrocarbons occurring at high temperature results in carbon deposition on the catalyst and tube walls. The consequent insulation of the heat transfer surfaces and encapsulation of the catalyst particles (which reduces the rate of the endothermic reactions) increase the temperature inside the reformer, speeding up the phenomenon. Finally, deposition of polymeric film may occur with heavy charge, rich in aromatic compounds, operating at low temperature and steam-to-carbon ratio.

15.3 Syngas conversion and purification

15.3.1 Water gas shift reaction

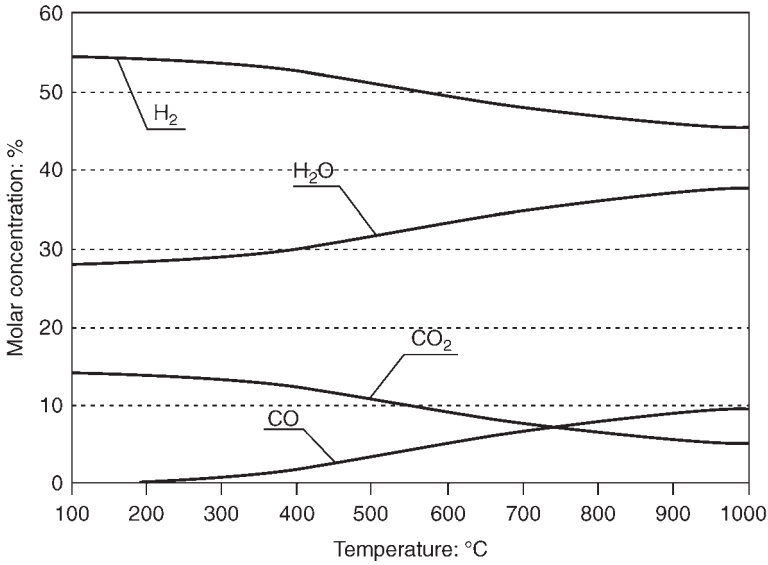
Syngas produced by steam reforming, catalytic partial oxidation and gasification always contains substantial fractions of carbon monoxide. Syngas composition can be considered at equilibrium with respect to WGS reaction (equation [15.5]) at the synthesis reactor exit, but hydrogen production can be substantially enhanced by achieving the equilibrium at lower temperature, as shown in Fig. 15.7. Being moderately exothermic (standard reaction enthalpy ΔH_0 at 25°C is −41.1 kJ/kmol), the WGS reaction is favored at low temperature and its equilibrium is described by the relation

$$\log_{10}(K_p) = \log_{10}\left(\frac{p_{CO_2} \cdot p_{H_2}}{p_{CO} \cdot p_{H_2O}}\right) = \frac{1961}{T} - 1.807 \qquad [15.8]$$

(where T is expressed in K) with a relative error on K_p estimation lower than 8% in the 200–900°C range. Hydrogen conversion is also increased by a water vapor excess whereas pressure does not affect the equilibrium because the reaction occurs at constant number of moles.

Different catalysts are used in order to promote the WGS reaction in the different temperature ranges. Within the temperature range of about 330–

© Woodhead Publishing Limited, 2010



15.7 Equilibrium composition of the water gas shift reaction as a function of temperature for a typical feed from a fired tubular steam reformer (CO: 8.7%, CO_2: 5.5%, H_2: 45.8%, H_2O: 36.8%, the balance being mainly composed of CH_4).

510°C, the catalyst is typically chromium-stabilized iron oxide promoted by small addition of copper (1–2% by weight) which is relatively insensitive to sulfur compounds. Copper- and zinc-based catalysts are active in the 180–330°C temperature range and are much more vulnerable to poisoning by sulfur, and also by chlorides and silica, which may be contained in boiler feedwater entrained with steam used in the process.

In hydrogen plants the arrangement of WGS reactors is actually related to the steam-to-carbon ratio in the charge. At high ratios, it is usually convenient to split the overall conversion into different (usually two) adiabatic reactors with intermediate cooling in order to combine a high H_2 conversion in the colder stage with faster kinetics and high-temperature heat recovery in the hot stage. At very low steam-to-carbon ratio (approximately corresponding to less than 2.5 in the initial charge to the reformer) the iron-based catalysts suffer from deactivation due to the formation of iron carbonyl, which promotes the synthesis of complex hydrocarbons and alcohols. In this case the preferred arrangement consists of a copper catalyst in a single medium-temperature shift reactor operating in the range of 210–330°C.

Hydrogen separation membranes may find useful application also in a WGS reactor, providing the same benefits mentioned for the reformers.

© Woodhead Publishing Limited, 2010

15.3.2 Acid gas removal (AGR)

At the exit of the WGS section, syngas from light charges has a hydrogen content of about 70–75% (molar, dry basis), 17–20% of CO_2 and few percent of CH_4, CO and other contaminants. Therefore syngas may be optionally treated to remove CO_2 and/or other species depending on the final destination of the hydrogen stream and possible options for CO_2 sequestration.

Removal of CO_2 from a gaseous stream is usually carried out by means of selective solvents which present much greater affinity for acid species (like CO_2 and H_2S) than the other ones. Processes may be divided into two categories according to the nature of the interactions between solvent and absorbed species.

- Physical absorption is where components to be removed are more soluble in the liquid absorbent than other ones, but they do not react chemically with the solvent. Rectisol and Selexol processes, which respectively use methanol and a mixture of polyethylene glycol dimethyl ethers as solvent, are examples of this category.
- Chemical absorption involves a reversible reaction between species to be removed and the solvent to form weakly bonded compounds. All the processes using amines, such as monoethanolamine (MEA) or methyldiethanolamine (MDEA), and alkaline salts solutions belong to this category.

In any case CO_2 absorption is carried out at syngas pressure and low temperature (ambient or colder by means of proper chillers) in trayed towers or packing towers where the gas stream is brought into direct contact with the CO_2-poor solvent. The CO_2-rich solvent collected at the absorber bottom is then regenerated at low pressure. For up to about 90% CO_2 removal efficiency, physical solvents may be regenerated by straightforward pressure reduction in consecutive flash drums. For higher removal efficiencies and chemical solvents, regeneration occurs at higher temperature in a stripping column and requires a significant steam consumption to feed the reboiler. Regardless of the regeneration solution, the CO_2 stream is typically released almost pure or in a mixture with water vapor which can be easily removed by condensation in a knock-out drum.

Since the capture efficiency of physical processes is strongly dependent on the partial pressure of CO_2 in the gas phase, chemical processes are better suited for application in hydrogen production from light charges because, in the usual cases, CO_2 partial pressure in the syngas stream is about 5 bar. Actually, in modern hydrogen production plants from light feedstocks, the AGR section is usually missing because CO_2 is directly removed in the pressure swing adsorption system (see section 15.3.3). Conversely, the AGR

© Woodhead Publishing Limited, 2010

section is conveniently adopted in configurations with CO_2 sequestration and in hydrogen production plants from heavy feedstocks where removing CO_2 from the syngas is worthwhile, even if CO_2 is vented, because it reduces the flow rate to the pressure swing adsorption system and substantially increases the heating value of the pressure swing adsorption off-gas stream.

15.3.3 Hydrogen recovery and purification

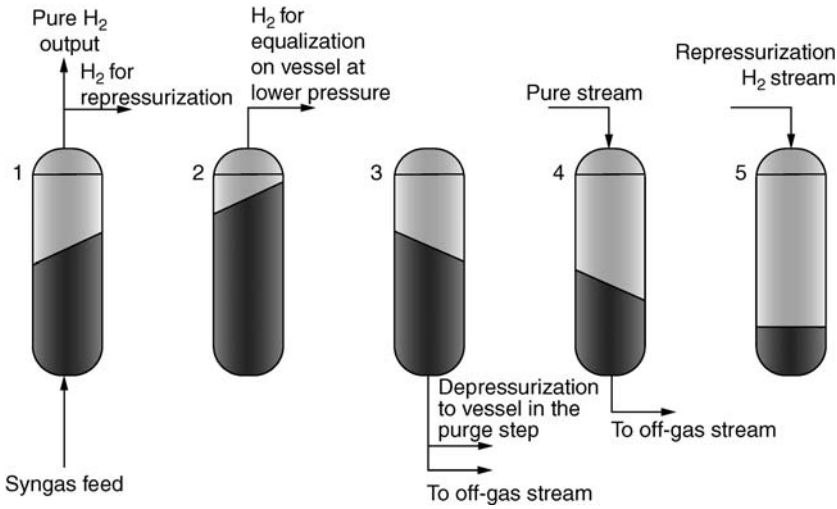
Different options can be applied to recover and purify hydrogen after the WGS or the AGR section. The choice is made based on plant requirements in terms of hydrogen purity, recovery efficiency, and the pressure of feed syngas, hydrogen and off-gas streams.

Pressure swing adsorption (PSA) is the preferred option to purify the syngas stream generated by steam reforming of light charges. The technique is based on the principle of selective concentration of gaseous species at the surface of microporous solid adsorbents such as zeolites and activated carbons. In particular, the materials adopted for hydrogen purification present the capability to adsorb species different from hydrogen and helium, showing an impurity loading proportional to partial pressure of contaminants. Therefore, the PSA operates at constant temperature 'swinging' between two pressures, adsorbing impurities at the higher one and releasing them at the lower one. Since the operating cycle is composed of at least two phases (production and regeneration), in theory a minimum of two beds in parallel are needed to ensure continuous operations. In industrial practice PSA plants are arranged on a higher number of beds (typically 8–12) in order to reduce the consumption of high-pressure, high-purity hydrogen during the repressurization phase. The overall operating cycle may be conceptually divided into five steps, as shown in Fig. 15.8.

1 Production, where a high-pressure feed stream is introduced to the bed, contaminants are adsorbed and a pure hydrogen output is produced.
2 Co-current depressurization; the hydrogen released in this step is used to partially pressurize another unit (pressure equalization phase).
3 Counter-current phase, where the bed is taken to the minimum pressure. Part of the entrapped impurities are released in this step and become part of the off-gas stream.
4 Purge, where a hydrogen flow released at the beginning of step 3 strips the contaminants remaining in the bed. The effluent gas represents the residual fraction of the off-gas stream.
5 Counter-current repressurization, carried out with hydrogen, at first removed in phase 2 and then coming from a vessel in production.

In a multi-bed PSA unit each step may be in turn divided over different beds. The resulting process produces hydrogen at a pressure slightly lower

© Woodhead Publishing Limited, 2010



15.8 Conceptual steps of the operating cycle of a multi-bed PSA plant.

than the feed stream (less than 1 bar drop), with a purity higher than 99.9% and with a recovery efficiency in the range 80–92%, the lower values typically being achieved in the lower pressure ratio configurations. The residual hydrogen fraction is included together with all the impurities in the off-gas stream, leaving the PSA at nearly ambient pressure. Simultaneous recovery of a substantial fraction (85–95%) of the CO_2 contained in the feed gas in a high-purity (more than 99%) stream can be achieved by particular bed arrangements, as shown by Sircar.[7]

Membrane systems are based on a specific characteristic, shown by a variety of polymeric materials, whereby they present different rates of permeation between hydrogen and other species in the mixture. Industrial membranes have an asymmetric structure meaning that the selective thin layer is coupled to a pressure-resistant support, usually arranged as spiral-wound or hollow-fiber modules. Feed gas has to be free of contaminants like ammonia, hydrogen sulfide, methanol, particulates and entrained liquid that may affect performance and lifetime of the membranes. Maximum allowable temperature for polymer membranes is typically below 100°C while safe operation is possible for feed pressures up to 160 bar. Considering that membrane surface is proportional to pressure drop across the membrane while permeate recompression work is proportional to pressure ratio, membrane separation is especially suited to recovering hydrogen from high-pressure off-gas streams. Performance of the separation process depends on membrane selectivity and process operating conditions, but a hydrogen recovery efficiency in the range 85–95% and a purity of the

© Woodhead Publishing Limited, 2010

permeate stream of about 90–98% can be achieved on a stream with 40–60% hydrogen concentration.

Low-temperature processes rely on the different boiling points of the species contained in the treated syngas. These processes are often used to separate hydrogen from hydrocarbons in refinery off-gas streams with a hydrogen content below 50%, but have been supplanted by PSA in hydrogen purification from steam reforming, unless simultaneous recovery of high-purity carbon monoxide is requested. Simple condensation is the most common cryogenic separation process. Preliminary removal of species like water or CO_2 that are solid at the separation temperature is required to prevent blockage of the cold section of the plant. After that, the gas mixture is cooled down below the condensation temperature of the high boiling species, which are therefore removed as liquid phase. Refrigeration required to achieve the condensation temperature can be obtained in different ways: by expanding the recovered hydrogen stream in a turbine, by using the Joule–Thomson effect throttling the separated liquid through a valve, or by means of an external chiller.

The purity of hydrogen recovered, which increases as separation temperature reduces, is usually in the range 90–96%.[8] The recovery efficiency depends on hydrogen solubility in the liquid phase and on the fraction of removed liquid. Hydrogen recovery, usually in the range 90–98%, can be increased by depressurizing the condensate and recycling the hydrogen-rich blow off.

Hybrid solutions composed by combining two different processes among PSA, membrane or cryogenic systems, can be adopted to enhance the performance of the process.

Methanation is a finishing technique which, unlike the ones mentioned before, does not aim to carry out a bulk separation of hydrogen from contaminants in the mixture, but simply to eliminate the traces of CO (and eventually CO_2) remaining in the syngas, which could be harmful in final hydrogen users like fuel cells or chemical processes. Methanation is suitable for purification of streams having a content of oxides up to about 2.5% and it is realized by performing the following reactions

$$CO + 3H_2 \leftrightarrow CH_4 + H_2O \qquad [15.9]$$

$$CO_2 + 4H_2 \leftrightarrow CH_4 + 2\ H_2O \qquad [15.10]$$

within the 250–350°C temperature range on a nickel catalyst. Methanation consumes part of the produced hydrogen but, under normal operating conditions, equilibrium is almost completely shifted towards the reaction products, which permits the reduction of carbon oxides concentration to less than 10 ppm.

© Woodhead Publishing Limited, 2010

Preferential oxidation is used selectively to convert traces of CO to CO_2 without significantly involving side oxidation of hydrogen that is present in a much greater concentration. The reaction is performed in an adiabatic reactor on noble metal (Pt, Pd, Rh and Ru) catalysts at low temperature (approximately 100°C) in order to avoid the reverse water gas shift that consumes hydrogen and produces more CO.[9] This novel technique is especially suited for hydrogen production for PEM fuel cells, given that these cells are extremely sensitive to CO poisoning but are not affected by CO_2 presence. Since it does not require a preliminary CO_2 removal, preferential oxidation represents a simple and cost-effective technique that can be adopted even for on-board hydrogen production for fuel cell vehicles. Selective CO methanation to remove only CO in hydrogen processing for fuel cells is also under investigation.[10]

15.4 Syngas and hydrogen from heavy feedstocks

The preferred route to produce syngas from heavy feedstocks like coal, petcoke and refinery residues, or from biomass, is gasification. The term 'gasification' includes a large number of technologies and licensed processes so it is impossible to provide here an exhaustive overview of the subject. Leaving this task to the specialized literature,[11] this chapter only briefly deals with the technologies applied in large-scale plants for production of hydrogen or synthesis gas from coal.

15.4.1 Entrained flow gasifiers

Gasification is a process involving a feedstock, an oxidizer and water (or steam) as temperature moderator. Exothermic and endothermic reactions occur during the process. All the exothermic fuel oxidation reactions may be considered complete while the other reactions involving steam and carbon dioxide are never complete because of thermodynamic limitations and eventually control the final composition. Most successful examples of large-scale, hard coal gasifiers are based on oxygen-blown, entrained flow technology, whose main characteristics are listed below.

- High operating temperature (1250–1500°C), which entails short residence time (a few seconds) and compact gasifiers accordingly. Operation above the ash melting temperature also allows recovery of coal ashes in the form of slag, a sort of inert, vitrified material.
- Production of clean, tar-free syngas with carbon conversion of over 99%.
- Limited (about 75%) cold gas efficiency, defined as the ratio between the

© Woodhead Publishing Limited, 2010

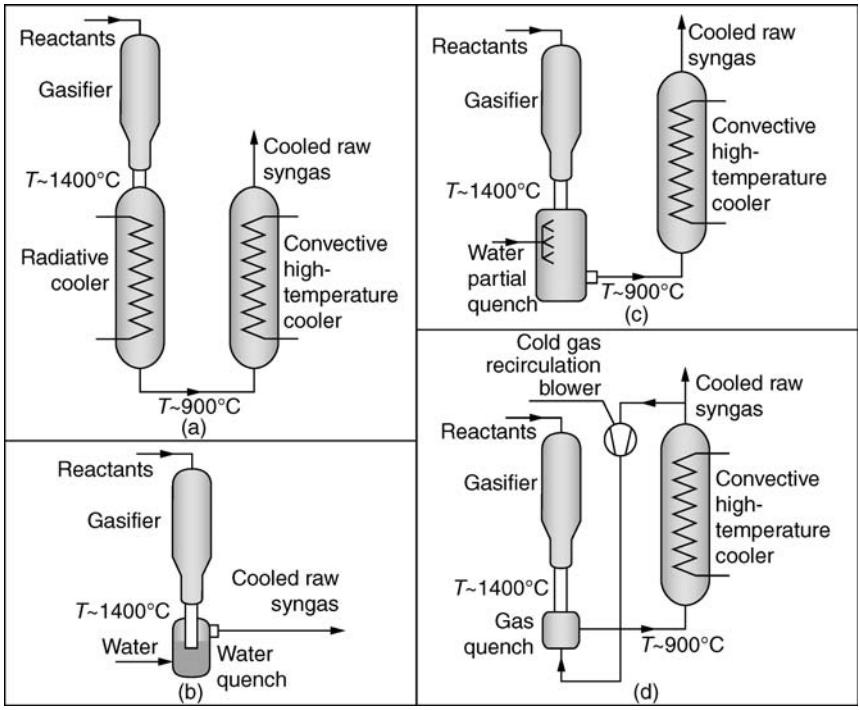
thermal power (flow rate by heating value) of the syngas output and fuel input.
- High oxygen demand to achieve the specified operating temperatures. Operation on air is virtually unacceptable since it would further decrease the cold gas efficiency by introducing a significant amount of inert nitrogen to be taken to high temperature. Presence of an air separation unit prevents any possibility of achieving small-sized plants.
- Requirement for fine grinding of coal to a size lower than 100 μm.
- No technical limitations on the type of coal used as feedstock, even if application to low-rank coals with a high moisture or ash content may be uneconomical due to the high level of oxygen consumption.

The actual applications of the entrained flow technology lead to different solutions in various design aspects. In two-stage processes, a proportion of the reactants is added in the non-slagging second stage where endothermic gasification reactions are driven by high-temperature gas produced in the first stage. This brings about a lower syngas outlet temperature (in the range 1000–1100°C), a higher cold gas efficiency and lower oxygen consumption, but also drawbacks such as reduced carbon conversion and a possible carry over of ash, char and tars in the syngas flow. Feed may be introduced in two different ways: by coal–water slurry injection or by means of inert gas pressurized lock-hoppers. The former is a simpler and more reliable option. It allows higher feed pressures to be achieved (up to 200 bar as opposed to 50 bar for dry-feed systems) but results in a lower cold gas efficiency due to the latent heat absorbed during evaporation of water in the slurry (whose maximum solid concentration is about 2/3 by weight, in order to ensure it can be pumped). Gasification processes differ also in respect of vessel protection against high temperatures (refractory containment or membrane wall cooling), flow direction (top or bottom feed) and mainly in the solutions adopted to recover sensible heat from the raw syngas.

Cooling is necessary in any case because all the dependable techniques to clean up syngas from sulfur operate at ambient temperature or lower. Given that in an entrained flow gasifier about 20% of the input fuel energy is present as sensible heat in the syngas stream, cooling is a capital-intensive task, made complicated by the fact that, in the range between softening (~900°C) and melting points, the ash is sticky and tends to agglomerate on convective heat exchange surfaces. The problem may be avoided through one of the different options sketched in Fig. 15.9. In Fig. 15.9a cooling is first carried out in a radiant cooler from the gasifier outlet temperature to a value below the ash softening point, and then completed in a convective heat exchanger. Both the coolers produce high-pressure steam for efficient heat recovery.

In Fig. 15.9b syngas is fully quenched with water and leaves the bottom

© Woodhead Publishing Limited, 2010



15.9 Schematic configuration of the different options to cool high-temperature raw syngas at the exit of an entrained bed gasifier.

chamber in saturated condition at about 250°C. This option gets rid of expensive high-temperature coolers but gives up the possibility of an efficient thermal recovery. Only low-pressure steam can be generated by recovering the latent heat of the water vapor contained in the syngas stream downstream of the quench and an expensive water treatment is required to handle the purge flow released by the process. In Fig 15.9c the partial water quench helps to increase the heat recovery efficiency by reducing the amount of water evaporated in the syngas stream and recovering heat for high pressure water generation at temperatures below the ash softening point. In Fig 15.9d quench by recirculated cold gas restores the efficient heat recovery of the first case (Fig. 15.9a) with full generation of high-pressure steam.

15.4.2 Other gasifier arrangements

Besides the entrained flow technology, two more different conceptual gasifier designs may be devised.

- In *moving beds* (sometimes called fixed beds), the coal moves slowly

© Woodhead Publishing Limited, 2010

down by gravity, usually flowing countercurrent to the gas produced in the bed. Along the top–bottom path, coal is first preheated and pyrolized as the remaining char proceeds to the bottom gasification zone, where the reactions with oxidizer and steam take place at slagging temperature. The countercurrent arrangement leads to low oxidizer consumption and low outlet syngas temperature (450–550°C), which are both beneficial to cold gas efficiency, but this also causes products of the pyrolysis to be carried over and remain in the syngas stream as liquid tars. Handling of liquor, which must be removed and treated or recycled to the bed, greatly complicates the plant and is one of the most critical points of this technology, along with the difficulty of using coals with a high content of fines that tend to block the passage of the syngas stream.

- In *fluid beds*, the feedstock is uniformly distributed in a bed of inert particles (the ash itself in the case of coal) made fluid by the blast injected at proper velocity from the bottom. Their operating temperature must be kept below the softening point of the ashes since their agglomeration inhibits the correct bed fluidization. This limits the reaction kinetics and makes fluid beds the reference technology for gasification of reactive feedstocks, such as low-rank coals and biomass rather than hard coal. The uniform distribution of material in the reactor results in partially reacted fuel being removed with the ash, leading to limited carbon conversion – lower than 97% in even the best process with strong recirculation of solids.

15.4.3 Syngas treatment and hydrogen production

Independent of the gasification process adopted, after the raw syngas stream has been cooled, it has to be cleaned up to allow its reliable and environmentally safe utilization. The first step of cleaning is water scrubbing, which is carried out at the end of the cooling process to remove particulates and water-soluble species. WGS reactors may be placed after the scrubber if the ratio H_2 to CO of the syngas has to be corrected. In the case of coal, the significant content of sulfur in the syngas stream precludes using the same catalysts mentioned for natural gas reforming but sulfur-tolerant Co–Mo catalysts are available and have been successfully operated for years in several synthesis gas plants. In case of heavy feed, the high CO content in the syngas stream calls for a proportional water vapor concentration. The full water quench definitely provides enough water to drive the WGS reaction to completion, while a significant amount of steam has to be added in the case of dry cooling. Given the high content of CO in the syngas, substantial heat is released in the WGS reaction and this suggests the opportunity to arrange a two-stage process as discussed in section 15.3.1.

© Woodhead Publishing Limited, 2010

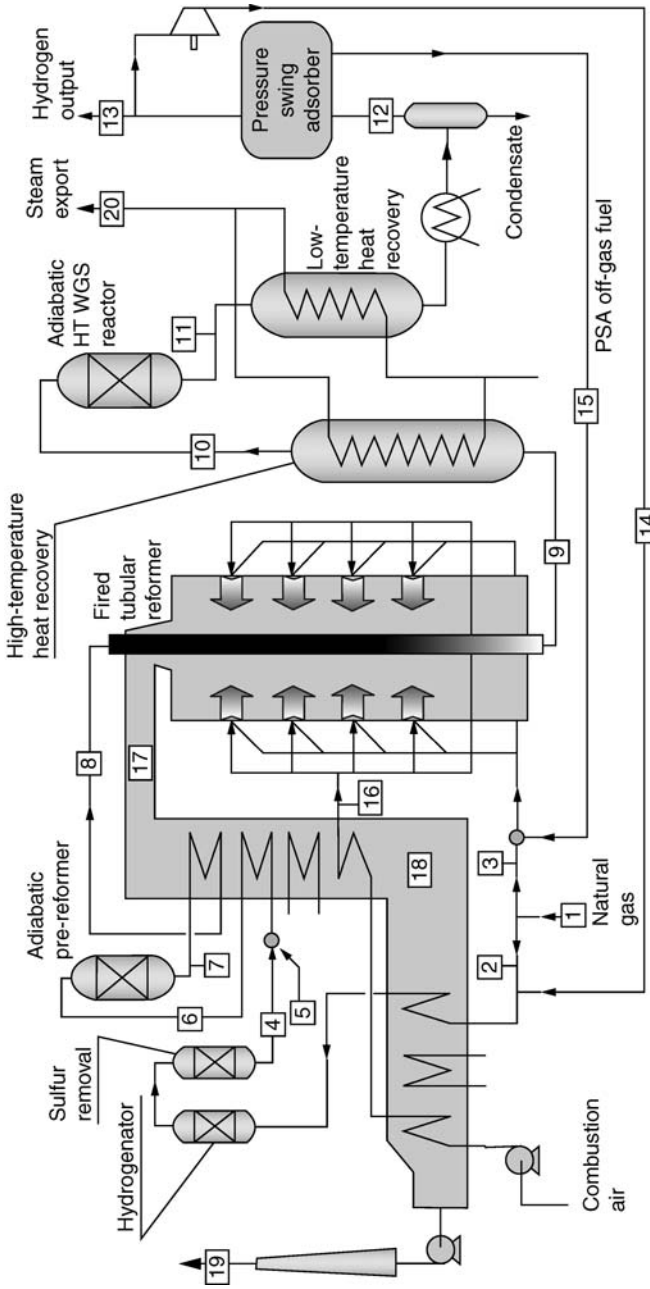
Sulfur in the raw coal is mainly converted to H_2S (and in a limited degree to COS) in the gasifier. Co–Mo WGS catalysts drive the conversion of COS contained in the syngas to H_2S, which is eliminated from syngas essentially by means of the same acid gas removal processes described in section 15.3.2. In plants without CO shift, if the selected AGR process is not effective on COS capture, COS is typically hydrolyzed to H_2S in a catalytic bed at about 200°C to enhance sulfur removal. Sulfur removal efficiency required in this case usually exceeds 99%, a value achievable by means of complete solvent regeneration in a stripping column. Since in the absorption tower a significant co-capture of CO_2 occurs along with H_2S absorption, particular care should be addressed to avoiding venting CO_2 in the plants where CO_2 sequestration is in place. Sulfur recovery is usually completed in a unit comprising an air-blown Claus plant for oxidizing H_2S to elemental sulfur. Claus plant tail gas, still rich in sulfur compounds, is then treated in a SCOT plant where those elements are catalytically converted to H_2S, which is removed by an amine absorption unit and recycled back to the absorption column of the AGR unit. Alternatively, concurrent capture and storage of CO_2 and H_2S may be a convenient option that allows elimination of the Claus and SCOT plants. Advantages related to a capital cost reduction must be weighed against possible increased risks and costs associated with transporting and storing CO_2 contaminated with a few percent H_2S. The clean syngas may finally be burned in a combined-cycle power plant as it occurs in IGCC plants or submitted to hydrogen recovery and purification treatments according to the final use.

15.5 Thermal balance of hydrogen production processes

15.5.1 Hydrogen production from natural gas

Figure 15.10 shows the complete layout of a plant based on a direct flame tubular reformer for production of high-purity hydrogen from natural gas.[12] Conditions at the most relevant points of the scheme are reported in Table 15.1 where the mass flow rates refer to a size of 30 000 Nm^3/h of hydrogen output. Input natural gas is divided into two streams: the 83% fraction allocated to hydrogen reforming is initially treated to remove sulfur traces and then mixed with steam. The charge having a 3.4 steam-to-carbon ratio is fed to an adiabatic pre-reformer and eventually to the fired reformer. Syngas at the reformer outlet is cooled to 330°C and shifted in an adiabatic reactor to enhance the hydrogen content. The syngas is then taken to ambient temperature for hydrogen recovery. Heat recovered in syngas cooling, along with additional heat from furnace flue gas, is used to produce 40 bar steam, which is partially exported from the plant. An 89% efficiency PSA is

© Woodhead Publishing Limited, 2010



15.10 Scheme of a mid-size plant for high-purity hydrogen production from natural gas based on a direct flame tubular reformer. Properties of points are listed in Table 15.1.

© Woodhead Publishing Limited, 2010

Table 15.1 Properties of significant streams in plant shown in Fig. 15.10 (lower heating value is reported in column 6). Compositions are given as mole percent of the total flow

	°C	bar	kg/s	kmol/s	MJ/kg	Ar	CH_4	C_{2+}	CO	CO_2	H_2	H_2O	N_2	O_2
1	20	45.0	2.73	0.1452	45.55	0.14	84.22	10.87		0.46			4.31	
2	20	45.0	2.26	0.1206	45.55	0.14	84.22	10.87		0.46			4.31	
3	20	45.0	0.463	0.0247	45.55	0.14	84.22	10.87		0.46			4.31	
4	365	40.0	2.27	0.1236	45.75	0.14	82.16	10.61		0.45	2.44		4.20	
5	294	41.0	8.11	0.4504								100.00	0.00	
6	490	36.6	10.38	0.5740	10.00	0.03	17.69	2.28		0.10	0.53	78.46	0.90	
7	440	35.6	10.38	0.6002	10.09	0.03	19.87		0.02	2.25	6.27	70.69	0.86	
8	620	35.1	10.38	0.6002	10.09	0.03	19.87		0.02	2.25	6.27	70.69	0.86	
9	890	32.7	10.38	0.7995	11.95	0.02	2.46		8.66	5.51	45.91	36.79	0.65	
10	330	31.7	10.38	0.7995	11.95	0.02	2.46		8.66	5.51	45.91	36.79	0.65	
11	401	31.0	10.38	0.7995	11.74	0.02	2.46		1.92	12.25	52.65	30.05	0.65	
12	31	30.0	6.07	0.5600	20.07	0.03	3.50		2.73	17.49	75.16	0.15	0.93	
13	36	29.0	0.75	0.3718	119.67		0.05				99.95		0.00	
14	85	44.0	0.0061	0.0030	119.67		0.05				99.95		0.00	
15	21	1.30	5.31	0.1852	5.86	0.09	10.49		8.27	52.89	25.00	0.46	2.80	
16	27	1.07	18.70	0.6480		0.92				0.04		1.03	77.28	20.73
17	1010	0.99	24.47	0.8289		0.74				19.32		17.27	61.17	1.49
18	525	0.98	24.47	0.8289		0.74				19.32		17.27	61.17	1.49
19	140	1.01	24.47	0.8289		0.74				19.32		17.27	61.17	1.49
20	300	40.0	4.45	0.2469								100.00		

Table 15.2 Performance of the plant for high-purity hydrogen production shown in Fig. 15.10.

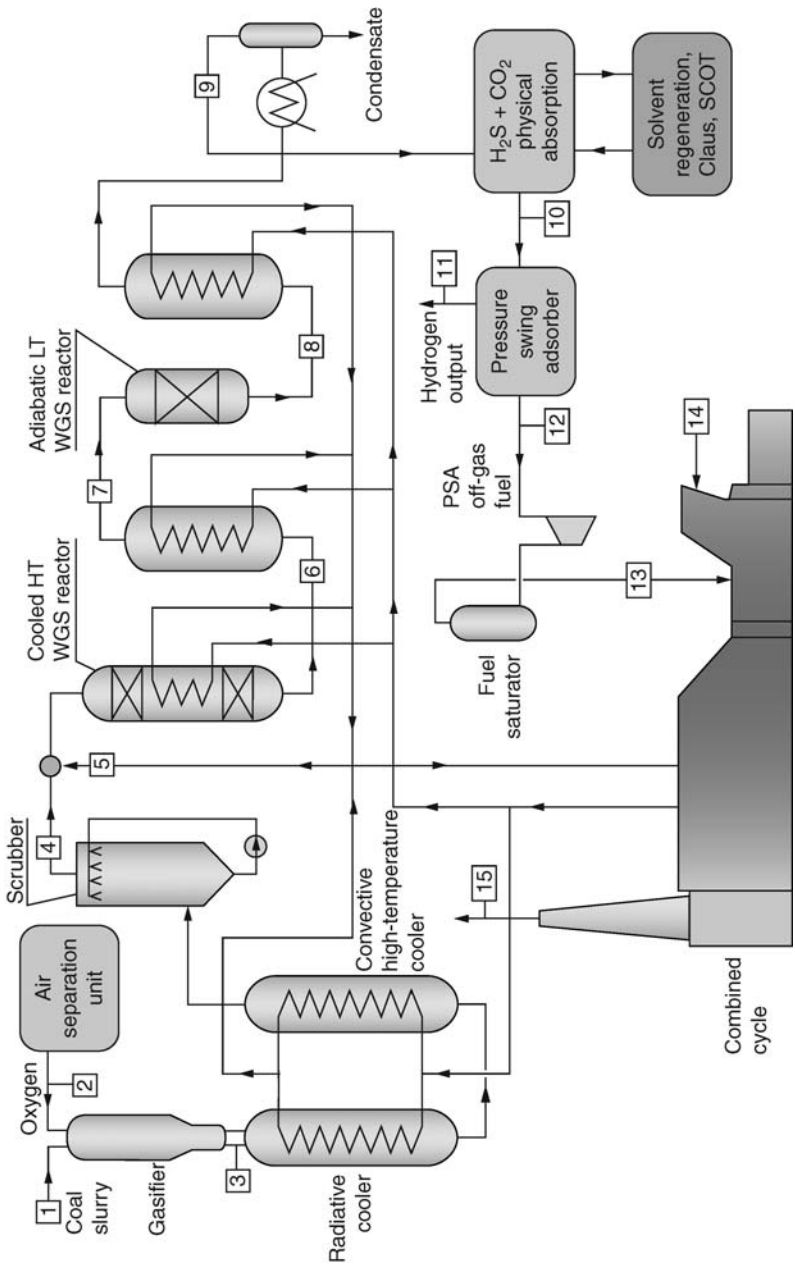
Natural gas input (LHV), MW	124.2
H_2 output flow rate, Nm^3/h	30 000
H_2 output (LHV), MW	90.0
Heat exported as steam flow, MW	12.8
H_2 production efficiency (LHV), %	72.45
Thermal efficiency (LHV), %	10.30

adopted to purify hydrogen, while the off-gas stream is burned with additional natural gas in the furnace to sustain reforming. Table 15.2 summarizes the overall plant performance. The process is able to convert 72% of the heating value of the whole natural gas input into hydrogen (lower heating value (LHV) basis). The overall efficiency rises to 83% when the energy value of the exported steam is considered.

15.5.2 Co-production of hydrogen and electricity from coal

Figure 15.11 shows the conceptual layout of an integrated large-scale plant for co-production of high-purity hydrogen and electricity from coal. The oxygen-blown entrained flow gasifier operates at 70 bar and it is fed with a slurry of two-third solids, one-third water produced by grinding Illinois #6

© Woodhead Publishing Limited, 2010



15.11 Scheme of a large-size plant for co-production of high-purity hydrogen and electricity from coal. Properties of points are listed in Table 15.4.

© Woodhead Publishing Limited, 2010

Table 15.3 Composition (% by weight) and heating value of the Illinois #6 coal assumed as the feedstock for the plant depicted in Fig. 15.11.

C	61.27	Moisture	12.00
H	4.69	Ash	8.70
O	8.83		
N	1.10	HHV, MJ/kg	26.143
S	3.41	LHV, MJ/kg	24.826

Table 15.4 Properties of significant streams in plant shown in Fig. 15.11 (lower heating value is reported in column 6). Compositions are given as mole percent of the total flow

	°C	bar	kg/s	kmol/s	MJ/kg	Ar	CH_4	CO	CO_2	H_2	H_2O	H_2S	N_2	O_2
1	15	1.01	95.4	—	19.96	Coal slurry: 75.8% coal with composition of tab. 2 + 24.2% water by weight								
2	207	84.0	58.1	1.804	0.00	3.65							1.35	95
3	1327	70.0	147.2	7.246	9.58	0.908	0.037	42.192	8.639	28.754	17.681	1.060	0.729	0.000
4	194	65.9	151.3	7.476	9.25	0.873	0.036	40.567	8.306	27.647	20.851	1.019	0.701	
5	440	70.0	72.3	4.011	0.00						100			
6	400	64.6	223.5	11.487	5.78	0.568	0.023	3.641	28.167	40.755	25.725	0.663	0.456	
7	207	63.3	223.5	11.487	5.78	0.568	0.023	3.641	28.167	40.755	25.725	0.663	0.456	
8	242	62.7	223.5	11.487	5.72	0.568	0.023	0.580	31.228	43.816	22.664	0.663	0.456	
9	35	60.2	176.8	8.892	7.23	0.734	0.030	0.750	40.342	56.604	0.094	0.857	0.589	
10	35	59.3	21.3	5.337	57.98	1.222	0.050	1.248	2.182	94.220	0.097	0.000	0.981	
11	35	58.0	8.6	4.265	119.95					100				
12	35	1.5	12.7	1.071	16.14	6.086	0.251	6.217	10.868	71.207	0.485		4.887	
13	180	22.3	28.0	1.916	7.35	3.403	0.140	3.476	6.076	39.813	44.360	0.000	2.732	0.000
14	15	1.01	152.3	5.278	0.00	0.92			0.037		1.028		77.282	20.733

coal (Table 15.3). Syngas is then cooled in radiative and convective syngas coolers, water scrubbed and mixed with steam to ensure the correct steam-to-carbon ratio for the following sulfur-tolerant shift reactors. Given the high CO content in the syngas, a cooled high-temperature WGS reactor is adopted to prevent the catalyst from overheating. After completing CO conversion in a low-temperature shift reactor, the syngas is cooled to ambient temperature and treated for acid gas removal by physical absorption. Preliminary removal of CO_2 increases the heating value of the PSA purge gas to a point that makes feasible its use in a gas turbine, with a benefit in efficiency of the plant. An 84.8% efficiency PSA finally separates the high-purity hydrogen stream from the off-gas addressed to the combined-cycle power plant. Properties at the most significant points of the plant are listed in Table 15.4, where the mass flow rates have been selected to match a thermal input of an $80\,MW_{EL}$ high-performance industrial gas turbine engine. The resulting hydrogen output is over $340\,000\,Nm^3/h$ and the complete plant energy balance is reported in Table 15.5.

© Woodhead Publishing Limited, 2010

Table 15.5 Performance of the plant for co-production of high-purity hydrogen and electricity shown in Fig. 15.11

Electric power, MW	80.1
Gas turbine	165.7
Steam turbine	−84.3
Air separation units	−17.9
Gasification auxiliaries	−4.4
Power island auxiliaries	−14.7
CO_2 removal + H_2 purification	−12.4
PSA off-gas compressor	−3.3
Heat rejection	
Net power output	108.7
Coal input (LHV), MW	1794.0
H_2 output flow rate, Nm^3/h	344 171
H_2 output (LHV), MW	1031.4
Heat released to ambient, MW	326.1
Electric efficiency (LHV), %	6.06
H_2 production efficiency (LHV), %	57.49

15.6 Future trends

15.6.1 Application of advanced techniques in decentralized small-scale plants

The current interest in hydrogen mainly originates from the possibility of distributing a carbon-free energy carrier which could substitute fossil fuels in power generation with the aim of reducing CO_2 emissions. On the other hand, hydrogen penetration in the transportation sector could promote diffusion of fuel cell technology causing a remarkable decrease in fossil fuel consumption by vehicles when compared to present engines. Creation of the hydrogen distribution infrastructures is the main hurdle to such evolution, especially in the first phases, when consumption is low and thinly spread over a wide territory. Decentralized small-scale plants could be a transitory solution to provide hydrogen for the embryonic fuel cell car market. Such small plants set requirements in terms of capital cost, size and starting transient completely different from the large ones previously described. Catalytic partial oxidation could find convenient application in such plants, along with membrane reformers and WGS reactors that allow integration of hydrogen production and separation, getting rid of some plant components. Decentralized plants could be fed by natural gas, methanol (in areas not supplied by the natural gas grid) or syngas from gasification of biomass, whose distributed production precisely matches such a pattern. The extreme outcome of such a concept leads to compact on-board devices capable of producing hydrogen in a vehicle directly starting from gasoline or diesel fuel.

© Woodhead Publishing Limited, 2010

15.6.2 CO_2 capture strategies for hydrogen production

Responses to climate change could lead in the longer term to massive production of decarbonized energy carriers from fossil fuels in combination with CO_2 capture and sequestration (CCS) strategies. Hydrogen will eventually be one of these carriers with prospects of penetration in the transportation sector or distributed via pipeline. CO_2 capture calls for centralized production, given that it is unrealistic to build a decentralized CO_2 sequestration system and too expensive to deploy a dense grid to collect CO_2. All the hydrogen production systems considered above are appropriate for CO_2 sequestration given that most of the carbon contained in the initial charge is eventually converted to CO_2. Capture efficiencies higher than 85% may be easily achieved in plants based on ATR reformers or gasification processes. In FTR reformers a substantial additional CO_2 emission may come from fuel used in the furnace that accounts for approximately 15–20% of the overall input fuel. To cut this CO_2 source the simplest solution is to heat the furnace with a fraction of the hydrogen produced.

To allow sequestration CO_2 has to be removed separately from other contaminants but, as already discussed, this does not entail dramatic changes in the scheme of hydrogen production plants or a significant addition of new components (limited to the CO_2 compression train). This makes a considerable difference compared to electric power stations where CO_2 capture involves substantial modifications of the basic plant. The resulting cost of the avoided CO_2 is therefore much lower for hydrogen plants than for electricity production plants suggesting that the former could be the forerunner in implementation of CO_2 sequestration techniques. A possible integrated approach has been proposed[13,14] for co-production of hydrogen and electricity. No significant advantages have been observed in such integration compared to plants for separate production in terms of conversion efficiency. Nevertheless the solution could be appealing from the economic perspective if production could be modulated to generate more electricity in peak hours, and more hydrogen in off-peak periods.

15.7 Sources of further information

Syngas and hydrogen production have been discussed in several publications. A recent book[15] deals systematically with hydrogen production and utilization, and treats in detail also hydrogen production from nuclear and renewable sources, transportation, storage and safety issues which have been neglected for the sake of brevity in the present chapter. A simpler textbook[16] covers the same subjects. A complete review of material requirements for handling hydrogen in all the phases from production to utilization is provided by Jones and Thomas.[17] A wide assessment

© Woodhead Publishing Limited, 2010

concerning gasification of coal, biomass and heavy liquid fuels is given by Dybkjaer and Winter Madsen,[12] which also deals with practical issues regarding the design of components. The *Ullmann's encyclopedia of industrial chemistry* contains two very comprehensive chapters about syngas[18] and hydrogen[19] production. The reader may also find helpful a classic textbook[1] to get deeper into the theoretical fundamentals about the ancillary technologies (such as charge purification, acid gas removal, hydrogen separation, etc.) always present in synthesis gas generation plants. Finally the DOE/NETL website[20] represents an excellent source of free information, especially concerning on-going research activities about advanced technologies.

Great emphasis is also given to the prospects for using hydrogen as a low-carbon energy vector in a sustainable economy facing the incumbent global climate change. The best known textbook addressing these subjects is probably by Rifkin,[21] but interesting analyses, partly covering more technological aspects, can also be found elsewhere.[22,23]

15.8 References

1 Kohl A.L., Nielsen, R.B., *Gas purification*, 5th edn., Gulf Publishing Company, Houston, Texas, USA, 1997, ISBN 0-88415-220-0.

2 Basini L. 'Issues in H2 and synthesis gas technologies for refinery, GTL and small and distributed industrial needs', *Catalysis Today* 2005, 106, 34–40, doi: 10.1016/j.cattod.2005.07.179.

3 Aasberg-Petersen K., Bak Hansen J.-H., Christensen T.S., Dybkjaer I., Seier Christensen P., Stub Nielsen C., Winter Madsen S.E.L., Rostrup-Nielsen J.R., 'Technologies for large-scale gas conversion', *Applied Catalysis A: General* 2001, 221, 379–387.

4 Dybkjaer I., Rostrup-Nielsen T., Aasberg Petersen K., 'Hydrogen and synthesis gas', in *ENI encyclopedia of hydrocarbons*, vol. 3, pp. 469–500, Treccani, Rome, Italy, 2007.

5 Grunwaldt J.-D., Basini L., Clausen B.S., 'In situ EXAFS study of Rh/Al2O3 catalysts for catalytic partial oxidation of methane', *Journal of Catalysis* 2001, 200, 321–329, doi: 10.1006/jcat.2001.3211.

6 Bredesen R., Jordal K., Bolland O., 'High-temperature membranes in power generation with CO_2 capture', *Chemical Engineering and Processing* 2004, 43, 1129–1158, doi: 10.1016/j.cep.2003.11.011.

7 Sircar S., 'Pressure swing adsorption technology', Proceedings of NATO Advanced Study Institute on *Adsorption science and technology*, Vimerio, Portugal, July 1988.

8 Di Luozzo M., 'The hydrogen cycle', in *ENI encyclopedia of hydrocarbons*, vol. 3, pp. 59–69, Treccani, Rome, Italy, 2007.

9 Bion N., Epron F., Moreno M., Mariño F., Duprez D., 'Preferential oxidation of carbon monoxide in the presence of hydrogen (PROX) over noble metals and transition metal oxides: advantages and drawbacks', *Top Catalysis* 2008, 51, 76–88, doi: 10.1007/s11244-008-9116-x.

© Woodhead Publishing Limited, 2010

10. Dagle R.A., Wang Y., Xia G.-G., Strohm J.J., Holladay J., Palo D.R, 'Selective CO methanation catalysts for fuel processing applications', *Applied Catalysis A: General* 2007, 326, 213–218, doi: 10.1016/j.apcata.2007.04.015.
11. Higman C., van der Burgt M., *Gasification*, Elsevier Science, USA, 2003, ISBN 0-7506-7707-4.
12. Dybkjaer I., Winter Madsen S., 'Advanced reforming technologies for hydrogen production', *The International Journal of Hydrocarbon Engineering*, December/January 1997/1998.
13. Chiesa P., Consonni S., Kreutz T., Williams R., 'Co-production of hydrogen, electricity and CO_2 from coal with commercially ready technology. Part A: performance and emissions', *International Journal of Hydrogen Energy* 2005, 30/7, 747–767, doi: 10.1016/j.ijhydene.2004.08.002.
14. Kreutz T., Williams R., Consonni S., Chiesa P., 'Co-production of hydrogen, electricity and CO_2 from coal with commercially ready technology. Part B: economic analysis', *International Journal of Hydrogen Energy* 2005, 30/7, 769–784, doi: 10.1016/j.ijhydene.2004.08.001.
15. Gupta R.B. (ed.): *Hydrogen fuel, production, transport and storage*, CRC Press, Boca Raton, USA, 2008, ISBN 978-1-4200-4574-8.
16. Rand D.A.J., Dell R. M., *Hydrogen energy: challenges and prospects*, RSC Publishing, UK, 2008, ISBN 978-0-85404-597-6.
17. Jones R.H., Thomas G.J, *Materials for the hydrogen economy*, CRC Press, Boca Raton, USA, 2008, ISBN 0-8493-5024-7.
18. Hiller H *et al.*, 'Gas production', in *Ullmann's encyclopedia of industrial chemistry*, Wiley-VCH, 2006, doi: 10.1002/14356007.a12_169.pub2.
19. Häussinger P., Lohmüller R., Watson A.M., 'Hydrogen', in *Ullmann's Encyclopedia of Industrial Chemistry*, Wiley-VCH, 2002, doi: 10.1002/14356007.a13_297.
20. DOE NETL website: http://www.netl.doe.gov/publications/index.html.
21. Rifkin J., *The hydrogen economy*, Tarcher/Penguin, USA, 2003, ISBN 1-58542-254-1.
22. Kruger P., *Alternative energy resources*: *The quest for sustainable energy*, John Wiley & Sons, USA, 2006, ISBN 0-471-77208-9.
23. Cipiti B., *The energy construct: Achieving a clean, domestic, and economical energy future*, Booksurge Publishing, USA, 2007, ISBN 1-4196-6978-8.

© Woodhead Publishing Limited, 2010

Index

acid gas removal, 71–4, 395–6
  applications and characteristics, 72
acoustic pressure, 251–2
activated carbon injection systems, 209–12
  demonstrated mercury removal at 2 or 5 lb/MMacf, 211
  mercury removal as function of concentration
    activated carbon injection concentration, 210
    activated carbon injection concentration using TOXECON II, 212
    chemically-treated activated carbon injection concentration, 211
advanced hybrid particulate collector, 236–7
  schematic diagram, 237
advanced optimised lignite technologies, 306
aero engines, 9, 18
  vs heavy industrial gas turbines requirements, 5
agglomeration technology, 303
air-based method utilising dense-medium fluidised bed, 296
air-blown gasification, 339–40
air separation unit, 340, 348
algae, 318
all-volatile treatment, 102–3
aluminosilicates, 370–1
amines, 348, 349
ammonia, 67, 207
ammonium bisulphate, 204
ammonium sulphate, 204
Angren power station, 347
anhydrous ammonia, 206
animal fats, 317
aquatic biomass, 317
aqueous trapping, 370
aquifer storage and recovery, 368
ARRA *see* Federal American Recovery and Reinvestment Act
Arrhenius relationship, 153
ASTM A193 GR B16, 14
asymmetric membrane, 114
ATR *see* autothermal reformers
Australian Victorian brown coal, 300
autothermal reformers, 387–9, 409
  schematic diagram, 387
autotuning techniques, 280
AVT (O), 102–3
AVT (R), 102

baghouse filters, 71, 203, 229
  see also fabric filters
Bayesian belief networks model, 261
binderless briquetting, 305
biomass
  available resources, 318–19
  chemical constituents in biomass fuels, 320–3
    herbaceous biomass, 321
    MSW, 321
    residual resources, 323
    woody biomass, 321
  conversion technologies classification, 317–18
  energy potentials and usage in 2004, 319
  fuel flexibility improvement in advanced power plants, 312–30
  fuels physical preparation, 324–8
    Danish wheat straw fired at Studstrup Power Station, 327

© Woodhead Publishing Limited, 2010

different biomasses comminution energy consumption, 325
palletising plant, 326
pellet production energy and costs, 327
pellet types, 328
pre-processing system Studstrup Power Station, 328
wood chip classifications, 324
functional biomass mixes, 329–30
ash properties changes through functional mixing, 329
residual resources, 319
resource to product conversion paths, 316
sketch of atmospheric CO_2 increase, 314
types and conversion technologies, 316–17
world biomass energy flows in 2004, 315
biomass mixes, 329
BoA *see* Braunkohlekraftwerk mit optimierter Anlagentechnik
boiler–turbine system, 280
bottom hole assemblies, 345
Braunkohlekraftwerk mit optimierter Anlagentechnik, 306
Brayton cycle, 4, 33, 48
briquetting, 303–5
British Gas/Lurgi slagging gasifier, 64
brown coal, 292, 297–8
Brownian motion, 221

calcium sulphate, 197, 199
see also gypsum
calcium sulphite, 192, 201
calcium sulphite hemihydrate, 191–2, 193
candle filters, 70–1
capacity factor, 26
capillary condensation, 151
capillary membrane module, 162
carbon capture and storage technologies, 333, 366, 409
carbon deposition, 393
carbon dioxide, 7, 143, 308
applicable capture technologies, 67–9
cryogenic separation, 69
membrane separation, 68–9
physical and chemical absorption, 67–8
capture, 143–8
overview, 146
principles, 145
trends, 81
emissions control technologies, 42–6
post-combustion control, 44–6
amine based CO_2 capture, 45
oxy-combustion, 45–6
potential sequestration into abandoned UCG cavities, 353
precombustion control, 42–4
selected studies for enhanced oil recovery, 367
storage in UCG process vicinity, 353–4
total and partial capture from product gas, 348–50
partial capture, 349–50
total capture, 349
transport properties/parameters and selected references, 367
carbon dioxide separation membrane
advanced development for power plants, 143–77
CO_2 capture principles, 145
CO_2/N_2 selectivity vs CO_2 permeability, 154
CO_2 separation and capture processes, 146
cost considerations, 175–7
costs as a function of pressure, 176
membrane system performance, 148–55
molecular weight and kinetic diameter of some gases, 151
Robeson's curve for CO_2/CH_4 separation, 155
design for power plant integration, 169–75
CO_2 permeate concentration, 172, 173
CO_2 recovery ratio vs stage cut, 171
feed mixture concentration, 175
membrane properties, 173
permeate concentration vs CO_2 recovery fraction, 174
gas absorption principle, 160
materials and design, 156–61
facilitated transport membranes, 159
hybrid membranes, 158–9
membrane contactors, 159–61
mixed-matrix membranes, 157–8

© Woodhead Publishing Limited, 2010

specific surface area of some contactors, 161
membrane modules, 161–9
capillary membrane module, 162, 165
characteristics, 168
comparison, 166–9
conceptual scheme, 162
costs, concentration polarisation control, and applications, 168
equipment configuration, 164
hollow-fibre membrane cross-section, 167
hollow-fibre membrane modules, 163, 165–6
other design parameters, 169
shell-side and bore-side feed hollow-fibre modules, 166
spiral-wound membrane in multi-module vessel, 165
spiral-wound module, 163, 165
carbon dioxide storage
advanced power plants environmental improvement, 364–79
alternatives to geologic storage, 376–7
CO_2 capture and sequestration from power plants, 365–6
enhanced oil/gas and coalbed methane recovery, 371–2
future trends, 377–9
sealing and monitoring to ensure CO_2 containment, 376
subsurface CO_2 flow and transport fundamentals, 366–8
deep saline formations, 372
emissions vs potential subsurface storage capacity, 375
general site selection criteria, 373–5
oil/gas vs coal vs deep saline, 372–3
subsurface CO_2 storage
fundamentals, 368–71
aqueous or solubility trapping, 370
chemical or mineral trapping, 370–1
general or traditional fluid storage in subsurface, 369
hydrodynamic or stratigraphic trapping, 370
residual gas or phase trapping, 371
carbon molecular sieve, 121
carbon molecular sieve membrane, 121
carbon monoxide
control, 41–2
emission trends, 28
carbonic acid, 370
carbonyl sulphide, 384
carrageenan, 329
casings, 14–15
catalyst deactivation, 393
catalytic combustor, 52
catalytic partial oxidation, 389, 408
caustic gouging, 96
CCS *see* carbon capture and storage technologies
ceramic coatings, 50
ceramic composites, 50
ceramic matrix composites, 29
ceramic membrane, 117–20
cermet membranes, 114
chemical-looping combustion, 144
chemical trapping, 370–1
chromium carbide, 11
cigar waste, 329
Claus plant, 348, 403
Claus process, 74
Clean Air Act Amendments (1970), 188
Clean Air Act Amendments (1977), 188
Clean Air Act Amendments (1990), 188
Clean Air Mercury Rule (2005), 188
co-current flow, 122–3
CO_2-EOR methods, 371, 373
coal
characteristics, 343
structure and physical properties, 343–4
coal bed methane, 345
coal cleaning, 295
coal-fired power plants
advanced control, 279–82
fuel splitting control, 280
furnace and boiler control, 280–2
imaging and neural net based combustion control system, 281
pulverising mill control, 279–80
advanced monitoring and process control technology, 264–84
3D flame temperature measurement, 278
distribution in Utah and their respective annual CO_2 emissions, 374
flame stability monitoring, 272–3
flame-eye-based, 273
multi-channel monitoring system, 273

© Woodhead Publishing Limited, 2010

fuel tracking
basic neural network for on-line tracking, 275
monitor basic sensing arrangement, 274
on-line tracking, 273–5
future trends, 282–4
on-line monitoring and measurement sensors, 266–79
3D plot of first three principal components, 275
electrostatic particle fineness sensors under test, 271
flame imaging, 276–9
flame parameters definitions, 276
fuel bunker monitoring, 266–7
on-line particle sizing, 270–2
pulverised fuel flow metering, 269–70
pulverising mill monitoring, 267–8
root and middle regions of flame field, 277
typical fuel supply and distribution system, 265
coal gasification, 60–4, 332, 366
see also underground coal gasification
entrained-glow gasifier, 61–3
fluidised-bed gasifier, 63
future trends, 79–81
moving-bed gasifier, 63–4
coal washing, 295
CoalTek, 302
coal–water slurry injection, 400
coarse homogeniser, 324
coffee, 329
COHPAC *see* compact hybrid particulate technology
COHPAC I, 236
COHPAC II, 236
combined cycle, 32–3
combined-cycle gas turbine, 347
combustion
behaviour, 246–8
experimental combustor, 247
high-temperature and smart sensor networks for power plants monitoring, 244–62
system, 10–11
combustor, 10
developments, 51–2
catalytic combustor, 52
pressure gain combustor, 51
trapped vortex combustor, 51–2
dynamics, 10
Co–Mo catalyst, 402–3
compact hybrid particulate technology, 236
compressor, 9–10
compressor coatings, 10
computational fluid dynamics, 282
contactors, 159–61
controlled retraction injection point, 338
Cool Water IGCC, 55
countercurrent flow, 123
CRIP *see* controlled retraction injection point
cross-flow, 123
cryogenic separation, 69
Cunningham correction factor, 222
cyclone filters, 69–70

Danish wheat straw, 327
Darcy's equation, 231
dense membranes *see* non-porous membranes
dense phase reburn, 214
Deutsch–Anderson equation, 222
diffusivity coefficient, 149
diode-laser-based-absorption sensors, 248
disk pelletizers, 303
drift velocity, 222
drilling and completion technology, 338
drop-in-core microcontroller, 257
dry ESPs, 219
dry flue gas desulfurisation technology, 194–203
duct sorbent injection, 202–3
economiser injection, 201
furnace sorbent injection, 197–201
hybrid systems, 203
other sorbent injection process, 197
simplified process schematic diagram, 198–9
SO_2 capture regimes for hydrated calcitic lime, 200
spray dry scrubbers, 194–6
spray dryer absorber and particulate control system components, 195
dry low nitrogen oxide burners, 66
dry sorbent injection *see* duct sorbent injection
dual-mode sorption model, 153
duct sorbent injection, 202–3

economiser injection, 201

© Woodhead Publishing Limited, 2010

electrical conductivity, 106
electromagnetic interference, 250
electrostatic precipitators, 193, 201, 219–28
  ash removal, 223
  charging and collecting particles basic concept, 221
  collection efficiency, 223
  construction materials, 228
  factors affecting performance, 224–7
    ash composition on fly ash resistivity for coals, 226
    temperature on resistivity based on coal sulphur content, 224
  future trends, 236–41
    mid- to long-term technologies, 238–41
    near- to mid-term technologies, 236–8
  generalised schematic diagram, 220
  operating principles, 220–1
  particle charging, 221
  particle collection, 222–3
  performance enhancement, 227
  precipitator efficiency by number of fields, 223
  wet ESPs, 227–8
electrostatic sensors, 271
enhanced coal bed methane, 353
enhanced oil recovery, 371
entrained-flow gasifier, 61–3, 399–401
ESP *see* electrostatic precipitators
European Groundwater Directive, 352
European UCG programme, 334
European wood chip classification, 324
extrusion, 303

fabric filters, 229–36
  cleaning mechanisms simplified diagrams, 233
  construction materials, 234
  filtration fabrics, 234–6
  future trends, 236–41
    mid- to long-term technologies, 238–41
    near- to mid-term technologies, 236–8
  generalised schematic diagram, 230
  materials composition for various filter media, 241
  media characteristics, 235
  operating principles, 229–32
  performance enhancement, 234
  specific designs, 232–4
Fabry–Perot sensor, 251, 256
facilitated transport membranes, 159
fast Fourier transform, 252–3
Federal American Recovery and Reinvestment Act, 377
FGD *see* flue gas desulfurisation
fibre Bragg grating sensors, 250–1
fibre optic sensors, 250–1
filters *see* fabric filters
fired tubular reformers, 386–7, 409
firing temperature, 6, 49, 50
fixed bed gasifiers *see* moving-bed gasifier
flame
  3D temperature measurement, 278
  imaging, 276–9
  parameters definitions, 276
  root and middle regions definitions, 277
  stability monitoring, 272–3
    flame-eye-based, 273
    multi-channel monitoring system, 273
flame eyes, 272, 283
flue gas cleaning systems
  activated carbon injection systems, 209–12
  desulfurisation, 189–203
    dry FGD technology, 194–203
    wet FGD technology, 189–94
  future trends, 212–15
    mercury capture, 214–15
    NO_x control, 213–14
  hybrid SNCR/SCR, 208
  selective catalytic reduction, 203–7
    configuration and catalyst composition, 206
    operation, 206–7
    process description, 204–5
  selective non-catalytic reduction, 207–8
  sulphur oxides, nitrogen oxides and mercury emissions control in power plants, 187–215
flue gas dedusting systems
  ash and particulate emissions control in power plants, 217–41
    electrostatic precipitators, 219–28
    fabric filters, 229–36
  future trends, 236–41
  materials, design, and development for particulate control, 219

© Woodhead Publishing Limited, 2010

flue gas desulfurisation, 189–203, 297
fluid beds, 402
fluidisation, 298
fluidised-bed dryer, 297–8
fluidised-bed gasifier, 63
fossil-fuel power plant
  hydrogen membrane shift reactor, 128
  precombustion CO_2 capture, 127
frequency-modulated continuous wave, 267
FTR *see* fired tubular reformers
fuel bunker monitoring, 266–7
fuel dilution, 67
functional biomasses, 329
furnace sorbent injection, 197, 199–201
FutureGen plant, 55
fuzzy reasoning, 280

gamma prime, 14
gas-fired combined-cycle power plant
  advantages and limitations, 46–8
  applicable criteria pollutants control technologies, 41–2
    ammonia control, 42
    CO and volatile organic compounds, 41–2
    NO_x control, 41
  carbon dioxide emissions control technologies
    post-combustion control, 44–6
    precombustion control, 42–4
  design and technology, 32–52
    efficiency gain over a simple cycle, 33
    fuel specifications, limits and variability, 36–7
    gas turbine with and without reheat, 34
    single and dual pressure ideal steam cycles, 35
    steam cycle types, 34
    types of gas turbines for applications, 33–4
    typical plant process description, 37–41
  future trends, 48–52
    combustor developments, 51–2
    gas turbine firing temperature, pressure ratio and intercooling, 49–50
    materials development, 50
    reheat gas turbines, 50
    steam-cooled gas turbine and triple pressure reheat steam cycle, 38
gas permeation rate, 149
gas separation, 148, 149
gas turbine, 47–8, 347
  advanced materials, design and technology, 3–30
    future trends, 29–30
    NGCC power plant levelised cost of electricity, 6
    trends in output and efficiency, 7
  components development of materials and coatings
    casings, 14–15
    combustion system, 10–11
    compressor, 9–10
    materials and technology historical trend, 13
    rotating turbine blade cross-section, 12
    rotors, 15
    SGT6-6000G, 8
    through-thickness temperature gradient, 13
    turbine, 11–14
  components materials and coatings development, 8–15
  design for hydrogen-rich gases, 21–6
    compressor characteristic, 22
    compressor operability, 22–3
    correlation of relative NO_x with stoichiometric flame temperature, 24
    design and materials for high hydrogen, 25–6
    high-hydrogen combustion, 23–5
    predicted turbulent flame speed, 24
    syngas and natural gas heating values, 21
    turbine enthalpy diagram, 26
  design to run at variable generation rates, 26–9
    load following over a 24 hour period, 27
    NO_x and CO emission trends, 28
    operating regimes based on ISO-3977-2, 27
  firing temperature, pressure ratio and intercooling, 49–50
  higher temperature efficiency operation, 15–21
    cooling circuit, 19

© Woodhead Publishing Limited, 2010

efficiency vs engine pressure ratio, 16
high temperature combustion, 19–21
increasing pressure ratio, 17
NO_x emissions and combustor temperature, 20
turbine design for high inlet temperature, 18–19
turbine inlet temperature on combined cycle efficiency, 17
IGCC power plant, 65–7
future trends, 82–3
hydrogen-rich syngas-fired gas turbine, 65–6
NO_x emissions control, 66–7
schematic representation, 4
vs aero engines requirements, 5
with and without reheat, 34
gas turbine test, 66
gasification, 55, 383, 399
geologic carbon sequestration, 364
technical and practical aspects, 378
German moist lignite, 300
German Rhenish coal, 298
glass membranes, 155
glass transition temperature, 152
GORE-TEX, 235
graphite, 235
gravity segregation, 367
gypsum, 190, 192, 193

Hazelwood power plant, 306
heat exchange steam reformers, 389, 390, 391
heat recovery steam generator, 21, 37, 39, 57–8
Hebbian learning, 278
Henry's law, 152
herbaceous biomasses, 317, 320, 321
agricultural straws, 322
grasses, 322
HESR *see* heat exchange steam reformers
high-temperature ceramic filters, 240
high-temperature shift reactors, 64–5
high-temperature Winkler process, 298
hollow-fibre membrane modules, 121, 163, 165–6, 167, 169
honeycomb briquettes, 304
hot gas filtration vessel
schematic diagram, 239
vessel internals photograph, 240
hybrid membranes, 158–9
hybrid SNCR/SCR, 208
hydrated lime, 194, 200, 202
hydrodynamic trapping, 370
hydrogen, 23, 111–12, 132–3
adiabatic pre-reformer and fired tubular reformer, 386
from fossil-fuel feedstocks in power plants, 383–409
from heavy feedstocks, 399–403
entrained flow gasifiers, 399–401
other gasifier arrangements, 401–2
production and syngas treatment, 402–3
large-size plant
high-purity hydrogen production, 406
properties of significant streams, 407
midsize plant
high-purity hydrogen production, 404
properties of significant streams, 405
plant performance
co-production of high-purity hydrogen and electricity, 408
high-purity hydrogen production, 405
production processes thermal balance, 403–7
co-production of hydrogen and electricity from coal, 405–7
composition and heating value of Illinois #6 coal, 407
from natural gas, 403–5
recovery and purification, 396–9
hydrogen damage, 96
hydrogen disulphide, 348
hydrogen flux, 115
hydrogen separation membrane
advanced development for power plants, 111–34
future trends, 133–4
hydrogen metal membrane separation targets, 125
hydrogen storage and transportation, 132–3
integration with power plant, 125–32
membrane flow patterns, 122
natural gas membrane reformer, 131

© Woodhead Publishing Limited, 2010

SOFC power plant, 130
system design and performance, 121–4
fossil-fuel power plant
incorporating hydrogen membrane shift reactor, 128
with precombustion carbon dioxide capture, 127
materials, 113–21
atomic hydrogen transport in metal membrane, 115
carbon molecular sieve membrane, 121
ceramic membrane, 117–20
gas molecules kinetic diameters, 118
metallic membrane, 115–17
mixed proton/electron conducting membrane, 119
multiphase ceramic/metal membrane, 120
polymeric membrane, 114–15
zeolite membrane, 120
two-stage membrane enhancement
enhancing permeate product purity, 124
enhancing residue product purity, 123
hydrogen sulphide, 384, 403

IGCC plants *see* integrated gasification combined cycle plants
induct dry injection *see* duct sorbent injection
industrial gas engines, 347
inseam drilling method, 346
integrated gasification combined cycle plants, 7, 23, 54–5, 112, 147, 218, 238–40, 333, 366
applicable CO_2 capture technologies, 67–9
cryogenic separation, 69
membrane separation, 68–9
physical and chemical absorption, 67–8
applicable emissions control technology, 69–75
acid gas removal, 71–4
mercury removal, 71
particulate matter removal, 69–71, 70
sulphur recovery and tail gas treatment, 74–5
coal IGCC plants advantages and limitations, 75–9
advantages, 75–9
estimated levelised cost of electricity for power plants, 78
limitations, 79
conceptual diagram
IGCC with CO_2 capture, 59
IGCC without CO_2 capture, 57
design and main processes
technologies, 60–7
coal gasification, 60–4
gas turbine, 65–7
gasification technologies characteristics, 61
water-gas shift reaction, 64–5
design and technology, 54–83
future trends, 79–83
CO_2 capture, 81
coal gasification, 79–81
F, G, and H class gas turbines major specifications, 82
gas turbine technologies, 82–3
types, 54–60
commercial and demonstration coal IGCC power plants, 56
with CO_2 capture, 58
without CO_2 capture, 55, 57–8
vs pulverised coal power plants, 76
Integrated Pollution Prevention Control, 351–2
intercooling, 49, 50
ion transport membranes, 348

Joule–Thomson effect, 115, 398

K-Fuel, 302
kaolinite, 329, 330
Kellogg Rust Westinghouse gasifier, 63
Knudsen diffusion, 151
Knudsen separation, 150–1

Langmuir adsorption, 153
Large Combustion Plant Directive, 352
levelised cost of electricity, 5, 78
NGCC power plant, 6
life cycle analysis, 313
lignin, 329
lignite, 292, 300
lignocellulosic biomass, 318
lime, 194
lime spray dryer process, 196
limestone, 193

© Woodhead Publishing Limited, 2010

scrubbing with forced oxidation, 192–3, 200–1
liquefied petroleum gas, 384
Longannet Power Station, 271
low-NO_x burners, 213
low-rank coal
advanced power plant fuel flexibility improvement, 291–309
chemical composition of various grades of coal, 292
dried lignite utilisation effect in Coal Creek power plant, 307
future trends in coal upgrading, 307–9
influence on design and efficiency of boilers, 294
preparation, 294–6
properties, 292–3
relative moisture and ash contents and calorific value, 293
upgrading technologies, 296–305
briquetting, 303–5
low-rank coal drying, 296–302
low-temperature lignite drying system, 301
steam tubular dryer, 297
utilisation in advanced power plants, 305–7
low-temperature shift reactors, 64–5
Lurgi dry ash gasifier, 64

Mach numbers, 18
Majuba coal field, 357
Markov models, 261
MDEA process, 72, 73
measure-while-drilling system, 346
Mechanisch-Thermische Entwasserung, 300
membrane contactors, 159–61
membrane flux, 113
membrane modules, 121, 161–9
membrane permeability, 113
membrane separation, 68–9, 148
MerCAP, 215
mercury, 71, 188
capture, 214–15
FGD systems, 214–15
innovative techniques, 215
removal, 71, 210, 211, 212
metal dusting, 391, 392
metallic membrane, 115–17
methanation, 385, 398
methane, 372
converted in a steam reforming process, 385
converted in an autothermal reforming process, 388
methane de-NO_x, 214
methyldiethanolamine, 395
micro-opto-electromechanical system, 256, 257
microprocessor, 257
migration velocity, 222
mineral trapping, 370–1
mineralisation, 376–7
Mining and Petroleum Acts, 352
mixed-matrix membranes, 114, 157–8
mixer agglomeration, 303
modified Wobbe Index, 36
module, 121
MOEMS *see* micro-opto-electromechanical system
monoethanolamine, 395
monolith modules, 121, 167–8
moving-bed gasifier, 63–4, 401–2
MTE *see* Mechanisch-Thermische Entwasserung
multipollutant control systems, 237–8
municipal solid waste (MSW), 317
chemical constituents, 320, 321
composition based on data from five Danish cities, 323
1200 MW Nuon Magnum IGCC plant, 55

nano-scale gas sensors, 251
National Energy Technology Laboratory, 372, 375
National Renewable Energy Laboratories (NREL), 29
natural gas, 19, 372, 384
natural gas combined cycle plants, 6, 27
natural gas reformer, 129
using air sweep to supply combustion heat, 131
using hot exhaust gas to supply heat, 131
natural gas storage, 368
NGCC plants *see* natural gas combined cycle plants
nitrogen oxides, 19, 28, 65
control, 41, 213–14
next generation low-NO_x burners, 213
novel enhanced combustion, 214

© Woodhead Publishing Limited, 2010

oxygen-enhanced combustion, 213–14
rich reagent injection/advanced layered technology approach, 213
SCR optimisation, 214
emission control, 66–7
emissions trends, 28
relationship of emissions with combustor temperature, 20
Nomex, 236
non-porous membranes, 150
Nu-Fuel process, 308

oceanic sequestration, 377
oxy-combustion, 45–6, 365–6
oxy-fuel combustion, 147
oxygen-enhanced combustion, 213–14
oxygen firing, 340, 347
oxygenated treatment, 103

palladium, 116
palletising process, 329
particulate control device, 238
perm-selectivity, 149, 150
permeability, 149
phase transition zone, 98–9
phase trapping, 371
pinch point effect, 294
PiT Indicator/Navigator, 282
planar membrane module, 121, 122
plate-and-frame device, 122
Pockel constants, 251
polymeric membranes, 114–15, 151–2
CO_2/N_2 selectivity vs CO_2 permeability, 154
performance, 157
polyphenylene sulphide, 236
polypropylene, 238
porous membranes, 150
post-combustion capture, 144–5, 176
power plants
advanced CO_2 gas separation membrane development, 143–77
cost considerations, 175–7
membrane materials and design, 156–61
membrane modules, 161–9
membrane system performance, 148–55
power plant integration design, 169–75
advanced hydrogen gas separation membrane development, 111–34
future trends, 133–4
hydrogen membrane integration with power plant, 125–32
hydrogen membrane materials, 113–21
hydrogen storage and transportation, 132–3
system design and performance, 121–4
biomass for fuel flexibility improvement, 312–30
available biomass resources, 318–19
chemical constituents, 320–3
conversion technologies classification, 317–18
functional biomass mixes, 329–30
physical preparation, 324–8
residual biomass resources, 319
types and conversion technologies, 316–17
CO_2 storage for environmental impact improvement, 364–79
alternatives to geologic storage, 376–7
capture and sequestration from power plants, 365–6
emissions vs potential subsurface storage capacity, 375
enhanced oil/gas and coalbed methane recovery, 371–2
future trends, 377–9
general site selection criteria, 373–5
sealing and monitoring to ensure CO_2 containment, 376
storage in deep saline formations, 372
storage options comparison, 372–3
subsurface flow and transport fundamentals, 366–8
subsurface storage fundamentals, 368–71
flue gas cleaning systems for SO_x, NO_x and mercury emissions control, 187–215
activated carbon injection systems, 209–12
flue gas desulfurisation, 189–203
future trends, 212–15
hybrid SNCR/SCR, 208
selective catalytic reduction, 203–7

© Woodhead Publishing Limited, 2010

selective non-catalytic reduction, 207–8
flue gas dedusting systems and filters
for ash and particulate emissions, 217–41
electrostatic precipitators, 219–28
fabric filters, 229–36
future trends, 236–41
materials, design, and development for particulate control, 219
high-temperature sensors and smart sensor networks for combustion monitoring, 244–62
combustion behaviour, 246–8
sensor considerations, 248–51
sensor information processing, 260–1
sensor response, 251–4
smart sensor networks vision, 255–60
low-rank coal for fuel flexibility improvement, 291–309
syngas and hydrogen production from fossil-fuel feedstocks, 383–409
future trends, 407–9
hydrogen and syngas from heavy feedstocks, 399–403
hydrogen production processes thermal balance, 403–7
syngas conversion and purification, 393–9
syngas production from gas and light liquids, 383–93
thermal cycle efficiency improvement, 89–107
advanced thermal power cycles characteristics, 91–3
challenges for future ultrasupercritical power cycles, 105–7
deposits and corrosion, 94–100
volatility, partitioning and solubility, 93–4
water and steam chemistry, 100–4
UCG for environmental impact improvement, 332–59
brief history, 334
drilling technologies and well construction, 344–6
environmental issues and benefits, 350–4
future trends, 354–8
integration with power plant, 346–50
process, 335–41
siting and geology criteria, 341–4
powered activated carbon injection, 238
precombustion capture, 145, 147, 177
precombustion gas processing, 346
preferential oxidation, 399
pressure drop, 231
pressure gain combustor, 51
pressure ratio, 9, 49
vs gas turbine efficiency, 16
pressure swing adsorption, 126, 396
pressurised fluidised-bed combustion, 238–40
principal component analysis, 274
Prism®, 114
proportional–integral–derivative controllers, 280
proton exchange membrane, 133
PSA *see* pressure swing adsorption
pulse-jet fabric filters, 233–4, 236
pulverised coal, 296
pulverised fuel, 320
flow metering, 269–70, 283
cross-correlation velocity measurement principle, 270
different electrostatic sensors for the velocity measurement, 270
power stations, 325
pulverising mill monitoring, 267–8, 282

qualified carbon dioxide, 377
quicklime, 197, 202

Rankine cycle, 4, 33, 35
recovery ratio, 170–1
Rectisol process, 67, 73, 395
refuse-derived fuels, 317
residual biomasses, 323
residual gas trapping, 371
resistivity, 224
reverse-gas fabric filters, 232, 235
rich reagent injection, 213
roll press, 303
rotors, 15
rubbery membranes, 152–3
vs glass membranes CO_2/CH_4 separation, 155

SCOT plant, 403
SCR *see* selective catalytic reduction
scrubbers, 365

© Woodhead Publishing Limited, 2010

selective catalytic reactor, 228
selective catalytic reduction, 21, 67, 203–7
  configuration and catalyst composition, 206
  configurations with typical system temperatures, 205
  operation, 206–7
  process description, 204–5
  unit slippage, 42
selective non-catalytic reduction, 207–8
Selexol process, 67, 73, 77, 348, 349, 395
semidry flue gas desulfurisation technology, 195
sensors
  coal-fired power plants on-line monitoring and measurement, 266–79
  combustion monitoring in power plants, 244–65
    experimental combustor, 247
    University of Maryland test combustor, 252
  consideration, 248–51
  information processing, 260–1
    computational sensor calibration model, 260–1
    data aggregation, 261
  novel micro-scale and nano-scale sensors, 249–51
    fibre optic sensors, 250–1
    nano-scale gas sensors, 251
  response, 251–4
    differential SPLs spectra, 254
    differential SPLs variation vs vertical and angular locations, 255
  smart sensor networks vision, 255–60
    envisioned smart MOEMS multifunctional sensor platform, 257
    hierarchical network structure, 258–9
    schematic diagram of hierarchical network structure, 258
    sensor coverage problem, 259–60
    smart multifunctional sensor platform, 256–8
  state-of-the-art for combustion monitoring, 248–9
    optical absorption and emission sensors, 248
    solid state gas sensors, 249
separation factor, 150
sewage sludge, 317
SGT6-6000G, 8, 10
shake-deflate baghouse, 232–3
shea chips, 329
Shell Claus off-gas treating process, 74
Shell gasifier, 62
shift reaction, 125, 126
  see also water gas shift reaction
shredder, 324
silicone, 235
SITRANS LR460, 267
Siveret's law, 116
sludge dewatering system, 200
SNCR *see* selective non-catalytic reduction
SO_2 Emissions Regulations (1983), 188
SOFC *see* solid oxide fuel cell
solid oxide fuel cell, 129
  power plant incorporating hydrogen membrane shift reactor, 130
solid state gas sensors, 249
solubility trapping, 370
sound pressure levels, 253
spallation, 12
specific collection area, 223
specific fuel consumption, 5
spiral module, 122
spiral-wound module, 163, 165, 169
SPL *see* sound pressure levels
spreader–stokers, 324
stage cut, 170
Stationary Emissions Standards (1970), 188
steam soot blowers, 206
steam tubular dryer, 297
steam turbine, 34–5
  corrosion, 97–9
    chemical environment in phase transition zone, 98–100
    deposits on turbine surfaces, 97
    liquid films in superheated parts, 97–8
  technology, 306
stratigraphic trapping, 370
Studstrup Power Station, 327, 328
sub-bituminous coals, 293
Sulfinol-D, 73
Sulfinol-M, 73–4
Sulfinol process, 73
sulphur, 403
sulphur trioxide, 199
supercritical power plant, 89

© Woodhead Publishing Limited, 2010

water and steam chemistry in the thermal cycle, 100–4
surface-modified inorganic membranes *see* hybrid membranes
surge margin, 22–3
syngas, 55, 65, 347, 366
composition for three CO_2 capture stages, 350
conversion and purification, 393–9
acid gas removal, 395–6
hydrogen recovery and purification, 396–9
multi-bed PSA plant operating cycle, 397
water gas shift reaction, 393–4
WGS equilibrium composition, 394
fossil-fuel feedstocks in power plants, 383–409
future trends, 408–9
CO_2 capture strategies for hydrogen production, 409
decentralised small-scale plants advanced techniques, 408
heavy feedstocks, 399–403
entrained flow gasifiers, 399–401
high-temperature raw syngas cooling options, 401
other gasifier arrangements, 401–2
treatment and hydrogen production, 402–3
production from gas and light liquids, 383–93
adiabatic pre-reformer and fired tubular reformer, 386
adiabatic pre-reforming, 385–6
advanced technologies, 389, 392
ATR reactor diagram, 387–9
autothermal reformers, 387–9
charge purification, 383–4
fired tubular reformers, 386–7
heat exchange steam reformers, 389
HESR + ATR reactors parallel arrangements, 391
HESR + FTR reactors and HESR + ATR reactors, 390
methane converted in a steam reforming process, 385
operational problems occurring in reformer reactors, 392–3
reforming reactions, 384–5
syngas cooler, 62

T-800, 11
tail gas treatment, 74
Teflon, 235
terrestrial sequestration, 376–7
thermal barrier coatings, 10–11
thermal cycle
challenges for future ultrasupercritical power cycles, 105–7
physical and thermodynamic properties of solutions, 105–6
transport properties of solutions, 106–7
deposits and corrosion, 94–100
boiler corrosion, 95–7
deposits, 94–5
deposits on an IP turbine, 99
HP turbine corrosion damage, 100
LP turbine corrosion damage, 98
other components in the water/steam cycle, 100
steam turbine corrosion, 97–9
supercritical turbine expansion curve and NaCl solubility, 97
improving efficiency in advanced power plants, 89–107
key characteristics, 91–3
Mollier diagram with turbine expression curves, 92
NaCl solubility in steam, 94
simplified fossil cycle with once-through boiler, 90
volatility, partitioning and solubility, 93–4
water and steam chemistry on supercritical and ultrasupercritical plant, 100–4
all-volatile treatment, 102–3
chemistry specifications for feedwater and steam, 103
EPRI specifications for feedwater and steam, 104
oxygenated treatment, 103
VGB specifications for feedwater and steam, 104
thermal mechanical fatigue, 26
time domain reflectometry, 267
TOXECON I, 209, 238
TOXECON II, 209, 238
TOXECON process, 238
TOXECON technology, 210
transition, 10
trapped vortex combustor, 51–2
tripper car system, 266
tubular dryer, 297

© Woodhead Publishing Limited, 2010

tubular membrane, 121, 122
tubularone, 297–8
turbine, 11–14

UBC process, 308
UCG *see* underground coal gasification
UK Clean Coal Programme, 342
UK Coal Authority, 352
ultrasupercritical boilers, 95
ultrasupercritical power plant
  future challenges, 105–7
  water and steam chemistry in the thermal cycle, 100–4
underground coal gasification
  advanced power plants environmental impact improvement, 332–59
  basic configuration, 335
  brief history, 334
  CO_2 potential sequestration into abandoned UCG cavities, 353
  depth of field trial 1960–2008, 339
  directional drilling and moveable injection, 338
  drilling technologies and well construction, 344–6
    directional drilling in coal, 345
    downhole assembly for directional drilling in coal, 345
    process walls underground engineering, 346
    steering in coal, 345–6
  environmental issues and benefits, 350–4
    CO_2 storage in UCG process vicinity, 353–4
    hydrology and ground water contamination, 351
    licensing requirements, 352
    regulatory requirements, 351–2
  estimated share of world coal resources, 356
  existing vs additional coal and gas reserves with UCG, 356
  future trends, 354–9
    Asia and South Africa, 357–8
    Australia, 358
    coal resources, 355–6
    current developments in 2009, 357
    Europe, 358
  gas composition of dry syngas from oxygen-fired UCG, 349
  gasification and cleanup basic flow chart, 348
  glossary, 360
  integration with power plant, 346–50
    power generation, 347
    surface plant for gas processing and cleaning, 348
    total and partial CO_2 capture from product gas, 348–50
  outstation possible layout, 341
  process, 335–41
    basic principles, 335–6
    commercial-scale operation, 341
    gasification reactions kinetics, 336–9
    modeling, 340
    oxygen vs air-blown UCG, 339–40
  reaction zone close-up, 337
  siting and geology criteria, 341–4
    coal characteristics, 343
    coal seams depth, 342–3
    selection criteria for UCG target sites, 342
    structure and physical properties of coal, 343–4
  stressed strata above UCG cavity, 354
  typical cavity shape, 336

viscous fingering, 367
volatile organic compounds, 41–2

water gas shift reaction, 58, 64–5, 125–6, 385, 393–4
  equilibrium composition, 394
water quench, 62
wet electrostatic precipitators, 219, 227–8
wet flue gas desulfurisation technology, 189–94
  alloy materials for wet FGD service, 194
  construction materials, 193–4
  generic wet scrubber system components, 190
  limestone and lime-based scrubbers, 190–3
WGS *see* water gas shift reaction
wheel speed, 18
White Coal technology, 304–5
  briquetting plant schematic diagram, 304
White Energy Company, 304
Wirbelschicht-Trocknung mit interner Abwarmenutzung, 298
  with external heating, 299

© Woodhead Publishing Limited, 2010

with integrated mechanical vapour compression, 299
woody biomasses, 316–17, 320
chemical constituents, 321
composition, heating values and ash properties, 321
WTA *see* Wirbelschicht-Trocknung mit interner Abwarmenutzung

zeolite membrane, 120
zeolites, 120

© Woodhead Publishing Limited, 2010